SUMO-dependent nuclear positioning safeguards replication fork integrity and competence

Kamila Schirmeisen

THÈSE DE DOCTORAT

NNT : 2023UPASL125

université PARIS-SACLAY

SUMO-dependent nuclear positioning safeguards replication fork integrity and competence

Positionnement nucléaire et SUMOylation dans le maintien de l'intégrité des fourches de réplication

Thèse de doctorat de l'université Paris-Saclay

École doctorale n° 577
Structure et Dynamique des Systèmes Vivants (SDSV)
Spécialité de doctorat : Sciences de la vie et de la santé
Graduate School : Life Sciences and Health
Référent : Faculté des sciences d'Orsay

Thèse préparée dans l'unité de recherche **Intégrité du Génome, ARN et Cancer** (Université Paris-Saclay, CNRS), sous la direction de **Sarah LAMBERT**, Directrice de recherche

Thèse soutenue à Paris-Saclay, le 14 Décembre 2023, par

Kamila SCHIRMEISEN

Composition du Jury

Membres du jury avec voix délibérative

Manuel MENDOZA Directeur de recherche INSERM, Université de Strasbourg	Président & Rapporteur
Marie-Noëlle SIMON Directrice de recherche CNRS, Université Aix-Marseille	Rapporteur & Examinatrice
Gerard MAZÓN Chargé de recherche CNRS, Université Paris-Saclay	Examinateur
Catherine FREUDENREICH Professeure, Tufts University	Examinatrice

Titre : Positionnement nucléaire et SUMOylation dans le maintien de l'intégrité des fourches de réplication.

Mots clés : réplication, recombinaison homologue, mobilité de la chromatine, sumoylation, réparation de l'ADN

Résumé : La transmission fidèle du patrimoine génétique est un processus cellulaire essentiel à la vie. Des accidents survenant au cours de la réplication, nommés stress de réplication, sont une source majeure d'instabilité génétique alimentant la tumorigenèse. La prise en charge du stress réplicatif survient dans un noyau présentant des compartiments avec des capacités de réparation différentes. Chez les eucaryotes, certains dommages de l'ADN présentent une mobilité accrue, un phénomène qui leur permet de changer de compartiment nucléaire afin de terminer le processus de réparation. De même, des fourches de réplication, dont la progression est altérée, se déplacent vers la périphérie pour s'ancrer aux complexes du pore nucléaire (CPN). Ces changements de compartiments sont régulés par le métabolisme de petits modificateurs de type ubiquitine (SUMO), qui jouent un rôle essentiel pour réguler spatialement les activités de la voie de réparation par la recombinaison homologue (RH). Nous avons précédemment établi, chez la levure *Schizossacharomyces pombe*, qu'une fourche de réplication bloquée par une protéine liée à l'ADN se relocalise et s'ancre au CPN de manière SUMO-dépendante. La formation de chaînes SUMO déclenche la relocalisation mais limite l'efficacité de redémarrage de la réplication par la RH. Un routage vers le CPN permet aux intermédiaires conjugués SUMO d'être éliminés par la protéase Ulp1 et le protéasome, dont les activités sont enrichies à la périphérie nucléaire.

Mon projet de thèse vise à décrypter comment le métabolisme SUMO et le CPN contribuent à la protection des fourches et à leur redémarrage. Pour cela, j'ai utilisé une approche de biologie synthétique pour bloquer la progression d'une seule fourche de réplication et étudier son devenir dans l'espace nucléaire de *S. pombe*. Tout d'abord, j'ai caractérisé le rôle du panier nucléaire, un sous-complexe du CPN, dans la réactivation des fourches par la RH.

J'ai découvert que la nucléoporine Nup60 assure la stabilité et la séquestration de la protéase SUMO Ulp1 à la périphérie nucléaire. J'ai aussi révélé que la nucléoporine Alm1 est importante pour la relocalisation et/ou l'ancrage des fourches bloquées au CPN. L'analyse de ces nucléoporines m'a permis de démêler les fonctions distinctes de Ulp1 et du protéasome dans la dynamique de redémarrage des fourches par la RH. J'ai montré, par une approche génomique cartographiant l'utilisation des ADN polymérases (Pu-seq), que les CPN associés à Ulp1 agissent sur la reprise de la synthèse d'ADN au niveau des fourches bloquées, tandis que les CPN associés au protéasome maintiennent la vitesse des fourches redémarrées. Les activités d'Ulp1 et du protéasome ne sont pas interchangeables et affectent différemment la dynamique du redémarrage des fourches par la RH. De plus, j'ai caractérisé la vague de SUMOylation qui se produit au site d'arrêt des fourches : la monoSUMOylation est insuffisante pour relocaliser les fourches à la périphérie nucléaire mais suffisante pour assurer la protection des fourches dans le nucléoplasme. En étudiant les rôles des deux SUMO ligases connues chez *S. pombe*, j'ai montré que, contrairement à Pli1, Nse2 n'est nécessaire ni pour la protection des fourches ni pour leur relocalisation à la périphérie nucléaire. Enfin, j'ai découvert que le compartiment nucléoplasmique est moins efficace dans la protection des fourches lorsque Ulp1 n'est pas séquestré à la périphérie nucléaire, alors que cette dernière fournit un environnement "protecteur des fourches" par des mécanismes encore inconnus.

L'ensemble de mes résultats suggèrent que la répartition spatiale du métabolisme SUMO et le positionnement nucléaire des sites de stress de réplication sont des déterminants clés de l'intégrité et du redémarrage des fourches de réplication. Ce travail permet de comprendre comment l'altération du métabolisme SUMO, fréquemment observée dans diverses maladies comme le cancer, influence le maintien de l'intégrité du génome.

Title : SUMO-dependent nuclear positioning safeguards replication fork integrity and competence

Keywords : replication, homologous recombination, chromatin mobility, sumoylation, DNA repair

Abstract : The maintenance of genome stability is crucial to ensuring the high-fidelity transmission of genetic information. Flaws in the DNA replication process, known as replication stress, has emerged as a major source of genome instability that fuels cancer development. Resolving replication stress occurs within a compartmentalized nucleus that exhibits distinct DNA repair capacities. In different eukaryotic organisms, DNA damage sites exhibit increased chromatin mobility, a phenomena that allow DNA damages to shift away from their nuclear compartment to achieve DNA repair. Similarly, replication forks whose progression is altered, were previously shown to shift to the nuclear periphery for anchorage to nuclear pore complexes (NPCs). These changes in nuclear positioning is regulated by small ubiquitin-like modifier (SUMO) metabolism, which is pivotal to spatially segregate the activities of the homologous recombination (HR) pathway. Our previous work in the fission yeast *Schizossacharomyces pombe*, has established that a replication fork blocked by a DNA-bound protein relocates and anchors to NPC in a SUMO-dependent manner. SUMO chains trigger the relocation of but also limit the efficiency of replication restart by HR. These SUMO conjugates can be cleared off by the SENP protease Ulp1 and the proteasome, whose activities are enriched at the nuclear periphery. Thus, a routing towards NPCs allows HR-dependent replication restart by counteracting the toxicity of SUMO chains.

My thesis project aims at deciphering how the spatial segregation of SUMO metabolism, together with NPCs, safeguard the integrity of replication fork and their replication competence. To reach this objective, I have exploited a synthetic biology approach to block the progression of a single replication fork and to investigate its fate within the nuclear space of the yeast *S. pombe*. First, I characterized the role of the nuclear basket, a sub-complex of the NPC, in facilitating recombination-dependent replication restart.

I discovered that the nucleoporin Nup60 ensures the stability and the sequestration of the SUMO protease Ulp1 at the nuclear periphery. Also, I revealed that the nucleoporin Alm1 is important for the efficient relocation and/or anchorage of arrested forks. The analysis of these two nucleoporins allowed me to disentangle the distinct functions of the SUMO protease Ulp1 and the proteasome in the dynamics of fork restart by HR. Using a genomic approach to map the usage of DNA polymerases (Pu-seq), I revealed that Ulp1-associated NPCs ensure an efficient initiation of DNA synthesis at restarted forks whereas proteasome-associated NPCs sustain the speed of restarted forks. The activities of Ulp1 and the proteasome cannot compensate each other but rather affect differently the dynamics of HR-dependent fork restart. Moreover, I have better characterized the wave of SUMOylation that occurs at site of fork arrest. While monoSUMOylation is insufficient to trigger the relocation towards the nuclear periphery, it is sufficient to safeguard fork integrity in the nucleoplasm. By investigating the division of labour of the two known SUMO ligases in fission yeast, I found that unlike Pli1, Nse2-dependent SUMOylation is dispensable for both relocation and protection of arrested forks. Finally, I found that the lack of Ulp1 sequestration at the nuclear periphery makes the nucleoplasmic compartment less efficient at ensuring fork protection, whereas the nuclear periphery provides a better "fork protective" environment by mechanisms that remain unknown.

Taken together, my results suggest that a spatially segregated SUMO metabolism and the nuclear positioning of replication stress sites are key determinants of replication forks integrity and restart. This thus shed light on how the distortion of SUMO equilibrium, frequently reported in a variety of human diseases including cancer, influences the maintenance of genome integrity at replication stress sites.

Acknowledgements

After the wonderful PhD journey at Institut Curie, it is time to acknowledge all the people who have participated in this amazing experience.

My first words go to my thesis director and supervisor, Sarah Lambert, who accepted me in her lab, first as an Erasmus student and then as a PhD student. Sarah, I am immensely grateful for your support, guidance, and encouragement, which have been invaluable throughout this journey. I greatly appreciate the immeasurable contribution you have made to shape my scientific development. The independence you gave me helped me discover my strengths, but also my weaknesses. You allowed me to contribute to different projects in the team, to participate in many conferences, to gain experience in writing scientific publications and review articles. It helped me grow and go beyond my initial skills to become better. I am convinced that everything I learned from you will be extremely useful during my future scientific adventures.

I would like to express my gratitude to all the members of my Jury for having accepted to evaluate my work. I sincerely thank Marie-Noëlle Simon and Manuel Mendoza, for the considerable investment and time they afford me by accepting to be reporters of this manuscript; Catherine Freudenreich and Gerard Mazón, for their willingness to be the examiners at my thesis defence. I am also thankful to the members of my thesis committee: Emmanuelle Fabre and Benoit Palancade, whose constructive comments and suggestions were always helpful and provided me with new ideas for my project. I would also like to thank our collaborators Tony Carr and Karel Naiman for joining our efforts in advancing this project.

I am thankful to the financial support I received from La Ligue contre le cancer for the first three years and Fondation ARC pour la recherche sur le cancer that financed my 4th year.

All this would not have been possible without the support of the team members. In particular, a special word goes to Karol Kramarz, who with patience guided me through my first years in the lab. Karol, you took me under your wing, devoted so much time to

mentor me, always believed in me and for that I thank you enormously. It was a real pleasure working with you and I am very grateful for everything you taught me. In line with our motto: "work hard, play hard", we spent many weekends and holidays in the lab back then, but I think we both agree that it paid off. I will come back to the second part of the motto a little later. I had the chance to spend three years in the company of Shrena, with whom I laughed a lot together. I am very grateful for your generosity and the support you have given me on a daily basis. Thank you for sharing not only the cool and happy moments but also the difficult and stressful ones. I hope to remain your favourite officemate. Even though we only worked together for a year, I am very glad that I had the opportunity to meet Lucie. You have no idea how inspiring and motivating you are to me. I will miss our long discussions, they were the moments where laughter was guaranteed unless the topic of the day was a difficult ideological or political issue. Thank you for being my sports buddy and for all the effort you put into teaching me how to fall safely while climbing. An enormous merci goes to Karine for all her efforts and help she provided me, especially in the last stage of my PhD. Combining forces and developing an efficient work system allowed us to break the lab record (and perhaps the world record as well) in the number of 2D gels done over the course of several months. Vincent, thank you for your availability and willingness to lend a helping hand whenever needed. For all the moments of laughter and joy we shared in and outside the lab. I am also grateful to Anne, whose unwavering kindness and contagious enthusiasm always created a positive and motivating work environment. Another thank you goes to Anissia for helping with the English/French corrections of the manuscript. I wish also to thank a lot other past and present members of the lab: Virginie, Dingli, Julien, Charlotte, Wafa, Typhaine, Maxime, Anusha, Eve, Elena, Kazi, Luca. It has been a pleasure to share bench, lunch, beers, scientific (and not so scientific) discussions.

I would also like to thank Marie-Noelle Soler and Laetitia Besse from Imaging Facility for their support, availability and always being friendly. Laetitia thank you for helping me so much with your great professional skills. I cannot forget to thank the kitchen (laverie) staff for their valuable work.

A huge thank you to all current and former members of UMR3348 for the friendly working environment, support, feedback received during our meetings and the great time spent together.

I would especially like to thank Anna, with whom I started my PhD thesis at the same time and we will finish it together. Due to the pandemic situation, we did not have much contact at the beginning, but nothing strengthened our friendship as much as the unforgettable train ride in Toulon. I am a big fan of your sense of humor and have always been impressed by all of your pranks & jokes. Tristan, Shreiyangi, Jenny and Armand, thank you for being also a part of this adventure. By being "external" to the lab, you had the unique ability of switching my mindset to a different point of view.

Enormous thanks goes to my Polish "family" here in France: Ania, Marysia and Karol. Each of you supported and helped me so much that I would never find enough words to thank you. Especially, that without you, I would have no chance in the fight against the French administration. I greatly appreciate all the moments we spent together, many hours of hiking, countless parties in Puchaczówka and Filia, celebrations of Polish holidays and traditions, conversations that could last forever.... Thank you Damesy for making all these years some of the most intense and unforgettable in my life! I would also like to thank Marco, for all the fruitful discussions we had and great moments we shared.

To my dear friend Ola for always finding a way to visit me in Gif (whenever possible and whatever it takes) and for all the crazy stories we had together. Thank you for your constant motivation, energy and spontaneity that always helped me recharge my batteries. To Laura and Aga with whom even from the distance I shared all the important moments of this journey. Thanks for all your encouragement and support.

Finally, last but by no means least, I deeply thank my family back in Poland, who always believed in me and strongly supported, even though it was not an easy time for them either. I would like to thank my parents Marzanna and Bernard for always making me feel that they are proud of me. Thanks to Adam and Agata for supporting me during this path and for being my eyes on Mum, Dad and Grandpa during this time. A special thanks to my little Ola, the latest arrival in our family, for making this last period happier and easier to face.

Table of contents

List of Figures

List of Tables

Abbreviations

A	adenine
ALT	Alternative Lengthening of Telomeres
alt-EJ	alternative End-Joining
Aos1	Activator of SUMO 1
APH	aphidicoline
ARS	Autonomously Replicating Sequence
ATM	Ataxia-Telangiectasia Mutated
ATPase	Adenosine Triposphate
ATR	Ataxia Telangiectasia and Rad3-related
ATRIP	ATR-interacting protein
BIR	Break Induced Repair
BLM	Bloom Syndrome RecQ Like Helicase
Bp	base pair
BPDE	benzo(a)pyrene diol epoxide
BRCA (1 and 2)	Breast Cancer
C	cytosine
Cas9	CRISPR associated protein 9
Cdt1	Chromatin Licensing and DNA replication factor 1
CDC (6, 25, 45…)	Cell Division Cycle
CDK (1 and 2)	Cyclin-dependent kinase
ChIP	Chromatin Immunoprecipitation
CHK (1 and 2)	Checkpoint Kinase
CMG	Cdc45-MCM-GINS complex
CPT	camptothecin
CRISPR	Clustered Regularly Interspaced Short Palindromic Repeats
CtIP	CtBP-interacting protein
Dbf4	Dumbbell former 4 protein

DDK	DBF4-Dependent Kinase
DDT	DNA Damage Tolerance pathways
dHJ	double Holliday Junction
D-loop	Displacement loop
dNTPs	deoxyribonucleotides
DPCs	DNA–protein Cross-link
DRC	DNA Repair Checkpoint
DSB	Double-Strand Break
dsDNA	double-stranded DNA
DSBR	Double-Strand Break Repair
E.coli	*Escherichia coli*
EM	Electron Microscopy
EME1	Essential Meiotic Structure-Specific Endonuclease 1
ERCC1	Excision Repair Cross-Complementation group 1
ETAA1	Ewing Tumor-Associated Antigen 1
EXO1	Exonuclease 1
FACS	Fluorescence Activated Cell Sorting
Fbh1	F-Box DNA Helicase 1
G	guanine
GEN1	Gen Endonuclease Homolog 1
GFP	Green Fluorescent Protein
GINS	go-ichi-ni-san complex
HJ	Holliday Junction
HLTF	Helicase Like Transcription Factor
HR	Homologous Recombination
HU	hydroxyurea
ICLs	Interstrand Crosslinks
IR	Ionizing Radiation
Kap (60 and 121)	karyopherins

Kb, **Mb**	kilo- and mega- base
Ku	Ku70-Ku80 heterodimer
MCM	Minichromosome Maintenance Complex
Mec1	Mitosis Entry Checkpoint 1
MiDAS	Mitotic DNA synthesis
Mlp (1 and 2)	Myosin-Like Proteins
MMS	Methyl-Methanesulfonate
Mms21	Methyl Methanesulfonate sensitivity 21
MRE11	Meiotic Recombination 11
MRN/MRX	Mre11-Rad50-Nbs1/Xrs2
MSD	Mean-Square Displacement
Msh (2, 3, 6)	Mitochondrial Targeting Sequence
MUS81	MMS and UV Sensitive 81
NBS1	Nijmegen Breakage Syndrome 1
NHEJ	Non-Homologous End Joining
NP	Nuclear Periphery
NPC	Nuclear Pore Complex
Nup (1, 37, 84…)	nucleoporins
ORC	Origin Recognition Complex
PARP1	Poly (ADP-ribose) polymerase 1
PCNA	Proliferating Cell Nuclear Antigen
Pc2	Polycomb 2
Phase G1	Phase Gap1
Phase G2	Phase Gap2
Phase M	Phase of mitosis
Phase S	Phase of synthesis
PIAS	Protein Inhibitor of Activated STAT
Pif1	Petite Integration Frequency 1
Pol (δ, η…)	DNA polymerase

preRC	pre-Replication Complex
POT1	Protection of Telomeres 1
pre-mRNA	precursor messenger RNA
PRIMPOL	human DNA polymerase-primase
Pu-seq	Polymerase Usage Sequencing
Rad (50, 51 …)	radiation sensitive
RANBP2	RAN Binding Protein 2
rDNA	ribosomal DNA
RDR	Recombination-Dependent Replication
RecA	Recombinase A
RecQ5	RecQ-like type 5
RFB	Replication Fork Barrier
RF-C	Replication Factor C
RIF1	Replication Timing Regulatory Factor 1
RING	Really Interesting New Gene
RNAi	RNA interference pathway
RNase	Ribonuclease
RNF4	Ring Finger Protein 4
RNR	Ribonucleotide Reductase
rNTP	Ribonucleotide Triphosphates
ROS	Reactive Oxidative Species
RPA	Replication Protein A
RS	Replication Slippage
RSR	Replication Stress Response
Rtf (1 and 2)	Replication termination factors
RTS1	Replication Terminator Sequence 1
SAE (1 and 2)	SUMO-Activating Enzyme Subunit 1 and 2
Sc	*Saccharomyces cerevisiae*
SD	Standard Deviation

SDSA	Synthesis-Dependent Strand Annealing
SENP (1, 2, 3…)	SUMO-specific proteases
Sgs1	Slow Growth Suppressor 1
SIM	SUMO Interaction Motif
SLX (1, 2, 5, 8)	Synthetic Lethal of unknown (X) function
SMARCAL1	SWI/SNF Related, Matrix Associated, Actin Dependent Regulator Of Chromatin, Subfamily A Like 1
SNF2	Sucrose Non-Fermentable
Sp	*Schizosaccharomyces pombe*
Srs2	Suppressor of Rad Six 2
SSA	Single Strand Annealing
ssDNA	single-stranded DNA
STUbL	SUMO-Targeted Ubiquitin Ligase
SUMO	Small Ubiquitin-Like Modifier
Swi2	SWItch 2
T	thymine
TAD	Topologically Associating Domains
TLS	Translesion Synthesis Polymerases
TOPBP1	Topoisomerase II Binding Protein 1
TOPORS	TOP1 Binding Arginine/Serine Rich protein
TPR	Translocated Promoter Region
TRCs	Transcription-Replication Conflicts
TS	Template Switch
Ubc9	Ubiquitin conjugating enzyme 9
UFBs	Ultrafine Anaphase Bridges
Ulp (1 and 2)	Ubiquitin-like specific protease 1 and 2
Uls1	Ubiquitin Ligase for SUMO conjugates 1
UV	Ultraviolet
WT	Wild Type

XP (C, F, G)	Xeroderma pigmentosum group
XRCC (1, 2, 3, 4)	X-ray Repair Cross-Complementing protein
ZNF451	Zinc Finger Protein 451
ZRANB3	Zinc Finger RANBP2-Type Containing 3
µM, nM, mM	micro-, nano- and mili-meter
2DGE	bi-Dimensional Gel Electrophoresis
53BP1	p53-Binding Protein 1

INTRODUCTION

Figure 1: **Double helix model and base pairing.** Left: The double-helical structure of DNA elucidated by James Watson and Francis Crick in 1953. Right: The sugar-phosphate backbones (in grey) run in opposite directions and the 3′ and 5′ ends of the two strands are aligned. Attached to each sugar is one of four bases: adenine (A), cytosine (C), guanine (G) or thymine (T). Hydrogen bonds between the complementary bases connect the two anti-parallel DNA. (Adapted from Pray, 2008)

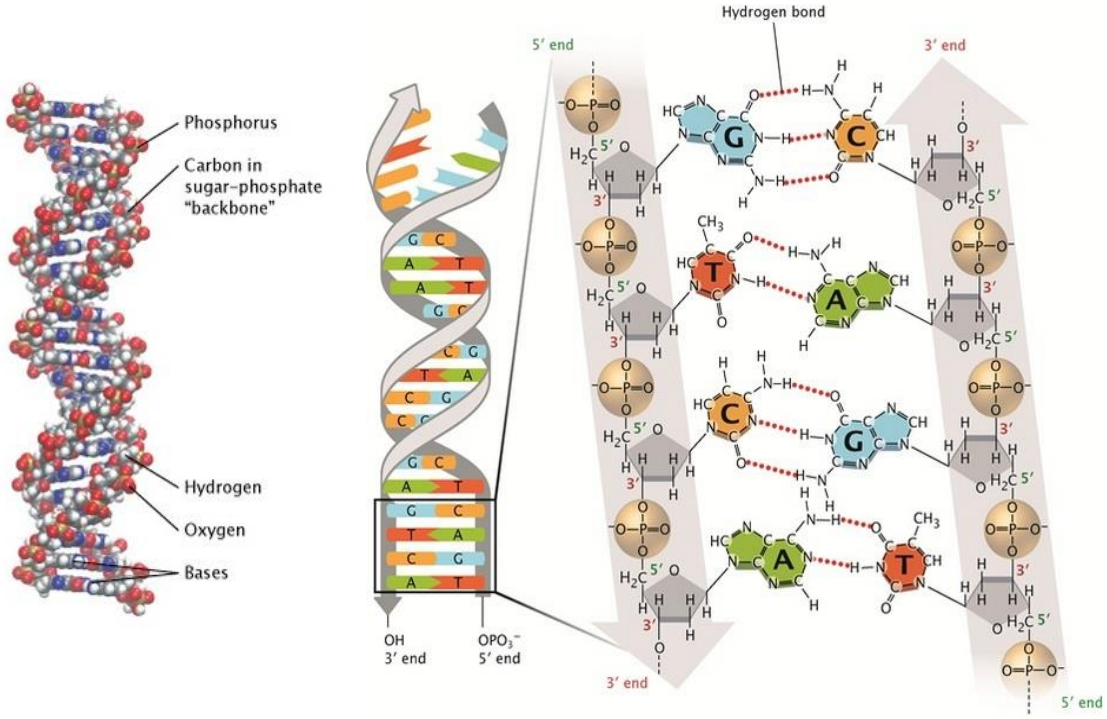

I. Replication stress as a source of genome instability

A: Mechanistic overview of DNA replication

At the core of every living organism lies a symphony of molecular events, orchestrated with precision and purpose. Within the complex world of cellular processes, few events are as fundamental and vital as cell division. This ability of cells to undergo division and proliferation, gives rise to the generation of new tissues, repair the damaged ones, and facilitates the constant renewal of life. About 330 billion cells are replaced daily (most of them being blood cells), which represents about 1% of all our cells (Sender and Milo, 2021). This relentless division requires an immaculate mechanism to ensure the faithful transmission of genetic information through generations.

In 1953, Watson and Crick made one of the most important breakthroughs in the history of biology, by providing the missing pieces to the puzzle of how genetic information is stored and passed on in living organisms. They not only deciphered the double helix structure of DNA, but also proposed the specific base pairing rules (A-T and G-C), giving an elegant explanation for a semi-conservative model of DNA replication (Figure 1) (Watson and Crick, 1953). Each parent strand of the DNA molecule acts as a template for synthesis of a complementary daughter strand, resulting in two identical DNA molecules. The process of DNA replication is highly regulated and extremely accurate to ensure that each new DNA molecule is an exact copy of the original, thereby preserving the integrity of the genome (Bell and Labib, 2016; Burgers and Kunkel, 2017).

Like many other processes of molecular biology, the course of DNA replication has been conventionally divided into three main stages known as initiation, elongation and termination (Masai et al., 2010).

1. Initiation

DNA synthesis begins at particular sites that have been named origins of replication (Fragkos et al., 2015). Replication origins, which consist of short sequences within DNA that are recognized by initiator proteins, have been well characterized in bacteria and yeast. In budding yeast, DNA replication is initiated at well-defined DNA sequence motifs called autonomously replicating sequence (ARS) (Xu et al., 2006). However, more recent research has shown that the situation in budding yeast may be in fact an exception, as in most of the eukaryotic cells (including fission yeas and human) replication is initiated at non-specific sequences. Specifically, replication of the human

Figure 2: **Initiation of DNA replication in *S. cerevisiae*.** Replication initiation occurs in two temporally separated steps. During origin licensing ORC, Cdc6 and Cdt1 cooperate to load onto chromatin an inactive double MCM2-7 hexamer to form the pre-replication complex (preRC). This step occurs from late mitosis to the end of G1. During the subsequent S phase, CDK and DDK kinases drive the activation of the pre-RC complex in a process called origin firing. The conversion of an inactive double MCM2-7 complex into two functional replisomes requires Sld2, Sld3, Sld7, Mcm10, Dpb11 and DNA polymerase ε. These firing factors promote the recruitment of Cdc45 and GINS to form the CMG complex, which stimulates the helicase activity of the MCM2-7 complex. (Adapted from Hills and Diffley, 2014)

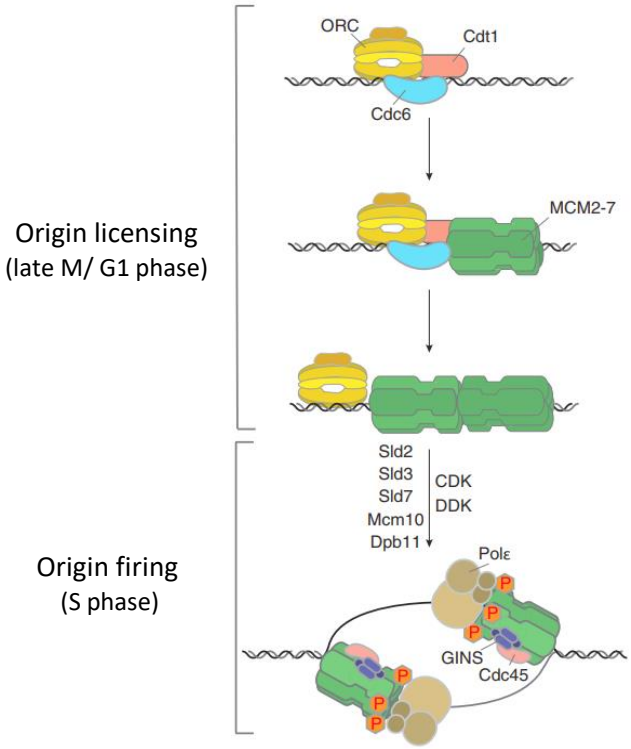

genome initiates within kilobase-sized broad zones and the exact position of the individual DNA replication origins within this zones, as well as the firing timing remain a matter of debate. Therefore, it becomes more and more common to use the term replication initiation zone instead of origin in the case of replication in human cells (Lubelsky et al., 2011; Petryk et al., 2016; Wang et al., 2021; Guilbaud et al., 2022).

The number of replication origins in a genome is dependent on chromosome size. In contrast to small, circular bacterial genomes that have one single origin of replication, eukaryotic linear genomes contain multiple origins, varying from 400 in yeast to 20 000-50 000 in humans (Nieduszynski et al., 2007; Cvetic and Walter, 2005; Méchali, 2010). Moreover, in metazoan the location of origins is specified by the context of local chromatin organisation, and may vary between rounds of replication or from one tissue to the other one.

During the late M to early G1 phase of the cell cycle, Origin Recognition Complex (ORC) binds to potential origin DNA sequences and, with the help of CDC6 and CDT1 proteins, loads the MCM2-7 complex (replicative helicase) onto the chromosome (Figure 2) (Bell and Stillman, 1992; Bochman and Schwacha, 2008; Deegan and Diffley, 2016). This process generates the pre-replicative complex (pre-RC), which licences the origin for potential activation in the subsequent S phase. In the next step, the licensed origins are activated in a process called origin firing. As cells progress into S-phase, the activity of CDKs and DDKs promotes the recruitment of proteins like CDC45 and GINS to the origin, leading to the formation of an active CMG helicase complex (Heller et al., 2011; Moyer et al., 2006; Douglas et al., 2018). Importantly, the separation of origin licensing and activation into distinct cell cycle phases ensures that the genome is copied exactly once during the cell cycle. Activation of the helicase allows unwinding and separating the DNA helix into ssDNA, which serves as templates for replication. As the DNA opens up, Y-shaped structures called replication forks are formed. Because two helicases bind per one origin of replication, two replication forks are formed and proceed bi-directionally along the genome, creating replication bubbles (Georgescu et al., 2017; Douglas et al., 2018).

2. Elongation

During elongation, DNA replicative polymerases add nucleotides to the growing DNA chain (Pavlov et al., 2020). The template strand specifies which of the four nucleotides (A, T, C, or G) is added along the newly synthesised strand. Importantly, DNA polymerases are only able to incorporate free nucleotides to the 3' end of an existing polynucleotide chain; therefore, the new strand will be formed in a 5’ to 3’ direction

Figure 3: **Simplified model of replication elongation with the focus on the composition of eukaryotic replisome.** At each replication origin, two replication forks are formed and proceed in opposite directions. DNA synthesis starts with the synthesis of RNA-primed DNA fragments by Pol alpha and Primase. They are further elongated by two different DNA polymerases (δ and ε) that are recruited for the DNA synthesis on lagging and leading strands, respectively. (Adapted from Méchali, 2010 and McCulloch and Kunkel, 2008)

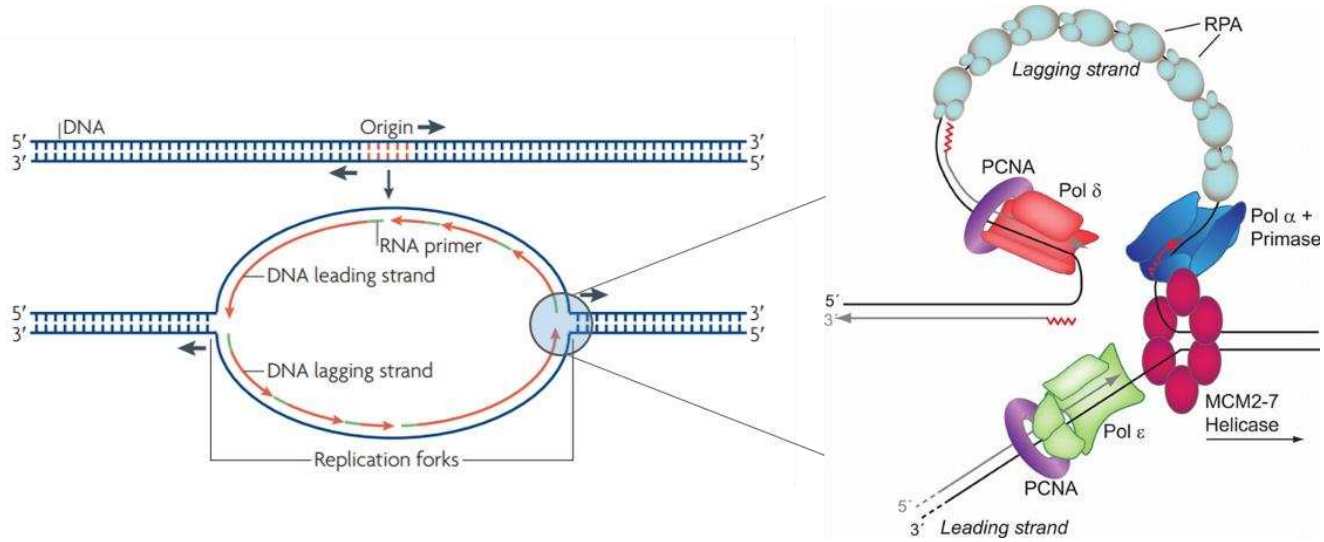

(Figure 3). This process will continue until the DNA polymerase reaches the end of the template strand or meet a converging fork. Among the multiple known eukaryotic DNA polymerases, three are at the main ones required to duplicate the bulk of eukaryotic genomes: DNA polymerase alpha (Pol α), DNA polymerase delta (Pol δ) and DNA polymerase epsilon (Pol ε). Besides the main activity of synthesising a new DNA strand at a generally high accuracy, most polymerases also possess a 3′-5′ exonuclease activity (Simon et al., 1991). It enables the removal of nucleotides that have just been synthetized at the 3′ end. This so-called proofreading function is to correct for occasional base pairing errors that may occur during strand synthesis. Moreover, DNA replication requires additional replication factors: the single-stranded DNA-binding protein (RPA), the clamp (PCNA) with its loader (RF-C) (Waga et al., 1998; Burgers and Kunkel, 2017). Replicative helicases, while unwinding DNA, cause torsional strain inducing super-positive supercoils ahead of replisome. Removal of these supercoils by topoisomerases I and II is essential for continued fork progression.

The above-described properties of DNA polymerases cause two major complications during the replication process. First, DNA polymerase adds a nucleotide to the pre-existing 3' end, therefore is unable to initiate the DNA synthesis *de novo,* in the absence of a free 3′ end on a single-stranded molecule. Therefore, primers are needed to facilitate the complementary strand synthesis (Figure 3). They are made by primase, a DNA-dependent RNA polymerase that has no difficulties with dealing with single stranded template to provide the needed primers (Pellegrini et al., 2012). These RNA primers are quite short and consist of approximately 7-12 ribonucleotides. Second, in a double stranded DNA molecule, the two strands run antiparallel to one another. Therefore, during replication the two newly synthesised strands grow in opposite directions as DNA polymerases can only synthesise new strands in the 5′ to 3′ direction (Georgescu et al., 2014; Miyabe et al., 2015). One strand, called the “leading” one is copied in a continuous manner, toward the replication fork as helicase unwinds the double-stranded DNA template. Replication of the other one, termed "lagging strand" has to be carried out in a discontinuous manner, in the direction away from the replication fork. The lagging strand is composed of short segments (typically about 100-200 nucleotides long), called Okazaki fragments, that are further ligated together to produce an intact daughter strand (Okazaki et al., 1968).

3. Termination

After a successful elongation, replication has to be terminated to give two copies of the DNA. Unlike initiation and elongation, replication termination has received

Figure 4: **Replication terminaton.** Before termination, replication forks encounter each other and the topological stress is relieved by the formation of catenanes. Converging CMG helicases bypass each other and continue to translocate until they encounter the last Okazaki fragments on the lagging strands. Once associated with dsDNA, CMGs undergoe ubiquitination on their MCM7 subunits, which promotes CMGs extraction from chromatin and Cdc48-dependent disassembly. Of note, CMG is unloaded only after has been fully ligated. (Dewar et al., 2015)

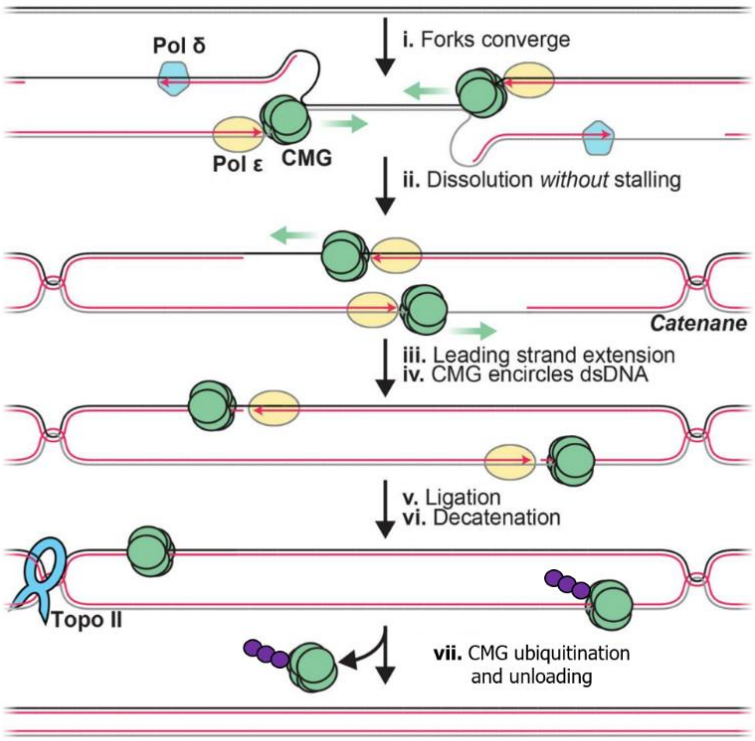

relatively little attention, especially in eukaryotic cells, although these events are just as abundant as initiations (Dewar and Walter, 2017). Termination occurs when two replication forks, moving in opposite direction from neighbouring origins, meet each other on the same stretch of DNA (Figure 4). This process called fork convergence is an essential prerequisite for replisome dissociation from the DNA. Initiated by ubiquitination of the MCM7 subunit, replisome disassembly prevents re-replication and interference with other chromatin-based processes (Maric et al., 2017; Moreno et al., 2014). The replicated sister chromatids are still linked by catenanes that are removed utilising topoisomerase II so that chromosome segregation can proceed successfully during the forthcoming mitosis (Keszthelyi et al., 2016).

Linear chromosomes face an issue that is not seen in circular DNA replication (Maestroni et al., 2017; Brenner and Nandakumar, 2022). When the replication fork reaches the end of the chromosome, the position and the removal of the RNA primer, which initiates the last Okazaki fragment, creates a gap at the lagging strand. Such incomplete replication would accelerate telomere shortening at each passage of the replication fork, thus limiting replicative lifespan. This DNA end-replication problem is handled in eukaryotic cells by *de novo* synthesis of telomeric repeats by telomerase: a specialised DNA polymerase that possesses a RNA template and a reverse transcriptase subunit. Extension of the telomeric DNA ensures that the ends of chromosomes are successfully duplicated with each round of DNA replication and cell division.

B: Replication stress

1. Sources

Any hindrance to DNA replication, which thought to be a faithful process ensuring accurate duplication of the genome, can have profound consequences for genome stability. The phenomenon of impeded replication forks progression and altered dynamics of DNA replication is termed replication stress and can be caused by a wide variety of endogenous and exogenous sources that either stalls, blocks, or terminates DNA polymerization (Figure 5) (Zeman and Cimprich, 2014).

1.1. Replication forks barriers

The major cause of replicative stress is slowing or stalling replication fork progression by various types of physical obstacles/barriers or under limited metabolic ressources. These replication blocks arise from distinct endogenous and exogenous sources, which will be briefly described below.

Figure 5: **Sources of DNA replication stress.** See text for details. (Willaume et al., 2021)

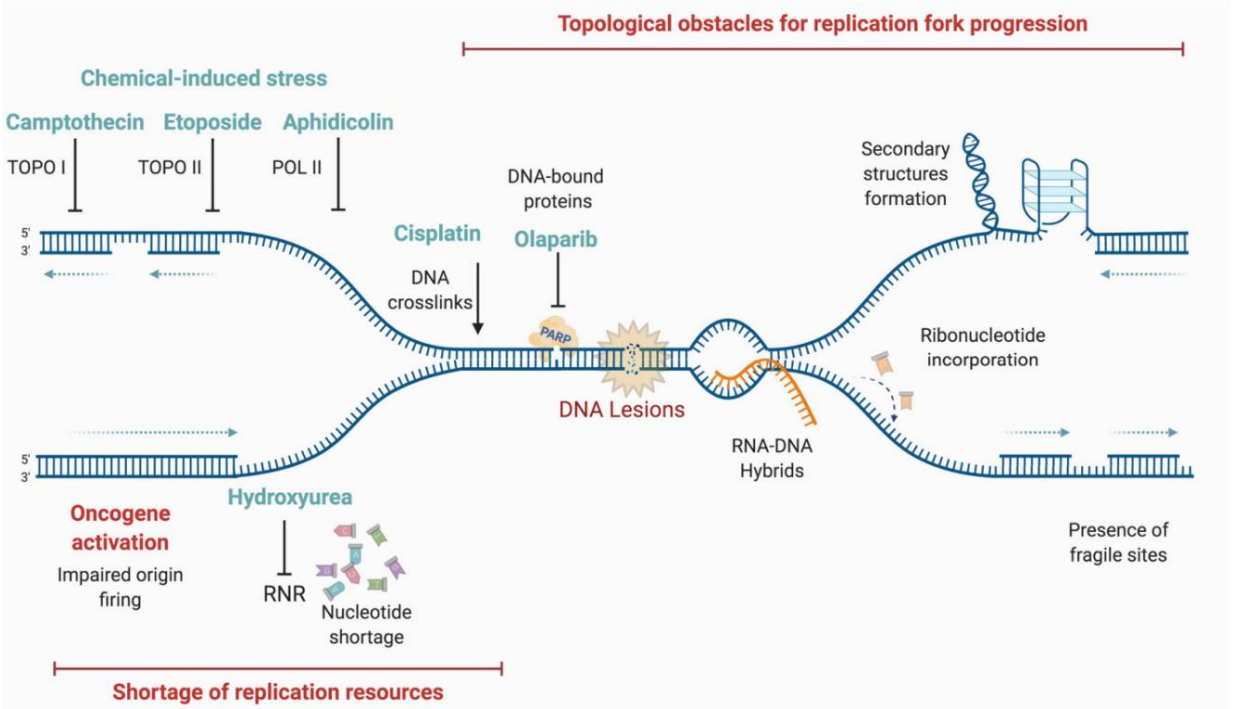

DNA lesions. One of the sources of replication stress are DNA lesions or adducts generated spontaneously during DNA metabolism or induced by environmental agents (Ashour and Mosammaparast, 2021; Ciccia and Elledge, 2010). Spontaneous DNA alterations (estimated to happen up to 10^5 times per cell per day) may result from dNTP misincorporation during DNA replication, interconversion between DNA bases caused by deamination, loss of DNA bases following DNA depurination alkylation (Lindahl and Barnes, 2000). Additionally, reactive oxidative species (ROS) derived from normal cellular metabolism processes can cause oxidation of DNA bases, strand breaks and removal of bases (Hoeijmakers, 2009). Nicks and gaps that occur in the course of several DNA repair pathways or some common DNA transactions (e.g. release of topological stress) can also be sources of replicative stress.

Environmental DNA damage arises from physical or chemical sources. Most common physical genotoxic agents are all wavelengths of ultraviolet (UV) and ionising radiation (IR). Exposure to UV (from sunlight) or IR (from cosmic radiation, medical treatments employing X-rays or radiotherapy) leads to the formation of DNA damage by inducing oxidation of DNA bases and subsequent introduction of single-strand and double-strand DNA breaks (SSBs and DSBs, respectively) (Hoeijmakers, 2009; Cadet and Wagner, 2013; Vallerga et al., 2015). Chemical mutagens also cause a broad spectrum of DNA lesions. Alkylating agents such as methyl-methanesulfonate (MMS) transfers methyl groups or other small alkyl groups to the DNA base, which becomes an obstacle to replication fork progression (Beranek, 1990). Crosslinking agents introduce covalent links between nucleotides of the same strand (intra-strand crosslinks), like cisplatin, or different strands (inter-strand crosslink), like mitomycin C (Schärer, 2005; Noll, 2006). Crosslinks make the strands unable to separate and/or uncoil, thus physically blocking normal progression of the replisome.

Misincorporation of ribonucleotides. In addition to ensuring high fidelity base pairing, replicative DNA polymerases are challenged by the discriminating between deoxyribonucleotides (dNTPs) and ribonucleotides (rNTPs). These are two types of nucleotides containing a similar, but not identical sugar-phosphate backbone. The high concentration of ribonucleotides, as well as the failure of DNA polymerases to perfectly determine the right nucleotide leads to misincorporation of ribonucleotides into the newly replicated DNA (Joyce et al., 1997). In human cells, the average frequency of ribonucleotide misincorporation into replicating DNA has been estimated to be one ribonucleotide per 1.5–2 kb. As it occurs at a strikingly high rate, ribonucleotide misincorporation is the most common type of replication error in normal cells (McElhinny et al., 2010; Clausen et al., 2013; Zong et al., 2020). However, ribonucleotide's presence in a DNA template stalls the replicative polymerases during

semi-conservative replication. Removal of misincorporated rNTPs is catalysed by the specialised ribonucleotide enzyme RNase H2, which loss has been linked to replication stress, mutation rate increase and genome instability (Lazzaro et al., 2012). Notably, mutations in RNase H2 leads to the Aicardi Goutières syndrome, which is an autosomal recessive inflammatory brain disorder that resembles congenital viral infection (Crow et al., 2006).

Non-B DNA structures. Canonical B-DNA is a right-handed double helix made of two antiparallel strands. During replication, the DNA strands must be separated to expose the DNA template, which gives an opportunity for alternative DNA structures to form. Several types of unusual secondary structures have been characterised, pointing to their ability to cause replication fork stalling, chromosomal fragility, and genome instability (Brown and Freudenreich, 2021).

G-quadruplexes are four-stranded intermolecular structures which form in GC-rich regions by Hoogsteen base pairing between guanine residues (Sen and Gilbert, 1988; Mirkin, 2007). It has been suggested that they arise as a consequence of replication, as their abundance is increased in S-phase (Biffi et al., 2013; Di Antonio et al., 2020). Hairpins or stem-loop structures are fold-back structures that rely on classic Watson–Crick base pairing within one DNA strand. They can be formed by many different types of sequences like inverted repeats, expandable trinucleotide repeats and palindromes. Hairpin, like G-quadruplex, forms on one DNA strand, leaving the complementary DNA strand single-stranded (Bochman et al., 2012). When two hairpins are located directly across from one another, a cruciform structure is formed. This phenomenon occurs much more frequently within AT rich sequences, in which the double helix can be easily unwound. In order to overcome the appearance of secondary structures during replication, a number of specialised helicases and structure-specific nucleases are engaged to unwind and disassemble them. Loss of these enzymes or the chemical stabilisation of the secondary structures can lead to slower replication fork progression and deletions of sequences at which these structures are predicted to form (Sharma, 2011; Paeschke et al., 2013).

In addition to secondary structures, compacted chromatin could also be problematic for the replication machinery. Heterochromatin regions within the genome, like centromeres and telomeres, inherently challenge replication, thus demand specialised mechanisms for chromatin remodelling to guarantee smooth progression of the replication fork (Ivessa et al., 2003; Sfeir et al., 2009; Zaratiegui et al., 2011). Furthermore, replication forks can stall at regions where the DNA topological stress

accumulates during opening up of the DNA double helix (replicated or transcribed regions) (Gaillard et al., 2015).

Transcription-Replication Conflicts. As transcription and replication both happen on DNA, they are spatially and temporally separated. Any perturbation of this coordination leads to collision between the transcription and replication machineries termed Transcription-Replication Conflicts (TRCs), which is a known source of replication stress (Wei et al., 1998; García-Muse and Aguilera, 2016). Regions of TRCs are marked by the appearance of R-loops: three-stranded polynucleotide structures consisting of DNA-RNA hybrids and the complementary strand being displaced as ssDNA. Since R-loops can serve as transient replication blocks, DNA topoisomerases, RNA-binding proteins and the exosome actively prevent their formation. If still formed, R-loops can be cleaved by specific DNA-RNA nucleases, removed by the RNase H family of enzymes or dismantled by specific DNA-RNA helicases (Gan et al., 2011; Helmrich et al., 2013, Sollier and Cimprich, 2014; Hamperl et al., 2017; Matos et al., 2020).

DNA-protein crosslink. The covalent binding of proteins to DNA causes the formation of another common source of replication stress (Tretyakova and Groehler, 2015; Vaz et al., 2017; Fielden et al., 2018). DNA-protein crosslinks (DPCs) can arise in an enzymatic manner, when a DNA-based enzyme, such as topoisomerases, becomes trapped and cannot complete the reaction it catalyses. It becomes not only a physical obstacle to the replisome but also often exposes single- or double-stranded breaks. Stabilisation of such intermediates can happen spontaneously in case of DNA damage, or be enhanced in the presence of specific chemotherapeutic drugs. For example, camptothecin and etoposide inhibit topoisomerase I or II, respectively, by trapping topoisomerase-DNA cleavage complexes. DNA polymerases and PARP1 can also become DPCs when trapped by aphidicolin and Olaparib, respectively (Ide et al., 2011; Vare et al., 2012; Pommier and Marchand, 2011). On the other hand, non-enzymatic DPCs define covalent crosslinking of any protein in the vicinity of DNA after exposure to agents such as UV light or aldehydes (Stingele et al., 2017).

1.2. Defects in the replication machinery

Faithful and dynamic DNA synthesis requires a balanced supply of dNTPs, generated by conversion of ribonucleotides to deoxyribonucleotides. This process is catalysed by the ribonucleotide reductase (RNR) which activity is highly regulated (Nordlund and Reichard, 2006; Zhang et al., 2009; Mathews, 2016). Alterations in RNR expression or its activity change the intra-cellular dNTP levels affecting replication dynamics in different ways. Increased dNTP pools interferes with initiation and induces mutagenesis by

reducing the fidelity of DNA polymerase proofreading (Chabes and Stillman, 2007; Kumar et al., 2010). In contrast, shortage of dNTPs induces a sharp transition to a slow-replication mode thus impeding fork progression (Bester et al., 2011; Chabosseau et al., 2011; Poli et al., 2012). Furthermore, mutations affecting replisome components are also associated with replication stress, as they give rise to reduced number, stability or fidelity of replication forks. This applies, among others, to mutations that disturb the stability and catalytic activity of DNA polymerases, helicases or RPA (Heitzer and Tomlinson, 2014; Alvarez et al., 2015; Bellelli and Boulton, 2021).

1.3. Dysregulation in origin firing

Most replication origins (more than 50% in yeast and about 90% in humans) that are licensed during G1 phase do not fire during unperturbed S phase, remaining as dormant origins to provide a backup mechanism to buffer replication perturbations (Heichinger et al., 2006; McIntosh and Blow, 2012).

Indeed, upon replication stress, these dormant origins are activated, leading to a higher origin firing density on chromatin to achieve complete and timely duplication of the genome (Ibarra et al., 2008; Moiseeva et al., 2019). However, recent studies suggest that alterations in origin firing program are not just a consequence but also a source of replication stress.

Defective replication origin firing results in genomic regions that are prone to under-replication, meaning chromosomal regions that remain un-replicated when cells enter mitosis. Such regions often refer to as chromosomal fragile sites (CFS). Mice and human models showed dormant origin deficiency due to reduced levels of loaded MCM onto the chromatin in both unchallenged S phase and in response to treatment with low doses of APH or HU (Kunnev et al., 2010; Kawabata et al., 2011). The inability to activate dormant origins, combined with a slowing down of fork progression, can lead to chromosomal regions in which the converging forks have not enough time to merge, resulting in incomplete DNA replication when cells enter mitosis. Such unresolved replication intermediates interfere later with chromosome segregation during mitosis leading to chromosome breakage and instability.

On the other hand, increased origin firing (for example in checkpoint-defective cells) causes shortage of DNA building blocks (dNTPs, histones) leading to replication fork stalling due to limited substrate availability (Beck et al., 2012). Moreover, an uncontrolled firing of replication origins results in an abundance of ssDNA and a potential exhaustion of the cellular pool of RPA. Such RPA exhaustion results in

unprotected ssDNA and genome-wide breakage of replication forks, a phenomenon termed replication catastrophe (Toledo et al., 2013; 2017). Upregulated origin firing gives also rise to extensive re-replication of DNA. In this circumstances, forks are characterised by a slow elongation rate, so even if multiple origins are re-fired, it does not help to fully duplicate the genome (Fujita, 2006; Fu et al., 2021).

2. Consequences of replication stress

Replication stress can be defined as any challenge that is encountered by the replication machinery and disrupts the normal progression of replication. As described above, it can be caused by a wide range of factor. However, in most cases, one of the earliest consequences, and a hallmark of replication stress, is the accumulation of single-stranded DNA (ssDNA) (Zeeman and Cimprich, 2014). The generation of ssDNA stretches at replication forks result from the uncoupling of the helicases and DNA polymerases: when the latter stalls and the former continues to unwind the parental DNA (Buyn et al., 2005; Branzei and Foiani, 2005). Other mechanisms can also generate ssDNA, such as the degradation of newly synthesised DNA through the concerted action of nucleases and DNA helicases. For instance, enzymes like MRN, CtIP, EXO1, and BLM, known for their role in resecting DNA ends at double-strand breaks (DSBs), can also act at stalled forks, contributing to the accumulation of ssDNA. Consequently, this leads to exposure of long tracks of ssDNA, which are extremely vulnerable to DNA damaging agents and hypermutation. Moreover, ssDNA accumulation is a precursor to chromosome breakage and a common precursor to DSBs (Saini and Gordenin, 2020; Feng et al., 2011).

Replication stress compromises the fulfilment of chromosome duplication leaving under-replicated regions. When these loci enter mitosis, each of the intertwined DNA strands already belongs to a separate sister chromatid. During chromosome segregation in anaphase, they form ultra-fine bridges (UFBs), which are subjected to increasing mechanical tensions and may therefore break. Such breakages challenge even chromosome segregation and poses a risk that the resulting damage will be transmitted to the daughter cell (Moreno et al., 2016; Chan et al., 2018).

All these scenarios endanger genome stability, therefore cells are equipped with mechanisms that prevent the formation, escalation or transmission of damage caused by replication stress.

Table 1: **Factors involved in DNA damage response.** The table contains examples of the key players of the DNA damage signaling pathway in human cells, along with their yeast counterparts.

Function	Human	*S.cerevisiae*	*S.pombe*
Sensors	MRN	MRN	MRX
	RPA	RPA	RPA
	RAD9/RAD1/HUS1	Ddc1/Rad17/Mec3	Rad9/Rad1/Hus1
	RAD17	Rad24	Rad17
Kinases	ATM	Tel1	Tel1
	ATR	Rad3	Mec1
	ATRIP	Ddc2	Rad26
Mediators	MDC1	-	Mdb1
	53BP1	Rad9	Crb2
	TopBP1	Dbp11	Cut5/Rad4
	Claspin	Mrc1	Mrc1
Effectors	CHK1	Chk1	Chk1
	CHK2	Rad53	Cds1
	p53	-	-
	CDC25	Mih1	Cdc25
	CDK1	Cdc28	Cdc2
	WEE1	Swe1	Wee1/Mik1

C: How to prevent and deal with replication stress?

1. Replication Stress Response

1.1. DNA replication checkpoint

Cells have evolved dedicated quality control mechanisms to detect problems on DNA template, referred to as cell cycle checkpoints. Among others, the DNA replication checkpoint (DRC) monitors the formation of ssDNA at replication fork during DNA synthesis. The excess of ssDNA is a primary signal of replication stress that activates the DNA replication checkpoint (Hartwell and Weinert, 1989; Paulsen and Cimprich, 2007; Branzei and Foiani, 2008). Homologues of human and yeast proteins involved in DNA replication checkpoint activation are listed in Table 1.

As mentioned before, the hallmark of replication stress is the persistence of ssDNA exposed at stalled replication forks. When bound by the replication protein A (RPA), it creates a structure that serves as a platform to recruit various sensor proteins (Figure 6). This includes the ATR-interacting protein (ATRIP), the 9-1-1 DNA clamp complex (RAD9-RAD1-HUS1), the topoisomerase II binding protein 1 (TOPBP1), and the Ewing tumor-associated antigen 1 (ETAA1). These factors recruit and activate the central replication stress response kinase ATR (ataxia telangiectasia and Rad3-related) (Mec1 in budding yeast, Rad3 in fission yeast). Once activated, ATR phosphorylates various substrates, including the effector kinase CHK1. Subsequently, the activated CHK1 is released from the fork, diffuse and amplify the checkpoint response signal in order to reach its cellular targets. The ATR-CHK1 axis of signalling is the keystone of the replication checkpoint and orchestrates the replication stress response through several distinct mechanisms, which can be divided into a global and a local response (Buyn et al., 2005; Nam and Cortez, 2011; Haahr et al., 2016; Saldivar 2017).

Global response. The best understood role of the DNA replication checkpoint is to control the progression of cell-cycle. Activation of ATR-CHK1-dependent response results in a drastic slowing of replication rates, which occurs in large part through suppression of origin firing through several mechanisms (Paulovich and Hartwell, 1995; Yekezare et al., 2013). In human S phase cells, CHK1 reduces CDK2 activity through suppression of cell division cycle 25 (CDC25A), a phosphatase that regulates CDK2 phosphorylation. Inhibition of the CDK2-dependent phosphorylation at origins, blocks the loading of pre-IC factors, thus restricting origins firing (Shechter et al., 2004; Bartek et al., 2004). Furthermore, CHK1 phosphorylates and activates the negative regulator of CDK1/2, WEE1-like protein kinase (WEE1). However, in budding yeast, the inhibition

Figure 6: **Replication stress response induced by ATR.** During replication stress, replisome is probe to slow or stall, which leads to the exposure of ssDNA. ATR kinase senses RPA-bound ssDNA at the stressed replication forks and orchestrates a global and local response to DNA replication stress. (Adapted from Charlier and Martins, 2020)

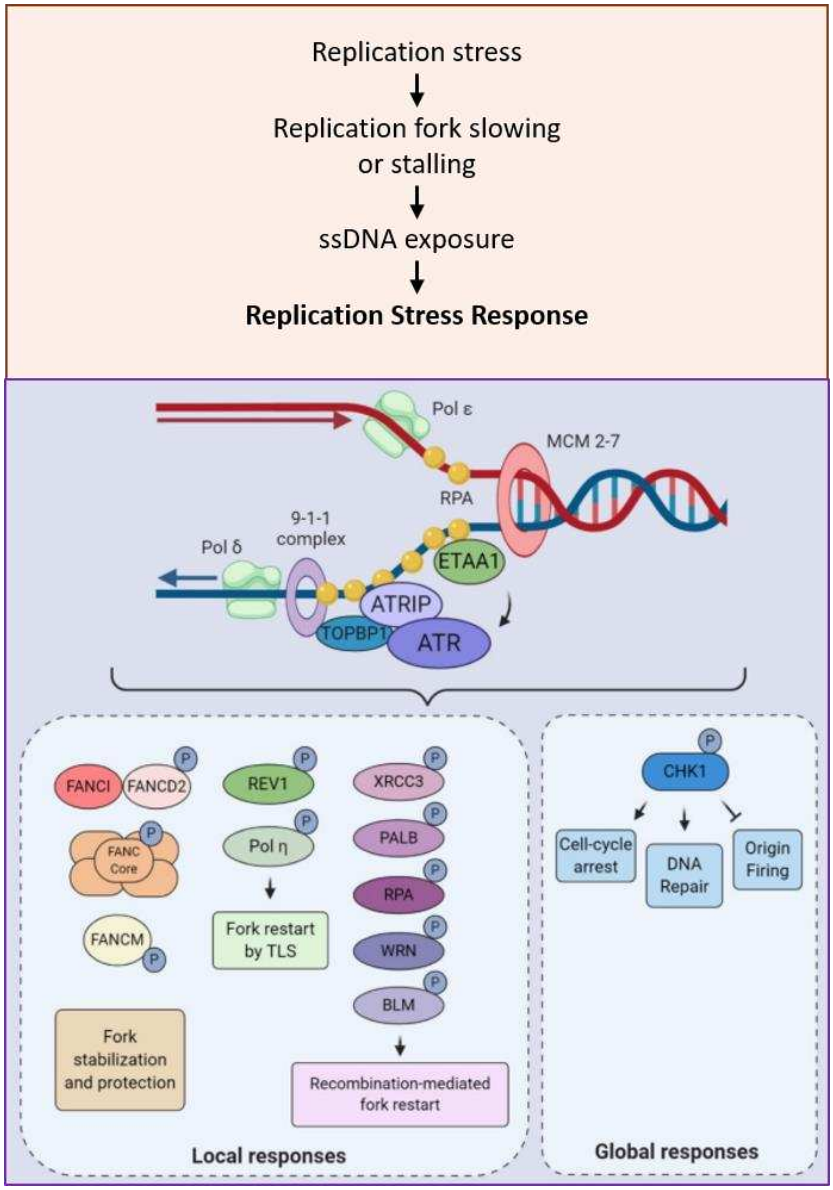

of CDK activity is by-passed by Rad53, which directly inhibits two replication initiation factors: Dbf4 and Sld3 (Lopez-Mosqueda, 2010; Zegerman and Diffley, 2010). The transient suppression of origin firing and cell-cycle progression limits the number of replication forks potentially exposed to stress, thereby preventing ssDNA accumulation, exhaustion of RPA and replication catastrophe (Toledo et al., 2013; Moiseeva et al., 2019).

Local response. Early studies proposed that, in addition to its global function in limiting the number of active replication forks, the checkpoint has also a local function at individual replication forks (Enoch et al., 1992). Later research provided evidences for such local function. Checkpoint-deficient yeast exposed to HU revealed an accumulation of aberrant replication forks, which were unable to resume DNA synthesis (Lopes et al., 2001; Sogo et al., 2002). Further studies allowed distinguishing three main ways by which ATR is thought to locally protect replication forks.

One function of the S-phase checkpoint is to maintain the structure and replicative competency of stalled forks, so they will be able to resume DNA synthesis once the block/inhibition is released (Dungrawala et al., 2015; Cortez, 2015). ATR checkpoint can directly target components of the replication machinery to prevent its dissociation from fork and/or to maintain the replisome in a competent state. Additionally, a number of proteins driving fork remodelling has been identified as ATR-Chk1 substrates. When encountering DNA lesion, forks can reverse their course by annealing the two newly synthesized strands, leading to four way junction structures resembling Holliday junctions. This protective mechanism stabilize stalled replication forks and ensure their ability to continue or resume replication without chromosomal breakage. Fork reversal was initially seen as a pathological structure but emerging evidence suggested that it is indispensable for maintaining genome stability (Neelsen and Lopes, 2015; Quinet et al., 2017). For example, impairing fork reversal by PARP inhibition leads to the formation of DSBs, indicating that fork reversal prevents fork collapse at camptothecin-induced lesions (Ray Chaudhuri et al., 2012).

However, when the source of replication stress cannot be eliminated, it results in persistent fork stalling. The exact mechanisms by which ATR might enable local firing of dormant origins are not yet fully understood. One proposed scenario is that checkpoint activation allows to fire a neighbouring dormant origin by inhibiting CHK1 activity in the vicinity of the stalled polymerase. This allows the completion of DNA synthesis within an actively replicating region in a process called compensation (Ge et al., 2010; Techer et al., 2017). Although at first glance this may seem contradictory to

Figure 7: **ATM-mediated signaling in the context of replication stress.** Persistent replication stress results in fork collapse and DSB formation. This leads to the recruitment of the MRN complex and ATM. Activated ATM phosphorylates subsequently a variety of substrates and coordinates a variety of cellular responses. (Adapted from Charlier and Martins, 2020)

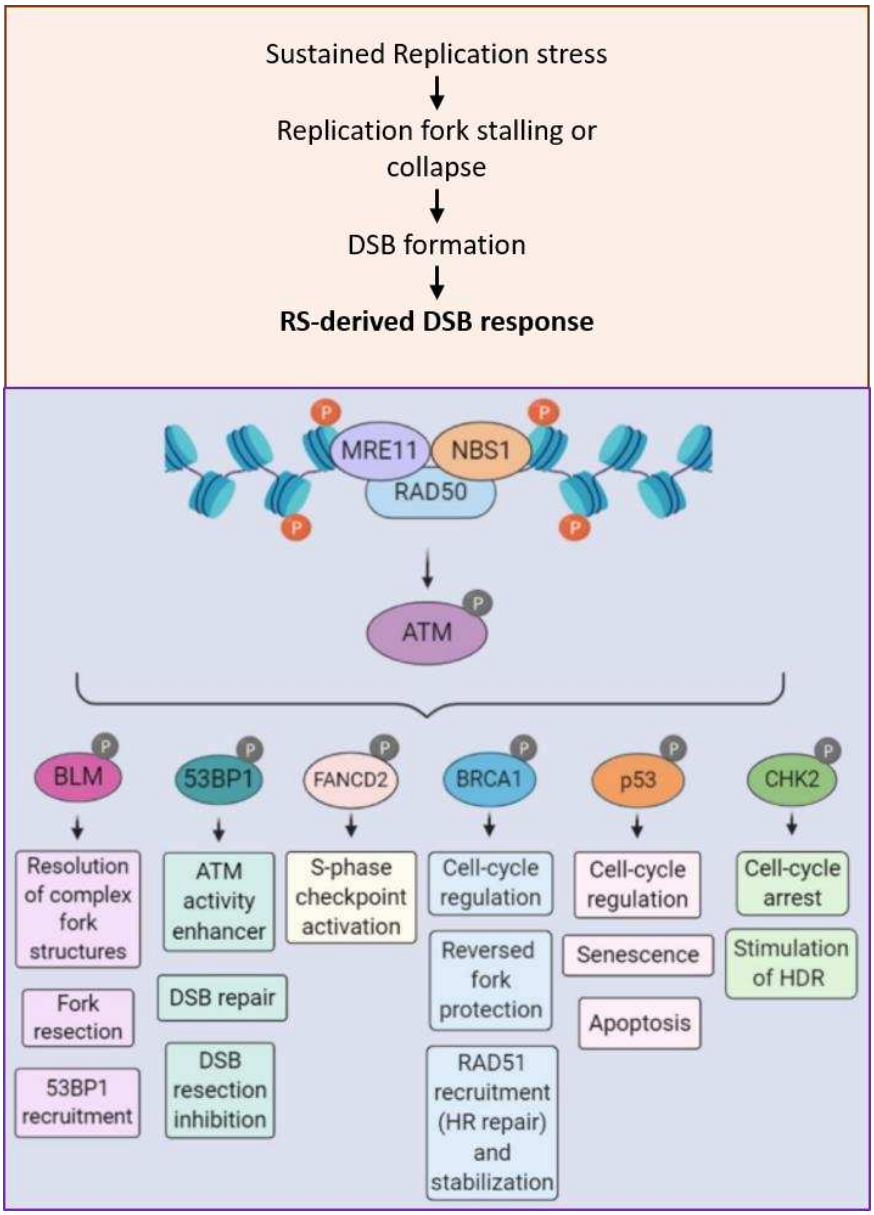

the above described global shutdown of origin firing, it only emphasizes the dependence of origin firing regulation on their proximity relative to the stalled forks.

A third way to contribute to genome integrity upon replication stress in the ATR-mediated activation of the DNA damage tolerance pathways (DDT) which is crucial to promote replication completion upon prolonged stalling. Two mechanistically distinct DDT branches have been characterized. One involves the temporary usage of translesion synthesis DNA polymerases (TLSs), which unlike replicative polymerases are capable to replicate directly across the lesions (Waters et al., 2009; Sale, 2012). However, TLSs activity is often linked to an increased risk of introducing mutations, thus the bypass occurs in an intrinsically error-prone manner (Friedburg, 2005). The other DDT mode involves the use of a homologous template, usually the sister chromatid, to copy the information from an undamaged region. This recombination - mediated mechanism is referred to as template switch (TS). TS is a complex but preferable process for bypassing DNA lesions, as it is generally accurate and error-free in the outcome (Branzei, 2011, Giannattasio et al., 2014). Replisome can skip the lesion and re-initiate DNA synthesis downstream of it. In vertebrates, repriming and further replication resumption is catalysed by PrimPol, which possesses both primase and polymerase activities (Mourón et al., 2013; Mehta et al., 2022). Repriming creates ssDNA gaps that are post-replicatively fill in by the two mechanisms described above (TLS and TS).

1.2. DNA damage checkpoint

Prolonged stalling of replication forks or inhibition of the ATR - CHK1 signalling axis leads to fork collapse which is a known source of replicative DSBs (Petermann et al., 2010; Dungrawala et al., 2015). The generation of replication stress-induced DSBs triggers the activation of other signalling kinases, including the ataxia-telangiectasia-mutated (ATM) kinase (Figure 7). Importantly, in contrast to ATR, it is not essential for cell survival (Durocher and Jackson, 2001; Jackson and Bartek, 2009; Harrigan et al., 2011).

The MRE11-RAD50-NBS1 complex, called MRN, is the sensor of DSBs and one of the first factor recruited to the site of DSB. Furthermore, MRN is required for the rapid recruitment of ATM and its subsequent activation (Uziel et al., 2003, Paull and Lee, 2005; Lee and Paull 2005). Both the exo and endonuclease activities of MRN were implicated in ATM activation by *in vitro* studies, however mouse cells expressing a nuclease-deficient mutant of MRE11 were still able to activate ATM (Jazayeri et al., 2008; Buis et

Table 2: **Human syndromes related to replication stress.**

Syndrome	Clinical sympthoms	Mutated gene
Xeroderma pigmentosum variant	Heurodegeneration, microcephaly, photosensitivity, skin cancer	Pol n
Bloom's syndrome	Microcpehaly, short stature, mild mental retardation, predisposition to cancer	BLM
Werner's syndrome	Premature agening, cancer predisposition	WRN
Aicardi-Goutieres syndrome (AGS)	Microcephaly, brain calcification, interferonpathy	RNASEH2
Heditary Breast and Ovarian Cancer	Breast and ovarian cancer	BRCA1, BRCA2
Fanconi anemia (FA)	Congenital abnormalities, progressive bone marrow failture, scuamous carcinomas of head and neck	FANCA-FANCL, BRCA2
Ataxia telangiectasia (AT)	Cerebellar ataxia, immune defects, predisposition to maligancy	ATM
Ataxia telangiectasia-like disorder (ATLD)	Mild AT like features, posibbly cancer predispositions	MRE11
Nijmegen breakage syndrome (NBS)	Microcephaly, growth retardation, immunodeficiency, cancer predisposition	NBS1
Nijmegen breakage syndrome-like disorder (NBSLD)	Microcephaly, growth retardation, immunodeficiency, cancer predisposition	RAD50
Seckel syndrome	Marked microcephaly, primordial dwarfism, dysmorphic facial features and mental retardation	ATR, SCKL2, SCKL3
Primary microcephaly 1 (MCPH1)	Microcephaly	MCPH1
Cockayane syndrome (CS)	Microcephaly, progressive neurodegeneration	CSA, CSB

al., 2008). ATM phosphorylates a number of downstream target proteins, which in turn trigger specific cellular consequences (Lavin et al., 2008).

Cell-cycle arrest. ATM's activation results in the phosphorylation and activation of CHK2. Activated CHK2 can then phosphorylate various downstream targets, including the Cdc25 family of phosphatases. Phosphorylated CDC25 undergoes degradation and therefore can no longer dephosphorylate CDK1-cyclin B resulting in cell-cycle arrest, mainly at the G1/S and G2/M transitions. This safeguard mechanism provides to the cell the time to repair replication-associated DNA damages before continuing with DNA replication and cell division (Xiao et al., 2003).

DNA repair. Following the initial activation, ATM triggers a cascade of events on the chromatin flanking DSBs. At damaged replication forks, ATM has a crucial role in orchestrating the repair of replicative single-ended DSBs at multiple levels. It was proposed that ATM could collectively control resection speed as well as counteract toxic DNA end-joining (Balmus et al., 2019). In a recent study, proteomics profiling of damaged replication forks revealed that ATM indeed promotes DNA end resection and facilitates homologous recombination repair. Additionally, the authors showed that ATM restricts the accumulation of non-homologous end joining factors by suppressing the canonical DSB-associated ubiquitin signaling (Nakamaura et al., 2021)

2. Dealing with DNA replication stress: implications in human diseases

In response to replication stress cells activate a complex set of downstream pathways essential to ensure the maintenance of genome stability. Defective Replication Stress Response (RSR) leads to the accumulation of DNA damage and ultimately provokes development of various congenital human diseases (Abugable et al., 2019; Schmit and Bielinsky, 2021).

As summarized in Table 2, patients carrying mutations in RSR genes display broad spectrum of clinical phenotypes. One overriding pathology seen in most of these syndromes is a development defect. This include growth restriction, short stature and brain development defects (microcephaly) (Katyal and McKinnon, 2008; Kerzendorfer and O'Driscoll, 2009). In addition, mutated variants of numerous DNA repair proteins were linked to multiple neurodegenerative disorders, as persistence of replication stress-induced DSBs lead to ATM-dependent apoptosis of damaged neural cells. For instance, degeneration of cerebellar neurons is a common feature of ataxia or apraxia (impaired motor coordination and eye movement defect, respectively) (O'Driscoll and Jeggo, 2008; Katyal and McKinnon, 2008). The implication in developmental defects

Figure 8: **Oncogene-induced replication stress.** (Adapted from Sarni and Kerem, 2017)

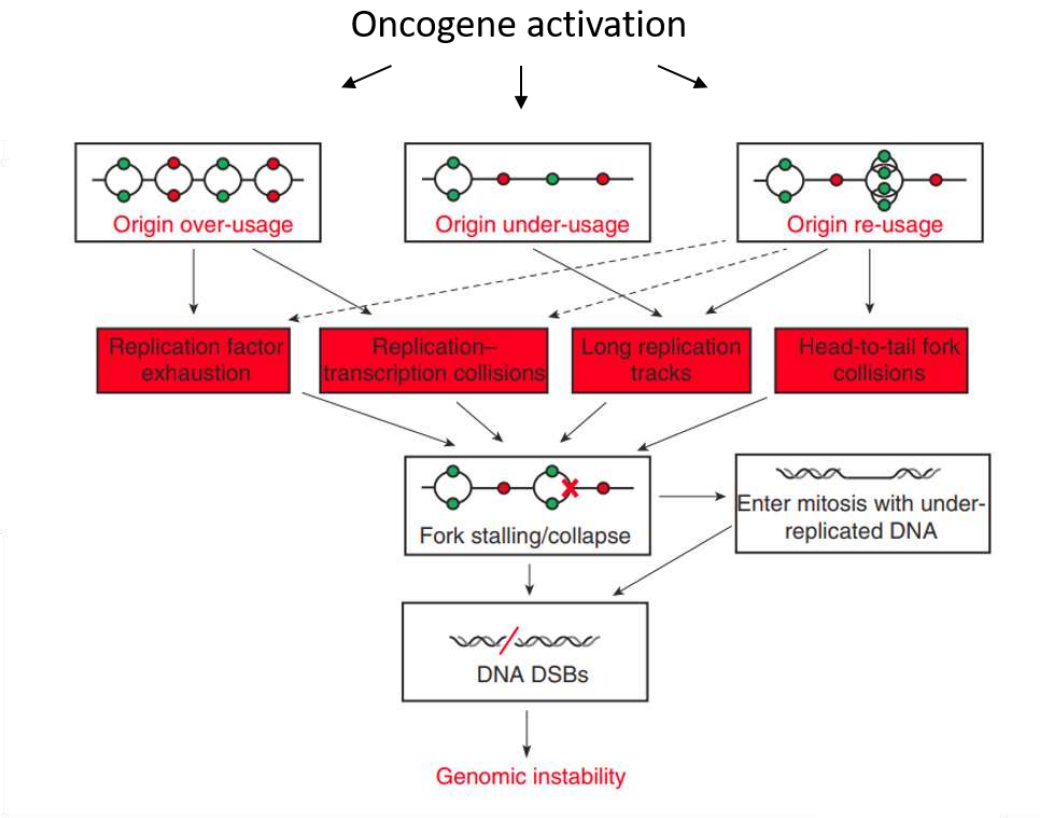

and neurological disorders emphasize the importance of an efficient RSR during cell proliferation. Furthermore, unresolved replication stress is a potent driver of dysfunctional stem cells differentiation, preventing tissue regeneration and haematopoiesis. Cells deficient for the RSR show also enhanced production of inflammatory cytokines that fosters the innate immune response (Ragu et al., 2020).

Moreover, an enhanced RSR has been associated with oncogene activation. Various oncogenes, known for their ability to promote sustained proliferation, may also drive replication perturbation by several mechanisms (Figure 8). These include deregulating origin licensing and/or firing, as well as affecting the faithful progression of replication forks. In addition, even a single oncogene can induce replication stress by more than one mechanism, further emphasizing the complex nature of oncogene-induced replication stress (Hills and Diffley, 2014; Sarni and Kerem, 2017). Nonetheless, in all scenarios oncogene-induced unbalanced DNA replication accelerates chromosomal aberrations and contributes to genomic instability that eventually fuels early tumorigenesis (Bartkova et al., 2006; Di Micco et al., 2006; Halazonetis et al., 2008).

Taken together, the importance of an efficient replication stress response and appropriate DNA replication for human health is highlighted by the variety of genetic disorders and increased cancer predisposition, associated with alterations in genes that participate in these processes.

II. Homologous recombination: the replication fork safeguard

A: Homologous recombination – an overview

1. Key steps and players

Homologous recombination (HR) is one of the most evolutionarily conserved processes, relying on the exchange of genetic information between two DNA molecules sharing extensive sequence homology. Beyond its role in driving evolutionary adaptability and genetic diversity, it is crucial for preservation of genome stability. HR is an efficient and high-fidelity mechanism for repairing a diversity of DNA damages including DNA gaps, DNA double-stranded breaks (DSBs) and DNA inter-strand crosslinks (ICLs). Moreover, it plays a significant role in telomere maintenance and provides critical support for DNA replication (Costes and Lambert, 2012; Jasin and Rothstein, 2013).

Figure 9: **Key steps of HR-mediated DSB repair.** (Prado, 2021)

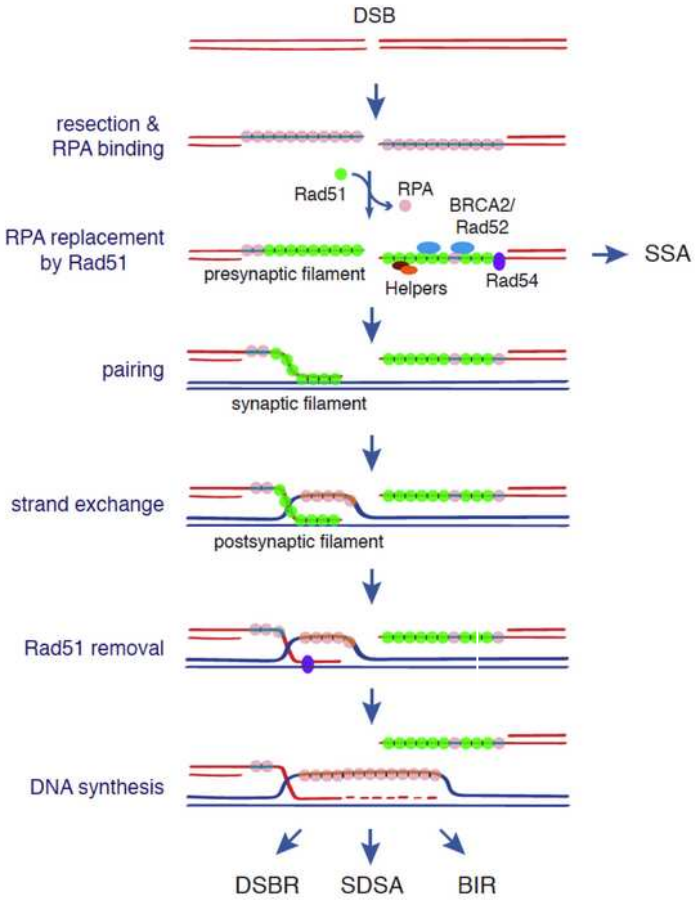

Figure 10: **Model of two-steps resection of DSB.** The initial resection of a DSB is initiated and regulated by MRN-CtIP complex that promotes the nucleolytic degradation in 3′-5′ direction (a). Next, EXO1 and DNA2-BLM/WRN are engaged in the long-range resection by degrading the 5′ DNA overhangs (b). (Zhao et al., 2020)

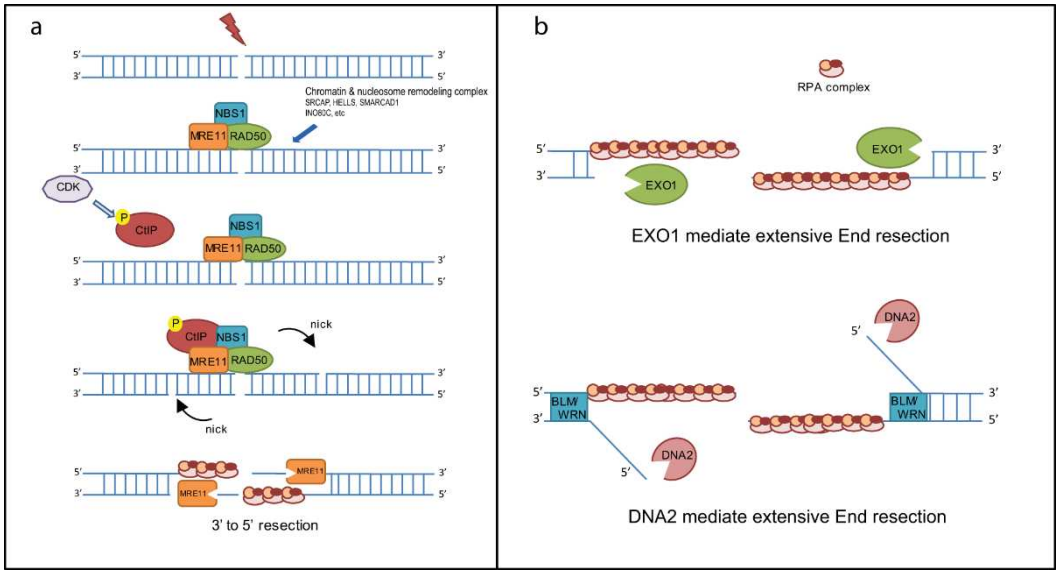

Homologous recombination at DNA damage sites makes use of an intact DNA copy (called the donor molecule) for the repair. The preferable template comes from the sister chromatid, as it provides the exact homologous sequence over long stretches of homology. However, templates located on a homologous chromosome or at an ectopic site can also be used (Johnson and Jasin, 2000). HR consists of multiple interconnected sub-pathways resulting in distinct outcomes in term of genetic exchanges, however the initial steps are functionally similar and rely on a core group of proteins. This includes the central recombinase Rad51 that is highly conserved among organisms.

Eukaryotic Rad51 is structurally and functionally similar to its bacterial homologue RecA in *E. coli* (Shinohara et al., 1992). Moreover, budding yeast ScRad51 and human hsRAD51 share over 80% sequence identity over the core domain (Baumann and West, 1998). The recombinase activity of Rad51 drives the pivotal steps of most HR events: homology search and DNA strand invasion and exchange. At the biochemical level, HR can divided into three stages: presynapsis, synapsis, and postsynapsis (Figure 9).

1.1 Presynaptic phase

As proposed by the classical model of DSB repair by HR, DNA end resection is the key step to produce a 3' single stranded DNA end that serves as a platform for the recruitment of factors involved in the homology-directed repair (Szostak et al., 1983). DSB is recognized by the MRN complex (composed of SpMre11/SpRad50/SpNbs1 in fission yeast, ScMre11/ScRad50/ScXrs2 in budding yeast and hsMRE11/hsRAD50/hsNBS1 in human) that binds to each side of the break to initiate the repair (Petrini and Stracker, 2003; Lee and Paul, 2004). The subsequent end-resection occurs in two steps (Figure 10). First, in a process termed the initial short range resection, the MRN complex together with its co-factor (ScSae2/SpCtp1 in yeast and CtIP in human) trims the broken ends to produce short (100-300 bp) 3′ single stranded overhangs (Mimitou et al., 2017; Garcia et al., 2011). Then, during the long-range resection, the short ssDNA overhangs up to several kilobases by the action of Exo1 and SpRqh1/ScSgs1/hsBLM – SpDna2/ScDna2/hsDNA2 (Mimitou and Symington, 2008; Zhu et al., 2008; Nimonkar et al., 2011).

Once generated, ssDNA overhangs are immediately coated by the replication protein A (RPA), to protect them from further nucleolytic degradation and to prevent the formation of secondary DNA structures. RPA is a highly conserved heterotrimeric protein complex composed of RPA1, RPA2, RPA3 subunits in humans (ScRfa1, Rfa2, Rfa3 / SpSsb1, Ssb2, Ssb3 in buddying and fission yeast, respectively) (Wold and Kelly, 1988; Wold, 1997). Next, Rad51 nucleates and oligomerizes on ssDNA to form a helical nucleoprotein filament referred to as the presynaptic complex (Conway et al., 2004;

Figure 11: **Mechanisms of accelerated homology search during recombination.** The search for a donor template is principally based on random probing events, but can be also regulated by additional parameters depending on the context such as: cohesion-mediated spatial proximity already juxtaposed before DSB formation (a); increased mobility of the DSB and/or the undamaged chromatin if probing in a larger volume is needed to enable ectopic recombination (b); accelerated filament probing by intersegmental contact sampling or sliding (c). (Renkawitz et al., 2014)

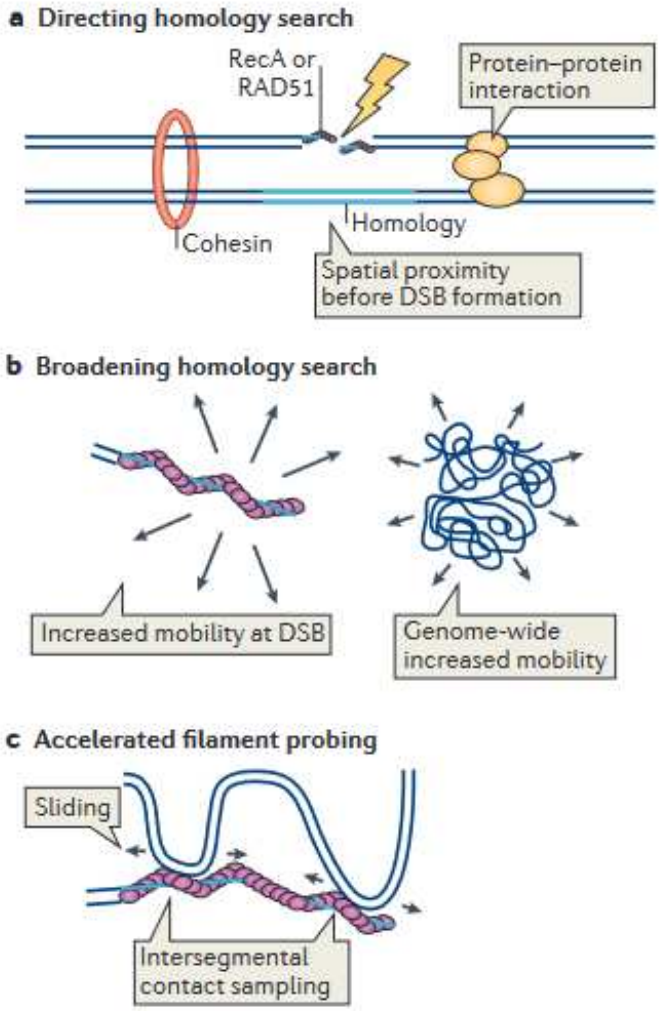

Short et al., 2016). As RPA is more abundant and has a higher affinity for ssDNA than Rad51, both factors competes for binding to ssDNA. Therefore, the loading of Rad51 requires to displace RPA from ssDNA and this step is achieved thank to the so called mediators factors.

In yeast, Rad52 displaces RPA form ssDNA and loads Rad51 on ssDNA (Sung, 1997; Milne and Weaver, 1993; Benson et al., 1998; New et al; 1998; Shinohara and Ogawa, 1998). Cells lacking Rad52 cannot form detectable DNA damage-induced Rad51 foci and are deficient in HR-mediated DSB repair, suggesting that Rad52 is required for *in vivo* filament assembly (Sugawara et al., 2003; Miyazaki et al., 2004). However in mammalian cells, loss of RAD52 does not lead to a strong DNA repair defects as observed in yeast (Rijkers et al., 1998; Yamaguchi-Iwai et al., 1998; Kan et al., 2017). This indicated that RAD52 has a secondary role in recombination, and the tumor suppressor BRCA2 was identified as the main RAD51 loader in human cells (Davies et al., 2001; Carreira et al., 2009; Jensen et al., 2010). Through its BRC repeats, BRCA2 recruits RAD51 to the site of DSBs to facilitate the formation of the nucleoprotein filament (Pellegrini et al., 2002; Yang et al., 2005; Jensen et al., 2010).

Another group of mediators are the yeast Rad51 paralogs (Rad55-Rad57 and Shu1-Psy3) working downstream of Rad52 to enhance the stability of already formed Rad51 filament and/or to facilitate Rad51 nucleation (Liu et al., 2011). In mammals, five RAD51 paralogues have been described: RAD51B, RAD51C, RAD51D, XRCC2 and XRCC3. They function in the same pathway as BRCA2 to promote RAD51 activity (Suwaki et al., 2011).

Additionally, a member of Swi2/Snf family, Sp/ScRad54 in yeast and hsRAD54 in human, was also found to promote nucleation of Rad51 in an ATPase activity-independent manner (Wolner et al., 2005; Ceballos and Heyer, 2011).

An additional function of the above mentioned mediators is to counteract the activity of helicases and translocases (called anti-recombinases), which effectively promote the dissociation of Rad51 from ssDNA to recycle Rad51 molecules or eliminate the undesirable HR intermediates. These include Sp/ScSrs2 and SpFbh1 in yeast and hsFBH1 in humans. Although there is no human orthologue of yeast Srs2, several helicases share similar functions like hsBLM and hsRecQ5 (Kohzaki et al., 2007; Burgess et al., 2009; Qiu et al., 2013). Thus, the interplay between Rad51 filament assembly and disassembly provides a mechanism to regulate HR initiation.

1.2 Synaptic phase

Once formed, the Rad51-ssDNA nucleoprotein filament begins the search for a homologous sequence. How this donor sequence is efficiently and timely found within a genome where most of its sequences are unrelated? Key insights from *in vitro* and *in vivo* single molecule studies helped to explain how is it facilitated (Figure 11). First, if the DSB and the region of homology sequence are already brought in close proximity before DSB formation (for example sister chromatids hold together by cohesion) the efficiency of recombination is significantly increased. Second, the increased mobility of damaged chromosomes enhanced the probability of contacts between the broken molecule and a more distant donor templates (Dion et al., 2012; Mine´-Hattab and Rothstein, 2012; Neumann et al., 2012). Third, a model called "intersegmental contact sampling" propose that the RecA/Rad51-ssDNA filament simultaneously probes different dsDNA regions, exploiting multiple weak, temporary contacts to rapidly search for homology within the genome (Forget and Kowalczykowski, 2012; Piazza et al., 2017). Additionally, Rad51 employs a length-based recognition strategy to efficiently identify 8 consecutives homologue nucleotides in the donor molecule. This selective mechanism streamlines the search process by disregarding shorter matches, ensuring a higher likelihood of accurate homologous target selection (Qi et al., 2015).

Upon successful identification of homology, the 3′-end of the nucleofilament invades the intact dsDNA. This strand invasion reaction generates a Rad51-bound heteroduplex in which the invading strand is base-paired with its complementary strand from the donor molecule. The non-complementary strand is displaced, thus a three-stranded structure called a displacement loop (D-loop) is formed. Rad54 then promotes the disassembly of Rad51 from the heteroduplex so that DNA repair synthesis can be initiated (Solinger et al., 2002; Thoma et al., 2005; Li et al., 2007; Wright and Heyer, 2014).

Despite the unconventional 5′-end strand invasion has been observed in vitro, it is considered as unproductive and undesirable, because DNA polymerases cannot extend the 5′ DNA end (Bachrati et al., 2006).

1.3 Postsynaptic phase

The initiation of DNA synthesis from the invading 3′-end commences the final, post-synaptic phase. In yeast, the polymerase delta (Pol δ) catalyses the recombination-associated DNA synthesis with the help of its processivity clamp PCNA (Wang et al., 2004; Maloisel et al., 2008; Li et al., 2009). In humans, POLδ is additionally supported by the translesion synthesis polymerase eta (POLη) (McIlwraith et al., 2005; Sneeden et

Figure 12: **Pathways of homologous recombination in DSB repair**. After strand invasion and formation of a D-loop intermediate, three different pathways can be utilized during the post-synaptic step of homologous recombination. In black: protein names of budding yeast HR factors, in red: protein names of human HR factors. SDSA: synthesis dependent strand annealing, DSBR: double-strand break repair, BIR: break induced repair. (Adapted from Godin, 2016)

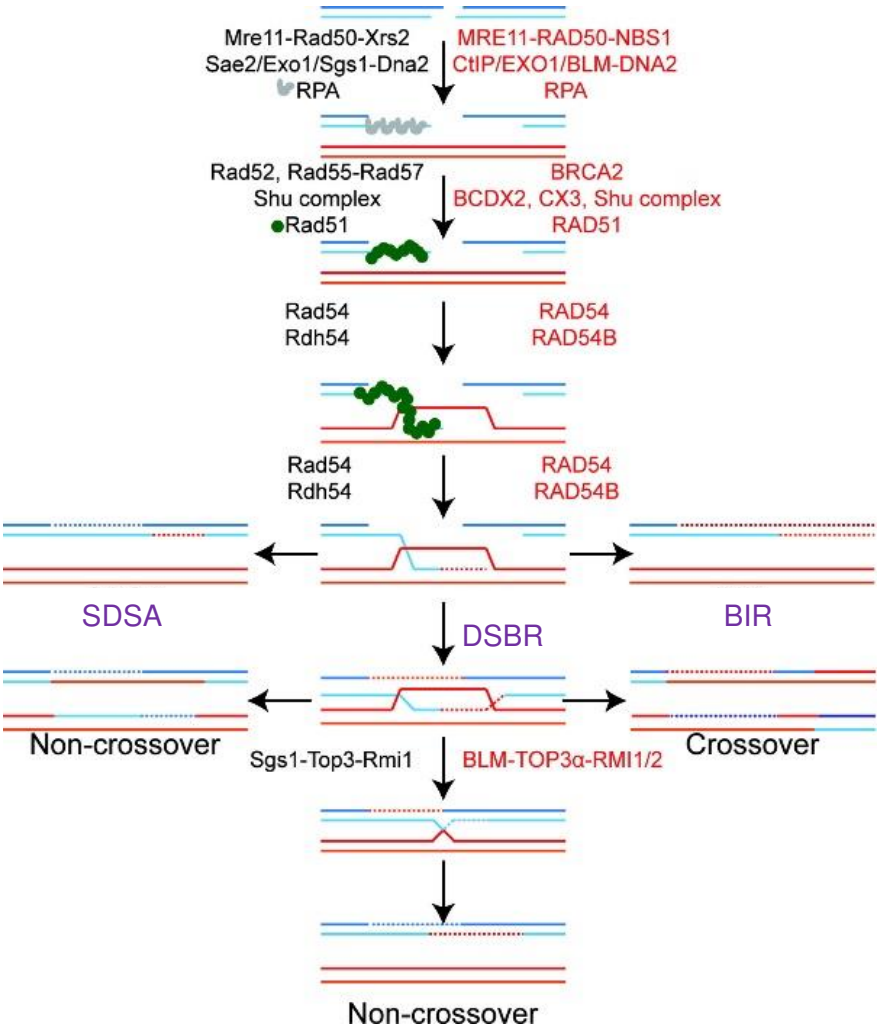

al., 2013). Copying the complementary sequence (in a continuous manner) extends both the heteroduplex and D-loop, leading to the formation of a structure called Holliday junction (HJ). Ultimately, it results in the recovery of the missing genetic information at the site of the DSB of the acceptor molecule that results in gene conversion in term of genetic exchange. After DNA synthesis is completed, recombination proceeds through different mechanisms that may or may not involve DNA strand crossover (Figure 12). A crossover event is described as swapping the distal arm of the broken DNA with the distal arm of the template molecule, resulting in a reciprocal genetic exchange between the acceptor and the donor DNA molecule

1.3.1 SDSA

In the synthesis-dependent strand annealing (SDSA) pathway, the extended invading strand is displaced from the D-loop, a mechanism call D-loop dissociation (Figure 12). Then, the stretch of repaired DNA synthesis allows to capture homology with the broken molecule and to reanneal with the ssDNA on the other break end, which is followed by gap-filling and ligation. A number of motor proteins have been implicated in the process of D-loop dissociation. These include yeast Srs2 and Sgs1-Top3-Rmi1 (STR) complex (Chavdarova et at., 2015; Fasching et al., 2015). Similarly, BLM-TOPOIIIa-RMI1/2 (known as the BTRR complex) promotes the unwinding of D-loop intermediate in humans (Bugreev et al., 2007; Bachrati et al., 2006; Harami et al., 2022). The joint action of helicases and topoisomerases prevents the formation of double Holliday junctions and give rise to a non-crossover product exclusively. This recombination outcome makes the SDSA pathway one of the least mutagenic HR sub-pathway and thus the predominant one in somatic or vegetative cells.

However, when the second broken end is not available for reannealing, another pathway called Break Induced Repair (BIR) takes over (Kramara et al., 2018). BIR will be described in more detail in the subchapter B (section 3.1) in the context of broken fork repair.

1.3.2 DSBR

In the double strand break repair (DSBR) pathway, the D-loop is stabilized and the displaced strand anneals with the second resected dsDNA end (Figure 12). This phenomenon, referred to as “second end capture”, leads to the formation of an intermediate termed a double Holliday junction (dHJ) (Duckett et al., 1988). These dHJs needs to be processed prior to separation of both physically linked DNA molecules. This occurs by two enzymatically distinct processes, leading to distinct genetic outcomes (Figure 13). In one scenario, dHJs are dissolved by the above mentioned

Figure 13: **Processing of the double Holliday junction.** Two enzymatically distinct processes lead to the resolution of Holliday junction with distinct genetic outcomes. The dHJ can be disengaged by dissolution leading to generation of non-crossover recombinants. On the other hand, dHJ can be resolved by endo-nucleolytic cleavage that give rise to both non-crossovers and crossovers depending on the strand cleaved (indicated by arrows). (Matos and West, 2004)

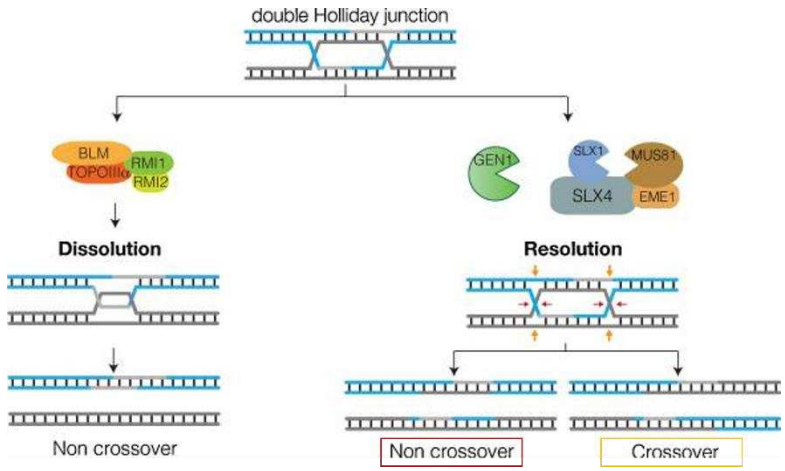

Figure 14: **Overview of DSB repair pathways.** Scheme illustrating the major DSB repair approaches: homologous recombination (HR), non-homologous end joining (NHEJ), alternative end-joining (alt-EJ), and the single strand annealing (SSA). DSB repair relies primarily on whether the DNA end resection occurs. When end resection takes place, HR, alt-EJ, and SSA can compete for the repair of DSBs. When end resection is inhibited, NHEJ is favoured. Key repair factors for each pathway are indicated. (Ackerson et al., 2021)

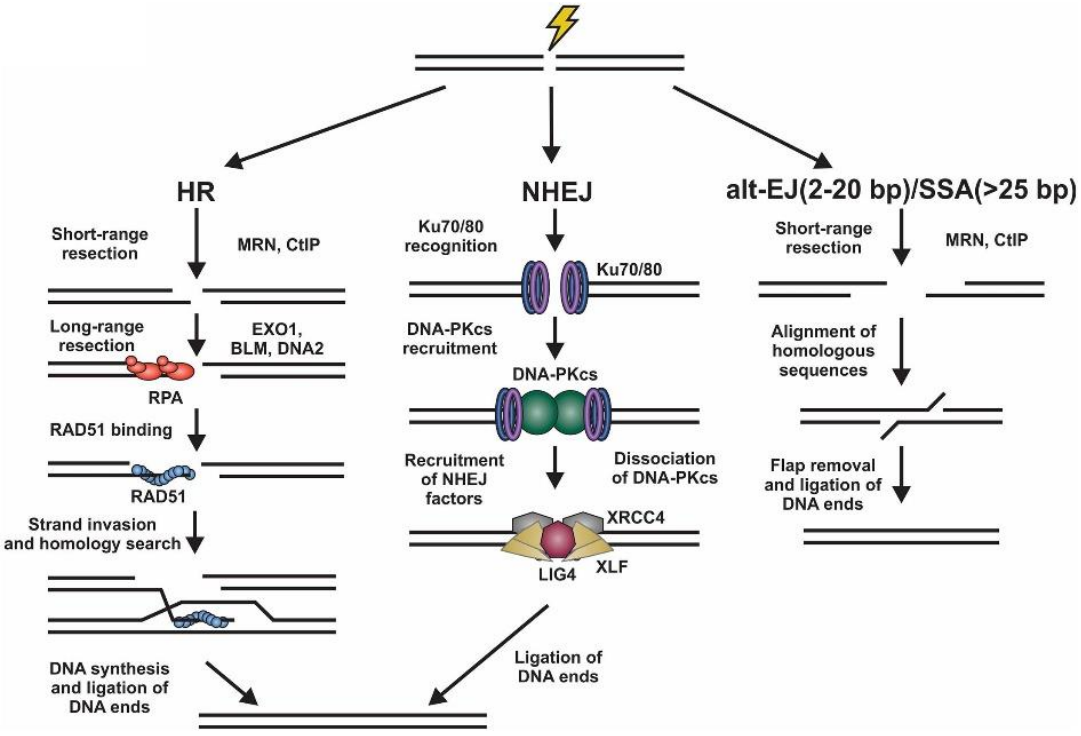

STR/BTR complexes in yeast and human respectively (Wu and Hickson, 2003; Cejka et al., 2010). Dissolution separates the recombining molecules without exchanging the flanking sequences, thus generating exclusively non-crossover products. Alternatively, these structures are resolved by specific nucleases called resolvases. These include mammalian MUS81-EME1, SLX1-SLX4, GEN1 and their yeast orthologues: ScMus81-Mms4, ScSlx1-Slx4, Yen1 (absent in fission yeast) (Boddy et al., 2001; Chen et al., 2001; Ciccia et al., 2003, Fricke and Brill, 2003; Rass et al., 2010; Wyatt et al., 2013). Depending on the strand cleaved within the dHJs, this resolution pathway leads to either crossover or non-crossover products.

1.3.3 SSA

Single-strand annealing (SSA) pathway is used to repair DSBs when it occurs between two repeated sequences. Although it does not require Rad51, it is still usually grouped together with other HR pathways. This is due not only to enzyme requirements, but also because the repair is initiated by an extensive resection, a feature shared among all recombination pathways, and the repair requires sequence homology (Bhargava et al., 2016). The end-resection exposes homology within the two repeats, so the resulting 3' overhangs anneal to each other in a Rad52-dependent manner. This requires the single strand annealing activity of Rad52 but not its interaction with Rad51. Then, the unpaired single-strands (flaps) are cleaved by endonucleases like yeast ScRad1-Rad10 and ScMsh2-Msh3 (XPF–ERCC1 in mammals) (Fishman-Lobell and Haber, 1992; Sugawara et al., 1997). DNA synthesis fills in any gaps and subsequent ligation successfully restores the integrity of the DNA duplex. The SSA pathway is a mutagenic process, since the sequences between the two direct repeats and one of the two copies are lost. However, it serves as a safeguard mechanism when other options are not available.

2. HR in DSB repair: competition with NHEJ

DSBs are not exclusively repaired by HR. Other repair pathway with distinct outcomes, like the previously mentioned SSA or non-homologous end joining (NHEJ) are in competition with HR for DSB repair (Figure 14) (Rouet et al., 1994; Liang et al., 1998; Johnson and Jasin, 2000; Chapman et al., 2012). NHEJ is a relatively simple, template-independent repair mechanism that involves blunt-end ligation of DNA extremities, regardless of sequence homology. Little or no DNA processing around the break is ensured by the Ku70/80 complex, which binds both ends of the break, protecting them from resection before being ligated (Chang et al., 2017). It is fast and efficient and often

not mutagenic when no DNA end processing is engaged. However, the repair of dirty DSBs that require processing to make them prone to ligation, often results in limited loss of genetic information at the damage locus, accompanied by short deletions that can disrupt the reading frame of a gene, thus resulting in a loss of function. This error-prone NHEJ repair of DSBs is exploited during gene inactivation by CRISPR-Cas9-based strategy.

The balance between the repair of DSB by HR or NHEJ is essential for genome stability and thus heavily regulated by many mechanisms (Shrivastav et al., 2008). One of the main determinant of repair pathway usage is the cell cycle phase. HR requires an homologous sequence as an intact donor, which in most cases is provided by the sister chromatid. This restricts recombination to S and G2 phases, when the preferred template is available (Ira et al., 2004, Escribano-Diaz et al., 2013; Orthwein et al., 2015). In contrast, for NHEJ, a repair template is not required, so it can occur throughout the cell cycle excepted in M phase. Thus, NHEJ dominates in G1, HR is most active in S phase, whereas they appear to compete in G2 phase (Rothkamm et al., 2003; Branzei and Foiani, 2008; Karanam et al., 2012).

Processing of the DNA break is another critical turning point for directing repair (Cejka, 2015). While NHEJ requires little or no DNA end processing, all HR subpathways are initiated by DNA resection to expose long tracts of ssDNA, which are eventually used for homology search and stand invasion. Therefore, extensive DNA end resection channels DSB repair towards HR and allows it to be initiated only when the repair template is available (Symington and Gautier, 2011; Chapman et al., 2012; Shibata, 2017). This robust regulation is also modulated in a cell-cycle dependent manner, as key resection factors are activated by S/G2 specific CDK (Caspari et al., 2002; Ira et al., 2004, Huertas et al., 2008). In human cells, the repair pathway choice is also highly regulated via antagonistic interplay between 53BP1 and BRCA1 which repress or promote resection, respectively (Bouwman et al., 2010, Bunting et al., 2010; Feng et al., 2015; Nacson et al., 2018).

Whether HR or NHEJ is used also depends on the complexity of damage at the DNA break ends. Heavy ion radiation result in complex DNA lesions, and these DSBs are preferentially repaired by HR in G2 phase (Shibata et al., 2011). Moreover, replication associated DNA lesions (one-ended DSBs at broken replication forks or protein blocks) are mainly dealt with by HR, as NHEJ can only repair two-ended DSBs. These broad replicative functions of HR will be discussed in more details in the following subsections

Figure 15: **The multifaceted functions of homologous recombination in DSB and replication-associated DNA damage.** See text for details. (Chakraborty et al., 2023)

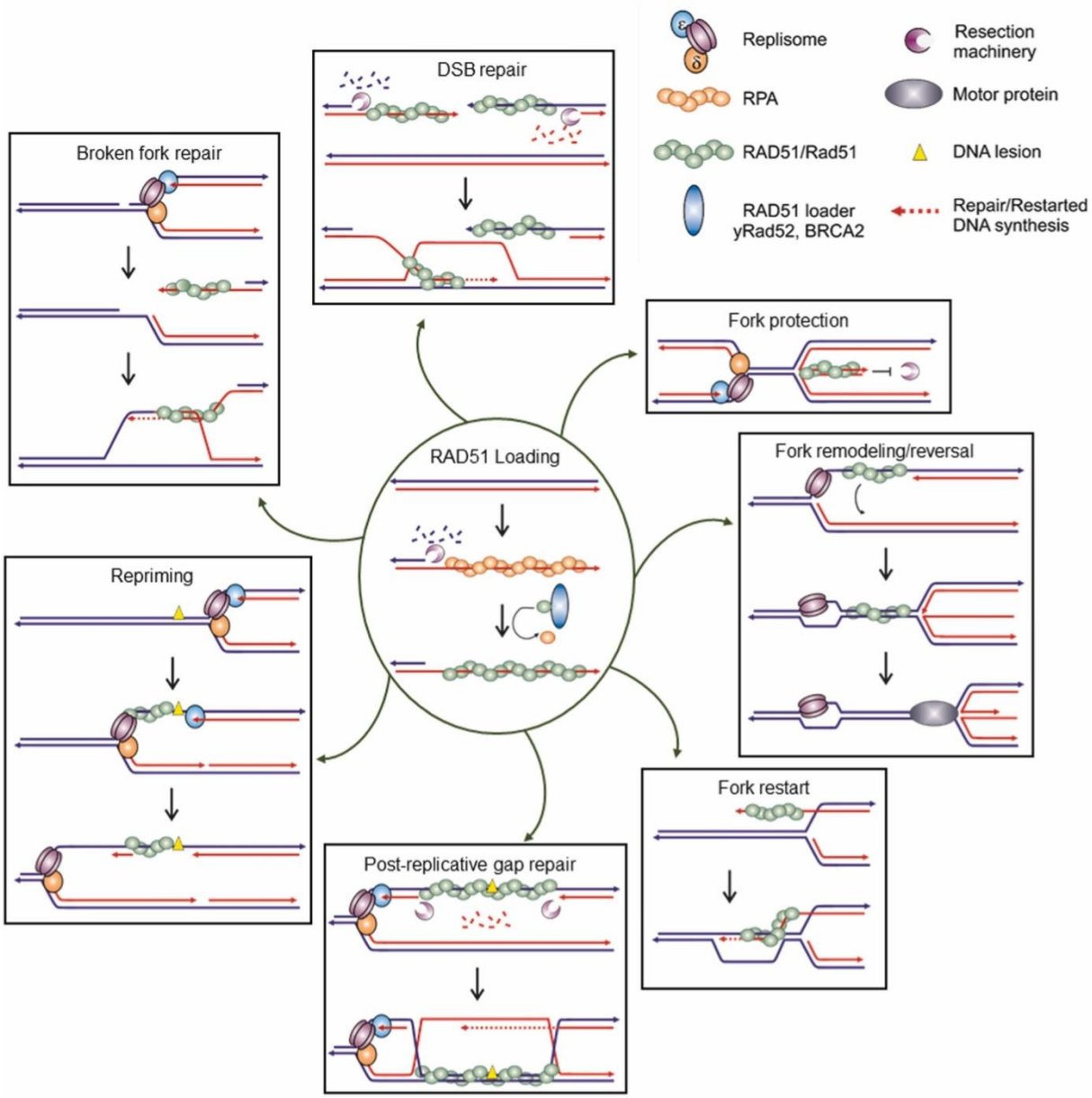

B: Roles of HR pathway in dealing with replication-associated DNA damages

Loss of replicative capacity often leads to mitotic catastrophe. To avoid incomplete chromosome replication, cells exploit distinct repair pathways to i) re-establish replication competence at dysfunctional or broken forks, ii) protect the integrity of stalled replication forks RF, iii) seal the ssDNA gaps behind the replication forks (Figure 15). How HR machinery regulates these mechanisms, thus ensuring continuous DNA synthesis and complete genome duplication, will be summarized below.

1. Fork remodelling

Upon global replication stress, perturbed replication forks can undergo architectural changes such as fork reversal, which allows to restrain DNA synthesis. Replication fork reversal is defined as the conversion of a replication fork into a 4-branched DNA structure equivalent to a Holliday junction (also known as chicken-foot). At reversed forks, the newly synthesized strands are annealed together forming a regressed arm. This is coordinated with the re-annealing of the parental strands that are back into a duplex form.

Fork reversal was extensively studied in bacteria. In *E. coli,* fork reversal occurs upon replication perturbation and is followed by an enzymatically cleavage to generate a replicative DSB that becomes toxic in the absence of HR (Seigneur et al., 1998; Michel et al. 2007; De Septenville et al., 2012).

Early studies in budding yeast using electron microscopy showed that checkpoint-deficient mutants treated with HU accumulated four-branched structures, which reflected reversed forks (Lopes et al., 2001; Sogo et al., 2002). In fission yeast, it was reported that Dna2 phosphorylation by the Cds1 kinase and the nuclease activity of Dna2 are required to prevent fork reversal (Hu et al., 2012). Thus in yeast, the DNA replication checkpoint plays an important role in preventing fork reversal. More recently, it was showed that in yeast cells treated with CPT-induced accumulation of positive supercoils ahead of replication forks led to fork reversal in yeast cells (Menin et al., 2018, Ray Chaudhuri et al., 2012). Electron microscopy analyses of replication forks purified from mammalian cells treated with agents that induce nucleotide depletion, oxidative base damage, UV photoproducts, topoisomerase cleavage complexes, or DNA crosslinks revealed that around 25% of analysed forks were reversed (Zellweger et al., 2015).

In mammals, several motor proteins promote fork reversal (Quinet et al., 2017). Electron microscopy (EM) and single-molecule DNA fiber approaches demonstrated that the translocase activities of the SNF2 family chromatin remodelers are required for replication fork reversal. These include SMARCAL1, ZRANB3 and HLTF which have been shown to catalyse replication fork remodelling both *in vitro* and *in vivo* (Blastyak et al., 2010; Achar et al., 2011; Betous et al., 2012; Poole and Cortez, 2017). Additionally, the RAD51 recombinase is also involved in replication fork reversal, as depleting RAD51 resulted in reduced proportion of reversed replication structures (Zellweger et al., 2015; Mijic et al., 2017). Interestingly, fork reversal does not require a stable RAD51 nucleofilament but strictly depends on the Rad51's strand exchange activity (Mijic et al., 2017; Liu et al., 2023).

A very recent report proposed that RAD51-mediated fork reversal allows bypassing the CMG helicase by annealing the parental strands behind the stalled fork while SMARCAL1 further extends this parental duplex, resulting in nascent strands being annealed together (Liu et al., 2023). Such mechanism allows achieving fork reversal without the need to unload the replication machinery. Especially, in this way the helicase is kept in a position ready to resume DNA synthesis once replication has started.

Fork reversal is indispensable for maintaining genome stability via multiple ways (Berti et al., 2013; Neelsen and Lopes, 2015). First, such remodelling of replication forks provides sufficient time for the DNA repair machinery to resolve perturbations and prevent DSB formation (Neelsen and Lopes, 2015; Ray Chaudhuri et al., 2012, Vujanovic et al., 2017, Mutreja et al., 2018). Moreover fork reversal also triggers template switching, where the nascent strand is used for error-free DNA synthesis (Zellweger et al., 2015). Thus, fork reversal is considered as a "holding state", but is fully reversible and can be rapidly restored into the three-way junction with normal replication speed and competence. In human cells, two exclusive pathways has been described to restore reversed fork in a 3-way DNA structure. The first one involves the RECQ1-dependent branch migration that is activated only once DNA lesion or replication stress source are removed (Berti et al., 2013; Zellweger et al., 2015). The second mechanism depends on the degradation of the reversed arm by the WRN helicase and the DNA2 nuclease, but is independent of EXO1, MRN and CtIP resection (Thangavel et al., 2015).

2. Fork protection

In the reversed fork structure, nascent strands assembled into a reversed arm, providing one-ended DNA end that can be somehow detected as a DSB and processed by nucleases such as MRE11, EXO1, DNA2, and MUS81 (Thangavel et al., 2015; Lemacon et al., 2017; Mijic et al., 2017, Berti et al., 2020). Also stalled replication forks are accompanied by the exposure of ssDNA and thus subjected to nucleolytic degradation. HR factors, in particular BRCA2 and RAD51 have emerged as key regulators of replication fork degradation, maintaining replication fork integrity and genomic stability. In their absence, replication forks are extensively and rapidly degraded by MRE11 as it was detected by DNA fiber assay and EM approaches in human and Xenopus cells, respectively (Schlacher et al., 2011; Ying et al., 2012; Ray Chaudhuri et al., 2016; Hashimoto et al., 2010). In fission yeast, Rad51-mediated fork protection was also shown to be important to maintain stalled replication forks in a structure that allows its merging with the opposite fork (Lambert et al., 2005; Lambert et al., 2010). The DNA-binding mutant RAD51-T131P, that forms an instable filament, was ineffective to protect replication forks against nucleases attack (Kolinjivadi et al., 2017; Mijic et al., 2017). Consistent with this, human cells expressing RAD51-II3A which retains DNA binding, but not strand exchange activity, were proficient in fork protection (Mason et al., 2019). This suggests that the protective effect of RAD51 is recombination independent: it requires stable filament formation, whereas the strand exchange activity remains dispensable. However, it still remains unclear how exactly RAD51 protects regressed forks from degradation by nucleases. Possible explanations include physical blocking of nuclease binding or co-operation with other inhibitory proteins. Interestingly, BRCA2 is required to stabilize the RAD51 filament on the regressed arm of a reversed fork. It has been also shown that BRCA2 deficient cells suffers from unprotected forks that are alleviated by downregulating RAD51 (Lemacon et al., 2017; Kolinjivadi et al., 2017; Mijic et al., 2017). Thus, RAD51 has a BRCA2-independent function in promoting fork reversal followed by a BRCA2-dependent function in protecting the reversed fork from excessive degradation.

3. Fork repair and restart

When a replication fork stalls or collapses to become dysfunctional, it is likely to be rescued by a converging fork that arrives upon activation of a nearby dormant origin. As mentioned above, HR factors protect the integrity of halted replication forks. However, when a converging fork is not available to resolve the dysfunctional fork, it

Figure 16: **Models of Break-induced Replication (BIR) and Recombination-dependent-replication (RDR).** Left: BIR can initiate from broken replication fork during S-phase or G2/M phase. Mechanisms of both Rad52-dependent and Rad51-independent BIR are illustrated. Right: RDR is initiated from ssDNA gap generated by the control degradation of nascent strand (at reversed fork or not). (Chakraborty et al., 2023)

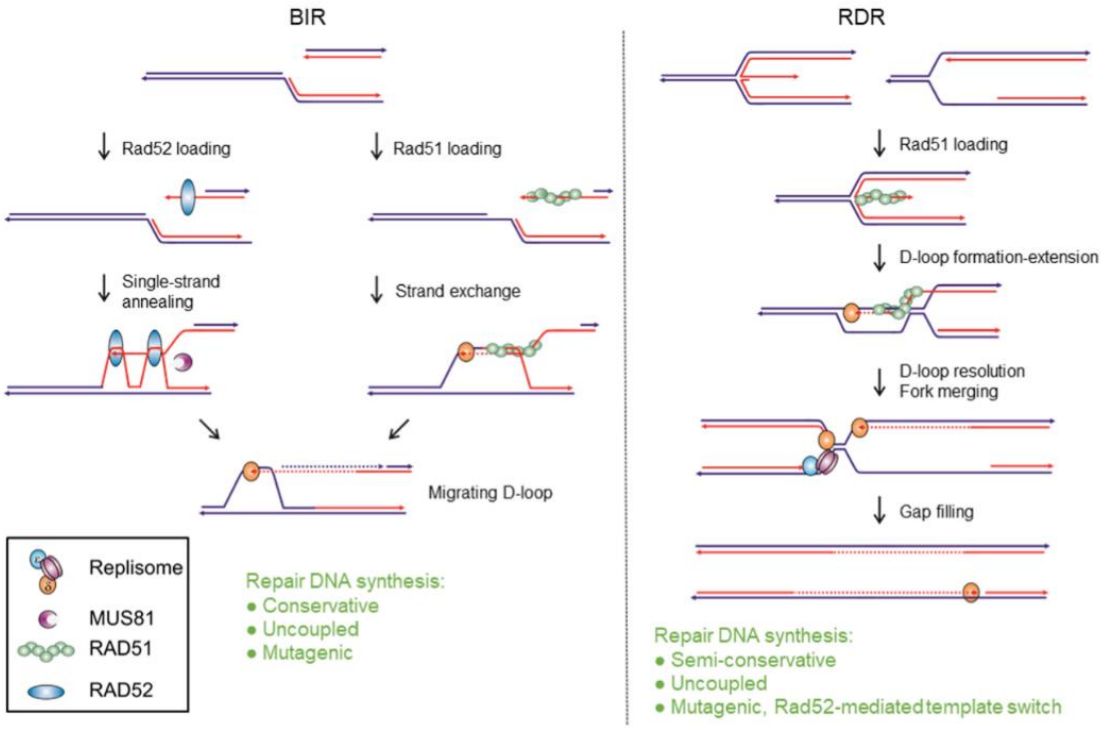

must be restarted to minimize unfinished DNA replication and to avoid under-replication. Studies in yeast, using site-specific fork arrest assays, reported that HR contributes to complete DNA replication by re-establishing the replication competence of dysfunctional forks via two mechanisms, namely Break-Induced Replication (BIR) mechanisms and Recombination-Dependent Replication (RDR) (Carr and Lambert, 2021). Notably, the repair DNA synthesis established by either BIR or RDR exhibits distinct features from the canonical DNA replication, as described below.

3.1 BIR

When a replication fork encounters a lesion or nick, it is converted into a broken fork that exhibits one-ended DSB. If not rescued by a converging fork, such dysfunctional broken fork can be repaired by BIR to ensure the resumption of DNA synthesis (Ait Saada et al., 2018) (Figure 16). BIR has been extensively studied in yeast systems, upon induction of a DSB in G2 cells with only one DNA end able to search for homology. BIR initiates generally in G2/M phase several hours after DSB induction from an extensive 5'-to-3' end resection at the break. The generated 3' ssDNA overhang is coated by the Rad51 filament and invades into a homologous template. The DNA synthesis proceeds in the context of a migrating D-loop and can continue over hundreds of kilobases until reaching the end of the chromosome (Saini et al., 2013; Wilson et al., 2013; Donnianni and Symington, 2013). The newly synthesized leading strand is constantly extruded from the D-loop generating an extensive region of nascent ssDNA. It is subsequently used as a template for copying the lagging strand. Thus, DNA synthesis during BIR is mechanistically distinct from the canonical one during replication. First, due to its unique mechanism, BIR is conservative rather than semi-conservative (Saini et al., 2013). Second, the synthesis of leading and lagging stands occurs asynchronously and both of them are synthesized by Polδ with the assistance of the non-essential subunit Pol32 (Lydeard et al., 2007; Donnianni et al., 2019; Liu et al., 2021). Moreover, in place of the CMG replicative helicase, BIR utilizes the alternative helicase Pif1 to unwind the DNA duplex and extrude the newly synthesized DNA from the D loop (Wilson et al., 2013). Pif1 allows the progression of BIR-mediated DNA synthesis, however at a slower rate that the canonical replication: 0.5Kb/min vs 2Kb/min (Liu et al., 2021).

In line with yeast studies, the MRE11 nuclease and RAD51 are required to restore replisome integrity upon fork collapse and breakage in Xenopus egg extract. Thus a HR-mediated mechanism is also necessary to restart broken replication forks in vertebrates (Hashimoto 2011).

Another less-efficient BIR mechanism has been reported in Rad51 deficient yeast cells (Malkova et al., 1996). In contrast to Rad51-dependent BIR, this Rad51-independend

pathway requires much less homology to initiate repair. Moreover, this initiation relies on Rad52's single strand annealing activity that anneals the resected broken DNA with a homologous region (Davis et al., 2001; Malkowa et al., 2001). While being a minor pathway in budding yeast, recent evidences suggest that a RAD51-independent form of BIR plays a more prominent role in human cells during mitotic DNA synthesis (MiDAS). MiDAS is viewed as the "last chance" mechanism to resume DNA synthesis and complete genome duplication before chromosome segregation initiates (Minocherhomji et al., 2015; Bhowmick et al., 2016). It is initiated at "difficult-to-replicate" sites, such as common fragile sites, by MUS81- and EME1-dependent cleavage of unresolved and late replication intermediates (Minocherhomji et al., 2015; Bhowmick et al., 2016; Bhowmick et al., 2017). It was initially reported as a RAD51 and BRCA2 independent but RAD52 and POLD3 dependent form of BIR (Sotiriou et al., 2016; Bhowmick et al., 2017). However, a recent report identified an unexpected role of RAD51 in promoting MiDAS, which relies on protecting the under-replicated DNA in mitotic cells (Wassing et al., 2021).

An important feature of BIR is the increased frequency of mutations arising through various processes: (1) complex genome rearrangements and frameshift mutations resulting from frequent template switches; (2) accumulation of mutations and DNA damage at the exposed ssDNA; (3) translocations resulting from ectopic invasion; (4) half-crossovers resulting from the resolution of BIR intermediates ; (5) loss of heterozygosity (Deem et al., 2011; Costantino et al., 2014; Sakofsky et al., 2014; Elango et al., 2019; Osia et al., 2022).

3.2 RDR

Evidences gathered over the last decade shows that HR-dependent replication fork restart can be initiated independently of DSBs (Figure 16) (Mizuno et al., 2009; Petermann et al., 2010; Lambert et al., 2010, Zellweger et al., 2015). Recombination-dependent-replication (RDR), as this mechanism is called, has been characterised mainly in fission yeast with the use of a site-specific replication fork barrier (RFB), which triggers replication fork collapse without inducing a DSB (Mizuno et al., 2009; Lambert et al., 2010).

In the first phase of RDR, dysfunctional forks undergo fork reversal, which provides a single DNA end for Ku binding. Then, an initial resection mediated by MRN-Ctp1 generates short ssDNA overhang, removing Ku from the reversed arm and allowing long-range resection to occur (Lambert et al., 2010; Teixeira-Silva et al., 2017; Miyabe et al., 2015). The subsequent Rad51-dependent strand invasion is followed by a DNA

synthesis during which both the leading and lagging strands are synthesized by the DNA polymerase delta, likely in an uncoupled manner. However, in contrast to BIR, the DNA synthesis remains semi-conservative (Naiman et al., 2021; Miyabe et al., 2015). As showed in fission yeast system, fork restart by RDR is achieved in 15-20 minutes in S-phase and such restarted fork can travel up to 20 Kb, before merging with a canonical, converging fork (Nguyen et al., 2015; Naiman et al., 2021, Miyabe et al., 2015).

Recent reports indicated that although the initial step of RDR is driven mainly by the Rad51 recombinase, the template switch during the progression of the restarted fork relies on Rad52's single strand annealing activity (Kishkevich et al., 2022). Interestingly, this resulting non-canonical form of DNA synthesis is associated with various types of genetic instability. First, ectopic recombination events can restart the fork at the wrong locus causing rearrangements such as translocations (Mizuno et al., 2009). On the other hand, forks restarted at the correct locus are intrinsically more error prone, showing elevated replication slippage events, recombination between direct repeats and formation of dicentric and acentric isochromosomes at inverted repeats (Iraqui et al., 2012; Mizuno et al., 2013; Jalan et al., 2019).

According to another latest research, the RDR may contribute to complete DNA replication in human cells. It was shown that cells exposed to mild replication stress use a RAD51 and RAD52-mediated HR pathway to continue DNA synthesis until G2-M transition, thus minimizing genome under-replication and replication stress-induced mitotic abnormalities. Contrary to MiDAS model, this resilient DNA synthesis does not rely on MUS81, suggesting that fork breakage is unrequired to preserve DNA replication in G2 cells (Mocanu et al., 2022).

There is a tendency to alternately use the BIR and RDR terms, which may not be completely correct. Hence, it seems important to emphasize that BIR should be rather considered as a specialized form of RDR, which is initiated by a DSB instead of an ssDNA gap. However in both cases, the non-canonical form of DNA synthesis during BIR and RDR results in higher mutation frequency, compared to the bulk of DNA synthesis. This indicates, that upon replication failures, the completion of chromosome duplication comes at the cost of using mutagenic replication-based DNA repair mechanisms that can lead to increased genome instability.

4. Repriming and gap filling

When the replisome encounters a DNA lesion that cannot be replicated by the replicative polymerases, distinct tolerance or bypass pathways are activated to ensure

continuous fork progression. These include switching to TLS polymerases that can replicate throughout the lesion or the re-initiation of *de novo* DNA synthesis downstream of the DNA lesion (Sale et al., 2012). The latter, called also repriming, requires the DNA polymerase PRIMPOL in human cells and the Primase-Pol alpha-Ctf4 complex in budding yeast (Mouron et al., 2013; Garcıa-Gomez et al., 2013; Bianchi et al., 2013; Fumasoni et al., 2015). Emerged evidences support the idea that HR factors can regulate repriming by their non-recombinogenic functions (Benureau et al., 2022). An increased accumulation of RAD51 behind replication forks was observed upon UV irradiation in human cells deficient for the TLS polymerase Eta. Interestingly, it was not associated with parallel increase in the formation of recombination-like DNA intermediates. Moreover, by treating the cells with the inhibitor B02, that destabilizes RAD51 filament formation and inhibits its subsequent strand exchange activity, the authors proposed that RAD51 plays a strand invasion-independent role to ensure efficient repriming. This non-recombinogenic function at a fork stalled by DNA lesion may involve an interaction with Pol alpha (Kolinjivadi et al., 2017; Di Biagi et al., 2023).

However, repriming leads to the formation and accumulation of ssDNA stretches behind the replication fork, called also daughter-strand gaps. If not sealed, they may be processed into DSBs and hence represent a source of potential genomic instability (Lopes et al., 2006; Hashimoto et al., 2010). These gaps are filled in either by the TLS polymerases or by template switch (TS), an HR sub-pathway (Wong et al., 2021). Analysis in yeast cells and Xenopus egg extracts treated with UV light or MMS, showed that ssDNA gaps accumulate behind the fork in the absence of Rad51 (Hashimoto et al., 2010; Joseph et al., 2022). Extensive studies in yeast provided insights into our understanding of the mechanisms by which post-replicative ssDNA gaps are repaired by HR. First, ssDNA gaps are enlarged by the activities of the exonuclease Exo1 and the helicase Pif1, in cooperation with the 9-1-1 and PCNA respectively (Karras et al., 2013; García-Rodríguez et al., 2018). In such manner, gap expansion facilitates the access of recombination factors in preparation for strand invasion (Vanoli et al., 2010; Giannattasio et al., 2014). However, in contrast to DSB-induced HR, the strand exchange is not initiated by an 3′-end ssDNA. In this case, the Rad51-coated ssDNA gap invades the sister chromatid and reanneals with the parental strand. This in turn displaces the newly synthetized strand, which serves as a template for the blocked 3′-end, further being extended by Pol delta (Giannattasio et al., 2014). The X-shaped recombination intermediates generated in this process are called sister chromatid junctions (SCJs) and can be easily detected in MMS-treated yeast cells lacking the STR dissolvase (Vanoli et al., 2010; Mankouri et al., 2011). Rad51-mediated gap filling is not coupled to replication fork progression but rather restricted to the G2/M phase by the DNA

Figure 17: **Replicative HR functions ensure complete genome duplication.** (Chakraborty et al., 2023)

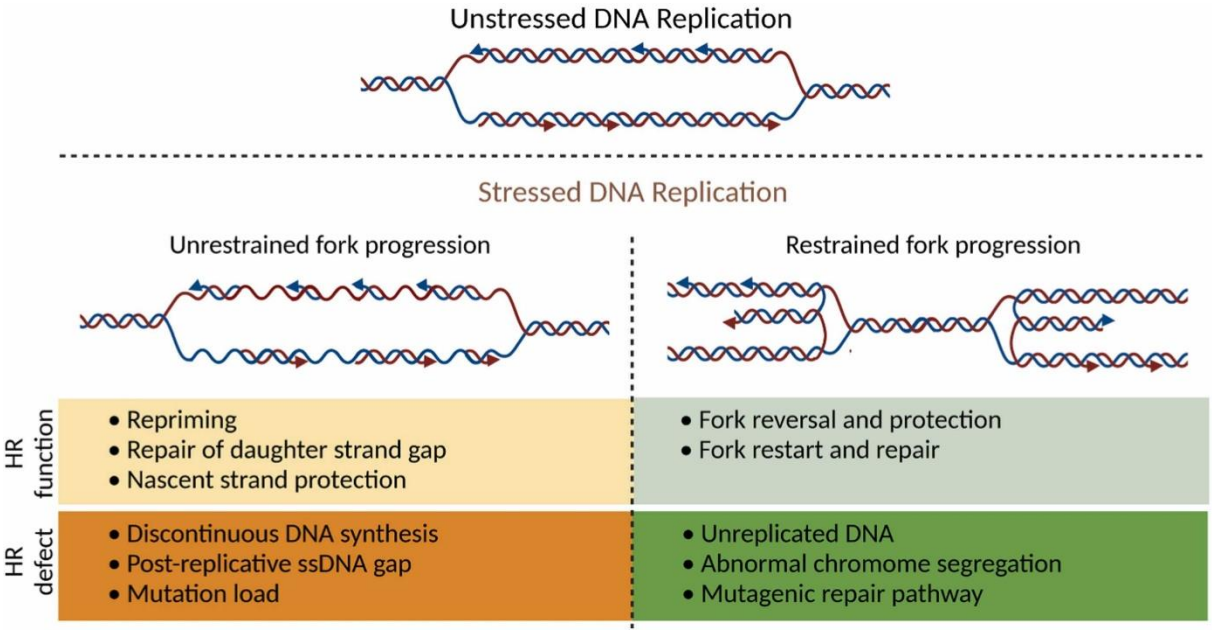

replication checkpoint (González-Prieto et al., 2013). Interestingly, another study in yeast model revealed that the repair of these gaps occurs in specific repair territories (PORTs), that are not only temporally, but also spatially distant from ongoing replication forks (Wong et al., 2020).

HR-mediated repair of post-replicative gaps has been also reported in human cells. Upon mild BPDE (benzo(a)pyrene diol epoxide) treatment, RAD51 was shown to form foci in response to bulky DNA adducts. RAD51 recruitment under these conditions occurs at post-replicative gap formed by PRIMPOL repriming and MRE11 and EXO1 – dependent resection, independently of replication fork stalling or collapse (Piberger et al., 2020).

The emerging picture is that Rad51 binds to unperturbed fork to support continuous DNA synthesis via repriming and subsequently uses its recombinogenic activity to promote post-replicative gap repair. Consistently, BRCA1 or BRCA2 deficient cells accumulate post-replicative gaps that can arise from various origins, including both defective repriming and unrepaired post-replicative gaps (Panzarino et al., 2021; Quinet et al., 2020; Taglialatela et al., 2021; Belan et al., 2022).

Taken together, the completion of genome duplication relies on the replicative functions of HR by several means (Figure 17). First, by protecting the integrity of halted replication forks to ensure accurate termination and by promoting fork repair and restart, HR prevents an under-replication of the genome at the time when cells enter mitosis. Second, by limiting the accumulation of post-replicative gaps, HR ensures a continuous DNA synthesis.

III. Role of the nuclear architecture and dynamics in homologous recombination-mediated DNA repair

A: Spatial organization of chromatin within the nucleus.

In eukaryotic cells, genomic DNA is divided into several units called chromosomes, the number of which varies from one organism to another (e.g. 46 in humans, 16 in buddying yeast, and 3 in fission yeast). However, fitting the chromosomal DNA into a confined nuclear space becomes challenging given the ratio between total DNA length and the nucleus size. For example, a typical human cell contains roughly 2 meters of DNA that needs to be accommodated in a nucleus with a diameter of ~ 5–10 µM. Therefore, eukaryotic genomes exhibit hierarchical levels of spatial organization in

Figure 18: **Schematic representation of hierarchical chromatin organization.** In eukaryotic nuclei, DNA double-helix is wrapped around nucleosomes forming the chromatin fiber, which further folds into loops. Such loops are then organized into topologically associating domains (TADs). At a higher scale, DNA fibers separate into clusters of active and inactive chromatin, defined as A compartment and B compartment, respectively. At the highest topological level, individual chromosomes occupy a distinct subspace in the nucleus termed chromosome territories. (Doğan and Liu, 2018)

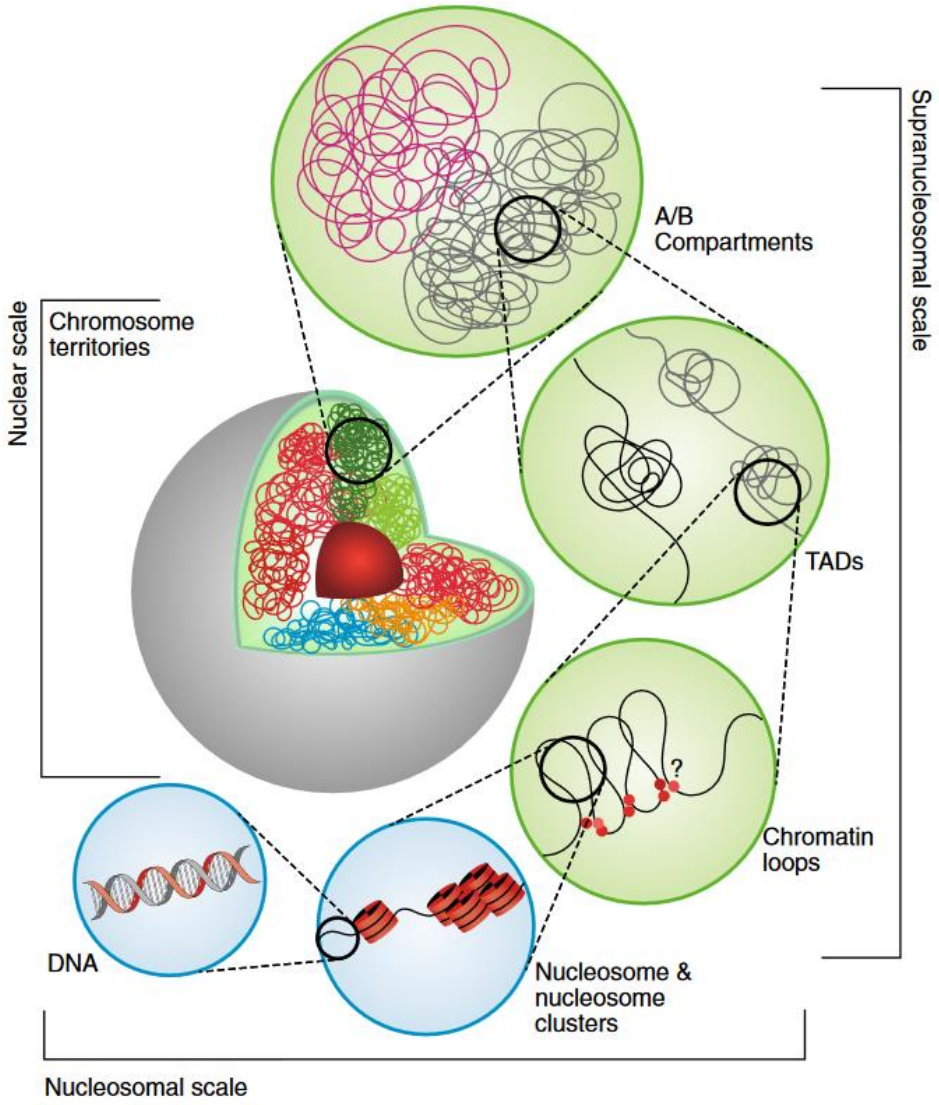

order to be packed into a more condensed structure (Figure 18) (Woodcock, 2006; Rowley et al., 2017; Misteli, 2020; Dekker et al., 2023).

In mammalian nuclei, the linear double helix DNA is wrapped around histone octamers to form nucleosomes – the basic unit of chromatin. Then, the string of nucleosomes is coiled into an even shorter and thicker chromatin fiber (Felsenfeld and Groudine, 2003; Bassett et al., 2009; Pombo and Dillon, 2015). Further interactions between chromatin fibers and chromosome scaffold proteins (CTCF/cohesion complex, condensins, topoisomerase II) lead to the formation of chromatin domains such as chromatin loops and topologically associating domains (TADs) (Dixon et al., 2012; Sexton and Cavalli, 2012; Dekker and Heard, 2015; Rowley and Corces, 2018). At a higher scale, these domains are segregated into two types of chromatin regions, termed "A" and "B" compartments. The A compartment represents transcriptionally active and open chromatin (euchromatin), while the B compartment corresponds to a repressed and more compacted state (heterochromatin) (Lieberman-Aiden et al., 2009; Rao et al., 2014; Wang et al., 2016; van Steensel and Belmont, 2017).

Eventually, the aggregation of chromatin compartments reflects the highest level of chromatin organization. At this large scale, each chromosome occupies a distinct nuclear area called chromosome territory (Boyle et al., 2001; Cremer et al., 2008; Cremer and Cremer, 2010; Fritz et al., 2019). Interestingly, the positions of chromosome territories are not completely random but rather correlate with their gene density and size. It was observed that smaller, gene-rich chromosomes tend to occupy more internal positions, whereas larger, gene-poor chromosomes are located near the nuclear periphery. Such radial organization has been observed in many eukaryotic cells, including human and mice (Croft et al., 1999, Tanabe et al., 2002; Mayer et al., 2005).

The spatial organization of yeast genomes preserves some of the basic organizational features of mammals. However, a few unique and defining features have also been identified. First, chromatin organization into topologically associating domains in yeast is still under debate (Carré-Simon and Fabre, 2022). Second, at a large scale, yeast chromosomes follow a Rabl-like spatial configuration, which is a slightly different mode of spatial organization compared to mammalian chromosomes. (Figure 19) (Rabl, 1885). In this conformation, all centromeres are clustered at one side of the nucleus, interact with components of the spindle pole body that is embedded in the nuclear envelope (Jin 2000; Bystricky et al., 2004; Winey and Bloom, 2012). Telomeres are also attached to the nuclear envelope while forming multiple clusters, the position of which is dictated by the length of the chromosome arms (Gotta et al., 1996, Taddei et al., 2004; Therizols et al., 2010; Marcomini and Gasser, 2015). Importantly, the Rabl-like

Figure 19: **Rabl-like configuration of chromosomes in fission yeast nucleus during interphase.** Chromosomes are tethered underneath the spindle pole body by their centromeres, while telomeres cluster distantly at several spots on the nuclear envelope. (Gallardo 2019)

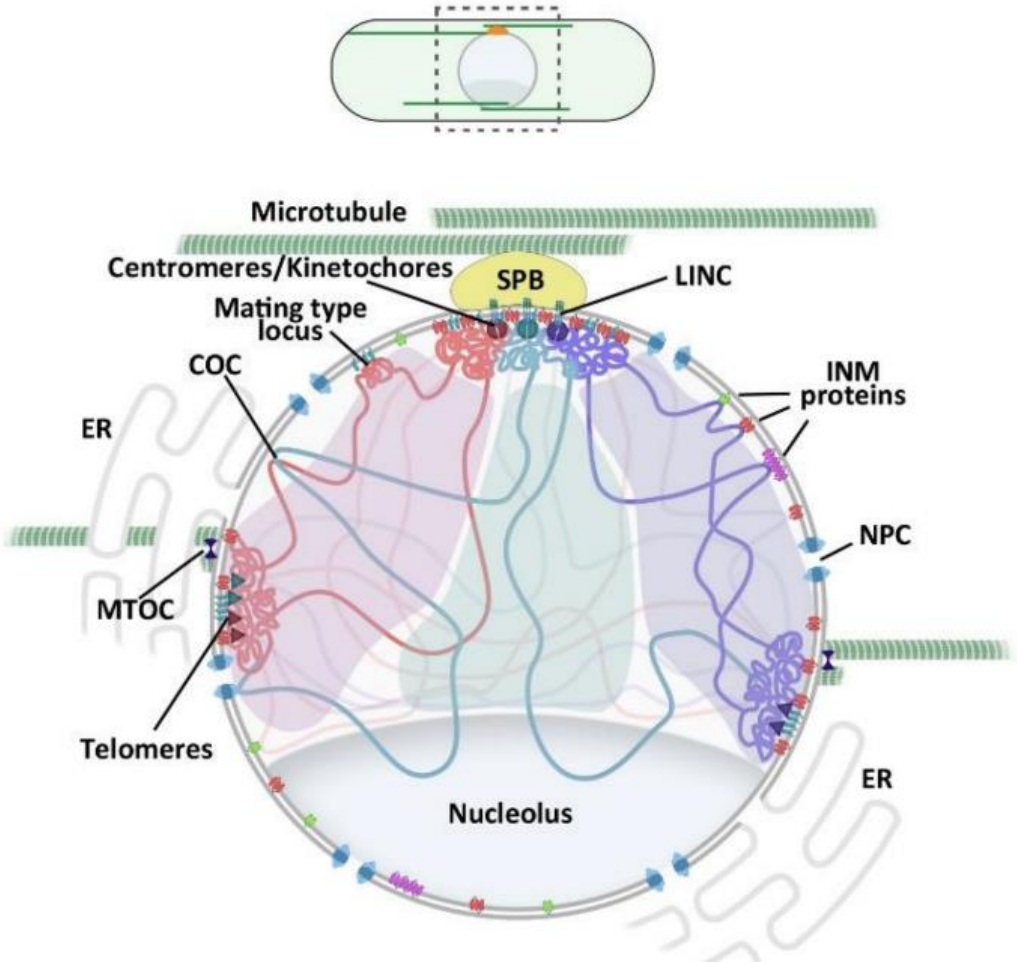

configuration was shown to reduce the topological entanglement of chromatin fibers (Pouokam et al., 2019).

The compartmentalized organization of chromosomes described above is restricted to interphase, i.e. when the cell is not dividing. At this stage, the chromatin is tightly packed, although flexible enough to allow processes such as transcription and replication to take place. However, as cells progress through the cell cycle into mitosis, the duplicated chromosomes dramatically change their structure. They become highly condensed and form structures with well-defined shapes and sizes that can be visualized with a light microscope. It is worth mentioning that the folding state of mitotic chromosomes is homogenous, locus-independent and common to all chromosomes among all cell types. The main reason for such strong condensation is the shortening of chromosomes' size before cell division. This, in turn, allows an efficient segregation of the sister chromatids to the opposite poles, thus ensuring a faithful transmission of the duplicated genome to the daughter cells.

B: Programmed chromatin mobility in response to DNA damage

Eukaryotic genomes are hierarchically structured in the nucleus, yet far from being static. In addition to chromosomes undergoing global morphological changes during the cell cycle, the chromatin exhibits various degrees of physical movement in response to DNA damage, a phenomenon that contributes to the maintenance of genome stability. To study and investigate chromosome mobility in different model systems, a common quantitative method has been employed. It involves marking chromosomal loci with fluorescent tags, tracking their movement by time-lapse microscopy and calculating the mean-square displacement (MSD). MSD plots the average volume a tagged locus has explored in the nucleus (Berg, 1993).

Using this approach, studies in yeast showed that the induction of a single DSB, either by HO or I-SceI endonucleases, led to an increased motion of the damaged locus. (Miné-Hattab and Rothstein, 2012; 2013; Dion et al., 2013; Miné-Hattab et al., 2017). Notably, the chromatin away from DSBs also moves, albeit to a lesser extent than the broken locus. Several groups have studied the dynamics of damaged versus undamaged chromosomes, in both haploid and diploid yeast cells (containing only one or two sets of chromosomes, respectively). An HO-induced DSB in a haploid cell increased the movement of an ectopic region located on a different chromosome (Strecker et al., 2016; Cheblal et al., 2020). A single DSB introduced by the endonuclease

I-SceI similarly led to an elevated motion of the unbroken homologous chromosome in diploid yeast cells. Interestingly, the dynamics of unbroken non-homologous chromosomes was also increased in the presence of a DSB, indicating that the increased motion is not an intrinsic property of homologous chromosome pairs (Miné-Hattab and Rothstein, 2012). In support of this view, the induction of multiple random breaks by γ-irradiation also led to a similar effect on global mobility (Miné-Hattab and Rothstein, 2012; Miné-Hattab et al., 2017; Smith et al., 2019). This enhanced chromosome mobility positively correlates with the kinetics and efficiency of recombination-mediated repair which is the dominant repair pathway in yeast (Neumann et al., 2012; Hauer et al., 2017, Challa et al., 2021).

In mammals, the amplitude of chromatin motions has been reported to correlate with break complexity, cell cycle stage and the choice of the repair pathway. DSBs induced by endonucleases or ionizing radiation, classified as simple breaks, are predominantly repaired by NHEJ in mammalian cells (Manivasakam et al., 2001; Mahaney et al., 2009). Live-cell imaging of a single DSB induced by the I-SceI endonuclease demonstrated none or limited motions of the tagged broken ends (Aten et al., 2004; Soutoglou et al., 2007; Neumaier et al., 2012; Roukos et al., 2013). Similar results were observed with X-ray, UV and γ-irradiated genome regions, which remain positionally stable (Nelms et al., 1998; Kruhlak et al., 2006; Jakob et al., 2009). Deprotected mammalian telomeres are an exception, as their significantly increased mobility was suggested to promote NHEJ-dependent chromosome end-to-end fusions (Lottersberger et al., 2015; Dimitrova et al., 2008). In contrast, mammalian DSBs repaired by recombination-mediated pathways showed enhanced dynamics, similar to what was observed in yeast. This includes repair of complex lesions resulting from trapped protein–DNA adducts during S phase. For example, DSBs generated by the topoisomerase II inhibitor etoposide exhibited high mobility in human cells (Krawczyk et al., 2012). Similarly, DSBs induced by neocarzinostatin (a radiomimetic drug) showed higher mobility in the G2 phase when repaired by HR than in G1 when repaired by NHEJ (Schrank et al., 2018). Moreover, a particular type of telomeres becomes highly mobile in response to DSBs. Indeed, in the absence of telomerase, telomeres can be maintained through a recombinogenic mechanism called alternative lengthening of telomeres (ALT) and it was shown in human cells, that ALT telomeres become highly mobile in response to DSBs (Fasching et al., 2007; Cho et al., 2014).

Global chromatin mobility has not been extensively studied in mammals and the so far obtained results are ambiguous. Analysis of DSBs induced by irradiation (mouse cells) or by cytotoxic drugs (human cells) both led to similar observations: there is a minor

Figure 20: **Chromatin dynamics upon DNA damage.** Examples of damage-induced changes in chromatin mobility include: extensive nuclear exploration of both damaged (A) and undamaged loci (B); clustering of multiple repair sites (C); directed motions to new nuclear locations (D). (Miné-Hattab and Chiolo, 2020)

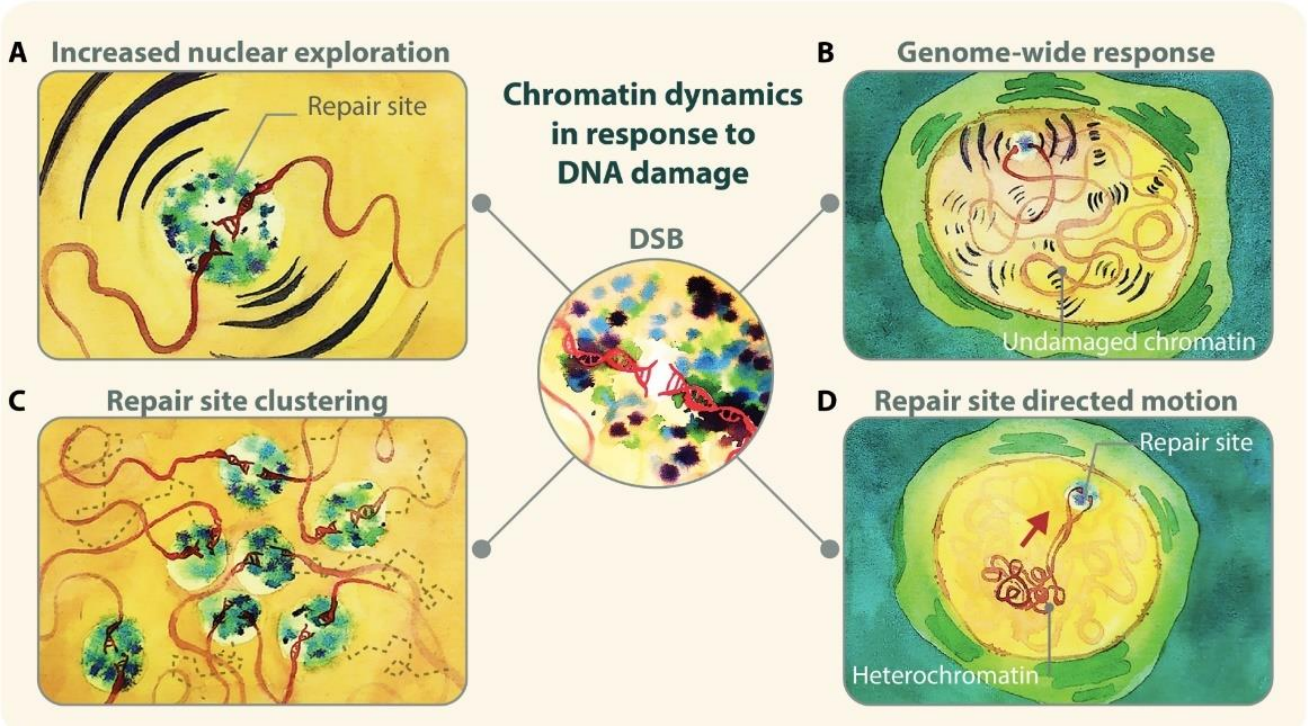

increase in the mobility of undamaged chromatin, compared to the damage site (Zidovska et al., 2013; Lottersberger et al., 2015). However, other studies did not report any change in the motion of undamaged chromatin (Dimitrova et al., 2008, Krawczyk et al., 2012).

Overall, this evidence supports the idea that a profound chromatin mobility is associated with DSBs destined for HR-dependent repair and to a lesser extent with those undergoing repair by NHEJ. What are then the functional consequences of enhanced chromatin mobility on DNA repair? It has been proposed that the increased mobility is implicated in certain processes such as homology search, DSB clustering and a direct motion of the damage site to a repair-prone nuclear compartment (Figure 20).

1. Chromosome mobility and homology search

In yeast nucleus, a locus experiencing a DSB explores an area 10 times larger than the area occupied before the damage (Lisby et al., 2003; Dion et al., 2012; Mine-Hattab and Rothstein, 2012). The DNA damage-induced chromosome mobility depends on checkpoint activation and HR factors. However, the requirement for Rad51 was not related to its recombinase activity (Dion et al., 2012; Smith et al., 2018). A very recent study in budding yeast used the first fully functional tagged version of Rad51 and reported that Rad51 nucleofilament is exceedingly long and highly dynamic, undergoing cycles of compaction and extension (Liu et al., 2023). Both of these features make homology searches faster and more efficient because they allow simultaneous scanning of sequences located in different nuclear regions. It is particularly important when the sister chromatid is not available and searching for a distant template is required (homologous chromosome or ectopic sequence). Indeed, increased mobility of DSBs positively correlated with homolog pairing and higher rates of recombination (Dion et al., 2012; Neumann et al., 2012; Miné-Hattab et al., 2017; Smith et al., 2018). Thus, spanning a larger nuclear volume facilitates the search for a donor sequence during homology-directed repair.

In humans, the DSB response at ALT telomeres triggers their movement across long distances to facilitate the association with recipient telomeres and homology-directed repair. Like in yeast, this process requires the HR machinery including RAD51 (Cho et al., 2014).

Hence, as the distance between the donor and the break increases, greater chromatin mobility becomes a requirement. This concept explains also the rather static nature of lesions repaired by NHEJ, where homology search is not part of the process and both broken ends are kept close together before ligation.

Figure 21: **The concept of repair centres.** Upon damage induction, DSBs tend to cluster together, forming so called repair centres. These repair centres are characterized by increased concentration of DNA repair factors and DNA damage signalling kinases, which facilitate efficient repair by HR. (Mackenroth and Alani, 2020)

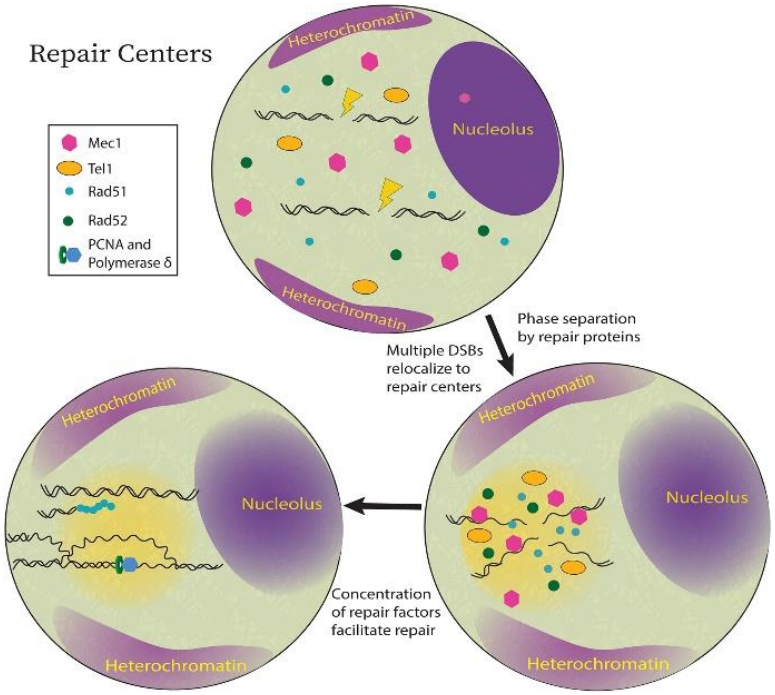

2. Chromosome mobility and clustering of repair sites

The increased motion of DSBs drives also the clustering of DNA damage sites into larger units. It was first observed in yeast that the generation of numerous random breaks by irradiation did not lead to the formation of an equivalent number of Rad52 foci. Instead, multiple breaks fused to form few repair centres in the nucleus (Lisby et al., 2003; Dion et al., 2013; Miné-Hattab et al., 2021). Further investigations revealed that HR proteins relocate from a diffuse nuclear distribution to aggregate at the DNA-damaged site (Figure 21). These include Rad51, Rad52, Rad54, the large subunit of the RPA complex, along with components of the DNA damage response machinery such as Mre11, and Tel1 (Lisby et al., 2004). Formation of these repair centres likely increases the local concentration of checkpoint and repair proteins, thus facilitating efficient DSB signalling, DNA end processing and repair of the break.

Similarly, studies in mammalian cells revealed that DSBs induced either by irradiation or endonucleases also had the tendency to merge into clusters (Aten et al., 2004; Krawczyk et al., 2012; Schrank et al., 2018). Their formation was associated with the accumulation of certain repair factors including ATM, 53BP1, and RIF1, thereby ensuring an optimal and efficient DNA damage response (Jakob et al., 2009; Neumaier et al., 2012; Roukos et al., 2013).

Besides facilitating repair, bringing multiple DSBs into close proximity may also be deleterious. It was reported that DSB clustering promoted chromosomal rearrangements in yeast and chromosomal translocations in mammalian cells (Roukos et al., 2013, Zhang 2012).

3. Chromosome mobility and direct motion of repair sites

The eukaryotic nucleus consists of different chromatin compartments showing distinct capacities for DNA repair. Moreover, DNA repair machineries are also spatially segregated (Kalousi and Soutoglou, 2016; Lemaitre et al., 2014). Thus, two types of genomic domains can be distinguished. Repair-prone domains correspond to the nuclear periphery and the nuclear pore complex (NPC) environment, while the nucleolus and heterochromatin regions are reported as repair-repressive domains. Therefore, in some cases the damaged chromatin exhibits non-random, but direct motions in order to change the nuclear compartment and facilitate efficient repair. A damaged locus either shifts away from the repair-repressive region and/or moves toward the repair-prone one.

Reports from several model organisms provided insights into the spatial regulation of DNA repair pathways activated in response to distinct types of DNA damage.

Breaks occurring within the heterochromatin escape their compartment to achieve faithful repair through homologous recombination. Such escape prevents ectopic recombination and rearrangements between repetitive sequences that are present in heterochromatin regions. Studies in Drosophila cells showed that DSBs in the pericentromeric heterochromatin relocated to the NPC (Chiolo et al., 2011; Ryu et al., 2015; Janssen et al., 2016; Caridi et al., 2018). In mouse cells, the same type of break moved to the periphery of the heterochromatin domain. However, in this case, a directed motion towards the NPC was not reported (Jakob et al., 2011; Tsouroula et al., 2016). Ribosomal DNA (rDNA), another example of a repetitive region, is localized in the nucleolus and kept in a heterochromatin state. DSBs induced within these rDNA repeats escaped the nucleolus compartment, as reported in yeast and human cells (Torres-Rosell et al., 2007; Harding et al., 2015; Van Sluis and Mac Stay, 2015; Horigome et al., 2019).

Another type of DNA damage that exhibits direct motion is represented by hard-to-repair DSBs. This includes *persistent DSBs (*due to permanent damage induction*)* and unrepairable DSBs (due to the absence of a homologous donor template*)*. In yeast, these types of breaks relocate towards the nuclear periphery, either to the inner nuclear membrane or to NPCs, where salvage pathways may help to complete their repair (Nagai et al., 2008; Oza et al., 2009; Kalocsay et al., 2009; Horigome et al., 2014; Oshidari 2018). Eroded telomeres, which are caused by telomerase inactivation and mimic one-ended DSBs, also move to NPCs to ensure the maintenance of telomere lengths by recombination (Khadaroo et al., 2009; Chung et al., 2015; Churikov et al., 2016). The phenomenon of relocation towards the nuclear periphery has also been observed in situations where replication is acutely restrained. In yeast, replication forks stalled by structure-forming sequences, DNA-bound proteins or within telomere repeats, as well as collapsed forks, move to the nuclear periphery for NPC anchorage (Figure 22) (Nagai et al., 2008; Su et al., 2015; Whalen et al., 2020; Aguilera et al., 2020; Kramarz et al., 2020). Likewise, replication stress induced within telomeric repeats in human cells led to the association of telomeres with the NPC (Pinzaru et al., 2020). Forks stalled upon the inhibition of mammalian DNA polymerase by aphidicolin treatment also shifted to the nuclear periphery (Lamm et al., 2020). It is important to note that not all types of stalled replication forks relocate to the nuclear periphery or NPC. For instance, fork stalling can be induced in yeast by treatment with hydroxyurea (HU), which leads to nucleotide depletion, but the replisome remains intact and is able to restart once the drug is removed. Such transiently stalled replication forks did not relocate to the NPC

Figure 22: **Various types of stalled forks relocate to the nuclear periphery and anchor to the NPCs.** Replication forks stall upon replication stress caused by various mechanisms. This includes structure-forming sequences (CAG repeats), DNA-bound protein complexes (*RTS1*-RFB), telomeric repeats, treatment with HU+MMS or aphidicolin. If the replisome dissociates from stalled forks, they turn into collapsed forks. These, in turn, give rise to different structures like reversed or broken replication forks. Both structures can undergo resection, generating ssDNA stretches bound by RPA. Repair proteins bind to the ssDNA and if SUMOylated, these proteins interact with the SUMO-targeted Ubiquitin Ligases (STUbL) (see chapter IV). The interaction of Slx5 STUbL with the NPC (for example via Nup84 in budding yeast) promotes relocation and anchorage to the NPC. (adapted from Whalen et al., 2020)

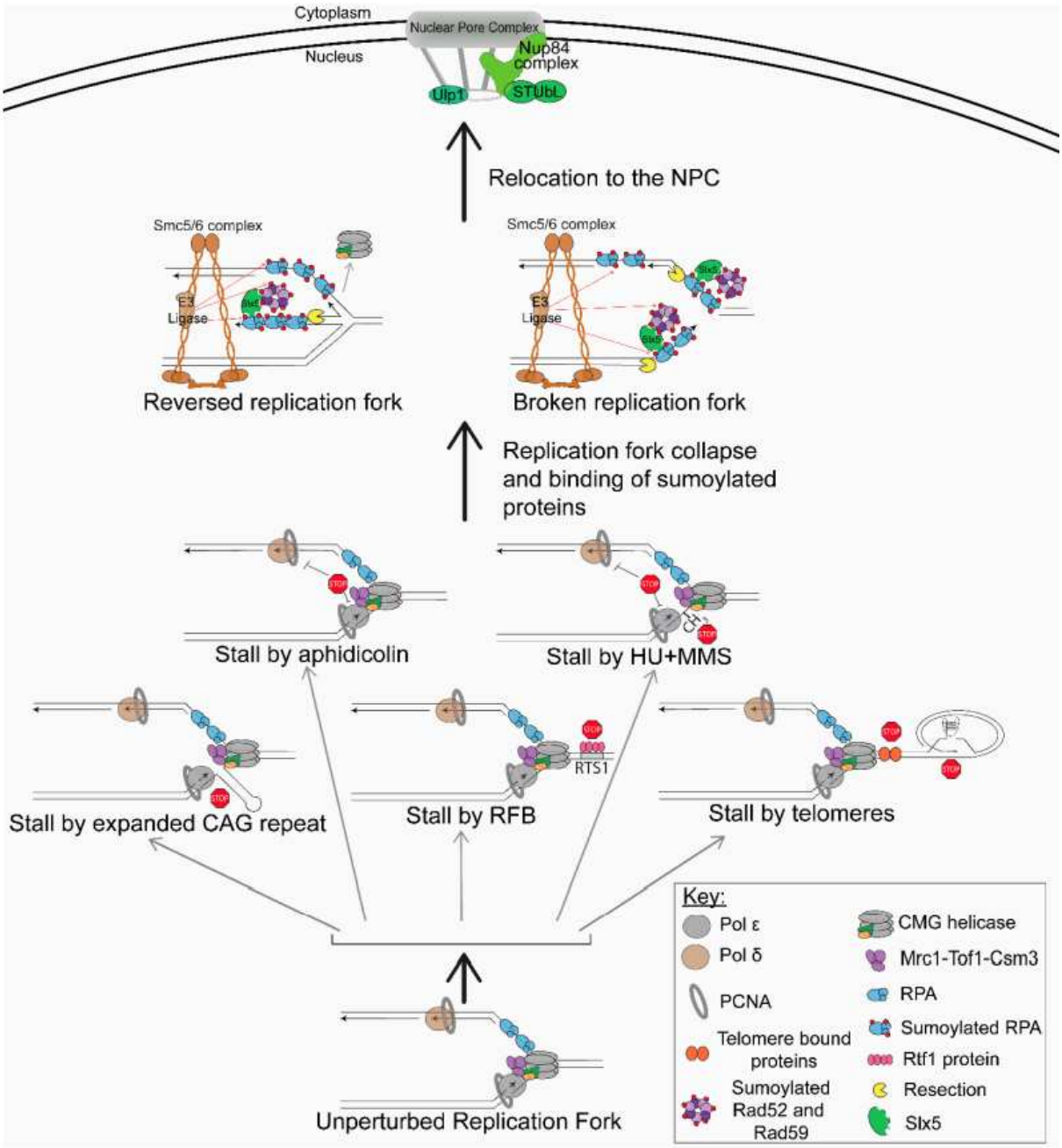

(Nagai et al., 2008; Su et al., 2015). However, relocation to the NPC occurred when cells were treated with HU for longer times or with both HU and alkylating agent MMS (methyl methane sulfonate) (Nagai et al., 2008). This suggests that prolonged or severe stall, leading to fork collapse is required to trigger relocation. Forks stalled upon the inhibition of mammalian DNA polymerase by aphidicolin treatment also shifted to the nuclear periphery (Lamm et al., 2020). It is important to note that not all types of stalled replication forks relocate to the nuclear periphery or NPC. For instance, fork stalling can be induced in yeast by treatment with hydroxyurea (HU), which leads to nucleotide depletion, but the replisome remains intact and is able to restart once the drug is removed. Such transiently stalled replication forks did not relocate to the NPC (Nagai et al., 2008; Su et al., 2015). However, relocation to the NPC occurred when cells were treated with HU for longer times or with both HU and alkylating agent MMS (methyl methane sulfonate) (Nagai et al., 2008). This suggests that prolonged or severe stall, leading to fork collapse is required to trigger relocation.

Taken together, the nuclear dynamics plays an important role in recombination-mediated repair particularly by facilitating homology search, driving the formation of repair centres, segregating lesions from compartments that jeopardize faithful repair or providing access to alternative rescue pathways in specific nuclear sub-compartments.

Figure 23: **Schematic illustration of the NPC.** NPCs are composed of multiple copies of nucleoporin proteins, organized in several different subcomplexes (indicated by boxes). The NPC is embedded in the nuclear envelope via transmembrane nucleoporins. The symmetric core of NPC is comprised of two outer rings (green) and an inner ring (violet) which forms the central channel of the NPC. This so-called scaffold layer provides structure and serves as an anchor for other nucleoporins. FG-nucleoporins inside the central channel regulate cargo traffic by forming a diffusion barrier which prevents passive diffusion of macromolecules. On the outside, the symmetric core is decorated with eight filaments extend into the cytoplasm; on the inside, the symmetric core is associated with nuclear basket nucleoporins projecting into the nucleoplasm (adapted from Burdine et al., 2020).

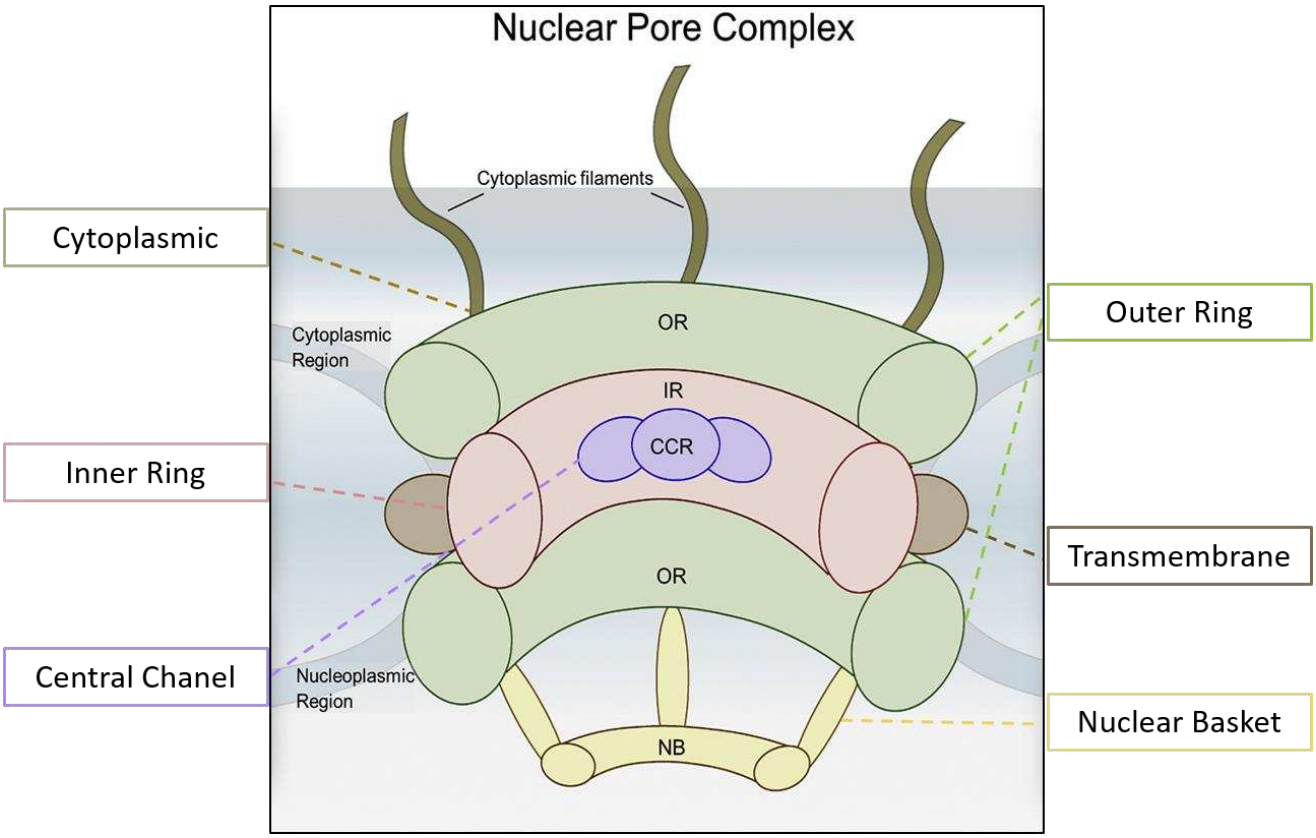

C: Nuclear organization and replication stress sites

1. Nuclear pore complexes and genome stability

The nuclear periphery is a bilayer membrane that separates the nuclear compartment from the cytoplasm. However, the macromolecular traffic between these two compartments is still possible and achieved through NPCs that are embedded in the membrane. NPCs are large protein complexes composed of multiple copies of around 30 different nucleoporins (Table 3). Electron microscopy studies revealed that the structural features of NPCs are conserved from yeast to mammals. Specific sets of nucleoporins are further arranged into distinct sub-complexes that serve as the main building block of the NPC (Figure 23) (Schwartz, 2016). The largest sub-complex is the Y-shaped mammalian Nup107-Nup160 complex and its counterpart Nup84 complex in budding yeast. Oligomerized Y-complexes form two substructures called outer rings (cytoplasmic and nucleoplasmic), which, together with the inner ring, build up the core scaffold of the NPC. Moreover, numerous filamentous structures extend from the outer rings facing the cytoplasm or the nucleoplasm. Nucleoplasmic filaments form a basket-like structure that is therefore called the nuclear basket. Beyond its canonical role in the selective passage of RNAs and proteins, NPCs have been implicated in transport-independent functions including DNA repair and genome stability maintenance (D'Angelo and Hetzer, 2008; Hoelz et al., 2011).

Particularly, the Y complex plays an important role in the DNA damage response. In budding yeast, the deletion of several nucleoporins of the Nup84 complex (e.g., *nup84*Δ or *nup133*Δ) resulted in high sensitivity to genotoxic drugs and replication stress (Bennett et al., 2001; *Nagai et al., 2008;* Loeillet et al., 2005). Loss of Nup133 led to an accumulation of DNA repair foci visualized by Rad52 (Loeillet et al., 2005). Moreover, mutations within the Nup84 complex caused synthetic lethality when combined with impaired HR-mediated DNA repair or DNA replication (induced by *rad52*Δ and *rad27*Δ, respectively) (Loeillet et al., 2005). A recent study demonstrated that the disruption of Nup84 was linked to a delayed progression of replication forks in the presence of DNA damage (Gaillard et al., 2019). In fission yeast, cells lacking Nup132 were sensitive to replication stress but not to DSBs or UV-induced DNA damage. Nup132 has been also shown to promote the recovery of transiently stalled forks (Kramarz et al., 2020). Similarly, the knockdown of NUP133 or NUP107 in human cells led to an accumulation of spontaneous DNA damage (Paulsen et al., 2009).

The integrity of another NPC sub-complex, namely the nuclear basket, is also required to prevent the accumulation of DNA damage. For example, studies in budding yeast showed an accumulation of Rad52 foci in the absence of Nup60 or both TPR (for

Table 3: **List of nucleoporins in yeast and human.**

Subcomplex	*S.pombe*	*S.cerevisiae*	Human
Cytoplasmic region	Nup146	Nup159	NUP214
		Nup42	NUP2
		Nup42	NUP12
			NUP358
	Nup82	Nup82	NUP88
			ALADIN
		Gle1	GLE1
		Nsp2	NUP62
			CG1
	Rae1	Gle2	RAE1
Core scaffold: outer ring (Y-complex)	Nup85	Nup85	NUP85
	Nup120	Nup120	NUP160
	Nup107	Nup84	NUP107
	Nup189	Nup145C	NUP96
	Nup131/Nup132	Nup133	NUP133
		Sec13	SEC13
	Seh1	Seh1	SEH1
	Nup37		NUP37
			NUP43
	Ely5		ELYS
Core scaffold: inner ring (Nic69-complex)	Nup97	Nic96	NUP93
		Nup188	NUP188
		Nup192	NUP205
		Nup157/170	NUP155
	Nup40	Nup53/59	NUP35
Central chanel (FG nucleoporins)	Nsp1	Nsp1	NUP62
		Nup49	NUP58
	Nup44	Nup57	NUP54
		Nup145N	NUP98
		Nup116	
		Nup100	
Transmembrane	Cut11	Ndc1	NDC1
	Tts1	Pom33	FMEM33
	Pom34	Pom34	NUP210
	Pom152	Pom152	GP210
		Pom152	POM121
Nuclear basket	Alm1	Mlp1	TPR
	Nup211	Mlp2	TPR
	Nup124	Nup1	NUP153
	Nup61	Nup2	NUP50
	Nup60	Nup60	
Mobile nucleoporins		Nup145C	Nup98

Translocated Promoter Region) homologs, Mlp1 and Mlp2 (Palancade et al., 2007). Importantly, such foci were not detected in mutants lacking nucleoporins involved in protein import or mRNA export. Thus, the accumulation of DNA damage is unlikely to result from defective transport but is rather linked to a function of the nuclear basket, similar to the Nup84 complex, in maintaining genome stability. In human cells, depletion of the nuclear basket component NUP153 caused ionizing radiation sensitivity. NUP153 has been shown to regulate DNA repair mostly by promoting the nuclear import of 53BP1 linking the macromolecular transport to DNA repair (Moudry et al., 2012, Lemaitre et al., 2012).

Taken together, the integrity of NPCs is vital for dealing with DNA damage and replication stress in both yeast and mammalian cells.

As mentioned before, NPC was demonstrated to act as a docking site and repair hub for different types of DNA lesions, including hard-to-repair DSB and collapsed replication forks. Several reports from different model systems have provided insights into the mechanism and functional consequences of relocating collapsed forks to NPCs, which will be summarized in the following sections.

2. Replication fork collapse at structure-forming sequences

Tri-nucleotide repeats, such as CAG repeats, have the tendency to form secondary DNA structures that can interfere with DNA replication and repair (Polleys et al., 2017). In budding yeast, replication forks that encounter long tracts of CAG repeats are prone to stall and collapse (Figure 22) (Freudenreich et al., 1998; Fouche et al., 2006; Nguyen et al., 2017). Such collapsed forks transiently shift to the nuclear periphery in the late S-phase, where they anchor to NPCs but not to the nuclear envelope (Su et al., 2015; Whalen et al., 2020; 2021; Polleys and Freudenreich, 2021). Chromatin immunoprecipitation experiments confirmed the association of CAG tracts with the nucleoporin Nup84 (NPC component) and not with Mps3 (nuclear envelope protein). Moreover, a later report showed that the relocation depends also on Nup1, a nuclear basket protein (see section 5, Aguilera et al., 2020).

The relocation and NPC anchorage require forks to be processed by the Mre11 exonuclease and further resected by Exo1 and Sgs1/Dna2 (Su et al., 2015). It has been proposed that the ssDNA generated in this process is then bound by RPA and other HR proteins. Indeed, Rad52 was found to bind the CAG repeats before their relocation but was removed afterwards to promote fork restart. On the contrary, Rad51 foci co-localized with CAG tracts only at the nuclear periphery and were excluded from the

Figure 24: **Spatially segregated steps of recombination-dependent replication in fission yeast.** Replication forks stalled at the RTS1-RFB shift transiently to the nuclear periphery where they associate with the nuclear periphery for the time necessary to achieve the HR-mediated fork restart (~ 20 min). In contrast to CAG repeats, relocation of RTS1-arrested forks requires Rad51 loading and enzymatic activity, supporting that joint-molecules, such as D-loops are relevant positioning signals. NPCs helps to sustain DNA synthesis upon replication stress by facilitating the removal of SUMO conjugates from the relocated joint-molecules (see Chapter IV). (Carr and Lambert, 2021)

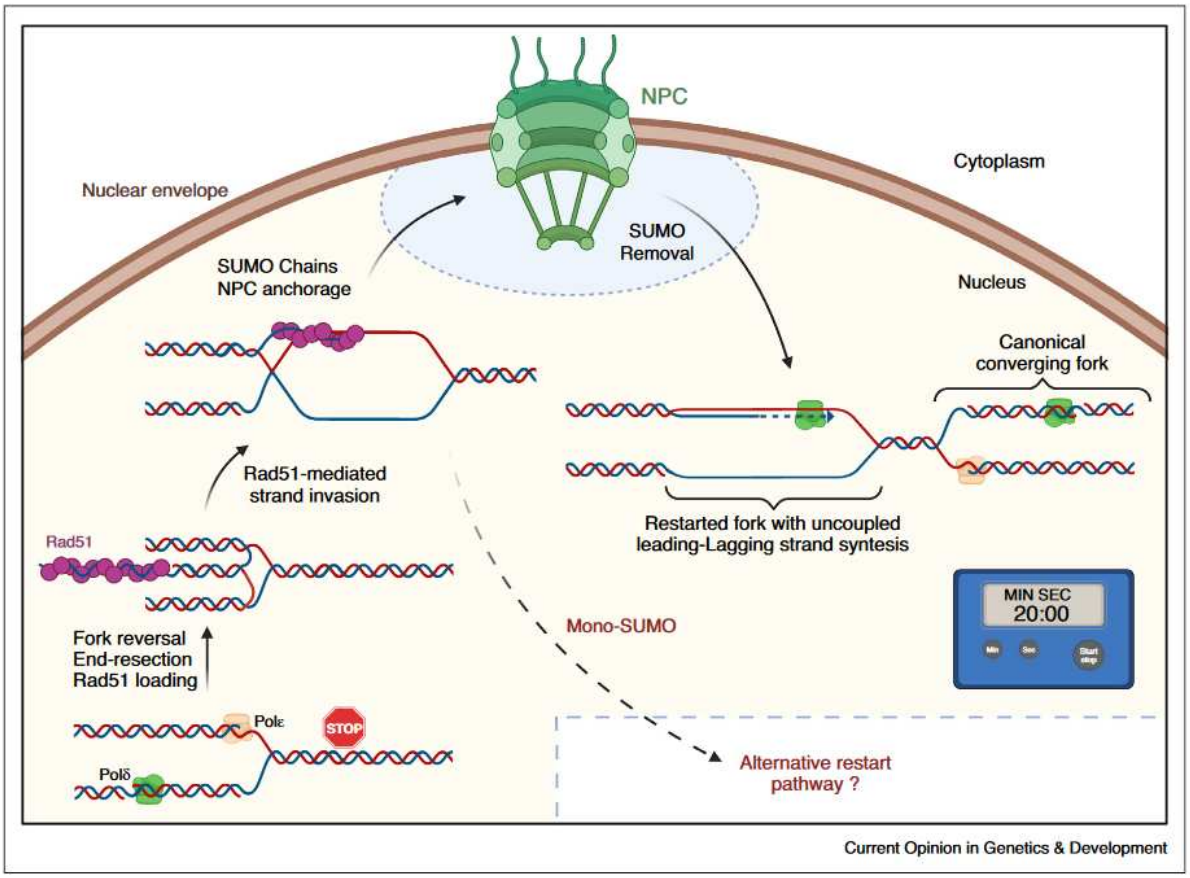

CAG repeats in the nuclear interior. Consistently, Rad51 was found to not be required for relocation (Su et al., 2015). Thus, recombination may be restrained at the early stages of fork stalling, but at the NPC this inhibition is alleviated to promote recombination-mediated fork restart (Whalen et al., 2020).

Mutants defective for relocation to NPCs (i.e. *nup84*Δ) showed an increased frequency of chromosomal breaks resulting in expansions and contractions of CAG tracts. This CAG fragility and instability, resulting from impaired relocation, occurred through a Rad52-dependent mechanism (Su et al., 2015; Whalen et al., 2020).

Together, these data indicate that routing towards NPCs helps to prevent a detrimental Rad52-dependent recombination pathway at collapsed forks, favouring the more accurate Rad51-mediated fork restart pathway. Such spatial segregation of the HR mechanism seems pivotal to maintain the stability and replication competence of repeats-induced collapsed forks.

3. Replication fork stalling at a DNA-bound protein complex

To investigate the fate of stalled forks in fission yeast, a site-specific replication fork barrier (*RTS1*-RFB) was employed (Kramarz et al., 2020). In this system, the activity of the RFB is mediated by the Rft1 protein that binds to the *RTS1* sequence to block the progression of the replisome in a polar manner. Forks arrested by such protein-mediated RFB become dysfunctional and can be rescued in two ways. They are either resolved by a converging fork or, if this is not coming on time, restarted by Recombination Dependent Replication (RDR) within 20 min. As mentioned before, RDR is associated to a non-canonical DNA synthesis with both strands being replicated by the polymerase delta (Lambert et al., 2010; Mizuno et al., 2013; Tsang et al., 2014; Miyabe et al., 2015; Nguyen et al., 2015).

Microscopy analysis revealed that replication forks arrested by the *RTS1*-RFB relocated to the nuclear periphery in S-phase (Figure 24). Similar to CAG repeats, the NPC was identified as the anchorage site of the active RFB, which was bound to Npp106 (a component of NPC) but not Sad1 nor Man1 (nuclear envelope proteins) (Kramarz et al., 2020).

It is worth mentioning that these forks are dysfunctional but not broken, thus DSB formation is not a prerequisite for triggering relocation. In line with this notion, it was previously observed that forks encountering a nick do not relocate to the nuclear periphery (Dion et al., 2012). In addition, the relocation and NPC anchorage of forks arrested at the *RTS1*-RFB requires the initial-resection machinery (Rad50 and Ctp1), and

the HR factors Rad52 and Rad51. To specify which Rad51 function is important, *rad51-II3A* mutant that binds DNA but lacks strand exchange activity (Cloud et al., 2012) was analyzed. The active RFB did not shift to the nuclear periphery in this mutant, which indicates that relocation requires the fork to be remodeled by the Rad51 enzymatic activity (Kramarz et al., 2020). Since the initial resection machinery was intact in *rad51-II3A* mutant, the authors concluded that nascent strand processing is necessary for Rad51 loading, but not sufficient to promote fork relocation *per se*. On the other hand, Rad51 binding to the active RFB was not affected in nucleoporin mutant defective for relocation (double mutant *nup131*Δ *nup132*Δ), supporting the notion that Rad51 loading and enzymatic activity occur prior to relocation and NPC anchorage. Together, this suggests that the formation of joint molecules, such as D-loop intermediate, constitutes a relevant signal for shifting the arrested forks towards the nuclear periphery (Figure 24).

This scenario differs from the one described for CAG repeats, where Rad51 loading was prevented in the nucleoplasm and facilitated only upon NPC anchorage. Differences between these two systems imply that the type of replication obstacle and likely the sequence environment affect the molecular transactions events at arrested forks. In repetitive sequences, premature loading of Rad51 is of great importance for potential rearrangements, whereas it remains a relatively safe mechanism within a unique sequence (Whalen et al., 2020; Kramarz et al., 2020).

Time-lapse microscopy analysis allowed to estimate that forks arrested at the RFB shift to the nuclear periphery for around 20 min, a timing that corresponds to the time of HR-mediated fork restart, suggesting that NPCs anchorage is an integral part of the RDR process (Kramarz et al., 2020). Indeed, the lack of relocation and subsequent anchorage led to a significant decreased in the RDR efficiency, thus impairing fork restart. Such correlation was observed in the above-mentioned mutants devoid of the initial-resection machinery, but also in the double mutant lacking two central components of the Y-complex Nup131 and Nup132. In the latter case, the NPC structure is likely impeded and no longer functional to anchor arrested forks.

Interestingly, in the single *nup132*Δ mutant arrested forks were properly anchored to the NPC but the efficiency of fork restart was still decreased. This defect did not result from faulty early steps of RDR, as fork resection and Rad51 loading were not affected in this genetic background. Thus, Nup132 is dispensable to anchor remodeled forks but is important for efficient fork restart by RDR (Kramarz et al., 2020). Taken together, these data revealed a novel function of NPCs in which Nup132 promotes HR-

dependent DNA synthesis downstream Rad51 binding, in a post anchoring manner. It also reinforces the notion that the subsequent steps of RDR are spatially segregated.

4. Replication fork stalling within telomeric repeats

Telomeres length can be maintained by a *reverse* transcriptase called telomerase. In yeast, telomerase inactivation led to a progressive shortening of telomeres at each cell cycle. This gradual telomere erosion proceeds until telomeres became critically short and their protective function was impaired. Eventually, unprotected telomeres are recognized as DSBs and activate a permanent cell cycle arrest, leading to replicative senescence (IJpma and Greider, 2003; Hector et al., 2012). While the majority of the cells die or remain arrested, a small fraction of survivors is able to bypass senescence by rearranging their telomeres via recombination events (Lundblad et al., 1993). Two distinct types of survivors have been distinguished: type I that depends on Rad51 and type II that is Rad51-independent (Chen et al., 2001; McEachern and Haber, 2006). Similar to the mammalian ALT pathway, both types of repair depend on the mechanism of break-induced replication to maintain functional telomeres (Lydeard et al., 2007; Dilley et al., 2016; Roumelioti et al., 2016). A study in budding yeast reported that eroded telomeres, which arise in the absence of telomerase, shifted from their nuclear membrane anchor sites toward NPCs (Khadaroo et al., 2009). Later it was found that this relocation favors the formation of type II survivors (Churikov et al., 2016).

Furthermore, it was noticed that in telomerase-deficient cells, some telomeres were detected at NPCs early after telomerase inactivation, but prior erosion and senescence (Khadaroo et al., 2009; Churikov et al., 2016). This was suggested to correspond to telomere repeats undergoing replication stress. Indeed, telomerase also prevents replication-induced damage at telomeres since its inactivation resulted in stochastic replication fork stalling and transient cell-cycle arrest (Simon et al., 2016; Maestroni et al., 2017; Xie et l., 2015, Xu et al., 2015; Aguilera et al., 2020).

Another study in budding yeast further characterized the relocation of telomeres under replication stress in telomerase-negative cells (Aguilera et al., 2020). First, it was confirmed that telomeric stalled forks anchored to NPCs in S-phase, where they were repaired by a conservative pathway to resume replication. Moreover, disruption of the nuclear basket component Nup1 (either by using a C-terminal truncation mutant or by fusing with a DNA-binding protein LexA) was shown to affect the peripheral localization of telomeric stalled forks, as well as fork stalled at CAG repeats. Consequently, when relocation and anchoring were hindered, stalled forks became engaged in a low-fidelity Rad51-dependent pathway to maintain telomere length. It was emphasized that this

Figure 25: **The role of NPC in the repair of fork stalled at telomeres.** In telomerase negative strain (*est2*Δ) replication forks stalled at telomeres relocalize to the nuclear pore complex, which favors conservative (error free) fork restart (left panel). When relocation fails (for example when Nup1 is fused to Lex), unrepaired stalled fork engage in error-prone Rad51-dependent repair through sister chromatid recombination (right panel). (Aguilera et al., 2020)

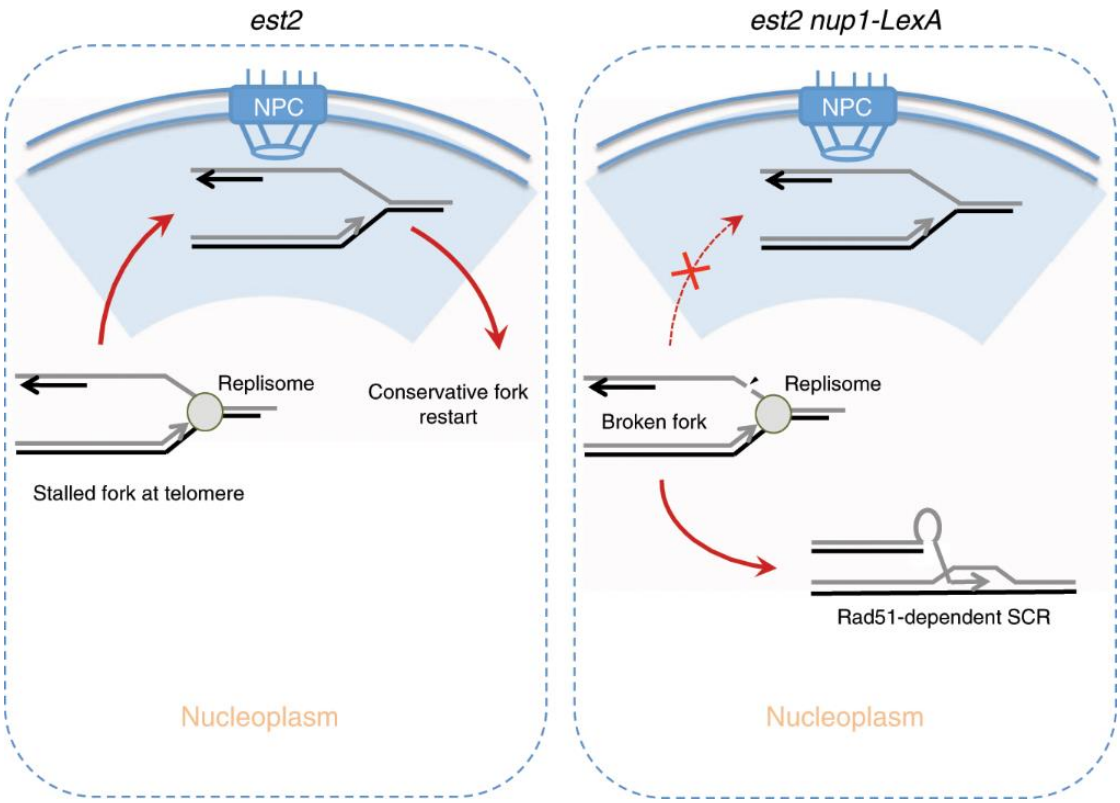

HR pathway differs from the ones involved in survivor formation. Particularly, it uses the sister chromatid as a template instead of another telomere. It does not generate long telomeres as observed in type II survivors; by contrast, it preserves a minimal telomere length sufficient to prevent replicative senescence. The authors therefore concluded that the lack of anchorage promotes telomere maintenance by unequal sister chromatid recombination, which is usually restricted upon relocation to the NPC.

To address this possibility, a single telomere was tethered to the NPC in order to evaluate the frequency of recombination events. As expected, the rate of sister chromatid recombination was significantly decreased. Moreover, such tethering restored the odds of type II recombination events, favoring conservative fork restart. Taken together, these results reveal an unsuspected role of the NPC in suppressing error-prone recombinogenic events at telomeric stalled forks (Figure 25).

The mechanisms engaged in resolving telomere-specific replication defects have also been investigated in human cells. POT1 is a component of the mammalian sheltering complex, playing a key role in telomere length regulation but also in telomere protection. Its depletion in human cells led to the activation of the DNA damage response at telomeres (Loayza and De Lande, 2003; Hockemeyer et al., 2005). Moreover, cancer-associated POT1 mutations, enriched within the OB fold domain, disrupted POT1 binding to telomeric ssDNA in vitro (Ramsay et al., 2013; Robles-Espinoza et al., 2014; Pinzaru et al., 2016). These POT1 oncogenic mutations were associated with telomere replication stress, fragility and increased frequency of mitotic DNA synthesis at telomeres (Pinzaru et al., 2016). A later study revealed that in cells expressing POT1 allele lacking the OB-fold domain (POT1-ΔOB), dysfunctional telomeres relocated to NPCs. Moreover, few nucleoporins were identified to be enriched at telomeres undergoing replication stress. These include the nuclear basket proteins TPR and NUP153, as well as NUP62. Inhibition of relocation to NPCs increased telomere dysfunction and fragility, which is a mark of telomere replication stress (Sfeir et al., 2009; Pinzaru et al., 2020). Additionally, preventing telomere-NPC interactions resulted in an elevated frequency of telomere sister chromatid exchange when POT1 was impaired. Collectively, these data emphasize that shifting replication-defective telomeres to the NPC prevents recombination between telomeric sister chromatids and facilitates fork restart. Thus, the direct role of NPCs in maintaining telomere stability upon replication stress seems to be evolutionary conserved from yeast to mammals.

5. Replication fork stalling upon DNA polymerase inhibition

Relocation of stalled forks in human cells has also been noticed in another experimental setup. In this system, cells were exposed to aphidicolin (DNA polymerase inhibitor) to induce global replication fork stalling. Upon aphidicolin treatment, foci marking stalled forks displayed increased mobility to eventually localize at the nuclear periphery in late S-phase (Lamm et al., 2020). When the relocation was inhibited, replication fork speed decreased, fork restart was impaired and the duration of S-phase was significantly extended. Additionally, an increase in micronuclei and anaphase abnormalities was observed, which reflects chromosome segregation errors arising from unresolved replication stress.

Thus, the peripheral positioning of stalled forks promotes replication stress response to ensure fork restart and prevent mitotic abnormalities. This study did not address the question of whether these stalled replication forks are anchored to the NPC. However, stalled replication forks in aphidicolin-treated mouse embryonic cells interact with some NPC components (unpublished data, mentioned in Whalen et al., 2020).

Taken together, the relocation to the nuclear periphery and anchorage to NPCs appear to be a universal phenomenon to favour the usage of the most conservative fork restart pathways and protect genome integrity. Especially, NPCs provide a nuclear environment that helps to restrict aberrant recombination events between repeated sequences.

D: Factors affecting chromatin mobility during DNA repair

Chromatin mobility during the response to DSBs and replication stress is a regulated phenomenon. The main molecular mechanisms, that underlie enhanced mobility of damaged DNA within the nucleus, will be briefly discussed.

1. Checkpoint signaling

Checkpoint activation is one of the contributing factors to chromatin mobility during DNA repair. Both ATR and ATM kinases, the key transducers of DNA damage signals, are necessary for the relocation of heterochromatic DSBs in Drosophila, persistent DSBs and eroded telomeres in budding yeast (*Nagai et al., 2008*; Chiolo et al., 2011; Churikov et al., 2016).

Figure 26: **INO80-mediated increase in chromatin mobility.** Upon DNA damage, nucleosome remodeling complex INO80 is recruited to chromatin in a checkpoint-dependent manner. INO80 promotes then the eviction of nucleosomes. Such nucleosome remodeling leads to reduction in the persistence length of chromatin fibers, thus enhancing their flexibility. (Seeber et al., 2014)

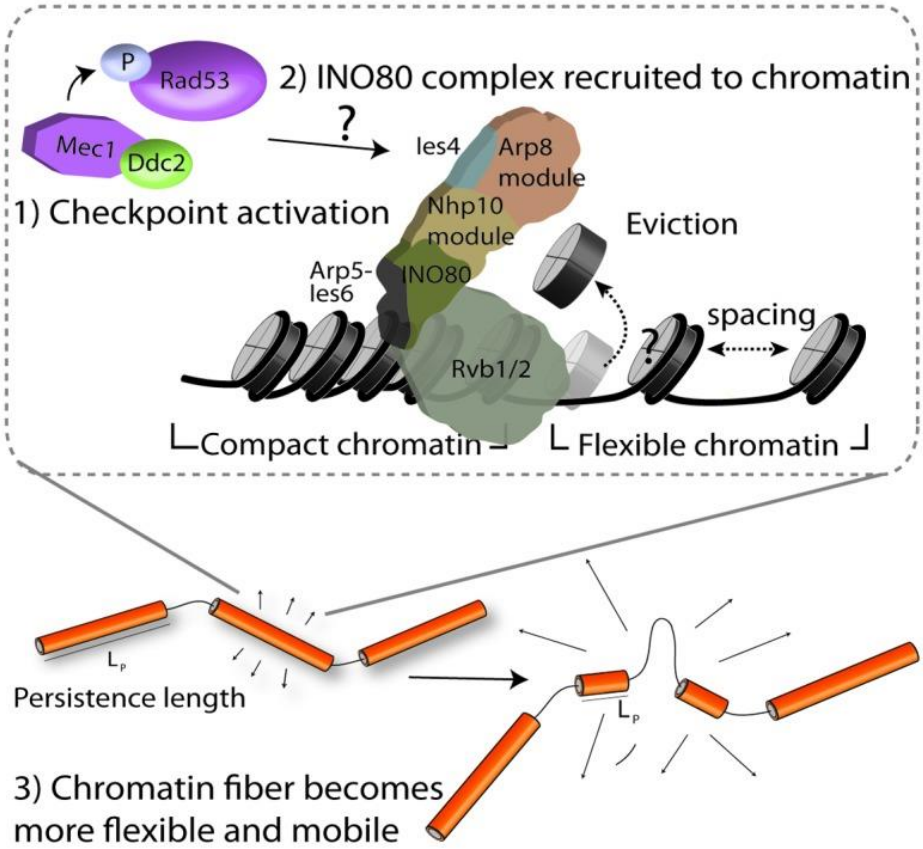

Checkpoint requirement has also been reported in the case of halted replication forks. In human cells treated with aphidicolin, stalled forks no longer localized to the nuclear periphery when the kinase activity of ATR was inhibited (Lamm et al., 2020). A similar observation has been made in mouse embryonic fibroblasts, where ATR inhibition led to a delayed interaction between aphidicolin-induced stalled forks and the NPC (unpublished data, mentioned in Whalen et al., 2020). Consistently, ATR facilitates the shift of replication-defective telomeres to the NPC in cells expressing POT1-ΔOB, but the ATM kinase was not found to be involved in this case (Pinzaru et al., 2020).

Conversely, the deletion of the yeast Mec1 (ATR homolog) or Tel1 (ATM homolog) had no impact on the relocation of forks stalled at the CAG repeats (Su et al., 2015). However, later experiments showed that deletion of other checkpoint proteins impairs relocation (unpublished data, mentioned in Whalen et al., 2020). Thus, the checkpoint response may be required, but the details remain to be clarified.

2. Physical features of the DNA lesion

The range of chromatin dynamic appears to be also affected by its physical state. The major features that enhance the mobility of the damaged locus include histone loss, chromatin decompaction and stiffening (Amitai et al., 2017; Hauer et al., 2017; Herbert et al., 2017).

A study in yeast has identified histone loss as a relatively quick response to DNA damage (Hauer et al., 2017). Their proteasome-mediated degradation required also checkpoint activation and the Ino80 nucleosome remodeler. The resulting reduction in nucleosome occupancy was accompanied by chromatin decompaction and increased flexibility (Figure 26). This, in turn, led to enhanced chromatin accessibility and mobility, facilitating homology search and/or DNA repair (Neumann et al., 2012; Mine-Hattab and Rothstein, 2013).

However, another report has also proposed a model in which global chromatin stiffening is responsible at least in part for the enhanced chromatin mobility after DNA damage in yeast. This increase in chromatin rigidity is mediated in part by the phosphorylation of the histone H2A (Herbert et al., 2017; Miné-Hattab et al., 2017). Although this seems contradictory, it may indicate a different degree of relaxation/stiffening at distinct genomic locations or time points upon damage induction. Therefore, further investigation is needed to determine the relative contribution of chromatin stiffening and relaxation to increased chromatin mobility.

Figure 27: **Actin-driven movements facilitates the isolation of DSBs to provide 'safe' repair.** The recombination-driven repair of heterochromatin in Drosophila is tightly regulated in space and time. Proteins required for DSB detection and resection are efficiently recruited to repair sites inside the heterochromatin domain, while Rad51 recruitment is temporarily halted. Checkpoint kinases and resection factors facilitate heterochromatin expansion. Next, actin is recruited to the repair site and upon activation polymerases toward the nuclear periphery. Damaged DNA that associated with the myosin-Smc5/6 complex slides with directed motions along actin filaments and eventually anchors to NPCs or inner membrane proteins. At the nuclear periphery, Rad51 is recruited to the repair site to enable 'safe' repair using the undamaged template that also relocalize in concert with the damaged locus. (Rawal et al., 2019)

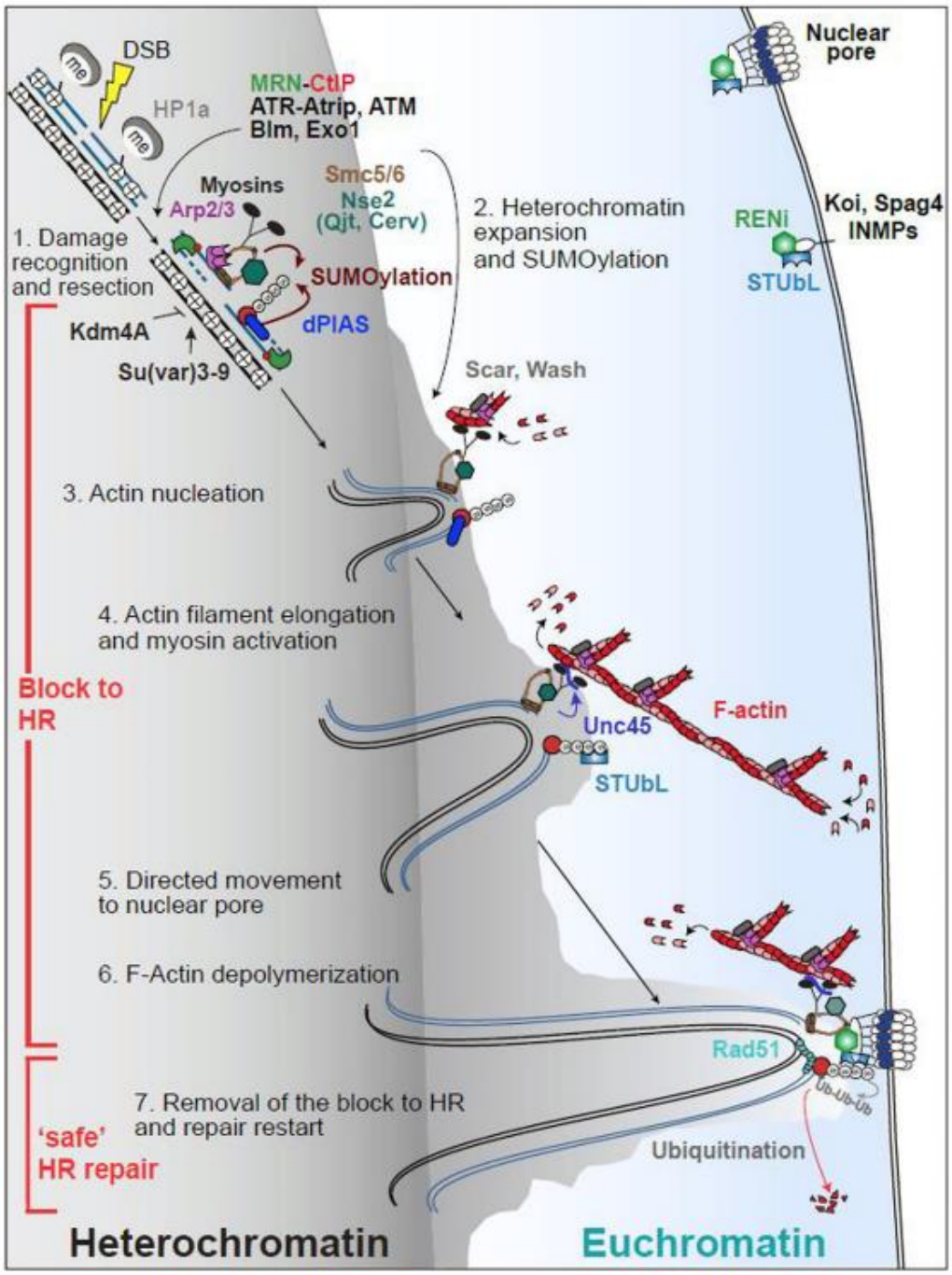

Moreover, the loss of external constraints imposed by DSB tethering to the centromere and/or to the telomeres was proposed as another mechanism affecting chromatin mobility (Strecker et al., 2016).

3. Mechanical forces

Additional determinants of enhanced chromatin mobility are intrinsic mechanical forces propagated by nuclear or cytoskeleton factors such as actin and microtubules.

Actin is a well-characterized cytoskeletal protein involved in the regulation of multiple cellular functions, such as the maintenance of cell structure and shape, cell migration, cargo transport, and cell division (Cooper and Schafer, 2000). The biological influences of actin stem mainly from its ability to polymerize into filaments (F-actin), complemented by the interaction with myosin motor proteins (Davidson and Cadot, 2021). Whereas F-actin is traditionally thought to be cytoplasmic, emerging evidence reveals that nuclear-specific F-actin is linked to diverse aspects of genome maintenance, at least in metazoan. These include chromatin reorganization, DNA repair and replication stress response (Parisis et al., 2017; Schrank et al., 2018; Caridi et al., 2018).

Nuclear F-actin is dynamically polymerized in response to DSBs. This was shown to drive the clustering of DSBs in human cells and promote their homology-directed repair (Schrank et al., 2018). In Drosophila and mouse cells, heterochromatic DSBs require nuclear F-actin and myosin to relocate to the nuclear periphery. In particular, the repair sites "slide" with directed movements along actin filaments that extend from the heterochromatin domain towards the nuclear periphery (Figure 27) (Caridi et al., 2018; Zagelbaum et al., 2023).

Recent reports in human cells have pointed to the role of F-actin in the relocation of replication stress to the nuclear periphery. Replication stress induced by aphidicolin caused an increase in the nuclear accumulation of actin. Furthermore, it was found that nuclear F-actin is polymerized through a pathway regulated by ATR (Lamm et al., 2020). Live cell imaging revealed that foci reflecting aphidicolin-induced stalled forks associated with nuclear F-actin and moved along these filaments toward the nuclear periphery. This is consistent with the previous observation made for heterochromatic DSBs in Drosophila, thus highlighting the role of F-actin as "highways" for relocation. Accordingly, upon treatment with an inhibitor of actin polymerization (Latrunculin B), stalled forks no longer moved to the nuclear periphery, which in turn impaired their restart and led to mitotic abnormalities (Spector et al., 1983; Lamm et al., 2020).

Figure 28: **Comparison of the structure of ubiquitin and SUMO based on the example of human SUMO-1.** Both proteins contain a characteristic tightly packed ββαββαβ ubiquitin-like fold Notably, SUMO is distinguished by a long and flexible N-terminal tail, not found in ubiquitin (Dohmen, 2004).

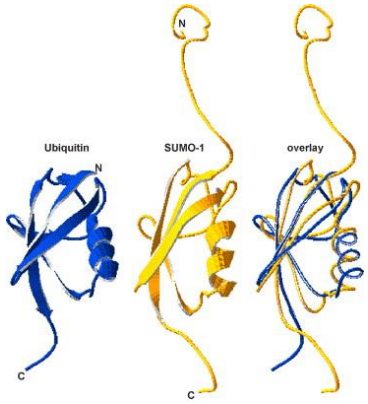

Table 4: **SUMO pathway players in humans, budding yeast *S. cerevisiae* and fission yeast *S. pombe*.** (Schirmeisen et al., 2021)

SUMO Pathway Component		Humans	*S. cerevisiae*	*S. pombe*
Small Ubiquitin-like Modifier (SUMO)		SUMO-1, SUMO-2, SUMO-3, SUMO-4, SUMO-5	Smt3	Pmt3
Activating Enzyme (E1)		SAE1 SAE2	Aos1 Uba2	Rad31 Fub2
Conjugating Enzyme (E2)		Ubc9	Ubc9	Hus5
SUMO Ligase (E3)	SP-RING type	PIAS1, PIAS2, PIAS3, PIAS4, Mms21	Siz1, Siz2, Mms21, Zip3	Pli1, Nse2
	other	RanBP2* HDAC4, KPA1, Pc2, Topors		
SUMO-targeted ubiquitin ligase (STUbL)		RNF4 RNF11	Slx5-Slx8 Uls1	Rfp1/Rfp2-Slx8 Rrp2 (predicted)
Sentrin/SUMO-specific protease (SENP)		SENP1°*, SENP2°*, SENP3, SENP5°, SENP6, SENP7	Ulp1°* Ulp2	Ulp1°* Ulp2

F-actin drives also the relocation of telomeres to the NPC in response to replication stress caused by POT1 dysfunction. Again, inhibiting F-actin polymerization decreased the number of replication-defective telomeres at the nuclear periphery, leading to increased telomere dysfunction and fragility (Pinzaru et al., 2020).

To date, it is not known whether F-actin is also required for the directed mobility of DNA lesions in the much smaller yeast nucleus. However, another type of cytoskeleton protein has been reported in yeast to mobilize DSBs and enhance their repair (Oshidari et al., 2018). Specifically, intranuclear microtubule filaments facilitate the interactions between subtelomeric DSBs and the NPC to ensure cell survival via break-induced replication. Thus, it remains to be determined which yeast cytoskeletal components are involved in relocating the distinct types of collapsed forks to the NPC.

4. Post-translational modification

SUMOylation, a post-translational modification, is an important regulator of the dynamic of DNA lesions. However, since SUMOylation is an important aspect of my thesis, a separate chapter will be devoted to it. This will allow for a more extensive description of the SUMO cycle, the key players of the pathway and in particular their importance in the relocation of collapsed replication forks to NPCs.

IV. SUMO: a powerful regulator of DNA lesion dynamics

A: SUMOylation at a glance

1. Mechanism and players

Post-translational modifications increase the functional repertoire of the proteome by rapidly changing the properties of the modified targets. These include covalent addition of small ubiquitin-like modifier (SUMO) to target proteins (Figure 28). Similar to ubiquitination, SUMOylation is highly conserved in all eukaryotes. Some organisms, such as yeast, express a single SUMO polypeptide (ScSmt3 and SpPmt3), while several SUMO paralogs are found in mammalian cells (SUMO 1-5) (Geiss-Friedlander and Melchior, 2007; Celen and Sahin, 2020). Players of the SUMO pathway in humans and yeast model organisms are listed in Table 4.

Figure 29: **The SUMO pathway.** Top: The overview of enzymes involved in the covalent attachment of SUMO to its substrates. First, SUMO undergoes processing by SUMO specific proteases (Step 1) and is subsequently transferred to the E1 activating enzyme (Step 2) and E2 conjugating enzyme (Step 3). Finally, E3 SUMO ligase catalyzes the conjugation of SUMO to a substrate (Step 4). SUMOylation can be reversed by the action of SUMO specific proteases (Step 5). Bottom: Different types of SUMO modifications. (Schirmeisen, 2021)

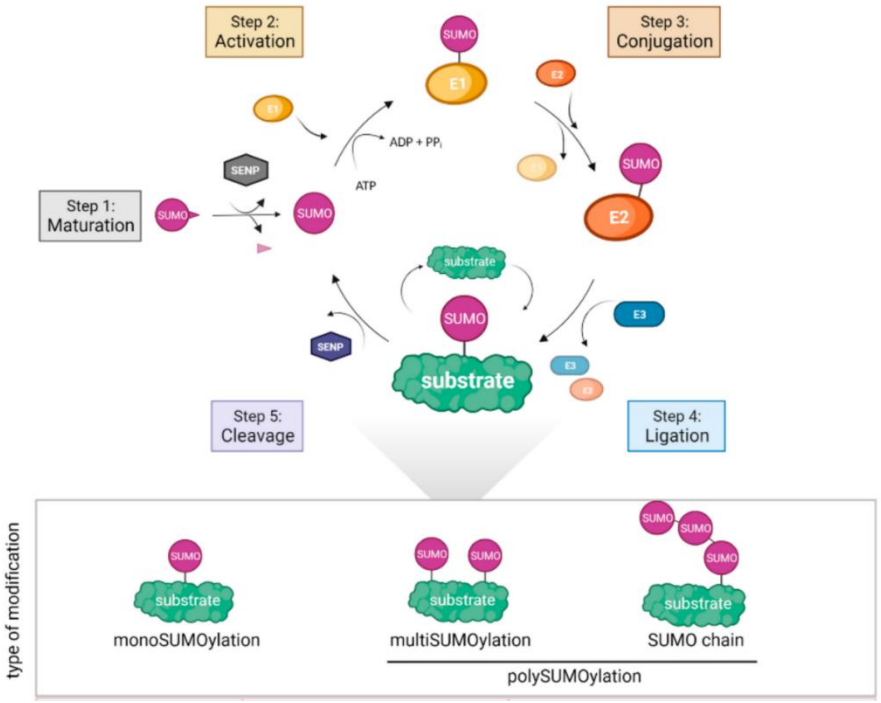

Figure 30: **Schematic representation of SP-RING family E3 SUMO ligases in yeast and humans.** The common motif required for E3 activity is the SP-RING. Other shared domains include SAP, PINIT and the SIM motif. Yeast Nse2 and mammalian MMS21 only share the SP-RING but are otherwise different. (Adapted from Pichler, 2017)

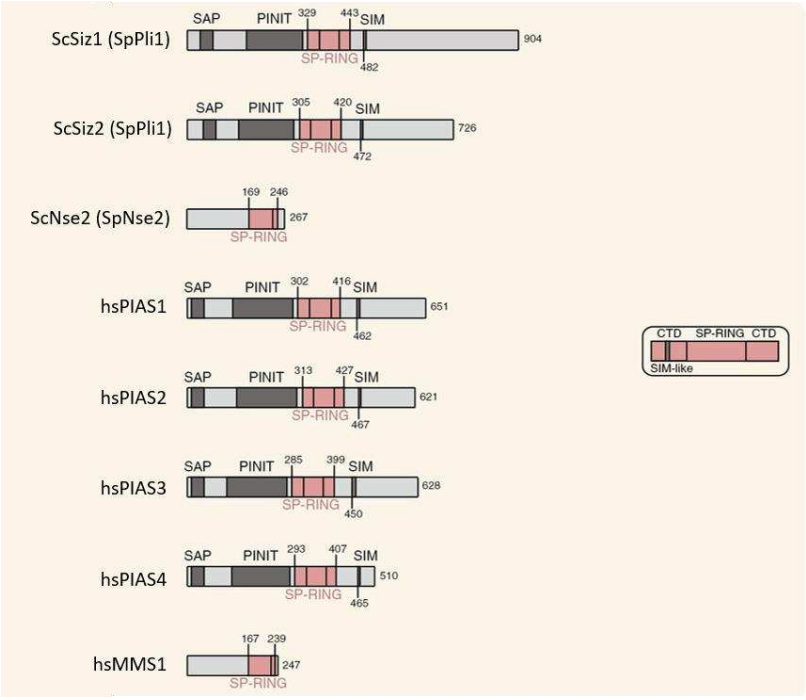

All SUMO proteins are synthesized in the form of immature precursors. Therefore, they must be first cleaved by specific proteases to expose a C-terminal di-glycine motif, which is critical for further conjugation (Pichler et al., 2017). Once processed, mature SUMO enters the SUMOylation cycle that occurs through an enzymatic cascade (Figure 29). The initial step involves SUMO adenylation, followed by the formation of a thioester bond with the E1 activating enzyme. The heterodimeric E1 enzyme is composed of SAE1-SAE2 subunits in humans, Aos1-Uba2 in budding yeast and Rad31-Fub2 in fission yeast (Table 4). Next, SUMO is transferred to the sole E2 conjugating enzyme (UBC9/ScUbc9 in human and budding yeast respectively, SpHus5 in fission yeast) forming as well a thioester bond (Desterro et al., 1999; Lois and Lima, 2005; Olsen et al., 2010).

Although the E2 enzyme is able to recognize and interact with some substrates, the efficient SUMO transfer is enhanced by E3 ligases through two mechanisms. Most often, E3 ligases bridge the SUMO-loaded E2 and the substrate to bring them into close proximity (Hay, 2005; Pichler and Melchior, 2004). On the other hand, when the E2 enzyme can interact directly with the substrate, the E3 ligase binds the E2–SUMO complex and stimulates its ability to discharge SUMO to the substrate (Reverter and Lima, 2005). Thus, E3 ligases promote the formation of an isopeptide bond between the C-terminal glycine of SUMO and the acceptor lysine of the target. This way, the E3 ligases guarantee the substrate specificity of the reaction (Gareau and Lima, 2010; Tozluoglu et al., 2010).

In a striking contrast to ubiquitination, where hundreds of distinct E3 ligases are required for specific target selection, only a few dozens of SUMO E3 ligases have been described. According to their structure and mechanism, they can be divided into distinct families.

The Siz/PIAS-type proteins are the major and probably the most studied family of SUMO E3 ligases. They possess a conserved SP-RING (Siz/PIAS-RING) domain, that is essential for their SUMO ligase activity (Johnson and Gupta, 2001; Takahashi, 2001; Hochstrasser et al., 2001). Several members exist in human cells (PIAS 1-4), two in budding yeast (ScSiz1 and ScSiz2) and one in fission yeast (SpPli1) (Watts et al., 2007; Rytinki et al., 2009). Additionally, MMS21 in human, ScMms21 and SpNse2 in yeast, also show SUMO E3 activity. Despite carrying the characteristic SP-RING domain, they are otherwise unrelated to the Siz/PIAS family (Figure 30). Importantly, both SpNse2 and ScMms21 are part of a large, essential Smc5/6 complex involved in DNA repair (Potts and Yu, 2005; Zhao and Blobel, 2005; Andrews et al., 2005). To date, only the SP-

Figure 31: **SUMO consensus motifs.** Left: Schematic representation of the main SUMOylation consensus motifs. Grey shading: hydrophobic residues; blue shading: lysine modified by SUMO; red shading: negatively charred residues. Right: Visualization of all known SUMOylation consensus motifs. Amino acids enriched are displayed above the x-axis whereas amino acids depleted displayed around SUMOylation site are below the x-axis. The degree of enrichment or depletion of a particular amino acid is reflected by the height of the corresponding letter. (Hendriks, 2016)

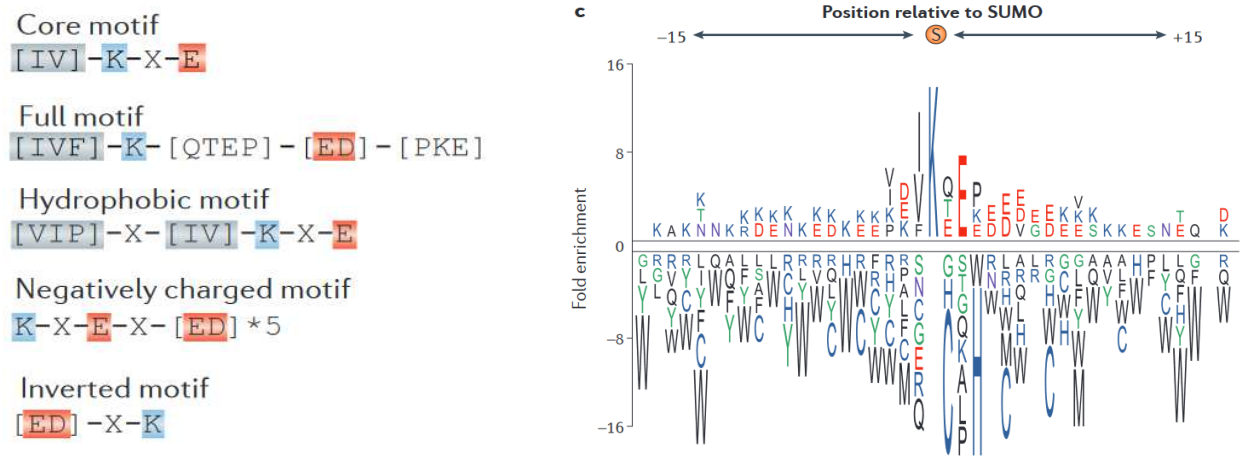

Figure 32: **Activities of SUMO specific proteases.** The Ulp/SENP proteases are involved in SUMO maturation process as they catalyze the processing of SUMO precursor in order to reveal the C-terminal di-glycine motif (dashed black box). Moreover, Ulp/SENP proteases are required for deconjugating distinct SUMO forms from substrates (dashed red box) and chain editing (solid red box). (Nayak, 2014)

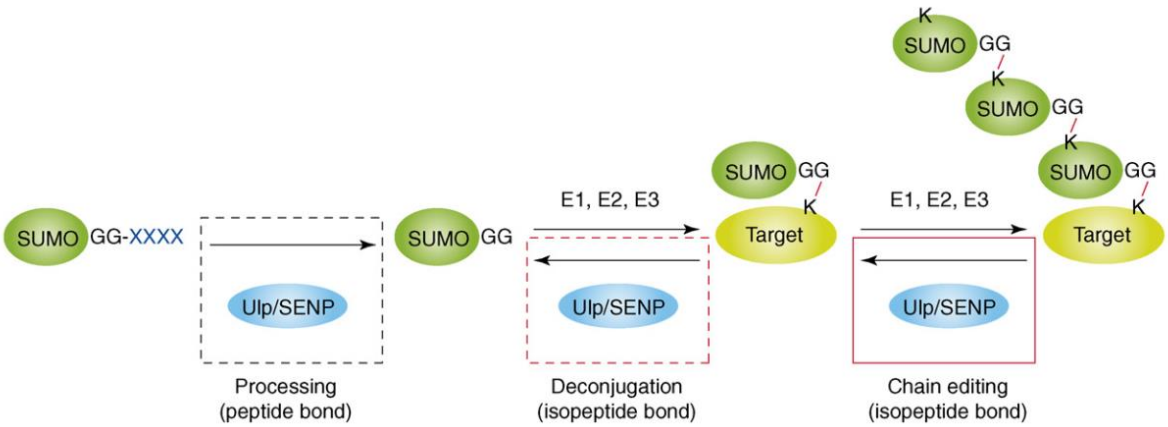

RING family of SUMO E3 ligases has been shown to be evolutionarily conserved from yeast to human.

The second type of SUMO E3 ligases is a well characterized, mammals-specific nucleoporin RANBP2. Structurally, it lacks homology to SP-RING-type E3 ligases but contains two internal repeats (IR1 and IR2) that can bind to UBC9 (Pichler et al., 2004). Biochemical studies showed that RANBP2 makes no contacts to its substrates, but enhances SUMOylation by positioning the SUMO-loaded E2 in an optimal orientation for efficient transfer (Reverter and Lima, 2005; Werner et al., 2012).

Besides the above-mentioned E3 ligases, enhanced SUMOylation in human cells has been associated with additional proteins, including PC2, TOPORS, KPA1, ZNF451 and HDACA4 (Kagey et al., 2003; Weger et al., 2005, Peng and Wysocka, 2008; Cappadocia et al., 2015).

Under normal conditions, the SUMO machinery predominantly targets lysines that reside within the SUMOylation consensus motif of [I/V/L]KXE (square brackets denote that any one of these large hydrophobic amino acids may be present and X denotes any residue) (Rodriguez et al., 2001; Sampson et al., 2001). Later analysis of data available from several mass spectrometry studies revealed additional various consensus motifs (Figure 31). These include inverted or extended core motifs that further strengthen the E2 affinity and lead to increased modification *in vitro* (Hendriks and Vertegaal, 2016). Moreover, upon stress such as heat shock and proteasome inhibition, SUMOylation was reported to become less stringent and promiscuously modify lysines at non-consensus motifs (Hendriks et al., 2014). On the other hand, it was noticed that many non-SUMOylated proteins also contain the SUMOylation consensus motifs. Therefore, the mere presence of such motifs alone does not necessarily designate a SUMO substrate.

SUMO might be attached as a monomer on single acceptor lysine generating monoSUMOylation (Figure 29). Substrates can be also modified with a monoSUMO particle on multiple lysine, which is referred to as multiSUMOylation. Additionally, SUMO has the ability to form polymeric chains (polySUMOylaton) in which successive SUMO particles are conjugated to an internal lysine of the previous SUMO particle in the chain (Tatham et al., 2001; Jansen and Vertegaal, 2021).

Similarly to other posttranslational modifications, SUMOylation is highly dynamic and reversible (Figure 32). Deconjugation of SUMO from the targets is carried out by SUMO-specific proteases. These enzymes cleave precisely the isopeptide bond

between the terminal glycine of SUMO and the substrate lysine. Additionally, certain SUMO proteases can fulfil another essential function via their hydrolase activity, namely processing the precursor SUMO to its mature form. All known SUMO proteases belong to the Ulp/SENP family of cysteine proteases, which share a conserved catalytic domain typically located at the C terminus end of the protein (Mukhopadhyay and Dasso, 2007; Hickey et al., 2012; Kunz et al., 2018).

The first discovered and described SUMO protease was the budding yeast ScUlp1 (UBL-specific protease 1) and later the second one ScUlp2 was identified (Li and Hochstrasser, 1999; 2000). Similarly, fission yeast contains two deSUMOylases: SpUlp1 and SpUlp2. Genetic studies in budding yeast revealed that different SUMOylated substrates accumulated in ScUlp1 or ScUlp2 deficient strains and that these mutants showed discrete phenotypes. Hence, the two yeast SUMO proteases appear to have distinct substrate specificities and only partially overlapping functions (Schwienhorst, 2000). Indeed, in addition to its deSUMOylating activity, Ulp1 (but not Ulp2) is required to generate the conjugatable mature SUMO in both yeast organisms. Additionally, ScUlp2 has been shown to preferentially cleave SUMO chains, negatively regulating substrate polySUMOylation (Hickey et al., 2012; Eckhoff and Dohmen, 2015). On the other hand, substrate specificity of Ulp1 and Ulp2 is in large part influenced by their different spatial localization (see below).

In human cells, six members of the SENP (sentrin-specific protease) family have been reported (Mukhopadhyay and Dasso, 2007; Geiss-Friedlander and Melchior, 2007). SENP1, SENP2, SENP3, and SENP5 are evolutionary related to yeast Ulp1, while SENP6 and SENP7 are closer to Ulp2 (Hickey et al., 2012; Kunz et al., 2018). As in yeast, mammalian SENPs have a dual enzymatic function in both SUMO maturation and deconjugation, however in a paralog-specific manner (Table 2). In the first case, SENP1 is most active on SUMO-1, SENP2 prefers SUMO-2 and SENP5 has significant processing activity for SUMO-3 precursor. When it comes to substrate deSUMOylation, SENP1 and SENP2 efficiently release all SUMO isoforms, whereas SENP3 and SENP5 favours the removal of SUMO2/3. In contrast, SENP6 and SENP7 preferentially cleave SUMO2/3 chains (Kunz et al., 2018).

Hence, SUMO proteases control the balance between free and conjugated SUMO particles. Moreover, their antagonistic interaction with SUMO E3 ligases determines the dynamic cellular levels of SUMOylated proteins.

2. Functions

Despite the similarities in the structure and conjugation pathways of ubiquitin and SUMO, the functions of both pathways are unique as they are not able to compensate for each other. At the molecular level, SUMOylation may lead to several non-exclusive consequences for the target protein (Figure 33). SUMO modification can elicit various biological consequences by affecting the activity, localization and/or stability of the target protein (Geiss-Friedlander and Melchior, 2007; Zhao, 2007; Wilkinson and Henley, 2010).

First, attachment of SUMO can mask the binding surface of target proteins thus blocking the interactions with different cofactors. This may alter the enzymatic activity, prevent transcription factors from binding to chromatin or prevent another post-translational modification. For example, SUMOylation of the E2 ubiquitin-conjugating enzyme inhibits its interaction with the E1 ubiquitin enzyme, resulting in a reduction in the effective ubiquitination of substrate proteins (Hardeland et al., 2002; Pichler et al., 2005).

Secondly, and conversely, SUMOylation may provide a new binding sites for partners harbouring specific SUMO interaction motifs (SIMs). The non-covalent interaction between SUMO and SIM is generally rather weak, but can be enhanced by the binding of several SIMs to SUMO chains (Hecker et al., 2006; Husnjak et al., 2016). Many SUMO:SIM-mediated interactions have been characterized and various downstream outcomes are possible. A typical example is the budding yeast *Srs2* helicase being recruited to replication *forks* by SUMOylated *PCNA to prevent recombination* (Pfander et al., 2005). SUMO-mediated interactions with transport complexes were shown to promote both nuclear import and export of certain cargo proteins (Santiago et al., 2013).

Interestingly, such interactions can also act as a double-edged sword when it comes to substrate stability. On one hand, SUMO chains may attract SIM-containing E3 ubiquitin ligase leading to ubiquitination and degradation of the substrate (see next section). On the other hand, other proteins interacting with SUMOylated substrates can prevent their deSUMOylation or degradation by competing with SUMO proteases or ubiquitin ligases respectively, thereby limiting their access to the substrate (Wei et al., 2017; Psakhye et al., 2019). These include SIM-containing ATPases or segregases that are able to extract SUMOylated proteins from the chromatin via their potential translocase activities (for example budding yeast Uls1 and fission yeast Rrp1/2) (Lescasse et al., 2013; Wei et al., 2017).

Figure 33: **Molecular consequences of SUMOylation.** SUMOylation affects protein-protein interactions via three non-mutually exclusive ways: a) masking of an interaction site; b) Formation of a new binding site; c) structural changes in the substrate's protein structure. (Geiss-Friedlander and Melchior, 2007)

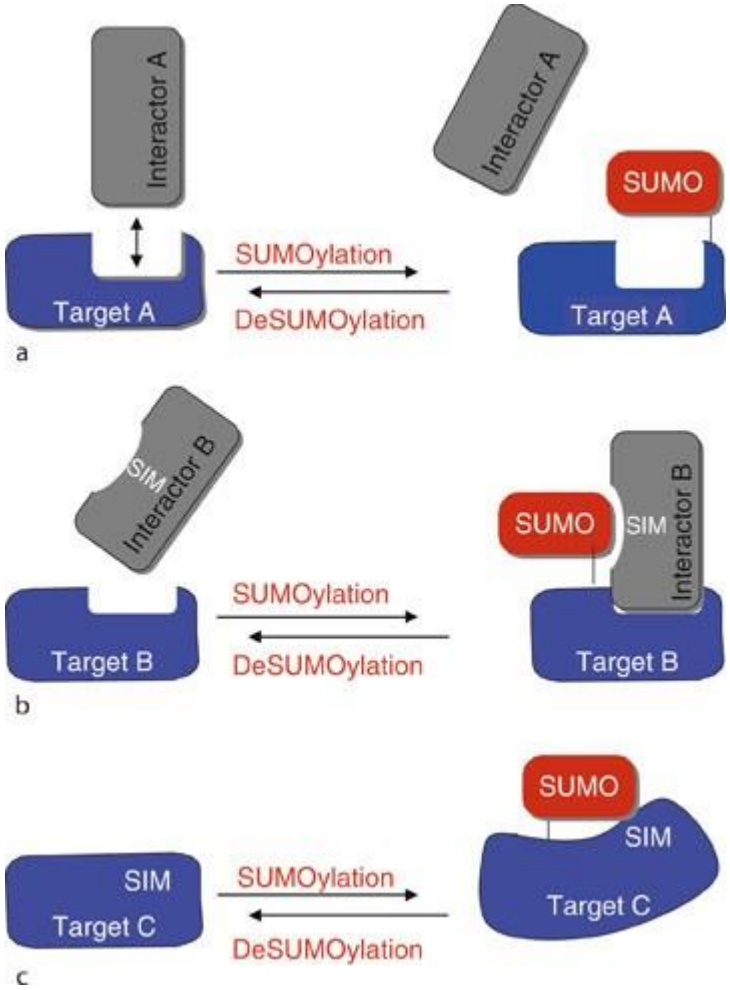

Alternatively, SUMOylation may also induce a conformational change of the modified target, for example via the interaction between an internal SIM motif and the conjugated SUMO particles. Such structural changes in the SUMOylated target may reveal a new binding site or destroy the existing one, which in both scenarios can directly affect its functions by modifying interactions with a partner protein or DNA binding affinity (Geiss-Friedlander and Melchior, 2007).

SUMOylation is implicated in a wide range of fundamental cellular processes including but not limited to DNA replication, DNA damage repair, chromatin remodelling, nuclear trafficking, protein degradation, cell cycle progression, gene expression, signal transduction (Seeler and Dejea, 2003; Johnson, 2004; Hay, 2005). Hence, the diversity of SUMO-regulated cellular processes underscores the significant role played by SUMOylation in cell fitness and survival.

This multitude of functions suggests also the existence of numerous targets. Indeed, a study from 2017 provided proteomic evidence for the SUMOylation of more than 6700 proteins in human cell, which constitutes almost 25% of the human proteome (Hendriks et al., 2017). However, for most substrates, only a small fraction of their total cellular pool is SUMOylated (often less than 1%) at a particular time point, especially in unstressed cells (Johnson, 2004; Hay, 2005).

An important question therefore arose, namely how can a small pool of SUMOylated protein lead to the dramatic effects that have been assigned to SUMOylation? First, it is important to keep in mind that SUMOylation is a reversible modification and can occur through cycles of SUMOylation and deSUMOylation, rather than being persistent. Although a rapid deconjugation by SENPs might shift the equilibrium to the side of the unmodified form (thus explaining the low detectable level of SUMOylation at a given time) a maximal downstream response can be still achieved. In this model, SUMO conjugation would promote a single event, whose consequences would persist after deSUMOylation. Several hypotheses have been put forward to explain this phenomenon.

One proposed model is that an initial wave of SUMOylation modifies a large fraction of the target pool and subsequently serves to recruit other interactors (for example additional post-translational modifiers) which remain on the substrate even after SUMO cleavage. Another possibility suggests that SUMOylation could drive the substrate to a functional complex or a subcellular compartment, where the protein remains even after deSUMOylaiton. In addition, some processes require synchronous and concerted action by multiple components in a given assembly (i.e. DNA damage

Figure 34: **Domain structures of SUMO-targeted Ubiquitin Ligases from yeast, flies and humans**. (Adapted from Chang, 2021)

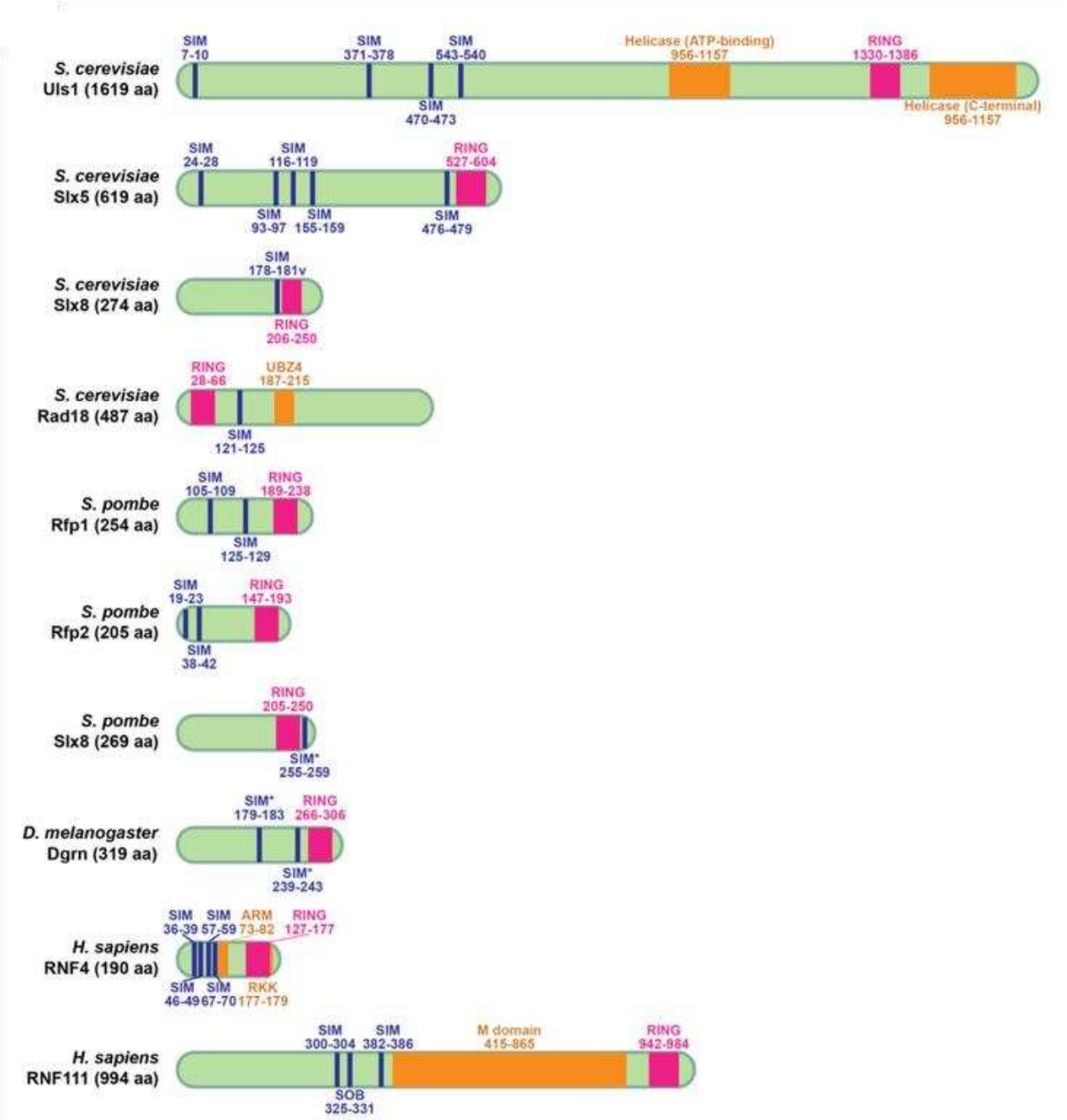

repair, chromatin remodelling, and transcription). Thus, the whole population of a given substrates could be modified over time, where the effect of each component SUMOylation adds up synergistically leading to a cumulative downstream effect. It is also common for some DNA metabolism factors to become SUMOylated "on-site", namely only when engaged with chromatin, which could also explain low levels of in vivo SUMOylation (Sarangi and Zhao, 2015).

3. When SUMOylation meets ubiquitination – the STUbL pathway

As mentioned above, SUMOylation can serve as a recruitment signal for other proteins. These include a specific class of ubiquitin E3 ligases called SUMO-targeted ubiquitin ligases (STUbL), that link the SUMO and ubiquitin systems (Figure 34) (Prudden et al., 2007; Uzunova et al., 2007; Perry et al., 2008).

To date, several STUbLs have been characterized in eukaryotic cells. In budding yeast, three STUbLs have been identified: the heterodimeric ScSlx5-Slx8, the large protein ScUls1 and the ubiquitin ligase ScRad18 that exhibits the hallmarks of a STUbL (Uzunova et al., 2007; Parker and Ulrich, 2012). In fission yeast, two different STUbL complexes are formed, SpSlx8 can interact with either SpRfp1 or SpRfp2 (Prudden et al., 2007; Kosoy et al., 2007). Following the identification of a STUbL in yeast, RNF4 (Ring Finger Protein 4) was the first STUbL identified in mammals and Arkadia (RNF111) the second one. However, Arkadia and RNF4 do not form a complex, indicating that they act independently (Kumar et al., 2017, Sriramachandra et al., 2019). Interestingly, the phenotypes observed in yeast cells lacking SpRfp1, SpRfp2 and SpSlx8 could be rescued by the expression of human hsRNF4 (Kosoy et al., 2007; Sun et al., 2007). These observations demonstrated that yeast and mammalian STUbLs are evolutionarily conserved and are functional homologs.

In general, all STUbLs are characterized by two key structural elements that determine their enzymatic functions (Figure 34). A tandem array of SUMO-interacting motifs (SIMs), allows the recruitment and binding to multiSUMOylated and polySUMOylated substrates, whereas a RING-type E3 finger domain is required for the ubiquitin ligase activity. Thus, by interacting with SUMOylated substrate, STUbLs catalyze the transfer of ubiquitin onto the covalently bound SUMO particle and/or the SUMOylated protein itself (Kerscher et al., 2007; Chang et al., 2021; Jansen and Vertegaal, 2021).

Genetic and biochemical studies showed that STUbLs regulates SUMOylation homeostasis by targeting SUMOylated proteins for proteasome-mediated degradation (Uzunova et al., 2007; Lallemand-Breitenbach et al., 2008; Miteva et al., 2010). Deletion of either ScSlx5 *or* ScSlx8, as well as ScUls1 led to the accumulation of SUMOylated proteins in budding yeast (Wang et al., 2006; Xie et al., 2007). Similarly, defects in fission

yeast STUbLs activity resulted in a drastic increase in SUMO conjugates (Sun et al., 2007; Prudden et al., 2007). Additionally, a proteomic study showed that hsRNF4 targets a large number of proteins for proteasomal destruction in human U2OS cells (Boulanger et al., 2021).

Besides triggering degradation, ubiquitynation of SUMOylated proteins can also affect their localisation and activity (Sriramachandran and Dohmen, 2014). The accumulation of SUMO conjugates in STUbL-deficient cells has been linked to an increased sensitivity of cells to DNA damage and global cellular dysfunctions. This underlies STUbLs functions in the maintenance of genome stability, by promoting the chromatin extraction and/or degradation of SUMOylated proteins involved, among others, in DNA replication and repair or transcription (Kosoy et al., 2007; Prudden et al., 2007). For example, SUMOylated RPA is recognized by hsRNF4, which then mediates RPA turnover on ssDNA (see below, Galanty et al., 2012).

Importantly, the homeostasis of key SUMOylated factors depends on the balance between the STUbLs activity and SUMO proteases that trim SUMO chains thus counteracting the STUbL pathway (Psakhye et al., 2019; Liebelt et al., 2019).

4. Spatial segregation of SUMO pathway

Similar to other cellular processes, the SUMO metabolism is spatially segregated in eukaryotic cells. The distinctive localization of SUMO metabolism related enzymes determines their substrate specificity, thus providing another remedy to control SUMOylation levels.

Two enzymes involved in SUMO conjugation have been found to be localized at the nuclear pore complexes (NPC) in mammals. First of them is the E3 ligase RANBP2. RANBP2 (called also NUP358) is a large nucleoporin localized at the cytosolic filaments of the NPC (Matunis et al., 1996; Mahajan et al., 1997). Structural studies have further revealed the formation of a tight RanBP2-SUMOylated RanGAP1-Ubc9 complex that is required for the SUMO E3-ligase activity of RanBP2 (Reverter and Lima, 2005; Werner et al., 2012). Thus, UBC9, the E2-conjugating enzyme, is the other SUMO-specific factor localized at the NPC. Although UBC9 has a predominant nuclear localization, a fraction of it was detected at both, cytoplasmic and nucleoplasmic sides of the NPC (Zhang et al., 2002; Saitoh et al., 2002). Importantly, UBC9 has been found at the NPC only in mammalian cells.

The spatial segregation of SUMO-proteases was reported in both yeast and mammals. In budding yeast, the SUMO-protease ScUlp1 is tethered to the NPC, whereas its

paralog ScUlp2 is mainly localized inside the nucleus (Li and Hochstrasser, 2000; Panse et al., 2003; Srikumar et al., 2013). Similarly, the peripheral localization is also a feature of the fission yeast SpUlp1, with SpUlp2 being mostly observed within the nuclear space. However, the sequestration of SpUlp1 at the nuclear periphery is cell-cycle dependent, with an association with NPC components during the S and G2 phases and a nuclear localization during anaphase (Taylor et al., 2002; Jongjitwimol et al., 2014). Anchorage of the yeast Ulp1 to the NPC requires multiple determinants. Early studies in budding yeast demonstrated that the N-terminus of Ulp1 mediates unconventional interactions with ScKap60 and ScKap121, the nuclear transport receptors termed karyopherins. These interactions together with the Ulp1's nuclear localization signal (NLS) were shown to be required for the proper localization of ScUlp1 at the NPC (Li and Hochstrasser, 2003; Panse et al., 2003; Makhnevych et al., 2007).

Later studies revealed that the proper localization of ScUlp1 in budding yeast requires also the Nup84-complex nucleoporins such as ScNup133 and ScNup120, together with the nuclear basket components ScNup60 and ScMlp1/2. Deletions of these nucleoporins led to a major lack of Ulp1 sequestration at the nuclear periphery and correlated also with a significant drop in the ScUlp1 protein level (Zhao et al., 2004; Palancade et al., 2007). Notably, inhibition of the proteasome partially restored the peripheral localisation of ScUlp1 in cells lacking ScNup133 and ScNup60 (other nucleoporin mutants were not tested). Hence, in nucleoporin mutants, the impaired anchorage of ScUlp1 at the NPCs led to its mislocalisation into the nucleoplasm and subsequent proteasome-mediated degradation.

Importantly, the link between nucleoporins and karyopherins was further analysed. First, microscopy analysis revealed that the two karyopherins, previously shown to be important for Ulp1 localization, were stable and functional in cells lacking ScNup133 or ScNup60. Moreover, in the absence of the karyopherins, ScUlp1 was no longer sequestrated at the NPC, but was not targeted for degradation and was found localized in the cytoplasm (Palancade et al., 2007; Makhnevych et al., 2007).

Together, these data indicate that distinct consecutive molecular mechanisms are involved in ensuring Ulp1 localization and stability at NPCs. Karyopherins seems to be involved in promoting Ulp1 import into the nucleus, whereas nucleoporins from Nup84-complex and nuclear basket ensure the stability of Ulp1 by facilitating (independently or alternately) its anchorage to the NPC. However, direct interactions between nucleoporins and Ulp1 have not been yet reported.

What are then the functional purposes of Ulp1 sequestration to the NPC? It was observed in budding yeast that ScUlp1 mutants impaired for tethering to the NPC, showed both increased and reduced SUMOylation level of some proteins (Zhao et al., 2004; Palancade et al., 2007; Lewis et al., 2007). Additionally, expressing an N-terminal truncated form of ScUlp1, that contained only the catalytic domain but that was mislocalized within the nucleus, was sufficient to counteract the accumulation of SUMO conjugates observed in the absence of the second SUMO-protease ScUlp2. This suggests that Ulp1 is able to process Ulp2-substrates when expressed in the nucleoplasm (Li and Hochstrasser, 2003). Hence, the complex alterations in global SUMOylation patterns may result from either Ulp1's inability to target genuine substrates or from its increased access to normally inaccessible nucleoplasmic SUMO conjugates.

Interestingly, overexpressing this N-terminal truncated form of ScUlp1 resulted in a dominant-lethal effect on cell growth. This phenotype was rescued when the catalytic domain of ScUlp1 was forced to localize in the cytoplasm (Mossessova and Lima, 2000; Panse et al., 2003). Therefore, exclusion from the nucleoplasm, rather than NPC localization, could be of predominant importance over the interaction of Ulp1 with NPCs. Moreover, it should be noted that in budding yeast, mislocalization of Ulp1 causes a defect in the retention of unspliced pre-mRNA within the nucleus (Lewis et al., 2007), showing that the association of Ulp1 with NPCs may be important to regulate nucleocytoplasmic trafficking.

In fission yeast, SpUlp1 is localized to the nuclear periphery and interacts with the NPC. In cells lacking the nucleoporin SpNup132 (ScNup133), Ulp1 was delocalized from the nuclear rim and its protein level was strongly decreased (Nie et al., 2015). Surprisingly, the global SUMOylation level in this mutant was significantly reduced, which is in striking contrast with the selective and relatively mild SUMOylation defects in the corresponding budding yeast mutant (Zhao et al., 2004; Palancade et al., 2007; Lewis et al., 2007).

As mentioned before, Ulp1 is responsible for the processing of SUMO precursors. Therefore, it could be hypothesized that the observed global reduction in the level of SUMO conjugates result from inefficient SUMO maturation. To test this possibility, the full-length or mature SUMO were expressed in SpNup132 deficient cells. In both cases the global level of SUMO conjugates remained unchanged, indicating that a SUMO maturation defect does not result from reduced SUMOylation when SpUlp1 is delocalized and destabilized. Instead, it was shown that delocalized SpUlp1 led to an

accumulation of SUMO chains on the SUMO E3 ligase SpPli1. This in turn promoted SpPli1 degradation in a STUbL- and proteasome-dependent manner, leading to a reduction in the global accumulation of SUMO conjugates. Thus, in fission yeast, Ulp1-associated NPCs protect SpPli1 from degradation by removing SUMO conjugates that could potentially attract STUbLs (Nie et al., 2015).

Altogether, despite that the Ulp1's sequestration at the NPC is important in both yeast models, the consequences of its delocalization and destabilization are different.

In human cells, each of the SUMO proteases localizes to a distinct subcellular compartment domain. Namely, SENP1 is localized to the nucleoplasm, SENP2 is enriched at NPCs, SENP3 and SENP5 in the nucleolus, and SENP6 is found in both the nucleus and the cytoplasm (Gong et al., 2000; Zhang et al., 2002; Nishida et al., 2000). Such differential localization likely contributes to the SUMO substrate specificity of these enzymes. SENP2 has been reported to concentrate at the nucleoplasmic face of NPCs through interactions with the karyopherins NUP153 (nuclear basket component) and the NUP107-160 subcomplex via its N-terminal domain. Similar to the yeast Ulp1, the N-terminal truncated form of SENP2 accumulated in the nucleus and led to an overall decrease in global SUMOylation (Zhang et al., 2002; Hang et al., 2002; Goeres et al., 2011).

Taken together, these reports across different model organisms highlight a non-canonical role of NPCs as a broadly conserved centre for SUMO-mediated signalling. Sustaining the SUMO homeostasis is a critical regulator of many cellular processes. How exactly the spatially segregated SUMO metabolism is critical for the maintenance of genome stability and more specifically for recombination-mediated DNA repair, will be discussed in the following section.

B: Crosstalk between SUMOylation and the Replication Stress Response

1. SUMO-based regulation of homologous recombination

The unique feature of SUMOylation, namely its ability to rapidly and reversibly change the properties of target proteins (stability, activity and localization) makes it an ideal fine-tuning regulator of many pathways implicated in genome maintenance. Indeed, for most eukaryotes, SUMO is essential for viability, with an exception in fission yeast where S*cpmt3* deleted cells are viable but extremely sick. An imbalanced SUMO metabolism led to extreme and pleiotropic phenotypes, up to lethality (Geiss-

Friedlander and Melchior, 2007). In this section, the focus will be put on the SUMO-based regulation of the HR machinery involved in the processing of DSBs or stalled replication forks.

Early studies in yeasts have revealed that defects in SUMO pathway caused a hypersensitivity to DNA-damaging agents and replication inhibitors. These include mutations in the E2 conjugating enzymes (ScUbc9 and SpHus5) as well as in the SUMO E3 ligases (ScSiz1-2, ScMms21 and SpNse2) (Maeda et al., 2004; Sacher et al., 2005; Zhao and Blobel, 2005; Watts et al., 2007; Cremona et al., 2012; Jentsch and Psakhye, 2013). A study in budding yeast provided evidences that Ubc9- and Mms21-mediated SUMOylation serves as a regulatory mechanism to prevent the pathological accumulation of Rad51-dependent cruciform structures at damaged forks during replication resumption (Branzei et al., 2006).

In human cells, many players of the SUMO pathway such as UBC9, PIAS and MMS21, together with SUMO1 and SUMO2/3, are rapidly recruited to sites of DSB and fork stalling (Galanty et al., 2009; Morris et al., 2009; Vyas et al., 2013). Similarly to yeast, mutations in these genes resulted in cells sensitivity toward reagents that generate DSBs or replication stress.

It was also shown that mutated UBC9 inhibited the formation of DNA damage-induced RAD51 nuclear foci (Shima et al., 2013). Moreover, depletion of the E3 SUMO ligase PIAS1 (or PIAS4) impaired DSB repair by HR, whereas MMS21 was required to protect cells from DNA-damage induced apoptosis (Galanty et al., 2009; Morris et al., 2009; Potts and Yu, 2005). Together this implies that a supply of SUMO conjugates is needed at the site of DNA damage.

However, SUMOylation acts as a double-edged sword as mutations leading to the accumulation of SUMO conjugates also sensitized cells to DNA damage and replication stress (Srikumar et al., 2013; Schwienhorst, 2000; Maeda et al., 2004; Zhao and Blobel, 2005; Branzei et al., 2006; Galanty et al., 2009; Morris et al., 2009). For example, fission yeast lacking two STUbL subunits, SpRfp1 and SpRfp2, showed a slow growth phenotype and sensitivity to treatment with HU or MMS (Prudden et al., 2007; Sun et al., 2007; Kosoy et al., 2007). Similarly, deletion of the other STUbL subunit SpSlx8 also led to a high sensitivity toward genotoxic agents like MMS, HU or CPT. In all cases, a subsequent deletion of the fission yeast SUMO ligase SpPli1 was sufficient to rescue these phenotypes, suggesting that they are caused by a toxic accumulation of SUMO conjugates (Prudden et al., 2007; Steinacher et al., 2013). Also, it was shown in human that inactivation of STUbL, by the depletion of RNF4, led to a defective in DSB repair by HR (Galanty et al., 2012).

Thus, any dysregulation in the SUMO homeostasis can influence DNA repair capacities and be deleterious for cells survival.

In line with this, studies in both yeast and mammals described numerous SUMO targets among replisome components and DNA repair proteins, including HR factors. Importantly, their SUMOylation level increases in response to replication stress or DNA damage (Zhao and Blobel, 2005; Watts et al., 2007; Psakhye and Jentsch, 2012; Cremona et al., 2012; Jentsch and Psakhye, 2013).

Few examples of the key SUMOylated factors will be briefly described below to illustrate how SUMOylation fine-tunes the distinct steps of recombination-mediated repair and differently influencing the fate of modified targets (Figure 35). These reports provide a biochemical basis important for understanding the various molecular mechanisms associated with the relocation of replication stress sites toward the nuclear periphery (see section 2.1 and 2.2).

Resection

As described before, DNA end processing occurs in two stages. An initial trimming by MRN and CtIP (MRX and ScSae2/SpCtIP in yeast) is followed by an extensive resection carried out either by EXO1 or BLM-DNA2 (Sc/SpExo1, ScSgs1/SpRqh1, Sc/SpDna2 in yeast) (Mimitou and Symington, 2011). In budding yeast, the MRX complex is required for the SUMOylation of many HR factors acting downstream of the resection, likely by generating ssDNA which allows for the recruitment of SUMO ligases (Cremona et al., 2012, Psakhye and Jentsch, 2012, Chung and Zhao, 2015). Furthermore, components of the resection machinery are also SUMOylated.

DNA damage-induced SUMOylation of the budding yeast ScSae2 was shown to increase its solubility, thereby promoting DNA end resection (Sarangi et al., 2015). The nuclease-helicase ScDna2 is SUMOylated at multiple sites, which was suggested to promote its targeting to damage sites and facilitate DNA end resection. On the other hand, SUMOylation specifically attenuates ScDna2 nuclease activity, whereas its helicase activity is not impaired. Moreover, ScDna2 SUMOylation appears to promote its degradation, which generates a feedback loop to prevent over-resection (Ranjha et al., 2019).

The human CtIP modification by SUMO was first described to promote its recruitment to the DSB site and thus favouring DNA end resection (Soria-Bretones et al., 2017). Further studies revealed that CtIP SUMOylation protects the integrity of stalled replication forks (Locke et al., 2021). The latter can be explained by the fact that

Figure 35: **SUMO-based control of the homologous recombination machinery.** For simplicity, the scheme provides an overview of DSB repair by homologous recombination only with budding yeast proteins. See text for the details. (Dhingra and Zhao, 2019)

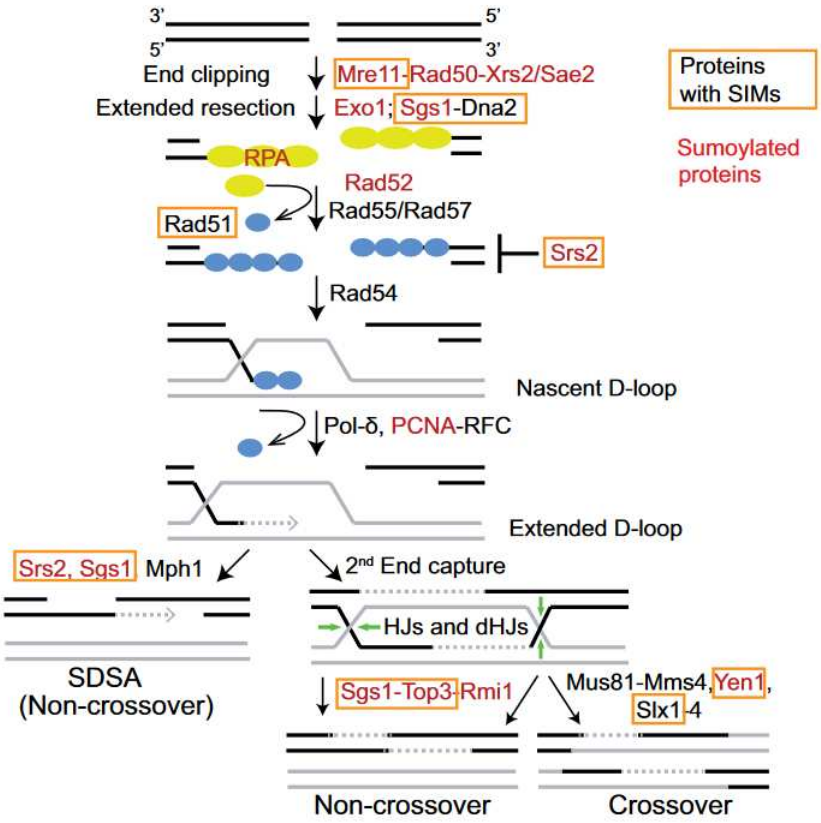

SUMOylated CtIP is targeted for STUbL-mediated ubiquitination and degradation to prevent the over-resection of DNA upon replication fork stalling (Han et al., 2021). Additionally, SUMOylation also controls the stability of human EXO1 in both unperturbed and stressed conditions. EXO1 is SUMOylated in vivo by the E3-SUMO ligases PIAS1/PIAS4 and it is a prerequisite for ubiquitin-mediated EXO1 degradation. On the other hand, EXO1 interacts with the SENP6 SUMO protease, whose depletion is promoting EXO1 degradation. Thus, a joint action of SUMO-conjugating and deSUMOylating enzymes provides a novel regulation layer of EXO1 stability (Bologna et al., 2015).

Rad51 filament formation

In both yeast and human, the RPA complex that binds the ssDNA overhang become SUMOylated. In budding yeast, SUMOylation of RPA occurred in a manner dependent on the SUMO ligase ScSiz2 upon exposure to DNA damaging agents (Cremona et al., 2012; Psakhye and Jentsch, 2012; Chung and Zhao, 2015; Dhingra et al., 2019). The mammalian RPA complex is modified by SUMO-2 and -3, which was shown to be involved in RAD51 foci formation. In more detail, the SENP6 SUMO protease interacts with RPA during unperturbed S-phase, thus keeping it hypoSUMOylated. Upon replication stress, the complex dissociates and allows the accumulation of SUMO2/3-modified RPA. This enhances the recruitment of RAD51 but also accelerates RPA replacement by RAD51 (Dou et al., 2010). Later study reported that in cells expressing the non-SUMOliable RPA or in cells depleted for RNF4, RAD51 failed to replace RPA (Galanty et al., 2012). Thus, the STUbL-mediated turnover of RPA at the DNA damage site is important to efficient HR initiation.

SUMOylation of Rad52 seems to be a conserved process as it has been observed in both fission and budding yeast, as well as in human cells (Ho et al., 2001; Sacher et al., 2006). In budding yeast, SUMO modification of ScRad52 is enhanced by the MRX complex, the SUMO-conjugating enzyme ScUbc9 and the SUMO ligase ScSiz2 (Johnson, 2004; Zhao and Blobel, 2005; Sacher et al., 2006). It was later shown that RPA-bound ssDNA promoted ScRad52 SUMOylation, this was not the case for Rad51-coated ssDNA. This suggests that ScRad52 SUMOylation occurs prior Rad51 nucleofilament formation (Altmannova et al., 2010). Although SUMOylation did not alter ScRad52 oligomerization or interactions with RPA and Rad51, it significantly lowered ScRad52 affinity towards ssDNA and dsDNA, reducing its DNA annealing activity. This was suggested to prompt ScRad52 dissociation from DNA either to favour appropriate pathways over others or to provide a mechanism for a dynamic exchange

of ScRad52 on DNA. (Altmannova et al., 2010). Later on, it was found that SUMOylated ScRad52 recruits the Cdc48 segregase to promote ScRad52 displacement from DNA by disfavouring its interaction with Rad51 (Bergink et al., 2013).

In addition to the above-mentioned evidences, additional observation suggest a strong interplay between SUMOylation and Rad51 functions. Early studies showed that mammalian RAD51 interacts with the UBC2 SUMO conjugating enzyme and SUMO-1 (Shen et al., 1996; Saitoh et al., 2002). The interaction with the latter has been suggested to be non-covalent and to occur via the SIM of Rad51 (Song et al., 2004). Later it was found that this SIM has an important role in DNA repair by attracting RAD51 to DNA damage sites. Moreover, Rad51 accumulation at DNA damage sites also requires the E2 ligase UBC9 and the E3 ligases PIAS1/PIAS4 (Shima et al., 2013). However, the question of whether RAD51 is directly SUMOylated upon DNA damage has been only recently resolved (Hariharasudhan et al., 2020). In this study, it was demonstrated that the SUMO E3 ligase activity TOPORS promoted RAD51 SUMOylation both *in vitro* and *in vivo*. Knockdown of TOPORS led to a decrease in the recruitment of RAD51 to DNA lesions and reduced efficiency of HR-mediated repair. Interestingly, the SUMOylation-deficient RAD51 was less capable to associate with BRCA2, likely explaining the HR repair deficiency of the cells expressing this mutant. Altogether, RAD51 SUMOylation is critical for its recruitment to DNA lesions and promotes HR-mediated repair.

The Srs2 helicase, an antagonist of the HR mediator proteins, can both bind to SUMO and be SUMOylated. Budding yeast ScSrs2 contains a SIM domain, best known for binding to SUMOylated PCNA. This interaction was initially shown to recruit ScSrs2 to stalled replication forks where it can remove ScRad51 from DNA (Papouli et al., 2005; Pfander et al., 2005). Later, ScSlx5/8 and ScUls1 were shown to associate with SUMOylated Srs2 and reduce its level at stalled replication forks by targeting it for degradation (Urulangodi et al., 2015; Kramarz et al., 2017). This was proposed to limit Srs2-mediated inhibition of Rad51 in situations when HR is needed to rescue replication defects.

The "ensemble effect"

Yeast harbouring mutations in the SUMOylation pathway are exclusively sensitive to assaults that induce DSBs, yet abrogating SUMO acceptor sites on individual HR proteins results only in mild phenotypes (Psakhye and Jentsch, 2012). This paradoxal discrepancy between strong phenotypes displayed by mutations in SUMO metabolism-related enzymes and the lack of notable phenotypes of SUMOylation-defective mutants seems to be characteristic of the SUMO pathway and can be

Figure 36: **Protein-group SUMOylation fosters DNA repair protein association and activity.** (Psakhye and Jentsch, 2012)

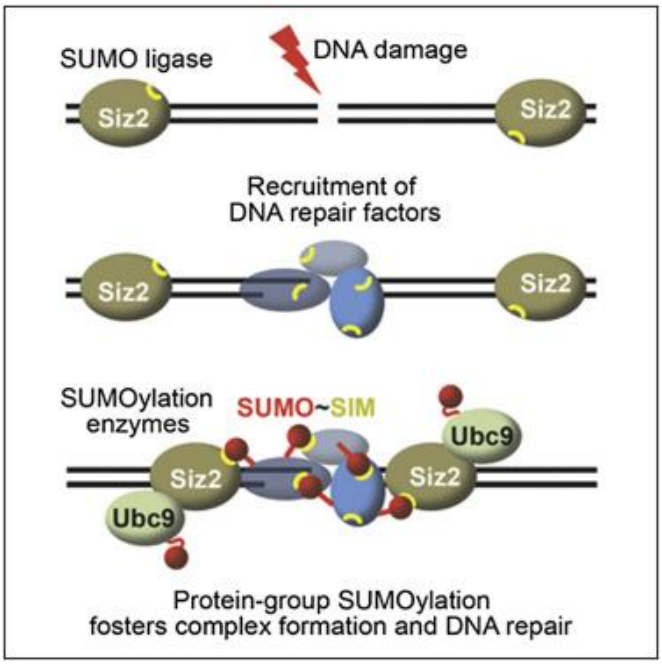

explained by so called "ensemble effect". When SUMOylation is restricted to a specific local area, it promotes modification of a group of proteins. These SUMOylated proteins then act synergistically through a combination of SUMO:SIM interactions. This is particularly important in the case of processes which require concerted action of multiple components. For instance, DNA damage triggers a SUMOylation wave that leads to simultaneous multisite modifications of a whole set of DNA damage checkpoint, replication, and repair proteins. Thus, the site of the DNA lesion shows the tendency to rapidly transform into hot spots of high SUMOylation activity that regulates DNA repair (Figure 36) (Burgess et al., 2007; Cremona et al., 2012; Psakhye and Jentsch, 2012; Sacher et al., 2006; Dhingra et al., 2019).

2. SUMOylation mediates DNA lesion mobility and repair at the NPC

In order to maintain the integrity of the genome, difficult to repair lesions and collapsed replication forks have been shown to relocate to the nuclear periphery and interact with NPCs, facilitating their recombination-dependent repair or restart, respectively. Many key players of homologous recombination pathways become SUMOylated in response to DNA damage or replication stress and the regulation of their SUMOylation levels appears to be critical for their activity (Psakhye and Jentsch, 2012; Cremona et al., 2012). Importantly, NPCs are known to serve as "SUMOylation activity centres", as they are enriched for multiple proteins linked to the SUMO pathway, including SIM-containing STUbLs and SUMO proteases (Nagai et al., 2008). Thus, it becomes more evident that SUMOylation provides the important link between NPCs and the spatially segregated recombination-mediated repair. Indeed, many studies in different systems revealed that the relocation mechanism is dependent on SUMOylation occurring at the DNA lesion site.

2.1. DSBs

In Drosophila cells, the SUMO ligase Nse2 and the STUbL enzyme Dgrn are required for relocation and NPC anchoring of heterochromatic DSBs. Additionally, SUMOylation impedes HR progression in heterochromatin domains by blocking the recruitment of Rad51 and thus prevents potential aberrant recombination between repeated sequences. At the nuclear periphery, STUbL likely mediates the ubiquitination and subsequent degradation of so far unidentified SUMOylated proteins, which may in turn promote Rad51 loading and repair (Ryu 2015, 2016, Caridi 2018, Chiolo 2011).

In budding yeast, DSBs that occur within the ribosomal DNA upon irradiation move outside the nucleoli region to complete HR repair. This relocation occurs in a manner

dependent on the ScMms21 and ScSiz2 SUMO ligases, with ScRad52 identified as an important SUMOylated target. Preventing ScRad52 SUMOylation resulted in the formation of ScRad52 foci within the nucleolus and hyper-recombination. Thus, ScRad52 SUMOylation limits deleterious recombination events within the rDNA by promoting nucleolar exclusion (Torres-Rosell 2007). Another work from yeast showed that persistent DSBs are recruited to the nuclear periphery in a SUMO-dependent manner. In S-phase, monoSUMOylation by ScMms21 promotes DSBs relocation towards the nuclear envelope protein ScMps3. On the other hand, polySUMOylation in G1 recruits the SUMO targeted ubiquitin ligase ScSlx5/Slx8 which promotes the relocation of persistent DSBs to the NPC. In this context, the formation of SUMO chains depends on both ScMms1 and ScSiz2 and deletion of either SUMO ligase inhibits the relocation of DSBs to the NPCs (Nagai et al., 2008; Horigome et al., 2016).

Furthermore, eroded telomeres in budding yeast accumulate SUMO-conjugates on RPA and several telomeric components. Then, the ScSlx5/Slx8 STUbL targets such modified telomeres to NPCs, where ScUlp1 SUMO protease facilitates their deSUMOylation. This has been shown to promote the repair of telomeres by a Rad51-independent pathway and generation of type II survivors (Khadaroo et al., 2009; Géli and Lisby, 2005; Churikov et al., 2016).

Hence, these pioneering studies indicate that SUMOylation serves as a major signal to coordinate the nuclear positioning of DSBs, providing a mechanism to ensure that their HR-mediated repair occurs in a safer environment. Interestingly, this model has been extended to collapsed forks, which relocation and anchorage to NPCs in yeast models was reported to depend on SUMOylation and is presented below.

2.2. Replication stress sites

Forks stalled by tri-nucleotides repeats

Replication forks collapsed at structure-forming CAG repeats in budding yeast relocate and anchor to the NPC (Su et al., 2015). This occurs in a SUMO-dependent mechanism that involves Smc5/6-associated ScMms21 and ScSlx5 STUbL (Figure 37) (Whalen et al., 2020). Notably, expressing a mutated SUMO particle, which eliminates polySUMOylation did not decrease the relocation rates. This indicates that monoSUMOylation is sufficient to promote the relocation of collapsed forks. Some specific targets undergoing SUMOylation upon fork collapse were identified and include ScRad52, ScRad59 and RPA subunit. Importantly, individual SUMOylation-deficient mutants in either protein did not completely impair relocation as,

Figure 37: **SUMO-driven routing of replication stress sites towards the nuclear periphery.** Left panel: DNA-bound, protein-mediated fork arrest in fission system. Right panel: structure-forming-mediated fork stalling in budding yeast. (Schirmeisen et al., 2021)

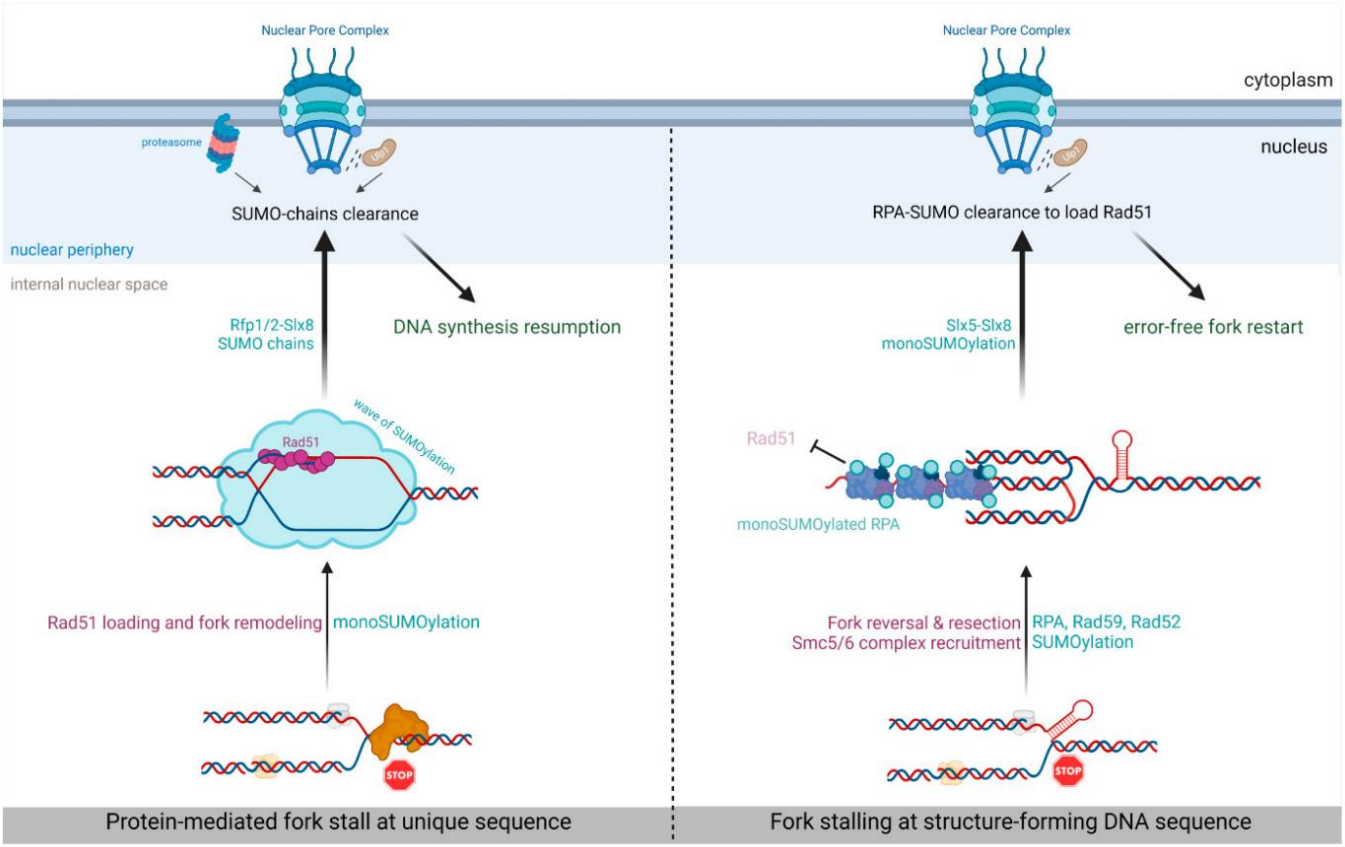

modification of all three proteins is required for relocation, but double mutants showed additive effects (Whalen et al., 2020). Thus, their SUMOylation may mediate the interaction with Nup84-bound ScSlx5, tethering the collapsed fork to the NPC. ScRad59 and RPA were shown to be SUMOylated by Mms21. No differences were observed in the SUMOylation pattern of Rad52 in Mms21 mutant lacking its ligase domain. The authors pointed out that this can result from the fact that the SUMOylation was examined in cells treated with zeocin, that induces DSBs but may trigger different modifications that structure-induced replication barrier. However, they did not exclude a minor role for the other SUMO ligase ScSiz2.

Besides promoting relocation, SUMOylation at the collapsed fork has another role. SUMOylated RPA, loaded onto previously processed ssDNA overhang, prevents ScRad51 loading before NPC anchorage. Possibly, SUMOylation of RPA subunits may inhibit ScRad51 filament formation by changing the kinetics of the RPA filament disruption, or alternatively by modifying ScRad51's interaction with its loader ScRad52 (Whalen et al., 2020). The exclusion of ScRad51 from stalled forks in the interior of the nucleus is thought to prevent recombination events that might be detrimental at the early stages of fork stalling. At the NPC, ScSlx5/Slx8 STUbL enzyme can ubiquitinate SUMOylated proteins at the fork, leading to their degradation. This in turn could alleviate the inhibition of Rad51 binding and facilitate its access to ssDNA to stimulate HR-mediated fork restart (Whalen et al., 2020).

Thus, SUMOylation drives the relocation of repeats-induced stalled forks towards NPCs to allow a Rad51-dependent pathway of fork restart.

Forks stalled at DNA-bound protein complex

In fission yeast, forks stalled at a site-specific replication fork barrier (RFB) relocate to the nuclear periphery in S-phase and anchor to the NPC (Kramarz et al., 2020). Similar to the above-mentioned budding yeast system, SUMOylation regulates the fate of such arrested forks, and interestingly can have both profitable and deleterious outcomes (Figure 37).

SUMOylation mediated by the SpPli1 SUMO E3 ligase is necessary to safeguard the integrity of dysfunctional forks and to promote their shift towards the nuclear periphery. In contrast to forks collapsed at CAG tracts, monoSUMOylation is not sufficient to trigger relocation, pointing out to the requirement of SUMO chains formation. Subunits of STUbL, SpSlx8 as well as SpRfp1 and SpRfp2 (ScSlx5 orthologues), were also shown to be involved in promoting the shift of arrested forks

to the nuclear periphery. Intriguingly, in a strain mutated for ScSlx8, the active RFB showed increased mobility (a phenomena reflecting a lack of anchorage), while this was not observed in the absence of Pli1. Thus, SUMO chains accumulating at the arrested fork promote chromatin mobility and facilitate their NPC anchorage in a STUbL-dependent manner. However, no specific SUMO targets have been identified yet.

Although the wave of SUMOylation promotes fork integrity and triggers relocation, at the same time SUMO chains were found to limit HR-mediated DNA synthesis. Indeed, in the absence of SUMO chains formation or upon destabilizing the interaction between SUMO particle and the E2 conjugating enzyme, fork restart occurs more efficiently. In this genetic background, the need for relocation and NPC anchorage was suppressed. Therefore, NPCs become critical to allow the resumption of DNA synthesis by clearing off SUMO conjugates from the arrested forks. It is ensured by the action of two factors enriched at the nuclear periphery: the Ulp1 SUMO protease and the proteasome. When SpUlp1 is delocalized from the NPC in the SpNup132 deficient cells or in the absence of a proteasome regulatory subunit Rpn10, arrested forks successfully relocate to the NPC but cannot be efficiently restarted.

Altogether, these data have established an important function of NPCs in the clearance of DNA repair/replication factors which when SUMOylated could hamper the resumption of DNA synthesis at stalled forks.

SUMO-driven relocation of perturbed replication forks is an important protective mechanism to maintain genome stability. The discrepancies in the above-described scenarios likely reflect different mechanisms engaged at various types of stalled forks; however, the basis and overall outcomes of the phenomena are consistent through the studied systems.

V. Experimental system

A: Fission yeast as a powerful model for studying eukaryote biology

Model organisms are simple non-human species, widely used as accessible and convenient systems to study particular aspects of biology. The most used model organisms include: i) unicellular organisms (bacteria, yeast), ii) invertebrate animal models (roundworms, fruit flies), iii) vertebrate animal models (frog, zebrafish, chicken), iv) mammalian model organisms (mice, rats) (Figure 38). All these species share

Figure 38: **Common model organisms used in molecular biology**. (Adapted from www.chegg.com/learn/topic/model-organisms).

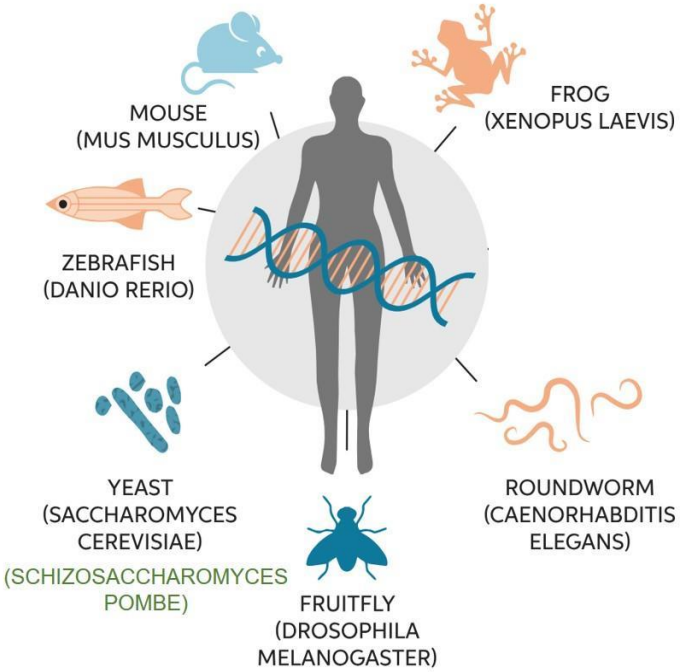

Figure 39: **Cellular morphology of fission yeast.** Transmission electron microscopy (top) and bright field microscopy (bottom) images of fission yeast cells. Comparison of the size and shape of budding and fission yeast cells (bottom right). (www.mpg.de, www.fast.kumamoto-u.ac.jp)

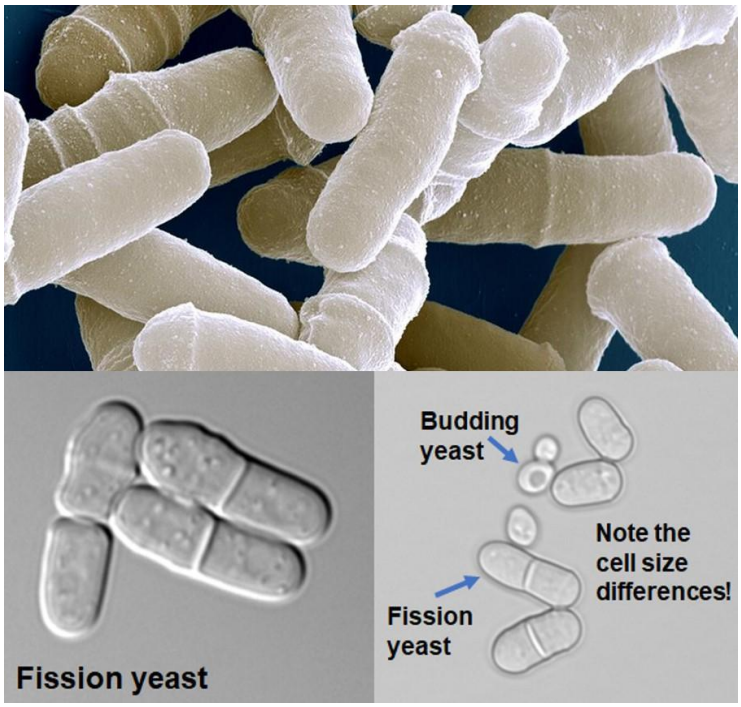

important biological similarities with humans, fuelling the assumption that observations made in model organisms will provide insight into the molecular mechanisms of human cells. Thus, studies in model organisms have the potential to improve our understanding of the molecular aetiology of human diseases and speed their diagnosis and treatment.

In basic research, two yeast species are commonly employed to elucidate the molecular functions of the eukaryotic cell: the budding yeast *Saccharomyces cerevisiae* and the fission yeast *Schizosaccharomyces pombe* (Figure 39). Although they diverged from a common ancestor, they are evolutionarily very distinct from one another as separated by ~ 400 million years (Heckman et al., 2001; Hedges 2002). However, the evolutionary distance between budding and fission yeast is the same as between yeast and mammals. Therefore, both yeast species are as close to humans as they are to each other (Vyas et al., 2021). Moreover, due to its rapid evolution, budding yeast may have lost some genes and functions that fission yeast and metazoans retained from their common ancestor. One example is the RNA interference (RNAi) pathway, the loss of which allows budding yeast to maintain dsRNA killer viruses (Drinnenberg et al., 2011).

Therefore, fission yeast offers unique advantages for investigating the biological processes in complex eukaryotes including humans, making it a valuable "micromammal" model (Aravind et al., 2000; Wood et al., 2002; Forsburg and Rhind , 2006).

Fission yeast was initially isolated from East African beer and described in 1893 by Paul Linder, who named the organism *Schizosaccharomyces pombe*. The term "*shizo*" means split/fission reflecting how these yeast cells divide, whereas "*pombe*" means beer in Swahili language (Lindner, 1893). The research using fission yeast as an experimental laboratory organism began in 1946 when Urs Leupold employed *S. pombe* for genetic analysis of the mating-type system (Leupold, 1950). Around the same time in Edinburg, Murdoch Mitchison used fission yeast to investigate the growth and division processes (Mitchison, 1957; 1990). The two fields of genetics and cell biology came together in the mid-1970s, when Paul Nurse, having first spent time in Leupold's group learning yeast genetics methods, joined Mitchison's lab to investigate how the cell cycle is controlled. Together with his colleagues, Paul Nurse isolated yeast mutants blocked in their cell cycle progression and altered in size and division (Fantes, 1989). Their studies were awarded in 2001 with a Nobel Prize in Physiology or Medicine to Paul Nurse, Leland Hartwell and Tim Hunt, for the discovery of key regulators of the cell cycle.

During the following decades, the fission yeast community expanded worldwide, providing valuable knowledge in the molecular mechanisms of many cellular processes such as DNA replication, DNA repair, and cell cycle (Fantes and Hoffman, 2016). This was largely due to the fact, that in 2002 the complete genome sequence of *S. pombe* was published, making it the sixth eukaryotic species with the entire genome sequenced (Wood et al., 2002). Akin to budding yeast, the fission yeast genome has a size of 13.8 Mb. However, it is divided into three relatively large chromosomes of 5.7 Mb, 4.6 Mb and 3.5 Mb, in contrast to 16 smaller chromosomes in budding yeast. Out of 5 118 protein-encoding genes identified in the fission yeast, 3 539 (69%) have homologs in human cells including 1 244 genes that are related to human disease (pombase.org).

Moreover, chromatin organization in fission yeast has several mammalian-like features that are absent or changed in budding yeast (Wood et al., 2002). These include higher levels of chromosome condensation during mitosis, conserved heterochromatin proteins, large origins of replication and large centromeres comprising repetitive sequences, and highly ordered complexity in telomere organization. Another common feature shared with mammals is the structure of genes. In human cells, most protein-coding genes consist of exons and introns. Similarly, more than 50% of fission yeast genes harbor one or more introns while this value is only 5% for budding yeast. Also, gene splicing and epigenetic silencing mechanisms in fission yeast display high similarity with those in mammalian cells, indicating a functional conservation in gene expression processes (Yvas et al., 2021).

Fission yeast has cylindrical and rod-shaped cells of around 4 µm in width and 8-15 µm in length. The cells grow by tip elongation and divide by medial fission, maintaining the same shape and diameter. The generation time varies with media (rich or minimal media) and temperature (25°C – 36°C) but is generally ranging from 2 to 4 hours for wild-type cells. The fission yeast mitotic (vegetative) cell cycle consists of subsequent G1, S, G2, and M phases (Figure 40) (Mitchison and Nurse, 1985; Forsburg and Rhind, 2006). Predominantly, cells grow during the G2 phase. It is the longest phase as it constitutes about 70% of the cycle time. When the cell reaches a desired size, it enters the mitotic (M)-phase where the nucleus divides into two smaller nuclei. Importantly, the nuclear envelope remains intact throughout nuclear division; hence this process is called closed mitosis (McCully and Robinow, 1971; Ding, 1997). The M-phase is followed by G1 during which a medial septum is generated to cleave the cell at its midpoint (Hoffman et al., 2015). However, the cytokinesis is not completed during the relatively short G1 phase. Instead, it occurs after the DNA replication at the end of the

Figure 40: **Schematic representation of the fission yeast cell cycle.** The circle reflects the duration and relative positions of the different cell cycle phases: G1 (gap phase 1), S (DNA replication), G2 (gap phase 2) and M (mitosis). Sketches outside the circle indicate the morphology of cells at the corresponding phase. Black spots inside the cells represent the nuclei and the numbers indicate the total amount of DNA per cell (e. g. 1C = single complete genome). (Adapted from Knutsen et al., 2011)

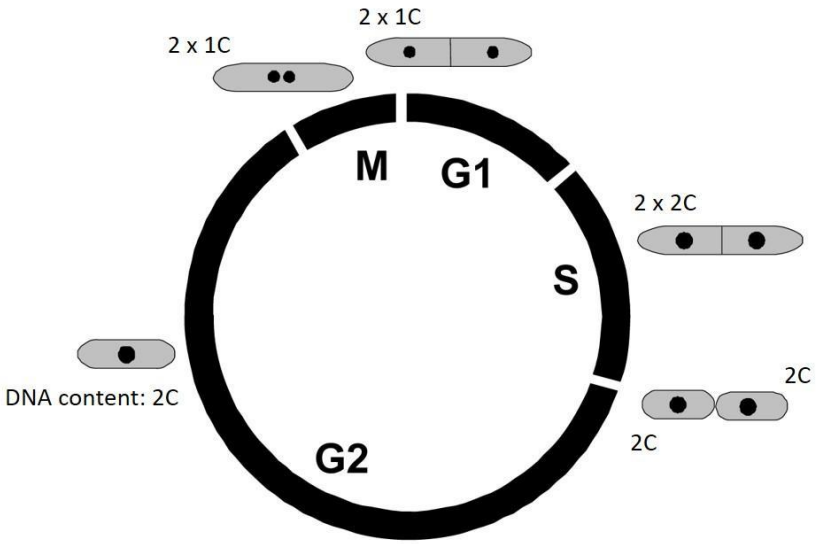

following S phase, leading to the formation of two identical G2 daughter cells. For this reason, cells in G1 (two nuclei, each with a single complete genome: 2x1C) and G2 phase cells (one nucleus with duplicated genome: 1x2C) contain the same amount of total DNA. Therefore, these two phases cannot be distinguished by measuring the cellular DNA content by flow cytometry.

Fission yeast tends to be in the haploid form through the mitotic cycle. However, when nutrients become limited cells can enter either a stationary phase upon glucose starvation, or the meiotic cycle upon nitrogen starvation (Hagan et al., 2016). The latter requires a conjugation between two haploid cells of opposite mating types (h+ and h-). Their fusion results in the formation of a diploid zygote (Forsburg and Rhind, 2006). Then, meiosis is initiated, leading to the formation of four haploid spores, the yeast equivalent of human gametes. When appropriate nutrients are restored, the spores germinate and re-enter the mitotic life cycle to proceed into vegetative growth. However, if the conjugated cells are supplied with nutrients before the meiotic cycle starts (at the diploid zygote stage), they can continue the vegetative growth as diploids (Egel and Mitani, 1974; Hayles and Nurse, 2016).

What makes fission yeast a great model organism? In addition to the above-mentioned similarities shared between fission yeast and mammalian cells, there are a few additional advantages. First, *S. pombe* is a non-pathogenic organism and its cell cycle is relatively short which makes it convenient to handle under standard laboratory conditions. Moreover, the small and easily editable fission yeast genome contributed to the development of versatile experimental approaches for genomics and proteomics analyses. Thus, over the last decades, fission yeast has become a prominent eukaryotic model to decipher the fundamental molecular mechanisms that govern not only cell division or morphology but also DNA replication, repair and recombination.

B: Conditional replication fork barrier in fission yeast

Replication forks can pause at accidental or programmed replication fork barriers (RFBs) during the replication process. In bacteria, RFBs coordinate for example the replication termination by stalling replication forks. The Tus protein binds defined “Ter” sites and inhibits the activity of the replicative helicase (Khatri et al.,1989; Lee et al., 1989; Hill and Marians, 1990). In eukaryotic cells, one of the most-studied RFBs was found in yeast. In budding yeast, programmed barriers within rDNA repeats prevent the collision between the replication and transcription machineries by ensuring a largely unidirectional replication of the rDNA repeats (Brewer et al., 1992; Kobayashi and Horiuchi, 1996; Krings and Bastia, 2005). In fission yeast, a natural replication fork

Figure 41: **Schematic representation of the *RTS1*-RFB construct in fission yeast.** The *RTS1* sequence (in dark blue) has been integrated at the *ura4* locus (red) on chromosome III. Cen3 indicates the position of the centromere. Ori indicates the position of origins of replication. Numbers indicate the distance in kilobases between the replication origins and the RFB. When Rtf1 is expressed, it binds to the *RTS1* sequence and blocks the progression of replication forks migrating from Cen3 towards the telomere. Such arrested forks may be either rescued by the opposite forks or restarted by homologous recombination mechanisms (see text for details).

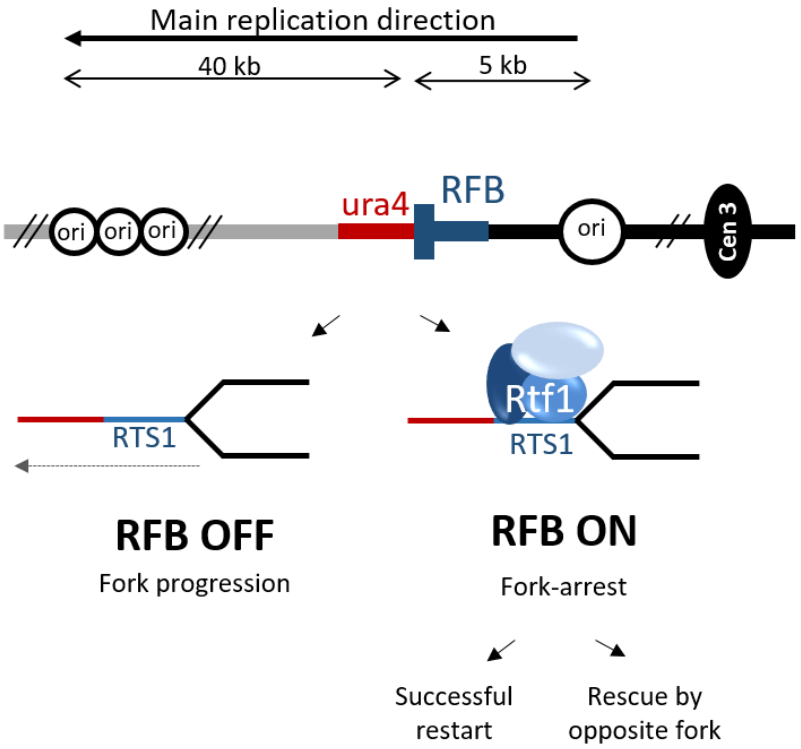

barrier was found at the mating type locus (*mat*) on chromosome II. The located Replication Termination Sequence (*RTS1*) ensures a unidirectional replication of the *mat* locus which is necessary for optimal mating type switching (Dalgaard and Klar, 2001; Codlin and Dalgaard, 2003).

The fork arrest at *RTS1* strictly depends on the binding of a protein complex with the main protein Rtf1 (Replication termination factor 1). In the absence of Rtf1, the *RTS1* sequence is replicated normally, without blocking the progression of replication forks (Dalgaard and Klar, 2001; Eydmann, 2008). *RTS1* is an 859 base pair long sequence, composed of two regions (Codlin and Dalgaard, 2003). The larger region B contains four binding sites of Rtf1 and is thus essential for the barrier activation. Region A is believed to reinforce the blocking activity of region B. Rtf1 binds the *RTS1* sequence and interacts with other proteins of the complex (Swi1 and Swi3), thus constituting a physical constraint for the replication fork. A characteristic feature of the *RTS1* barrier is its ability to block the replicating fork in a polar manner: it only blocks the progression of forks traveling in one direction, whereas the progression of the opposite fork is unaffected by the barrier (Dalgaard and Klar, 2001). The distinction between the "restrictive" and "permissive" replication direction depends on the orientation of the *RTS1* sequence.

This natural fission yeast RFB system has been engineered to serve as a genetic tool to induce site-specific fork stalling and investigate the molecular mechanisms of events occurring at arrested, collapsed and restarted replication forks (Lambert et al., 2005). For this purpose, the *RTS1* sequence has been introduced on chromosome III at the *ura4* locus, whose replication dynamics has been well characterized (Figure 41). Most of the forks replicating this region originate from a strong origin of replication located 5 kilobases upstream of the *ura4* locus and travel from the centromere-proximal side toward the telomere. On the telomere-proximal side of the *ura4* locus, the closest origins are located more than 40 kilobases away and are considered as so-called weak origins. In order to create an inducible system, the endogenous gene encoding Rtf1 was placed under a thiamine-repressible *nmt41* promoter. If thiamine is present in the culture medium, Rtf1 is not expressed and the *RTS1*-RFB remains inactive (a condition referred to as OFF). Inversely, after thiamine removal *nmt41* is no longer repressed and the expressed Rtf1 activates the *RTS1*-RFB (a condition referred to as ON). Rtf1 expression reaches the maximal expression level 16 hours after thiamine removal from the media. In this context, the active *RTS1*-RFB blocks the progression of around 90% of the forks coming from the strong origin on the centromeric-proximal side. Such dysfunctional forks can be either rescued by merging with the converging fork or restarted by homologous recombination. The recombination-dependent

replication restart occurs in 20 min after being initiated by the Exo1-mediated resection and subsequent Rad52 and Rad51 recruitment. Importantly, restarted forks are associated with a semi-conservative but non-canonical DNA synthesis, where both strands are replicated by polymerase delta. Moreover, this non-canonical DNA synthesis is liable to replication errors, including replication slippage on microhomology regions, intra and inter-chromosomal template switches and reversal of DNA replication orientation during replication trough palindromic sequence (U-turn). Finally, restarted forks are insensitive to the *RTS1* barrier (Lambert et al., 2005; 2010; Mizuno et al., 2009; 2013, Iraqui et al., 2012; Tsang et al., 2014; Miyabe et al., 2015; Nguyen et al., 2015; Ait Saada et al., 2017; Teixeira-Silva et al., 2017; Naiman et al., 2021).

Complementary genetic, cellular and molecular assays have been developed in the lab to study the molecular mechanisms and the key players involved in the events occurring at the replication fork blockage at the *RTS1*-RFB locus. These techniques allow to: (1) measure the recombination-mediated fork restart efficiency (proxy-restart genetic assay); (2) analyze replication intermediates generated at the blocked forks (bi-dimensional gel electrophoresis, 2DGE); (3) monitor the recruitment of proteins to the stressed locus in single cells (microscopy combined with a fluorescent reported system) or in a cell population (chromatin immunoprecipitation, ChIP); (4) track *in vivo* the fate and nuclear positioning of the locus (microscopy combined with a fluorescent reported system) (Ait Saada et al., 2017; Teixeira-Silva et al., 2017; Hardy et al., 2019; Kramarz et al., 2020).

OBJECTIVES

Studies across several model organisms demonstrated that different types of stressed replication forks shift to the nuclear periphery and anchor to NPCs in a SUMO-dependent manner. A recent work from our team revealed that, in fission yeast , replication forks blocked by a DNA-bound protein relocate and anchor to NPCs to achieve the resumption of DNA synthesis (Kramarz et al., 2020). This shift towards the nuclear periphery depends on Pli1-dependent SUMOylation and more specifically SUMO chains formation. However, SUMO chains limit the efficiency of replication restart by homologous replication, thereby requiring to be cleared off by the SENP protease Ulp1 and the proteasome, whose activities are enriched at the nuclear periphery. We have previously found that the Y-complex of the NPC is critical to prime the recombination-mediated DNA synthesis resumption in a post-anchoring manner. This function has been linked to the nucleoporin Nup132 role in promoting the localization of Ulp1 at the nuclear periphery. Moreover, we have shown that SUMOylation by Pli1 safeguards fork integrity in the nucleoplasm. However, due to some limitations of our previous work, many aspects of the proposed model remained unexplored. Therefore, by combining different molecular and genetic approaches I have sought to address several fundamental questions that are listed below:

Which sub-complexes of the NPC are involved in facilitating recombination-dependent replication restart?

- Are the components of the nuclear basket, which protrude into the nucleoplasm, also involved in promoting efficient restart of arrested replication forks?
- If so, is the mechanism similar to the function of Y-complex nucleoporins in ensuring SUMO protease Ulp1 localization at the nuclear periphery?

How the NPC ensures the dynamic of the recombination-dependent DNA synthesis at arrested forks?

- What is the role of Ulp1 and the proteasome in promoting the fork restart?
- Can these functions compensate for each other?

What are the features of the SUMOylation wave that occurs at the fork arrest site?

- Does Nse2, the second E3 SUMO ligase in fission yeast, contribute to the formation of the SUMOylation that is required for fork protection and relocation?
- What is the type of SUMOylation that is critical for protecting forks from extensive degradation (monoSUMOylation vs polySUMOylation)?

How does a dynamic repositioning within a compartmentalized nucleus affect the maintenance of replication fork integrity?

- How would an unceasing presence at the nuclear periphery impact the integrity of arrested forks?
- On the contrary, what are the consequences of the lack of anchorage of arrested forks to NPCs?
- How does the interplay between Ulp1 sequestration and nuclear positioning affect the integrity of arrested replication forks?

Globally, during my PhD in how the spatial segregation of SUMO metabolism, together with NPCs, safeguard the integrity of replication fork and their replication competence.

RESULTS

The results obtained during my PhD are presented in four sections as follows:

Section I: Publication #1

When I first joined the team of Sarah Lambert, I collaborated with Karol Kramarz, a former post-doc of the lab. We worked together on a project that was focused to investigate the spatial control of Recombination-Dependent Replication at arrested replication forks in fission yeast. Data obtained during that period allowed us to publish a scientific article entitled "*The nuclear pore primes recombination-dependent DNA synthesis at arrested forks by promoting SUMO removal*", that I signed as second author. Importantly, this work paved the way to my main PhD project, in frame of which I aimed to decipher the unexplored aspects of the model proposed in Publication #1.

Section II: Publication #2

The great part of my PhD project was dedicated to better understand the dynamics aspect of the mechanisms engaged at the nuclear periphery that are involved in restarting the arrested forks by recombination-dependent mechanism. Data in this section are presented in the form of a manuscript entitled "*SUMO protease and proteasome recruitment at the nuclear periphery differently affect replication dynamics at arrested forks*" that I sign as the first co-author and that is ready for submitting.

Section III and IV: **Additional data**

Moreover, during my PhD I sought to characterize the SUMOylation wave that occurs at the fork arrest site. I also addressed the key determinants of replication forks integrity within a compartmentalized nucleus. The two last sections include some unpublished results that require additional experiments to consolidate the already obtained data and to strengthen the conclusions and hypothesis.

I: Publication #1

The nuclear pore primes recombination-dependent DNA synthesis at arrested forks by promoting SUMO removal

nature COMMUNICATIONS

ARTICLE

https://doi.org/10.1038/s41467-020-19516-z OPEN

The nuclear pore primes recombination-dependent DNA synthesis at arrested forks by promoting SUMO removal

Karol Kramarz[1,2,3], Kamila Schirmeisen[1,2,3], Virginie Boucherit[1,2,3], Anissia Ait Saada[1,2,3], Claire Lovo[1,2], Benoit Palancade[4], Catherine Freudenreich[5] & Sarah A. E. Lambert[1,2,3]✉

Nuclear Pore complexes (NPCs) act as docking sites to anchor particular DNA lesions facilitating DNA repair by elusive mechanisms. Using replication fork barriers in fission yeast, we report that relocation of arrested forks to NPCs occurred after Rad51 loading and its enzymatic activity. The E3 SUMO ligase Pli1 acts at arrested forks to safeguard integrity of nascent strands and generates poly-SUMOylation which promote relocation to NPCs but impede the resumption of DNA synthesis by homologous recombination (HR). Anchorage to NPCs allows SUMO removal by the SENP SUMO protease Ulp1 and the proteasome, promoting timely resumption of DNA synthesis. Preventing Pli1-mediated SUMO chains was sufficient to bypass the need for anchorage to NPCs and the inhibitory effect of poly-SUMOylation on HR-mediated DNA synthesis. Our work establishes a novel spatial control of Recombination-Dependent Replication (RDR) at a unique sequence that is distinct from mechanisms engaged at collapsed-forks and breaks within repeated sequences.

[1] Institut Curie, PSL Research University, UMR3348, F-91405 Orsay, France. [2] CNRS UMR3348 "Genome integrity, RNA and Cancer", "Equipe labellisée LIGUE 2020", F-91405 Orsay, France. [3] University Paris Sud, Paris-Saclay University, UMR3348, F-91405 Orsay, France. [4] Université de Paris, CNRS, Institut Jacques Monod, F-75006 Paris, France. [5] Department of Biology, Tufts University, Medford, MA 02155, USA. ✉email: sarah.lambert@curie.fr

Flaws in the DNA replication process, known as replication stress, lead to fragile replication fork structures prone to chromosomal rearrangement and mutation, contributing to human diseases including cancer[1,2]. The resolution of replication stress occurs within a compartmentalized nucleus. How the distinct nuclear compartments operate to ensure faithful resolution of replication stress is far from understood.

The completion of DNA replication is continuously threatened by numerous obstacles. Replication obstacles hinder fork elongation and occasionally cause dysfunctional forks, deprived of their replication competence[3]. Replication-based pathways have evolved to ensure DNA replication completion and avoid genome instability. Dysfunctional forks are either rescued by opposite forks or, if a converging fork is not available in a timely manner, restarted and repaired. Homologous recombination (HR) is a ubiquitous DNA repair pathway involved in the repair of double strand breaks (DSBs), and in the protection and restart of dysfunctional forks[3]. This last pathway is referred to as recombination-dependent replication (RDR), a DSB-free mechanism allowing efficient fork-restart. The pivotal HR protein is the recombinase Rad51 that is loaded onto single-stranded DNA (ssDNA) with the help of its loader Rad52 in yeast. At compromised forks, the combined action of nucleases promotes the resection of newly replicated strands to generate ssDNA gaps and the subsequent loading of Rad51[4]. Then, the strand exchange activity of Rad51 builds a particular DNA structure, called a D-loop, from which DNA synthesis is primed allowing fork-restart[5,6]. A feature of RDR is its mutagenic DNA synthesis prone to chromosomal rearrangements[7–10]. How the subsequent steps of RDR are spatially segregated within the nuclear architecture is unknown.

The nuclear periphery (NP) constitutes a boundary between the nucleus and cytoplasm and is formed of a double membrane nuclear envelope (NE) and multiple nuclear pore complexes (NPCs)[11]. NPCs are highly conserved macromolecular structures, composed of multiple copies of 30 different nucleoporins, most of which associate in stable sub-complexes[12–14]. A central channel (referred to as the core of NPCs) allows macromolecule exchange between the cytoplasm and the nucleus. The largest NPC sub-complex is the Y-shaped mammalian Nup107-Nup160 complex (called Nup84 complex in budding yeast), located both at the cytoplasmic and nuclear side[15].

In budding yeast, DNA lesions (persistent DSBs, eroded telomeres, and collapsed forks) shift to the NP to associate with two distinct perinuclear anchorage sites: either the inner nuclear membrane SUN protein Mps3 or NPCs (extensively reviewed in ref. [16]). DSB-NPC association occurs in all cell cycle phases whereas DSB-Mps3 association is restricted to S/G2 cells. Relocation of DSBs to either Mps3 or the NPC requires distinct signaling mechanisms to promote distinct DNA damage survival pathways[17–24]. The fission yeast homologue of Mps3, Sad1, was shown to co-localize with DSBs, indicating an evolutionarily conserved role of the NE in DSB repair[25].

Anchoring of DNA lesions to NPCs requires SUMOylation events, a type of post-translational modification[17,20,22,23,26]. The SUMO (Small Ubiquitin-like Modifier) particle is covalently bound to lysines of target proteins by the joint action of SUMO-activating (E1) and -conjugating (E2) enzymes, a process enhanced by SUMO E3 ligases[27,28]. Persistent DNA damage and eroded telomeres are subject to SUMOylation waves that target DNA repair factors[29,30]. SUMOylated proteins are key substrates for the SUMO Targeted Ubiquitin Ligase (STUbL) family of E3 ubiquitin ligases such as the yeast Slx8-Slx5 and human RNF4, that target DNA lesions to NPCs[17,20,22,23,26,31–33]. SUMOylated proteins can undergo degradation or direct SUMO removal by SENP proteases, which are spatially segregated within the nucleus[34]. In yeasts, the SENP protease Ulp1 is constitutively attached to NPCs, whereas Ulp2 is found in the nucleoplasm[35,36].

The NPC has emerged as a central player in the maintenance of genome integrity[37,38]. Mutations in the budding yeast Nup84 complex lead to a defective DNA repair and replication stress response[11,17,36,39–41]. The outcome of relocation of damage is often deduced from the phenotypes arising from the ablation of anchorage sites at NPCs. Budding yeast NPCs favor the repair of DSBs by Break Induced Replication (BIR)[20,42]. Eroded telomeres relocate to NPCs in a SUMO-dependent manner to allow recombination-mediated elongation of telomeres, generating type II survivors[23]. A failure in anchoring forks stalled at expanded CAG repeats leads to chromosomal fragility of CAG tracts[22]. Also, delocalization of Ulp1 caused by mutations in the Nup84 complex results in DNA damage sensitivity[36] but how Ulp1-associated NPCs safeguard genome integrity is poorly understood. In eukaryotes, breaks within repeated sequences (Heterochromatin, rDNA) shift away from their chromatin environment, in a SUMO-dependent manner, to allow Rad51 loading and the completion of HR repair[26,43–46]. Thus, an emerging scenario suggests that NPCs are involved in both SUMO homeostasis and anchoring of DNA lesions to spatially segregate DNA repair events and avoid inappropriate HR repair. However, failures in uncoupling SUMO homeostasis from anchorage did not allow interrogating the relative contributions of these two NPC functions in maintaining genome integrity.

Using a site-specific replication fork barrier (RFB), we report that DSB-free and dysfunctional forks relocate and anchor to NPCs, in a poly-SUMO and STUbL-dependent manner, for the time necessary to complete RDR. Relocation occurs after Rad51 binding and enzymatic activity, suggesting that D-loop intermediates anchor to NPCs. We reveal a novel post-anchoring function of NPCs in promoting the removal of SUMO chains by Ulp1 and the proteasome. Indeed, the E3 SUMO ligase Pli1 safeguards fork-integrity and generates SUMO chains that trigger NPC anchorage but further limit the efficiency of HR-mediated DNA synthesis. Selectively preventing Pli1-dependent SUMO chains is sufficient to bypass the need for NPC anchorage in promoting HR-mediated DNA synthesis. We uncovered a novel SUMO-based regulation that spatially segregates the subsequent steps of RDR and that is distinct from mechanisms engaged at DSBs and collapsed forks within repeated sequences.

Results

To investigate the spatial regulation of RDR, we exploited the *RTS1*-RFB that allows a single replisome to be blocked in a polar manner at a defined locus on *S. pombe* chromosome III (Fig. 1a). The RFB activity is mediated by the *RTS1*-bound protein Rtf1 whose expression is repressed in the presence of thiamine[47]. Forks arrested at the RFB become dysfunctional and are rescued by opposite forks or, if not available in a timely manner, restarted; both pathways require the binding of Rad51 to the active RFB[6]. Replication fork restart occurs by RDR within ~20 min and is initiated by an end-resection machinery to generate ssDNA gaps onto which RPA, Rad52, and Rad51 are loaded[4,5,48,49]. RDR is associated with a non-processive DNA synthesis liable to replication slippage and GCRs, during which both strands are synthetized by Polymerase delta, making the progression of restarted forks likely insensitive to the RFB[7,49].

Dysfunctional forks associate with NPCs for ~20 min during S-phase. To follow the sub-nuclear location of the active RFB in living cells, we employed a *LacO*-marked RFB visualized by *LacO*-bound mCherry-LacI foci in yeast expressing the endogenous tagged Npp106-GFP, a component of the inner ring complex of

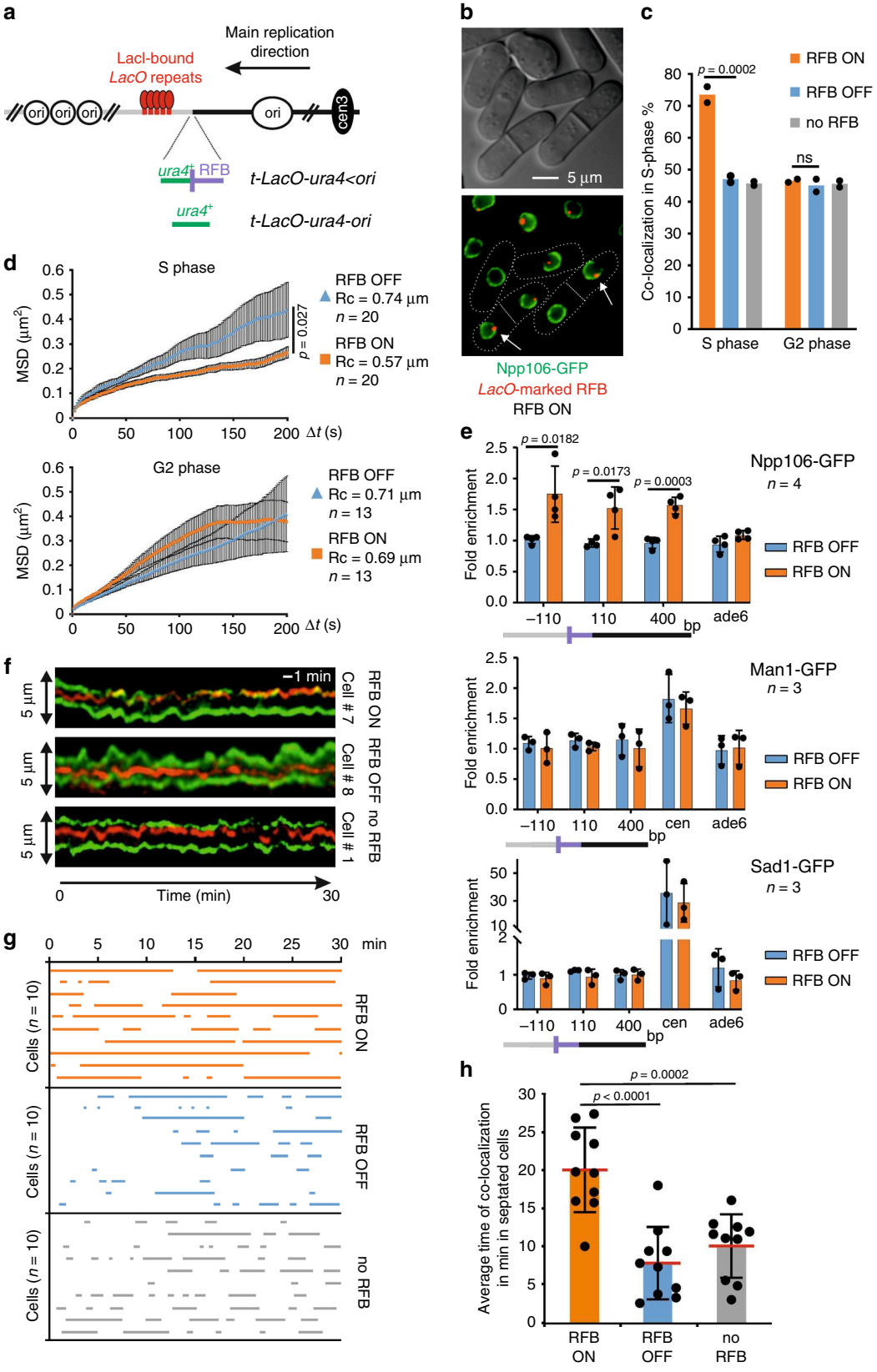

NPCs (Fig. 1a, b)[6]. The shape of the nucleus in S and G2-phase cells was often irregular, preventing us to apply a classical zoning approach[17] to assign the nuclear positioning of the *LacO*-marked RFB. Instead, we monitored co-localization between the NP and the *LacO*-marked RFB (Fig. 1b, c). When the RFB was inactive (RFB OFF) or absent from the *ura4*$^+$ locus (no RFB, Fig. 1a), LacI-foci co-localized with the NP in ~45% of both S and G2-phase cells (Fig. 1c). Upon activation of the RFB (RFB ON), the *LacO*-marked RFB was located more frequently at the NP in S-phase cells, ~70% of the time, but not in G2 cells. Thus, forks

Fig. 1 The active *RTS1*-RFB transiently relocates to NPCs in S-phase. a Scheme of the *LacO*-marked *RTS1*-RFB (purple) integrated at the *ura4*$^+$ locus (green, *t-LacO-ura4 < ori*) or not (*t-LacO-ura4-ori*). Cen3: centromere position. *LacO* arrays (red) bound by mCherry-LacI (ellipses) are integrated ~7 kb away from *ura4*$^+$. When Rtf1 is expressed (RFB ON, 24 h induction for cell imaging experiments) and binds to *RTS1*, 90% of forks moving from *cen3* to *t* are blocked. **b** Example of co-localization between Npp106-GFP and the *LacO*-marked RFB. Mono-nucleated cells and septated bi-nucleated cells correspond to G2 and S-phase cells, respectively. Arrows indicate co-localization events. **c** Quantification of co-localization events in indicated conditions: *t-LacO-ura4-ori*, Rtf1 expressed (no RFB), *t-LacO-ura4 < ori*, Rtf1 repressed (RFB OFF) and *t-LacO-ura4 < ori*, Rtf1 expressed (RFB ON). $n = 250$ cells in both S and G2 phase. Two-sided Fisher's exact test was used for group comparison to determine the *p* value (ns non-significant). Dots represent values from two independent biological experiments. **d** The mobility of the RFB in OFF and ON conditions is presented as a mean square displacement (MSD) over the indicated time interval (Δt) for n independent cells. R_c radius of constraint. *p* value was calculated as a one sided *t*-test based on MSD curves. Black bars correspond to standard error of the mean (SEM). **e** Binding of the RFB to Npp106-GFP (top), Man1-GFP (middle) and Sad1-GFP (bottom) analyzed by ChIP-qPCR. Distances from the RFB are presented in bp. A centromere locus, known to interact with Man1 and Sad1 was used as a positive control. Primers targeting *ade6* gene were used as unrelated control locus. Values are mean of n independent biological repeats, with standard deviation (SD) as error bars. *p* value was calculated using two-sided *t*-test. **f** Representative kymographs over 30 min of single S phase nucleus in indicated conditions. Green and red signals correspond to the Npp106-GFP marked nuclear periphery and the *LacO*-marked RFB, respectively. **g** Co-localization time from the analysis of kymographs in indicated conditions. Each line corresponds to an individual S-phase nucleus. Ten cells per conditions were analyzed. **h** Average co-localization time obtained from **f**. Each dot represents one sample, red bar indicate the mean from 10 independent S-phase cells ± SD. *p* value was calculated using two-sided *t*-test.

arrested by a DNA-bound protein complex transiently relocate to the NP in S-phase cells.

To examine if the dynamics of the active RFB changes with NP enrichment, we monitored the mobility of the GFP-LacI focus by single-particle tracking (SPT) in living cells (Supplementary Fig. 1a) and calculated the range of nuclear volume explored by the *LacO*-marked RFB by mean square displacement (MSD) analysis (Fig. 1d) as reported for other types of damage[50]. Upon RFB activation, the overall mobility of the *LacO*-marked RFB decreased, exclusively in S-phase cells, compared to the RFB OFF control. The radius of constraint (Rc, radius of maximum volume of particle movement) in the OFF condition was significantly higher than the one obtained in the ON condition in S phase cells ($p < 0.05$) while no significant difference was detected in G2 cells, indicating that dysfunctional forks exhibit a reduced mobility in S-phase, consistent with an anchorage to a perinuclear structure. To identify the anchorage site, we performed Chromatin Immunoprecipitation (ChIP) experiments against Npp106-GFP, Sad1-GFP (the Mps3 orthologue) and Man1-GFP (a Lap-Emerin-Man domain protein of the inner nuclear envelope) to test their binding to the RFB. Man1 and Sad1 were found enriched at centromeres, as reported[51,52], but not at the active RFB (Fig. 1e). Npp106-GFP was significantly enriched at the active RFB, indicating that NPCs are acting as anchorage sites as reported for extended CAG repeats[22]. In these experiments, we used strains devoid of the nearby *LacO* array to ensure the binding of NP components to the active RFB is not a consequence of proximal *LacO* arrays that may influence sub-nuclear positioning.

To investigate the dynamics of the association of the RFB with the NP in single cell, we performed time-lapse microscopy for 30 min to build up kymographs over time (See "Methods" and Supplementary Fig. 1a). The analysis of 10 individual S-phase nuclei showed short and intermittent co-localizations between the NP and the unstressed locus (RFB OFF and no RFB controls), indicating transient and dynamic interactions (Fig. 1f, g and Supplementary Fig. 1b–d). The average time of co-localization was ~10 min (Fig. 1h). Consistent with an anchorage to NPCs, the active RFB co-localized with the NP in a less sporadic manner, with interactions lasting for most of the acquisition time in the majority of S-phase cells analyzed. The average time of co-localization was ~20 min (Fig. 1h), and correlated with the time needed to restart replication forks[48,49]. We conclude that dysfunctional forks transiently anchor to NPCs in S-phase, for a time that coincides with the time needed to complete RDR.

Relocation to NPCs requires Rad51 loading and enzymatic activity. Collapsed forks but not stalled forks associate to NPCs[17,22]. Because the exact nature of DNA structures underlying collapsed versus stalled forks remains debated, we addressed the role of fork processing in anchoring the RFB to NPCs. The resection of nascent strands at arrested forks primes RDR. It occurs as a two-step process: a short-range resection by MRN-Ctp1 that generates ~110 bp sized gaps obligatory for replication restart followed by an Exo1-mediated long-range resection[5]. One role of MRN-Ctp1 is to remove the heterodimer KU from dysfunctional forks to overcome its anti-resection activity. Consequently, the lack of KU results in extensive fork-resection. We observed a lack of correlation between the extent of fork-resection and the capacity of the active RFB to shift to the NP and bind to NPCs (Fig. 2a, b, see Supplementary Fig. 2 for location in G2-phase). Instead, we noticed that RFB relocation was abrogated in mutants exhibiting a delay in replication restart (*i.e. rad50Δ*, *ctp1Δ* and *pku70*[5]) raising the possibility that replication/recombination intermediates formed during RDR trigger relocation to NPCs. Consistent with this, Rad51 and Rad52 were necessary to shift the active RFB to the NP (Fig. 2c and Supplementary Fig. 2). Rad51 promotes replication restart at arrested forks and protects them from uncontrolled end-resection to facilitate merging with opposite forks. To distinguish between these two Rad51 functions, we analyzed the *rad51-II3A* mutant that binds DNA to protect forks but is unable to facilitate restart because of its defective strand exchange activity[6]. The active RFB did not shift to the NP nor bind to NPCs in *rad51-II3A* cells (Fig. 2b, c and Supplementary Fig. 2), reinforcing the notion that relocation occurs after fork remodeling by Rad51 enzymatic activity. Since MRN-Ctp1 is active in *rad51-II3A* cells, we propose that short-range resection mediated by MRN-Ctp1 is necessary but not sufficient to shift arrested forks to NPCs and that building Rad51-mediated joint-molecules at arrested forks is necessary for stable association with NPCs.

RDR and anchorage, but not fork-integrity, are impaired by the loss of the Slx5-Slx8 STUbL pathway. Depending on the nature of DNA lesions, the *S. pombe* Slx8 STUbL either suppresses or promotes genome instability[53]. Also, Slx8 prevents uncontrolled HR at the constitutive *RTS1*-RFB[54]. Thus, it was worthwhile to address the role of SUMO and Slx8 activity in the spatial regulation of RDR. SUMO (encoded by the non-essential *S. pombe* gene *pmt3*$^+$) was necessary to shift the active RFB to the NP in S-phase (Fig. 3a and Supplementary Fig. 3a). In the temperature-sensitive *slx8-29* mutated strain[55], the active RFB did not shift to the NP at 32 °C (Fig. 3a and Supplementary Fig. 3a) and MSD analysis showed an

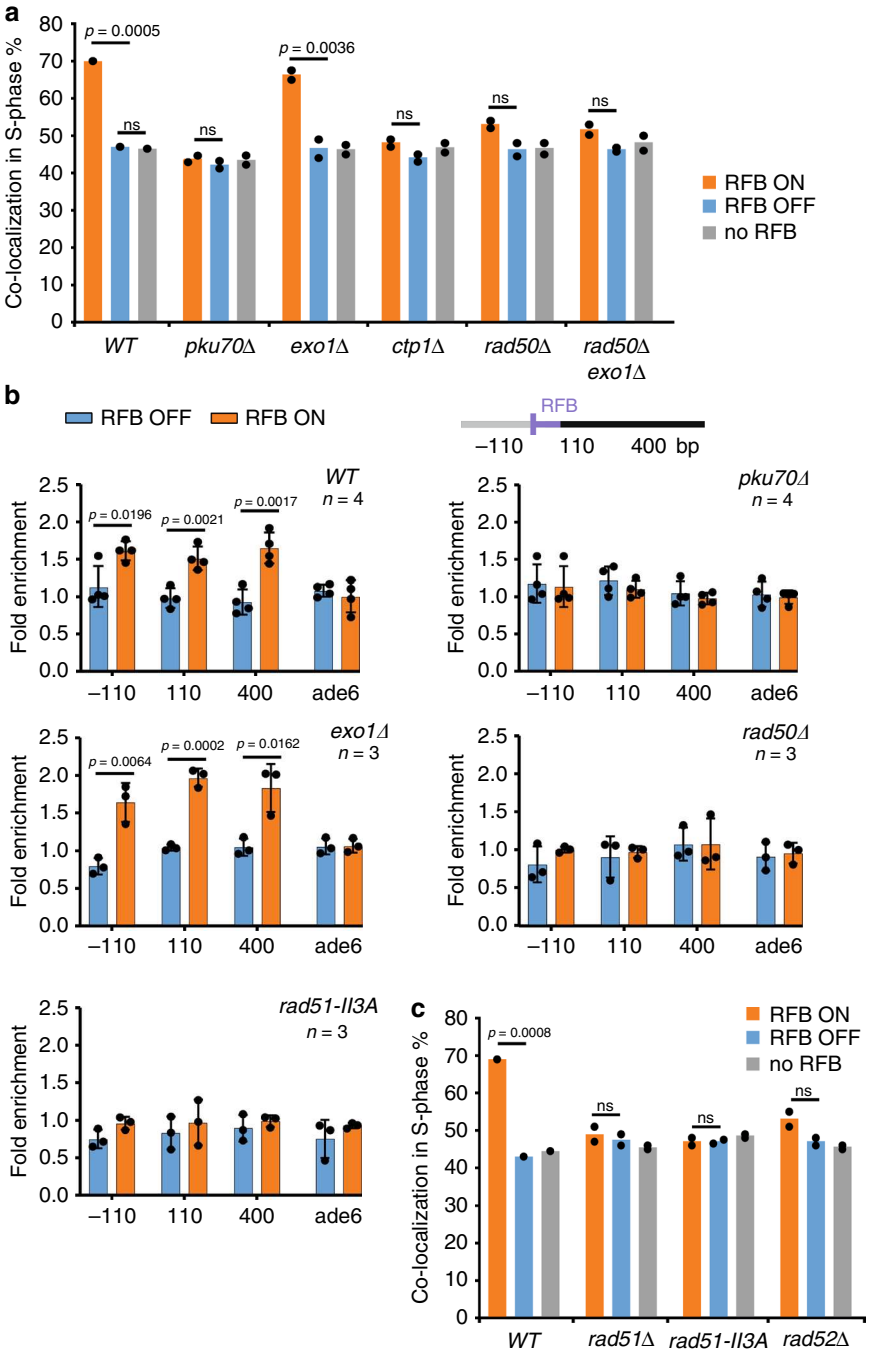

Fig. 2 Relocation to NPCs requires Rad51 enzymatic activity. a Co-localization events in S-phase cells in indicated conditions and strains, as described on Fig. 1b, c. *p* value was calculated by Fisher's exact test for OFF and ON groups for each mutant and condition. In all, 200 cells were analyzed for each strain and condition. Dots represent values obtained from two independent biological experiments. For each set of data, *WT* strain was analyzed alongside mutants. **b** Binding of Npp106-GFP to the RFB in indicated strains. Upstream and downstream distances from the RFB are presented in bp (top). Primers targeting *ade6* gene were used as unrelated control locus. Values are mean of n independent biological repeats, with SD as error bars. *p* value was calculated using two-sided *t*-test. **c** Co-localization events in S-phase cells in indicated conditions and strains, as in **a**.

increased mobility of the active RFB (Fig. 3b), indicating a lack of anchorage to NPCs when Slx8 is not functional. At permissive temperature (25 °C), the *slx8-29* mutated strain behaved as *WT* control (Figs. 3b and 1d). Rfp1 and Rfp2 are two orthologues of Slx5 and they form two independent heterodimers with Slx8[31]. The active RFB did not shift to the NP in the absence of either Rfp1 or Rfp2 (Fig. 3a and Supplementary Fig. 3a), reinforcing the notion that the Slx8 STUbL anchors arrested forks to NPCs.

To address the consequences of this lack of relocation, we investigated the efficiency of RDR. HR-mediated fork restart is associated with a non-processive DNA synthesis liable to replication slippage (RS). We developed genetic assays to monitor RFB-induced RS, based on the restoration of a functional *ura4*$^+$ gene to select for Ura$^+$ cells (Fig. 3c and details in the legend)[7]. The frequency of Ura$^+$ reversion is used as readout of the frequency at which the *ura4-sd20* allele is replicated by a restarted fork in the cell population. At 32 °C, the frequency of

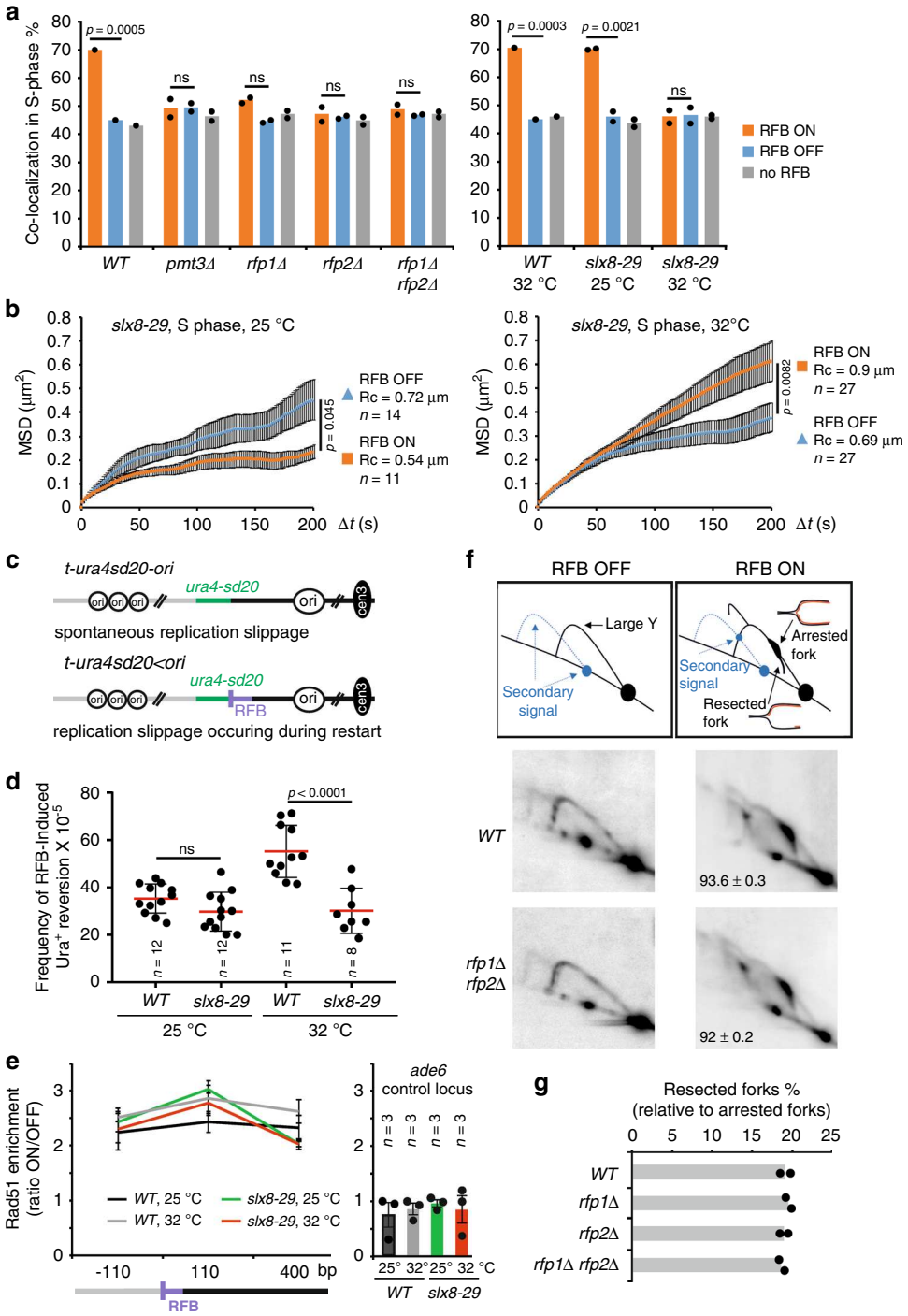

RFB-induced RS in *slx8-29* cells was decreased by nearly 50%, compared to *WT* (Fig. 3d) indicating that Slx8 promotes RDR. This defect was not caused by a less efficient Rad51 binding to the active RFB (Fig. 3e). Finally, we investigated the integrity of fork arrested by the RFB. We analyzed replication intermediates by bi-dimensional gel electrophoresis (2DGE) to examine the resection of nascent strands at arrested forks (referred to as resected forks, Fig. 3f)[5]. The lack of a functional Slx8 pathway (in *slx8-29*, *rfp1Δ*, *rfp2Δ* or double mutants) did not impede or enhance the level of resected forks (Fig. 3f, g and Supplementary Fig. 3b, c). Hence, the lack of Slx8-mediated anchorage to NPCs impedes HR-mediated DNA synthesis downstream of fork-resection and Rad51 loading, suggesting that the processing of SUMO conjugates is necessary to complete RDR.

Nup132 promotes HR-dependent DNA synthesis in a post-anchoring manner. To elucidate the mechanisms engaged at NPCs, we focused on the two fission yeast orthologues of Nup133, a component of the Y-shaped Nup107-Nup160 complex: Nup132 that is the most abundant (~3000 molecules/cell), and localized at the nuclear side of NPCs, whereas Nup131 is less expressed (~200 molecules/cell) and is localized at the cytoplasmic side[56]. Interestingly, *nup132Δ* cells, but not *nup131Δ* cells, were sensitive to a broad range of replication-blocking agents, including hydroxyurea (HU), but not to DSBs induced by bleomycin or to UV-induced DNA damage (Fig. 4a). A major function of NPCs being the transport of macromolecules, we further analyzed protein import and mRNA export in these mutants. Neither the absence of Nup131 nor Nup132 affected

Fig. 3 Slx8 STUbL is necessary for anchoring to NPCs and RDR but not for safeguarding fork-integrity. a Co-localization events in S-phase cells in indicated conditions and strains, as described on Fig. 2a. *p* value was calculated by Fisher's exact test. **b** MSD of the RFB in OFF and ON conditions in n S phase cells of *slx8-29* mutant grown at permissive (25°C, left panel) and restrictive (32 °C, right panel) temperature over indicated time interval (Δt). *p* value was calculated as a one sided *t*-test based on MSD curves. Black bars correspond to SEM. **c** Diagram of constructs containing the reporter gene *ura4-sd20* (green) associated (*t-ura4sd20* < *ori*) or not (*t-ura4sd20-ori*) to the RFB. The non-functional *ura4-sd20* allele, containing a 20-nt duplication flanked by micro-homology, is located downstream of the RFB. Upon activation of the RFB, a restarted fork can replicate the *ura4-sd20* and the HR-mediated non-processive DNA synthesis favors the deletion of the duplication, resulting in a functional *ura4*$^+$ gene, generating Ura$^+$ cells. As control, the construct devoid of RFB is used to monitor the spontaneous frequency of RS that is then subtracted to obtain the frequency of RFB-induced RS. **d** Frequency of RFB-induced Ura$^+$ reversion in indicated strains and conditions. Each dot represents one sample from n independent biological replicate. Bars indicate mean values ± SD. *p* value was calculated by two-sided *t*-test. **e** Binding of Rad51 to the RFB in *WT* and *slx8-29* strains at indicated temperature. ChIP-qPCR results are presented as RFB ON/OFF ratio for each mutant. Distances from the RFB are presented in bp. Values are mean from three independent biological replicates ± SEM. **f** Top panel: Scheme of replication intermediates (RI) analyzed by neutral-neutral 2DGE of the *AseI* restriction fragment in RFB OFF and ON conditions. Partial restriction digestion caused by psoralen-crosslinks results in a secondary arc indicated on scheme by blue dashed lines. Bottom panels: Representative RI analysis in indicated strains and conditions. The *ura4* gene was used as probe. Numbers indicate the percentage of forks blocked by the RFB ± SD. **g** Quantification of resected forks. Values are mean of two independent biological repeats.

nuclear shape and protein import, but *nup132Δ* cells exhibited a very mild defect in mRNA export (Supplementary Fig. 4) albeit moderate when compared to the strong defect reported upon heat shock[57].

We tested the role of Nup132 in the recovery from HU-stalled forks. Strains were blocked in early S-phase by exposing exponentially growing cells to HU for 4 hours and then released into HU-free media. Flow cytometry analysis indicated that the *WT* and *nup131Δ* strains reached a G2 DNA content within 45 min after release whereas *nup132Δ* and *nup131Δ nup132Δ* cells exhibited an additional 15 min delay (Supplementary Fig. 5a, left panel). Chromosome analysis by Pulse Field Gel Electrophoresis (PFGE) showed that HU treatment prevented chromosomes from migrating into the gel because of the accumulation of replication intermediates (Supplementary Fig. 5b). Sixty minutes after release, *WT* chromosomes were able to migrate into the gel and their intensity doubled 90 minutes after release, indicating that the *WT* genome was fully duplicated and replication intermediates were resolved (Supplementary Fig. 5b, c). In contrast, chromosomes from *nup132Δ* cells showed a clear delay in their ability to migrate fully into the gel. Even 90 minutes after release, chromosomes intensity did not double, indicating that *nup132Δ* genome failed to be fully duplicated because of an accumulation of unresolved replication intermediates. Our data reveal a critical role for Nup132 in promoting DNA replication upon transient fork stalling.

We asked if Nup132 and Nup131 are involved in RDR. We detected a reduced frequency of RFB-induced RS only in the absence of Nup132 and no further reduction was observed in the double *nup131Δ nup132Δ* mutant (Fig. 4b). This defect was not correlated with a less efficient Rad51 binding to the active RFB (Fig. 4c), indicating that the early step of RDR, fork-resection and Rad51 loading, are functional. The active RFB was enriched at the NP in S-phase cells in the absence of either Nup131 or Nup132, but not in the absence of both nucleoporins (Fig. 4d and Supplementary Fig. 2). Supporting this result, the active RFB bound properly to NPCs in *nup132Δ* cells but not in the double *nup131Δ nup132Δ* mutant by ChIP (Fig. 4e). Thus, Nup132 is dispensable to anchor remodeled forks to NPCs. However, the absence of both nucleoporins may modify the NPC structure, making it inefficient for anchoring. These data reveal a novel function for NPCs in which Nup132 promotes HR-dependent DNA synthesis, downstream of Rad51 binding, in a post-anchoring manner.

HR-dependent DNA synthesis is non-processive, liable to mutation, and GCR. We monitored the rate of RFB-induced mutagenesis and GCR, including translocation and genome deletion (Supplementary Fig. 6a, b for detailed explanations)[7]. Briefly, we selected *ura4* loss events after RFB induction or not and analyzed the events by PCR to discriminate between mutation, translocation, and genomic deletion; all these events occur in an HR-dependent manner. In *WT* cells, the induction of the RFB resulted in a 4.5, 10, and 14-fold increase in the rate of mutagenesis, deletion, and translocation, respectively (Supplementary Fig. 6c, d). The rate of translocation and genomic deletion were unaffected in the absence of Nup131 and Nup132, but RFB-induced mutagenesis was abolished in *nup131Δ* and *nup132Δ* single mutants or in the double mutant, indicating a role of both nucleoporins in promoting mutagenic HR-mediated DNA synthesis. Altogether, our data reveal a novel NPC function, via Nup132 and to a lesser extent Nup131, in promoting HR-dependent DNA synthesis. The distinct contribution of Nup131 and Nup132 to this pathway might reflect their different localization within NPCs and/or their relative abundance[56].

Pli1-dependent SUMO chains are toxic to HR-dependent DNA synthesis. Our data indicate that anchoring to NPCs is not sufficient to promote RDR, as exemplified in the *nup132Δ* mutant. In the absence of Nup132, the SUMO deconjugating enzyme Ulp1 is delocalized from NPCs and can no longer antagonize the PIAS family E3 ligase Pli1 that promotes 90% of bulk SUMOylation and SUMO chain formation. As a consequence, both Ulp1 and Pli1 expression are lowered, resulting in a low global SUMOylation level[35]. Surprisingly, the deletion of *pli1* partly rescued the sensitivity of *nup132Δ* cells to replication stress (Fig. 5a), suggesting a toxicity of Pli1 activity in the absence of Nup132. We asked if this toxicity might also underlie the RDR defect. The active RFB did not shift to the NP nor bound to NPCs in the absence of Pli1 (Fig. 5b, c and Supplementary Fig. 2). MSD analysis confirmed an absence of reduced mobility of the active RFB and thus a lack of anchorage in *pli1Δ* cells (Fig. 5d). However, the lack of Pli1 did not affect RFB-induced RS (Fig. 5e), indicating that RDR is fully completed without anchorage to NPCs when Pli1 is absent. Interestingly, the lack of Pli1 partly rescued the defect in RFB-induced RS of *nup132Δ* cells (Fig. 5e), even though the active RFB was still unable to bind NPCs (Fig. 5b, c). A similar rescue was observed in *slx8-29 pli1Δ* cells (Fig. 5e), consistent with Pli1 causing genome instability in the absence of STUbL activity[54,55]. Of note, the deletion of *pli1* did not rescue the mRNA export defect of *nup132Δ* cells, showing that the role of Nup132 in promoting RDR and mRNA export are uncoupled (Supplementary Fig. 4d, e). Thus, Pli1 activity is necessary to anchor arrested forks to NPCs but is toxic to HR-dependent DNA synthesis, in the absence of Nup132 and STUbL activity, suggesting a role for NPCs in counteracting this toxicity.

To gauge the type of SUMOylation involved in relocation but becoming toxic to HR-mediated DNA synthesis, we manipulated the level and type of SUMO conjugates by several means. We employed a "Low SUMO" strain in which the endogenous SUMO

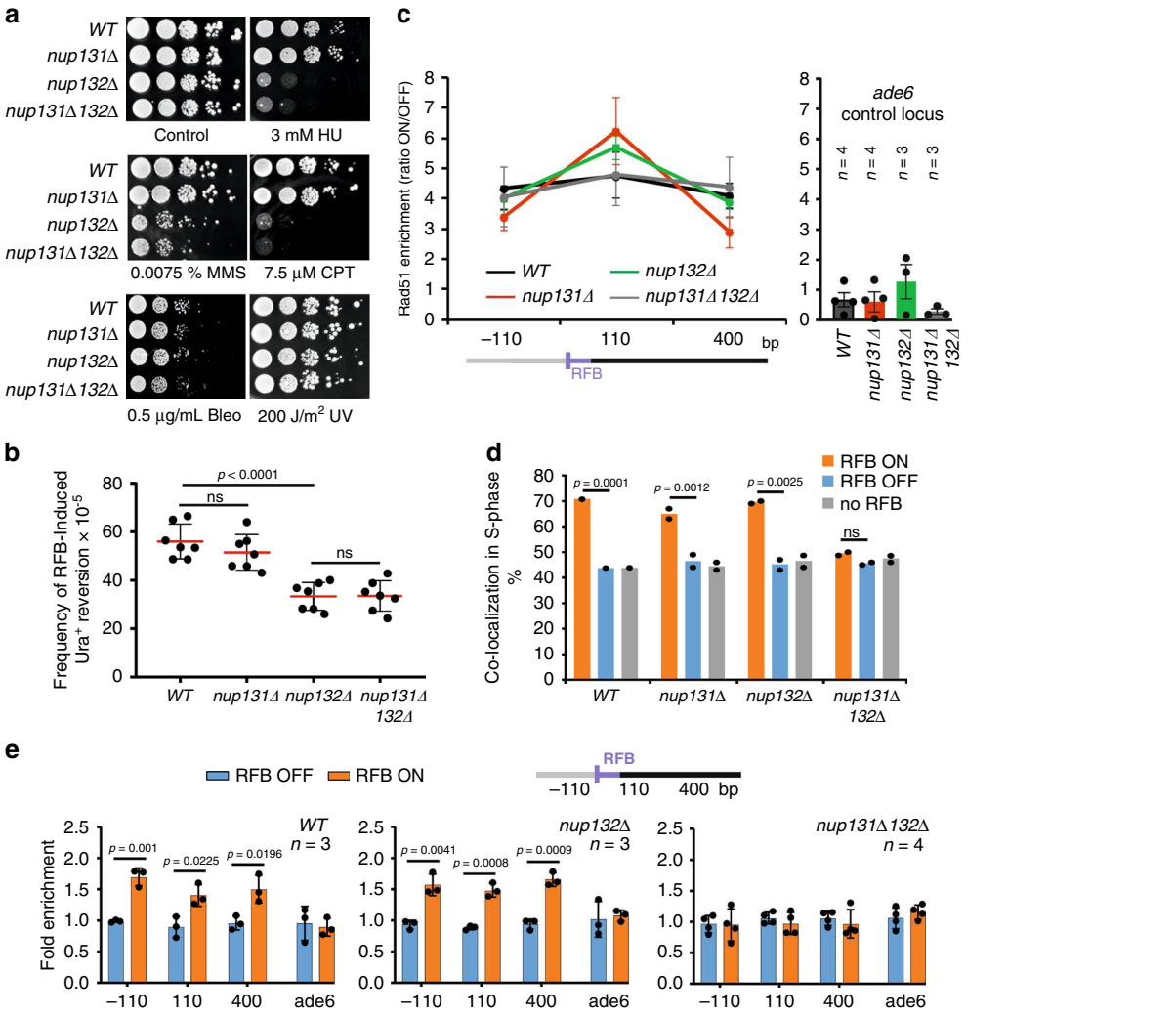

Fig. 4 Nup132 promotes HR-mediated DNA synthesis, downstream of Rad51 binding, in a post-anchoring manner. a Sensitivity of indicated strains to indicated genotoxic drugs. Ten-fold serial dilution of exponential cultures were dropped on appropriate plates. Bleo bleomycin; CPT camptothecin; HU hydroxyurea; MMS methyl methane sulfonate and UV: Ultra Violet-C. See supplementary Fig. 4 for the characterization of macromolecules transport and supplementary Fig. 5 for replication defect upon HU-fork stalling. **b** Frequency of RFB-induced Ura$^+$ reversion in indicated strains and conditions. Each dot represents one sample from seven independent biological replicate for each strain. Bars indicate mean values ± SD. *p* value was calculated by two-sided *t*-test. **c** Binding of Rad51 to the RFB in indicated strains as described on Fig. 3e. Values are mean from n independent biological replicates ± SEM. **d** Co-localization event in S-phase cells in indicated conditions and strains. In all, 250 cells were analyzed for each condition and strain. *p* value was calculated by Fisher's exact test for OFF and ON groups for each mutant and condition. Dots represent values obtained from two independent biological experiments. For each set of data, *WT* strain was analyzed alongside mutants. **e** Binding of Npp106-GFP to the RFB in indicated strains. Upstream and downstream distances from the RFB are presented in bp. Primers targeting *ade6* gene were used as unrelated control locus. Values are mean of n independent biological repeats ± SD. *p* value was calculated using two-sided *t*-test.

promoter was replaced by a weaker constitutive promoter[53] and a *pmt3-KallR* mutant (SUMO-*KallR*) in which all internal Lys are mutated to Arg to prevent poly-SUMOylation[55]. Pli1-dependent SUMO chain formation is enhanced by the interaction between the single E2 SUMO conjugating enzyme Ubc9 and SUMO. Thus, we took advantage of the *pmt3-D81R* mutant (SUMO-D81R) that impairs Ubc9-SUMO interaction and allows mono and di-SUMOylation to occur in a Pli1-dependent manner but impairs the chain-propagating role of Pli1 that is toxic in the absence of STUbL[55]. In all conditions, the active RFB did not shift to the NP and RFB-induced RS was slightly increased (Fig. 5f, g), indicating that poly-SUMOylation is instrumental in relocating the RFB but impedes HR-dependent DNA synthesis. Moreover, all conditions restored RFB-induced RS in *nup132Δ* cells, indicating SUMO chains are the source of toxicity to RDR (Fig. 5g). Hence, relocation requires Pli1-dependent SUMO chain formation which then limits HR-mediated DNA synthesis, generating a need to overcome this inhibitory effect by events occurring at NPCs. In addition, limiting the SUMO chain-propagating role of Pli1 is sufficient to bypass the necessity for relocation to NPCs to ensure efficient RDR.

Relocation to NPCs allows SUMO chains removal by Ulp1 and the proteasome. Relocation to NPCs is necessary to overcome the inhibitory effect of SUMO chains when priming HR-mediated DNA synthesis. STUbLs promote the ubiquitylation of SUMO conjugates for proteolysis by the proteasome, whose activity is enriched at the NP[33]. We focused on Rpn10, a regulatory subunit of the proteasome, whose absence results in defective degradation of ubiquitinated proteins[58]. In *rpn10Δ* cells, the active RFB shifted to the NP but the frequency of RFB-induced RS was severally

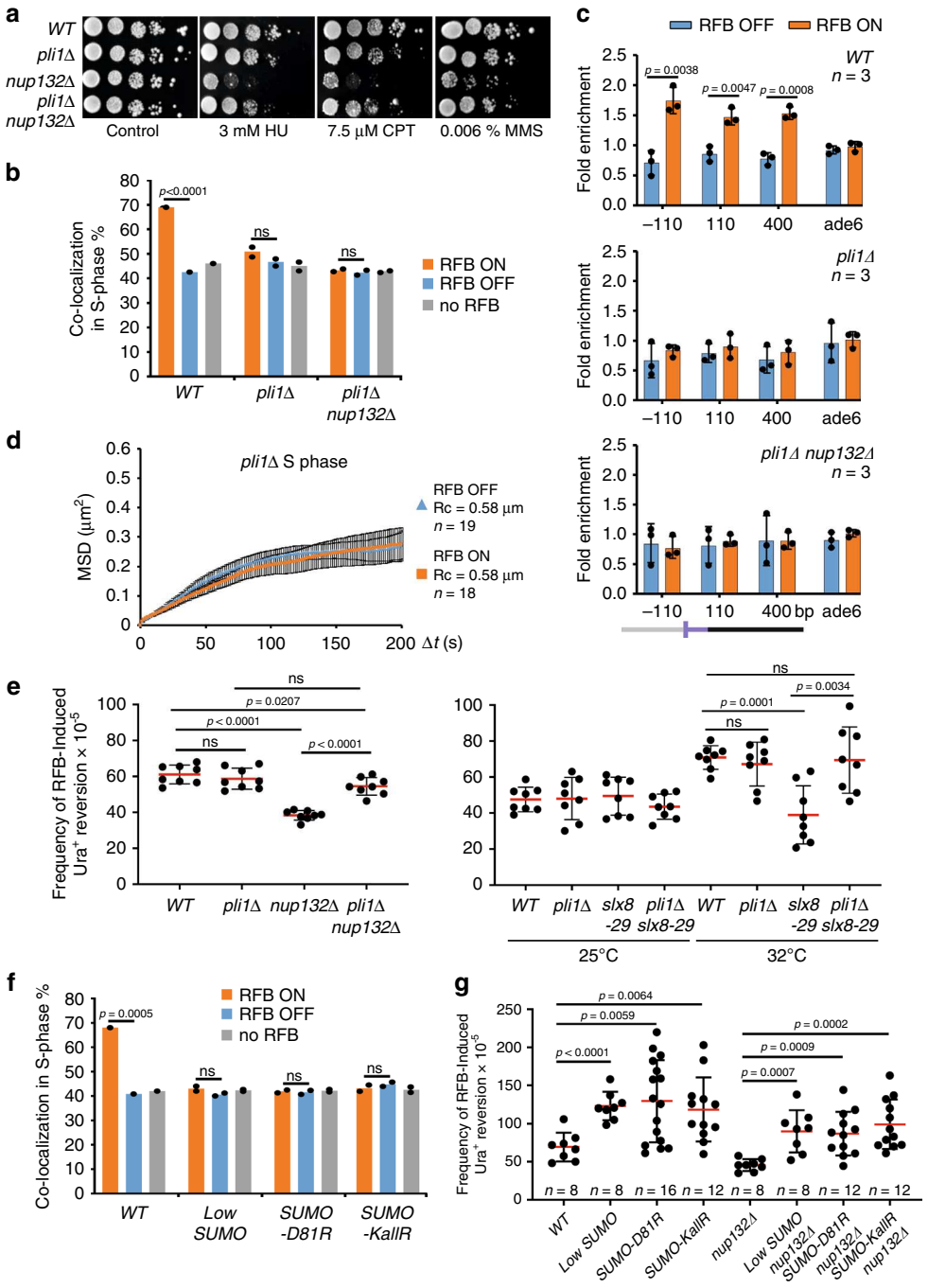

Fig. 5 Pli1-dependent SUMO chain promotes relocation to NPCs but are toxic to RDR. a Sensitivity of strains to indicated genotoxic drugs. Ten-fold serial dilution of exponential cultures were dropped on appropriate plates as described in Fig. 4a. **b** Co-localization event in S-phase cells in indicated conditions and strains as on Fig. 2a. *p* value was calculated by Fisher's exact test for OFF and ON groups for each mutant and condition. **c** Binding of Npp106-GFP to the RFB in indicated strains. Upstream and downstream distances from the RFB are presented in bp. Primers targeting *ade6* gene were used as unrelated control locus. Values are mean of three independent biological repeats ± SD. *p* value was calculated using two-sided *t*-test. **d** MSD of the RFB in OFF and ON conditions in S phase cells of *pli1Δ* mutant over indicated time interval (Δt) calculated for *n* independent cells, as described on Fig. 1d. Black bars correspond to SEM. **e** Frequency of RFB-induced Ura$^+$ reversion in indicated strains and conditions. Each dot represents one sample from eight independent biological replicate for each strain. Bars indicate mean values ± SD. *p* value was calculated by two-sided *t*-test. **f** Co-localization event in S-phase cells in indicated conditions and strains as in Fig. 2a. *p* value was calculated by Fisher's exact test for OFF and ON groups for each mutant and condition. **g** Frequency of RFB-induced Ura$^+$ reversion in indicated strains and conditions. Each dot represents one sample from n independent biological replicate for each strain. Bars indicate mean values ± SD. *p* value was calculated by two-sided *t*-test.

decreased and a slight additivity was observed in *nup132Δ rpn10Δ* cells (Fig. 6a, b). Thus, the proteasome activity is necessary for efficient RDR but this might not be under regulation by Nup132.

In the absence of Nup132, Ulp1 is delocalized from NPCs that are no longer able to counteract the toxicity of SUMO chains to promote RDR. Thus, we investigated the role of Ulp1 in RDR. The overexpression of Ulp1 rescued the defective RFB-induced RS of *nup132Δ* cells (Fig. 6b), indicating that low Ulp1 expression is detrimental to efficient RDR. We employed a LexA-based tethering approach to artificially target Ulp1 to the RFB[23] (Fig. 6c). Expression of Ulp1-LexA did not lead to sensitivity to genotoxic agents in striking contrast to *ulp1Δ* cells (Fig. 6d), indicating the fusion protein is functional. Ulp1-LexA was enriched in the vicinity of the RFB only in the presence of 8 LexA binding sites (at the *t-LexBS-ura4sd20 < ori* construct, Fig. 6e). Consistent with the role of Nup132 in anchoring Ulp1 at the NP, the inactive RFB shifted to the NP, in a Nup132 manner. When activated, the RFB shifted to the NP in the absence of Nup132, confirming that Ulp1 is not necessary for anchorage (Fig. 6f). Remarkably, tethering Ulp1-LexA to the active RFB, anchored to NPCs, resulted in an increased frequency of RFB-induced RS in the absence of Nup132, reinforcing the notion that Ulp1-associated NPCs are required to overcome the inhibitory effect of poly-SUMOylation on HR-mediated DNA synthesis (Fig. 6g).

Pli1 safeguards the integrity of nascent strands at arrested forks. A question arising from our work is the positive effect of Pli1 activity at sites of replication stress. Although *pli1Δ* cells were insensitive to replication-blocking agents, they exhibited a clear defect in the recovery from HU-stalled forks and in chromosomes duplication, suggesting an accumulation of unresolved replication intermediates (Supplementary Fig. 5). We thus investigated the integrity of the fork arrested at the RFB by 2DGE and observed an increased level of resected forks in *pli1Δ cells* (Fig. 7a, b). RPA-ChIP confirmed an extensive recruitment of RPA, up to 3 Kb upstream of the RFB, supporting the formation of larger ssDNA gaps in the absence of Pli1 (Fig. 7c). Thus, Pli1 activity is critical to negatively regulate the resection of nascent strands and safeguard fork-integrity.

Discussion

Collapsed forks anchor to NPCs but the mechanisms engaged at NPCs to ensure fork integrity and restart were not understood. Here, we reveal the beneficial and detrimental functions of SUMOylation at replication stress sites. We propose that Pli1 activity engages at arrested forks to control the extent of nascent strand resection. Pli1 generates SUMO chains that signal for a STUbL-dependent anchorage to NPCs, but hinder the priming of HR-mediated DNA synthesis. Hence, NPCs become critical to allow the resumption of DNA synthesis by clearing off SUMO conjugates in a post-anchoring manner, via Ulp1 and proteasome activities. Selectively preventing Pli1-mediated SUMO chains bypasses the need for anchorage to NPCs while maintaining efficient RDR. Thus, SUMO-regulated mechanisms spatially segregate the subsequent steps of RDR from Rad51 loading and activity occurring in the nucleoplasm and the restart of DNA synthesis occurring after anchorage to NPCs (Fig. 7d).

We establish that DSB formation is not a requirement to anchor arrested forks to NPCs. Instead, it requires forks to be remodeled by Rad51 enzymatic activity. Relocation requires nascent strand resection to occur for Rad51 loading, but is not sufficient per se. SUMOylation of HR factors is necessary to anchor expanded CAG tracts to NPCs[59] and therefore their absence at the RFB may impair the wave of SUMOylation necessary for relocation. However, the lack of relocation in the Rad51-II3A mutant indicates that joint-molecules, such as D-loops from which DNA synthesis is primed, are also relevant positioning signals to relocate arrested forks to NPCs. In several eukaryotes, relocation of DSBs to the NP requires end-resection and Rad51, suggesting that Rad51-mediated repair progression stabilizes repair intermediates to facilitate anchorage[59]. Breaks within repeated sequences (heterochromatin in flies, mouse peri-centromere, rDNA in budding yeast) shift away from their compartments to continue HR repair and load Rad51 at mobilized DNA damage sites[26,43,45,60]. Relocation of forks collapsed at expanded CAG repeats requires nuclease activities to engage SUMO-RPA onto ssDNA which prevents Rad51 loading. Anchorage to NPCs then facilitates Rad51 loading[59]. Here, we report a distinct situation when forks arrest within a unique sequence. Relocation requires Rad51 loading and enzymatic activity and the lack of anchorage (in STUbL or nucleoporin mutants) does not affect Rad51 loading, supporting that Rad51 loading and enzymatic activity occur prior to anchorage to NPCs. These distinct situations likely reflect different mechanisms engaged at unique sequence versus repeated sequences, where controlling Rad51 loading is of major importance to avoid potential rearrangements for the latter.

STUbL binds to SUMO modified DNA repair factors via its SIM domains to tether DNA lesions to NPCs[16,59]. Our data are consistent with this and highlight the positive and negative effects of bulk SUMOylation mediated by Pli1. Though the potential mode of Pli1 recruitment to replication stress sites remain to be identified, we show that Pli1 engagement at arrested forks is vital to safeguard fork-integrity. We noticed that the lack of Pli1 did not increase RDR efficiency whereas preventing SUMO chains does, suggesting that Pli1-dependent mono-SUMOylation events remain necessary to RDR. The Ubc9-SUMO interface may help to increase the local concentration of SUMO particles to enhance Pli1-mediated SUMO chains and mediate anchorage to NPCs. In contrast to forks collapsed at CAG tracts[59], relocation requires poly-SUMOylation as reported for persistent DSBs in budding yeast[20]. However, those SUMO chains limit HR-mediated DNA synthesis, possibly the DNA synthesis primed from D-loops, a step necessary to ensure efficient fork restart. A selective defect in Pli1-mediated SUMO chain or preventing poly-SUMOylation bypasses the need for relocation to NPCs and alleviates the toxicity of SUMO conjugates. A remaining question is whether the SUMO-targets responsible for relocation and preventing the priming of HR-mediated DNA synthesis are similar or distinct.

A possible scenario is that SUMO-dependent relocation to NPCs occurs when arrested forks are not rescued in a timely manner by opposite forks: this would lead to safeguarding fork-integrity by Pli1, and thus engaging the relocation process to NPCs. Interestingly, the lack of STUbL resulted in increased mobility of arrested forks, a phenomena not observed in the absence of Pli1, suggesting that SUMOylation promotes chromatin mobility of replication stress sites and STUbL promotes their anchorage to NPCs.

Collectively, this study uncovers how anchorage to NPCs helps to sustain DNA synthesis upon replication stress. The lack of Nup132 provides a unique genetic situation to uncouple the role of NPCs in anchoring arrested forks from their role in promoting DNA synthesis upon stress conditions. We establish that Nup132 is necessary to prime HR-mediated DNA synthesis, downstream of Rad51 binding and activity, in a post-anchoring manner. This function is linked to the role of Nup132 in recruiting Ulp1 at NPCs and is uncoupled from the transport of macromolecules. We propose that Ulp1-associated NPCs, as well as proteasome activity, are critical to remove SUMO conjugates from joint-molecules to allow DNA synthesis resumption. Consistent with

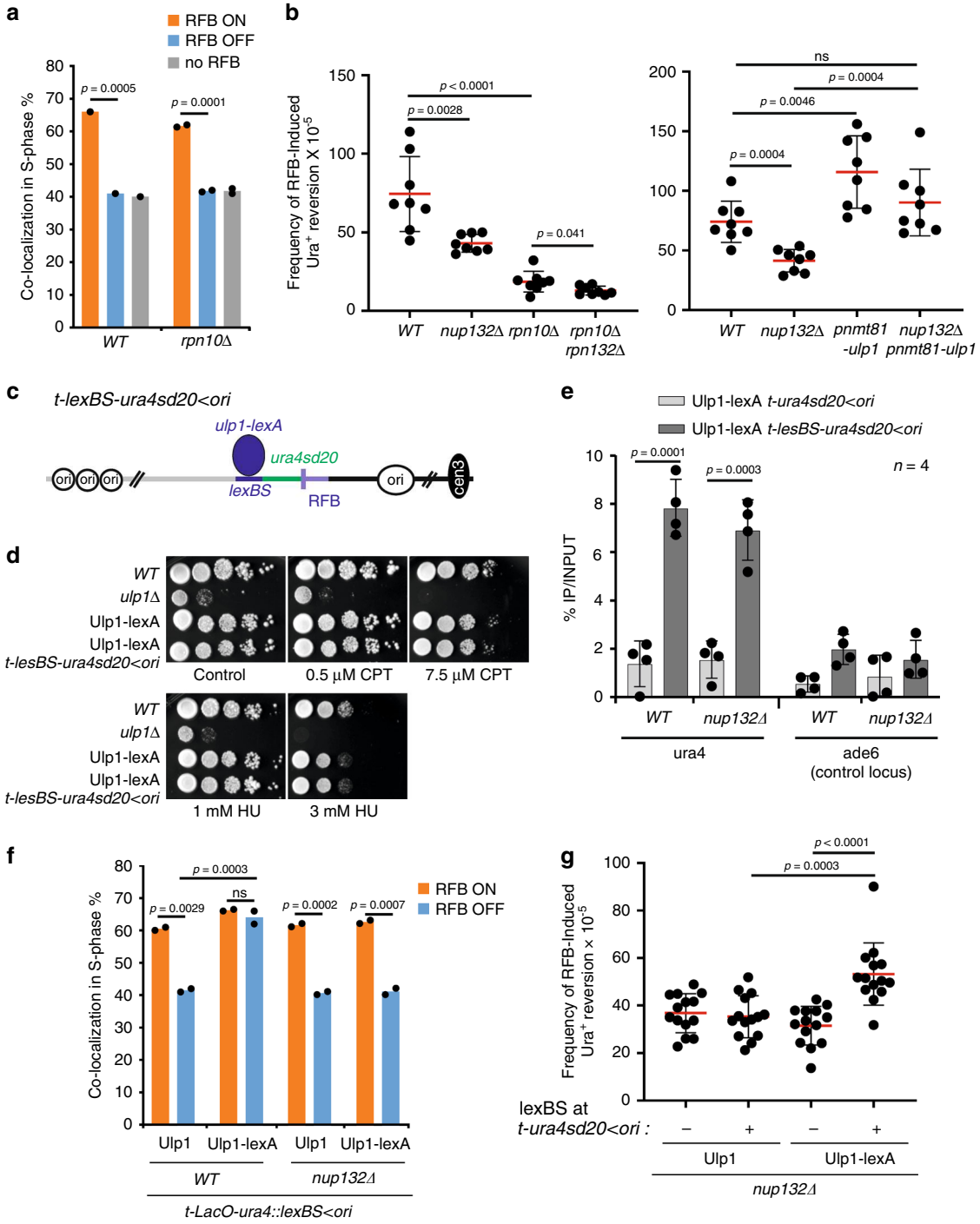

Fig. 6 Proteasome and Ulp1 activity are necessary to clear off SUMO conjugates to promote RDR. a Co-localization event in S-phase cells in indicated conditions and strains as on Fig. 2a. *p* value was calculated by Fisher's exact test for OFF and ON groups for each mutant and condition. **b** Frequency of RFB-induced Ura$^+$ reversion in indicated strains and conditions. Each dot represents one sample from eight independent biological replicate for each strain. Bars indicate mean values ± SD. *p* value was calculated by two-sided *t*-test. **c** Diagram of construct containing lexA-binding site (lexBS, purple) that allows tethering of Ulp1-lexA to the *t-lexBS-ura4sd20 < ori* construct (**d**, **e**, **g**) or to the *t-Laco-ura4::lexBS < ori* construct (**f**). **d** Sensitivity of indicated strains to indicated genotoxic drugs. Ten-fold serial dilution of exponential cultures were dropped on appropriate plates. **e** Binding of Ulp1-LexA to *ura4* or ade6 (unrelated control locus) in the presence of LexBS (*t-lexBS-ura4sd20 < ori*) or not (*t-ura4sd20 < ori*). Values are mean of four independent biological repeats ± SD. *p* value was calculated using two-sided *t*-test. **f** Co-localization event in S-phase cells in indicated conditions and strains as on Fig. 2a. *p* value was calculated by Fisher's exact test for OFF and ON groups for each mutant and condition. **g** Frequency of RFB-induced Ura$^+$ reversion in indicated strains and conditions. Each dot represents one sample from 14 independent biological replicate for each strain. Bars indicate mean values ± SD. *p* value was calculated by two-sided *t*-test.

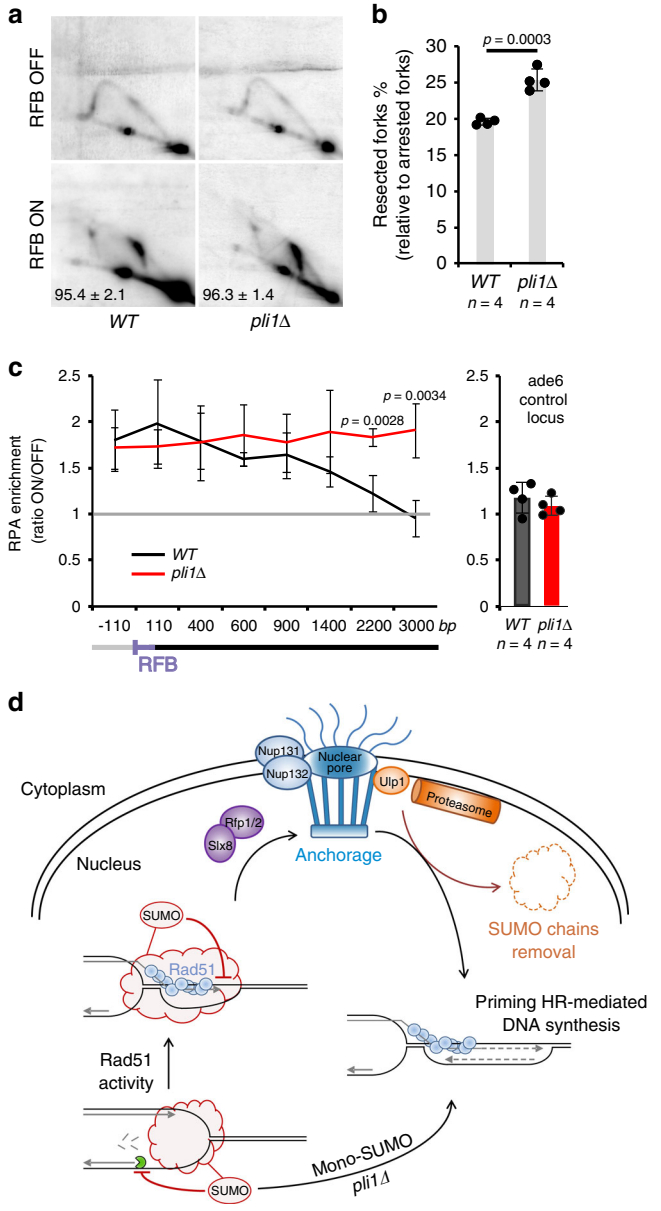

Fig. 7 Pli1 safeguards fork-integrity by limiting resection of nascent strands. a Representative RI analysis in indicated strains and conditions as described on Fig. 3. **b** Quantification of resected forks. Values are mean of four independent biological replicates ±SD. *p* value was calculated by two-sided *t*-test. **c** Binding of RPA (Ssb3-YFP) to the RFB in indicated strains. ChIP-qPCR results are presented as ON/OFF ratio for each mutant. Upstream and downstream distances from the RFB are presented in bp. Values are mean from four independent biological replicates ±SD. *p* value was calculated by two-sided *t*-test. Primers targeting *ade6* gene were used as unrelated control locus. **d** SUMO-based regulation of relocation of remodeled forks to NPCs to promote RDR. See text for explanations.

budding yeast Nup84 sustaining fork progression at stalled forks[41], Nup132 is necessary to sustain DNA replication upon HU treatment. The deletion of Pli1 did not rescue the defect in the recovery from HU-stalled forks in *nup132Δ* cells (Supplementary Fig. 5), indicating that Nup132 sustains DNA replication upon stress by distinct mechanisms according to the nature of stalled versus dysfunctional forks.

SUMOylation is a dynamic and reversible modification. At dysfunctional forks, our data establish a clear role of NPCs in counteracting the toxicity of SUMO chains to allow HR-mediated DNA synthesis. SUMO removal involves Ulp1 and the proteasome, two activities occurring at the NP. Although the role of NPCs in promoting the removal of SUMO conjugates has been previously proposed[17], our work reveals the versatile functions of SUMOylation in promoting fork integrity and relocation at the expense of limiting the step of HR-mediated DNA synthesis. We propose that SUMO-primed ubiquitylation promotes the clearance of DNA repair/replication factors at arrested forks to prime DNA synthesis, but the multiple targets remain unknown. Interestingly, the Branzei lab recently identified replication factors undergoing SUMOylation regulated by Ulp2 and STUbL to control replication initiation[61]. Similarly, we propose that key SUMOylated factors are controlled by Ulp1 and STUbL to regulate timely fork restart.

Methods

Standard yeast genetics. Yeast strains and primers used in this work are listed in Table S1 and S2 respectively. Gene deletion or tagging were performed by classical genetic techniques. Strain with *SUMO-KallR* was obtained by integration of synthetized mutated *pmt3* gene (Genscript) into *pmt3::ura4* and colonies were selected on 5-FOA. Mutation of all lysines to arginines was confirmed by sequencing. To assess the sensitivity of chosen mutants to genotoxic agents, midlog-phase cells were serially diluted and spotted onto plates containing hydroxyurea (HU), methyl methanesulfonate (MMS), campthotecin (CPT), bleomycin (bleo) or irradiated with an appropriate dose of UV. Strains carrying the *RTS1*, replication fork block sequence were grown in minimal medium EMMg (with glutamate as nitrogen source) with addition of appropriate supplements and 60 µM thiamine (barrier inactive, OFF). The induction of replication fork block was obtained by washing away the thiamine and further incubation in fresh medium for 24 h (barrier active, ON).

Live cell imaging. For snapshot microscopy, cells were grown in filtered EMMg with or without 60 µM thiamine for 24 h to exponential phase (RFB OFF and RFB ON), then centrifuged and resuspended in 500 µL of fresh EMMg. In all, 1 µL from resulting solution was dropped onto Thermo Scientific slide (ER-201B-CE24) covered with a thin layer of 1.4% agarose in filtered EMMg. 21 z-stack pictures (each z step of 200 nm) were captured using 3D LEICA DMRXA microscope, supplied with CoolSNAP monochromic camera (Roper Scientific) under 100X oil-immersion magnification with numerical aperture 1.4. Exposure time for GFP channel was 500 ms, for mCherry 1000 ms. Pictures were collected with METAMORPH software and analyzed with ImageJ software. Foci that merged or partially overlap were counted as colocalization event.

The mobility of arrested forks was investigated by collecting 3-dimensional 14-stack images every 1.5 s over 5 min. Cells were visualized with a Spinning Disk Nikon inverted microscope equipped with the Perfect Focus System, Yokogawa CSUX1 confocal unit, Photometrics Evolve512 EM-CCD camera, 100X/1.45-NA PlanApo oil immersion objective and a laser bench (Errol) with 491 diode laser, 100 mX (Cobolt). Images were captured every 1.5 s with 14 optical slices (each z step of 300 nm), 100 ms exposure time for single GFP channel at 15% of laser power using METAMORPH software. Time-lapse movies were mounted and analyzed with ImageJ software as described below.

To study the colocalization time between lacO/LacI RFB foci and Npp106-GFP cells grown in the above conditions were visualized with a Nikon inverted microscope described above, using two fluorescent channels with 491 and 561 nm diode lasers, 100 mX (Cobolt). Images were captured every 10 s with 14 optical slices (each z step of 300 nm) for 30 min with 100 ms exposure time both for GFP and mCherry channels at 15% of laser power using METAMORPH software. Time-lapse movies were mounted and analyzed with ImageJ software (description below).

Protein import-export from nucleus was monitored using *WT* and *nup131Δnup132Δ* strains expressing genomic LacI-NLS-GFP without *LacO* repeats integrated into the genome. Cells grown for 24 h with or without thiamine were visualized with Nikon inverted microscope described above. Snapshot pictures (21 stacks, each z of 200 nm and 100 ms exposure) were acquired using METAMORPH software and analyzed in ImageJ. Images were projected for maximum intensity. The nuclear/cytoplasmic ratio (N/C) was determined by measuring mean fluorescence intensity within constant square regions (ROI plugin from ImageJ) placed in the cytoplasm, center of nucleus and intercellular background. Nuclear/cytoplasm ratio stand for (Nucleus-background)/(Cytoplasm-background).

All image acquisition was performed on the PICT-IBiSA Orsay Imaging facility of Institut Curie.

Movie analysis. Movies have been mounted using ImageJ. For analysis of mobility of arrested forks after projection around *z*-axis, single-particle tracking was performed using ImageJ plugin SpotTracker[62]. Obtained coordinates for RFB foci were

then analyzed using MS Excel macro as in ref. [63]. Derived parameters were utilized to calculate mean square displacement and radius of constrains for each condition. The statistical significance was calculated based on MSD curves by one-tailed *t*-test.

For co-localization analysis of RFB foci and Npp106-GFP, first z projection was done for GFP and mCherry channels, then pictures have been denoised by subtracting background, compensated for bleaching over time (ImageJ plugin Stack Contrast Adjustment) and finally processed with filter Gaussian Blur. A kymograph was constructed over each S phase nucleus in indicated strains (Supplementary Fig. 1). First, all optical slices were projected around *z*-axis using average intensity parameter. Then a resulting 2D movie, consisting of 181 frames of 10 s interval was analyzed to pick up cells forming septum, which undergo S phase for analysis (Supplementary Fig. 1). Subsequently a projection over time-axis to form kymograph for GFP and mCherry channels was made. Next, to investigate the colocalization between Npp106-GFP-stained nuclear periphery and *lacO*-bound mCherry-LacI both channels were merged. The time of colocalization has been estimated based on the overlap of *RTS1*-RFB *lacO*/lacI-mCherry signal and Npp106-GFP signal (Supplementary Fig. 1).

Chromatin immunoprecipitation. ChIP against Npp106-GFP, Man1-GFP, Sad1-GFP, as well as RPA (ssb3-YFP) were performed as described in ref. [4] with following modifications. 200 mL of culture (at 1×10^7 concentration) for each condition (*RTS1*-RFB OFF/ON) was divided into 2 ×100 mL aliquots and then crosslinked with 10 mM DMA (dimethyl adipimidate, thermo scientific, 20660) and subsequently 1% formaldehyde (Sigma, F-8775). Next, cells from each 100 mL were then frozen in liquid nitrogen and lysed by bead beating in 400 µL of lysis buffer (50 mM HEPES pH 7.5, 1% Triton X100, 0.1% Nadeoxycholate, 1 mM EDTA with 1 mM PMSF and Complete EDTA-free protease inhibitor cocktail tablets (Roche, 1873580). Chromatin sonication was performed using a Diagenode Bioruptor in a mode High, 10 cycles of 30 s ON and 30 s OFF. Then sonicated chromatin fractions were pooled (400 µL + 400 µL) for each condition and immunoprecipitation over night was performed as follows: 300 µL was incubated with anti-GFP antibody (Invitrogen, A11122) at 1:150 concentration, 300 µL was incubated with Normal Rabbit IgG antibody (Cell Signaling Technology, #2729S) at concentration 1:75 and 5 µL was preserved as INPUT fraction. Next morning a Protein G Dynabeads (Invitrogen, 10003D) were added for 1 h and immunoprecipitated complexes have been decrosslinked for 2 h at 65° C. The DNA associated with respective protein was purified with a Qiaquick PCR purification kit (QIAGEN, 28104) and eluted in 400 µL of water. qPCR (iQ SYBR green supermix, Biorad, 1708882, primers listed in Table S2) was performed to determine the relative amounts of DNA (starting quantities based on standard curves for each pair of primers) using BIORAD CFX Maestro v1.1. For Npp106-GFP, Man1-GFP and Sad1-GFP enrichment, based on starting quantities, was normalized by dividing specific GFP signal over rabbit IgG control and then relative to an internal control locus at chromosome II (II.50). RPA enrichment, based on starting quantities, was calculated in the same way as Npp106-GFP, Man1-GFP, Sad1-GFP and presented as ratio ON/OFF.

Rad51 and Ulp1-lexA ChIP were performed with above protocol, but *rad51*Δ or strain devoid of Ulp1-lexA were used as a negative control, instead of normal rabbit IgG antibody[6]. Briefly, cells cross-linked with DMA and 1 % formaldehyde were subjected to ChIP protocol and immunoprecipitation was performed overnight using anti-Rad51 antibody (Abcam, ab63799) at 1:300 dilution or anti-lexA antibody (Abcam, ab174384) at 1:120 dilution. For qPCR starting quantities have been determined and the enrichment was calculated by subtracting negative control values and internal control locus at chromosome II (II.50).

2DGE analysis of replication intermediates. Exponential cells (2.5×10^9) were treated with 0.1% sodium azide and subsequently mixed with frozen EDTA (of final concentration at 80 mM). Genomic DNA was crosslinked with trimethyl psoralen (0.01 mg/mL, TMP, Sigma, T6137) added to cell suspensions for 5 min in the dark. Next, cells were irradiated with UV-A (365 nm) for 90 s at a constant flow 50 mM/cm^2. Subsequently, cell lysis was performed by adding lysing enzymes (Sigma, L1412) at concentration 0.625 mg/mL and zymolyase 100 T (Amsbio, 120493-1) at 0.5 mg/mL. Obtained spheroplasts were next embedded into 1 % low melting agarose (InCert Agarose 50123, Lonza) plugs and incubated overnight at 55 °C in a digestion buffer with 1 mg/mL of proteinase K (Euromedex EU0090). Then plugs were washed with TE buffer (50 mM Tris, 10 mM EDTA) and stored at 4 °C. Digestion of DNA was performed using 60 units per plug of restriction enzyme *Ase*I (NEB, R0526M), next samples were treated with RNase (Roche, 11119915001) and beta-agarase (NEB, M0392L). Melted plugs were equilibrated to 0.3 M NaCl concentration. Replication intermediates were purified using BND cellulose (Sigma, B6385) poured into columns (Biorad, 731-1550)[10]. RIs were enriched in the presence of 1 M NaCl 1.8% caffeine (Sigma, C-8960), precipitated with glycogen (Roche, 1090139001) and migrated in 0.35% agarose gel (1xTBE) for the first dimension. The second dimension was cast in 0.9% agarose gel (1xTBE) supplemented with EtBr. Next DNA was transferred to a nylon membrane (Perkin-Elmer, NEF988001PK) in 10x SSC. Finally, membranes were incubated with ^{32}P-radiolabeled *ura4* probe (TaKaRa *Bca*BEST^{TM} Labeling Kit, #6046 and alpha-^{32}P dCTP, Perkin-Elmer, BLU013Z250UC) in Ultra-Hyb buffer (Invitrogen, AM8669) at 42 °C. Signal of replication intermediates was collected in phosphor-imager software (Typhoon-trio) and quantified by densitometric analysis with ImageQuantTL software (GE healthcare). The 'tail signal' was normalized to the overall signal corresponding to arrested forks.

Replication slippage assay. The frequency of *ura4*+ revertants using *ura4-sd20* allele was performed as follows. 5-FOA (EUROMEDEX, 1555) resistant colonies were grown on plates containing uracil with or without thiamine for 2 days at 30 °C and subsequently inoculated into EMMg supplemented with uracil for 24 h. Then cultures were diluted and plated on EMMg complete (for cell survival) and on EMMg without uracil both supplemented with 60 µM thiamine. After 5–7 days incubation at 30 °C colonies were counted to determine the frequency of *ura4*$^+$ reversion. To obtain the true occurrence of replication slippage by the *RTS1*-RFB, independently of the genetic background, we subtracted the replication slippage frequency of the strain devoid of RFB (considered as spontaneous frequency) from the frequency of the strain containing *the t-ura4sd20 < ori* construct, upon expression of Rtf1.

Flow cytometry. Flow cytometry analysis of DNA content was performed as follows[64]: cells were fixed in 70% ethanol and washed with 50 mM sodium citrate, digested with RNAse A (Sigma, R5503) for 2 h, stained with 1 µM Sytox Green nucleic acid stain (Invitrogen, S7020) and subjected to flow cytometry using FACSCANTO II (BD Biosciences). Gating procedure is presented on Supplementary Fig. 5.

Pulse field gel electrophoresis. Yeast cultures were grown to logarithmic phase in rich YES medium to concentration 5×10^6/mL, synchronized in 20 mM HU for 4 hours, subsequently released to fresh YES medium. At each time point 20 mL of cell culture was harvested, washed with cold 50 mM EDTA pH 8 and digested with litycase (Sigma, L4025) in CSE buffer (20 mM citrate/phosphate pH 5.6, 1.2 M sorbitol, 40 mM EDTA pH 8). Next cells were embedded into 1% UltraPure^{TM} Agarose (Invitrogen, 16500) and distributed into 5 identical agarose plugs for each time point. Plugs were then digested with Lysis Buffer 1, LB1 (50 mM Tris-HCl pH 7.5, 250 mM EDTA pH 8, 1 % SDS) for 1.5 hour in 55 °C and then transferred to Lysis Buffer 2, LB2 (1% *N*-lauryl sarcosine, 0.5 M EDTA pH 9.5, 0.5 mg/mL proteinase K) o/n at 55 °C. Next day LB2 was change for fresh one and digestion was continued o/n at 55 °C. After, plugs were kept at 4 °C. To visualize intact chromosomes one set of plugs was run on a Biorad CHEF-DR-III pulse field gel electrophoresis (PFGE) system for 60 h at 2.0 V/cm, angle 120°, 14 °C, 1800 s single switch time, pump speed 70 in 1x TAE buffer. Separated chromosomes were stained in ethidium bromide (10 µg/mL) for 30 min, washed briefly in 1x TAE and visualized with UV transilluminator.

Ura4 loss assay. Mutant strains were grown on complete EMMg plates with or without 60 µM thiamine. Then 11 independent colonies from each strain and condition were inoculated into 5 mL of complete EMMg with or without thiamine and grown to stationary phase. Appropriate dilutions were plated on YES plates (for cell survival) and on 0.1% 5-FOA (EUROMEDEX, 1555) plates. After 5–7 days incubation at 30 °C colonies were counted. The rate of ura4+ loss was determined by the median and statistical significance was measured by nonparametric Mann–Whitney U test.

PCR assays for determination of the rates of genomic deletion, translocation, and mutation. 100 5-FOA resistant colonies per strain per condition were subjected for PCR analysis (primers for translocation junction, *ura4*+ and control gene *rng3*+ listed in Table S2) as reported in ref. [7]. Translocations, deletions and mutations were counted as percentages of all events and these values were used to balance the rates of *ura4* loss and subsequently to estimate the respective rates of translocations, deletions and mutations. Mann–Whitney U test was used to check the statistical significance of analyzed data.

Fluorescence in situ hybridization. Fluorescence in situ hybridization (FISH) was performed as described elsewhere[65] with following modifications. Strains were grown in complete EMMg media without thiamine and fixed with formaldehyde (Sigma, F8775) added to the final concentration of 4% for 45 min with rotation at RT. Next, cells were washed twice in Fixation buffer (1.2 M sorbitol, 100 mM $KHPO_4$, pH 7.5) and resuspended in fresh Fixation buffer containing 100 T zymolyase (MP Biomedicals, SKU08320932) at final concentration 0.5 µg/mL. Cells were then digested for 10 min at 30 °C. Spheroplasts were gently washed twice with ice-cold Fixation buffer. Next cells were stored in 70% ethanol for at least 3 h at 4 °C. Then ethanol was carefully removed after mild centrifugation (400 g) and cells were incubated for 5 min, RT in 2x SSC. Subsequently, cells were resuspended in Hybridization buffer (50% formamide, 10% dextran sulphate, 4x SSC, 0.02% polyvinyl pyrrolidone, 0.02% BSA, 0.02% Ficoll 400, 125 µg/mL of *E. coli* tRNA, 500 µg/mL salmon sperm DNA) and prehybridized at 37 °C for 1 h. Hybridization overnight, in the dark, was performed in Hybridization buffer with 10 µg/mL of Oligo-dT_{50}-Cy3 probe at 37 °C. Next day cells were incubated at RT for 30 min in 2X SSC and then 30 min 1X SSC. The last incubation with 0.5X SSC was carried at 37 °C. Subsequently cells were incubated with DAPI solution (diluted 1/4000 in 0.5x SSC) for 3 min. Next cells were washed with 0.5X SSC for 5 min to remove

excess of DAPI. Finally, cells were resuspended in 15 µL of VECTASHIELD® Antifade Mounting Medium and subjected to snapshot microscopy on glass slides using a DM6000B Leica microscope with a 100×, NA 1.4 (HCX Plan-Apo) oil immersion objective coupled to a piezo-electric motor (LVDT; Physik Instrument) and a CCD camera (CoolSNAP HQ; Photometrics). In all, 21 z-stacks of 200 nm, with 300 ms exposure time for Cy3 and 50 ms for DAPI channels were collected with METAMORPH and analyzed with ImageJ software. Percentage of cells with poly(A) + RNA accumulation was calculated from at least 200 cells per each strain and condition.

Statistical analysis. Quantitative densitometric analysis of Southern-blots after 2DGE was carried using ImageQuant software. The 'tail signal' of resected forks was normalized to the overall signal corresponding to arrested forks.

Quantification of PFGE was performed using ImageJ and presented as percenatge of migrating chromosomes relative to asynchronous profile.

Cell imaging was performed using METAMORPH software and processed and analyzed using ImageJ software.

The explanation and definitions of values and error bars are mentioned within the figure legends. Most experiments the number of samples is $n > 3$ obtained from independent experiments to ensure biological reproducibility. For all experiments based on the analysis of cell imaging, the number of nuclei analyzed is mentioned in the figure legends.

Statistical analysis was carried using Mann–Whitney U tests and Student's *t*-test.

Reporting summary. Further information on research design is available in the Nature Research Reporting Summary linked to this article.

Data availability

Data have been deposited to Mendeley data and are available at: https://doi.org/10.17632/4m7z3gy5yc.1. All relevant data are available from the corresponding author. Source data are provided with this paper.

Received: 26 February 2020; Accepted: 16 October 2020;
Published online: 06 November 2020

References

1. Zeman, M. K. & Cimprich, K. A. Causes and consequences of replication stress. *Nat. Cell Biol.* **16**, 2–9 (2014).
2. Magdalou, I., Lopez, B. S., Pasero, P. & Lambert, S. A. E. The causes of replication stress and their consequences on genome stability and cell fate. *Semin. Cell Dev. Biol.* **30**, 154–164 (2014).
3. Ait Saada, A., Lambert, S. A. E. & Carr, A. M. Preserving replication fork integrity and competence via the homologous recombination pathway. *DNA Repair* **71**, 135–147 (2018).
4. Tsang, E. et al. The extent of error-prone replication restart by homologous recombination is controlled by Exo1 and checkpoint proteins. *J. Cell Sci.* **127**, 2983–2994 (2014).
5. Teixeira-Silva, A. et al. The end-joining factor Ku acts in the end-resection of double strand break-free arrested replication forks. *Nat. Commun.* **8**, 1982 (2017).
6. Ait Saada, A. et al. Unprotected replication forks are converted into mitotic sister chromatid bridges. *Mol. Cell* **66**, 398–410.e4 (2017).
7. Iraqui, I. et al. Recovery of arrested replication forks by homologous recombination is error-prone. *PLoS Genet* **8**, e1002976 (2012).
8. Mizuno, K., Miyabe, I., Schalbetter, S. A., Carr, A. M. & Murray, J. M. Recombination-restarted replication makes inverted chromosome fusions at inverted repeats. *Nature* **493**, 246–249 (2012).
9. Jalan, M., Oehler, J., Morrow, C. A., Osman, F. & Whitby, M. C. Factors affecting template switch recombination associated with restarted DNA replication. *Elife* **8**, e41697 (2019).
10. Lambert, S. et al. Homologous recombination restarts blocked replication forks at the expense of genome rearrangements by template exchange. *Mol. Cell* **39**, 346–359 (2010).
11. Mekhail, K. & Moazed, D. The nuclear envelope in genome organization, expression and stability. *Nat. Rev. Mol. Cell Biol.* **11**, 317–328 (2010).
12. D'Angelo, M. A. & Hetzer, M. W. Structure, dynamics and function of nuclear pore complexes. *Trends Cell Biol.* **18**, 456–466 (2008).
13. Reichelt, R. et al. Correlation between structure and mass distribution of the nuclear pore complex and of distinct pore complex components. *J. Cell Biol.* **110**, 883–894 (1990).
14. Rout, M. P. et al. The yeast nuclear pore complex: composition, architecture, and transport mechanism. *J. Cell Biol.* **148**, 635–651 (2000).
15. Schwartz, T. U. The structure inventory of the nuclear pore complex. *J. Mol. Biol.* **428**, 1986–2000 (2016).
16. Seeber, A. & Gasser, S. M. Chromatin organization and dynamics in double-strand break repair. *Curr. Opin. Genet. Dev.* **43**, 9–16 (2017).
17. Nagai, S. et al. Functional targeting of DNA damage to a nuclear pore-associated SUMO-dependent ubiquitin ligase. *Science* **322**, 597–602 (2008).
18. Kalocsay, M., Hiller, N. J. & Jentsch, S. Chromosome-wide Rad51 spreading and SUMO-H2A.Z-dependent chromosome fixation in response to a persistent DNA double-strand break. *Mol. Cell* **33**, 335–343 (2009).
19. Oza, P., Jaspersen, S. L., Miele, A., Dekker, J. & Peterson, C. L. Mechanisms that regulate localization of a DNA double-strand break to the nuclear periphery. *Genes Dev.* **23**, 912–927 (2009).
20. Horigome, C. et al. PolySUMOylation by Siz2 and Mms21 triggers relocation of DNA breaks to nuclear pores through the Slx5/Slx8 STUbL. *Genes Dev.* **30**, 931–945 (2016).
21. Horigome, C. et al. SWR1 and INO80 chromatin remodelers contribute to DNA double-strand break perinuclear anchorage site choice. *Mol. Cell* **55**, 626–639 (2014).
22. Su, X. A., Dion, V., Gasser, S. M. & Freudenreich, C. H. Regulation of recombination at yeast nuclear pores controls repair and triplet repeat stability. *Genes Dev.* **29**, 1006–1017 (2015).
23. Churikov, D. et al. SUMO-dependent relocalization of eroded telomeres to nuclear pore complexes controls telomere recombination. *Cell Rep.* **15**, 1242–1253 (2016).
24. Khadaroo, B. et al. The DNA damage response at eroded telomeres and tethering to the nuclear pore complex. *Nat. Cell Biol.* **11**, 980–987 (2009).
25. Swartz, R. K., Rodriguez, E. C. & King, M. C. A role for nuclear envelope–bridging complexes in homology-directed repair. *Mol. Biol. Cell* **25**, 2461–2471 (2014).
26. Ryu, T. et al. Heterochromatic breaks move to the nuclear periphery to continue recombinational repair. *Nat. Cell Biol.* **17**, 1401–1411 (2015).
27. Jalal, D., Chalissery, J. & Hassan, A. H. Genome maintenance in Saccharomyces cerevisiae: the role of SUMO and SUMO-targeted ubiquitin ligases. *Nucleic Acids Res.* **45**, 2242–2261 (2017).
28. Watts, F. Z. et al. The role of *Schizosaccharomyces pombe* SUMO ligases in genome stability. *Biochem. Soc. Trans.* **35**, 1379–1384 (2007).
29. Sacher, M., Pfander, B., Hoege, C. & Jentsch, S. Control of Rad52 recombination activity by double-strand break-induced SUMO modification. *Nat. Cell Biol.* **8**, 1284–1290 (2006).
30. Cremona, C. A. et al. Extensive DNA damage-induced sumoylation contributes to replication and repair and acts in addition to the mec1 checkpoint. *Mol. Cell* **45**, 422–432 (2012).
31. Prudden, J. et al. SUMO-targeted ubiquitin ligases in genome stability. *EMBO J.* **26**, 4089–4101 (2007).
32. Perry, J. J. P., Tainer, J. A. & Boddy, M. N. A SIM-ultaneous role for SUMO and ubiquitin. *Trends Biochem. Sci.* **33**, 201–208 (2008).
33. Sriramachandran, A. M. & Dohmen, R. J. SUMO-targeted ubiquitin ligases. *Biochim. Biophys. Acta* **75–85**, 2014 (**1843**).
34. Hickey, C. M., Wilson, N. R. & Hochstrasser, M. Function and regulation of SUMO proteases. *Nat. Rev. Mol. Cell Biol.* **13**, 755–766 (2012).
35. Nie, M. & Boddy, M. N. Pli1 ^{PIAS1} SUMO ligase protected by the nuclear pore-associated SUMO protease Ulp1$^{SENP1/2}$. *J. Biol. Chem.* **290**, 22678–22685 (2015).
36. Palancade, B. et al. Nucleoporins prevent DNA damage accumulation by modulating Ulp1-dependent sumoylation processes. *Mol. Biol. Cell* **18**, 2912–2923 (2007).
37. Bukata, L., Parker, S. L. & D'Angelo, M. A. Nuclear pore complexes in the maintenance of genome integrity. *Curr. Opin. Cell Biol.* **25**, 378–386 (2013).
38. Freudenreich, C. H. & Su, X. A. Relocalization of DNA lesions to the nuclear pore complex. *FEMS Yeast Res.* https://doi.org/10.1093/femsyr/fow095. (2016).
39. Loeillet, S. et al. Genetic network interactions among replication, repair and nuclear pore deficiencies in yeast. *DNA Repair.* **4**, 459–468 (2005).
40. Therizols, P. et al. Telomere tethering at the nuclear periphery is essential for efficient DNA double strand break repair in subtelomeric region. *J. Cell Biol.* **172**, 189–199 (2006).
41. Gaillard, H., Santos-Pereira, J. M. & Aguilera, A. The Nup84 complex coordinates the DNA damage response to warrant genome integrity. *Nucleic Acids Res* **47**, 4054–4067 (2019).
42. Chung, D. K. C. et al. Perinuclear tethers license telomeric DSBs for a broad kinesin- and NPC-dependent DNA repair process. *Nat. Commun.* **6**, 7742 (2015).
43. Tsouroula, K. et al. Temporal and spatial uncoupling of DNA double strand break repair pathways within mammalian heterochromatin. *Mol. Cell* **63**, 293–305 (2016).
44. Marnef, A. et al. A cohesin/HUSH- and LINC-dependent pathway controls ribosomal DNA double-strand break repair. *Genes Dev.* **33**, 1175–1190 (2019).

45. Torres-Rosell, J. et al. The Smc5-Smc6 complex and SUMO modification of Rad52 regulates recombinational repair at the ribosomal gene locus. *Nat. Cell Biol.* **9**, 923–931 (2007).
46. Horigome, C., Unozawa, E., Ooki, T. & Kobayashi, T. Ribosomal RNA gene repeats associate with the nuclear pore complex for maintenance after DNA damage. *PLoS Genet* **15**, e1008103 (2019).
47. Lambert, S., Watson, A., Sheedy, D. M., Martin, B. & Carr, A. M. Gross chromosomal rearrangements and elevated recombination at an inducible site-specific replication fork barrier. *Cell* **121**, 689–702 (2005).
48. Nguyen, M. O., Jalan, M., Morrow, C. A., Osman, F. & Whitby, M. C. Recombination occurs within minutes of replication blockage by RTS1 producing restarted forks that are prone to collapse. *Elife* **4**, e04539 (2015).
49. Miyabe, I. et al. Polymerase δ replicates both strands after homologous recombination–dependent fork restart. *Nat. Struct. Mol. Biol.* **22**, 932–938 (2015).
50. Heun, P., Laroche, T., Shimada, K., Furrer, P. & Gasser, S. M. Chromosome dynamics in the yeast interphase nucleus. *Science* **294**, 2181–2186 (2001).
51. Steglich, B., Filion, G. J., van Steensel, B. & Ekwall, K. The inner nuclear membrane proteins Man1 and Ima1 link to two different types of chromatin at the nuclear periphery in S. pombe. *Nucleus* **3**, 77–87 (2012).
52. King, M. C., Drivas, T. G. & Blobel, G. A network of nuclear envelope membrane proteins linking centromeres to microtubules. *Cell* **134**, 427–438 (2008).
53. Nie, M., Moser, B. A., Nakamura, T. M. & Boddy, M. N. SUMO-targeted ubiquitin ligase activity can either suppress or promote genome instability, depending on the nature of the DNA lesion. *PLoS Genet* **13**, e1006776 (2017).
54. Steinacher, R., Osman, F., Lorenz, A., Bryer, C. & Whitby, M. C. Slx8 removes Pli1-dependent protein-SUMO conjugates including SUMOylated topoisomerase I to promote genome stability. *PLoS ONE* **8**, e71960 (2013).
55. Prudden, J. et al. DNA repair and global sumoylation are regulated by distinct Ubc9 noncovalent complexes. *Mol. Cell. Biol.* **31**, 2299–2310 (2011).
56. Asakawa, H. et al. Asymmetrical localization of Nup107-160 subcomplex components within the nuclear pore complex in fission yeast. *PLoS Genet* **15**, e1008061 (2019).
57. Tani, T., Derby, R. J., Hiraoka, Y. & Spector, D. L. Nucleolar accumulation of poly (A)+ RNA in heat-shocked yeast cells: Implication of nucleolar involvement in mRNA transport. *Mol. Biol. Cell* **6**, 1515–1534 (1995).
58. Boehringer, J. et al. Structural and functional characterization of Rpn12 identifies residues required for Rpn10 proteasome incorporation. *Biochem. J.* **448**, 55–65 (2012).
59. Whalen, J. M., Dhingra, N., Wei, L., Zhao, X. & Freudenreich, C. H. Relocation of collapsed forks to the nuclear pore complex depends on sumoylation of DNA repair proteins and permits Rad51 association. *Cell Rep.* **31**, 107635 (2020).
60. Chiolo, I. et al. Double-strand breaks in heterochromatin move outside of a dynamic HP1a domain to complete recombinational repair. *Cell* **144**, 732–744 (2011).
61. Psakhye, I., Castellucci, F. & Branzei, D. SUMO-chain-regulated proteasomal degradation timing exemplified in DNA replication initiation. *Mol. Cell* **76**, 632–645 (2019).
62. Sage, D., Neumann, F. R., Hediger, F., Gasser, S. M. & Unser, M. Automatic tracking of individual fluorescence particles: application to the study of chromosome dynamics. *IEEE Trans. Image Process* **14**, 1372–1383 (2005).
63. Dion, V., Kalck, V., Seeber, A., Schleker, T. & Gasser, S. M. Cohesin and the nucleolus constrain the mobility of spontaneous repair foci. *EMBO Rep.* **14**, 984–991 (2013).
64. Sabatinos, S. A., Forsburg, S. L. & Measuring, D. N. A. content by flow cytometry in fission yeast. *Methods Mol. Biol.* **521**, 449–461 (2009).
65. Bretes, H. et al. Sumoylation of the THO complex regulates the biogenesis of a subset of mRNPs. *Nucleic Acids Res.* **42**, 5043–5058 (2014).

Acknowledgements

We thank Joe Murray, Antony Carr, Dorota Dziadkowiec and Vincent Dion for exchanging reagents, and Xiaofeng Allen Su for performing initial pilot zoning assays with the RFB system. The Sad1-GFP strain was obtained from YGRC/NBRP Japan resource database (http://yeast.nig.ac.jp/yeast/top.xhtml). We are very grateful to Michael Boddy for providing *slx8-29*, "Low Sumo" and "SUMO-D81R" strains. We also thank the PICT-IBiSA@Orsay Imaging Facility of the Institut Curie and the Flow Cytometry Facility of the Orsay site of Institut Curie. We thank Marie-Noelle Simon and Vincent Géli for their criticisms and helpful comments on this work. This study was supported by grants from the Institut Curie, the CNRS, the *Fondation ARC* (Projet Fondation ARC PJA 20181208114), the *Fondation pour la Recherche Médicale* "Equipe FRM DEQ20160334889", LIGUE contre le cancer "Equipe Labellisée 2020 (EL2020LNCC/Sal), and the ANR grant NIRO (ANR-19-CE12-0023-01). AAS was funded by a French governmental fellowship and a 4th-year PhD grant from *Fondation ARC*, KK received a Postdoctoral fellow ship from *Fondation ARC* (PDF20171206749) and K.S. received a PhD fellowship from the LIGUE contre le cancer. C.H.F. is funded by NIH grant GM122880. The funders had no role in study design, data collection and analysis, the decision to publish, or preparation of the paper.

Author contributions

K.K., K.S., V.B., and A.A.S performed the experiments. B.P., K.K., C.F., and S.A.E.L contributed to experimental design and data analysis. C.L. provided expertise to perform MSD. K.K., and S.A.E.L wrote the paper. S.A.E.L and C.H.F edited the paper.

Competing interests

The authors declare no competing interests.

Additional information

Supplementary information is available for this paper at https://doi.org/10.1038/s41467-020-19516-z.

Correspondence and requests for materials should be addressed to S.A.E.L.

Peer review information *Nature Communications* thanks the anonymous reviewer(s) for their contribution to the peer review of this work. Peer reviewer reports are available.

Reprints and permission information is available at http://www.nature.com/reprints

Publisher's note Springer Nature remains neutral with regard to jurisdictional claims in published maps and institutional affiliations.

II: Publication #2

SUMO protease and proteasome recruitment at the nuclear periphery differently affect replication dynamics at arrested forks.

SUMO protease and proteasome recruitment at the nuclear periphery differently affect replication dynamics at arrested forks.

Kamila Schirmeisen[1,2,#], Karel Naiman[3,4 #], Karine Fréon[1,2], Laetitia Besse[5], Shrena Chakraborty[1,2], Antony M Carr[4], Karol Kramarz[6,*] and Sarah AE Lambert[1,2,7*]

1. Institut Curie, Université PSL, CNRS UMR3348, 91400 Orsay, France.
2. Université Paris-Saclay, CNRS UMR3348, 91400 Orsay, France.
3. INSERM U1068, CNRS UMR7258, Aix Marseille Univ U105, Institut Paoli-Calmettes, CRCM, Marseille, France
4. Genome Damage and Stability Centre, School of Life Sciences, University of Sussex, Falmer, BN1 9RQ, UK.
5. Institut Curie, Universite´ PSL, CNRS UAR2016, Inserm US43, Universite´ Paris-Saclay, Multimodal Imaging Center, 91400 Orsay, France.
6. Academic Excellence Hub - Research Centre for DNA Repair and Replication, Faculty of Biological Sciences, University of Wroclaw, 50-328 Wroclaw, Poland
7. Equipe Labelisée Ligue Nationale Contre le cancer, France

[#] Equal contribution.

* Co-corresponding author: sarah.lambert@curie.fr and karol.kramarz@uwr.edu.pl

Lead contact: Sarah Lambert, sarah.lambert@curie.fr

Running title:

replication restart dynamics at the nuclear periphery

Keywords: Homologous recombination, fork restart, SUMO, Nuclear basket, proteasome, Ulp1

Abstract

Nuclear pores complexes (NPCs) are genome organizers, defining a particular nuclear compartment enriched for SUMO protease and proteasome activities, and act as docking sites for DNA repair. In fission yeast, the anchorage of perturbed replication forks to NPCs is an integral part of the recombination-dependent replication restart mechanism (RDR) that resumes DNA synthesis at terminally dysfunctional forks. By mapping DNA polymerase usage, we report that SUMO protease Ulp1-associated NPCs ensure efficient initiation of restarted DNA synthesis, whereas proteasome-associated NPCs sustain the progression of restarted DNA polymerase. In contrast to Ulp1-dependent events, this last function occurs independently of SUMO chains formation. By analyzing the role of the nuclear basket, the nucleoplasmic extension of the NPC, we reveal that the activities of Ulp1 and the proteasome cannot compensate for each other and affect RDR dynamics in distinct ways. Our work probes the mechanisms by which the NPC environment ensures optimal RDR.

Highlights:

● Ulp1-associated NPCs ensure efficient initiation of restarted DNA synthesis, in a SUMO chain-dependent manner

● Proteasome-associated NPCs foster the progression of restarted DNA synthesis, in a SUMO chain-independent manner

● The nucleoporin Nup60 promotes the spatial sequestration of Ulp1 at the nuclear periphery

● Ulp1 and proteasome activities are differently required for optimal recombination-mediated fork restart.

Introduction

The eukaryotic genome is folded in 3D within a membrane-less compartmentalized nucleus. This constitutes a critical layer of regulation of DNA-associated transactions, making nuclear organization an important determinant of genome integrity[1]. The stability of the genome is at its most vulnerable during DNA replication; the progression of replisome being recurrently threatened by a broad spectrum of obstacles, that cause fork slowing, temporary fork stalling or terminal collapse of the replication fork[2]. Such alterations of fork progression are a hallmark of replication stress and failure to safeguard genome stability upon replication stress is a potent driving force behind the onset and progression of human diseases including cancer[3]. While multiple replication fork-repair pathways can be engaged at stressed forks to promote the completion of genome duplication, they result in variable outcomes for genome stability and thus must be carefully controlled and regulated. Our current knowledge of the regulatory functions played by nuclear organization in the usage of fork repair pathways remains in its infancy.

Among the fork-repair pathways, Homologous recombination (HR) is particularly active in protecting, repairing and restarting stressed forks, making HR an efficient tumor suppressor mechanism[4]. The central and universal factor of the HR machinery is the Rad51 recombinase that forms a nucleoprotein filament on single stranded DNA (ssDNA), with the assistance of a loader, known as Rad52 in yeast models. In a non-recombinogenic mode, the Rad51 filament inhibits the degradation of ssDNA by various nucleases, thus ensuring the protection and integrity of stressed forks. In a recombinogenic mode, HR repairs broken forks with a single-ended double strand break (DSB) by a mechanism called break-induced replication (BIR) and promotes replication resumption at DSB-free collapsed forks by a mechanism called recombination-dependent replication (RDR)[5]. Both BIR and RDR are associated with non-canonical DNA synthesis, which is up to 100 times more mutagenic that canonical replication. Furthermore, during BIR and RDR, both DNA strands are synthesized by DNA polymerase delta (Pol δ)[6,7]. These features allow experimental differentiation between DNA replicated by a repaired/restarted fork and DNA replicated by a canonical origin-born fork. Although stressed forks have the potential to relocate to the nuclear periphery (NP), little is known about the contribution of such nuclear reorganization in regulating the replicative functions of the HR machinery.

3D genome folding in the highly complex nuclear environment is a critical layer of DNA repair regulation. A striking example is the DNA damage response-dependent fate of DSBs that relocate to the NP or shift away from heterochromatin compartments to

achieve error-free repair (reviewed in [8,9]). This led to the concept that membrane-less nuclear compartments exhibit distinct DNA repair capacities and that DNA repair machineries are spatially segregated. Nuclear pore complexes (NPCs) are macromolecular structures embedded in the nuclear envelope (NE) that act as nuclear scaffolds to regulate a variety of cellular processes via a wide range of mechanisms[10]. The overall structure of NPCs is highly evolutionarily conserved in the eukaryote kingdom, being composed of multiples copies of 30 different nucleoporins that associate in stable sub-complexes. The core NPC defines a central channel composed of transmembrane and channel nucleoporins. This core complex assembles with the outer and inner rings at the cytoplasmic and nuclear sides, respectively. A Y-shaped structure, located both at the cytoplasmic and nuclear side of NPCs, called in fission yeast Nup107-Nup160 complex, is crucial for NPC organization and proper segregation of chromosomes in eukaryotes[11–13]. The final composition of individual NPCs is variable, depending on their position within the NE, suggesting that the NPC structure is dynamic. In particular, the nuclear basket, a nucleoplasmic extension of the core NPC, is the most dynamic part and NPCs localized in the nucleolar part of the NE are more frequently devoid of a nuclear basket[12]. The primary function of NPCs is the transport of macromolecules from the cytoplasm to the nucleus and mRNA export. NPCs have also emerged as genome organizers, defining a particular nuclear compartment enriched for the SUMO SENP protease and the proteasome and acting as docking sites for DSBs and perturbed replication forks[8].

Several groups have reported that stressed forks can relocate to the NP and, in some cases, to anchor at NPCs[14]. These include forks stalled by structure-forming DNA sequences, telomere repeats, DNA-bound proteins and replication inhibitors[15–21]. Although distinct scenarios arise depending of the source of the replication stress and the model organism, the common emerging theme is that the nuclear positioning of replication stress sites influences the usage of fork repair pathways. For example, in *Saccharomyces cerevisiae* (Sc), forks stalled within telomere repeats associate with NPCs to restrict error-prone HR events and maintain telomere length[18]. Forks stalled by CAG repeats, prone to form secondary DNA structures, also anchor to NPCs, in a SUMO-dependent manner[16]. In this instance, SUMOylated RPA on ssDNA at the stalled fork inhibits Rad51 loading, which is permitted only after NPC anchorage that subsequently favors error-free fork restart[17]. These changes in nuclear positioning are far from being a yeast-specific phenomenon. Upon DNA polymerases inhibition, stalled forks in human cells exhibit relocation to the NP to minimize chromosomal instability and to ensure timely fork restart[20]. Additionally, stressed forks at human telomeres relocate to NPCs to maintain telomere integrity[19].

We previously reported that, in the yeast *Schizosaccharomyces pombe* (Sp), dysfunctional forks relocate in a SUMO-dependent manner and anchor to NPCs for the time necessary to achieve RDR[15]. This change in nuclear positioning is critical to spatially segregate the subsequent steps of RDR, with dysfunctional forks being processed and remodeled in the nucleoplasm to load Rad51. SUMO chains that are generated by the E3 SUMO ligase, Pli1, trigger the relocation. However, they also limit the efficiency of HR-mediated DNA synthesis for fork restart. Relocating these dysfunctional forks towards NPCs allows the SUMO conjugates to be cleared by the SUMO deconjugating enzyme, Ulp1, which is sequestrated at the NP[22]. Therefore, NPCs are an integral part of RDR regulation to promote HR-dependent DNA synthesis at dysfunctional forks. However, the dynamics underlying this process remain unexplored. In particular, the contribution of NPCs to non-canonical Pol δ/Pol δ DNA synthesis, a hallmark of HR-restarted forks, has not been addressed. Here, by mapping DNA polymerase usage during HR-mediated fork restart, we reveal that the SUMO protease, Ulp1, and the proteasome differentially affect the dynamics of HR-dependent fork restart by ensuring efficient DNA synthesis resumption and by sustaining the dynamic progression of restarted fork, respectively. Moreover, by studying the role of the nuclear basket in RDR, we show that Ulp1 and the proteasome do not compensate for each other, with Ulp1 being critical to counteract the inhibitory effect of SUMO chains but not the proteasome. Our study uncovers mechanisms by which the NPC compartment acts as a critical environment for optimal HR-dependent fork restart.

Results

To investigate the contribution of the NP to the dynamics of HR-mediated fork restart, we exploited the *RTS1*-RFB that promotes the polar arrest of a single replisome at a specific genomic location (Fig. 1a)[23]. The activity of the RFB is fully dependent on the Rtf1 protein that binds to the *RTS1* sequence. The expression of Rtf1 can be artificially regulated by the *nmt41* promoter to allow Rtf1 repression in thiamine-containing media (RFB OFF condition) and its expression upon thiamine removal (RFB ON condition). Alternatively, the *rtf1* gene can be deleted and the results compared with an *rtf1*+ strain. Forks arrested at the RFB become fully dysfunctional and undergo controlled degradation of the nascent strand by the end-resection machinery to generate single stranded DNA gaps of ~ 1 Kb in length[24,25]. RPA, Rad52 and Rad51 are loaded onto these ssDNA gaps, ensuring fork protection until the arrested fork is either rescued by a converging fork or is actively restarted by RDR, which occurs approximately 20 minutes after the arrest[6,26–28]. The progression of the restarted fork is associated with a non-canonical, mutagenic DNA synthesis in which both strands are synthesized by Pol δ, making restarted fork insensitive to the RFB[26,27,29,30].

Ulp1-associated NPCs ensure the efficient priming of recombination-mediated DNA synthesis

We previously reported that the nucleoporin Nup132, which is part of the Y complex of the core NPCs, promotes RDR in a post-anchoring manner and acts downstream of Rad51 loading[15]. The RDR defect observed in *nup132* null cells is caused by the delocalization of Ulp1 from the NP since its artificial tethering to the RFB restored RDR efficiency. Thus, Ulp1-associated NPCs prime HR-dependent DNA synthesis to ensure efficient RDR, but the dynamics of this process are unknown. To address this, we employed the polymerase usage sequencing (Pu-seq) approach that allows the genome-wide mapping of the usage of Polymerases δ and epsilon (Pol ε) during DNA replication[31]. Pu-seq makes use of a pair of yeast strains mutated in either Pol δ or Pol ε that incorporate higher levels of ribonucleotides during DNA synthesis. The mapping of ribonucleotides in a strand-specific manner in strains mutated either for Pol δ or Pol ε allows the genome-wide tracking of polymerase usage. Combined with the *RTS1*-RFB, the Pu-seq method allows the monitoring of the usage frequency of each polymerase separately on both the Watson and Crick strands when the RFB is either inactive (RFB OFF, in an *rtf1Δ* genetic background) or constitutively active (RFB ON, Rtf1 being expressed under control of the *adh1* promoter to maximize fork arrest efficiency)[26].

At an inactive barrier site (RFB OFF), replication is canonical and unidirectional coming from an early replication origin (leading strand synthesized by Pol ε and lagging strand

synthesized by Pol δ) (Fig 1a-b, top panel). This division of labour between Pol δ and ε changed sharply in an RFB ON strain: at the barrier site, Pol ε in the leading strand is switched to Pol δ during the restart of the blocked fork (Fig 1b, bottom panel). The sharp transition characterizes the efficiency of the restart itself. It means that this creates a bias towards Pol δ on both strands (Watson and Crick) downstream of the *RTS1* barrier site due to the restart. The Pol δ/δ bias describes the time needed for the restart as well as the speed of the restarted fork relative to the canonical convergent fork from late replication origin[26]. Based on the Pol δ/δ bias (Fig. 1c), we estimated that, when compared to *WT* (*nup132+*) cells, only 60% of the expected number of forks were arrested and restarted in *nup132Δ* cells, while the remaining 40% were either not arrested or were arrested and did not restart before being rescued by an incoming leftward moving canonical fork. The increase in Pol ε usage on the Crick strand for ~10 Kb downstream of the *RTS1* barrier is indicative of this latter scenario (Fig. 1b). Remarkably, this fork-restart defect is consistent with our previous estimation using a proxy-restart assay that exploits the mutagenic DNA synthesis to provide a genetic readout of RDR efficiency. Using this proxy assay we reported a nearly two-fold reduction in RDR efficiency in *nup132Δ* cells compared to *WT*[15]. Finally, the relative slope of the Pol δ/δ bias disappearance over distance was similar between the two replicates from *nup132Δ* cells and the *WT* strain, indicating that the forks that succeeded to restart progress with similar speed (Fig. 1c).

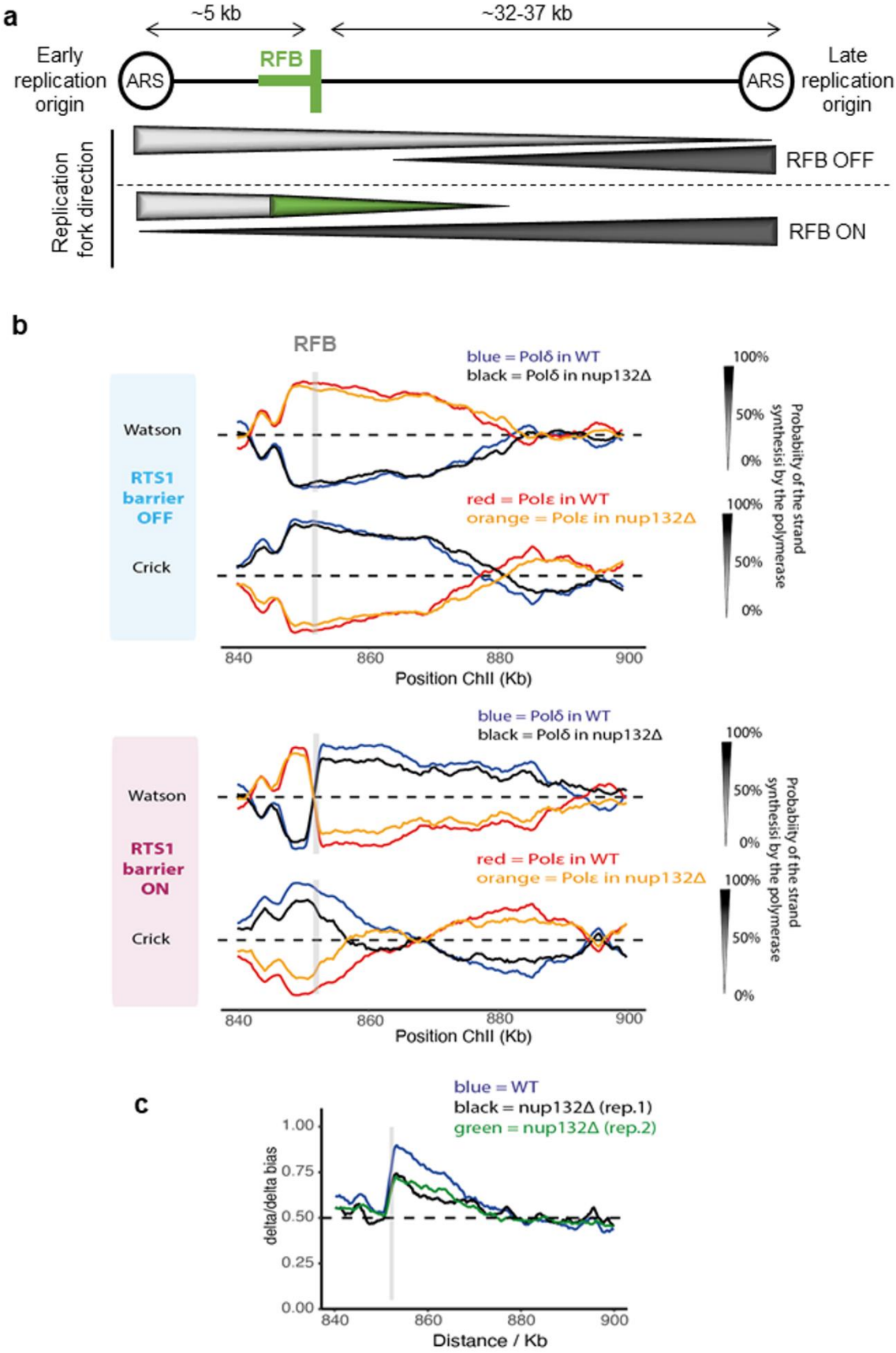
a
~5 kb
~32-37 kb
Early replication origin
ARS
RFB
ARS
Late replication origin
Replication fork direction
RFB OFF
RFB ON
b
RFB
blue = Polδ in WT
black = Polδ in nup132Δ
red = Polε in WT
orange = Polε in nup132Δ
Watson
RTS1 barrier OFF
Crick
100%
50%
0%
Probability of the strand synthesisi by the polymerase
840
860
880
900
Position ChII (Kb)
Watson
RTS1 barrier ON
Crick
c
blue = WT
black = nup132Δ (rep.1)
green = nup132Δ (rep.2)
delta/delta bias
1.00
0.75
0.50
0.25
0.00
Distance / Kb

Figure 1: Ulp1-associated NPC promotes the dynamic of recombination-mediated fork restart

a. Schematic of the *RTS1*-RFB locus on chromosome II. The position of the *RTS1*-RFB is indicated as green thick bars. The directional RFB blocks the progression of right-moving forks that initiate from the left autonomously replicating sequence (ARS). The direction of unperturbed (RFB OFF) and perturbed replication (RFB ON) forks is indicated by the thickness of arrows underneath. Light and dark gray bars indicate the progression of canonical right and left-moving fork, respectively. The green bar indicates the progression of restarted replication mediated by homologous recombination.

b. Pu-Seq traces of the ChrII locus in *RTS1*-RFB OFF (top panel) and ON (bottom panel) condition in *WT* and *nup132Δ* strains. The usage of Pol delta (in blue and black for *WT* and *nup132Δ* cells, respectively) are shown on the Watson and Crick strands. The usage of Pol epsilon (in red and orange for *WT* and *nup132Δ* cells, respectively) are shown on the Watson and Crick strands. Note the switch from Pol epsilon to Pol delta on the Watson strand at the RFB site (gray bar) is indicative of a change in polymerase usage on the leading strand in RFB ON condition.

c. Graph of Pol delta/delta bias over both strands (Watson and Crick) around RFB site in WT and two independent replicates of *nup132Δ* strains. The gray bar indicates the position of the *RTS*1-RFB.

The nuclear basket promotes RDR in pre and post-anchoring manner

We next investigated the role of the nuclear basket, the nucleoplasmic extension of the NPC, in dealing with replication stress. The *S. pombe* nuclear basket is composed of 4 non-essential nucleoporins: Nup60 (ScNup60), Nup61 (ScNup2, HsNup50), Nup124 (ScNup1, HsNup153) and Alm1 (ScMlp1/2, HsTPR)[12]. A fifth component is the essential nucleoporin Nup211, a second orthologue of ScMlp1/2 and HsTPR. Some of these components are known to contribute to resistance to DNA damage[32,33]. We confirmed that *alm1Δ* cells were highly sensitive to a wide range of replication-blocking agents and bleomycin-induced DSBs, whereas *nup60Δ* and *nup61Δ* cells exhibited mild sensitivity only to hydroxyurea (HU), a replication inhibitor that depletes dNTP pool (Supplementary Fig. 1a).

To establish if this HU sensitivity correlated with a defect in resuming replication following HU treatment, we arrested cells for 4 hours in 20mM HU and then followed DNA content by flow cytometry upon release into HU-free media. Of the nuclear basket mutants, only *nup61Δ* cells displayed a defect in the recovery from HU-stalled forks, a defect similar to the one previously reported for *nup132Δ* cells[15] (Supplementary Fig. 1b): the *WT* strain reached a G2 DNA content 45 minutes after release, whereas both *nup132Δ* and *nup61Δ* cells exhibited an additional 15 minutes delay. This observation is supported by the analysis of chromosomes by Pulse Field Gel Electrophoresis (PFGE) following release from HU arrest. HU treatment prevented chromosomes from migrating into the gel because of the accumulated replication intermediates (Supplementary Fig. 1c). *WT* chromosomes migrated into the gel and showed approximately twice the intensity of an asynchronous culture, 90 minutes after release, indicating that the *WT* genome was fully duplicated and recovered from HU-stalled forks (Supplementary Fig. 1d). Consistent with the flow cytometry data, only chromosomes from *nup132Δ* and *nup61Δ* cells showed a clear delay in their ability to migrate into the gel and to fully duplicate. This confirms a role for Nup61 in promoting DNA replication upon transient fork stalling by HU.

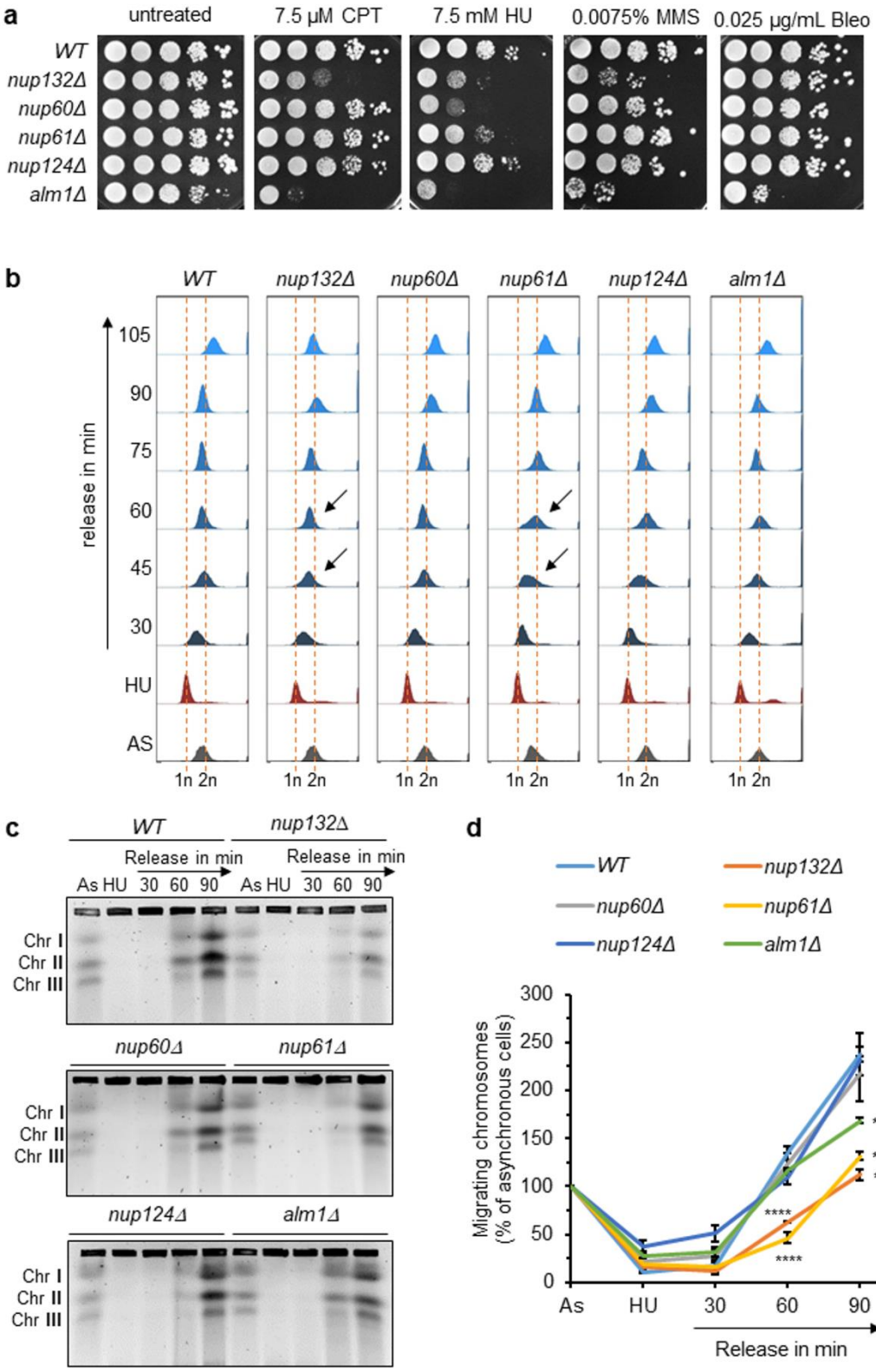
a
untreated
7.5 µM CPT
7.5 mM HU
0.0075% MMS
0.025 µg/mL Bleo
WT
nup132Δ
nup60Δ
nup61Δ
nup124Δ
alm1Δ
b
WT
nup132Δ
nup60Δ
nup61Δ
nup124Δ
alm1Δ
release in min
105
90
75
60
45
30
HU
AS
1n 2n
c
WT
nup132Δ
Release in min
As HU 30 60 90
Chr I
Chr II
Chr III
nup60Δ
nup61Δ
nup124Δ
alm1Δ
d
WT
nup132Δ
nup60Δ
nup61Δ
nup124Δ
alm1Δ
Migrating chromosomes (% of asynchronous cells)
300
250
200
150
100
50
0
As
HU
30
60
90
Release in min
****

Figure S1: Role of the nuclear basket in the recovery from HU-induced stalled forks.

a. Sensitivity of indicated strains to indicated genotoxic drugs. Ten-fold serial dilution of exponential cultures were dropped on appropriate plates. Bleo: bleomycin; CPT: camptothecin; HU: hydroxyurea; MMS: methyl methane sulfonate.

b. Flow cytometry analysis of indicated strains in indicated conditions. Logarithmically growing cells (AS: Asynchronous cells) were exposed to 20 mM HU for 4 hours (HU time point) and then released into fresh, HU-free, rich medium YES at 30°C to monitor S-phase progression at indicated time after release.

c. Analysis of chromosome by pulse field gel electrophoresis (PFGE) in the above mentioned conditions. Representative images of chromosomes migration during PFGE in indicated strains and conditions.

d. Quantification of % of chromosomes migrating into the gel after release from HU block. Values are means of two independent biological replicates ± standard deviation (SD). *p* value was calculated by two-sided Fisher's exact test (**** $p \leq 0.0001$).

To establish the role of the nuclear basket in promoting replication resumption at the RFB, we first measured replication slippage (RS) downstream of *RTS1*, the proxy measure of non-canonical replication resulting from RDR[30]. The absence of Nup60 and Alm1, but not of Nup124 or Nup61, led to a ~2-fold reduction in the frequency of RFB-induced RS, indicating a reduced RDR efficiency (Fig. 2 a-b). Analysis of replication intermediates by bi-dimensional gel electrophoresis (2DGE) showed that fork arrest and the formation of large ssDNA gaps (>100 bp) at the RFB (which are visualized as a specific "tail" DNA structure emanating from arrested fork signal and descending toward the linear arc; see red arrow on Fig. 2c)[28] were both normal in all four non-essential nucleoporin mutants (Fig. 2c-d). This indicates that the controlled degradation of nascent strand and Rad51-dependent fork protection are unaffected. Thus, the RDR defect observed in *nup60Δ* and *alm1Δ* is not related to defects in the early steps of RDR, such as ssDNA gaps formation to Rad51 loading.

We next investigated the ability of the RFB to relocate to the NP. We employed strain harboring a *LacO*-marked RFB, expressing LacI-mCherry and an endogenously GFP-tagged Npp106, a component of the inner ring complex of NPCs, to mark the NP (Fig.2e-f). We counted co-localization events between the NP and the *LacO*-marked RFB, visualized by a LacI-mcherry focus (see white arrows on Fig. 2f), as previously reported[15]. When the RFB was inactive (RFB OFF), LacI-foci co-localized with the NP in ~45 % of S-phase cells (Fig. 2g). Upon activation of the RFB (RFB ON), the *LacO*-marked RFB was more often (~70 %) localized at the NP in *WT* cells, as previously reported (REF). This shift of the active RFB to the NP was observed in all nuclear basket mutants with the exception of *alm1Δ* (Fig. 2g). The *nup61Δ* cells exhibited a slight increase in the frequency of co-localization in RFB OFF condition but reached a similar enrichment at the NP than *WT* cells in RFB ON condition. Thus, Alm1 and Nup60 promote RDR in a pre- and post-anchoring manner, respectively.

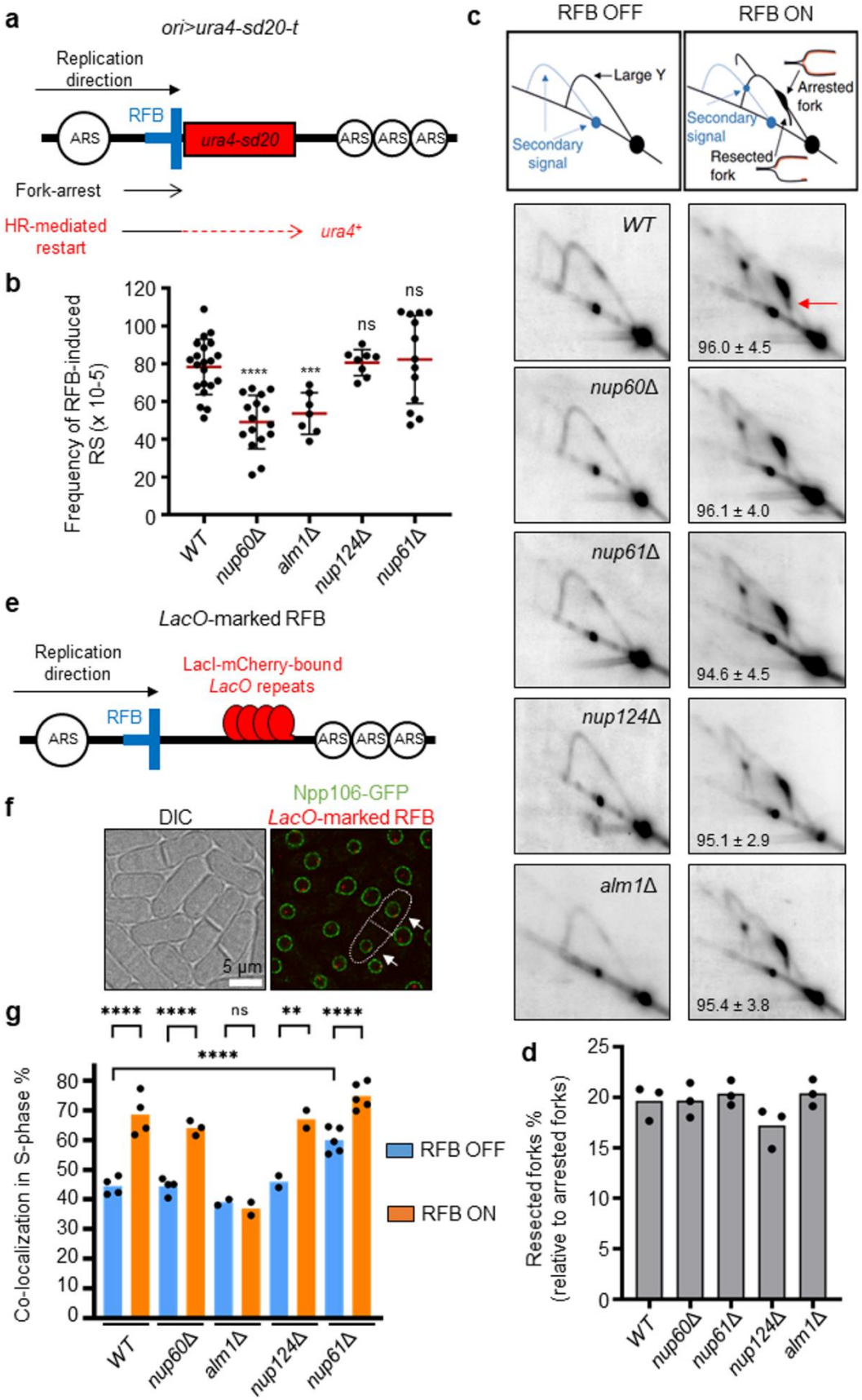
a
ori>ura4-sd20-t
Replication direction
RFB
ARS
ura4-sd20
ARS
ARS
ARS
Fork-arrest
HR-mediated restart
ura4+
b
Frequency of RFB-induced RS (x 10-5)
120
100
80
60
40
20
0
****
***
ns
ns
WT
nup60Δ
alm1Δ
nup124Δ
nup61Δ
c
RFB OFF
RFB ON
Large Y
Secondary signal
Arrested fork
Secondary signal
Resected fork
WT
96.0 ± 4.5
nup60Δ
96.1 ± 4.0
nup61Δ
94.6 ± 4.5
nup124Δ
95.1 ± 2.9
alm1Δ
95.4 ± 3.8
d
Resected forks %
(relative to arrested forks)
25
20
15
10
5
0
WT
nup60Δ
nup61Δ
nup124Δ
alm1Δ
e
LacO-marked RFB
Replication direction
LacI-mCherry-bound LacO repeats
RFB
ARS
ARS
ARS
ARS
f
DIC
Npp106-GFP
LacO-marked RFB
5 µm
g
**** **** ns ** ****
****
Co-localization in S-phase %
80
70
60
50
40
30
20
10
0
RFB OFF
RFB ON
WT
nup60Δ
alm1Δ
nup124Δ
nup61Δ

Figure 2: The nuclear basket promotes Recombination-dependent replication in pre- and post-anchoring manner.

a. Diagram of the *ori*>*ura4-sd20-t* construct on chromosome III (ori: replication origin, >: *RTS1*-RFB orientation that block right-moving forks, t: telomere). The non-functional *ura4-sd20* allele (red bar), containing a 20-nt duplication flanked by micro-homology, is located downstream of the RFB (blue bar). During HR-mediated fork restart, the *ura4-sd20* allele is replicated by an HR-associated DNA synthesis that is liable to replication slippage (RS) resulting in the deletion of the duplication and the restoration of a functional *ura4*$^{+}$ gene[30]. ARS: autonomously replicating sequence.

b. Frequency of RFB-induced RS in indicated strains and conditions. Each dot represents one sample from independent biological replicate. Red bars indicate mean values ± standard deviation (SD). *p* value was calculated by two-sided t-test (**** *p* ≤0.0001; *** p≤0.001 ns: non-significant).

c. Top panel: scheme of replication intermediates (RI) analyzed by neutral-neutral 2DGE of the *AseI* restriction fragment in RFB OFF and ON conditions. Partial restriction digestion caused by psoralen-crosslinks results in a secondary arc indicated on scheme by blue dashed lines. Bottom panels: representative RI analysis in indicated strains and conditions. The *ura4* gene was used as probe. Numbers indicate the % of forks blocked by the RFB ± standard deviation (SD). The red arrow indicates the tail signal resulting from resected forks.

d. Quantification of resected forks in indicated strains Dots represent values obtained from independent biological experiments. No statistical difference was detected between samples.

e. Diagram of the *LacO*-marked RFB**.** *LacO* arrays bound by mCherry-LacI (red ellipses) are integrated ~7 kb away from the *RTS1*-RFB (blue bar).

f. Example of fluorescence (right panel) and bright-field images (left panel) cells expressing the endogenous Npp106-GFP fusion protein and harboring the *LacO*-marked RFB. Mono-nucleated cells and septated bi-nucleated cells correspond to G2 and S-phase cells, respectively. White arrows indicate co-localization events in S-phase cells. Scale bare: 5µm.

g. Quantification of co-localization events in S-phase cells in indicated conditions and strains. Dots represent values obtained from independent biological experiments. At least 100 nuclei were analyzed for each strain and condition. Fisher's exact test was used for group comparison to determine the *p* value (****p≤0.0001; ** p≤0.01; ns: non-significant).

The nuclear basket promotes the sequestration of Ulp1 at the nuclear periphery.

In budding yeast, several components of the nuclear basket are critical for peripheral Ulp1 localization. This includes Nup60 and the synergistic action of Mlp1 and Mlp2[34,35]. We thus investigated the expression and the nuclear sub-localization of Ulp1 in the absence of a functional nuclear basket. Ulp1 was C-terminally tagged with GFP and tested for functionality (Supplementary Fig. 2a). We observed that, in the background of either a *nup60Δ* or *a nup132Δ* mutant, Ulp1-GFP levels were largely abrogated whereas a ~75 % and ~60 % reduction was observed in *nup124Δ* and *alm1Δ* backgrounds, respectively (Fig. 3a). Inhibiting the proteasome activity by treating cells with bortezomib, a proteasome inhibitor[36], partly restored Ulp1-GFP protein level in *nup132Δ* and *nup60Δ* cells, similarly to previous finding in budding yeast[34]. However, the sequestration of Ulp1-GFP at the NP was not restored (Supplementary Fig. 2b-c).

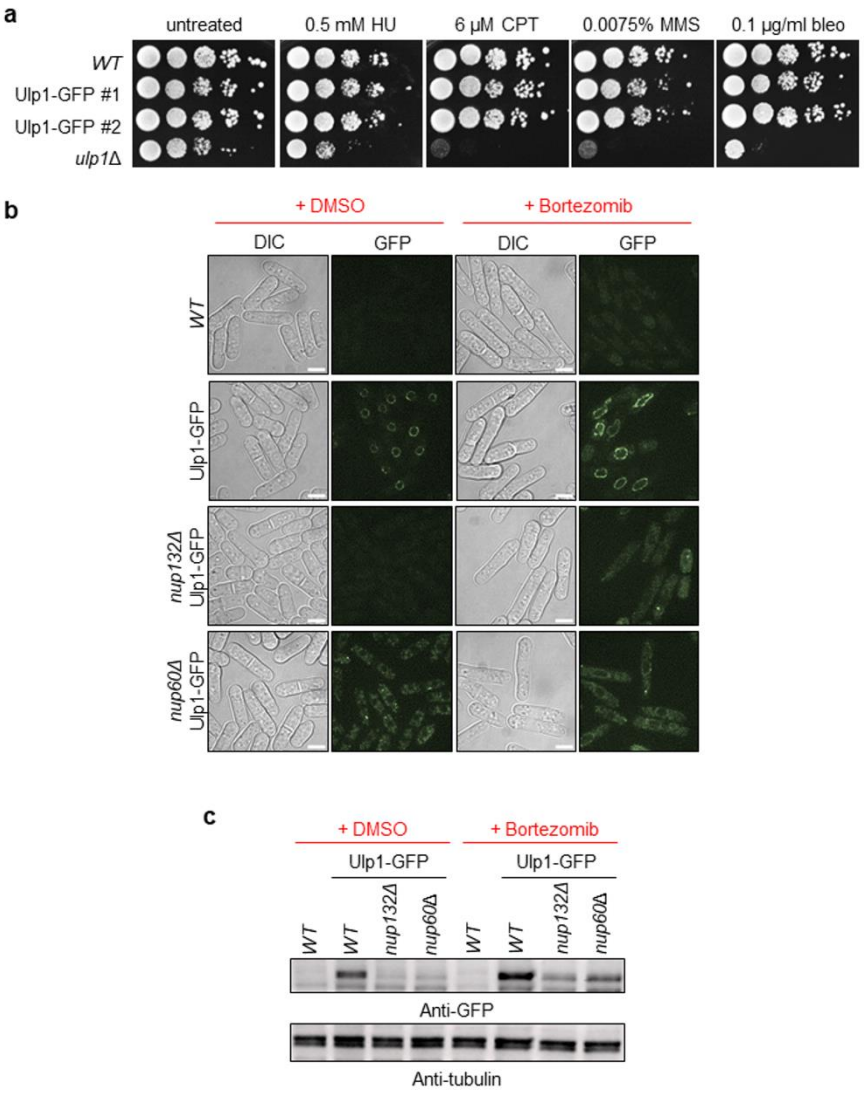

Figure S2: The down-regulation of Ulp1 expression is caused by the proteasome.

a. Ulp1-GFP is a functional fusion protein. Ten-fold serial dilution of exponential cultures were dropped on appropriate plates. Bleo: bleomycin; CPT: camptothecin; HU: hydroxyurea; MMS: methyl methane sulfonate.

b. Cell imaging of Ulp1-GFP in indicated strains and conditions. Representative cell images of Ulp1-GFP in indicated strains in presence or absence of bortezomib. Scale bar: 5µm.

c. Expression of Ulp1-GFP in indicated strains and conditions. An untagged WT strain was included as control for antibody specificity. Tubulin was used as loading control.

In *S. pombe*, the delocalization of Ulp1 leads to the degradation of SUMO chain-modified Pli1, an E3 SUMO ligase, resulting in a global decrease of SUMO conjugates[37]. Consistent with Ulp1 expression being severely lowered and delocalized from the NP in *nup132Δ* and *nup60Δ* (Fig. 3a-b and Supplementary Fig. 2b), we observed a global reduction in the accumulation of SUMO conjugates in these mutants, compared to *WT* (Fig. 3b). We noticed that the pattern of SUMO conjugates in *nup132Δ* and *nup60Δ* backgrounds was similar to the one observed in the strain expressing SUMO-KallR, in which all internal lysines are mutated to arginines to prevent SUMO chains formation[15]. The accumulation of SUMO conjugates was more adversely affected by the absence of Pli1 than in the *nup132Δ* and *nup60Δ* cells, suggesting that Pli1 conserved some activity in these genetic backgrounds, as previously reported for *nup132Δ* cells[15]. Consistent with Ulp1 expression being moderately in the absence of Nup61 or Nup124, the accumulation and the pattern of SUMO conjugates were less affected (Fig. 3b).

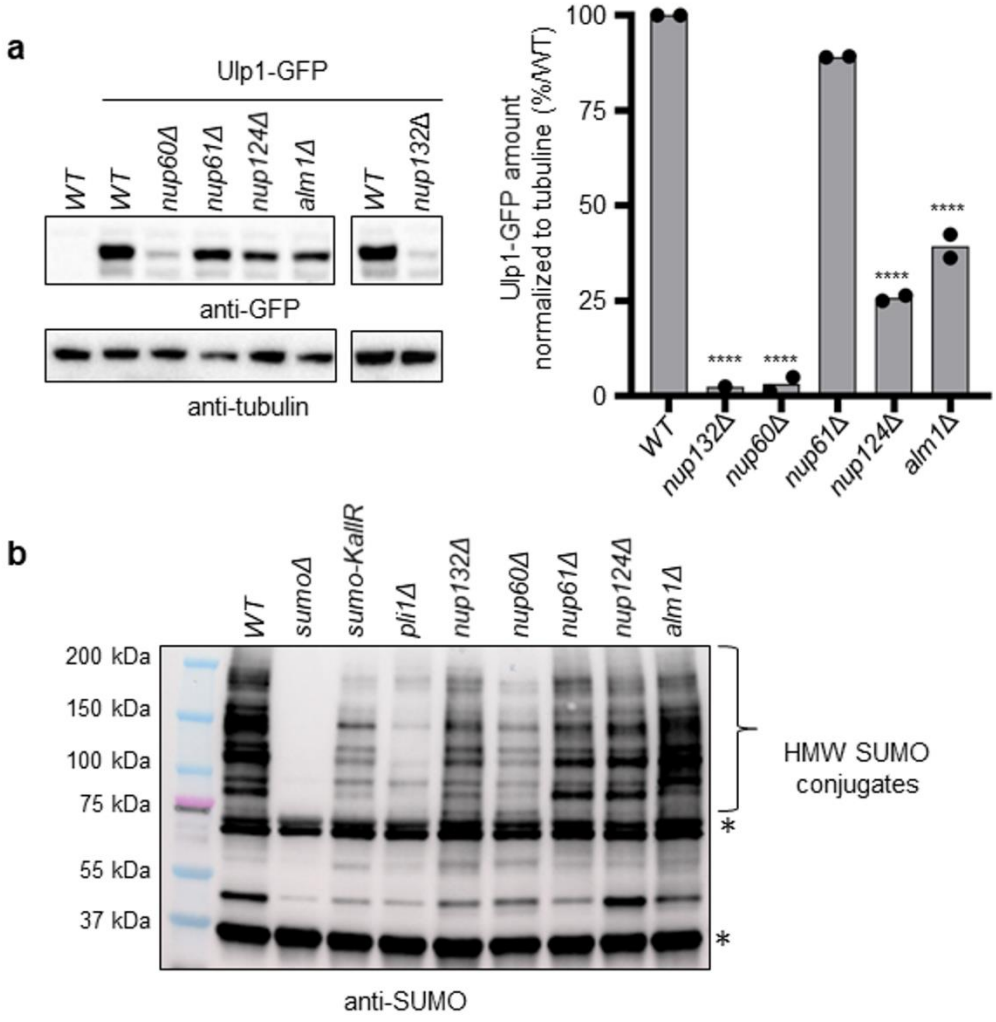

Figure 3: The nuclear basket regulates the expression of the SUMO SENP protease Ulp1

a. Left panel: expression of Ulp1-GFP in indicated strains. An untagged *WT* strain was included as control for antibody specificity. Tubulin was used as loading control. Right panel: quantification. The normalized amount of Ulp1 was calculated by dividing the GFP signal by tubulin signal. The normalized amount of Ulp1-GFP in mutants was indicated as a percentage of the *Wild type*. Dots represent values obtained from independent biological experiments. *p* value was calculated by two-sided t-test (**** $p \leq 0.0001$).

b. Expression of SUMO conjugates in indicated strains. A strain deleted for *pmt3* gene that encodes the SUMO particle (*sumoΔ*) was added as control for antibody specificity. * indicates unspecific signal.

To better assign the role of the nuclear basket in sequestrating Ulp1 at the NP, we employed a live cell imaging approach to image simultaneously Ulp1 at the NP in *WT* and relevant mutant backgrounds and quantified Ulp1 density at the NP. To ensure accuracy, we mixed an equal amount of exponentially growing *WT* cells expressing Ulp1-GFP with *WT* or nuclear basket mutated cells expressing both Ulp1-GFP and Cut11-mCherry (Fig. 4a). This approach allowed us to distinguish within the same microscopy field *WT* and mutated strains, and thus accurately quantify peripheral Ulp1 irrespective of exposure and acquisition parameters. In addition, as Cut11 is a transmembrane core NPC nucleoporin, we also could quantify the total amount and density of NPCs. As previously reported[38], the nuclear morphology of *alm1Δ* cells was affected compared to *WT*, with an increased in nuclear perimeter and size (Supplementary Fig. 3a). Consistent with our analysis of Ulp1 expression levels (Fig. 3a), the total amount of peripheral Ulp1 decreased in *nup132Δ*, *nup60Δ* and *nup124Δ* cells when compared to *WT* (Supplementary Fig. 3b), resulting in a reduced peripheral Ulp1 density (Fig. 4a-b). Although the total amount of peripheral Ulp1 was slightly increased in *alm1Δ* cells (Supplementary Fig. 3b), the increased nuclear size led to a significant reduction in term of peripheral Ulp1 density (Fig. 4b). The total amount of Cut11 was variable in all strains when compared to *WT* (Supplementary Fig. 3c) but we observed a clear reduction in peripheral Cut11 density in *alm1Δ* cells because of an increased nucleus size (Fig 4c). These defects in NPCs density and nuclear morphology may explain the lack of localization of the RFB at the NP in the absence of Alm1. Finally, we quantified co-localization between Cut11-mCherry and Ulp1-GFP signal as a read-out of Ulp1-associated NPCs, using both Manders overlap coefficient (Fig. 4d-e) and the Pearson coefficient correlation (Supplementary Fig. 3d). As a control, we first assigned co-localization between Cut11-mCherry and Npp106-GFP, two core components of NPCs. Between 80 to 90 % of Cut11 signal was associated with Npp106 under our microscopy conditions, validating our methodological approach (Fig. 4d-e and Supplementary Fig. 3d). In the absence of either Nup132 or Nup60, Ulp1 appeared no longer overlapping with Cut11 at the resolution achieved on the images, indicating that Ulp1-associated NPCs are abolished. Despite a lower NPCs density and a reduced Ulp1 expression in the absence of Alm1, Ulp1-associated NPCs were only moderately affected (~70 % compared to ~75 % in the *WT* background). In contrast, only ~50 % of Cut11 signal was correlated with Ulp1 in *nup124Δ* cells (Fig. 4e and Supplementary Fig. 3d), indicating that Ulp1-associated NPCs are less abundant. We concluded that Nup60 and, to a lesser extent, Nup124, are two key components of the nuclear basket that sequester Ulp1 at the NP.

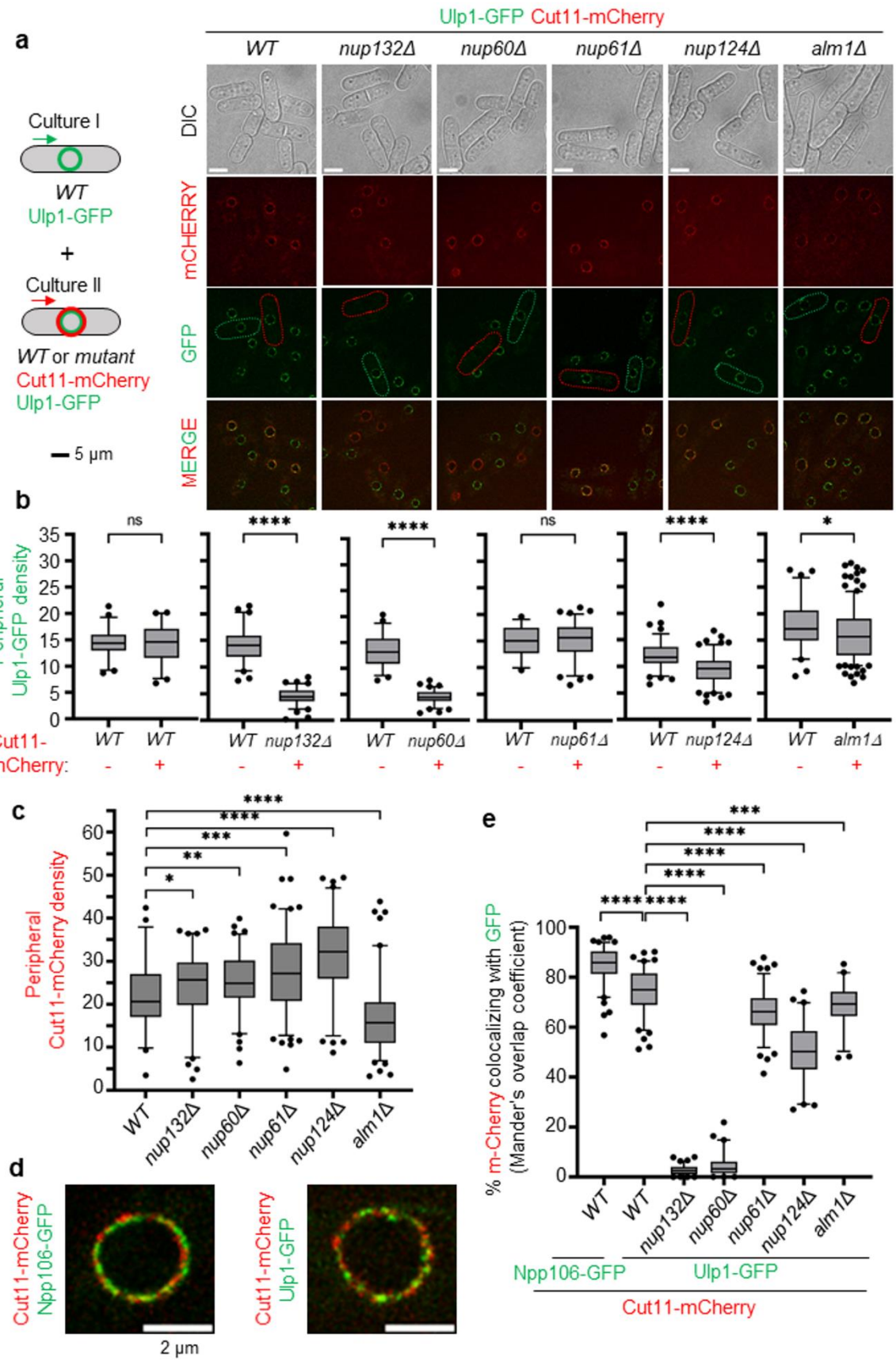
a
Ulp1-GFP Cut11-mCherry
WT
nup132Δ
nup60Δ
nup61Δ
nup124Δ
alm1Δ
DIC
mCHERRY
GFP
MERGE
Culture I
WT
Ulp1-GFP
+
Culture II
WT or mutant
Cut11-mCherry
Ulp1-GFP
5 µm
b
Peripheral Ulp1-GFP density
ns
****
****
ns
****
*
Cut11-mCherry:
WT WT WT nup132Δ WT nup60Δ WT nup61Δ WT nup124Δ WT alm1Δ
c
Peripheral Cut11-mCherry density
WT
nup132Δ
nup60Δ
nup61Δ
nup124Δ
alm1Δ
d
Cut11-mCherry Npp106-GFP
Cut11-mCherry Ulp1-GFP
2 µm
e
% m-Cherry colocalizing with GFP (Mander's overlap coefficient)
Npp106-GFP
Ulp1-GFP
Cut11-mCherry

Figure 4: The nuclear basket contributes to sequester the SUMO SENP protease Ulp1 at the nuclear periphery.

a. Left panel: schema of the strategy employed by equally mixing two genetically distinct cell cultures. Right panel: representative cell images of Cut11-mCherry and Ulp1-GFP in indicated strains. Green and Red cell borders indicate cels from culture I (expressing Ulp1-GFP) and culture II (expressing Ulp1-GFP Cut11-mCherry), respectively. Scale bare 5µm.

b. Box-and-whisker plots of Ulp1-GFP density (mean fluorescence intensity) at the nuclear periphery in indicated strains and conditions. Boxes represent the 25/75 percentile, black lines indicate the median, the whiskers indicate the 5/95 percentile and dots correspond to minimum and maximum values. *p* value was calculated by Mann-Whitney U test (**** $p \leq 0.0001$; *** $p \leq 0.001$; ** $p \leq 0.01$; * $p \leq 0.05$; ns: non-significant). At least 50 nuclei were analyzed for each strain.

c. Box-and-whisker plots of Cut11-mCherry density (mean fluorescence intensity) at the nuclear periphery in indicated strains. Boxes represent the 25/75 percentile, black lines indicate the median, the whiskers indicate the 5/95 percentile and dots correspond to minimum and maximum values. *p* value was calculated by Mann-Whitney U test (**** $p \leq 0.0001$; *** $p \leq 0.001$; ** $p \leq 0.01$; * $p \leq 0.05$; ns: non-significant). At least 50 nuclei were analyzed for each strain.

d. Example of the localization of Npp106-GFP and Cut11-mCherry (left panel) or Ulp1-GFP and Cut11-mCherry (right panel) on overlay images. Scale bare: 2 µm.

e. Box-and-whisker plots of co-localization between Cut11-mCherry and Ulp1-GFP (Mander's overlap coefficient) in indicated strains. The co-localization between the Npp106-GFP, an inner ring nucleoporin of NPC, and Cut11-mCherry, was performed as a control to show maximum correlation between intensities of those both proteins at the resolution achieve on the images. Boxes represent the 25/75 percentile, black lines indicate the median, the whiskers indicate the 5/95 percentile and dots correspond to minimum and maximum values. *p* value was calculated by Mann-Whitney U test (**** $p \leq 0.0001$; *** $p \leq 0.001$)

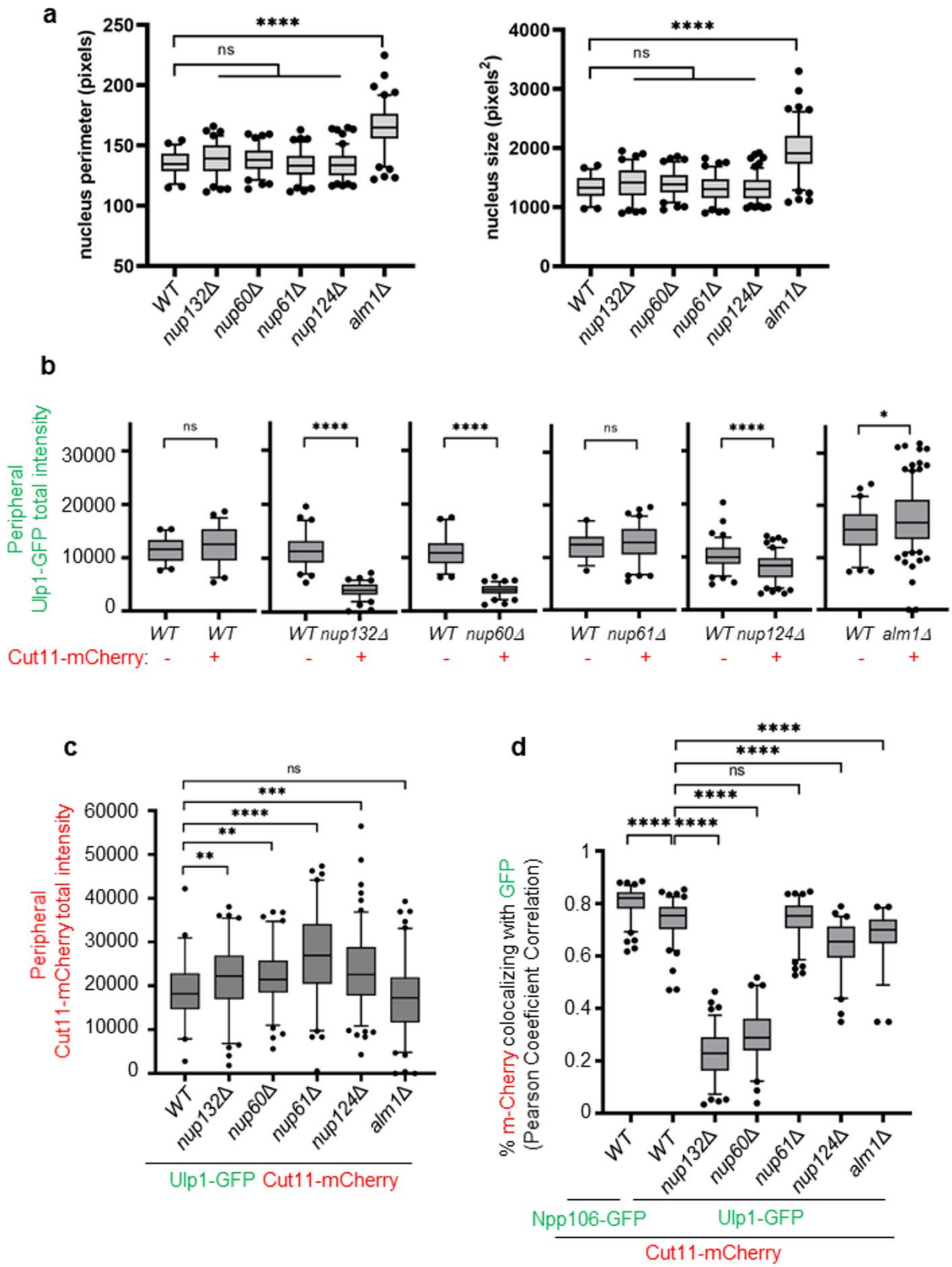
a
nucleus perimeter (pixels)
250
200
150
100
50
****
ns
WT
nup132Δ
nup60Δ
nup61Δ
nup124Δ
alm1Δ
nucleus size (pixels²)
4000
3000
2000
1000
0
****
ns
b
Peripheral Ulp1-GFP total intensity
30000
20000
10000
0
ns
****
****
ns
****
*
WT WT WT nup132Δ WT nup60Δ WT nup61Δ WT nup124Δ WT alm1Δ
Cut11-mCherry: - + - + - + - + - + - +
c
Peripheral Cut11-mCherry total intensity
60000
50000
40000
30000
20000
10000
0
ns
***
****
**
**
WT
nup132Δ
nup60Δ
nup61Δ
nup124Δ
alm1Δ
Ulp1-GFP Cut11-mCherry
d
% m-Cherry colocalizing with GFP (Pearson Coeficient Correlation)
1
0.8
0.6
0.4
0.2
0
****
****
ns
****
****
****
WT
WT
nup132Δ
nup60Δ
nup61Δ
nup124Δ
alm1Δ
Npp106-GFP
Ulp1-GFP
Cut11-mCherry

Figure S3: Image quantification of nuclear morphology parameters, Ulp1-GFP and Cut11-mCherry intensity.

a. Box-and-whisker plots of nucleus perimeter (left panel) and nucleus size (right panel) in indicated strains. Boxes represent the 25/75 percentile, black lines indicate the median, the whiskers indicate the 5/95 percentile and dots correspond to minimum and maximum values. *p* value was calculated by Mann-Whitney U test (**** $p \leq 0.0001$; ns: non-significant). At least 50 nuclei were analyzed for each strain.

b. Box-and-whisker plots of Ulp1-GFP total intensity (raw integrated density) at the nuclear periphery in indicated strains and conditions. Boxes represent the 25/75 percentile, black lines indicate the median, the whiskers indicate the 5/95 percentile and dots correspond to minimum and maximum values. *p* value was calculated by Mann-Whitney U test (**** $p \leq 0.0001$; * $p \leq 0.05$; ns: non-significant). At least 50 nuclei were analyzed for each strain.

c. Box-and-whisker plots of Cut11-mCherry total intensity (raw integrated density) at the nuclear periphery in indicated strains and conditions. Boxes represent the 25/75 percentile, black lines indicate the median, the whiskers indicate the 5/95 percentile and dots correspond to minimum and maximum values. *p* value was calculated by Mann-Whitney U test (**** $p \leq 0.0001$; *** $p \leq 0.001$; ** $p \leq 0.01$; ns: non-significant). At least 50 nuclei were analyzed for each strain.

d. Box-and-whisker plots of co-localization between Cut11-mCherry and Ulp1-GFP (using the Pearson correlation coefficient) in indicated strains. The co-localization between the Npp106-GFP, an inner ring nucleoporin of NPC, and Cut11-mCherry, was performed as a control to show maximum correlation between intensities of those both proteins at the resolution achieve on the images. Boxes represent the 25/75 percentile, black lines indicate the median, the whiskers indicate the 5/95 percentile and dots correspond to minimum and maximum values. *p* value was calculated by Mann-Whitney U test (**** $p \leq 0.0001$; ns: non-significant). At least 50 nuclei were analyzed for each strain.

In budding yeast, Mlp1 and Mlp2 act synergistically to spatially localized Ulp1 to the NP[35]. We therefore addressed the role of the second TPR orthologue, Nup211 that is an essential nucleoporin in *S. pombe*. We thus employed an auxin-inducible degron (AID) approach using the recently developed AID2 version that makes use of OsTIR1-F74A to target AID-tagged proteins for degradation[39]. Nup211-HA-mAID was efficiently degraded 30 minutes after addition of 5-adamantyl-IAA and no degradation was observed in the absence of TIR1-F74A (Supplementary Fig. 4a). We observed a ~40 % reduction in Ulp1-GFP expression 60 minutes after 5-adamantyl-IAA addition, compared to the control strain in which TIR1-F74A is not expressed (compared lines 3 and 4 on Supplementary Fig. 4b). However, we noticed that Ulp1-GFP expression was slightly decreased in the strain expressing TIR1-F74A in the absence of 5-adamantyl-IAA (compared lines 1 and 2 on Supplementary Fig. 4b). Consistently with this, these strains showed a significant growth defect when plated on media free of drug (Supplementary Fig. 4c), indicating that either the AID2 system applied to Nup211 is leaky or that the C-terminal degron tag partially compromised Nup211 function. When we quantified peripheral Ulp1-GFP by live-cell imaging, we observed that the addition of 5-adamantyl-IAA led to an increased density of peripheral Ulp1 in *WT* cells and no changes were observed upon degradation of Nup211 (Supplementary Fig. 4d). We concluded that Nup211 makes little contribution to Ulp1 expression and peripheral sequestration. We wanted to test the possibility that Alm1 and Nup211 act synergistically to regulate Ulp1 expression and localization, but we failed in generating viable spores combining *alm1* deletion with the *nup211-HA-mAID* locus.

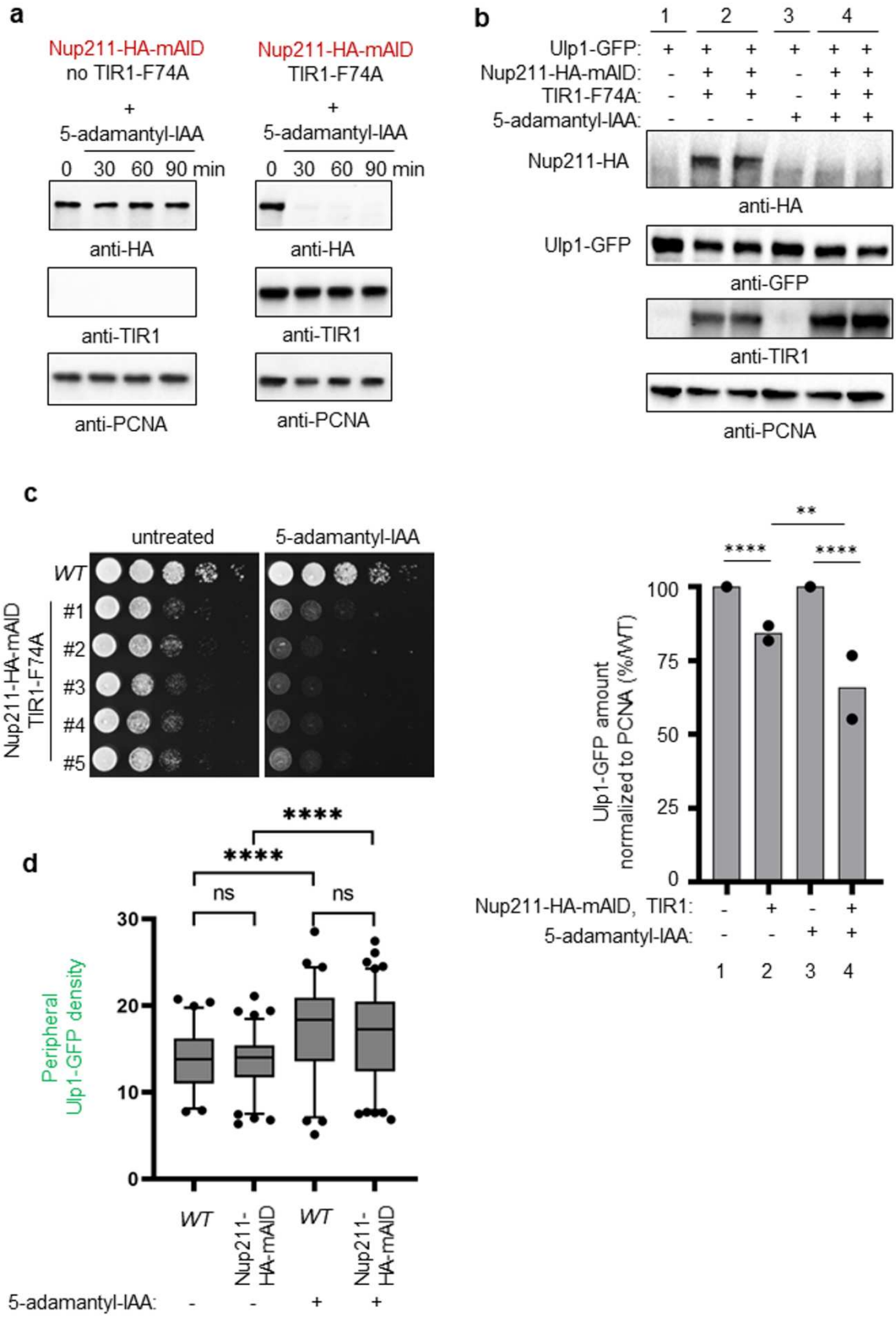
a
Nup211-HA-mAID
no TIR1-F74A
+
5-adamantyl-IAA
0 30 60 90 min
anti-HA
anti-TIR1
anti-PCNA
Nup211-HA-mAID
TIR1-F74A
+
5-adamantyl-IAA
0 30 60 90 min
anti-HA
anti-TIR1
anti-PCNA
b
1 2 3 4
Ulp1-GFP: + + + + + +
Nup211-HA-mAID: - + + - + +
TIR1-F74A: - + + - + +
5-adamantyl-IAA: - - - + + +
Nup211-HA
anti-HA
Ulp1-GFP
anti-GFP
anti-TIR1
anti-PCNA
c
untreated
5-adamantyl-IAA
WT
Nup211-HA-mAID TIR1-F74A
#1
#2
#3
#4
#5
**
****
****
Ulp1-GFP amount normalized to PCNA (%WT)
100
75
50
25
0
Nup211-HA-mAID, TIR1: - + - +
5-adamantyl-IAA: - - + +
1 2 3 4
d
****
****
ns
ns
Peripheral Ulp1-GFP density
30
20
10
0
WT
Nup211-HA-mAID
WT
Nup211-HA-mAID
5-adamantyl-IAA: - - + +

Figure S4: An auxin-induced degron approach to conditionally downregulate Nup211

a. Expression of Nup211-HA-mAID fusion protein in strain expressing TIR1-F74A (right panels) or not (left panel) as a function of time (in minute) upon addition of 5-adamentyl-IAA. PCNA was used as loading control.

b. Top panels: expression of Ulp1-GFP, Nup211-HA-mAID and TIR1 in indicated conditions. PCNA was used as loading control. Bottom panel: quantification. Dots represent values obtained from independent biological experiments. The normalized amount of Ulp1 was calculated by dividing the GFP signal by PCNA. The normalized amount of Ulp1-GFP in mutants was indicated as a percentage of the wild type . *p* value was calculated by two-sided Fisher's exact test (**** $p \leq 0.0001$; ** $p \leq 0.01$).

c. Cell growth assay of indicated strains. Ten-fold serial dilution of exponential cultures were dropped on plate containing 5-adamantyl-IAA (right panel) or not (left panel). Five independent clones expressing Nup211-HA-mAID were tested alongside *WT* strain. Note the cell growth defect of Nup211-HA-mAID strains in the absence of 5-adamantyl-IAA is indicative of lack of Nup211 functionality.

d. Box-and-whisker plots of Ulp1-GFP density (mean fluorescence intensity) at the nuclear periphery in indicated strains and conditions. Boxes represent the 25/75 percentile, black lines indicate the median, the whiskers indicate the 5/95 percentile and dots correspond to minimum and maximum values. *p* value was calculated by Mann-Whitney U test (**** $p \leq 0.0001$; ns: non-significant). At least 50 nuclei were analyzed for each strain.

Restoring Ulp1-associated NPCs rescues RDR defect in *nup60Δ* whereas RDR defect in *alm1Δ* is not caused by the lack of shift to NP.

We previously established that SUMO chains trigger relocation of the RFB to NP but are also a source of toxicity that impedes HR-mediated DNA synthesis at arrested forks in the absence of Nup132[15]. Thus, when the active RFB shifts to the NP but Ulp1 is no longer recruited at NPCs to degrade SUMO conjugates, RDR is impeded. To test if the same scenario occurs in the absence of Nup60, we employed a previously successful approach to tether Ulp1-LexA to the RFB harboring 8 LexA binding sites (either *t-LacO-ura4:LexBS<ori* for nuclear positioning (Fig. 5a) or *t-ura4-sd20:lexA<ori* for RFB-induced RS[15] (Fig. 5a). In *WT* cells, the *LacO*-marked RFB was constitutively enriched at the NP upon expression of Ulp1-LexA, whatever its activity (OFF or ON), showing that Ulp1 is successfully tethered to the RFB (Fig. 5a). Consistent with the role of Nup60 in sequestrating Ulp1 at the NP, the inactive RFB did not shift to NP in *nup60Δ* cells, but was efficiently enriched at the NP in RFB ON condition, confirming that Ulp1 is not necessary for anchorage (Fig. 5a). Remarkably, tethering Ulp1-LexA to the active RFB, anchored to NPCs, resulted in an increased frequency of RFB-induced RS in *nup60Δ* cells, indicating that the lack of Ulp1-associated NPCs is a limiting step in promoting HR-mediated DNA synthesis (Fig 5b). In addition, we combined the *nup60* deletion with SUMO-KallR, which allows only mono-SUMOylation to occur, resulting in a profound reduction of global SUMO-conjugates (Fig. 3b). As previously reported[15], we observed a slight increase in RFB-induced RS in SUMO-KallR strain, indicating that SUMO chains limits RDR efficiency (Fig. 5c). As expected, preventing SUMO chains in *nup60Δ* cells restored RFB-induced RS to *WT* level, further confirming that Ulp1-associated NPCs are required to overcome the inhibitory effect of SUMO chains on HR-mediated DNA synthesis (Fig 5c).

Surprisingly, applying similar approaches to *alm1Δ* cells resulted in different outcomes, indicating a distinct scenario of RDR defect. Preventing SUMO chains formation did not rescue the RDR defect observed in the absence of Alm1 (compared *alm1Δ* and *alm1Δ* SUMO-KallR on Fig. 5d), indicating that this mutant does not suffer from the toxicity of SUMO chains against HR-mediated DNA synthesis. Moreover, tethering Ulp1 to the RFB did not rescue the RDR defect (Fig. 5b). The analysis of the nuclear positioning of the *LacO*-marked RFB showed that the RFB was efficiently shifted to the NP in *alm1Δ* cells whether the RFB was active or not, thus allowing bypassing the role of Alm1 in locating the active RFB at the NP (compare RFB ON condition with or without Ulp1-LexA in *alm1Δ* on Fig. 5a). In other words, the artificial anchorage of the RFB to Ulp1-associated NPCs is not sufficient to rescue the RDR defect of *alm1Δ* cells. This indicates that the lack of RFB relocation to NP is not the underlying cause of the RDR defect and

that Alm1 is probably required at NPCs to promote RDR in a SUMO chains-independent manner. Interestingly, Daga and colleagues have reported that Alm1 is required for proper localization of the proteasome to the NE. Several proteasomal subunits and anchor, such as Mts2, Mts4 and Cut8, are no longer properly localized at the NP in *alm1Δ* cells[38]. Interestingly, we previously proposed that RFB relocation to NPCs allows also access to proteasome to promote RDR[15]. Given the technical difficulty to restore a stoichiometric proteasome at the NP in *alm1Δ* cells, we turned our attention to a viable proteasome mutant to address its role in the dynamic of RDR.

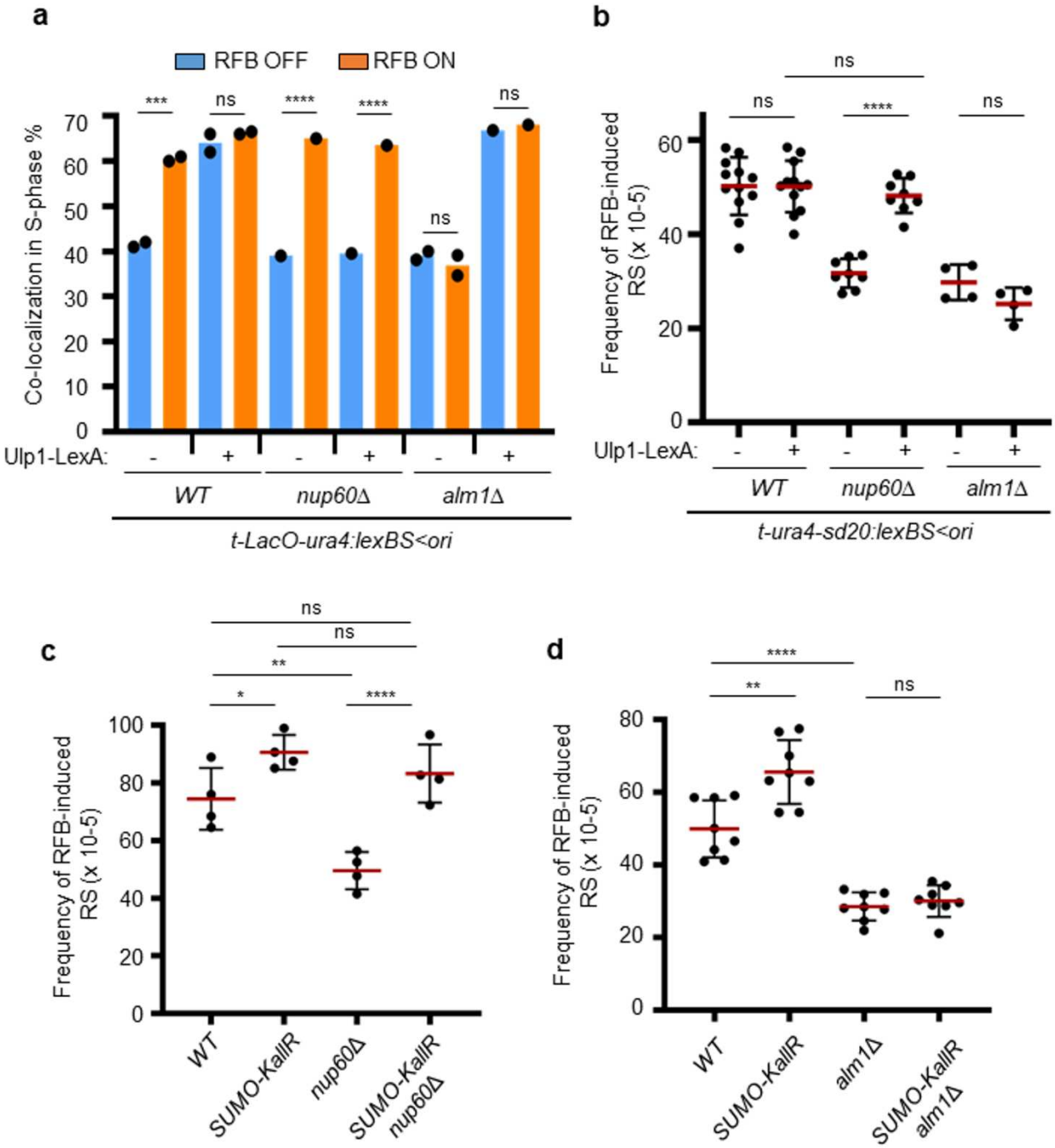
a
RFB OFF
RFB ON
Co-localization in S-phase %
Ulp1-LexA:
WT
nup60Δ
alm1Δ
t-LacO-ura4:lexBS<ori
b
Frequency of RFB-induced RS (x 10-5)
Ulp1-LexA:
WT
nup60Δ
alm1Δ
t-ura4-sd20:lexBS<ori
c
Frequency of RFB-induced RS (x 10-5)
WT
SUMO-KallR
nup60Δ
SUMO-KallR nup60Δ
d
Frequency of RFB-induced RS (x 10-5)
WT
SUMO-KallR
alm1Δ
SUMO-KallR alm1Δ

Figure 5: Restoring Ulp1-associated NPCs rescues RDR defect in *nup60Δ* but not in *alm1Δ*

a. Quantification of co-localization events in S-phase cells in indicated conditions and strains. Dots represent values obtained from independent biological experiments. At least 100 nuclei were analyzed for each strain and condition. p value was calculated by two-sided Fisher's exact test (**** p≤0.0001; *** p≤0.001; ns: non-significant).

b to c. Frequency of RFB-induced RS in indicated strains and conditions. Dots represent values obtained from independent biological experiments. Red bars indicate mean values ± SD. *p* value was calculated by two-sided t-test **** *p* ≤0.0001; ** p≤0.01,* p≤0.05 ns: non-significant).

Proteasome-associated NPCs sustain the dynamic of HR-restarted forks.

We previously reported that, in the absence of Rpn10, the active RFB shifts to the NP but RDR efficiency was severely decreased[15]. Rpn10 is located at the NP and is a regulatory subunit of the 19S proteasome that physically interacts with Mts4/Rpn1[40–42]. Rpn10 acts as an ubiquitin receptor of the proteasome and its absence results in the accumulation of Ubiquitin conjugates. Despite an accumulation of SUMO conjugates in *rpn10Δ* cells (Fig. 6a), we observed that defect in RFB-induced RS was not rescued by preventing SUMO chains formation (Fig. 6b), indicating a role of the proteasome in promoting RDR independently of counteracting the inhibitory effect of SUMO chains. To probe this function, we applied the Pu-Seq approach to the *rpn10* mutant to compare DNA polymerases usage at the barrier site and further downstream to *WT* profile. Based on the Pol δ/δ bias (Fig. 6c-d), we estimated that, when compared to *rpn10+* cells, approximately 85% of the expected number of forks were arrested and restarted in *rpn10Δ* cells (Fig. 6c). Remarkably, the relative slope of the Pol δ/δ bias disappearance over distance was much steeper in the two replicates from *rpn10Δ* cells than in *WT* strains, indicating a lower speed of restarted forks (Fig. 6d). This slow replication accounts for the increased number of leftward moving canonical forks evident in the Pu-seq traces (Fig. 6c). We estimated that approximately half of the restarted forks move at one third of the speed of *WT* restarted forks. This scenario contrasts with that observed in the *nup132Δ* cells, in which less forks were restarted but the speed of those that did restart was unaffected. We concluded that both the proteasome and Ulp1 are required at the NP to foster the dynamics of HR-mediated DNA synthesis by affecting, respectively, the efficient initiation of restarted DNA synthesis and the speed of the restarted fork.

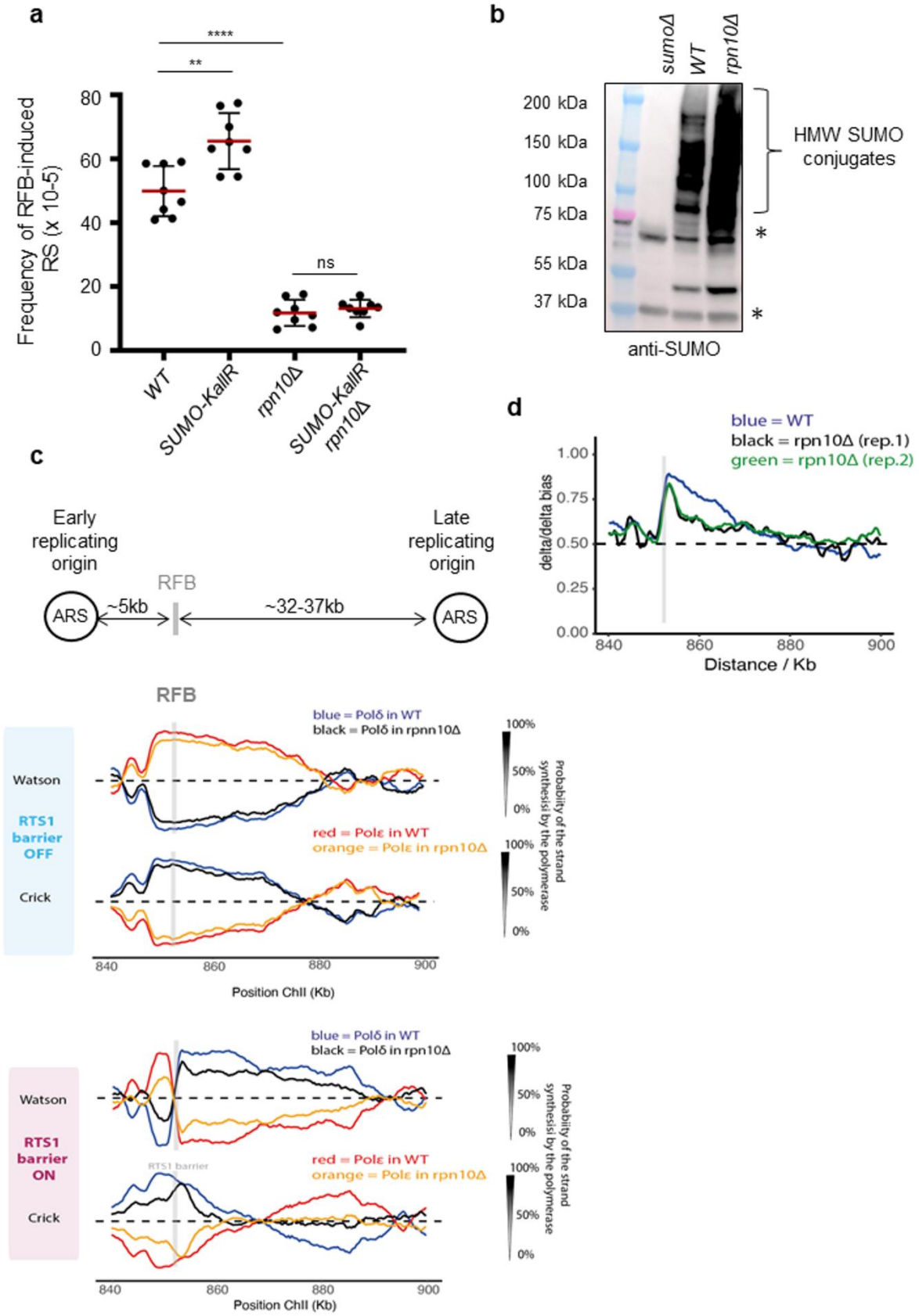
a
****
**
ns
Frequency of RFB-induced RS (x 10-5)
80
60
40
20
0
WT
SUMO-KallR
rpn10Δ
SUMO-KallR rpn10Δ
b
sumoΔ
WT
rpn10Δ
200 kDa
150 kDa
100 kDa
75 kDa
55 kDa
37 kDa
HMW SUMO conjugates
*
*
anti-SUMO
c
Early replicating origin
Late replicating origin
RFB
ARS
~5kb
~32-37kb
ARS
d
blue = WT
black = rpn10Δ (rep.1)
green = rpn10Δ (rep.2)
delta/delta bias
1.00
0.75
0.50
0.25
0.00
840
860
880
900
Distance / Kb
RFB
blue = Polδ in WT
black = Polδ in rpnn10Δ
red = Polε in WT
orange = Polε in rpn10Δ
Watson
RTS1 barrier OFF
Crick
100%
50%
0%
Probability of the strand synthesisi by the polymerase
840
860
880
900
Position ChII (Kb)
blue = Polδ in WT
black = Polδ in rpn10Δ
red = Polε in WT
orange = Polε in rpn10Δ
Watson
RTS1 barrier ON
RTS1 barrier
Crick
100%
50%
0%
Probability of the strand synthesisi by the polymerase
840
860
880
900
Position ChII (Kb)

Figure 6: Proteasome-associated NPCs promote the speed of restarted fork.

a. Frequency of RFB-induced RS in indicated strains and conditions. Dots represent values obtained from independent biological experiments. Red bars indicate mean values ± SD. *p* value was calculated by two-sided t-test (**** $p \leq 0.0001$; ** $p \leq 0.01$; ns: non-significant).

b. Expression of SUMO conjugates in indicated strains. A strain deleted for *pmt3* gene that encodes the SUMO particle (*sumoΔ*) was added as control for antibody specificity. * indicates unspecific signal.

c. Pu-seq traces of the ChrII locus in RTS1-RFB OFF (top panel) and ON (bottom panel) condition in *WT* and *rpn10Δ* strains. The usage of Pol delta (in blue and black for *WT* and *rpn10Δ* cells, respectively) are shown on the Watson and Crick strands. The usage of Pol epsilon (in red and orange for *WT* and *rpn10Δ* cells, respectively) are shown on the Watson and Crick strands. Note the switch from Pol epsilon to Pol delta on the Watson strand at the RFB site (gray bar) is indicative of a change in polymerase usage on the leading strand in RFB ON condition.

d. Graph of Pol delta/delta bias in RFB on condition according to chromosome coordinates in WT and two independent replicates of rpn10Δ strains. The gray bar indicates the position of the *RTS*1-RFB.

Discussion

Halted replication forks are diverted to the NP and can associate with NPC components to engage error-free DNA repair pathways[8,14–21] . How the NPC environment acts mechanistically to foster the dynamic of DNA repair pathways remains an open question. Here, we reveal that NPCs define a particular nuclear compartment that favors the dynamic of HR-dependent DNA synthesis at dysfunctional forks by two distinct mechanisms. The SUMO protease Ulp1 ensures an efficient initiation of restarted DNA synthesis by alleviating the inhibitory effect of SUMO chains. This mechanism requires the sequestration of Ulp1 at the NP, that is coordinated by the Y complex and the nuclear basket nucleoporin Nup60. The second mechanism relies on the ability of the nuclear basket to enrich proteasome component at the NP[38,42], to foster the speed of restarted DNA polymerases. Surprisingly, this last function cannot be bypassed by preventing SUMO chains formation. Moreover, we establish that Ulp1 and the proteasome affect differently the dynamics of HR-mediated DNA synthesis without compensating for each other.

We previously reported that the Y complex nucleoporin Nup132 promotes RDR in a post-anchoring manner, downstream Rad51 loading at dysfunctional forks, by sequestrating the SUMO protease Ulp1 at the NP, whose activity if necessary to alleviate the inhibitory effect of SUMO chains on HR-mediated DNA synthesis[15]. Here, we reveal that the nuclear basket contributes to this pathway. Akin to the budding yeast situation[34], the sequestration of Ulp1 at the NP requires the nuclear basket nucleoporin Nup60. Despite our effort, we could not address without ambiguity the synergistic functions of TPR homologues, Alm1 and Nup211, in the spatial segregation of Ulp1 at the NP. By mapping DNA polymerase usage during HR-dependent fork restart[26], we establish that Ulp1-associated NPCs are necessary to ensure efficient initiation of restarted DNA synthesis that is likely inhibited by Pli1-dependent formation of SUMO chains of unknown targets. In budding yeast, a similar inhibitory effect of SUMO chains on DNA replication initiation at origins has been reported[43]. The MCM helicase and other replication factors were identified as SUMO chains-modified substrates for targeting by the SUMO protease Ulp2 and proteasomal degradation. Although we did not formally address the role of the *S. pombe* Ulp2 in RDR, our data clearly highlight a role for Ulp1-associated NPCs in counteracting the inhibitory effect of SUMO chains on the initiation of restarted DNA synthesis. Docking studies predicted a higher affinity of SpUlp1 towards SUMO particle compared to ScUlp1 that could suggest a more specific role of *S. pombe* Ulp1 in targeting SUMO chains than Ulp2[44]. Moreover, we report that the abundance of Ulp1-associated NPCs is not a limiting

factor in promoting RDR, as their reduction by 40 % in *nup124* cells leads to no noticeable defect in RDR efficiency.

We previously reported that the proteasome, whose activity is enriched at the NP[42], promotes RDR in a post-anchoring manner[15]. The mapping of DNA polymerase usage during HR-dependent fork restart reveals that proteasome defect affects more severely the progression of restarted DNA polymerases, with a reduction of the speed by up to 70 %, than the initiation of restarted DNA synthesis. This contrasts with the role of Ulp1 that contributes only to the initiation of DNA synthesis with no apparent contribution to the dynamic progression of restarted DNA polymerases. This division of labour between the proteasome and the SUMO protease in ensuring the dynamics of HR-dependent fork restart is reinforced by the fact that these activities cannot compensate for each other. Indeed, the artificial tethering of the RFB to NPCs in the *alm1* mutant shows that Ulp1-associated NPCs are insufficient to promote efficient RDR without a functional proteasome at the NP. Moreover, our genetic analysis establish that the role of the proteasome in fostering the speed of restarted DNA synthesis is not related to counteracting the inhibitory effect of SUMO chains. This suggest distinct specificity of the proteasome and Ulp1 towards SUMOylated targets which affect differently the dynamics resumption of DNA synthesis at dysfunctional forks. We do not exclude that SUMO-independent poly-Ubiquitination, targeted by Rpn10 for proteasomal degradation, plays a role in promoting RDR. However, we previously identified that the SUMO Targeted Ubiquitin Ligase (STUbL) Slx8-Rfp1-Rfp2, a family of E3 ubiquitin ligases that targets SUMOylated proteins for degradation[45], promotes both the relocation of dysfunctional forks to NPCs and RDR efficiency in a Pli1-dependent manner[15]. This supports that mono-SUMOylated or chain-free multi-SUMOylated factors are potential targets of a proteasome and Slx8-dependent pathway that ensures the speed of restarted DNA polymerases. SUMO chains-independent function of STUBL have been reported. This includes the relocation of forks collapsed at CAG repeats via mono-SUMOylation recognized by the SUMO interacting motif (SIM) of Slx5[17]. The human STUBL RNF4 was shown to bind the substrate ETV4 mono-SUMOylated on multiple lysines, in a process requiring the multiple SIM domains of RFN4[46].

This work also identifies that in the absence of the nuclear basket nucleoporin Alm1, the RFB was no longer enriched at the NP. To our knowledge, TPR homologues have not been involved in anchoring DNA lesions to NPCs in yeast models. Upon telomeric replication stress, human telomeres relocate to the NP and associate with NPC components, including TPR, to resolve replication defects[19]. Depletion of human TPR is associated with a variety of replication defects and TPR was proposed to coordinate at

NPCs a network of factors involved in RNA metabolism to protect cells from RNA-mediated replication stress[47]. Given the nuclear morphology alterations in the absence of Alm1, we do not favor the hypothesis of a direct involvement of Alm1 in anchoring dysfunctional forks at NPCs. In human cells, the mobility of stressed forks towards the NP requires F-nuclear actin polymerization[8,20], but such mechanism has not been reported in yeasts. Thus, we estimated that, in the absence of Alm1, the RFB must explore a nuclear volume 40 % larger to reach the NP and associate with NPCs which abundance is reduced by one quarter. We therefore favor the hypothesis that the lack of relocation is an indirect effect due to alterations of nuclear morphology.

Overall, this work uncovers two mechanisms by which the NPC environment ensures the dynamic of HR-dependent replication restart, streamlining the need for dysfunctional forks to change nuclear positioning. Ulp1-associated NPCs contribute to efficient initiation of restarted DNA synthesis to engage a Polδ/Polδ DNA synthesis, by counteracting the inhibitory effect of SUMO chain, whereas proteasome-associated NPCs foster the progression of restarted DNA synthesis, in a SUMO chain independent manner. These two functions cannot compensate for each other, are differently required and control distinct dynamics of replication resumption at dysfunctional forks. Moreover, our work indicate that multiple SUMOylated targets are likely engaged to limit HR-dependent DNA synthesis.

Funding and Acknowledgements

The authors thank the Multimodal Imaging Center Imaging Facility of the Institut Curie - CNRS UMS2016 / Inserm US43 / Institut Curie / Université Paris- and the Flow Cytometry Facility of the Orsay site of Institut Curie.

This study was supported by grants from the Institut Curie, the CNRS, the Fondation LIGUE contre le cancer "Equipe Labellisée 2020 (EL2020LNCC/Sal), the ANR grant NIRO (ANR-19-CE12-0023-01). KS has recived a PhD fellowship from the fondation LIGUE contre le cancer and a 4th-year PhD grant from Fondation ARC. KK was supported by the program "Excellence Initiative - Research University" for the University of Wrocław of the Ministry of Education and Science from Poland, under grant number IDN.CBNDR 0320/2020/20. AC acknowledges Wellcome grant 110047/Z/15/Z

The funders had no role in study design, data collection and analysis, the decision to publish, or preparation of the manuscript.

Author contributions

K.K., K.S., K.N., S.C. and K.F. performed the experiments.
K.K. K.S. A.C. and S.A.E.L contributed to experimental design and data analysis.
L.B. provided expertise to perform and analyze cell imaging.
K.N. and A.C provide the expertise to analyse Pu-seq data.
K.K, A.C., K.N., L.B. and S.A.E.L wrote the manuscript.

Declaration of interests

The authors declare no competing interests.

Methods

Standard yeast genetics

Yeast strains used in this work are listed in Table S1. Gene deletion or tagging were performed by classical genetic techniques. To assess the sensitivity of chosen mutants to genotoxic agents, mid log-phase cells were serially diluted and spotted onto plates containing hydroxyurea (HU), methyl methanesulfonate (MMS), campthotecin (CPT), bleomycin (bleo). Strains carrying the *RTS1,* replication fork block sequence were grown in minimal medium EMMg (with glutamate as nitrogen source) with addition of appropriate supplements and 60 µM thiamine (barrier inactive, OFF). The induction of replication fork block was obtained by washing away the thiamine and further incubation in fresh medium for 24 hours (barrier active, ON).

Live cell imaging

For snapshot microscopy, cells were grown in filtered EMMg with or without 60 µM thiamine for 24 hours to exponential phase (RFB OFF and RFB ON), then centrifuged and resuspended in 500 µL of fresh EMMg. 1 µL from resulting solution was dropped onto Thermo Scientific slide (ER-201B-CE24) covered with a thin layer of 1.4 % agarose in filtered EMMg[15]. 21 z-stack pictures (each z step of 200 nm) were captured using a Nipkow Spinning Disk confocal system (Yokogawa CSU-X1-A1) mounted on a Nikon Eclipse Ti E inverted microscope, equipped with a 100x Apochromat TIRF oil-immersion objective (NA: 1.49) and captured on sCMOS Prime 95B camera (Photometrics) operated through MetaMorph® software (Molecular Devices). Confocal images were acquired with GFP and m-Cherry were excited with a 488 nm (Stradus® - Vortran Laser Technology, 150mW) and a 561 nm (Jive™ - Cobolt, 100mW) lasers, respectively. A quad band dichroic mirror (405/488/568/647 nm, Semrock) was used in combination with single band-pass filters of 525/50 or 630/75 for the detection of GFP and m-Cherry respectively. Fluorescence and bright-field 3D images were taken at every 0.3µm over a total of 4.5µm thickness. Exposure time for GFP channel was 500 ms, for mCherry 1000 ms. During the imaging, the microscope was set up at 25°C. For the experiment on Ulp1 and Cut11, the Gataca Live SR module (Müller et al., 2016, Gataca Systems), implemented on the Spinning Disk confocal system, was used to generates super resolution images with lateral image resolution improvement (around 120 nm).

Image analysis

Images were mounted and analyzed with Fiji software[48]. First, the 3D Z series are converted into 2D projection based on maximum intensity values. The quantification of Ulp1 and Cut11 was performed using a homemade macro. The user draw manually

all nuclear ring on the merge images as first step. Then automatically, 3 types of region were created from the manual annotation:

- the nucleus was obtained by enlarging the manual annotation of 3 pixels
- the nucleoplasm was obtained by shrinking the nucleus of 8 pixels
- the nuclear periphery has been extracted from the previous two regions by selecting only those pixels that are not common.

Several measurements were exported for all regions, such as perimeter of nuclei in pixels, area in pixels^2, the fluorescence density of a protein (annotated as "Mean fluorescence intensity" in Fiji: this value represent the Raw Integrated Density measured in the selection and normalized by the area of the same selection) and the total fluorescence intensity of the protein (annotated as "RawIntDen"(Raw Integrated Density) in Fiji: this value represent the sum of all pixels intensities in the selection). To assess the co-localization of Ulp1 and Cut11 proteins, the JACoP plugin[49] was used to study the correlation between the intensities of these two proteins in different NPC mutant strains. Pearson and Manders' coefficients were calculated for each nucleus obtained previously. Before running the analysis, pre-processing was applied (background subtraction using the rolling ball algorithm with a radius of 20 pixels and a Gaussian filter (sigma 1)) to reduce image noise and facilitate detection of the Ulp1 and Cut11 proteins needed to calculate Manders' coefficients. The "Default" thresholding method was used for the detection of Ulp1-GFP and Cut11-mCherry positive signals.

2DGE analysis of replication intermediates

Exponential cells ($2.5x10^9$) were treated with 0.1% sodium azide and subsequently mixed with frozen EDTA (of final concentration at 80 mM). Genomic DNA was crosslinked with trimethyl psoralen (0.01 mg/mL, TMP, Sigma, T6137) added to cell suspensions for 5 min in the dark. Next, cells were irradiated with UV-A (365 nm) for 90 s at a constant flow 50 mM/cm^2. Subsequently, cell lysis was performed by adding lysing enzymes (Sigma, L1412) at concentration 0.625 mg/mL and zymolyase 100 T (Amsbio, 120493-1) at 0.5 mg/mL. Obtained spheroplasts were next embedded into 1 % low melting agarose (InCert Agarose 50123, Lonza) plugs and incubated overnight at 55 ^oC in a digestion buffer with 1 mg/mL of proteinase K (Euromedex EU0090). Then plugs were washed with TE buffer (50 mM Tris, 10 mM EDTA) and stored at 4 ^oC. Digestion of DNA was performed using 60 units per plug of restriction enzyme *Ase*I (NEB, R0526M), next samples were treated with RNase (Roche, 11119915001) and beta-agarase (NEB, M0392L). Melted plugs were equilibrated to 0.3 M NaCl concentration. Replication intermediates were purified using BND cellulose (Sigma, B6385) poured into columns (Biorad, 731-1550)[50]. RIs were enriched in the presence of 1M NaCl 1.8%

caffeine (Sigma, C-8960), precipitated with glycogen (Roche, 1090139001) and migrated in 0.35 % agarose gel (1xTBE) for the first dimension. The second dimension was cast in 0.9 % agarose gel (1xTBE) supplemented with EtBr. Next DNA was transferred to a nylon membrane (Perkin-Elmer, NEF988001PK) in 10x SSC. Finally, membranes were incubated with ^{32}P-radiolabeled *ura4* probe (TaKaRa *Bca*BEST^{TM} Labeling Kit, #6046 and alpha-^{32}P dCTP, Perkin-Elmer, BLU013Z250UC) in Ultra-Hyb buffer (Invitrogen, AM8669) at 42°C. Signal of replication intermediates was collected in phosphor-imager software (Typhoon-trio) and quantified by densitometric analysis with ImageQuantTL software (GE healthcare). The 'tail signal' was normalized to the overall signal corresponding to arrested forks.

Replication slippage assay

The frequency of *ura4+* revertants using *ura4-sd20* allele was performed as follows. 5-FOA (EUROMEDEX, 1555) resistant colonies were grown on plates containing uracil with or without thiamine for 2 days at 30 °C and subsequently inoculated into EMMg supplemented with uracil for 24 h. Then cultures were diluted and plated on EMMg complete (for cell survival) and on EMMg without uracil both supplemented with 60 µM thiamine. After 5-7 days incubation at 30°C colonies were counted to determine the frequency of ura4+ reversion. To obtain the true occurrence of replication slippage by the *RTS1*-RFB, independently of the genetic background, we subtracted the replication slippage frequency of the strain devoid of RFB (considered as spontaneous frequency) from the frequency of the strain containing *the t-ura4sd20<ori* construct, upon expression of Rtf1.

Flow cytometry

Flow cytometry analysis of DNA content was performed as follows[51]: cells were fixed in 70 % ethanol and washed with 50 mM sodium citrate, digested with RNAse A (Sigma, R5503) for 2 hours, stained with 1µM Sytox Green nucleic acid stain (Invitrogen, S7020) and subjected to flow cytometry using FACSCANTO II (BD Biosciences).

Whole protein extract analysis

Aliquots of 1x10^8 cells were collected and disrupted by bead beating in 1 mL of 20 % TCA (Sigma, T9159). Pellets of denatured proteins were washed with 1M Tris pH 8 and resuspended in 2x Laemmli buffer (62.5 mM Tris pH 6.8, 20 % glycerol, 2 % SDS, 5 % β-mercaptoethanol with bromophenol blue). Samples were boiled before being subjected to SDS-PAGE on Mini-PROTEAN TGX Precast Gel 4-15 % (Biorad, 4561086). Western blot using anti-GFP (Roche, 11814460001), anti-HA (Santa Cruz Biotechnology, sc-57592), anti-TIR1 (MBL, PD048), anti-PCNA (Santa Cruz, sc-56) or anti-tubulin (Abcam, Ab6160) antibodies was performed. For the analysis of cellular

patterns of global SUMOylation, whole protein extraction was performed as follows: aliquots of $2x10^8$ cells were collected and resuspended in 400µl of water. The cell suspensions were mixed with 350 µl of freshly prepared lysis buffer (2M NaOH, 7% β-merkaptoethanol) and 350µl of 50% TCA (Sigma, T9159). After spin, pellets were further washed with 1M Tris pH 8 and resuspended in 2x Laemmli buffer (62.5 mM Tris pH 6.8, 20 % glycerol, 2 % SDS, 5 % β-mercaptoethanol with bromophenol blue). Samples were boiled before being subjected to SDS-PAGE on Mini-PROTEAN TGX Precast Gel 4-15 % (Biorad, 4561086). Western blot using anti-SUMO antibody (non-commercial, produced by Agro-Bio) was performed.

Pulse field gel electrophoresis

Yeast cultures were grown to logarithmic phase in rich YES medium to concentration 5 x 10^6/mL, synchronized in 20 mM HU for 4 hours, subsequently released to fresh YES medium. At each time point 20 mL of cell culture was harvested, washed with cold 50 mM EDTA pH 8 and digested with litycase (Sigma, L4025) in CSE buffer (20 mM citrate/phosphate pH 5.6, 1.2 M sorbitol, 40 mM EDTA pH 8). Next cells were embedded into 1% UltraPure™ Agarose (Invitrogen, 16500) and distributed into 5 identical agarose plugs for each time point. Plugs were then digested with Lysis Buffer 1, LB1 (50 mM Tris-HCl pH 7.5, 250 mM EDTA pH 8, 1 % SDS) for 1.5 hour in 55°C and then transferred to Lysis Buffer 2, LB2 (1 % N-lauryl sarcosine, 0.5 M EDTA pH 9.5, 0.5 mg/mL proteinase K) o/n at 55°C. Next day LB2 was change for fresh one and digestion was continued o/n at 55°C. After, plugs were kept at 4°C. To visualize intact chromosomes one set of plugs was run on a Biorad CHEF-DR-III pulse field gel electrophoresis (PFGE) system for 60 h at 2.0 V/cm, angle 120°, 14°C, 1800 s single switch time, pump speed 70 in 1x TAE buffer. Separated chromosomes were stained in ethidium bromide (10 µg/mL) for 30 min, washed briefly in 1x TAE and visualized with UV trans-illuminator.

Pu-Seq

The published protocol[52] was used with minor modifications: size selection was performed using a Blue Pippin (Sage Science). We used *rnh201-RED* instead of *rnh201::kan*[26]. Sequence files were aligned with Bowtie2 and alignment data converted to counts with custom Perl script[52]. Analysis of polymerase usage was performed with custom R script[52].

STATISTICAL ANALYSIS

Quantitative densitometric analysis of Southern-blots after 2DGE was carried using ImageQuant software. The 'tail signal' of resected forks was normalized to the overall signal corresponding to arrested forks.

Quantification of PFGE was performed using ImageJ and presented as % of migrating chromosomes relative to asynchronous profile. Cell imaging was performed using METAMORPH software and processed and analyzed using ImageJ software[48]. The explanation and definitions of values and error bars are mentioned within the figure legends. Most experiments the number of sample is n > 3 obtained from independent experiments to ensure biological reproducibility. For all experiments based on the analysis of cell imaging, the number of nuclei analyzed in mentioned in the figure legends. Statistical analysis was carried using Mann-Whitney U tests, Student's t test and Fischer's exact test.

DATA AVAILABILITY

Data have been deposited to Mendeley data and are available at. The source data underlying Figs 2a, 2c-d, 2b-d, 2g, 3a-b, 4b-c, 4e, 5a-c, and Supplementary Figs 1a, 1c-d, 2a, 2c, 3a-d, 4a-d are provided as a Source Data file. All relevant data are available and further information and requests for reagents and resources should be directed to and will be fulfilled by Dr. Sarah A.E. Lambert (sarah.lambert@curie.fr)

Strain number	Mating type	Genotype	Reference
KK1467	*h-*	*cdc6-L591G rtf1::Nat rnh201-RED:Kan Rura-ChrII RTS1::phleo ura4-D18 ade6-704 leu1-32*	this study
KK1470	*h-*	*cdc6-L591G Nat:ADH1:rtf1 rnh201-RED:Kan Rura-ChrII RTS1::phleo ura4-D18 ade6-704 leu1-32*	this study
KK1473	*h-*	*cdc20-M630F rtf1::Nat rnh201-RED:Kan Rura-ChrII RTS1::phleo ura4-D18 ade6-704 leu1-32*	this study
KK1475	*h-*	*cdc20-M630F Nat:ADH1:rtf1 rnh201-RED:Kan Rura-ChrII RTS1::phleo ura4-D18 ade6-704 leu1-32*	this study
KK1899	*h-*	*nup132::Hygro cdc6-L591G rtf1::Nat rnh201-RED:Kan Rura-ChrII RTS1::phleo ura4-D18 ade6-704 leu1-32*	this study
KK1901	*h-*	*nup132::Hygro cdc6-L591G Nat:ADH1:rtf1 rnh201-RED:Kan Rura-ChrII RTS1::phleo ura4-D18 ade6-704 leu1-32*	this study
KK1903	*h-*	*nup132::Hygro cdc20-M630F rtf1::Nat rnh201-RED:Kan Rura-ChrII RTS1::phleo ura4-D18 ade6-704 leu1-32*	this study
KK1905	*h-*	*nup132::Hygro cdc20-M630F Nat:ADH1:rtf1 rnh201-RED:Kan Rura-ChrII RTS1::phleo ura4-D18 ade6-704 leu1-32*	this study
KK1377	*h+*	*ade6-704 leu1-32 ura4-D18*	this study
KK1557	*h+*	*nup132::Nat ade6-704 leu1-32 ura4-D18*	this study
KK1561	*h+*	*nup60::Hygro ade6-704 leu1-32 ura4-D18*	this study

KK1578	*h-*	*nup61::Hygro ade6-704 leu1-32 ura4-D1*	this study
KK1599	*h-*	*nup124::Hygro ade6-704 leu1-32 ura4-D18*	this study
KK1384	*h+*	*alm1::Hygro ade6-704 leu1-32 ura4-D18*	this study
KK1707	*h+*	*nmt41:rtf1:sup35 ade6-704 leu1-32 t-ura4^{+}<ori (uraR)*	this study
KK931	*h+*	*nup60::Hygro nmt41:rtf1:sup35 ade6-704 leu1-32 t-ura4^{+}<ori (uraR)*	this study
KK953	*h+*	*nup61::Hygro nmt41:rtf1:sup35 ade6-704 leu1-32 t-ura4^{+}<ori (uraR)*	this study
KK1593	*h+*	*nup124::Hygro nmt41:rtf1:sup35 ade6-704 leu1-32 t-ura4^{+}<ori (uraR)*	this study
KK1464	*h-*	*alm1::Hygro nmt41:rtf1:sup35 ade6-704 leu1-32 t-ura4^{+}<ori (uraR)*	this study
KK300	*h+*	*npp106-GFP:Nat arg3::mCherry-LacI nmt41:rtf1:sup35 ade6-704 leu1-32 t-LacO 7,9Kb:Kan:ura4^{+}<ori (uraR)*	Kramarz et al., 2020
KK301	*h+*	*nup60::Hygro npp106-GFP:Nat arg3::mCherry-LacI nmt41:rtf1:sup35 ade6-704 leu1-32 t-LacO 7,9Kb:Kan:ura4^{+}<ori (uraR)*	this study
KK166	*h-*	*nup61::Hygro npp106-GFP:Nat arg3::mCherry-LacI nmt41:rtf1:sup35 ade6-704 leu1-32 t-LacO 7,9Kb:Kan:ura4^{+}<ori (uraR)*	this study
KK32	*h+*	*nup124::Hygro npp106-GFP:Nat arg3::mCherry-LacI nmt41:rtf1:sup35 ade6-704 leu1-32 t-LacO 7,9Kb:Kan:ura4^{+}<ori (uraR)*	this study
KK1579	*h-*	*alm1::Hygro npp106-GFP:Nat arg3::mCherry-LacI nmt41:rtf1:sup35 ade6-704 leu1-32 t-LacO 7,9Kb:Kan:ura4^{+}<ori (uraR)*	this study
KK697	*h-*	*ulp1::Kan nmt41:rtf1:sup35 ade6-704 leu1-32 t-ura4-SD20<ori (uraR)*	this study
KK1553	*h-*	*ulp1-GFP:Kan ade6-704 leu1-32 ura4-D18*	this study
KK1555	*h-*	*nup132::Kan ulp1-GFP:Kan ade6-704 leu1-32 ura4-D18*	this study
KK1560	*h-*	*nup60::Kan ulp1-GFP:Kan ade6-704 leu1-32 ura4-D18*	this study
KK1575	*h+*	*nup61::Kan ulp1-GFP:Kan ade6-704 leu1-32 ura4-D18*	this study
KK1596	*h+*	*nup124::Kan ulp1-GFP:Kan ade6-704 leu1-32 ura4-D18*	this study
KK1996	*h+*	*alm1::Kan ulp1-GFP:Kan ade6-704 leu1-32 ura4-D18*	this study
KK1564	*h-*	*pmt3 ::Kan-ura4 nmt41:rtf1:sup35 ade6-704 leu1-32 t-ura4^{+}<ori (uraR)*	this study
KK2018	*h+*	*SUMO-KallR (pmt3-KallR) ade6-704 leu1-32 ura4-D18*	this study
KK1965	*h-*	*ulp1-GFP:Kan cut11-mCherry :Hygro ade6-704 leu1-32 ura4-D18*	this study
KK1967	*h+*	*nup132::Kan ulp1-GFP:Kan cut11-mCherry :Hygro ade6-704 leu1-32 ura4-D18*	this study

KK1970	*h+*	*nup60::Hygro ulp1-GFP:Kan cut11-mCherry :Hygro ade6-704 leu1-32 ura4-D18*	this study
KK2287	*h-*	*nup61::Hygro ulp1-GFP:Kan cut11-mCherry :Hygro ade6-704 leu1-32 ura4-D18*	this study
KK2309	*h+*	*nup124::Hygro ulp1-GFP:Kan cut11-mCherry :Hygro ade6-704 leu1-32 ura4-D18*	this study
KK2071	*h+*	*alm1::Hygro ulp1-GFP:Kan cut11-mCherry :Hygro ade6-704 leu1-32 ura4-D18*	this study
KK2292	*h-*	*npp106-GFP:Kan cut11-mCherry :Hygro ade6-704 leu1-32 ura4-D18*	this study
KK1788	*h+*	nup211-mAID-HA-Turg1:Kan ade6-704 leu1-32 ura4-D18	this study
KK1790	*h+*	nup211-mAID-HA-Turg1:Kan arg3::bleMX6-arg3+-padh1-OsTIR1F74A-Tadh1 ade6-704 leu1-32 ura4-D18	this study
KK1780	*h+*	ulp1-GFP:kan nup211-mAID-HA-Turg1:Kan ade6-704 leu1-32 ura4-D18	this study
KK1782	*h-*	ulp1-GFP:kan nup211-mAID-HA-Turg1:Kan arg3::bleMX6-arg3+-padh1-OsTIR1F74A-Tadh1 ade6-704 leu1-32 ura4-D18	this study
KK2273	*h-*	*SUMO-KallR (pmt3-KallR) nmt41:rtf1:sup35 ade6-704 leu1-32 t-ura4-SD20<ori (uraR)*	Kramarz et al., 2020
KK2281	*h-*	*nup60::Hygro SUMO-KallR (pmt3-KallR) nmt41:rtf1:sup35 ade6-704 leu1-32 t-ura4-SD20<ori (uraR)*	this study
KK2403		*alm1::Hygro SUMO-KallR (pmt3-KallR) nmt41:rtf1:sup35 ade6-704 leu1-32 t-ura4-SD20<ori (uraR)*	this study
KK2391	*h+*	*rpn10::Hygro SUMO-KallR (pmt3-KallR) nmt41:rtf1:sup35 ade6-704 leu1-32 t-ura4-SD20<ori (uraR)*	this study
KK1631	*h-*	*nmt41:rtf1:sup35 ade6-704 leu1-32 t-Kan-lexBS:ura4-SD20<ori (uraR)*	Kramarz et al., 2020
KK1635	*h-*	*ulp1-lexA:Hygro nmt41:rtf1:sup35 ade6-704 leu1-32 t-Kan-lexBS:ura4-SD20<ori (uraR)*	Kramarz et al., 2020
KK1639	*h-*	*nup60::Hygro nmt41:rtf1:sup35 ade6-704 leu1-32 t-Kan-lexBS:ura4-SD20<ori (uraR)*	this study
KK1642	*h+*	*nup60::Hygro ulp1-lexA:Hygro nmt41:rtf1:sup35 ade6-704 leu1-32 t-Kan-lexBS:ura4-SD20<ori (uraR)*	this study
KK1769	*h-*	*alm1::Hygro nmt41:rtf1:sup35 ade6-704 leu1-32 t-Kan-lexBS:ura4-SD20<ori (uraR)*	this study
KK1770	*h-*	*alm1::Hygro ulp1-lexA:Hygro nmt41:rtf1:sup35 ade6-704 leu1-32 t-Kan-lexBS:ura4-SD20<ori (uraR)*	this study
KK1192	*h+*	*npp106-GFP:Nat arg3::mCherry-LacI nmt41:rtf1:sup35 ade6-704 leu1-32 t-LacO 7,9Kb:Kan:ura4::LexBS<ori (uraR)*	Kramarz et al., 2020
KK1193	*h-*	*ulp1-lexA:Hygro npp106-GFP:Nat arg3::mCherry-LacI nmt41:rtf1:sup35 ade6-704 leu1-32 t-LacO 7,9Kb:Kan:ura4::LexBS<ori (uraR)*	Kramarz et al., 2020
KK1854	*h-*	*nup60::Hygro npp106-GFP:Nat arg3::mCherry-LacI nmt41:rtf1:sup35 ade6-704 leu1-32 t-LacO 7,9Kb:Kan:ura4::LexBS<ori (uraR)*	this study
KK1857	*h-*	*nup60::Hygro ulp1-lexA:Hygro npp106-GFP:Nat arg3::mCherry-LacI nmt41:rtf1:sup35 ade6-704 leu1-32 t-LacO 7,9Kb:Kan:ura4::LexBS<ori (uraR)*	this study
KK1931	*h-*	*alm1::Hygro npp106-GFP:Nat arg3::mCherry-LacI nmt41:rtf1:sup35 ade6-704 leu1-32 t-LacO 7,9Kb:Kan:ura4::LexBS<ori (uraR)*	this study

KK1929	*h+*	*alm1::Hygro ulp1-lexA:Hygro npp106-GFP:Nat arg3::mCherry-LacI nmt41:rtf1:sup35 ade6-704 leu1-32 t-LacO 7,9Kb:Kan:ura4::LexBS<ori (uraR)*	this study
KK1527	*h-*	*rpn10::Hygro cdc6-L591G rtf1::Nat rnh201-RED:Kan Rura-ChrII RTS1::phleo ura4-D18 ade6-704 leu1-32*	this study
KK1868	*h-*	*rpn10::Hygro cdc6-L591G Nat:ADH1:rtf1 rnh201-RED:Kan Rura-ChrII RTS1::phleo ura4-D18 ade6-704 leu1-32*	this study
KK1526	*h-*	*rpn10::Hygro cdc20-M630F rtf1::Nat rnh201-RED:Kan Rura-ChrII RTS1::phleo ura4-D18 ade6-704 leu1-32*	this study
KK1894	*h-*	*rpn10::Hygro cdc20-M630F Nat:ADH1:rtf1 rnh201-RED:Kan Rura-ChrII RTS1::phleo ura4-D18 ade6-704 leu1-32*	this study

References

1. Misteli, T. & Soutoglou, E. The emerging role of nuclear architecture in DNA repair and genome maintenance. *Nature Reviews Molecular Cell Biology* **10**, 243–254 (2009).
2. Ait Saada, A., Lambert, S. A. E. & Carr, A. M. Preserving replication fork integrity and competence via the homologous recombination pathway. *DNA Repair* **71**, 135–147 (2018).
3. Berti, M., Cortez, D. & Lopes, M. The plasticity of DNA replication forks in response to clinically relevant genotoxic stress. *Nature Reviews Molecular Cell Biology* **21**, 633–651 (2020).
4. Chakraborty, S., Schirmeisen, K. & Lambert, S. A. The multifaceted functions of homologous recombination in dealing with replication-associated DNA damages. *DNA Repair (Amst).* **129**, 103548 (2023).
5. Carr, A. & Lambert, S. Recombination-dependent replication: new perspectives from site-specific fork barriers. *Current Opinion in Genetics and Development* **71**, 129–135 (2021).
6. Miyabe, I. *et al.* Polymerase δ replicates both strands after homologous recombination-dependent fork restart. *Nat. Struct. Mol. Biol.* **22**, 932–938 (2015).
7. Donnianni, R. A. *et al.* DNA Polymerase Delta Synthesizes Both Strands during Break-Induced Replication. *Mol. Cell* **76**, 371-381.e4 (2019).
8. Lamm, N., Rogers, S. & Cesare, A. J. Chromatin mobility and relocation in DNA repair. *Trends in Cell Biology* **31**, 843–855 (2021).
9. Stanic, M. & Mekhail, K. Integration of DNA damage responses with dynamic spatial genome organization. *Trends in Genetics* **38**, 290–304 (2022).
10. Pascual-Garcia, P. & Capelson, M. The nuclear pore complex and the genome: organizing and regulatory principles. *Current Opinion in Genetics and*

Development **67**, 142–150 (2021).
11. Asakawa, H. *et al.* Characterization of nuclear pore complex components in fission yeast Schizosaccharomyces pombe. *Nucl. (United States)* **5**, 149–62 (2014).
12. Varberg, J. M., Unruh, J. R., Bestul, A. J., Khan, A. A. & Jaspersen, S. L. Quantitative analysis of nuclear pore complex organization in Schizosaccharomyces pombe. *Life Sci. Alliance* **5**, e202201423 (2022).
13. Asakawa, H. *et al.* Asymmetrical localization of nup107-160 subcomplex components within the nuclear pore complex in fission yeast. *PLoS Genet.* **15**, e1008061 (2019).
14. Schirmeisen, K., Lambert, S. A. E. & Kramarz, K. SUMO-based regulation of nuclear positioning to spatially regulate homologous recombination activities at replication stress sites. *Genes* **12**, 2010 (2021).
15. Kramarz, K. *et al.* The nuclear pore primes recombination-dependent DNA synthesis at arrested forks by promoting SUMO removal. *Nat. Commun.* **11**, 5643 (2020).
16. Su, X. A., Dion, V., Gasser, S. M. & Freudenreich, C. H. Regulation of recombination at yeast nuclear pores controls repair and triplet repeat stability. *Genes Dev.* **29**, 1006–1017 (2015).
17. Whalen, J. M., Dhingra, N., Wei, L., Zhao, X. & Freudenreich, C. H. Relocation of Collapsed Forks to the Nuclear Pore Complex Depends on Sumoylation of DNA Repair Proteins and Permits Rad51 Association. *Cell Rep.* **31**, 107635 (2020).
18. Aguilera, P. *et al.* The nuclear pore complex prevents sister chromatid recombination during replicative senescence. *Nat. Commun.* **11**, 160 (2020).
19. Pinzaru, A. M. *et al.* Replication stress conferred by POT1 dysfunction promotes telomere relocalization to the nuclear pore. *Genes Dev.* **34**, 1619–1636 (2020).
20. Lamm, N. *et al.* Nuclear F-actin counteracts nuclear deformation and promotes fork repair during replication stress. *Nat. Cell Biol.* **22**, 1460–1470 (2020).
21. Nagai, S. *et al.* Functional targeting of DNA damage to a nuclear pore-associated SUMO-dependent ubiquitin ligase. *Science (80-.).* **322**, 597–602 (2008).
22. Taylor, D. L., Ho, J. C. Y., Oliver, A. & Watts, F. Z. Cell-cycle-dependent localisation of Ulp1, a Schizosaccharomyces pombe Pmt3 (SUMO)-specific protease. *J. Cell Sci.* **115**, 1113–1122 (2002).
23. Lambert, S. *et al.* Homologous recombination restarts blocked replication forks at the expense of genome rearrangements by template exchange. *Mol. Cell* **39**, 346–359 (2010).
24. Teixeira-Silva, A. *et al.* The end-joining factor Ku acts in the end-resection of double strand break-free arrested replication forks. *Nat. Commun.* **8**, 1982 (2017).
25. Tsang, E. *et al.* The extent of error-prone replication restart by homologous

recombination is controlled by Exo1 and checkpoint proteins. *J. Cell Sci.* **127**, 2983–2994 (2014).
26. Naiman, K. *et al.* Replication dynamics of recombination-dependent replication forks. *Nat. Commun.* **12**, 923 (2021).
27. Nguyen, M. O., Jalan, M., Morrow, C. A., Osman, F. & Whitby, M. C. Recombination occurs within minutes of replication blockage by RTS1 producing restarted forks that are prone to collapse. *Elife* **2015**, e04539 (2015).
28. Ait Saada, A. *et al.* Unprotected Replication Forks Are Converted into Mitotic Sister Chromatid Bridges. *Mol. Cell* **66**, 398-410.e4 (2017).
29. Mizuno, K., Miyabe, I., Schalbetter, S. A., Carr, A. M. & Murray, J. M. Recombination-restarted replication makes inverted chromosome fusions at inverted repeats. *Nature* **493**, 246–249 (2013).
30. Iraqui, I. *et al.* Recovery of Arrested Replication Forks by Homologous Recombination Is Error-Prone. *PLoS Genet.* **8**, e1002976 (2012).
31. Daigaku, Y. *et al.* A global profile of replicative polymerase usage. *Nat. Struct. Mol. Biol.* **22**, 192–198 (2015).
32. Pan, X. *et al.* Identification of novel genes involved in DNA damage response by screening a genome-wide Schizosaccharomyces pombe deletion library. *BMC Genomics* **13**, 662 (2012).
33. Deshpande, G. P. *et al.* Screening a genome-wide S. pombe deletion library identifies novel genes and pathways involved in genome stability maintenance. *DNA Repair (Amst).* **8**, 672–679 (2009).
34. Palancade, B. *et al.* Nucleoporins prevent DNA damage accumulation by modulating Ulp1-dependent sumoylation processes. *Mol. Biol. Cell* **18**, 2912–2923 (2007).
35. Zhao, X., Wu, C. Y. & Blobel, G. Mlp-dependent anchorage and stabilization of a desumoylating enzyme is required to prevent clonal lethality. *J. Cell Biol.* **167**, 605–611 (2004).
36. Takeda, K., Mori, A. & Yanagida, M. Identification of genes affecting the toxicity of anti-cancer drug bortezomib by genome-wide screening in S. pombe. *PLoS One* **6**, e22021 (2011).
37. Nie, M. & Boddy, M. N. Pli1PIAS1 SUMO ligase protected by the nuclear pore-associated SUMO protease Ulp1SENP1/2. *J. Biol. Chem.* **290**, 22678–22685 (2015).
38. Salas-Pino, S., Gallardo, P., Barrales, R. R., Braun, S. & Daga, R. R. The fission yeast nucleoporin Alm1 is required for proteasomal degradation of kinetochore components. *J. Cell Biol.* **216**, 3591–3608 (2017).
39. Watson, A. T., Hassell-Hart, S., Spencer, J. & Carr, A. M. Rice (Oryza sativa) tir1

and 5′adamantyl-iaa significantly improve the auxin-inducible degron system in schizosaccharomyces pombe. *Genes (Basel).* **12**, 882 (2021).

40. Wilkinson, C. R. M. *et al.* Analysis of a gene encoding Rpn10 of the fission yeast proteasome reveals that the polyubiquitin-binding site of this subunit is essential when Rpn12/Mts3 activity is compromised. *J. Biol. Chem.* **275**, 15182–15192 (2000).
41. Seeger, M. *et al.* Interaction of the anaphase-promoting complex/cyclosome and proteasome protein complexes with multiubiquitin chain-binding proteins. *J. Biol. Chem.* **278**, 16791–16796 (2003).
42. Wilkinson, C. R. M. *et al.* Localization of the 26S proteasome during mitosis and meiosis in fission yeast. *EMBO J.* **17**, 6465–6476 (1998).
43. Psakhye, I., Castellucci, F. & Branzei, D. SUMO-Chain-Regulated Proteasomal Degradation Timing Exemplified in DNA Replication Initiation. *Mol. Cell* **76**, 632-645.e6 (2019).
44. Babbal, Mohanty, S., Dabburu, G. R., Kumar, M. & Khasa, Y. P. Heterologous expression of novel SUMO proteases from Schizosaccharomyces pombe in E. coli: Catalytic domain identification and optimization of product yields. *Int. J. Biol. Macromol.* **209**, 1001–1019 (2022).
45. Chang, Y. C., Oram, M. K. & Bielinsky, A. K. Sumo-targeted ubiquitin ligases and their functions in maintaining genome stability. *International Journal of Molecular Sciences* **22**, 5391 (2021).
46. Aguilar-Martinez, E., Guo, B. & Sharrocks, A. D. RNF4 interacts with multiSUMOylated ETV4. *Wellcome Open Res.* **1**, (2017).
47. Kosar, M. *et al.* The human nucleoporin Tpr protects cells from RNA-mediated replication stress. *Nat. Commun.* **12**, 3937 (2021).
48. Schindelin, J. *et al.* Fiji: An open-source platform for biological-image analysis. *Nature Methods* **9**, 676–682 (2012).
49. Bolte, S. & Cordelières, F. P. A guided tour into subcellular colocalization analysis in light microscopy. *Journal of Microscopy* **224**, 213–232 (2006).
50. Lambert, S. *et al.* Homologous recombination restarts blocked replication forks at the expense of genome rearrangements by template exchange. *Mol. Cell* **39**, 346–359 (2010).
51. Sabatinos, S. A. & Forsburg, S. L. Measuring DNA content by flow cytometry in fission yeast. *Methods Mol. Biol.* **1300**, 79–97 (2015).
52. Keszthelyi, A., Daigaku, Y., Ptasińska, K., Miyabe, I. & Carr, A. M. Mapping ribonucleotides in genomic DNA and exploring replication dynamics by polymerase usage sequencing (Pu-seq). *Nat. Protoc.* **10**, 1786–1801 (2015).

Figure 42: **Pli1 E3 SUMO ligase promotes the dynamic of recombination-mediated fork restart.** Top panels: Pu-Seq traces of the ChrII locus in *RTS1*-RFB OFF (left) and ON (right) condition in *WT* and *pli1Δ* strains. The usage of Pol delta (in blue and black for *WT* and *pli1Δ* cells, respectively) are shown on the Watson and Crick strands. The usage of Pol epsilon (in red and orange for *WT* and *pli1Δ* cells, respectively) are shown on the Watson and Crick strands. Bottom panels: Graph of Pol delta/delta bias over both strands (Watson and Crick) around RFB site in *RTS1*-RFB OFF (left) and ON (right) condition in *WT* and two independent replicates of *pli1Δ* strains. The gray bar indicates the position of the *RTS*1-RFB.

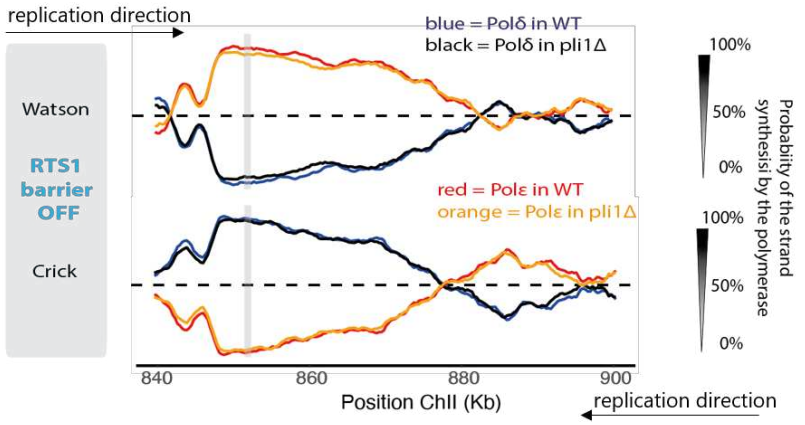

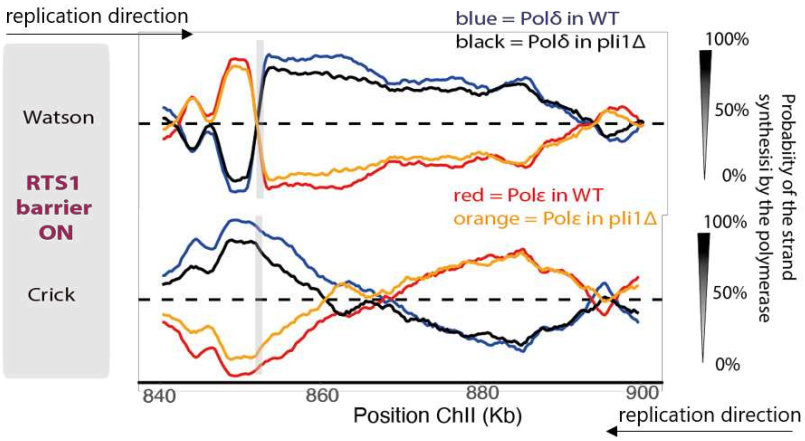

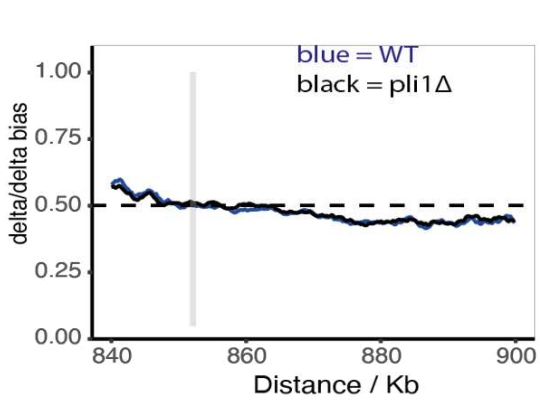

RFB OFF

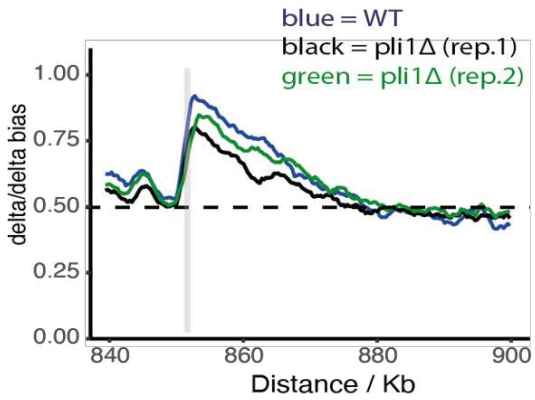

RFB ON

III. What are the features of the SUMOylation wave that occurs at the site of fork arrest?

Relocation to the nuclear periphery and association with NPCs have been reported as a phenomenon emerging in response to halted replication forks. Notably, SUMOylation plays a key role in regulating the nuclear positioning of stressed replication forks as well as the mechanisms that are further engaged to repair and/or restart the fork (Nagai et al., 2008; Su et al., 2015; Whalen et al., 2020; Kramarz et al., 2020; Aguilera et al., 2020). Previous works from our team revealed that such SUMO-based mechanism is also involved in the spatial segregation of the subsequent steps of recombination-dependent fork restart when forks are stalled by DNA-bound proteins. By employing the *RTS1*-RFB system in fission yeast, I revealed that SUMO chains trigger relocation of the arrested replication fork to the nuclear periphery, where it associates with the NPC. At the nuclear periphery, the removal of SUMO-chains by Ulp1 protease and proteasome activity unrelated to SUMO-chains were proposed to allow HR-mediated RF restart to occur (**Publication #1**, **Publication #2**).

1. Pli1 SUMO ligase fine-tunes the dynamics of HR-mediated fork restart in the nucleoplasm.

We previously showed that preventing Pli1-mediated SUMOylation is sufficient to bypass the need for anchorage to nuclear pore complexes while maintaining *Wild Type* level of recombination-dependent replication (**Publication #1**: Figure 5E and 5G). Interestingly, we noticed that preventing SUMO chains formation (*SUMO-KallR* mutant) resulted in increased efficiency of recombination-dependent replication in the nucleoplasm, whereas the lack of Pli1 did not lead to similar increase. This suggested that while SUMO chains have an inhibitory effect on fork restart, Pli1-dependent monoSUMOylation events may be important to promote the restart of arrested forks that failed to relocate to the nuclear pore complexes.

However, a direct evidence that would strengthen our conclusions was missing. Therefore, I decided to employ the polymerase usage sequencing (Pu-Seq) technique, which allows obtaining more information about the dynamics of HR-mediated fork restart than the previously used proxy-restart assay. Briefly, Pu-Seq tracks the usage frequency of each polymerase on both the Watson and Crick strands across the

Figure 43: **SUMO conjugates accumulate at the active RFB in Pli1-dependent manner.** Analysis of SMO recruitment to the *RTS1*-RFB by ChIP-qPCR in indicated strains. Upstream and downstream distances from the RFB are indicated by arrows and presented in base pairs (bp). Primers targeting ade6 gene were used as unrelated control locus. Each dot represents one sample from independent biological replicate. Red bars indicate mean values ± standard deviation (SD). *p* value was calculated by two-sided t-test (*** p≤0.001; ** p≤0.01; * p≤0.05).

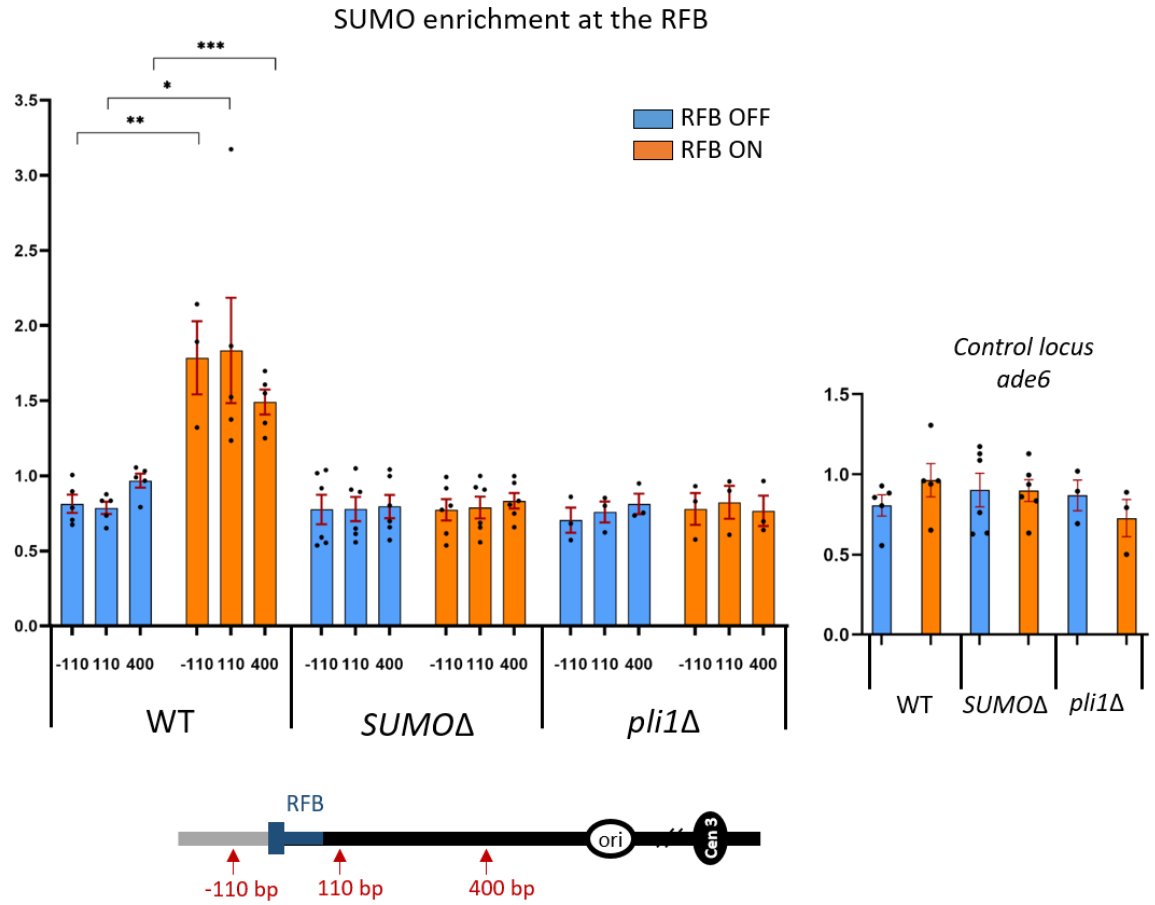

genome (see **Publication #2**: Figure 1 and corresponding paragraph). Using the Pu-Seq approach, I monitored replication dynamics around the *RTS1* blocking site in *Wild Type* and *pli1*Δ mutant (Figure 42). When the RTS1 barrier was inactive (RFB OFF), replication forks were coming from an early replication origin and synthetized the leading strand by Pol epsilon and lagging strand by Pol delta (Figure 42, top left). Upon barrier activation (RFB ON), Pol epsilon on the leading strand was switched at the barrier site to polymerase delta during the restart of the blocked replication fork. This transition creates a bias towards Pol delta on both strands downstream of the *RTS1* barrier site due to the restart.

Based on the Pol delta/delta bias (Figure 42, bottom right), it was estimated that when compared to *Wild Type*, between 85-75% of the expected number of forks were arrested and restarted in *pli1*Δ cells while the remaining 15-25% were either not arrested or did not restart before being rescued by an incoming leftward moving canonical fork. The increase in Pol epsilon usage on the Crick strand for ~10 Kb downstream of the *RTS1* barrier is indicative of this latter scenario (Figure 42, top right). Moreover, the forks that succeeded to restart progress with a speed similar to *Wild Type*, as indicated by the comparable relative slope of the Pol delta/delta bias disappearance over distance in *Wild Type* and *pli1*Δ cells (Figure 42, bottom right). Thus, the data suggest that the E3 SUMO ligase Pli1 promotes the efficient HR-mediated restart of arrested forks, but is not involved in regulating the speed of these restarted forks.

2. Forks arrested at the RFB undergo a local wave of Pli1-dependent SUMOylation.

Pli1-dependent SUMOylation events are involved in promoting relocation of RFB-arrested forks towards the nuclear periphery, their anchoring to nuclear pore complexes and to some extend Pli1 regulates the recombination-dependent replication in the nucleoplasm. However, the contribution of Pli1 to the accumulation of SUMO conjugates at arrested forks remains unaddressed.

Therefore, I aimed to optimize a technique that would allow to detect for the first time the local SUMOylation events at the RFB. In addition, it would help to establish the genetic dependency of SUMO intermediates formation at a single arrested fork resolution. To do so, I employed an anti-SUMO antibody generated in our lab to perform chromatin immunoprecipitation in *Wild Type*, *sumo*Δ and *pli1*Δ asynchronous

Figure 44: **Pli1-dependent SUMOylation at the RFB is highly dynamic.** A: Schematic representation of the experimental setup. Asynchronous cells harbouring the *cdc2-as* allele were treated with 3-Br-PP1 for 4h, then washed and released into fresh media. At each time point, two samples were collected: one for the flow cytometry analysis (FACS) and one for chromatin immunoprecipitation (ChIP). B: Flow cytometry analysis of *WT cdc2-as* and *pli1Δ cdc2-as* cells. C: Analysis of SUMO recruitment to the *RTS1*-RFB by ChIP-qPCR in indicated strains in RFB ON condition.

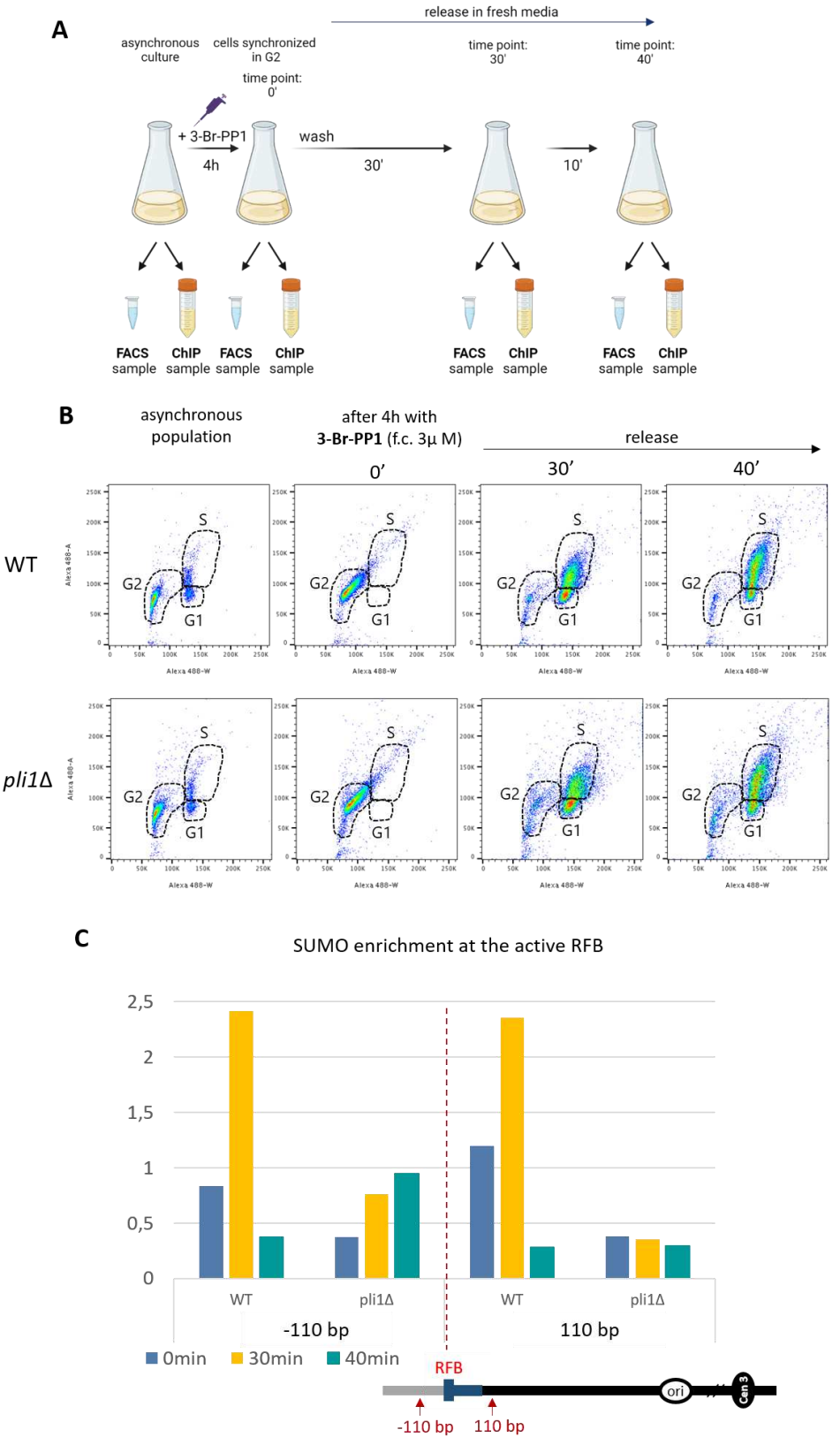

cells. By qPCR I analyzed the accumulation of SUMO conjugates in the vicinity of the RFB locus (exact positions of the used primers are indicated on the scheme on Figure 43). I observed a significant SUMO enrichment at the active RFB in *Wild Type* but not in SUMO depleted cells (Figure 43). This enrichment was also Pli1-dependent, indicating that Pli1 promotes the local SUMO wave that occurs upon RFB activation.

It is of note that in an asynchronous population of fission yeast only ~10-20 % of cells are in S-phase (undergoing replication) (Willis and Rhind, 2011). To increase the proportion of replicating cells, I took advantage of the *cdc2-asM17* allele which allows to synchronize cells in G2 using 3-Br-PP1, which can be further release into S phase. Upon the removal of 3-Br-PP1, samples were collected at the indicated times (Figure 44A). The cell cycle progression was monitored by flow cytometry (Figure 44B).

I performed SUMO-ChIP experiment in S-phase synchronized cells to address the level and kinetics of SUMOylation events at the RFB in *Wild Type* and *pli1*Δ mutant (Figure 44C). My preliminary data confirmed the accumulation of SUMO at the active RFB in a Pli1-dependent manner and revealed a transient accumulation of SUMO conjugates. In *Wild Type* cells a peak of SUMO enrichment was observed 30 min after release in S-phase and drastically diminished within the following 10 minutes. This suggest that SUMO conjugates formation and resolution is extremely fast. However, additional biological replicates including the analysis of the control locus *ade6* are needed to confirm these preliminary results. Also, it would be very informative to test the accumulation of SUMO conjugates at a greater distance from the RFB (upstream and downstream from the barrier). This would allow to determine the range of the SUMOylation events and their kinetics at the given position. Nonetheless, the already obtained data suggest that a highly dynamic Pli1-dependent SUMOylation occurs at the site of arrested forks.

3. Division of labour of the two fission yeast E3 SUMO ligases.

In fission yeast, two E3 SUMO ligases have been identified to date: Pli1 and Nse2. Each of them has specific targets and have at least some non-overlapping functions in maintaining genome stability (Watts et al., 2007).

We previously showed that Pli1 is involved in regulating the relocation, HR-mediated restart and nascent strand protection of replication forks arrested at the RFB. One aim of my PhD project was to verify whether these roles of Pli1 are indeed dependent on its SUMO ligase activity. Furthermore, I wanted to test if the second E3 SUMO ligase

Figure 45: **Sequence alignment of the SP-RING domains of the two E3 SUMO ligases in fission yeast.** Identical residues are boxed and similar residues are shaded. Stars indicate the positions of the residues forming the C2HC3 conserved SP-RING domain which were mutated in *pli1-RING* and *nse2-RING* catalytic-dead mutants.

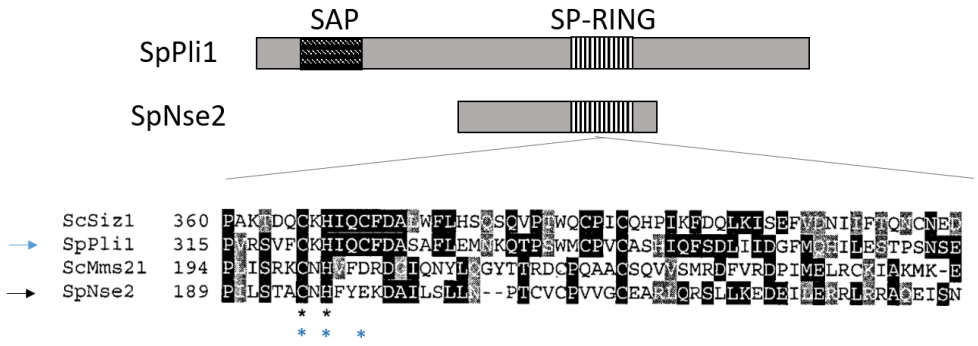

pli1-RING^{m} *(C321S-H323A-C326S) Xhemale et al. EMBO J. 2004*
nse2-RING^{m} *(C195S-H197A) Andrews et al. Mol Cell 2005*
sumo-KallR: all internal lysine acceptor for SUMO addition are mutated
sumoΔ: pmt3+ gene, encoding the only SUMO particle in fission yest, is deleted

Figure 46: **Comparison of the phenotypes of *pli1-RING* and *nse2-RING* mutants.** A: Sensitivity of indicated strains to indicated genotoxic drugs. Ten-fold serial dilution of exponential cultures were dropped on appropriate plates. CPT: camptothecin; HU: hydroxyurea; MMS: methyl methane sulfonate. B: Expression of SUMO conjugates in indicated strains grown in untreated conditions as well as in response to MMS-induced DNA damage (3h treatment with 0,03% MMM). A strain deleted for *pmt3* gene that encodes the SUMO particle (*sumoΔ*) was added as control for antibody specificity. * indicates unspecific signal.

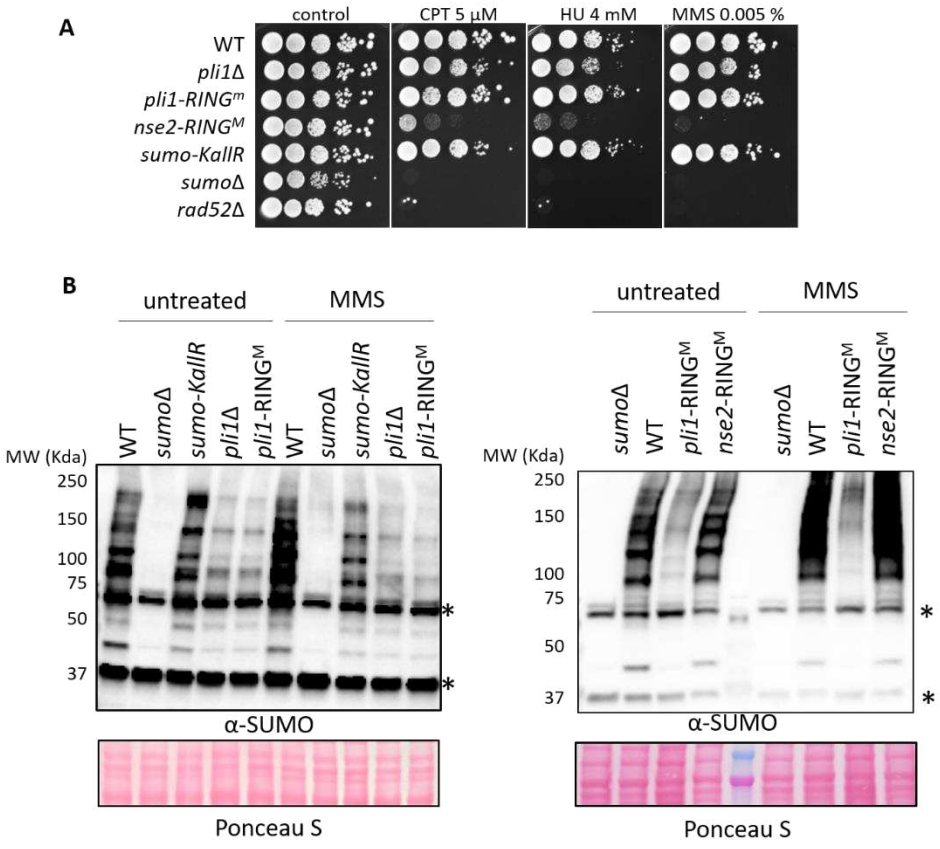

Nse2 also participates in the SUMO-based regulation of RFB relocation, fork restart or protection.

To do so, I generated ligase-dead mutants of Pli1 and Nse2 by introducing point mutations within their RING domains (Figure 45). These mutations have been reported to abrogate the SUMO ligase function of both ligases (Xhemalce et al., 2004; Andrews et al., 2005). First, I ensured that the ligase-dead mutants generated by me exhibit the same phenotypes as the ones previously described in the literature. By serial dilution assay, I compared the viability of the mutant cells to replication-blocking agents including CPT, HU and MMS. As reported previously, *nse2-RING*, but not *pli1-RING* cells, were sensitive to all tested drugs (Figure 46A). I also analysed by Western Blot the levels of SUMO conjugates in untreated cells as well as in response to MMS, a well-known inducer of SUMOylation. In both conditions, I observed a drastic decrease of SUMO conjugates in *pli1*Δ and *pli1-RING* when compared to *Wild Type*. On the contrary, *nse2-RING* showed a *Wild Type* level of global SUMOylation (Figure 46B).

3.1 RFB relocation to the NPC depends on the E3 SUMO ligase activity of Pli1 but not Nse2.

Then I investigated the nuclear positioning of the *LacO*-marked RFB in cells expressing the endogenous tagged Npp106-GFP (Figure 47A). I asked how frequently the *LacO*-marked RFB visualized by mCherry-LacI foci co-localizes with the nuclear periphery visualized by Npp106-GFP, as previously reported (Kramarz et al., 2020).

The active *LacO*-marked RFB (RFB ON) localized more frequently at the nuclear periphery in *Wild Type* cells during the S-phase, as previously reported (Figure 47B). This relocation was shown to be dependent on SUMO chains and Pli1, therefore I did not observe enrichment of the active RFB at the nuclear periphery in SUMO-KallR and *pli1*Δ mutants respectively. Moreover, I observed that Pli1 catalytic dead mutant showed the same phenotype as *pli1*Δ, regarding the nuclear positioning of the RFB (Figure 47B). In other words, defective relocation in the *pli1*Δ mutant does not result from the absence of Pli1 protein itself (and thus potential disturbances in some protein-protein interactions) but from the lack of its SUMO ligase activity. Conversely, the shift of the active RFB to the nuclear periphery was not impacted in the *nse2-RING* mutant.

Thus, I concluded that the formation of SUMO chains which trigger RFB relocation is indeed catalyzed by Pli1 and the catalytic activity of Nse2 is dispensable.

Figure 47: **E3 SUMO ligase activity of Pli1, but not Nse2, is necessary to promote RFB relocation.** A top: Diagram of the *LacO*-marked RFB. *LacO* arrays bound by mCherry-LacI integrated ~7 kb away from the *RTS1*-RFB. A bottom: Example Mono-nucleated cells (G2) and septated bi-nucleated cells (S-phase) expressing the endogenous Npp106-GFP and harboring the *LacO*-marked RFB. White arrows indicate co-localization events in S-phase cells. B: Quantification of co-localization events in S-phase cells in indicated conditions and strains. Dots represent values obtained from independent biological experiments. At least 100 nuclei were analyzed for each strain and condition. Fisher's exact test was used for group comparison to determine the *p* value (** p≤0.01; * p≤0.05; ns: non-significant).

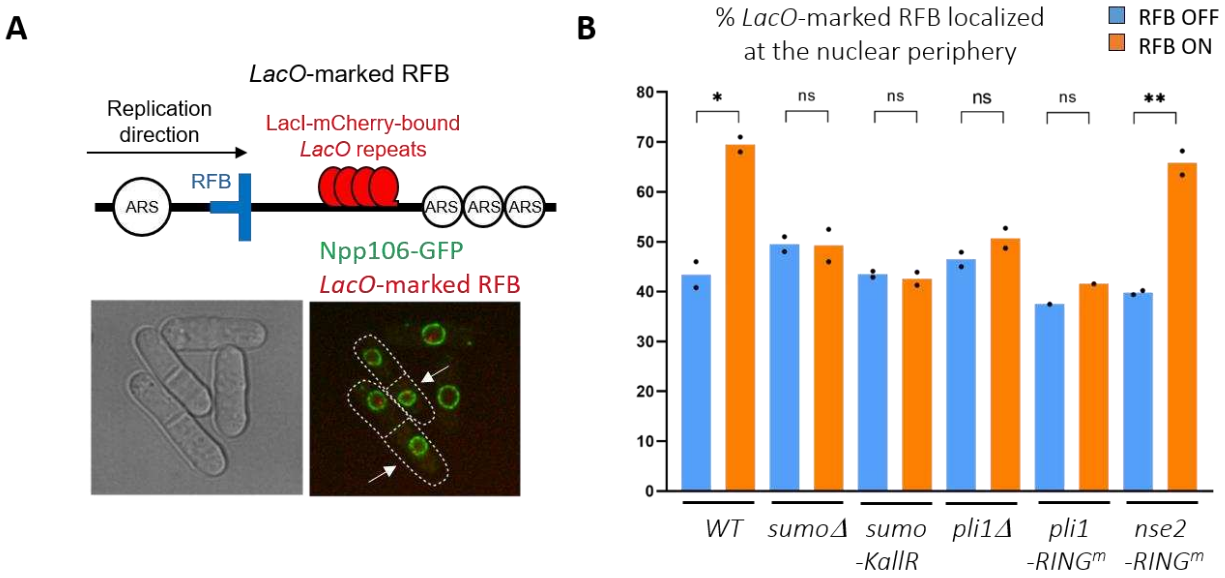

Figure 48: **Loss of SUMO E3 ligase activity in Pli1 or Nse2 had no effect on RDR efficiency.** A: Diagram of the *ori>ura4-sd20-t* construct on chromosome III (ori: replication origin, >: *RTS1*-RFB, t: telomere). The non-functional *ura4-sd20* allele (red bar), containing a 20-nt duplication flanked by micro-homology, is located downstream of the RFB (blue bar). ARS: autonomously replicating sequence. B: Frequency of RFB-induced RS in indicated strains and conditions. Each dot represents one sample from independent biological replicate. Red bars indicate mean values ± standard deviation (SD). *p* value was calculated by two-sided t-test (**** *p* ≤0.0001; *** p≤0.001; ** p≤0.01; * p≤0.05).

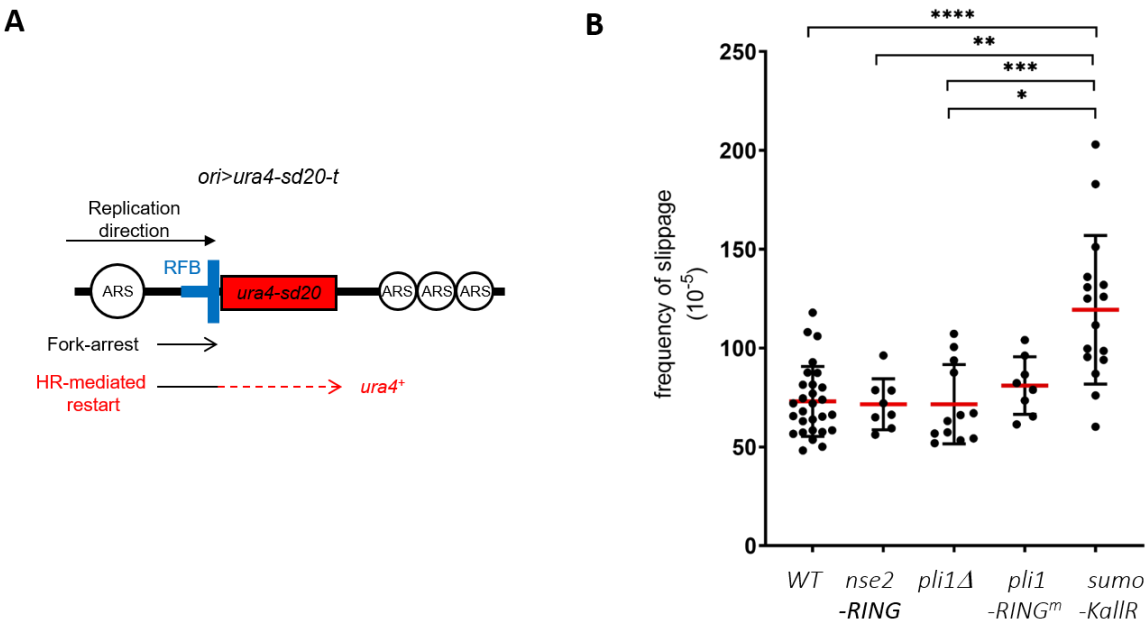

3.2 Recombination-dependent replication at arrested forks does not require Nse2-mediated SUMOylation.

Next, I investigated the role of Pli1 and Nse2 SUMO ligases activities in promoting replication resumption at the RFB. To do so, I employed a proxy-restart assay to measure the frequency of replication slippage occurring downstream the RFB, exploiting the mutagenic DNA synthesis as a readout of recombination-dependent replication efficiency (Figure 48A) (Iraqui et al., 2012).

As reported (**Publication #1**), the absence of Pli1 did not affect the RFB-induced replication slippage and *pli1-RING* showed the same result. Similarly, the frequency of RFB-induced replication slippage in *nse2-RING* ligase-dead mutants was at the *Wild Type* level (Figure 48B). *nse2-RING* phenotype can be simply explained by the fact that in this mutant the RFB still relocates to the nuclear periphery where the inhibitory effect of SUMO conjugates on HR-mediated DNA synthesis is alleviated. As mentioned before, the proxy-restart assay does not allow addressing the dynamics of recombination-dependent DNA synthesis. Therefore, it would be necessary to perform Pu-Seq analysis in the *nse2-RING* mutant to confirm that Nse2 is dispensable to promote fork restart by recombination-dependent replication.

4. Pli1-dependent monoSUMOylation safeguards replication fork integrity in the nucleoplasm.

By an unknown mechanism, Pli1 limits nascent strand degradation at arrested replication forks that fail to anchor to NPCs and remain in the nucleoplasm (**Publication #1**).

To verify whether this protection function is related to the SUMO ligase activity of Pli1, I examined the resection of nascent strands at the arrested forks (referred to as resected forks) in *pli1-RING* mutant (Figure 49). Analysis of replication intermediates by bi-dimensional DNA gel electrophoresis (2DGE) revealed that fork resection (visualized as a specific "tail" DNA structure; marked with a red arrow on Figure 49), was at the same level in *pli1*Δ and *pli1-RING* mutant, indicating that nascent DNA is more resected compared to Wild Type cells. Only one experiment has been performed for the *pli1-RING* mutant and this result needs to be repeated to validate the observations. Nonetheless, the preliminary data suggest that the Pli1 SUMO ligase activity is necessary to protect arrested replication forks from excessive nascent strand degradation when they are located in the nucleoplasm.

Figure 49: **Pli1-dependent monoSUMOylation limits the extent of nascent strand degradation at arrested replication forks.** Left panel: scheme of replication intermediates (RI) analyzed by neutral-neutral 2DGE of the *AseI* restriction fragment in RFB OFF and ON conditions. Partial restriction digestion caused by psoralen-crosslinks results in a secondary arc indicated on scheme by blue dashed lines. Middle panels: representative RI analysis in indicated strains and conditions. The *ura4* gene was used as probe. Numbers indicate the % of forks blocked by the RFB ± standard deviation (SD). The red arrow indicates the tail signal resulting from resected forks. Right panel: Quantification of resected forks in indicated strains. Dots represent values obtained from independent biological experiments. *p* value was calculated by two-sided t-test (** p≤0.01).

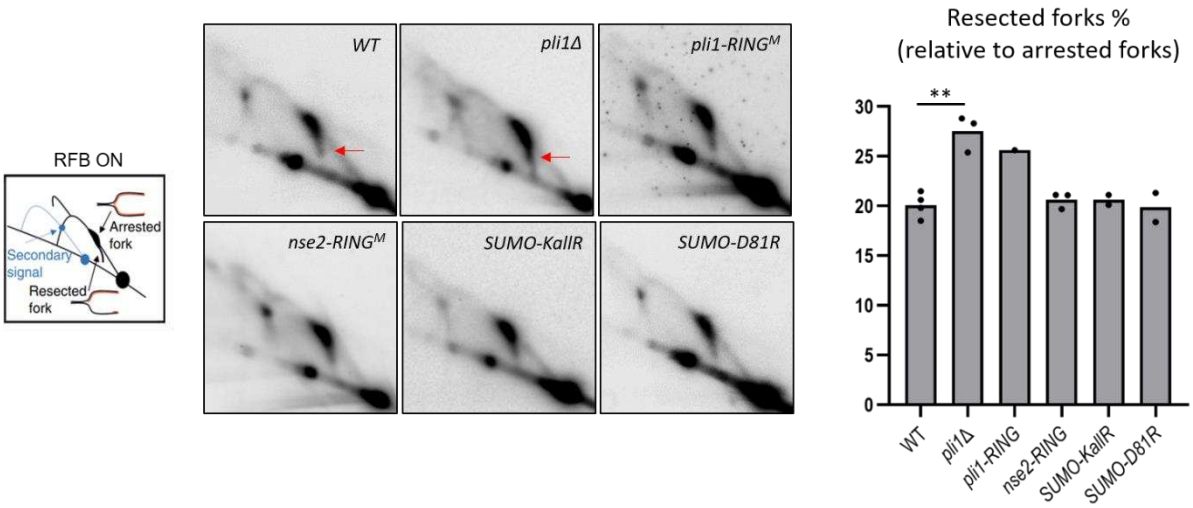

Figure 50: **Pli1 promotes Rad51 recruitment to the active RFB.** Analysis of Rad51 binding at the *RTS1*-RFB by ChIP-qPCR in indicated strains (ON/OFF ratio). Upstream and downstream distances from the RFB are indicated by arrows and presented in base pairs (bp). Primers targeting ade6 gene were used as unrelated control locus. Each dot represents one sample from independent biological replicate. Red bars indicate mean values ± standard deviation (SD). *p* value was calculated by two-sided t-test (** p≤0.01; * p≤0.05).

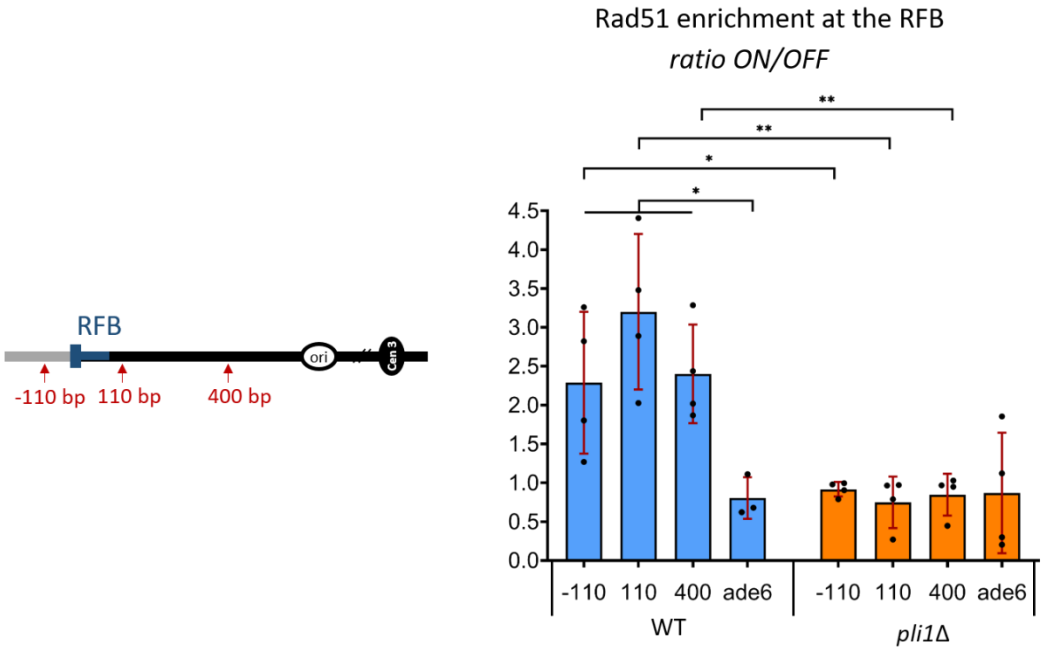

At the same time, the level of fork resection in the *nse2-RING* mutant was at the *Wild Type* level, indicating that Nse2-mediated SUMOylation is not required for maintaining the integrity of arrested forks (Figure 49).

To gauge the type of SUMO modification involved in fork protection, I took advantage of two mutants in which the level and type of SUMO conjugates has been manipulated by distinct means. In the *SUMO-KallR* mutant, all internal lysines of the SUMO particle are mutated to prevent the formation of SUMO chains, while monoSUMOylation still occurring. In the *SUMO-D81R* mutant, the interaction between the E2 SUMO conjugating enzyme Ubc9 and SUMO is impaired and only mono- and diSUMOylation can occur in a Pli1-dependent manner (Prudden et al., 2011). Interestingly, by 2DGE analysis, I found that in both mutants the level of resected forks was comparable to *Wild Type* level (Figure 49). Thus, preventing the formation of SUMO chains, while maintaining the possibility of mono- and diSUMOylation, did not lead to more extensive fork resection.

Therefore, I concluded that Pli1-mediated SUMOylation and more specifically monoSUMOylation is critical to negatively regulate the resection of nascent strand and safeguard fork-integrity in the nucleoplasm.

I also sought to decipher what could be the molecular mechanisms by which Pli1 protects arrested forks. One possibility is that Pli1-dependent monoSUMOylation favors recruitment and/or optimal binding of HR factors at arrested replication forks to protect them. To test this hypothesis, I analyzed Rad51 binding to the RFB by chromatin immunoprecipitation in *pli1*Δ mutant (Figure 50). Rad51 enrichment at the active RFB was decreased in the absence of Pli1 compared to *Wild Type* cells. This suggests that Pli1 protects arrested fork by favoring the recruitment and or stability of the Rad51 filament.

Contributions

Data presented in Figure 42 were obtained in collaboration with Tony Carr (University of Sussex) and Karel Naiman (Centre de Recherche en Cancérologie de Marseille). K.N performed the Pu-Seq experiment. K.N and T.C provided the expertise to analyse the Pu-Seq data. The ChIP experiments presented in Figure 43 were carried out in cooperation with Karol Kramarz, a former postdoc in the team. Western Blot experiment in Figure 46B (right panel) was performed by Shrena Chakraborty, a PhD student in the team.

Figure 51: **The nuclear periphery is proficient for the controlled resection of nascent strand and RDR.** A: Schematic representation of the LexA-based strategy to tether the RFB to the NPC. Nup60 (left) or Ulp1 (right) fused to LexA thether lexA-binding sites (lexBS, purple) inserted in a close proximity to *RTS1*-RFB site at the chromosome III. B: Quantification of co-localization events in S-phase cells in indicated conditions and strains. Dots represent values obtained from independent biological experiments. At least 100 nuclei were analyzed for each strain and condition. Fisher's exact test was used for group comparison to determine the *p* value (****p≤0.0001). C: Frequency of RFB-induced RS in indicated strains and conditions. Each dot represents one sample from independent biological replicate. Red bars indicate mean values ± standard deviation (SD). No statistical difference was detected between samples. D: Representative replication intermediates analysis in indicated strains and conditions. The *ura4* gene was used as probe. Numbers indicate the % of forks blocked by the RFB ± standard deviation (SD). E: Quantification of resected forks in indicated strains. Dots represent values obtained from independent biological experiments. No statistical difference was detected between samples.

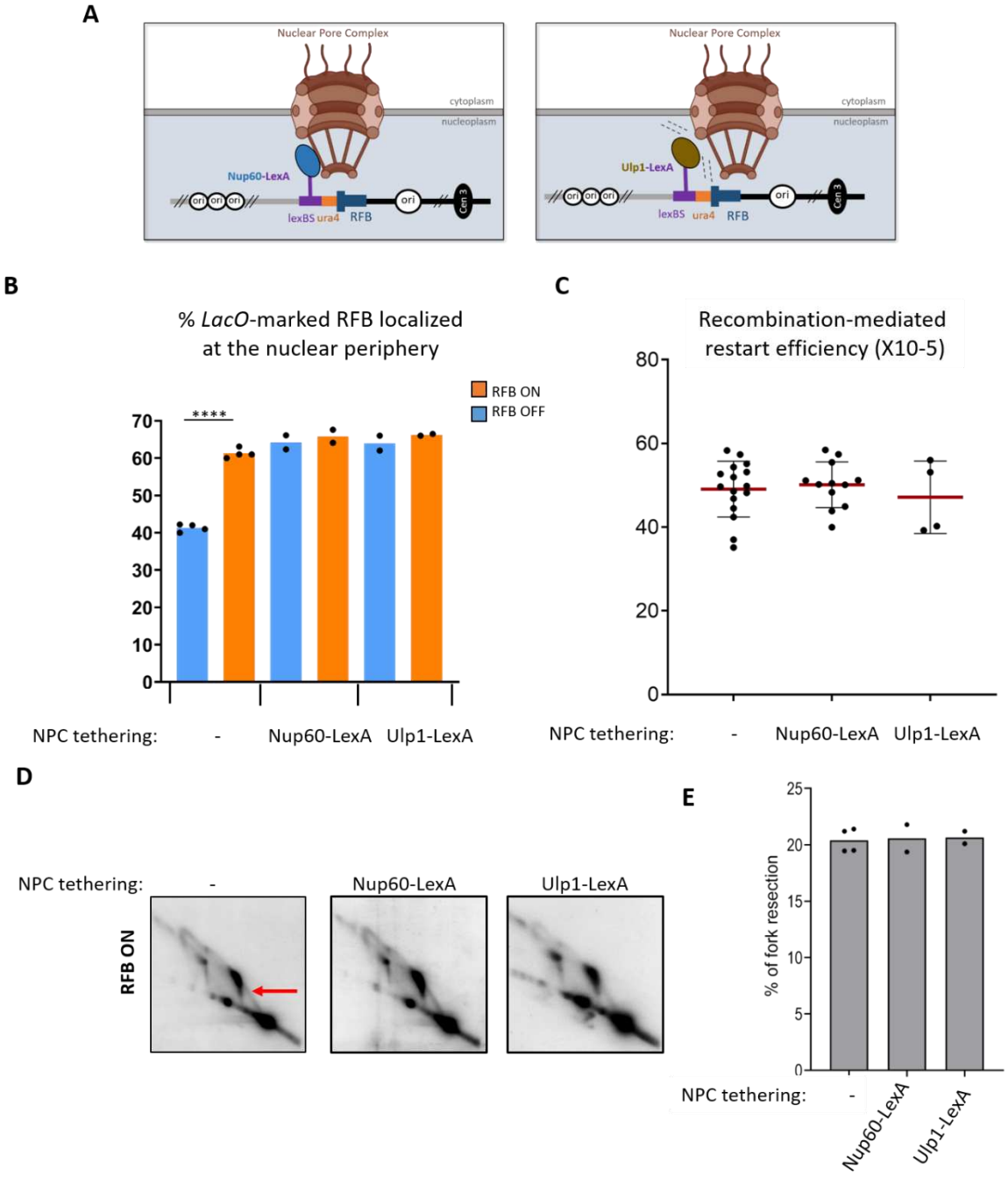

IV. How does a dynamic repositioning within a compartmentalized nucleus affect the maintenance of replication fork integrity?

Forks arrested at the RFB relocate to the nuclear periphery where they anchor to the NPC for around 20 minutes. This transient NPC association is critical to promote the HR-mediated fork restart (**Publication #1**, **Publication #2**), downstream the loading of recombination factors. During my PhD, I sought to decipher whether the shifting between different nuclear compartments has a role in maintaining the integrity of arrested replication forks.

1. The nuclear periphery is proficient for the controlled resection of nascent strand and RDR.

First, I investigated how an unceasing presence at the nuclear periphery would affect the integrity of arrested forks. To test this, I established a LexA-based strategy, where the RFB harbors eight LexA binding sites that are bound by LexA protein fused either to Nup60 (a nuclear basket component) or Ulp1 (SUMO protease located at the NP via interaction with NPC). This way, arrested forks were artificially tethered to the NPC (Figure 51A).

To validate the system, I analyzed the nuclear position of the RFB in *Wild Type* cells in which the tethering was applied or not. Upon expression of Nup60-LexA or Ulp1-Lex, the *LacO*-marked RFB was constitutively enriched at the nuclear periphery in both OFF and ON conditions (Figure 51B). This suggests that the NPC tethering works efficiently, regardless the barrier activation.

By employing the proxy-restart assay, I measured the frequency of RFB-induced replication slippage that indicates the HR-mediated DNA synthesis resumption at arrested forks. Remarkably, I observed that tethering the RFB to the NPC did not affect the efficiency of fork restart, (Figure 51C). Moreover, the analysis of replication intermediates by bi-dimensional gel electrophoresis (2DGE) showed that the artificial NPC anchorage of the RFB did not alter the extent of nascent strand degradation at arrested forks (Figure 51D and 51E).

Figure 52: **Loss of simultaneous loss of Nup131 and Nup132 results in uncontrolled exo1-dependent resection of nascent strands**. A: Representative replication intermediates analysis in indicated strains and conditions. The *ura4* gene was used as probe. Numbers indicate the % of forks blocked by the RFB ± standard deviation (SD). The red arrow indicates the tail signal resulting from resected forks. B: Quantification of resected forks in indicated strains. *p* value was calculated by two-sided t-test (** p≤0.01). C: Analysis of RPA binding at the *RTS1*-RFB by ChIP-qPCR in indicated strains (ON/OFF ratio). Upstream and downstream distances from the RFB are presented in base pairs (bp). Primers targeting ade6 gene were used as unrelated control locus. Bars indicate mean values ± standard deviation (SD). *p* value was calculated by two-sided t-test (* p≤0.05).

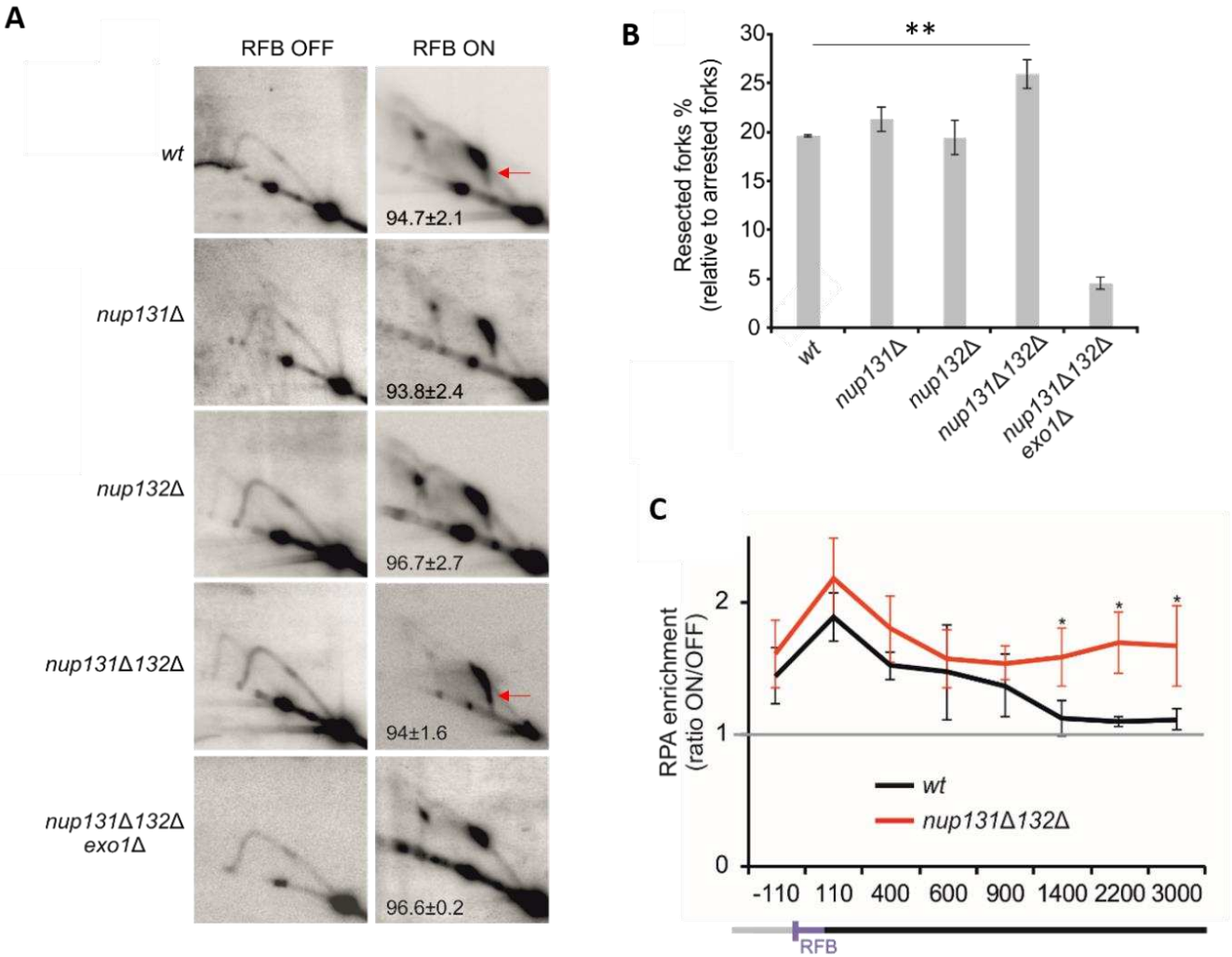

My data therefore indicate that the nuclear periphery is proficient for replication restart by homologous recombination and for the controlled degradation of nascent strand.

2. The lack of NPC anchorage results in unprotected forks in the nucleoplasm.

On the other hand, one unanswered question was to understand the consequences of a lack of NPC anchorage of arrested forks. We previously showed that upon severe disruption of the Y complex, the NPC is no longer able to anchor the RFB. As reported, the active *LacO*-marked RFB was enriched at the nuclear periphery in S-phase cells in the absence of either Nup131 or Nup132, however no relocation was observed in the absence of both nucleoporins (**Publication #1**: Figure 4D). Thus, I took advantage of the *nup131*Δ *nup132*Δ mutant to investigate the consequences of the lack of anchorage sites at the NPC on fork-integrity.

First, I examined the resection of nascent strands at RFB-arrested forks (referred to as resected forks). 2DGE analysis revealed that while the level of resected forks in the single *nup131*Δ or *nup132*Δ mutants was similar to the one of *Wild Type* cells, it was increased upon deletion of both nucleoporins (Figure 52A and 52B). The higher level of resected forks in the *nup131Δ nup132Δ* mutant was further suppressed by deleting the nuclease Exo1, suggesting that the nucleoplasm is a more permissive compartment to Exo1 activity.

To strengthen this conclusion, I analyzed the recruitment of the ssDNA-binding protein RPA to the RFB by ChIP-qPCR (Figure 52C). In *Wild Type* cells, RPA was recruited up to 1 kb upstream from the RFB as previously reported (Tsang et al., 2014). In *nup131Δ nup132Δ* mutant cells, I observed that RPA accumulated up to 3 kb upstream from the RFB, which suggest that indeed larger ssDNA gaps were formed at the RFB in the absence of Nup131 and Nup132. These results establish that the lack of anchorage sites at the NPC results in an uncontrolled Exo1-mediated fork-resection that impairs fork-integrity.

Figure 53: **Nuclear positioning of arrested forks influences the maintenance of replication fork integrity.** A: Representative images showing RPA foci (labeled with Ssb3-mcherry) colocalizing with GFP-LacI foci cells harboring the t-LacO-ura4<ori construct shown in Figure 47A. B: Quantification of cells showing the RPA-positive (orange) or RPA-negative (blue) *LacO*-marked-RFBs, according to their nuclear positioning. Fisher's exact test was used for group comparison to determine the *p* value (****p≤0.0001; **p≤0.01).

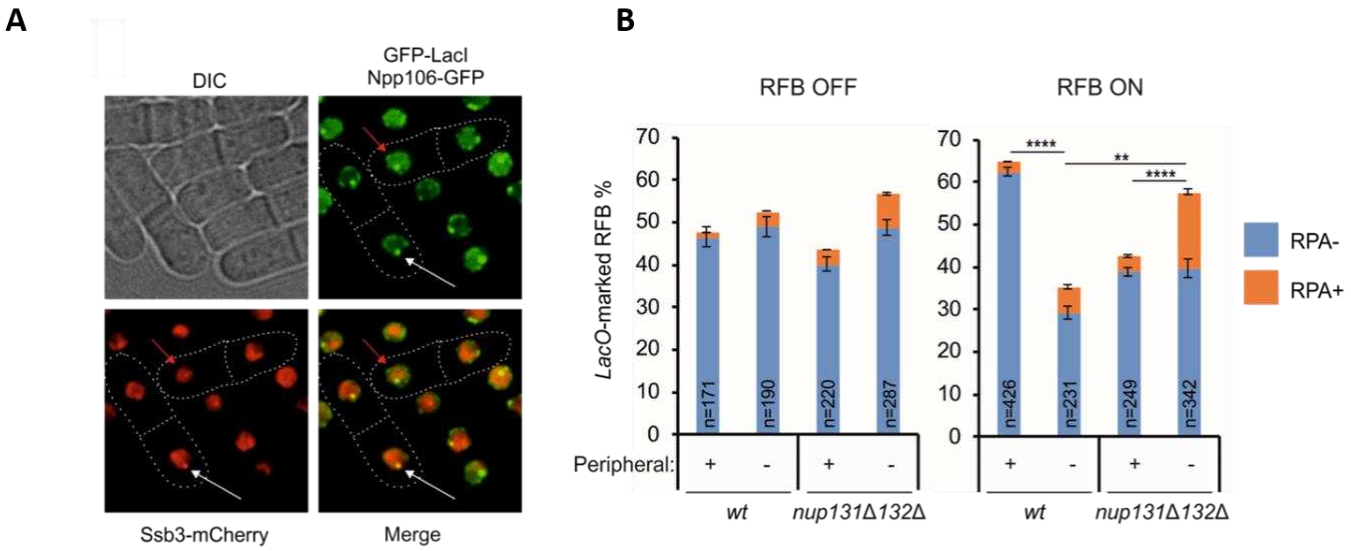

Previous study from our lab reported that the co-localization between the *LacO*-marked RFB and RPA is fully dependent on Exo1, indicating that those events mainly reflect the functionality of the Exo1-mediated long-range resection (Ait Saada et al., 2017). To further confirm that the uncontrolled Exo1-mediated long range resection occurs in the nucleoplasm, I analyzed by live cell imaging the *LacO*-marked RFB according to two criteria: their sub-nuclear position (*i.e.* being peripheral or not) and their association with RPA by addressing co-localization events between GFP-LacI and

Ssb3-mcherry, one of the subunit of the trimeric RPA (Figure 53A). Consistent with our previous findings, most of the active *LacO*-marked RFB became peripheral in *Wild Type* cells but not in the *nup132Δ nup131Δ* mutant (Figure 53B). Importantly, in the *Wild Type* cells, the induction of the RFB resulted in a ~ 2 fold increase in the frequency of RPA-positive *LacO*-marked RFBs (4,7% in RFB OFF vs 8,7% in RFB ON) with most of these forks being in the nucleoplasm, whereas peripheral RFB have the tendency to be less frequently associated with RPA. Namely, in ON condition the frequency of RPA-positive and non-peripheral RFB (6,3%) was higher than the frequency of RPA-positive but peripheral RFB (2,4%). This indicates that arrested forks anchored to the NPC have a clear tendency to be less associated with RPA that would be consistent with anchorage occurring after Rad51 loading, as previously proposed (Kramarz et al., 2020). Interestingly, in the *nup132Δ nup131Δ* mutant, the non-peripheral active RFBs were even more frequently RPA positive (17,9%) compared to *Wild Type* (6,3%). Notably, the frequency of RPA-positive RFBs positioned within the nucleoplasm increased by 2.3 fold upon RFB activation (7,9% in RFB OFF vs 17,9% in RFB ON), whereas the frequency of RPA-positive and peripheral RFB was unaffected (3,5% in RFB OFF vs 3,55% in RFB ON).

These data further suggest that the lack of anchorage sites at the NPC results in arrested forks being more frequently subjected to Exo1-mediated long-range resection and that this pathway occurs in the nucleoplasm.

Figure 54: **Artificial tethering of RFB to the NPC rescues the extensive resection in *nup131Δ nup132Δ* mutant.** A: Schematic representation of the LexA-based strategy to tether the RFB to the NPC. Nup60 (left) or Ulp1 (right) fused to LexA tether lexA-binding sites (lexBS, purple) inserted in a close proximity to *RTS1*-RFB site at the chromosome III. B: Quantification of co-localization events in S-phase cells in indicated conditions and strains. Dots represent values obtained from independent biological experiments. At least 100 nuclei were analyzed for each strain and condition. Fisher's exact test was used for group comparison to determine the *p* value (**p≤0.01). C: Representative replication intermediates analysis in indicated strains and conditions. The *ura4* gene was used as probe. Numbers indicate the % of forks blocked by the RFB ± standard deviation (SD). D: Quantification of resected forks in indicated strains. Dots represent values obtained from independent biological experiments. *p* value was calculated by two-sided t-test (** p≤0.01).

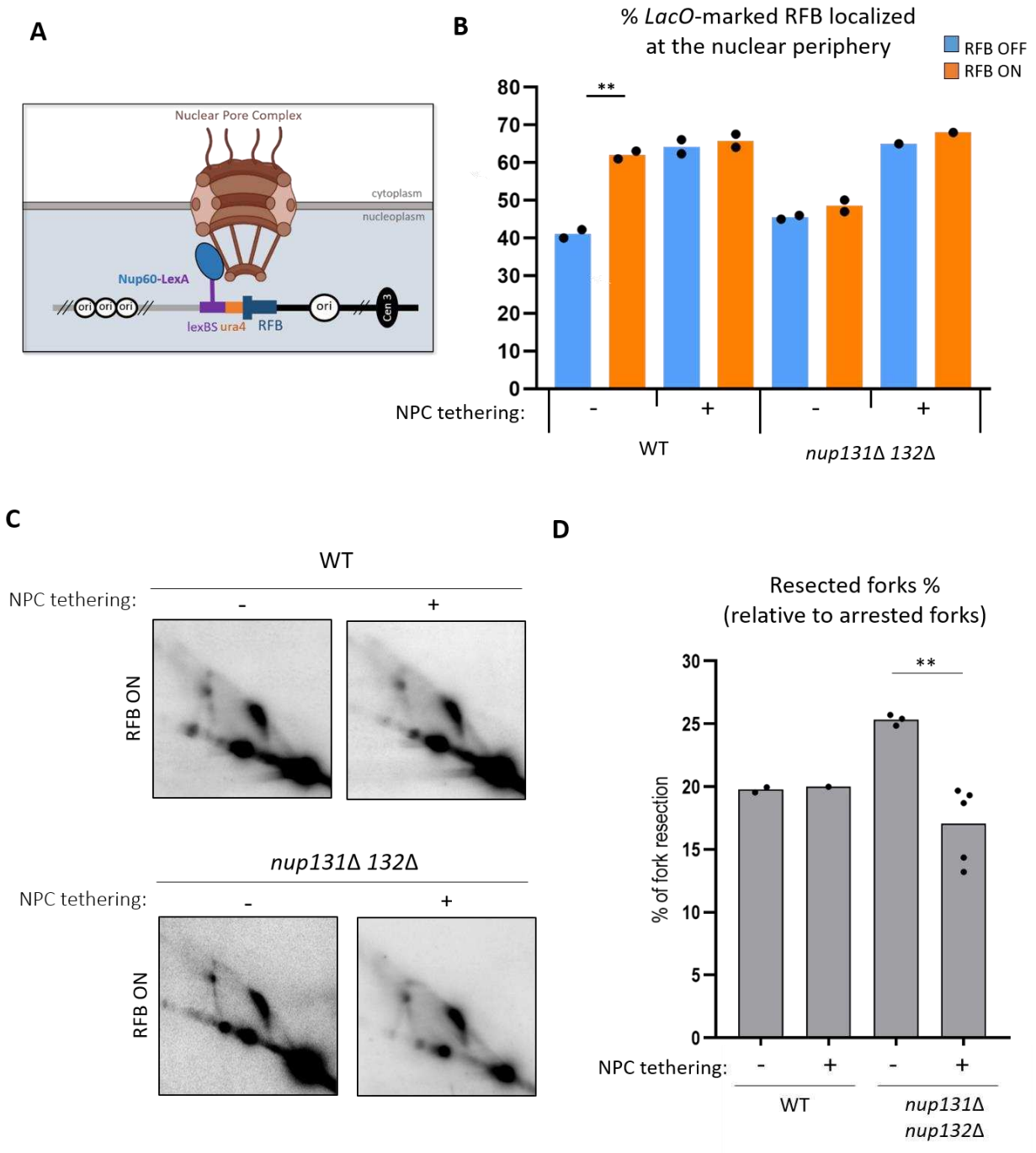

3. Spatially segregated SUMOylation and nuclear positioning affect the integrity of arrested replication forks.

To strengthen my hypothesis according to which unprotected forks, that remain in the nucleoplasm, are indeed a consequence of the lack of anchorage to NPCs, I took advantage of the above-described tethering approach to tether arrested forks to the NPC (Figure 54A).

Analysis of the nuclear positioning of the *LacO*-marked RFB showed that upon expression of Nup60-LexA, the RFB was constitutively enriched at the nuclear periphery whatever its activity (OFF or ON) in both *Wild Type* and *nup131Δ nup132Δ cells* (Figure 54B). This confirmed that in both genetic backgrounds the RFB is successfully tethered to the NPC.

Then I analysed the level of fork resection by 2DGE. I observed that the artificial tethering of the RFB to the NPC was sufficient to rescue the hyper-resection of nascent strands in the *nup132Δ nup131Δ* mutant, restoring fork protection to *Wild Type* level (Figure 54C and 54D). This data highlight that nuclear positioning contributes to safeguard the integrity of arrested replication forks.

This leads to the question, why does nucleoplasm become more permissive towards fork resection in this particular genetic condition. Interestingly, when I took a closer look at the different phenotypes of *nup131*Δ, *nup132*Δ and *nup132*Δ *nup131*Δ mutants, I noticed a striking dependency. Namely, the hyper-resection of nascent strands seems to correlate with the defective NPC anchorage and the lack of Ulp1 sequestration (Figure 55A). Moreover, I showed in Publication #2, that in the *alm1*Δ mutant, the active RFB is not enriched at the nuclear periphery without leading to an excessive resection of arrested forks (**Publication #2**: Figure 2D and 2G). This indicates that in this mutated background, the nucleoplasm is not more permissive to Exo1-mediated long range resection than in the *Wild Type*. Importantly, in the absence of Alm1, Ulp1 was properly sequestrated at the nuclear periphery (**Publication #2**: Figure 4). This highlights that not just the mere, but rather the simultaneous failure to shift the RFB to the NPC and to sequester Ulp1 at the nuclear periphery leads to an hyper-resection of forks located in the nucleoplasm. Thus, I hypothesized that maintaining arrested replication forks in the nucleoplasm when Ulp1 is no longer sequestered at the nuclear periphery is detrimental to fork integrity (Figure 55B).

Figure 55: **Unprotected forks correlate with the lack of RFB anchorage to NPC and Ulp1 mislocalization.** A: Representative cell images of Ulp1-GFP in indicated strains. B: Schematic illustration of the hypothesis that loss of Ulp1 sequestration may jeopardize fork protection in the nucleoplasm.

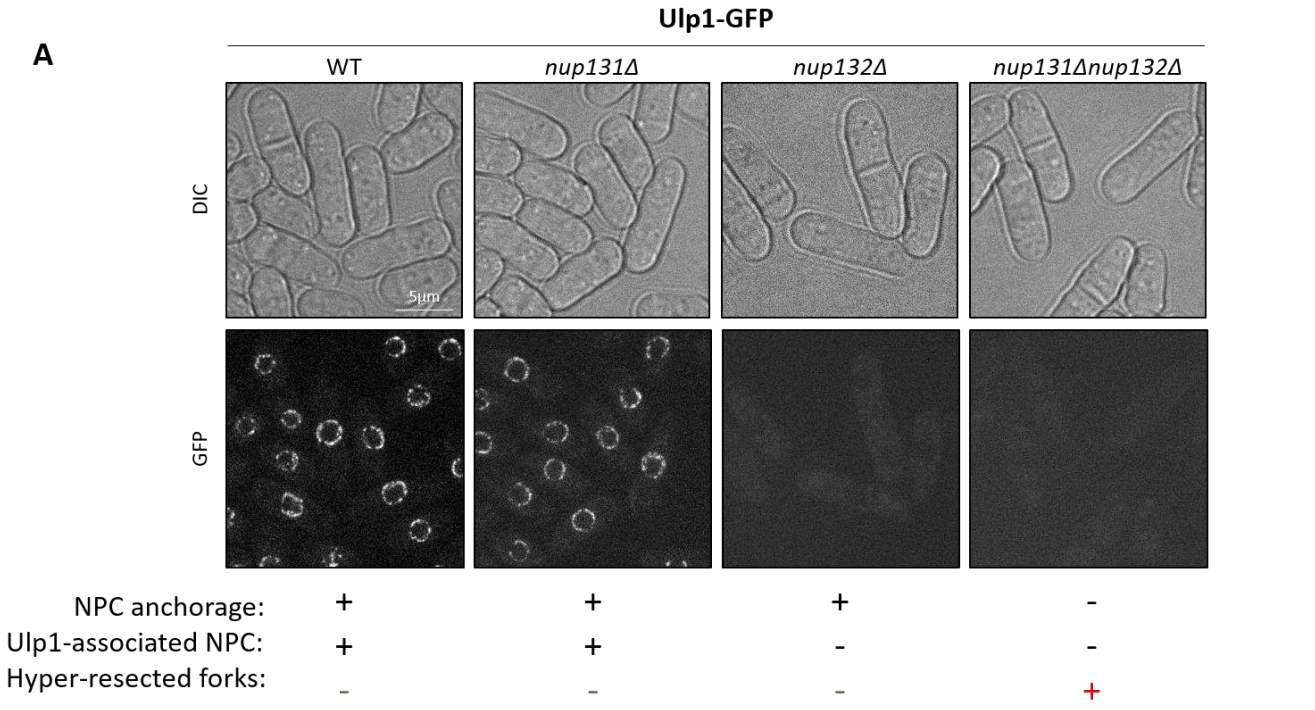

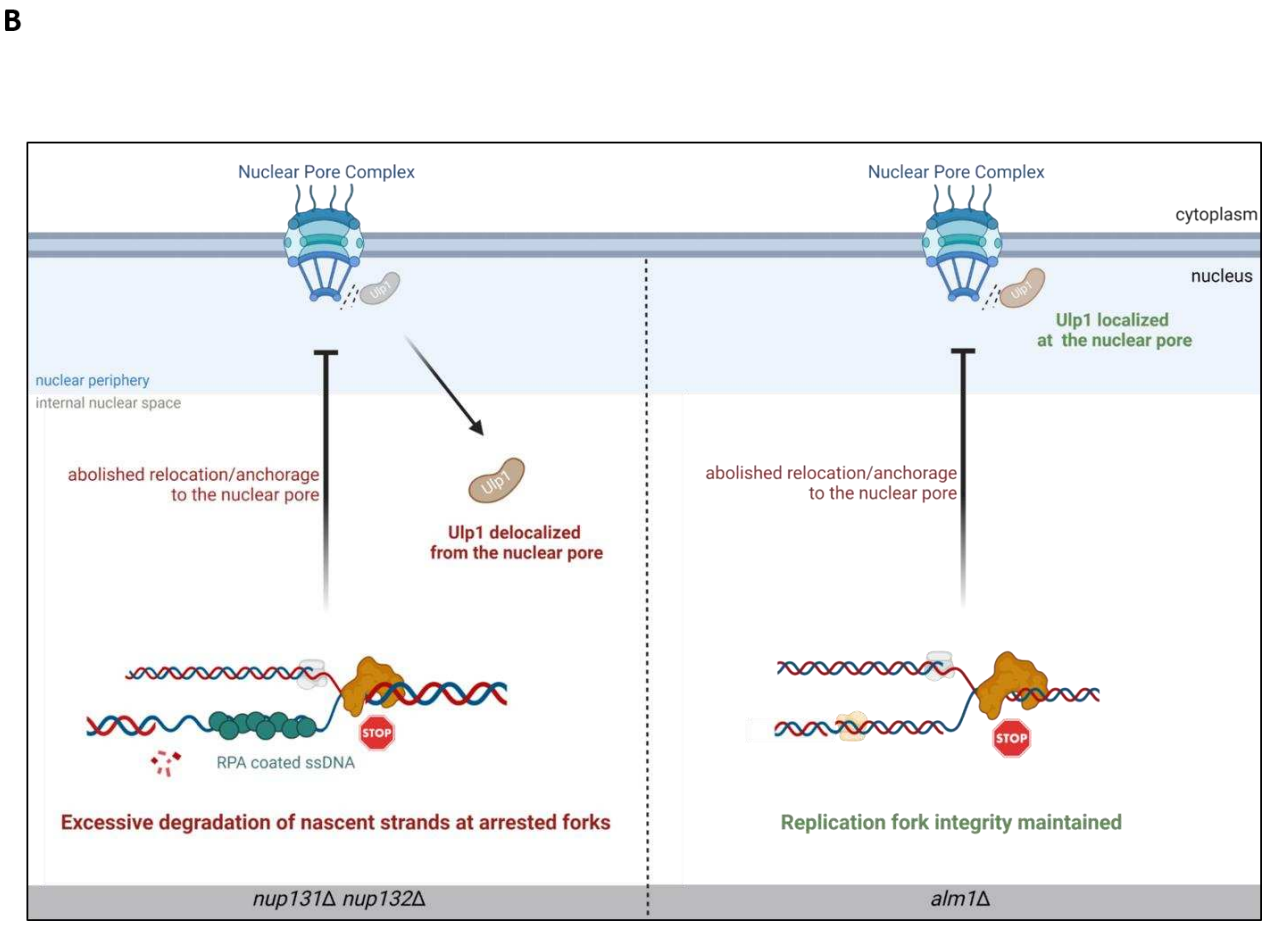

While additional experiments are required to clarify the molecular details of the underlying mechanism, two hypotheses of how Ulp1 delocalization may jeopardise fork protection will be discussed in the following section.

Contributions

The experiments, the results of which are presented in Figure 52, Figure 53 and Figure 55, were carried out in cooperation with Karol Kramarz, a former postdoc in the team.

DISCUSSION

I. Mechanisms engaged at Nuclear Pore Complexes to promote the restart of arrested replication forks

Different types of perturbed replication forks shift towards the nuclear periphery to associate with NPCs, which act as a DNA repair hub (Pinzaru et al., 2020; Lamm et al., 2020; Whalen et al., 2020; Kramarz et al., 2020). However, the precise mechanisms engaged at the nuclear periphery are not fully elucidated. In fission yeast, forks arrested at DNA-bound protein complexes relocate in a SUMO-dependent manner and anchor to NPCs to ensure fork restart by the recombination-dependent replication mechanism (RDR) (Kramarz et al., 2020). The resumption of DNA synthesis at arrested forks is facilitated by the action of two enzymatic activities being enriched at the nuclear periphery: the SUMO protease Ulp1 and the proteasome.

1. The nuclear basket promotes recombination-dependent replication in pre- and post-anchoring manners.

We previously reported that the nucleoporin Nup132 (ScNup133, HsNUP133), a component of the Y complex of the NPC, has a post-anchoring role in promoting recombination-mediated fork restart by ensuring the sequestration of Ulp1 at the nuclear periphery (**Publication #1**). This sequestration of Ulp1 is necessary to counteract the inhibitory effect of SUMO chains on the efficiency of RDR.

During my PhD, I have shown that nucleoporins of the nuclear basket are also involved in facilitating optimal recombination-mediated fork restart by at least two means. The Nuclear basket, a NPC sub-complex extending into the nucleoplasm, is composed of Nup60 (ScNup60), Nup61 (ScNup2, HsNUP50), Nup124 (ScNup1, HsNUP153) and Alm1 (ScMlp1/2, HsTPR). A fifth component is the essential nucleoporin Nup211, a second orthologue of ScMlp1/2 and HsTPR (Varberg et al., 2022). Combining our genetic assay and live cell-microscopy approach, I found that the nuclear basket nucleoporin Nup60 promotes efficient fork restart in a post-anchoring manner by ensuring the sequestration of Ulp1 at the nuclear periphery (**Publication #2**: Figure 2B, Figure 4). It is consistent with the situation in budding yeast, where ScNup60 was shown to be required to localize and stabilize the Ulp1 SUMO protease at the nuclear periphery (Zhao et al., 2004). Furthermore, the reduced efficiency of RDR and destabilization of Ulp1 in Nup60-deficient cells resembles the previously described phenotype of the *nup132*Δ mutant (**Publication #1**: Figure 4B; **Publication #2**: Figure 4). Interestingly,

in budding yeast, the *loss of ScNup84 (Y complex component)* led to a partial delocalization of ScNup60 from the NPC to the nucleoplasm. Moreover, *in vitro* data revealed that ScNup60 can directly interact with both ScNup133 and ScNup84 (Niño et al., 2016). A study in mouse cells reported that NUP133 is required for the proper nuclear basket assembly. Depletion of NUP133 specifically led to TPR-deficiency in approximately one-half of NPCs and perturbed the dynamics of NUP153 (Souquet et al., 2018). In the context of these data, it is therefore possible that the fission yeast SpNup132 contributes to the proper nuclear basket assembly by stabilizing SpNup60, thus establishing a binding interface between the NPC and Ulp1. To validate this model, the sub-nuclear localization and stability of Nup60 should be tested in *nup132*Δ mutant.

Noteworthy, I observed that in *nup124*Δ cells the reduction of Ulp1 level at the nuclear periphery by 40% did not correlated with a detectable defect in RDR efficiency (**Publication #2**: Figure 2B, Figure 4)**.** Hence, to some extent a lowered abundance of Ulp1-associated NPCs is not a limiting factor in promoting recombination-dependent fork restart.

I further demonstrated that another nuclear basket component, the nucleoporin Alm1, also contributes to replication resumption at RFB-arrested forks. Intriguingly, Alm1 promotes RDR in both a pre- and post-anchoring manner.

First, I identified that in the absence of Alm1, fork arrested by the RFB were no longer enriched at the nuclear periphery (**Publication #2**: Figure 2G). Upon *alm1* deletion, the nucleus volume increased by 40% thus the arrested forks would have to travel a longer distance to reach the nuclear periphery, where then the density of NPCs is lowered (**Publication #2**: Figure 4C, Figure S3A). Moreover, to date, the involvement of TPR homologues in anchoring DNA lesions to NPCs has not been reported in yeast models. Thus, I lean towards the hypothesis according to which the lack of relocation in Alm1-deficient cells is rather an indirect effect due to two features, namely the alterations of nuclear morphology and reduced NPCs abundance. To strengthen this hypothesis, the dynamics of the *LacO*-marked RFB could be compared in *WT* and *alm1*Δ cells. If the active RFB explores a comparable area in both cases, this might explain why arrested forks could not reach the nuclear periphery within an enlarged nucleus in *alm1*Δ mutant. Such inability to enhance the mobility of arrested replication forks could result from constraints in physical forces such as F-nuclear actin polymerization, although such mechanism has not been yet reported in yeasts models.

Second, the artificial anchorage of the RFB to NPCs was not sufficient to rescue the RDR defect of *alm1Δ* cells, indicating that Alm1 is also required to promote the restart of arrested forks upon their relocation to the NPC (**Publication #2**: Figure 5B). In contrast to Nup60, this post-anchoring role of Alm1 is not linked to ensuring the spatial sequestration of Ulp1 at the nuclear periphery. In budding yeast, the synergistic action of Mlp1 and Mlp2 (two orthologues of human TPR) is critical for the peripheral localization of Ulp1 (Zhao et al., 2004). Unfortunately, I could not address a similar possibility for the two fission yeast TPR orthologues, as I failed to generate a viable double mutant cells deficient for both, Alm1 and Nup211. Nonetheless, the RDR defect of *alm1Δ* cells was not bypassed by preventing SUMO chains formation, confirming that this mutant does not suffer from an inability to cancel the toxicity of SUMO chains. Interestingly, it was shown that several proteasome subunits are delocalized from the nuclear periphery in *alm1Δ* cells (Salas-Pino et al., 2017). We previously reported that the proteasome activity is required to promote RDR in a post-anchoring manner (**Publication #1**: Figure 6A and 6B). Hence, the second role of Alm1 likely relies on its ability to enrich proteasome components at the nuclear periphery.

Altogether, this work identifies distinct roles of nuclear basket components in promoting an efficient recombination-dependent restart of arrested forks, with Nup60 being involved in the spatial sequestration of Ulp1 and Alm1 ensuring the enrichment of proteasome subunits at the nuclear periphery.

2. Ulp1 and proteasome activities differently regulate the dynamic of restarted DNA synthesis at arrested replication forks

Previously, using a proxy-restart assay as a readout of RDR efficiency, we reported that both the Ulp1 SUMO protease and the proteasome are required for efficient recombination-mediated fork restart (**Publication #1**: Figure 6B). Here, by mapping DNA polymerases usage, we reveal that these two factors favor the optimal dynamic of DNA synthesis at restarted forks by two distinct mechanisms.

First, we identified a role for Ulp1 in counteracting the inhibitory effect of SUMO chains to engage the Polδ/Polδ DNA synthesis at restarted forks (**Publication #2**: Figure 1). This mechanism requires the sequestration of Ulp1 at the nuclear periphery, which is coordinated by the Y complex nucleoporin Nup132 and the nuclear basket nucleoporin Nup60, as discussed above. Thus, Ulp1-associated NPCs promote an efficient initiation

Figure 56: **SUMOylated PCNA and Srs2 downregulates the HR pathway at restarted replication forks.** PCNA SUMOylation targets Srs2 to stalled replication forks. At the D-loop intermediate, Srs2 promotes the dissociation of polymerase delta, which blocks the further progression of DNA synthesis at the restarted replication forks. (Adapted from Burkovics et al., 2013)

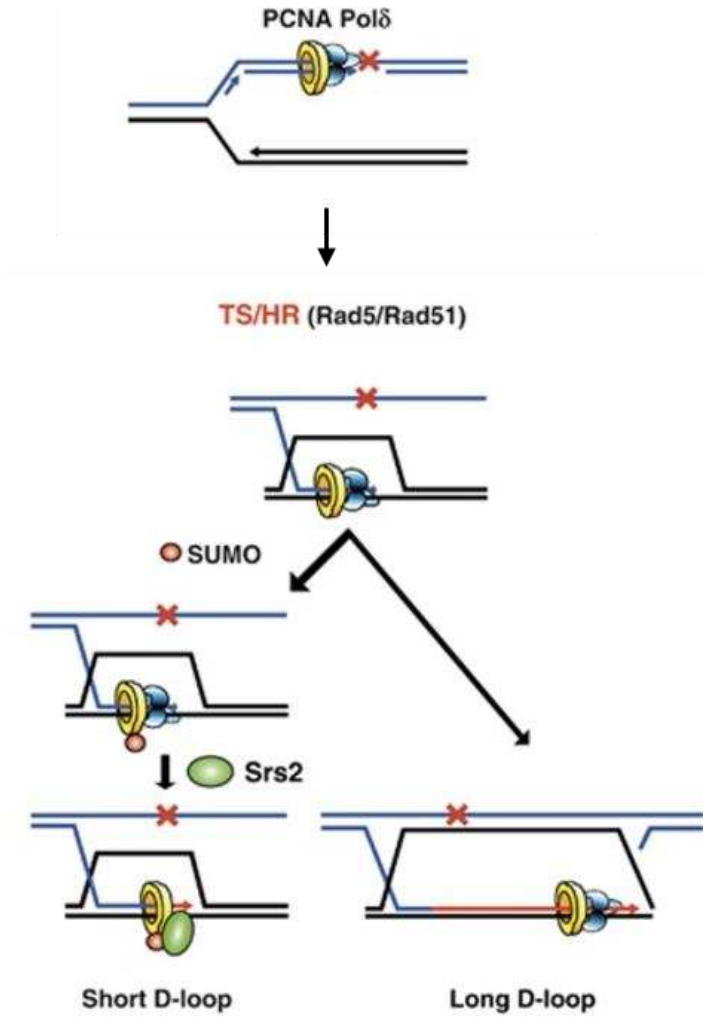

of DNA synthesis resumption, without affecting the speed of the successfully restarted replication forks.

To date, we have not identified a specific target(s) whose modification by SUMO chains would result in a negative regulation of recombination-dependent replication fork restart. However, other reports allow for speculation regarding a potential target that could be involved in this mechanism. In budding yeast, SUMOylated PCNA has the ability to recruit the anti-recombinase Srs2 to stalled replication fork in order to prevent unwanted recombination events (Papouli et al., 2005; Pfander et al., 2005). Srs2 is well known to restrict HR by disassembling Rad51 nucleofilaments, but a more recent study reported a novel mechanism by which SUMO-PCNA together with Srs2 can block the extension of DNA synthesis from a recombination intermediate. *In vitro* experiments showed that Srs2, through interaction with SUMOylated PCNA inhibited the D-loop extension by disrupting the elongation complex composed of polymerase δ and SUMOylated PCNA (Figure 56) (Burkovics et al., 2013). Interestingly, Ulp1-mediated deSUMOylation of PCNA restored the D-loop extension activity of polymerase δ. A similar mechanism could underline the inhibitory effect of SUMO-chains on the initiation of DNA synthesis at RFB-arrested forks in our system, as during RDR both DNA strands are synthesized by polymerase δ. Although SUMOylation of PCNA has not been yet demonstrated in fission yeast, different SUMOylated factor(s) present at the arrested forks could also attract Srs2 to inhibit polymerase δ. Thereafter, anchorage to Ulp1-associated NPCs would allow to overcome SUMO-mediated recruitment of Srs2 and facilitate an efficient resumption of DNA replication by Polδ/Polδ forks. Indeed, fission yeast Srs2 poses several putative SIM motifs, which could support the proposed model, however it requires to be further investigated.

Moreover, we established that proteasome activity helps to maintain the optimal dynamics of HR-mediated DNA synthesis by fostering the progression of restarted DNA polymerases (**Publication #2**: Figure 6C and 6D). This function occurs independently of counteracting the inhibitory effect SUMO chains (**Publication #2**: Figure 6A). Although, we previously identified a role of Slx8-Rfp1/Rfp2, the E3 ubiquitin ligase that targets SUMOylated proteins for degradation (STUbL), in promoting efficient fork restart by the RDR pathway (**Publication #1**: Figure 3D, Figure 5E). This can therefore indicate that monoSUMOylated or chain-free multiSUMOylated factors (modified with single SUMO moieties at multiple sites) can be the potential targets of STUbL- and proteasome-dependent pathway that ensures the speed of restarted DNA polymerases. Such SUMO chains-independent regulation of STUbL functions have been reported. In budding yeast, the monoSUMOylation occurring at forks collapsed at CAG repeats is sufficient for Slx5 to promote relocation

of these dysfunctional forks to the NPC (Whalen et al., 2020). Human STUbL RNF4 can also bind to a substrate that is monoSUMOylated on multiple lysines (Aguilar-Martinez et al., 2017). Nonetheless, I do not exclude that a proteasome-mediated degradation of polyubiquitinated but SUMO-free substrates also plays a role in promoting RDR.

So what could be the molecular link between the proteasome activity and fostering replication forks speed? One simple explanation would be the removal of chromatin bound proteins that directly impede the progression of the replicative helicase or DNA polymerase (Langston and O'Donnell, 2017). Alternatively, the proteasome could be involved in the degradation of factors that stabilize or promote the formation of topological barriers ahead of replication forks.

Overall, these data provide new mechanistic insights into the regulation of recombination-dependent replication restart at the NPC, hence attributing the need for dysfunctional forks to change their nuclear position. Ulp1-associated NPCs by counteracting the inhibitory effect of SUMO chains contribute to efficient initiation of restarted DNA synthesis, whereas proteasome-associated NPCs foster the progression of restarted DNA synthesis, in a SUMO chain independent manner. Interestingly, the activities of Ulp1 and the proteasome cannot compensate for each other, likely targeting distinct substrates.

3. Two spatially segregated sub-pathways of recombination-dependent replication restart?

Relocation towards the nuclear periphery and the anchorage of perturbed replication forks to NPCs ensure the resumption of DNA synthesis at terminally dysfunctional forks by promoting a recombination-dependent replication restart mechanism.

However, it was noticed that in some genetic backgrounds recombination-dependent replication restart can also occur without a routing towards the nuclear periphery and NPC anchorage. This applies to cells deleted for the main E3 SUMO ligase Pli1 (*pli1*Δ) and cells expressing the mutated allele of SUMO which is unable to form SUMO chains (*SUMO-KallR*) (Figure 48). In both cases SUMOylation is hampered, which likely bypass the need for anchorage to Ulp1-associated NPC to overcome the inhibitory effects of SUMO conjugates on the initiation of DNA synthesis. Interestingly, my genetic analysis established the efficiency of RDR in SUMO-KallR cells is drastically reduced upon

deletion of Rpn10, a proteasome subunit (**Publication #2**: Figure 6A). This indicates that when SUMO chains-mediated relocation is defective, the recombination-dependent fork restart in the nucleoplasm still relies on a functional proteasome.

Preventing SUMO chains increased the RDR efficiency as compared to Wild Type, whereas the lack of Pli1 did not (Figure 48). This suggested that while SUMO chains limit recombination-mediated DNA synthesis, Pli1-dependent mono-SUMOylation events remain necessary to promote replication restart. Indeed, the analysis of DNA polymerase usage during HR-dependent fork restart revealed that the loss of Pli1 affects the initiation of DNA synthesis at restarted forks but do not impair the progression of restarted DNA polymerases (Figure 42). Of note, *pli1* deletion is associated with decreased levels of Rad51 binding to arrested forks (Figure 43). It is thus possible that, at the early stages of fork arrest, Pli1-dependent monoSUMOylation ensures Rad51 recruitment, which is then pivotal for the efficient initiation of DNA synthesis to restart replication. A recent study in budding yeast reported that in the context of stalled replication forks, the monoSUMOylation of DDK stabilizes Rad51 on exposed ssDNA gaps to facilitate both recombination-mediated gap filling and DNA damage bypass (Joseph et al., 2020). In light of this, it would be important to test whether Rad51 is efficiently recruited to arrested forks in *SUMO-KallR* mutant that is proficient only in monoSUMOylation. Moreover, the analysis of DNA polymerase usage during HR-dependent fork restart would help to determine whether the increased level of RDR in the *SUMO-KallR* mutant is due to a more efficient initiation of restarted DNA synthesis or results from elevated speed of the restarted forks. Another remaining question is whether the level of recombination-mediated fork restart in SUMO chains-deficient cells would remain increased if the arrested forks were permanently located at the periphery?

On the other hand, the increased frequency of RDR in the relocation-deficient SUMO-KallR mutant, could also suggest the existence of two spatially distinct sub-pathways of HR-mediated fork restart. One pathway triggered by SUMO chains formation and followed by relocation to the nuclear periphery, and a second pathway signaled by mono-SUMOylation and occurring within the nucleoplasm. Previous work from our team demonstrated that in *rad51*Δ cells the effectiveness of recombination-dependent fork restart was decreased by 60-70% (Ait Saada et al., 2017). Such partial reduction indicates that the remaining fork restart occurs through a Rad51-independent pathway. Consistent with this observation, a recent study in fission yeast reported that replication forks arrested at the RFB can be restarted by a Rad51-independent pathway, which

relies on the single strand annealing (SSA) activity of Rad52 (Kishkevich et al., 2022). However, it is still unclear how frequently this pathway is used and how it is regulated. All the above insights lead to the hypothesis according to which a Rad51-independent sub-pathway of RDR may occur when the relocation of arrested forks to the nuclear periphery is impaired. Determining whether the replication fork restart occurring in the nucleoplasm relies on the SSA activity of Rad52, but not on its function of loader of the recombinase Rad51, is the subject of the PhD project of another student in our team – Shrena Chakraborty.

II. Key determinants of replication forks integrity within a compartmentalized nucleus

DNA end resection needs to be tightly regulated because insufficient or excessive resection threatens genome stability (Ronato et al., 2020; Cejka and Symington, 2021). Especially, large stretches of persistent single-stranded DNA, generated for example at halted replication forks, are extremely vulnerable to DNA damaging agents and hypermutation (Saini and Gordenin, 2020). Therefore, protecting replication forks from extensive degradation is essential to prevent genome instability, a major driving force at tumorigenesis.

1. Pli1-dependent monoSUMOylation protects fork integrity

I have observed that SUMOylation mediated by the E3 SUMO ligase Pli1 is critical for maintaining the integrity of arrested replication forks, while the second E3 SUMO ligase Nse2 seems to be dispensable (Figure 49). Importantly, I have confirmed that Pli1 function in protecting replication fork is dependent on its E3 SUMO ligase activity. More specifically, monoSUMOylation is sufficient to limit the extent of ssDNA at arrested replication forks that fail to anchor to NPCs and remain in the nucleoplasm.

What could be the mechanism by which Pli1 ensures the negative regulation of nascent strand degradation?

First, SUMOylation may recruit and/or promote the optimal binding of HR factors that are known for their role in the protection of replication forks. Indeed, I found that upon RFB activation, Pli1 promotes a local wave of SUMOylation and also favors the

enrichment of Rad51 at the active RFB (Figure 43, Figure 50). In support of the idea that Pli1-mediated SUMOylation promotes Rad51 recruitment to arrested replication forks, the human E3 SUMO ligases PIAS1 and PIAS4 were also shown to be required for RAD51 accumulation at sites containing DNA damage (Shima et al., 2013). However, SUMOylation appears to exert a complex control of Rad51 accumulation at sites of DNA damage.

RAD51 harbors a SIM motif that is required for the interaction with SUMO-1 and was identified as necessary for RAD51 DNA damage-induced accumulation on chromatin (Shima et al., 2013). Two putative SIM motifs were recently identified in budding yeast ScRad51. Mutations of these putative SIMs did not interfere with ScRad51 protein stability, however they drastically diminished the accumulation of Rad51 on damaged chromatin around replication regions (Joseph et al., 2022). In both yeast and human, Rad52 and RPA are known to be SUMOylated and may serve as the binding partners for Rad51 (Ho et al., 2001; Sacher et al., 2006; Dou et al., 2010; Dhingra et al., 2019). Thus one possibility is that such noncovalent SIM–SUMO interactions are involved in regulating Rad51 recruitment to arrested replication forks in fission yeast.

On the other hand, a recent study showed that RAD51 is itself SUMOylated by the E3 SUMO ligase TOPORS both *in vitro* and *in vivo* (Hariharasudhan et al., 2022). RAD51 SUMOylation by TOPORS is required for RAD51 chromatin recruitment at IR-induced DSBs. The authors provided also molecular insight into how SUMOylation regulates the RAD51's activity by revealing that SUMOylation of RAD51 has a critical role in regulating its associating with BRCA2. In budding yeast, Mms21-dependent mono-SUMOylation of Rad51 promotes its recruitment to DNA (Antoniuk-Majchrzak et al., 2023). It would be therefore important to know if monoSUMOylation is also sufficient to promote fission yeast Rad51 recruitment to arrested forks. If so, it would explain why the integrity of RFB-arrested replication forks was maintained in SUMO-chains deficient cells (*SUMO-KallR* mutant) but not in cells deficient for the E3 SUMO ligase Pli1.

Alternatively, nuclease activities may be subjected to a SUMO-based regulation via direct or indirect means to control the resection at arrested replication forks.

For example, human CtIP (a nuclease involved in the initial resection of DSB) is SUMOylated by the E3 SUMO ligase PIAS4 and this modification is important for its role in protecting stalled replication forks from excessive nucleolytic degradation by the DNA2 exonuclease (Przetocka et al., 2018; Han et al., 2021; Locke et al., 2021). On the other hand, SUMOylated CtIP is targeted by STUbL RNF4 for ubiquitination and subsequent proteasomal degradation. Such mechanism was showed to avoid uncontrolled extensive resection by preventing aberrant accumulation of CtIP at DSBs

(Han et al., 2021). CtIP's yeast counterparts, namely ScSae2 and SpCtp1, were also shown to be modified by SUMO (Sarangi et al., 2015). SUMOylation is also known to regulate the activity of enzymes involved in long range resection. Budding yeast ScDna2 is SUMOylated *in vivo* by the E3 SUMO ligase ScSiz2 and this modification moderately attenuates the nuclease activity of Dna2 *in vitro*, but does not affect the helicase activity. *In vivo*, SUMOylation of Dna2 facilitates its degradation leading to its reduced protein levels (Ranjha et al., 2019). Moreover, PIAS1/PIAS4-dependent SUMOylation of human EXO1 was shown to promote its ubiquitin-mediated degradation (Bologna et al., 2015). Taking advantage of an *in vitro* reconstituted system, the authors demonstrated the conservation of Exo1 SUMOylation in budding yeast by the ScSiz1/ScSiz2.

Thus, it is possible that Pli1-dependent SUMOylation inhibits the uncontrolled degradation of nascent strand at arrested forks in the nucleoplasm by either restricting the nucleolytic activity of nucleases or by promoting their STUbL-mediated degradation. In the context of our previous observations, the second possibility appears to be unlikely, because we did not observe any increase in extensive fork resection upon inactivation of the fission yeast STUBL complex (*rfp1*Δ *rfp2*Δ) (**Publication #1**: Figure 3F).

All of the above proposed scenarios are not exclusive, as the SUMOylation wave observed at the RFB may lead to simultaneous and multi-site modifications of different factors.

2. Spatially segregated SUMO metabolism safeguards the integrity of replication fork within a compartmentalized nucleus

My data indicate that the interplay between the localization of the SUMO protease Ulp1 and nuclear positioning contributes to maintain the integrity of arrested replication forks (Figure 56B). Arrested forks, that failed to anchor to the NPC, were being more frequently subjected to Exo1-mediated long-range resection if Ulp1 was no longer localized at the nuclear periphery (in the *nup131*Δ *nup132*Δ mutant). On the contrary, when Ulp1 was properly distributed at the nuclear periphery, arrested forks positioned within the nucleoplasm were not undergoing extensive degradation (in the *alm1*Δ and *sumo-KallR* mutants). How a defective Ulp1 sequestration at the nuclear periphery makes the nucleoplasmic compartment more permissive to Exo1-mediated

Figure 57: **Strategy to stabilize Pli1 in the *nup132Δ* genetic background.** Schematic diagram indicating the relative positions of three lysine residues, whose ubiquitination promotes degradation of Pli1 (A). Western Blot analysis of Pli1-Flag, or Pli1K3R –Flag protein levels in Wild Type and nup132Δ mutant (B). While the unmodified Pli1 is destabilized in *nup132Δ* cells, the levels of Pli1K3R levels remain high, indicating that mutating K15, K169 and K214 residues is sufficient to stabilize Pli1 in cells lacking Nup132. (Strachan et al. 2022)

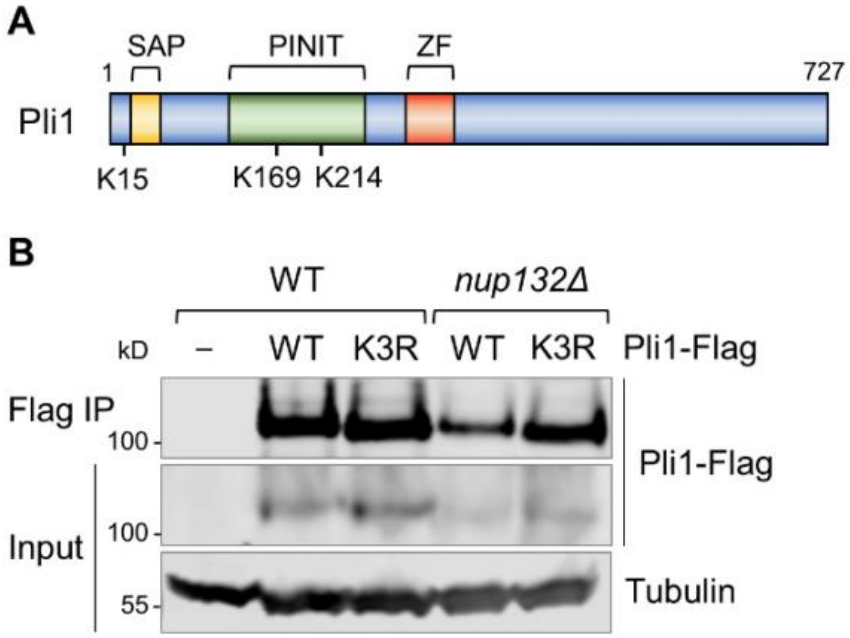

long range resection? Consistent with my observations, I propose that the lack of Ulp1 peripheral localization is detrimental to replication fork integrity by counteracting Pli1-dependent monoSUMOylation, which is essential for replication fork protection in the nucleoplasm. Two hypotheses that explain this phenomenon are discussed below.

Ulp1 destabilization leads to Pli1 degradation

The fission yeast E3 SUMO ligase Pli1 is auto-SUMOylated and accumulates SUMO chains that can serve as binding sites for STUbL (Nie et al., 2015). In normal conditions, Ulp1 deSUMOylates Pli1 to protect it from ubiquitinated-mediated proteasomal degradation. However, when delocalized, Ulp1 is degraded and can no longer counteract Pli1 SUMOylation. Consequently, polySUMOylated Pli1 is subjected to STUbL-mediated degradation, which causes profound defects in the SUMO pathway (Nie et al., 2015). Such global decrease in Pli1-dependent SUMOylation (similar to the one observed in *pli1*Δ mutant), may prevent the modification of key substrates involved in protecting nascent strands from degradation, when arrested forks are in the nucleoplasm.

Thus, the defect in fork protection in *nup131*Δ *nup132*Δ mutant could arise as a result of Pli1 destabilization, since in the absence of Nup132, Ulp1 is mislocalized from the NPC and subsequently degraded leading to ubiquitin-dependent degradation of Pli1. To verify this hypothesis, the level of fork resection could be checked in a condition, where Pli1 does not undergo degradation in the *nup131*Δ *nup132*Δ background.

Recently, Strachan *et al.* identified three residues of the fission yeast Pli1 (K15, K169 and K214), whose ubiquitination promotes degradation of Pli1 in *nup132*Δ cells (Strachan et al., 2022, preprint). Mutations of these three lysines to arginine were sufficient to stabilize the mutated Pli1 (Pli1-K3R) in the *nup132*Δ background (Figure 57). As part of the newly established collaboration with Joanna Strachan and Elizabeth Bayne (University of Edinburgh), we received strains caring wild-type or mutant Pli1 tagged with FLAG (Pli1-FLAG, Pli1-K3R-FLAG). The next step will be to test whether the stabilizing Pli1-K3R mutation is sufficient to rescue the defect in fork protection observed in *nup131*Δ *nup132*Δ cells. If so, it would support the first hypothesis that when Ulp1 is no longer sequester at the nuclear periphery, the inability to protect replication forks in the nucleoplasm is due to destabilizations of Pli1.

Ulp1 mislocalisation results in unscheduled deSUMOylation of nuclear targets

The loss of Ulp1 sequestration at the nuclear periphery leads to decreased levels of Ulp1, which in turn result in aberrant SUMOylation of some of its substrates (as in the

above discussed case of E3 SUMO ligase Pli1). However, it is also believed that mislocalized Ulp1, even in low amounts, could deSUMOylate some nuclear substrates and reduce the amount of their SUMOylated forms (Panse et al., 2003; Palancade et al., 2007). For example, a study in budding yeast showed that upon deletion of its N-terminal NPC-targeting domain, Ulp1 partially overcomes phenotypic abnormalities associated with loss of its paralogue Ulp2. It indicated that Ulp1 mislocalized in the nucleoplasm acquired the ability to deSUMOylate substrates that are normally restricted to Ulp2 (Li and Hochstrasser, 2003). Thus, Ulp1 sequestration can prevent the deSUMOylation of nucleoplasmic proteins in an unregulated manner.

Therefore, it is also likely that the delocalized Ulp1 in *nup131*Δ *nup132*Δ cells leads to an unscheduled deSUMOylation of a nucleoplasmic factor, which SUMOylation is crucial to promote fork protection. One way to verify this proposed model, would be to test whether eliminating the nucleoplasmic Ulp1 will rescue the hyper resection of arrested replication forks in the nucleoplasm in the *nup131*Δ *nup132*Δ genetic background. This could be done by fusing Ulp1 with a nucleoporin to reestablish the NPC-associated Ulp1. It is however important to note, that by applying such strategy, not only the peripheral localization of Ulp1 would be restored, but also its stability and protein level. Thus, while the possible rescue would confirm that the increased fork resection in *nup131*Δ *nup132*Δ is caused by Ulp1 mislocalization or instability, it could not allow distinguishing the contribution of these two specific mechanisms.

Alternatively, it could be directly checked whether Ulp1 activity in the close proximity of nucleoplasmic positioned arrested fork will enhance the nascent strand degradation. It should be tested in a genetic background where the following features are fulfilled: Ulp1 is localized at the nuclear periphery, the RFB do not relocate to the NPC and the integrity of arrested forks is maintained at the *WT* level (for example in the *alm1*Δ or *sumo-KallR mutant*). In these mutants, the LexA-based tethering strategy could be applied to tether the catalytic domain of Ulp1 to the RFB. Of note, tethering a truncated form of Ulp1 lacking its N-terminal NPC localizing domain will prevent the simultaneous tethering of RFB to the NPC. In this scenario, Pli1 level will be maintained by the retention of endogenous Ulp1 properly localized at the periphery. Hence, the potential rescue would confirm that the increased fork resection in *nup131*Δ *nup132*Δ is caused by the untimely access of Ulp1 to the arrested forks.

My data already indicate that the artificial anchorage of the RFB to Ulp1-associated NPCs does not alter replication fork protection. However, it still unclear whether the mechanisms of ensuring fork integrity at the nuclear periphery and in the nuclear interior are the same. Indeed, tethering arrested forks to the NPC restored fork integrity

in *nup131*Δ *nup132*Δ, even if Ulp1 still mislocalized and destabilized leading to a global decrease in Pli1-dependent SUMOylation (Figure 54). This may indicate that, in contrary to the nucleoplasmic compartment, at the nuclear periphery, SUMO is dispensable to regulate the mechanisms involved in ensuring the controlled degradation of nascent strands.

III. The maintenance of replication forks competence and integrity is likely regulated by multiple SUMOylated factors.

Several reports from different systems demonstrated that SUMOylation regulates the spatially segregated process of restarting/repairing dysfunctional replication forks. Our previous data and the results I obtained during my PhD revealed that in fission yeast, SUMOylation ensures the protection of arrested replication forks, triggers their relocation towards the nuclear periphery, fine-tunes the initiation of restarted DNA synthesis and is likely involved in ensuring the optimal progression of the restarted forks.

I have addressed the division of labor of the two fission yeast E3 SUMO ligases and I found that Pli1, but not Nse2, is required for the SUMO-based regulation of fork protection, relocation and restart (Figure 47, Figure 48, Figure 49).

Using a SUMO antibody generated in our laboratory, I demonstrated for the first time the local accumulation of SUMO conjugates at RFBs, indicating that indeed factors present at stalled forks undergo a wave of SUMOylation. This detectable enrichment of SUMOylation upon RFB activation supports the model according to which multiple targets, instead of a single one, are modified by SUMO. Indeed, upon DNA damage, SUMOylation is known to affect a protein group rather than individual proteins, leading to simultaneous multi-site modifications of different factors (Psakhye and Jentsch, 2012).

Moreover, my observations led me to hypothesize that the SUMO-based regulation of each of the above-mentioned aspects may rely on distinct SUMOylated factors. For example, in the absence of Nup131 and Nup132, nascent strands at arrested fork are subjected to an uncontrolled Exo1-mediated resection, which impairs fork integrity (Figure 52). As monoSUMOylation was shown to be sufficient to safeguard replication fork integrity in the nucleoplasm, it indicates that in this genetic background,

monoSUMOylation of an unidentified target(s) was lost. At the same time, the recombination-dependent restart of arrested forks was restrained in *nup131*Δ *nup132*Δ cells (**Publication #1**: Figure 4B), pointing to a scenario in which SUMO chains on another target(s) were still preserved and inhibit the initiation of DNA synthesis resumption.

Altogether, my data indicate that multiple SUMOylated targets are engaged to control different steps of the spatially segregated RDR pathway within the fission yeast nucleus.

IV. Conclusions

My PhD project aimed at deciphering how the spatial segregation of SUMO metabolism, together with NPCs, safeguard the integrity of replication fork and their replication competence within a compartmentalized nucleus in fission yeast. It was previously reported that a routing toward NPCs allows HR-dependent replication restart by the joint action of the SUMO protease Ulp1 and the proteasome, whose activities are enriched at the nuclear periphery.

Here, I characterized the role of the nuclear basket, a sub-complex of the NPC, in promoting efficient recombination-dependent replication restart. I discovered that the nucleoporin Nup60 ensures the stability and the sequestration of the SUMO protease Ulp1 at the nuclear periphery. Also, I revealed that the nucleoporin Alm1 that is important for proteasome enrichment at the nuclear periphery has likely an indirect function in facilitating successful relocation and/or anchorage of arrested forks to the NPCs.

Interestingly, I found that the SUMO protease Ulp1 and the proteasome have distinct functions in regulating the dynamics of fork restart by HR. By counteracting the inhibitory effect of SUMO chains, Ulp1 ensures an efficient initiation of restarted DNA synthesis while the proteasome activity is important to sustain the speed of restarted forks. Noteworthy, these two activities of Ulp1 and the proteasome cannot compensate for each other and multiple SUMOylated and/or ubiquitinated targets are likely engaged to fine-tune HR-dependent DNA synthesis.

Moreover, I showed that Pli1-dependent monoSUMOylation is crucial to safeguard fork integrity in the nucleoplasm. The loss of Ulp1 sequestration at the nuclear periphery

leads to alterations in the global SUMOylome pattern, alleviating also the monoSUMOylation of key factors involved in maintaining fork integrity. I hypothesize that, in this condition, the nucleoplasmic compartment becomes less efficient at ensuring fork protection, whereas the nuclear periphery provides a better “fork protective” environment by mechanisms that remain to discover.

Taken together, my results suggest that a spatially segregated SUMO metabolism and the nuclear positioning of replication stress sites are key determinants of replication forks integrity and restart. This shed light on how the distortion of SUMO equilibrium, frequently reported in a variety of human diseases including cancer, influences the maintenance of genome integrity at replication stress sites. Such fundamental research, deciphering in depth mechanisms by which cells could fight naturally against genetic instability, is critical for the development of optimal anti-cancer therapy.

Annexe

genes

MDPI

Review

SUMO-Based Regulation of Nuclear Positioning to Spatially Regulate Homologous Recombination Activities at Replication Stress Sites

Kamila Schirmeisen [1,2], Sarah A. E. Lambert [1,2,*] and Karol Kramarz [3,*]

[1] Institut Curie, Université PSL, CNRS UMR3348, 91400 Orsay, France; kamila.schirmeisen@curie.fr
[2] Ligue Nationale Contre le Cancer (Équipe Labélisée), Université Paris-Saclay, CNRS UMR3348, 91400 Orsay, France
[3] Academic Excellence Hub—Research Centre for DNA Repair and Replication, University of Wrocław, 50-328 Wrocław, Poland
* Correspondence: sarah.lambert@curie.fr (S.A.E.L.); karol.kramarz@uwr.edu.pl (K.K.)

Abstract: DNA lesions have properties that allow them to escape their nuclear compartment to achieve DNA repair in another one. Recent studies uncovered that the replication fork, when its progression is impaired, exhibits increased mobility when changing nuclear positioning and anchors to nuclear pore complexes, where specific types of homologous recombination pathways take place. In yeast models, increasing evidence points out that nuclear positioning is regulated by small ubiquitin-like modifier (SUMO) metabolism, which is pivotal to maintaining genome integrity at sites of replication stress. Here, we review how SUMO-based pathways are instrumental to spatially segregate the subsequent steps of homologous recombination during replication fork restart. In particular, we discussed how routing towards nuclear pore complex anchorage allows distinct homologous recombination pathways to take place at halted replication forks.

Keywords: DNA; replication stress; SUMO; genome stability; homologous recombination; nuclear pore complex; chromatin mobility; yeast

Citation: Schirmeisen, K.; Lambert, S.A.E.; Kramarz, K. SUMO-Based Regulation of Nuclear Positioning to Spatially Regulate Homologous Recombination Activities at Replication Stress Sites. *Genes* **2021**, *12*, 2010. https://doi.org/10.3390/genes12122010

Academic Editor: Thorsten Allers

Received: 1 December 2021
Accepted: 13 December 2021
Published: 17 December 2021

1. Replication Stressed Forks and Homologous Recombination

In an average human life span, each individual copies approximatively 2×10^{16} m of DNA, representing 130,000 times the distance between the earth and the sun. DNA replication is therefore a fundamental process necessary for cell division, organism development, tissue homeostasis, and cell renewal. Genome duplication occurs during S-phase, and the associated DNA synthesis is overall highly accurate. Nonetheless, many endogenous and exogenous factors can challenge the process of DNA replication, a phenomenon that is referred to as replication stress. Replication stress can be defined as any event that alters the rate of DNA replication. This includes the deceleration of replication fork progression, a well-recognized feature of replication stress, as consequence of a myriad of fork obstacles [1]. The rate of fork progression can be affected globally upon treatment with chemotherapeutics drugs targeting DNA replication, oncogene activation, or inherited mutations that impair DNA replication [2,3]. In addition, during each round of DNA replication, a myriad of fork obstacles have the potential to hinder DNA synthesis, making particular genomic regions difficult to replicate, such as telomeres, centromeres, and sites of transcription–replication conflicts [3]. Replication blocks can result in the slowdown, stalling, or collapse of the replisome. Stressed replication forks are fragile DNA structures prone to DNA breakage leading to mutation and gross chromosomal rearrangements. Beyond the challenge of maintaining genome stability, replication stress induces a cascade of cellular processes, such as inflammation, senescence, aging, and cell death affecting cell fate and identity [2,4]. Therefore, replication stress is an underlying cause of many human diseases, including cancer, in-born developmental defects, neurological disorders,

and accelerated aging. For example, the cancer risk of a given tissue is mathematically linked with the number of stem cell divisions, and cancer development and aggressiveness is associated with intrinsic replication stress [5,6]. The molecular processes that govern the accuracy of genome duplication upon physiological or pathological replication stress have been under intense research, at both the basic and clinical level, with the aim to target novel pathways to cure diseases.

The maintenance of genome stability upon replication stress relies on the completion of DNA replication and numerous replication fork repair pathways that have evolved with increasing genome sizes through evolution [7]. Among these pathways, homologous recombination (HR) is particularly active in protecting, repairing, and restarting stressed replication forks [8,9]. HR repairs broken replication forks through a mechanism called break-induced replication (BIR) and ensures replication resumption at double strand break-free (DSB-free) arrested forks through template switching or a mechanism called recombination-dependent replication (RDR) [10–12]. This last pathway is initiated by Rad51-coated single-stranded DNA gaps formed through the well-controlled degradation of newly replicated strands [13–16]. Both BIR and RDR are associated with mutagenic DNA synthesis, which distinguishes a restarted fork from a replication origin-born fork [12]. This feature might be particularly harmful when the fork arrests within repeated sequences. Akin to how nuclear positioning impacts the way a double-strand break (DSB) is repaired, recent advances support the hypothesis that molecular transactions engaged at arrested forks depend on nuclear positioning, in which SUMO-based mechanisms are critical. Here, we review how the spatially segregated SUMO metabolism in yeast nuclei regulates the distinct steps of HR-mediated fork restart and the relevance of this in human cells.

2. Replication Stress Sites Move to the Nuclear Periphery

Eukaryotic genomes are 3D folded in a highly compartmentalized nucleus that has a distinct chromatin environment and DNA repair capacity [17]. In the early 2000s, it was discovered that damaged chromatin exhibit increased mobility to allow DNA damages to shift away from their compartment to another one to complete DNA repair [18–20]. This includes DSBs occurring within heterochromatin in *Drosophila*, yeast, human nucleolus, and mouse peri-centromeres that escape their compartment to achieve DSB repair through HR [21–25]. This led to the concept that a given chromatin environment is refractory to DNA repair processes and that DNA repair machineries are spatially segregated [17,26]. In budding yeast, difficult to repair DSBs (*i.e.*, in the absence of donor template for HR repair) at unique sequence are mobilized to the nuclear periphery to anchor to components of the nuclear pore complex (NPC) or the nuclear envelope to achieve DNA repair by salvage pathways [20,27–29]. Eroded telomeres (i.e., in the absence of telomerase), which mimic one-ended DSB, also anchor to NPCs to ensure the maintenance of telomere length by HR (referred to as type II survivors) [30,31]. The necessity of changing nuclear compartment for NPC anchorage has been extended to halted replication forks. In yeast models, forks stalling within telomere repeats, forks stalled by tri-nucleotides repeats or DNA-bound proteins, and collapsed forks relocate to the nuclear periphery for NPC anchorage [20,32–34]. In human cells, forks stalled upon the inhibition of DNA polymerases exhibit relocation to the nuclear periphery, and replication stress at telomeres leads to telomeres' association with NPCs [35,36]. Preventing relocation results in chromosome breaks, delayed replication restarts, and abnormal mitotic chromosome segregation including micronuclei formation. The directed mobility of damaged chromatin to its relocation at the nuclear periphery requires nuclear forces provided by microtubules and nuclear filamentous actin, a subject recently reviewed in [37]. Of interest in this review, SUMO-based mechanisms are central to NPC anchorage and for the orchestration of the subsequent steps of DSB repair by HR [20,21,27,31–33,38]. Recent studies indicate that the anchorage of replication stress sites to NPCs is controlled by SUMO metabolism for a tight regulation of HR activity. In fission yeast, a novel spatial regulation of RDR was proposed based on two sub-pathways inside the nucleus: one that occurs within the nucleoplasm and one that involves NPC

anchorage [33]. This routing is regulated by SUMOylation and has a distinct outcome on the efficiency of RDR and the maintenance of fork integrity.

A long-standing question was if DSB formation was a prerequisite for NPC anchorage. Because collapsed forks are prone to breakage, it could not be excluded that forks arrested by secondary DNA structures or at telomere repeats undergo fork breakage before NPC anchorage. In fission yeast, a site-specific replication fork barrier (called *RTS*1-RFB) allows the polar block of a single replisome by a DNA-bound protein complex [39]. Forks arrested by the RFB are bound by HR factors, including the recombinase Rad51 and its loading mediator Rad52, independently of DSB formation. Instead, the binding of HR factors requires the controlled degradation of newly replicated strands by nucleases (i.e., MRN-Ctp1, Exo1) to generate a single-stranded DNA gap [16,40,41]. In such a system, the active RFB anchors to the NPC for the time necessary for HR to restart the arrested fork [33,42,43], supporting the hypothesis that DSB is not a prerequisite for the anchorage of replication stress sites.

3. SUMOylation in DNA Repair

SUMO (small ubiquitin-like modifier) is an essential particle present in all eukaryotic cells that triggers post-translational modifications (PTMs) (Figure 1). Akin to ubiquitin, SUMO is covalently attached to target proteins. SUMOylation affects the activity, localization, and stability of modified proteins. All SUMO particles are expressed as immature precursors, which must be cleaved at the C-terminus by sentrin/SUMO-specific proteases (SENPs) to expose two glycine residues essential for further conjugation [44]. Subsequently, after activation and transesterification by the E1 enzyme, SUMO is transferred onto target protein by the joint action of the E2 conjugating enzyme and a limited set of E3 SUMO ligases. Despite its great importance for cell fitness and survival, SUMOylation is not an abundant PTM, in contrast to ubiquitination. SUMO might be attached to its targets via a single acceptor lysine as a monomer, thus generating monoSUMOylation (Figure 1). If a monoSUMO particle is covalently attached to several lysines of a given substrate, it is referred to as multiSUMOylation, a type of polySUMOylation. An interesting feature of SUMO is its ability to form polymeric chains by attachment of the SUMO particle to the internal lysines of the initial SUMO particle. We will refer to this last type of modifications as a SUMO chain, another type of polySUMOylation [45]. In yeast models, SUMO is encoded by a single gene (*Saccharomyces cerevisiae SMT3* and *Schizosaccharomyces pombe pmt3*$^{+}$), whereas higher eukaryotes express a few conjugatable SUMO paralogs (SUMO1-5) [46–49].

Pioneering studies in yeasts have revealed that monoSUMOylation plays important roles in DNA repair with numerous DNA repairs factors being SUMOylated to regulate their activity and localization, including HR factors [50–52]. Furthermore, studies conducted on higher eukaryotes have also described numerous SUMO targets among DNA repair proteins. For instance, SUMOylation of human CtIP (*S. pombe* Ctp1, *S. cerevisiae* Sae2) favors DNA end resection at DSBs and the protection of replication forks [53,54]. The analysis of proteins associated with nascent DNA has revealed that several components of the replisome are SUMOylated in human cells [55]. This includes DNA polymerases, the MCM complex, PCNA, and RPA [56–58]. Replication stress is broadly connected to an increased level of SUMOylation for many of these factors, a phenomenon called SUMO stress response (SSR), which plays key roles in preserving genome stability upon perturbed replication conditions. For instance, in budding yeast, monoSUMOylation was shown to protect damaged forks through the accumulation of Rad51-dependent recombination DNA structures [59,60]. Furthermore, in budding yeast, RPA becomes polySUMOylated during replicative senescence. At stalled replisomes several factors of replication restart machineries undergo SUMOylation, such as Mre11, Ku, Sgs1, and Rad52 [61,62]. Nonetheless, the repertoire of SUMOylated factors at replication forks in response to a distinct type of replication stress largely remains to be established.

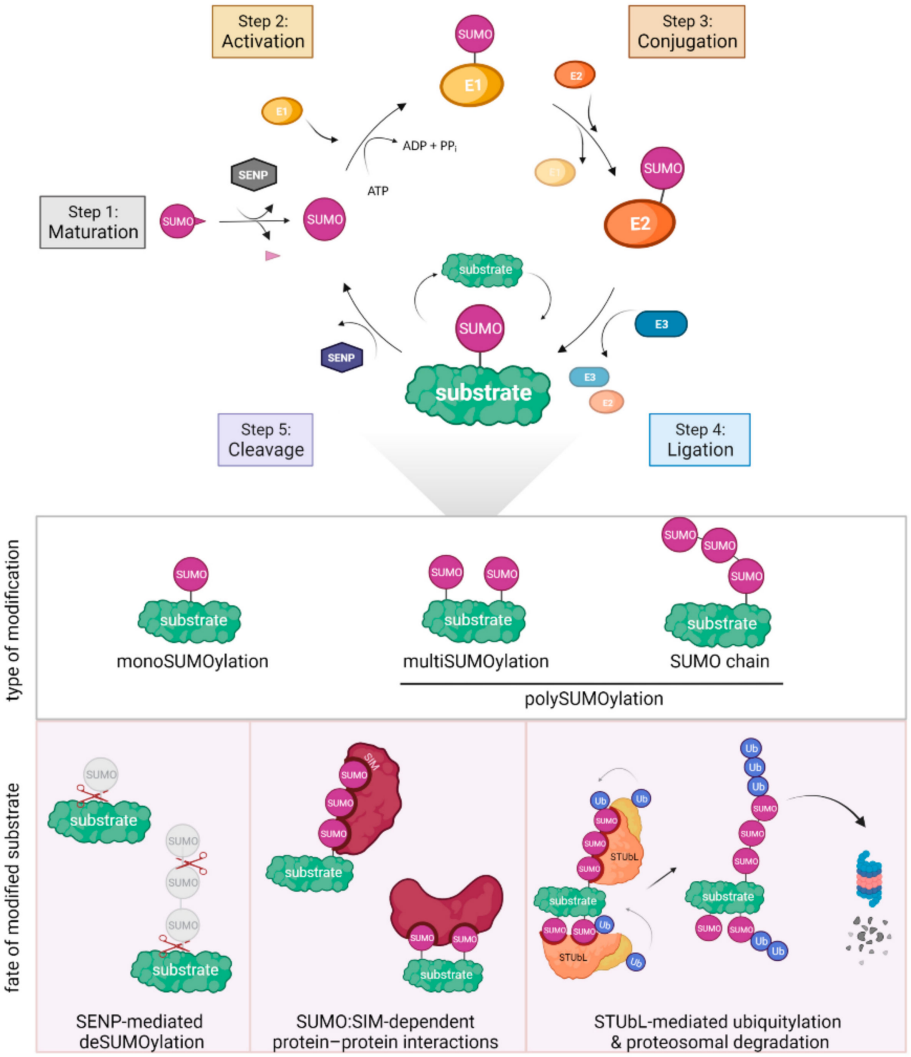

Figure 1. SUMO metabolism and functions. Top panel: cycle of SUMOylation. Bottom panel: function of the different types of SUMOylation.

SUMO chains are detectable in all eukaryotic organisms, especially in response to replication stress. Although SUMO chains help to target proteins for degradation by the proteasome, their potential contributions in regulating DNA repair or replication processes remain largely unfathomed [45,63]. Moreover, SUMOylation can act as a double-edged sword in sustaining genome stability; both ineffective SUMOylation and the accumulation of SUMO chains make cells sensitive to DNA damage and replication stress [64]. Any dysregulation in the SUMO level can be deleterious for cells' survival and influence DNA repair capacities, putting SUMO metabolism under tight regulation [65,66].

In budding yeast, SUMOylation is catalyzed by three E3 SUMO ligases (Table 1). The activity of the two paralogs Siz1 and Siz2 (human PIAS1-4, *S. pombe* Pli1) is responsible for bulk SUMOylation in *S. cerevisiae* cells [67]. The third E3 SUMO ligase Mms21 (human MMS21, *S. pombe* Nse2) has fewer substrates and mainly catalyzes monoSUMOylation. Mms21 is a part of the Smc5-6 complex and is critical for DNA repair and cell survival [38]. Similarly, the *S. pombe* Mms21 homologue, Nse2, is also part of the Smc5-6 complex and mainly catalyzes monoSUMOylation, which is critical for the maintenance of chromosome integrity [64]. Therefore, the lack of Nse2 is lethal, and the mutation of the catalytic RING domain leads to severe sickness [50,68]. In fission yeast, Pli1, which triggers the formation of both monoSUMOylation and SUMO chains, conducts the bulk SUMOylation. The mutation of *pli1+* does not lead to cellular sensitivity to DNA-damaging agents, in contrast

to *nse2* defects [50]. This suggest an apparent division of labor between distinct E3 SUMO ligases, but the underlying mechanisms are currently not understood.

Table 1. Players of the SUMO pathway in humans, *Saccharomyces cerevisiae* and *Schizosaccharomyces pombe*.

SUMO Pathway Component		Humans	*S. cerevisiae*	*S. pombe*
Small ubiquitin-like modifier (SUMO)		SUMO-1, SUMO-2, SUMO-3, SUMO-4, SUMO-5	Smt3	Pmt3
Activating enzyme (E1)		SAE1 SAE2	Aos1 Uba2	Rad31 Fub2
Conjugating enzyme (E2)		Ubc9	Ubc9	Hus5
SUMO ligase (E3)	SP-RING type	PIAS1, PIAS2, PIAS3, PIAS4 Mms21	Siz1, Siz2 Mms21 Zip3	Pli1 Nse2
	other	RanBP2 * [69] HDAC4 [70], KPA1 [71], Pc2 [72], Topors [73]		
SUMO-targeted ubiquitin ligase (STUbL)		RNF4 RNF11	Slx5-Slx8 Uls1	Rfp1/Rfp2-Slx8 Rrp2 (predicted)
Sentrin/SUMO-specific protease (SENP)		SENP1 °,*, SENP2 °,*, SENP3, SENP5 ° SENP6, SENP7	Ulp1 °,* Ulp2	Ulp1 °,* Ulp2

* Localized at the nuclear pore complex. ° Involved in SUMO maturation.

The action of E3 SUMO ligases is antagonized by SENP SUMO proteases (Ulp1 and Ulp2 in budding and fission yeast and six SENPs in humans, see Table 1) that can directly remove SUMOylation from target proteins. The activity of SENP SUMO proteases is spatially segregated in the nucleus in most organisms. Budding yeast Ulp1 is localized at the nuclear periphery through interactions with the Y-complex of the NPC (Nup84) and the nuclear basket (Nup60–Mlp1/2), whereas Ulp2 is located in the nucleoplasm [20,74]. Importantly, Ulp1 cleaves the SUMO precursor to make it prone to conjugation with the E1 enzyme. The mutation of *ULP1* is inviable in budding yeast and in *S. pombe*, it leads to extreme sickness together with a global decrease in SUMO levels because of the defect in the SUMO conjugation cycle [50]. Cells devoid of Ulp2 exhibit poor growth in both yeast models and accumulation of high-molecular-weight (HMW) SUMO conjugates, highlighting the distinct roles of Ulp1 and Ulp2 in SUMO regulation. In human cells, SENP1, SENP2, SENP3, and SENP5 are evolutionary related to yeast Ulp1, whereas SENP6 and SENP7 are derived from Ulp2 [75]. Among this group, SENP1 and SENP2 are enriched at the nuclear periphery, and both are required for the maturation of SUMO precursors [76].

PolySUMOylated proteins are recognized and bound by specific enzymes called SUMO-targeted ubiquitin ligases (STUbLs) that transfer ubiquitin onto SUMO for proteasomal degradation to modulate nuclear localization or activity (Table 1) [77]. In budding yeast, two STUbLs have been reported so far: the heterodimer Slx5-Slx8 and the large protein Uls1. In *S. pombe*, two distinct STUbL complexes are formed by the interaction between Slx8 and either Rfp1 or Rfp2 proteins. Human cells contain RNF4 and RNF111 enzymes exhibiting STUbL activities. In general, STUbLs are enzymes containing a RING domain characteristic of E3 ubiquitin ligases and several SUMO-interacting motifs (SIMs), that enable interactions with SUMOylated proteins [78]. Defects in STUbLs activity leads to a drastic increase in HMW-SUMO conjugates in cells [79,80]. Interestingly, budding yeast Ulp2 and human SENP6 were found to antagonize STUbLs by restraining SUMO chains' generation in the nucleoplasm [81–83]. Beyond triggering protein degradation, recent evidence indicates that SUMO chains act as regulators of chromatin dynamics and genome stability by affecting the composition and assembly of DNA repair complexes on chromatin during the replication stress response [63].

Beyond the function of SUMOylation in regulating DNA repair and replication factors' activity and cellular localization, SUMO metabolism is critical to the mobility of DNA lesions and their anchorage to NPC.

4. NPCs Anchor DNA Lesions in a SUMO-Dependent Manner to Promote DNA Repair

The double-layered nuclear membrane is penetrated by large macromolecular structures called NPCs that have an estimated mass of ~50 MDa in yeast and 112 MDa in vertebrates [84]. Cryo-electron microscopy has shown that the architecture of NPCs is highly conserved among eukaryotes [85]. Each NPC is assembled from multiple copies of ~30 different nucleoporins, which are called nucleoproteins or Nups. These proteins associate in distinct sub-complexes joined to each other, including eight cytoplasmic filaments, the symmetric central scaffold, and eight nucleoplasmic filaments, forming the nuclear basket [86]. The central scaffold is composed of an inner-ring complex surrounded by the outer rings containing cytoplasmic and nuclear domains. The inner ring constitutes a central channel abundant in FG-nucleoporins that facilitate the selective nucleocytoplasmic transport of molecules. The major building blocks of the outer rings are the Y-shaped Nup107-160 complexes (in humans and *S. pombe*), known as the Nup84 complex in budding yeast [86–88].

Beyond the canonical function of NPCs in the selective import/export of proteins and RNAs, those large structures contribute to the regulation of gene expression, 3D organization of the genomes, DNA repair processes, and maintenance of genome integrity [89–91]. Several studies have demonstrated that NPCs are an integral part of the DNA damage response (DDR), acting by promoting the transport of DNA repair factors by anchoring DNA lesions and by engaging alternative DNA repair pathways. Mutations in the Y-complex or the nuclear basket make yeast cells highly vulnerable to DNA damage and replication stress [74,91,92], although it is often not clear if this is a consequence of defective macromolecular transport or related to a direct function of NPCs in DNA repair. For example, the depletion of the human nuclear basket nucleoporin NUP153 leads to a defective import of the DDR mediator 53BP1 into the nucleus, resulting in an increased level of intrinsic replication stress and to cellular sensitivity to replication-blocking agents [93,94]. In buddying yeast, mutations in several nucleoporins of the Nup84 complex (e.g., *nup84*Δ or *nup133*Δ) lead to sensitivity to genotoxic drugs and replication stress [20,92]. Additionally, disruption of *NUP84* was reported to cause a delay in replication fork progression in the presence of DNA damage [95]. In fission yeast, the lack of Nup132 (*NUP133* in budding yeast and humans) leads to sensitivity to replication stress but not to DSBs or UV-induced DNA damage, and Nup132 promotes DNA replication recovery upon transient fork stalling [33].

Evidence gathered over the past two decades from numerous studies support the concept that NPCs act as docking sites for different types of DNA lesions. However, the exact NPC components involved in anchoring DNA lesions are unknown. The anchorage of DNA lesions is dependent on SUMO metabolism and both monoSUMOylation and SUMO chains' formation, indicating that SUMO constitutes the key signal for NPC anchorage (Table 2). A current model from a budding yeast study indicates that the STUbL factor Slx8 associates with the Y complex of the NPC, providing a physical link between SUMOylated proteins at DNA damage sites and the NPC [20]. The NPC anchorage of persistent DSBs, heterochromatic DSBs, and eroded telomeres in several organisms requires Slx8 [21,31,38,96]. SUMO interaction motifs (SIMs) of STUbL would allow bridging SUMOylated repair factors to NPCs [97]. However, there is no structural information regarding Slx8-NPC interactions to improve our understanding of the anchorage function of the NPC. In addition, it remains unknown whether this interaction is conserved in other eukaryotes, and/or additional mechanisms of anchorage do exist. Indeed, several Nups contain SIM domains that may be instrumental to anchor SUMOylated DNA repair factors to NPCs. The NPC anchorage of DSBs is necessary to maintain genome integrity, but the mechanisms engaged at NPCs remain not entirely uncovered. Studies from different model organisms support the concept that DSBs at repeated sequences and/or heterochro-

matin are subjected to SUMOylation events. This is necessary for DSBs to shift away from their compartments and to spatially regulate the subsequent steps of DSB repair by HR. In *Drosophila*, heterochromatic DSBs relocate to the nuclear periphery in an Nse2- and PIAS-dependent manner [21]. In this system, SUMOylation inhibits the loading of RAD51 before relocation. At the periphery, STUbL stabilizes the interaction with repair sites and promotes the loading of Rad51, but how this step is achieved is currently unknown.

Table 2. Comparison of systems of replication stress relocation to NPC/nuclear periphery.

Type of Obstacle	Protein-Mediated Fork Arrest	Structure-Forming DNA Sequence	Telomere-Specific Replication Stress		Aphidicolin Induced Replication Stress
System description	Site-specific RFB blocking a single replisome in a polar manner	Expanded trinucleotide repeats forming hairpin structures that stall replisomes	Stalled replisomes at telomere repeats in telomerase-negative cells	Telomere-specific replication stress induced by POT1 dysfunctions	Global replication fork stalling induced
Organism	*S. pombe*	*S. cerevisiae*	*S. cerevisiae*	human cell lines	human cell lines
Relocation and anchorage requirements	• Rad51-dependent fork remodeling • Pli1 • SUMO chain • Rfp1-Slx8, • Rfp2-Slx8 • NPC-anchorage site unknown	• Nascent DNA degradation (by Mre11, Exo1, Dna2) • Mms21 • SUMOylation of RPA, Rad52, Rad59 • Slx5-SUMO interaction • Nup1, Nup84	• Nup1	• F-actin polymerization • ATR pathway • Nup62, Nup153, TPR	• F-actin polymerization
Relocation outcomes	Ulp1-NPCs alleviate inhibitory effect of SUMO chains on HR-mediated fork restart	Rad51 loading to promote error free fork restart and preventing CAG repeat instability	Promoting conservative fork restart pathway to avoid error-prone Rad51-dependent SCR	Preventing SCR at telomeres to promote the maintenance of repetitive DNA	Promoting replication stress response to ensure fork restart and prevent mitotic abnormalities.
Reference	[33]	[32,34,97]	[34]	[36]	[35]

In budding yeast, SUMOylation plays a key role in the nucleolar dynamics by ensuring the compartmentalization of HR activities. Indeed, replication-born DSBs within rDNA sequences shift from the nucleolus to anchor to NPCs and maintain repeat integrity [23]. Recently, the mobility of individual rDNA repeats out of the nucleolus was shown to be dependent on the SUMOylation of factors that tether rDNA units to the nuclear periphery [98]. Moreover, the SUMOylation of the HR factor Rad52 enables its exclusion from the nucleolus, thus limiting deleterious recombination events within rDNA [99]. Preventing Rad52 SUMOylation leads to the formation of Rad52 foci inside the nucleolus and rDNA hyper-recombination. In budding yeast, eroded telomeres (i.e., in the absence of telomerase) undergo polySUMOylation and anchor to NPCs to facilitate the maintenance of telomeres lengths through a BIR type of repair, generating type II survivors [30,31,100]. PolySUMOylated telomeres are targeted to NPCs by the Slx5-Slx8 STUbL, and after anchorage to NPCs, they undergo deSUMOylation by the Ulp1 SUMO protease located at nuclear basket to unlock a Rad51-independent pathway [31]. Together, these pioneering studies point out how SUMOylation coordinates the nuclear positioning of DSBs and HR activities to maintain genome stability.

A recent study on budding yeast highlighted SUMO-independent alternative mechanisms by which NPCs regulate HR activity (Table 2). Replication forks that stall at telomere repeats relocate and anchor to the NPC, via the nucleoporin Nup1 of the nuclear basket, to promote a conservative HR type of repair [34]. In contrast, when anchorage to NPCs was prevented, stalled forks were subjected to a Rad51-dependent type of HR, leading to

error-prone sister chromatid recombination (SCR) to maintain telomere length and bypass replicative senescence. Interestingly, Siz1- or Siz2-dependent SUMOylation was not required to promote this last pathway. Instead, it was proposed that Nup1 prevents SCR by regulating karyopherin functions in escorting cargo to the site of the stalled fork to channel their repair toward a conservative restart pathway.

Both chromatin context and repeated sequences affect the scenario by which DSBs are repaired; SUMOylation events appear necessary to move DSBs away from their compartments and prevent RAD51 loading until DSBs are relocated in a "safer" environment to complete DNA repair. Both similar and distinct scenarios have emerged for the repair of arrested forks.

5. SUMO-Based Regulation of Nuclear Positioning Regulates Replication Fork Repair

Akin to SUMO's role as a nuclear positioning signal for DSBs, SUMO-dependent relocation of replication stress sites was recently discovered. In budding yeast, tri-nucleotide repeats, such as CAG, have a tendency to form secondary DNA structures prone to stall replication forks [101]. Such stalled forks relocate and anchor to NPCs in an Mms21-dependent SUMOylation and Slx5-dependent manner in late S-phase (Figure 2 and Table 2) [32]. Mutations of SIM domains of Slx5 were sufficient to prevent relocation, further supporting the role of STUbL in bridging SUMOylation and NPC anchorage [91,97]. This anchorage requires stalled forks to be processed by the end resection machinery to expose the ssDNA on which RPA is loaded. NPC anchorage requires the SUMOylation of RPA and the HR factors Rad52 and Rad59. As suggested at DSBs, SUMOylation and especially SUMO-RPA, which is known to interact with Slx8-Slx5 [31,102], prevent Rad51 loading before NPC anchorage. Indeed, Rad51 foci formation at stalled forks occurs only after relocation and anchorage [97], suggesting that not yet identified mechanisms are at work in the NPC to promote Rad51 engagement at forks stalled within repeated sequences. The relocation event is crucial for maintaining genome stability, as the lack of NPC anchorage leads to increased chromosomal fragility of CAG tracks [32], indicating that NPCs allow the engagement of specific mechanisms to maintain fork integrity. Thus, as observed for DSBs within repeated sequences, SUMOylation restrains Rad51-dependent HR events that can be detrimental when forks are arrested at repeated sequences. This routing of repeats-induced stalled forks toward NPCs could allow an error-free and Rad51-dependent fork restart pathway.

In fission yeast, forks arrested at the *RTS1*-RFB, which mediates a DNA-bound protein block to replisomes, were recently shown to relocate and anchor to NPCs in S-phase (Figure 2 and Table 2) [33]. This anchorage event requires the E3 SUMO ligase Pli1 and the Slx8 STUbL pathway, indicating that SUMOylation is the key nuclear positioning signal, but the exact SUMOylated targets are unknown. However, the underlying type of SUMOylation is the SUMO chain. Indeed, abrogating the formation of SUMO chains by mutating all acceptor lysine to arginine in *SUMO-KallR* mutant leads to a lack of relocation to the nuclear periphery. Moreover, anchorage to the NPC requires Rad51 binding to arrested forks, as well as its strand exchange activity, suggesting that arrested forks need to be remodeled by HR activity to be prone to anchorage. One possibility is that Rad51-dependent recombination/replication DNA structures trigger the recruitment of specific factors subjected to the SUMO chain formation critical to NPC anchorage. These data indicate that, contrary to the repeats-induced stalled forks, Rad51 binding occurs before anchorage to NPCs.

Although SUMO chains signal relocation, they negatively impact the efficiency of RDR. Indeed, the efficiency of RDR was increased in the absence of SUMO chains. Destabilizing the interaction between SUMO and the E2 conjugating enzyme Ubc9 (in the SUMO-D81R mutant) also stimulated the efficiency of RDR. NPC anchorage is then necessary to clear off SUMO conjugates by the proteasome and the SENP protease Ulp1, two activities enriched at the nuclear periphery. In the absence of Nup132, Ulp1 is delocalized from NPC and less expressed [103]. In this genetic context, arrested forks were properly anchored to NPCs

but RDR efficiency was decreased, revealing a novel post-anchoring function of NPCs in ensuring replication restart. The artificial tethering of Ulp1 to the RFB was sufficient to restore RDR efficiency. These data suggest the existence of at least two spatially segregated RDR pathways whose choice is under SUMO control. Pli1 would be recruited early at arrested forks to safeguard fork integrity by limiting the degradation of the nascent strand. SUMO chains, arising as a presumable consequence of Pli1 activity, may restrain a type of DNA synthesis for replication resumption, creating a commitment to NPCs anchorage to overcome the SUMO chain's inhibitory effect. When only monoSUMOylation occurs, the arrested forks remain in the cytoplasm, and the fork restart occurs efficiently. During the HR-mediated fork restart, the DNA polymerase delta synthetizes both strands of the restarted fork, in contrast to origin-born replication fork [42]. Whether SUMOylation events at the RFB influence the use of distinct DNA polymerases during fork restart is unknown. Interestingly, the defective STUBL pathway resulted in a marked increase in the mobility of the RFB, whereas the absence of Pli1 resulted in a global decrease in RFB's mobility, suggesting that the level of SUMOylation at sites of replication stress is critical for nuclear movement. Interestingly, the formation of liquid-like repair centers of Rad52, a SUMO target, requires the correct assembly of intracellular microtubule filaments in budding yeast [104]. It is unknown, however, if an interplay between nuclear filaments and SUMO metabolism exists and impacts the processing of DNA lesions.

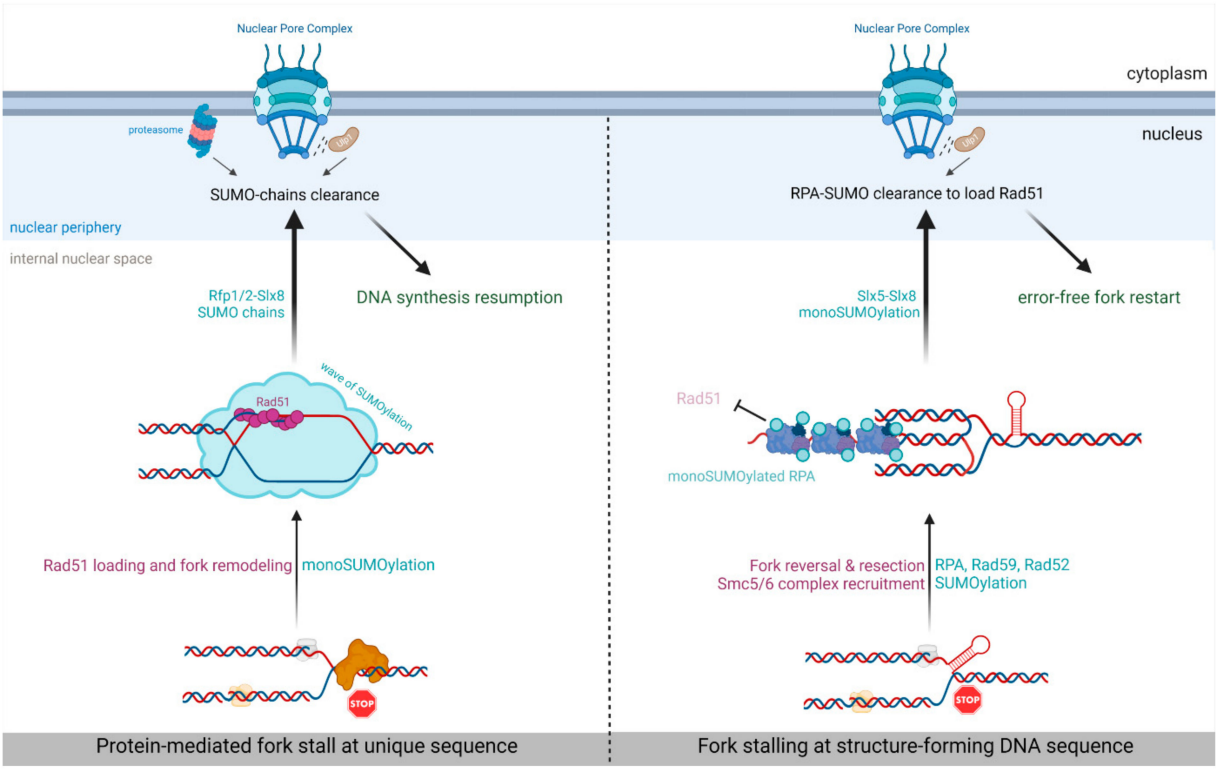

Figure 2. Routing towards NPCs for DNA-bound, protein-mediated fork arrest (**left** panel) and structure-forming-mediated fork stalling (**right** panel).

Overall, these finding reveal that the switch between monoSUMOylation and the SUMO chain formation at arrested replisomes likely constitutes a quality-control step that dictates the choice of replication fork repair pathways in the nuclear space. Moreover, the SUMO metabolism differentially influences the fate of arrested replisomes according to sequences' context; at repeated sequences, SUMOylation restrains Rad51 loading until the stalled forks anchor to NPCs, whereas at unique sequences, SUMOylation is necessary to maintain fork integrity until SUMO chains trigger NPC anchorage to allow an efficient fork restart. This suggests that additional features such as chromatin landscape influences SUMOylation features at sites of replication stress.

6. Concluding Remarks

SUMOylation connects replication stress sites to NPCs that act as molecular hubs to regulate HR activity. Different scenarios have emerged according to the type of fork obstacles and their surrounding sequences environment and organisms. The mechanisms triggering the relocation of forks arrested at repeated sequences, such as at expanded CAG, are presumably distinct from those involved in the relocation of protein-mediated fork stalling. It is evident that cells have evolved pathways to restrict the access of Rad51 at repeated sequences to limit deleterious HR events and preserve a constant size of repeats. Such pathways may limit fork-restart efficiency when the forks arrest at unique sequences. However, all the scenarios reveal that a spatially segregated SUMO metabolism is critical to ensure genome integrity at replication stress sites. Many questions remain to be addressed: How is the division of labor organized between distinct E3 SUMO ligases in yeast and human nuclei upon replication stress? What are the mechanisms engaged at the NPC or nuclear periphery that ensure an efficient and error-free fork restart? How are these NPC-related mechanisms coordinated with the global DDR response? How do chromatin organization and potential histone marks influence SUMO metabolism at sites of replication stress? Finally, most DSBs do not relocalize to the nuclear periphery or NPCs, raising questions about how the molecular and structural determinants make replication stress sites prone to relocation and NPC anchorage. Deciphering the repertoire of SUMOylated factors at replication forks upon various replication-blocking agents will certainly provide additional layers to answer these questions.

Author Contributions: Writing—original draft preparation, K.S., S.A.E.L. and K.K.; writing—review and editing, S.A.E.L. and K.K.; visualization—K.S. All authors have read and agreed to the published version of the manuscript.

Funding: This work was funded by the program "Excellence Initiative—Research University of the University of Wrocław" of the Ministry of Education and Science from Poland, under grant number IDN.CBNDR 0320/2020/20 to K.K.; the French ANR grant NIRO, under grant number ANR-19-CE12-0023-01, and the Fondation LIGUE contre le cancer Equipe Labellisée 2020, under grant number EL2020LNCC/Sal to S.A.E.L.; a PhD fellowship from the Fondation LIGUE contre le cancer to K.S.

Conflicts of Interest: The authors declare no conflict of interest.

References

1. Zeman, M.K.; Cimprich, K.A. Causes and consequences of replication stress. *Nat. Cell Biol.* **2014**, *16*, 2–9. [CrossRef] [PubMed]
2. Willaume, S.; Rass, E.; Paulafontanilla-Ramirez, P.; Moussa, A.; Wanschoor, P.; Bertrand, P. A link between replicative stress, lamin proteins, and inflammation. *Genes* **2021**, *12*, 552. [CrossRef] [PubMed]
3. Magdalou, I.; Lopez, B.S.; Pasero, P.; Lambert, S.A.E. The causes of replication stress and their consequences on genome stability and cell fate. *Semin. Cell Dev. Biol.* **2014**, *30*, 154–164. [CrossRef] [PubMed]
4. Lin, Y.L.; Pasero, P. Replication stress: From chromatin to immunity and beyond. *Curr. Opin. Genet. Dev.* **2021**, *71*, 136–142. [CrossRef] [PubMed]
5. Gaillard, H.; García-Muse, T.; Aguilera, A. Replication stress and cancer. *Nat. Rev. Cancer* **2015**, *15*, 276–280. [CrossRef]
6. Tomasetti, C.; Vogelstein, B. Variation in cancer risk among tissues can be explained by the number of stem cell divisions. *Science* **2015**, *347*, 78–81. [CrossRef] [PubMed]
7. Berti, M.; Cortez, D.; Lopes, M. The plasticity of DNA replication forks in response to clinically relevant genotoxic stress. *Nat. Rev. Mol. Cell Biol.* **2020**, *21*, 633–651. [CrossRef] [PubMed]
8. Ait Saada, A.; Lambert, S.A.E.; Carr, A.M. Preserving replication fork integrity and competence via the homologous recombination pathway. *DNA Repair* **2018**, *71*, 135–147. [CrossRef] [PubMed]
9. Scully, R.; Elango, R.; Panday, A.; Willis, N.A. Recombination and restart at blocked replication forks. *Curr. Opin. Genet. Dev.* **2021**, *71*, 154–162. [CrossRef]
10. Sakofsky, C.J.; Malkova, A. Break induced replication in eukaryotes: Mechanisms, functions, and consequences. *Crit. Rev. Biochem. Mol. Biol.* **2017**, *52*, 395–413. [CrossRef] [PubMed]
11. Hashimoto, Y.; Puddu, F.; Costanzo, V. RAD51-and MRE11-dependent reassembly of uncoupled CMG helicase complex at collapsed replication forks. *Nat. Struct. Mol. Biol.* **2012**, *19*, 17–24. [CrossRef] [PubMed]
12. Carr, A.; Lambert, S. Recombination-dependent replication: New perspectives from site-specific fork barriers. *Curr. Opin. Genet. Dev.* **2021**, *71*, 129–135. [CrossRef] [PubMed]

13. Neelsen, K.J.; Lopes, M. Replication fork reversal in eukaryotes: From dead end to dynamic response. *Nat. Rev. Mol. Cell Biol.* **2015**, *16*, 207–220. [CrossRef] [PubMed]
14. Quinet, A.; Lemaçon, D.; Vindigni, A. Replication Fork Reversal: Players and Guardians. *Mol. Cell* **2017**, *68*, 830–833. [CrossRef]
15. Lemaçon, D.; Jackson, J.; Quinet, A.; Brickner, J.R.; Li, S.; Yazinski, S.; You, Z.; Ira, G.; Zou, L.; Mosammaparast, N.; et al. MRE11 and EXO1 nucleases degrade reversed forks and elicit MUS81-dependent fork rescue in BRCA2-deficient cells. *Nat. Commun.* **2017**, *8*, 860. [CrossRef]
16. Teixeira-Silva, A.; Ait Saada, A.; Hardy, J.; Iraqui, I.; Nocente, M.C.; Fréon, K.; Lambert, S.A.E. The end-joining factor Ku acts in the end-resection of double strand break-free arrested replication forks. *Nat. Commun.* **2017**, *8*, 1982. [CrossRef] [PubMed]
17. Kalousi, A.; Soutoglou, E. Nuclear compartmentalization of DNA repair. *Curr. Opin. Genet. Dev.* **2016**, *37*, 148–157. [CrossRef] [PubMed]
18. Aten, J.A.; Stap, J.; Krawczyk, P.M.; Van Oven, C.H.; Hoebe, R.A.; Essers, J.; Kanaar, R. Dynamics of DNA Double-Strand Breaks Revealed by Clustering of Damaged Chromosome Domains. *Science* **2004**, *303*, 92–95. [CrossRef] [PubMed]
19. Seeber, A.; Gasser, S.M. Chromatin organization and dynamics in double-strand break repair. *Curr. Opin. Genet. Dev.* **2017**, *43*, 9–16. [CrossRef] [PubMed]
20. Nagai, S.; Dubrana, K.; Tsai-Pflugfelder, M.; Davidson, M.B.; Roberts, T.M.; Brown, G.W.; Varela, E.; Hediger, F.; Gasser, S.M.; Krogan, N.J. Functional targeting of DNA damage to a nuclear pore-associated SUMO-dependent ubiquitin ligase. *Science* **2008**, *322*, 597–602. [CrossRef] [PubMed]
21. Ryu, T.; Spatola, B.; Delabaere, L.; Bowlin, K.; Hopp, H.; Kunitake, R.; Karpen, G.H.; Chiolo, I. Heterochromatic breaks move to the nuclear periphery to continue recombinational repair. *Nat. Cell Biol.* **2015**, *17*, 1401–1411. [CrossRef] [PubMed]
22. Chiolo, I.; Minoda, A.; Colmenares, S.U.; Polyzos, A.; Costes, S.V.; Karpen, G.H. Double-strand breaks in heterochromatin move outside of a dynamic HP1a domain to complete recombinational repair. *Cell* **2011**, *144*, 732–744. [CrossRef] [PubMed]
23. Horigome, C.; Unozawa, E.; Ooki, T.; Kobayashi, T. Ribosomal RNA gene repeats associate with the nuclear pore complex for maintenance after DNA damage. *PLoS Genet.* **2019**, *15*, e1008103. [CrossRef]
24. Marnef, A.; Finoux, A.L.; Arnould, C.; Guillou, E.; Daburon, V.; Rocher, V.; Mangeat, T.; Mangeot, P.E.; Ricci, E.P.; Legube, G. A cohesin/HUSH- And LINC-dependent pathway controls ribosomal DNA double-strand break repair. *Genes Dev.* **2019**, *33*, 1175–1190. [CrossRef] [PubMed]
25. Tsouroula, K.; Furst, A.; Rogier, M.; Heyer, V.; Maglott-Roth, A.; Ferrand, A.; Reina-San-Martin, B.; Soutoglou, E. Temporal and Spatial Uncoupling of DNA Double Strand Break Repair Pathways within Mammalian Heterochromatin. *Mol. Cell* **2016**, *63*, 293–305. [CrossRef] [PubMed]
26. Lemaître, C.; Grabarz, A.; Tsouroula, K.; Andronov, L.; Furst, A.; Pankotai, T.; Heyer, V.; Rogier, M.; Attwood, K.M.; Kessler, P.; et al. Nuclear position dictates DNA repair pathway choice. *Genes Dev.* **2014**, *28*, 2450–2463. [CrossRef]
27. Kalocsay, M.; Hiller, N.J.; Jentsch, S. Chromosome-wide Rad51 spreading and SUMO-H2A.Z-dependent chromosome fixation in response to a persistent DNA double-strand break. *Mol. Cell* **2009**, *33*, 335–343. [CrossRef] [PubMed]
28. Oza, P.; Jaspersen, S.L.; Miele, A.; Dekker, J.; Peterson, C.L. Mechanisms that regulate localization of a DNA double-strand break to the nuclear periphery. *Genes Dev.* **2009**, *23*, 912–927. [CrossRef]
29. Horigome, C.; Oma, Y.; Konishi, T.; Schmid, R.; Marcomini, I.; Hauer, M.H.; Dion, V.; Harata, M.; Gasser, S.M. SWR1 and INO80 chromatin remodelers contribute to DNA double-strand break perinuclear anchorage site choice. *Mol. Cell* **2014**, *55*, 626–639. [CrossRef]
30. Khadaroo, B.; Teixeira, M.T.; Luciano, P.; Eckert-Boulet, N.; Germann, S.M.; Simon, M.N.; Gallina, I.; Abdallah, P.; Gilson, E.; Géli, V.; et al. The DNA damage response at eroded telomeres and tethering to the nuclear pore complex. *Nat. Cell Biol.* **2009**, *11*, 980–987. [CrossRef] [PubMed]
31. Churikov, D.; Charifi, F.; Eckert-Boulet, N.; Silva, S.; Simon, M.-N.; Lisby, M.; Géli, V. SUMO-Dependent Relocalization of Eroded Telomeres to Nuclear Pore Complexes Controls Telomere Recombination. *Cell Rep.* **2016**, *15*, 1242–1253. [CrossRef]
32. Su, X.A.; Dion, V.; Gasser, S.M.; Freudenreich, C.H. Regulation of recombination at yeast nuclear pores controls repair and triplet repeat stability. *Genes Dev.* **2015**, *29*, 1006–1017. [CrossRef] [PubMed]
33. Kramarz, K.; Schirmeisen, K.; Boucherit, V.; Ait Saada, A.; Lovo, C.; Palancade, B.; Freudenreich, C.; Lambert, S.A.E. The nuclear pore primes recombination-dependent DNA synthesis at arrested forks by promoting SUMO removal. *Nat. Commun.* **2020**, *11*, 5643. [CrossRef]
34. Aguilera, P.; Whalen, J.; Minguet, C.; Churikov, D.; Freudenreich, C.; Simon, M.N.; Géli, V. The nuclear pore complex prevents sister chromatid recombination during replicative senescence. *Nat. Commun.* **2020**, *11*, 160. [CrossRef]
35. Lamm, N.; Read, M.N.; Nobis, M.; Van Ly, D.; Page, S.G.; Masamsetti, V.P.; Timpson, P.; Biro, M.; Cesare, A.J. Nuclear F-actin counteracts nuclear deformation and promotes fork repair during replication stress. *Nat. Cell Biol.* **2020**, *22*, 1460–1470. [CrossRef]
36. Pinzaru, A.M.; Kareh, M.; Lamm, N.; Lazzerini-Denchi, E.; Cesare, A.J.; Sfeir, A. Replication stress conferred by POT1 dysfunction promotes telomere relocalization to the nuclear pore. *Genes Dev.* **2020**, *34*, 1619–1636. [CrossRef] [PubMed]
37. Lamm, N.; Rogers, S.; Cesare, A.J. Chromatin mobility and relocation in DNA repair. *Trends Cell Biol.* **2021**, *31*, 843–855. [CrossRef]
38. Horigome, C.; Bustard, D.E.; Marcomini, I.; Delgoshaie, N.; Tsai-Pflugfelder, M.; Cobb, J.A.; Gasser, S.M. PolySUMOylation by Siz2 and Mms21 triggers relocation of DNA breaks to nuclear pores through the Slx5/Slx8 STUbL. *Genes Dev.* **2016**, *30*, 931–945. [CrossRef] [PubMed]

39. Lambert, S.; Mizuno, K.; Blaisonneau, J.; Martineau, S.; Chanet, R.; Fréon, K.; Murray, J.M.; Carr, A.M.; Baldacci, G. Homologous recombination restarts blocked replication forks at the expense of genome rearrangements by template exchange. *Mol. Cell* **2010**, *39*, 346–359. [CrossRef]
40. Ait Saada, A.; Teixeira-Silva, A.; Iraqui, I.; Costes, A.; Hardy, J.; Paoletti, G.; Fréon, K.; Lambert, S.A.E. Unprotected Replication Forks Are Converted into Mitotic Sister Chromatid Bridges. *Mol. Cell* **2017**, *66*, 398–410.e4. [CrossRef] [PubMed]
41. Tsang, E.; Miyabe, I.; Iraqui, I.; Zheng, J.; Lambert, S.A.E.; Carr, A.M. The extent of error-prone replication restart by homologous recombination is controlled by Exo1 and checkpoint proteins. *J. Cell Sci.* **2014**, *127*, 2983–2994. [CrossRef] [PubMed]
42. Miyabe, I.; Mizuno, K.; Keszthelyi, A.; Daigaku, Y.; Skouteri, M.; Mohebi, S.; Kunkel, T.A.; Murray, J.M.; Carr, A.M. Polymerase δ replicates both strands after homologous recombination–dependent fork restart. *Nat. Struct. Mol. Biol.* **2015**, *22*, 932–938. [CrossRef]
43. Nguyen, M.O.; Jalan, M.; Morrow, C.A.; Osman, F.; Whitby, M.C. Recombination occurs within minutes of replication blockage by *RTS1* producing restarted forks that are prone to collapse. *Elife* **2015**, *4*, e04539. [CrossRef]
44. Pichler, A.; Fatouros, C.; Lee, H.; Eisenhardt, N. SUMO conjugation—A mechanistic view. *Biomol. Concepts* **2017**, *8*, 13–36. [CrossRef]
45. Ulrich, H.D. The Fast-Growing Business of SUMO Chains. *Mol. Cell* **2008**, *32*, 301–305. [CrossRef]
46. Flotho, A.; Melchior, F. Sumoylation: A regulatory protein modification in health and disease. *Annu. Rev. Biochem.* **2013**, *82*, 357–385. [CrossRef] [PubMed]
47. Cappadocia, L.; Lima, C.D. Ubiquitin-like Protein Conjugation: Structures, Chemistry, and Mechanism. *Chem. Rev.* **2018**, *118*, 889–918. [CrossRef] [PubMed]
48. Sriramachandran, A.M.; Meyer-Teschendorf, K.; Pabst, S.; Ulrich, H.D.; Gehring, N.H.; Hofmann, K.; Praefcke, G.J.K.; Dohmen, R.J. Arkadia/RNF111 is a SUMO-targeted ubiquitin ligase with preference for substrates marked with SUMO1-capped SUMO2/3 chain. *Nat. Commun.* **2019**, *10*, 3678. [CrossRef]
49. Liang, Y.C.; Lee, C.C.; Yao, Y.L.; Lai, C.C.; Schmitz, M.L.; Yang, W.M. SUMO5, a novel poly-SUMO isoform, regulates PML nuclear bodies. *Sci. Rep.* **2016**, *6*, 26509. [CrossRef] [PubMed]
50. Watts, F.Z.; Skilton, A.; Ho, J.C.Y.; Boyd, L.K.; Trickey, M.A.M.; Gardner, L.; Ogi, F.X.; Outwin, E.A. The role of Schizosaccharomyces pombe SUMO ligases in genome stability. In Proceedings of the Biochemical Society Transactions. *Biochem. Soc. Trans.* **2007**, *35*, 1379–1384. [CrossRef] [PubMed]
51. Sacher, M.; Pfander, B.; Jentsch, S. Identification of SUMO-protein conjugates. *Methods Enzymol.* **2005**, *399*, 392–404. [CrossRef] [PubMed]
52. Jentsch, S.; Psakhye, I. Control of nuclear activities by substrate-selective and protein-group SUMOylation. *Annu. Rev. Genet.* **2013**, *47*, 167–186. [CrossRef] [PubMed]
53. Soria-Bretones, I.; Cepeda-García, C.; Checa-Rodriguez, C.; Heyer, V.; Reina-San-Martin, B.; Soutoglou, E.; Huertas, P. DNA end resection requires constitutive sumoylation of CtIP by CBX4. *Nat. Commun.* **2017**, *8*, 113. [CrossRef] [PubMed]
54. Locke, A.J.; Hossain, L.; McCrostie, G.; Ronato, D.A.; Fitieh, A.; Rafique, T.A.; Mashayekhi, F.; Motamedi, M.; Masson, J.Y.; Ismail, I.H. SUMOylation mediates CtIP's functions in DNA end resection and replication fork protection. *Nucleic Acids Res.* **2021**, *49*, 928–953. [CrossRef]
55. Lopez-Contreras, A.J.; Ruppen, I.; Nieto-Soler, M.; Murga, M.; Rodriguez-Acebes, S.; Remeseiro, S.; Rodrigo-Perez, S.; Rojas, A.M.; Mendez, J.; Muñoz, J.; et al. A Proteomic Characterization of Factors Enriched at Nascent DNA Molecules. *Cell Rep.* **2013**, *3*, 1105–1116. [CrossRef]
56. Cremona, C.A.; Sarangi, P.; Yang, Y.; Hang, L.E.; Rahman, S.; Zhao, X. Extensive DNA damage-induced sumoylation contributes to replication and repair and acts in addition to the mec1 checkpoint. *Mol. Cell* **2012**, *45*, 422–432. [CrossRef]
57. Hoege, C.; Pfander, B.; Moldovan, G.L.; Pyrowolakis, G.; Jentsch, S. RAD6-dependent DNA repair is linked to modification of PCNA by ubiquitin and SUMO. *Nature* **2002**, *419*, 135–141. [CrossRef] [PubMed]
58. Golebiowski, F.; Matic, I.; Tatham, M.H.; Cole, C.; Yin, Y.; Nakamura, A.; Cox, J.; Barton, G.J.; Mann, M.; Hay, R.T. System-wide changes to sumo modifications in response to heat shock. *Sci. Signal.* **2009**, *2*, ra24. [CrossRef]
59. Branzei, D.; Sollier, J.; Liberi, G.; Zhao, X.; Maeda, D.; Seki, M.; Enomoto, T.; Ohta, K.; Foiani, M. Ubc9- and Mms21-Mediated Sumoylation Counteracts Recombinogenic Events at Damaged Replication Forks. *Cell* **2006**, *127*, 509–522. [CrossRef] [PubMed]
60. Klein, H.L. A SUMOry of DNA Replication: Synthesis, Damage, and Repair. *Cell* **2006**, *127*, 455–457. [CrossRef]
61. Psakhye, I.; Jentsch, S. Protein group modification and synergy in the SUMO pathway as exemplified in DNA repair. *Cell* **2012**, *151*, 807–820. [CrossRef]
62. Sarangi, P.; Zhao, X. SUMO-mediated regulation of DNA damage repair and responses. *Trends Biochem. Sci.* **2015**, *40*, 233–242. [CrossRef] [PubMed]
63. Keiten-Schmitz, J.; Schunck, K.; Müller, S. SUMO Chains Rule on Chromatin Occupancy. *Front. Cell Dev. Biol.* **2020**, *7*, 343. [CrossRef] [PubMed]
64. Prudden, J.; Perry, J.J.P.; Nie, M.; Vashisht, A.A.; Arvai, A.S.; Hitomi, C.; Guenther, G.; Wohlschlegel, J.A.; Tainer, J.A.; Boddy, M.N. DNA Repair and Global Sumoylation Are Regulated by Distinct Ubc9 Noncovalent Complexes. *Mol. Cell. Biol.* **2011**, *31*, 2299–2310. [CrossRef] [PubMed]
65. Bergink, S.; Jentsch, S. Principles of ubiquitin and SUMO modifications in DNA repair. *Nature* **2009**, *458*, 461–467. [CrossRef] [PubMed]

66. Jackson, S.P.; Durocher, D. Regulation of DNA Damage Responses by Ubiquitin and SUMO. *Mol. Cell* **2013**, *49*, 795–807. [CrossRef]
67. Reindle, A.; Belichenko, I.; Bylebyl, G.R.; Chen, X.L.; Gandhi, N.; Johnson, E.S. Multiple domains in Siz SUMO ligases contribute to substrate selectivity. *J. Cell Sci.* **2006**, *119*, 4749–4757. [CrossRef]
68. Xhemalce, B.; Riising, E.M.; Baumann, P.; Dejean, A.; Arcangioli, B.; Seeler, J.S. Role of SUMO in the dynamics of telomere maintenance in fission yeast. *Proc. Natl. Acad. Sci. USA* **2007**, *104*, 893–898. [CrossRef]
69. Pichler, A.; Gast, A.; Seeler, J.S.; Dejean, A.; Melchior, F. The nucleoporin RanBP2 has SUMO1 E3 ligase activity. *Cell* **2002**, *108*, 109–120. [CrossRef]
70. Yang, Q.; Tang, J.; Xu, C.; Zhao, H.; Zhou, Y.; Wang, Y.; Yang, M.; Chen, X.; Chen, J. Histone deacetylase 4 inhibits NF-κB activation by facilitating IκBα sumoylation. *J. Mol. Cell Biol.* **2020**, *12*, 933–945. [CrossRef]
71. Peng, J.; Wysocka, J. It takes a PHD to SUMO. *Trends Biochem. Sci.* **2008**, *33*, 191–194. [CrossRef] [PubMed]
72. Kagey, M.H.; Melhuish, T.A.; Wotton, D. The polycomb protein Pc2 is a SUMO E3. *Cell* **2003**, *113*, 127–137. [CrossRef]
73. Weger, S.; Hammer, E.; Heilbronn, R. Topors acts as a SUMO-1 E3 ligase for p53 in vitro and in vivo. *FEBS Lett.* **2005**, *579*, 5007–5012. [CrossRef]
74. Palancade, B.; Liu, X.; Garcia-Rubio, M.; Aguilera, A.; Zhao, X.; Doye, V. Nucleoporins prevent DNA damage accumulation by modulating Ulp1-dependent sumoylation processes. *Mol. Biol. Cell* **2007**, *18*, 2912–2923. [CrossRef] [PubMed]
75. Kunz, K.; Piller, T.; Müller, S. SUMO-specific proteases and isopeptidases of the SENP family at a glance. *J. Cell Sci.* **2018**, *131*, jcs211904. [CrossRef] [PubMed]
76. Palancade, B.; Doye, V. Sumoylating and desumoylating enzymes at nuclear pores: Underpinning their unexpected duties? *Trends Cell Biol.* **2008**, *18*, 174–183. [CrossRef] [PubMed]
77. Uzunova, K.; Göttsche, K.; Miteva, M.; Weisshaar, S.R.; Glanemann, C.; Schnellhardt, M.; Niessen, M.; Scheel, H.; Hofmann, K.; Johnson, E.S.; et al. Ubiquitin-dependent proteolytic control of SUMO conjugates. *J. Biol. Chem.* **2007**, *282*, 34167–34175. [CrossRef] [PubMed]
78. Chang, Y.C.; Oram, M.K.; Bielinsky, A.K. Sumo-targeted ubiquitin ligases and their functions in maintaining genome stability. *Int. J. Mol. Sci.* **2021**, *22*, 5391. [CrossRef]
79. Kramarz, K.; Litwin, I.; Cal-Bakowska, M.; Szakal, B.; Branzei, D.; Wysocki, R.; Dziadkowiec, D. Swi2/Snf2-like protein Uls1 functions in the Sgs1-dependent pathway of maintenance of rDNA stability and alleviation of replication stress. *DNA Repair* **2014**, *21*, 24–35. [CrossRef]
80. Prudden, J.; Pebernard, S.; Raffa, G.; Slavin, D.A.; Perry, J.J.P.; Tainer, J.A.; McGowan, C.H.; Boddy, M.N. SUMO-targeted ubiquitin ligases in genome stability. *EMBO J.* **2007**, *26*, 4089–4101. [CrossRef] [PubMed]
81. Psakhye, I.; Castellucci, F.; Branzei, D. SUMO-Chain-Regulated Proteasomal Degradation Timing Exemplified in DNA Replication Initiation. *Mol. Cell* **2019**, *76*, 632–645.e6. [CrossRef]
82. Liebelt, F.; Jansen, N.S.; Kumar, S.; Gracheva, E.; Claessens, L.A.; Verlaan-de Vries, M.; Willemstein, E.; Vertegaal, A.C.O. The poly-SUMO2/3 protease SENP6 enables assembly of the constitutive centromere-associated network by group deSUMOylation. *Nat. Commun.* **2019**, *10*, 3987. [CrossRef] [PubMed]
83. Mullen, J.R.; Das, M.; Brill, S.J. Genetic evidence that polysumoylation bypasses the need for a SUMO-targeted UB ligase. *Genetics* **2011**, *187*, 73–87. [CrossRef]
84. Kim, S.J.; Fernandez-Martinez, J.; Nudelman, I.; Shi, Y.; Zhang, W.; Raveh, B.; Herricks, T.; Slaughter, B.D.; Hogan, J.A.; Upla, P.; et al. Integrative structure and functional anatomy of a nuclear pore complex. *Nature* **2018**, *555*, 475–482. [CrossRef] [PubMed]
85. Von Appen, A.; Beck, M. Structure Determination of the Nuclear Pore Complex with Three-Dimensional Cryo electron Microscopy. *J. Mol. Biol.* **2016**, *428*, 2001–2010. [CrossRef] [PubMed]
86. Knockenhauer, K.E.; Schwartz, T.U. The Nuclear Pore Complex as a Flexible and Dynamic Gate. *Cell* **2016**, *164*, 1162–1171. [CrossRef] [PubMed]
87. Hoelz, A.; Debler, E.W.; Blobel, G. The Structure of the nuclear pore complex. *Annu. Rev. Biochem.* **2011**, *80*, 613–643. [CrossRef] [PubMed]
88. Schwartz, T.U. The Structure Inventory of the Nuclear Pore Complex. *J. Mol. Biol.* **2016**, *428*, 1986–2000. [CrossRef]
89. Ibarra, A.; Hetzer, M.W. Nuclear pore proteins and the control of genome functions. *Genes Dev.* **2015**, *29*, 337–349. [CrossRef] [PubMed]
90. D'Angelo, M.A.; Hetzer, M.W. Structure, dynamics and function of nuclear pore complexes. *Trends Cell Biol.* **2008**, *18*, 456–466. [CrossRef] [PubMed]
91. Whalen, J.M.; Freudenreich, C.H. Location, location, location: The role of nuclear positioning in the repair of collapsed forks and protection of genome stability. *Genes* **2020**, *11*, 635. [CrossRef] [PubMed]
92. Loeillet, S.; Palancade, B.; Cartron, M.; Thierry, A.; Richard, G.-F.; Dujon, B.; Doye, V.; Nicolas, A. Genetic network interactions among replication, repair and nuclear pore deficiencies in yeast. *DNA Repair* **2005**, *4*, 459–468. [CrossRef] [PubMed]
93. Moudry, P.; Lukas, C.; Macurek, L.; Neumann, B.; Heriche, J.K.; Pepperkok, R.; Ellenberg, J.; Hodny, Z.; Lukas, J.; Bartek, J. Nucleoporin NUP153 guards genome integrity by promoting nuclear import of 53BP1. *Cell Death Differ.* **2012**, *19*, 798–807. [CrossRef] [PubMed]
94. Lemaître, C.; Fischer, B.; Kalousi, A.; Hoffbeck, A.S.; Guirouilh-Barbat, J.; Shahar, O.D.; Genet, D.; Goldberg, M.; Betrand, P.; Lopez, B.; et al. The nucleoporin 153, a novel factor in double-strand break repair and DNA damage response. *Oncogene* **2012**, *31*, 4803–4809. [CrossRef] [PubMed]

95. Gaillard, H.; Santos-Pereira, J.M.; Aguilera, A. The Nup84 complex coordinates the DNA damage response to warrant genome integrity. *Nucleic Acids Res.* **2019**, *47*, 4054–4067. [CrossRef] [PubMed]
96. Amaral, N.; Ryu, T.; Li, X.; Chiolo, I. Nuclear Dynamics of Heterochromatin Repair. *Trends Genet.* **2017**, *33*, 86–100. [CrossRef]
97. Whalen, J.M.; Dhingra, N.; Wei, L.; Zhao, X.; Freudenreich, C.H. Relocation of Collapsed Forks to the Nuclear Pore Complex Depends on Sumoylation of DNA Repair Proteins and Permits Rad51 Association. *Cell Rep.* **2020**, *31*, 107635. [CrossRef] [PubMed]
98. Capella, M.; Mandemaker, I.K.; Martín Caballero, L.; den Brave, F.; Pfander, B.; Ladurner, A.G.; Jentsch, S.; Braun, S. Nucleolar release of rDNA repeats for repair involves SUMO-mediated untethering by the Cdc48/p97 segregase. *Nat. Commun.* **2021**, *12*, 4918. [CrossRef] [PubMed]
99. Torres-Rosell, J.; Sunjevaric, I.; De Piccoli, G.; Sacher, M.; Eckert-Boulet, N.; Reid, R.; Jentsch, S.; Rothstein, R.; Aragón, L.; Lisby, M. The Smc5-Smc6 complex and SUMO modification of Rad52 regulates recombinational repair at the ribosomal gene locus. *Nat. Cell Biol.* **2007**, *9*, 923–931. [CrossRef] [PubMed]
100. Géli, V.; Lisby, M. Recombinational DNA repair is regulated by compartmentalization of DNA lesions at the nuclear pore complex. *Bioessays* **2015**, *37*, 1287–1292. [CrossRef] [PubMed]
101. Polleys, E.J.; Freudenreich, C.H. Homologous recombination within repetitive DNA. *Curr. Opin. Genet. Dev.* **2021**, *71*, 143–153. [CrossRef] [PubMed]
102. Chung, I.; Zhao, X. DNA break-induced sumoylation is enabled by collaboration between a sumo ligase and the ssdnabinding complex rpa. *Genes Dev.* **2015**, *29*, 1593–1598. [CrossRef] [PubMed]
103. Nie, M.; Boddy, M.N. Pli1 ^{PIAS1} SUMO Ligase Protected by the Nuclear Pore-associated SUMO Protease Ulp1 $^{SENP1/2}$. *J. Biol. Chem.* **2015**, *290*, 22678–22685. [CrossRef] [PubMed]
104. Oshidari, R.; Huang, R.; Medghalchi, M.; Tse, E.Y.W.; Ashgriz, N.; Lee, H.O.; Wyatt, H.; Mekhail, K. DNA repair by Rad52 liquid droplets. *Nat. Commun.* **2020**, *11*, 695. [CrossRef] [PubMed]

DNA Repair 129 (2023) 103548

Contents lists available at ScienceDirect

DNA Repair

journal homepage: www.elsevier.com/locate/dnarepair

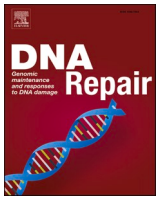

The multifaceted functions of homologous recombination in dealing with replication-associated DNA damages

Shrena Chakraborty [a,b,c,1], Kamila Schirmeisen [a,b,c,1], Sarah AE Lambert [a,b,c,*]

[a] Institut Curie, Université PSL, CNRS UMR3348, 91400 Orsay, France
[b] Université Paris-Saclay, CNRS UMR3348, 91400 Orsay, France
[c] Equipe Labelisée Ligue Nationale Contre le Cancer, France

ARTICLE INFO

Keywords:
Homologous recombination
Replication stress
Fork integrity and restart
Post-replicative gap repair
Cancer
Genome instability

ABSTRACT

The perturbation of DNA replication, a phenomena termed "replication stress", is a driving force of genome instability and a hallmark of cancer cells. Among the DNA repair mechanisms that contribute to tolerating replication stress, the homologous recombination pathway is central to the alteration of replication fork progression. In many organisms, defects in the homologous recombination machinery result in increased cell sensitivity to replication-blocking agents and a higher risk of cancer in humans. Moreover, the status of homologous recombination in cancer cells often correlates with the efficacy of anti-cancer treatment. In this review, we discuss our current understanding of the different functions of homologous recombination in fixing replication-associated DNA damage and contributing to complete genome duplication. We also examine which functions are pivotal in preventing cancer and genome instability.

1. Introduction

Homologous recombination (HR) is a DNA repair pathway involved in fixing accidental and programmed double strand break (DSB). Defects in the HR machinery predispose to cancer, in particular breast and ovarian cancers. The HR machinery is also connected to the DNA replication process to ensure complete and accurate DNA replication [1]. The bulk of DNA synthesis occurs in the S-phase, thanks to the firing and progression of thousands of replication forks. Accurate genome duplication is critical for cell division, development and tissue renewal. However, DNA replication is not an easy feat since many events of endogenous or exogenous origin can challenge replisome progression, a phenomena termed "replication stress" (RS) [2]. This includes replication obstacles such as protein-DNA complexes, DNA damage, transcription machinery and secondary DNA structures. The discovery that oncogene expression forces cell proliferation in the context of inadequate cell metabolism, a process called oncogene-induced unbalanced DNA replication, has further highlighted the causal relationship between RS, genome instability and cancer development [3,4]. Moreover, many drugs used in chemotherapies target the process of DNA replication, making it a relevant target to trigger replication catastrophe in cancer cells [5]. Therefore, understanding the molecular mechanisms by which the HR machinery regulates the accuracy of genome duplication under physiological or pathological RS conditions is of increasing interest.

2. Recombinogenic versus non-recombinogenic functions of HR during DNA replication

The HR process makes use of an intact and homologous DNA sequence as a template to repair DNA. The central and universal factor of the HR machinery is the recombinase Rad51 (hereafter named Rad51 for yeast models and RAD51 for mammalian cells) that exhibits multiple and inter-dependent biochemical activities (reviewed in [6]). ATP-bound Rad51 monomers bind to resected single stranded (ss) DNA in a process called nucleation with a stoichiometry of 1 monomer per 3 nucleotides. The cooperative binding mode of Rad51 allows the formation of a nucleoprotein filament coated onto ssDNA, viewed as the active form of HR, capable of homology search to find the appropriate DNA template. The Rad51 filament then allows strand invasion generating a joint molecule called displacement loop (D-loop) in which the complementary strand of the donor duplex is displaced as a ssDNA strand. Although Rad51 does not require a DNA end to promote strand exchange, most HR-based repair models assume that a 3'-end-invading

* Correspondence to: Institut Curie, Université PSL, Université Paris-Saclay, CNRS UMR3348, 91400 Orsay, France.
E-mail address: sarah.lambert@curie.fr (S.A. Lambert).
[1] Equal contribution.

https://doi.org/10.1016/j.dnarep.2023.103548
Received 23 June 2023; Received in revised form 26 July 2023; Accepted 27 July 2023
Available online 1 August 2023

strand, as opposed to a 5'end-invading strand, generates a productive D-loop for priming DNA synthesis and thus copies the missing genetic information or resume DNA replication. The loading of Rad51 onto DNA requires the assistance of a loader, known as Rad52 in yeast and BRCA2 in vertebrate, although these two loaders have different operating modes (Fig. 1). Rad51 has also a DNA-dependent ATPase activity that facilitates its dissociation from DNA. Regulating the ATPase activity of Rad51 is therefore critical to control filament formation and strand exchange, and several HR mediators are proposed to play such a function (discussed in [7]). Finally, Rad51 has a second low affinity dsDNA binding site that is critical for homology search and strand exchange [8].

The direct observation of DNA replication structures by electronic microscopy (EM) from cells defective for Rad51 (in Xenopus egg and yeast cells) revealed the presence of large ssDNA gaps both at the elongation point of replication forks and behind them [9,10]. Thus, continuous DNA synthesis is ensured by the recombinase Rad51 that couples lagging and leading strand synthesis and protects newly replicated DNA from nucleolytic degradation. Since then, several studies have revealed multiple functions of the core HR machinery in dealing with replicative DNA damage and fork obstacle, including the repair of broken fork, the restart of dysfunctional fork, fork protection, and the repair of daughter strand gap. Interestingly, some of these molecular transactions do not require the strand exchange activity of Rad51 and thus refer to as non-recombinogenic functions in contrast to strand exchange-based mechanisms that refer to as homology-directed repair (HDR). Below, we summarize the multifaceted functions of the HR machinery during DNA replication (Fig. 1), illustrate how these functions ensure key biological processes to complete genome duplication, and how these HR sub-pathways are regulated.

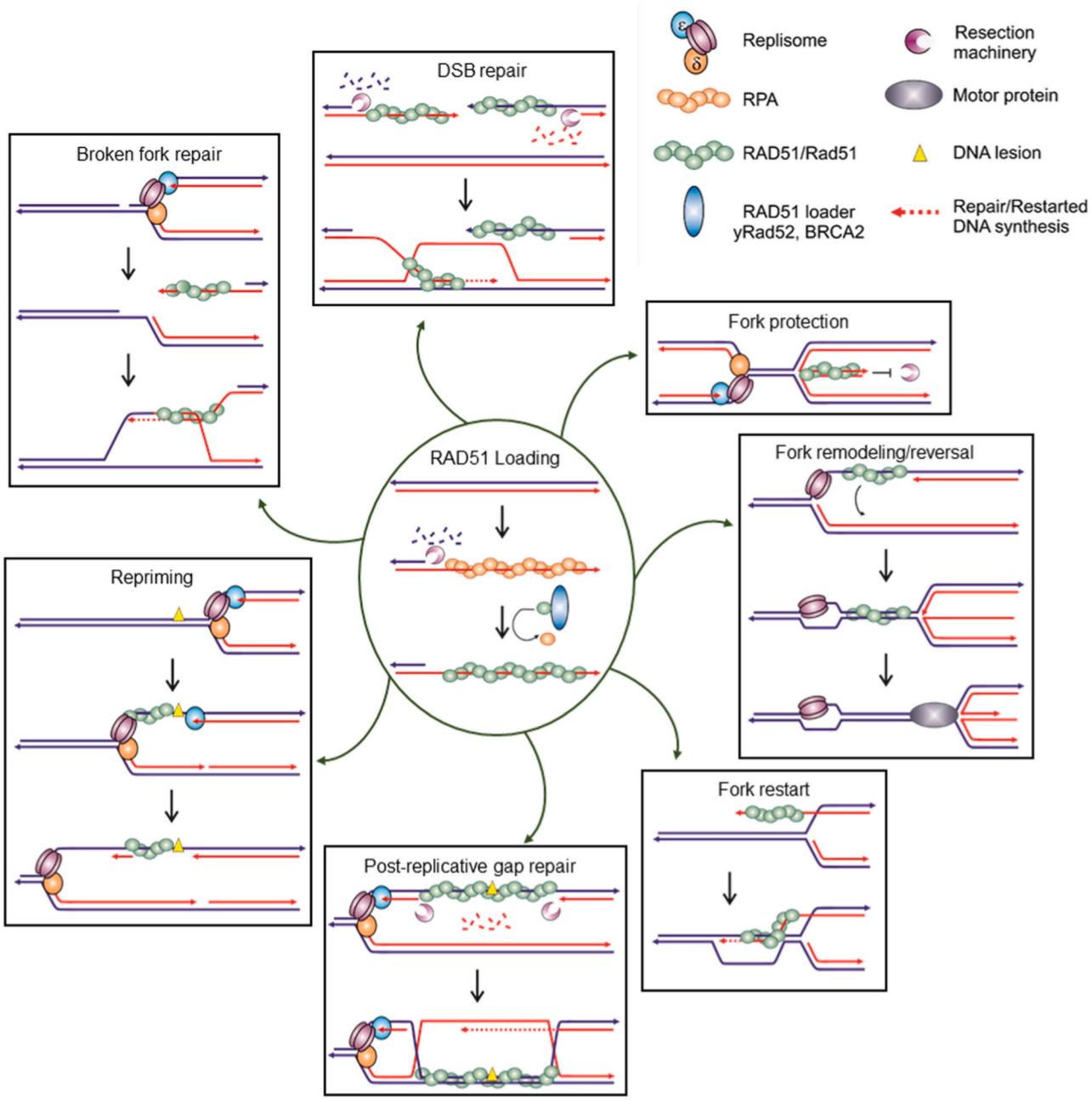

Fig. 1. The multifaceted functions of homologous recombination in DSB and replication-associated DNA damage (See text, Section 3 for details).

3. The homologous recombination machinery engages at replication fork for multiple functions

3.1. The repair and restart of replication fork require a recombinogenic function

When a replication fork encounters a nick or a ssDNA gap, it results in a broken fork exhibiting a one-sided DSB, a typical HDR substrate. The Rad51-coated filament initiates strand invasion within the parental duplex, followed by DNA synthesis, an HR pathway referred to as break-induced replication (BIR) (reviewed in [11]). BIR has been extensively studied in yeast models, upon induction of a DSB in G2 cells with only one DNA end able to search for homology. In this case, BIR can proceed with DNA synthesis over hundreds of kilobases until reaching the end of the chromosome, although this DNA synthesis step is highly mutagenic [12–17]. In Xenopus egg extract, broken forks lead to the loss of some components of the replicative helicase CMG (the GINS subunits) and the restoration of a functional replisome requires RAD51 and the nuclease MRE11, showing that an HR-dependent process is necessary to maintain replisome integrity upon fork collapse [18]. By definition, BIR initiates from an invading one-sided DSB end from which DNA synthesis is extended within a migrating D-loop [19–23]. The newly synthesized strand is extruded from the D-loop and is used as a template to copy the second strand. Thus, BIR synthesis is conservative and both strands are synthesized by the DNA polymerase delta with the assistance of the non-essential subunit Pol32 [12,24,25]. Pol alpha is proposed to be required for stabilizing the long leading strand but its exact function remains unclear [12]. This non-canonical form of DNA synthesis results in an 100- to 1000-fold increase in mutation frequency, compared to the bulk of DNA synthesis as well as frequent template switches resulting in complex genome rearrangement favoring cancer progression [13–17]. BIR events underlie Alternative Lengthening of Telomeres (ALT), a mechanism that allows maintaining telomere length in ~ 20% of cancer cells (reviewed in [26]). Many ALT pathways were found to be independent of RAD51 but relying on RAD52, which may exploit its strand annealing activity to recombine telomeric repeats, similarly to the RAD51-independent BIR described in budding yeast. BIR also underlies Mitotic DNA Synthesis (MiDAS), a process occurring on condensed chromosomes and viewed as the "last chance" to complete genome duplication before chromosome segregation initiates [27] (and reviewed in [28]). MiDAS is initiated by Mus81-mediated enzymatic cleavage of unresolved and late replication intermediates at "difficult-to-replicate" sites, such as common fragile sites, allowing BIR to resume DNA synthesis. MiDAS was initially described as RAD52 and POLD3 (the human orthologue of budding yeast Pol32) dependent but RAD51 and BRCA2 independent [29,30], consistent with these two last factors being excluded from the chromatin in mitosis. Nonetheless, a recent study established a role for RAD51 in promoting MiDAS, acting upstream of Mus81-dependent cleavage of late replication intermediates to complete DNA replication in mitosis [31].

In the last 10 years, evidences have accumulated to support that DSB is not a prerequisite to initiate HR-dependent replication fork restart [32–35]. This mechanism, called recombination-dependent-replication (RDR) is initiated by the controlled resection of newly synthesized strands to generate ssDNA gaps at the fork, further promoting the loading of the ssDNA binding protein RPA and HR factors (reviewed in [1]). Although there is a tendency to use the terms BIR and RDR interchangeably, BIR could be denoted as a specialized form of RDR, initiated by a DSB instead of an ssDNA gap (Fig. 2). Mutations in the second DNA binding site of RAD51, called RAD51-II3A, impair the strand exchange

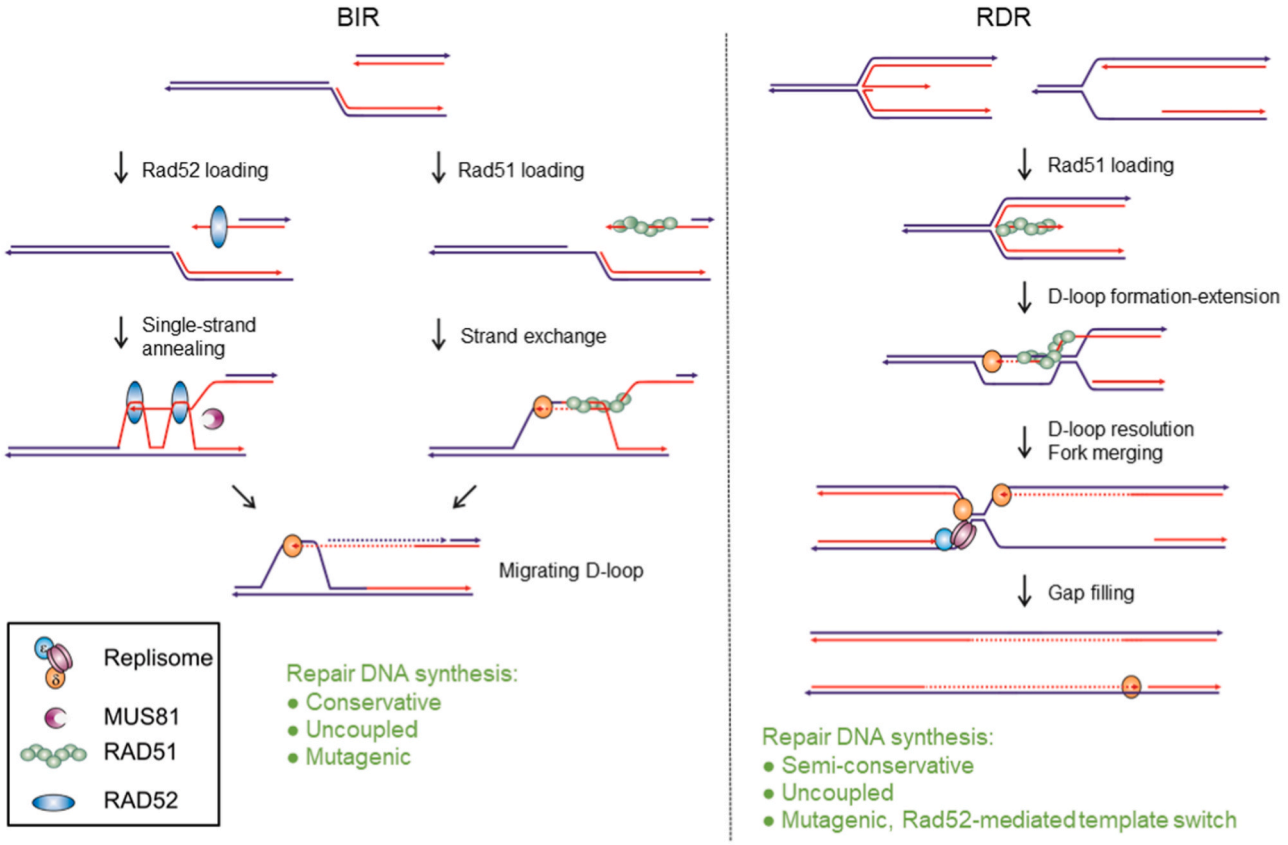

Fig. 2. Models of Break-induced Replication (BIR) and Recombination-dependent-replication (RDR). BIR: the left part illustrates the Rad52-dependent and Rad51-independent BIR and the right panel illustrates the Rad51 and Rad52-dependent RDR. BIR can initiate from broken replication fork after enzymatic cleavage or not during or outside S-phase. RDR is initiated from ssDNA gap generating by the control degradation of nascent strand initiated at reversed fork or not, resulting in a Rad51-bound extruded leading strand.

activity without affecting nucleoprotein filament formation or binding to DNA [8]. This mutant is defective in restarting dysfunctional forks induced by a site-specific replication fork barrier (RFB) in the fission yeast, *Schizosaccharomyces pombe* and in restarting forks stalled upon depletion of dNTP pool in human cells (*i.e.* upon hydroxyurea (HU) treatment) [36,37]. However, the expression of hsRAD51-II3A also resulted in the accumulation of collapsed forks, in a more severe way than in the RAD51 depletion condition, suggesting that a stable but unproductive RAD51 filament inhibits alternative fork restart/repair pathways or leads to enzymatic cleavage of stalled forks [36]. Extensively studied in the fission yeast *S. pombe*, collapsed forks can be restarted by RDR in 15–20 min and can travel over long distances, up to 20 Kb, before fusing with a canonical fork [38–40]. During RDR, the DNA synthesis remains semi-conservative but both strands are synthesized by the DNA polymerase delta, likely in an uncoupled manner [39,40]. Thus, similarly to BIR, this non-canonical form of DNA synthesis is mutagenic, leading to frequent dissociation of the nascent strand from the template, followed by template switches triggering chromosomal rearrangements, genomic duplications or deletions and replication slippages [33,34,41–44]. Although the initial step of RDR is largely dependent on the strand exchange activity of Rad51, a recent report demonstrated that the strand annealing activity of Rad52 makes significant contribution to template switches during the elongation step of RDR, thus modulating replication errors during the progression of the restarted fork [44]. RDR may contribute to complete DNA replication in human cells. Indeed, upon mild replication stress conditions, DNA synthesis persists during the transition of late S to G2/M phase to minimize unfinished DNA replication and RS-induced mitotic abnormalities. In contrast to MiDAS, this resilient DNA synthesis relies on RAD51 and RAD52 but not MUS81, suggesting that fork breakage is not required to sustain DNA replication in G2 cells [45].

3.2. Replication fork remodeling and protection

Reversed replication forks are 4-branched DNA structures in which the newly synthesized strands are annealed together, and the opened parental DNA strands are back into a duplex form (Fig. 1). Fork reversal occurs not only at a fork encountering any type of DNA lesion, but also as an overall response to RS to restrict fork elongation [35,46]. Thus, fork reversal is viewed as a "holding state" during which an active replication fork can undergo cycle of fork reversal and fork restoration, depending on RS signaling conditions. However, a reversed fork provides a one-ended DNA end that is somehow recognized and processed as a DSB end, leading to nascent strand degradation by the resection machinery (reviewed in [5]). This refers to as unprotected forks that are detected using a DNA fiber assay in which nascent strands are labelled by two successive rounds of distinguishable thymidine analogues incorporated into DNA. Unprotected forks are revealed, upon HU treatment, by the shortening of the DNA fiber length labeled during the second round, requiring both strands of the reversed arm to be degraded. Several motor proteins promote fork reversal in vivo and in vitro (reviewed in [47]) and RAD51 promotes both fork reversal and fork protection [35,48]. Although RAD51-dependent fork reversal is independent of BRCA2 [49–51], whether or not it is a recombinogenic function remains debated. Human cells expressing RAD51-II3A are able to protect the fork against degradation by the nuclease DNA2 [36]. A more recent study, in which the reversed fork was detected directly by EM, investigated the role of several RAD51 mutated forms affecting distinct biochemical activities in promoting fork reversal. The authors proposed that RAD51-mediated fork reversal allows bypassing the replicative helicase CMG by annealing the parental strands behind the stalled fork while the translocase SMARCAL1 further extends this parental duplex, resulting in nascent strands being annealed together. All mutants impaired for the strand exchange activity were found defective in promoting fork reversal [52]. One hypothesis is that RAD51 mediates fork reversal by multiple mechanisms, either by itself or by stimulating the activity of motor proteins.

In contrast, the strand exchange activity of RAD51 is dispensable for fork protection, which requires RAD51 DNA binding, its loader BRCA2 and nucleoprotein filament formation. RAD51-T131P, a heterozygous mutated allele identified in a Fanconi Anemia patient, acts as a dominant negative form when mixed with wild type RAD51, producing an unstable filament ineffective for fork protection, but sufficient to perform fork reversal [50,53]. Thus, the role of RAD51 in promoting fork reversal and fork protection engages distinct biochemical functions: fork reversal may require a few RAD51 molecules engaged at fork upon uncoupling between lagging and leading strand synthesis, whereas fork protection requires numerous monomers to form a filament onto the reversed arm, which can reach multiple kilobases in length. Surprisingly, RAD51-mediated fork reversal is BRCA2 independent whereas RAD51-mediated fork protection is BRCA2-dependent. Therefore, BRCA2 deficient cells suffers from unprotected forks that are alleviated by downregulating RAD51 [49–51]. The roles of BRCA2 in promoting HDR and fork protection are genetically separable and require distinct modes of interaction with RAD51 and its loading [48]. For example, BRC repeats of BRCA2 are critical to promote HDR but not fork protection whereas a single mutation in the C-terminal TR2 domain (S3291A) impairs fork protection but not HDR. It was recently shown in vitro that the protective function of RAD51 largely involves its capacity to bind dsDNA instead of ssDNA [54]. While BRC repeats abrogated RAD51-dependent DNA protection by removing RAD51 from dsDNA, the TR2 fragment restored DNA protection by stabilizing RAD51 onto dsDNA, a property not shared by a TR2-S3291A fragment. These results provide a better framework to understand the biology of separation-of-function mutants of RAD51 and BRCA2. Nonetheless, it remains key to understand how the full-length BRCA2 protein handles in vivo these different regulating functions to orchestrate RAD51 activity at the fork. Indeed, the same replication intermediate, a reversed fork, contributes to restrain fork progression while also being an entry point for the degradation of nascent strands, if unprotected. This suggests that RAD51-mediated fork reversal and fork protection must be tightly coupled to avoid genome instability.

3.3. The repair of post-replicative gaps and repriming

When the replisome encounters a DNA lesion that the replicative DNA polymerases cannot replicate, the DNA damage tolerance or bypass pathways ensure the completion of genome duplication, without repairing the damage. These mechanisms require priming *de novo* DNA synthesis downstream of the DNA lesion, ensuring continuous fork progression but leaving stretches of ssDNA behind the fork, named daughter-strand gaps. These gaps are then filled in either by the Translesion Synthesis (TLS) DNA polymerases or by template switch (TS), an HR sub-pathway (reviewed in [55]). Technical advances such as single-molecule analysis by EM or DNA fiber, have provided evidence of post-replicative gaps and their accumulation in the absence of a functional HR pathway in several organisms (yeast, Xenopus, human cells). In budding yeast, daughter-strand gaps are first enlarged by the nuclease Exo1, followed by a Rad51-mediated invasion of the ssDNA gap into the fully replicated sister chromatid [56,57]. This process is uncoupled from the bulk of DNA synthesis since Rad52 and Rad51 foci are mainly observed in the G2 phase, despite Rad51 being able to associate with unperturbed fork during S-phase [58,59]. The dynamic tracking of RPA foci relative to DNA synthesis sites concluded that the repair of post-replicative gaps is confined to specific territories that are spatially and temporally distant from ongoing replication forks [59]. HR-dependent repair of post-replicative gaps has also been reported in human cells upon treatment with BPDE (benzo(a)pyrene diol epoxide) that induces bulky adducts. In this situation, both MRE11 and EXO1 promote gap expansion to generate RAD51 foci, independently of fork stalling or collapse [60]. The current model of HR-dependent gap repair suggests that the intact sister chromatid is invaded by the ssDNA gap,

without the use of a 3' end extremity, thus a different mode of HR than the ones used to repair broken forks or DSBs (reviewed in [61]). How these distinct types of strand invasion are regulated remains largely unknown. Interestingly, a recent study in budding yeast identified physical interactions between the MCM complex, a component of the replicative DNA helicase, and Rad51-Rad52 to form a nuclease-insoluble nuclear scaffold in the G1 phase, in which MCM is bound to DNA but not Rad51 and Rad52 [62]. The authors uncovered a Rad51 mutant (Rad51m) that was no longer able to interact with MCM in vivo, although a direct interaction was not established. This mutant showed defective post-replicative gap repair and sensitivity to damaged replication fork-inducing agents but normal DSB repair, suggesting either a non-recombinogenic function of Rad51 in promoting gap repair or that the Rad51 strand exchange activity operates differently at DSBs versus ssDNA gaps. Physical interactions between human MCM and RAD51 were also reported without clear biological role (reviewed in [61]).

Repriming requires the DNA polymerase Primpol in human cells and the Primase-Pol alpha-Ctf4 complex in budding yeast [63,64]. Evidence has emerged supporting that HR factors ensure non-recombinogenic functions to regulate repriming. In the absence of the TLS polymerase Eta, mutations in which lead to the *Xeroderma pigmentosum* human syndrome, the analysis of replication intermediates by EM after exposure to UV irradiation, revealed a dual requirement for RAD51 at the fork and behind it [65]. First, RAD51 was detected in a limited amount at the fork, whereas its detection was greater behind the fork. Second, using the inhibitor B02 that disorganizes the RAD51 nucleoprotein filament in a way that is no longer functional to promote strand exchange activity, the authors suggested that RAD51 plays a non-recombinogenic function at a fork stalled by DNA lesion to ensure efficient repriming, a function that may involve an interaction with Pol alpha [50,66]. Given that restricting yeast Rad52 expression to G2 phase leads to defect in tolerating replicative DNA lesions [58], an emerging picture is that the recombinase Rad51 binds to unperturbed fork to promote continuous fork progression and DNA synthesis via repriming and then switches to a recombinogenic function to promote post-replicative gap repair. Consistently, mammalian cells defectives for BRCA1 or BRCA2 accumulate post-replicative gaps from multiple origins [67,68]. This includes a defect in a FEN1-independent pathway of Okazaki fragment maturation on the lagging strand that remains to be defined, unrepaired post-replicative gaps, and the inability to restrain repriming [68–75]. Indeed, BRCA2 interacts with the replication factor MCM10 to restrain PRIMPOL activity on the leading strand, independently of fork protection [76].

The replicative HR functions help to complete genome duplication by several means (Fig. 3). Two types of "unfinished DNA replication" can be considered: when some parts of the genome are not replicated at all or when the genome is replicated in a discontinuous manner. By ensuring fork restart and repair, especially at transcription-replication collisions, or fork protection to ensure accurate termination, HR prevents an under-replication of the genome and the formation of a particular type of mitotic bridges, named ultra-fine bridges, a hallmark of unreplicated DNA in mitosis [37,77–79]. By limiting the accumulation of post-replicative gaps, HR ensures a continuous DNA synthesis and avoid the excessive use of TLS activity that may contribute to increasing mutation load.

4. Regulation of the distinct replicative HR functions by nuclear positioning

The distinct replicative HR functions exhibit different outcomes on genome stability and must therefore be strictly kept in check. In addition to the above-mentioned cell-cycle regulations, nuclear positioning and chromatin context significantly influence the outcomes of HR on genome stability. We intentionally tend to avoid using the term "pathway choice" because, in our view, it implies an active process of choosing among all possible HR subpathways to deal with replication-associated DNA damage and that all mechanisms are equally available and effective. Instead, it appears that depending on the nuclear compartment, the availability of some repair factors may make one pathway more efficient than another one.

DNA repair occurs in the context of eukaryotic genomes organized into a compartmentalized nucleus. The quest to locate distant homologous regions can be a challenge, which may require advanced mechanisms like chromatin mobility both locally (at the damage site) and globally. Increased chromatin mobility is a phenomenon conserved across different organisms in response to DSBs (reviewed [80,81]). For example, DSBs occurring within repeated sequences or in heterochromatic regions shift away from their compartment to achieve HR repair

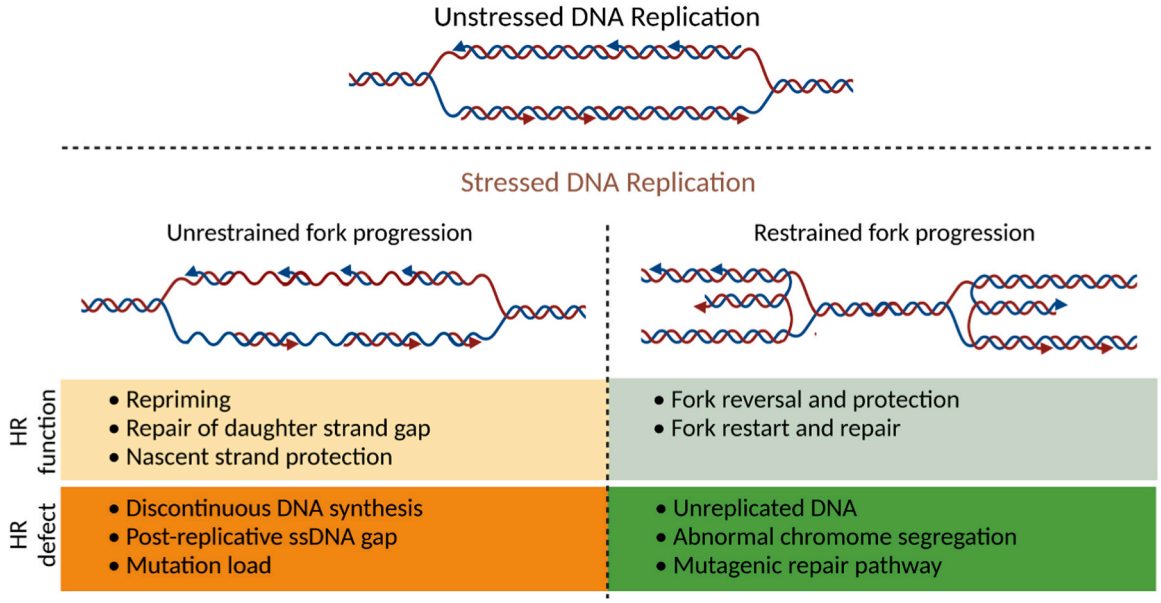

Fig. 3. Two types of "unfinished DNA Replication". The top panel illustrate the progression of canonical fork, including semi-discontinuous DNA synthesis on the lagging strand. A hallmark of unrestrained fork progression is discontinuous DNA synthesis on both sister chromatid, generating post-replicative daughter strand gaps. Fork reversal contributes to restrain fork progression upon stress, increasing the risk of "unreplicated DNA" when cells enter mitosis if no restart occurs.

(reviewed in [82,83]). As observed for DSBs, replication stress sites were reported to relocate to the nuclear periphery, and in some cases, to anchor to nuclear pore complexes (NPCs) to regulate and fine-tune HR-based mechanisms. This includes forks stalled by telomere repeats, structures forming sequences, DNA-bound proteins or replication inhibitors [84–89]. Relocation to NPCs and/or the nuclear periphery may create an environment more favorable to some replicative HR sub pathways. Diverse scenarios emerge depending on the type of fork obstacle and the model organism (Fig. 4).

4.1. Fork stalling within telomere repeats

Inactivation of telomerase in yeast leads to telomere erosion and replicative senescence. The relocation of eroded telomeres to NPCs facilitates the emergence of survivors (of type II) by a process similar to mammalian ALT [90]. However, telomerase is also essential to counteract replication-induced damage at telomeres, as its inactivation leads to stochastic replication fork stalling and transient cell-cycle arrests (reviewed in [91]). Thus, in the absence of telomerase, telomere replication becomes dependent on HR factors, as their deletion dramatically boosts senescence. In budding yeast, telomeric stalled forks relocate and associate with NPCs to resume replication. In the absence of anchorage, stalled forks engage in an error-prone Rad51-dependent pathway to maintain telomere length by recombination between sister chromatids [86]. This emphasizes an unsuspected role of NPCs in restricting error-prone HR events at stalled forks.

4.2. Forks stalled by tri-nucleotides repeats

In budding yeast, tri-nucleotide repeats, such as CAG, have the propensity to form secondary DNA structures prone to stall replication forks (reviewed in [92]). Such stalled forks transiently relocate and anchor to NPCs in late S-phase, in a SUMO-dependent manner [87]. SUMOylated RPA, loaded onto ssDNA, prevents Rad51 loading that is permitted only after NPC anchorage [93]. It was proposed that at the NPC, the Slx5–8 STUbL pathway promotes the degradation of SUMOylated proteins to alleviate the inhibition of Rad51 loading and favor HR-mediated fork restart. Impaired relocation leads to repeat instability in a Rad52-dependent manner [87]. This scenario exemplifies the concept of a spatially segregated mechanism to regulate the sequential loading of HR factors at stalled forks and ensure replication restart in an accurate manner.

4.3. Forks stalled at DNA-bound protein complex

Another study in fission yeast describes how relocation and anchorage to NPCs help to sustain RDR. A fork arrested by a protein-mediated RFB relocates to the nuclear periphery and anchors to NPCs during S-phase, for the time necessary to complete RDR [85]. Relocation depends on the recombinogenic function of Rad51, suggesting that joint molecules are important nuclear positioning signals and that Rad51 loading is not prevented at unique sequences, in contrast to repeated sequences. Relocation also requires the E3 SUMO ligase Pli1 and the STUBL pathway, although the exact SUMOylated targets are still unknown. It was proposed that the accumulation of SUMO chains limits the Rad51-dependent RDR, creating a need for the SUMO protease Ulp1 and the proteasome; two activities enriched at the NPC level, to eliminate SUMO conjugates and enable replication to restart. This exemplifies how a SUMO-based mechanism spatially segregates the subsequent RDR steps from Rad51 loading and activity occurring in the nucleoplasm and the restart of DNA synthesis occurring after anchorage to NPCs. One remaining question is the identification of the Rad51-independent RDR,

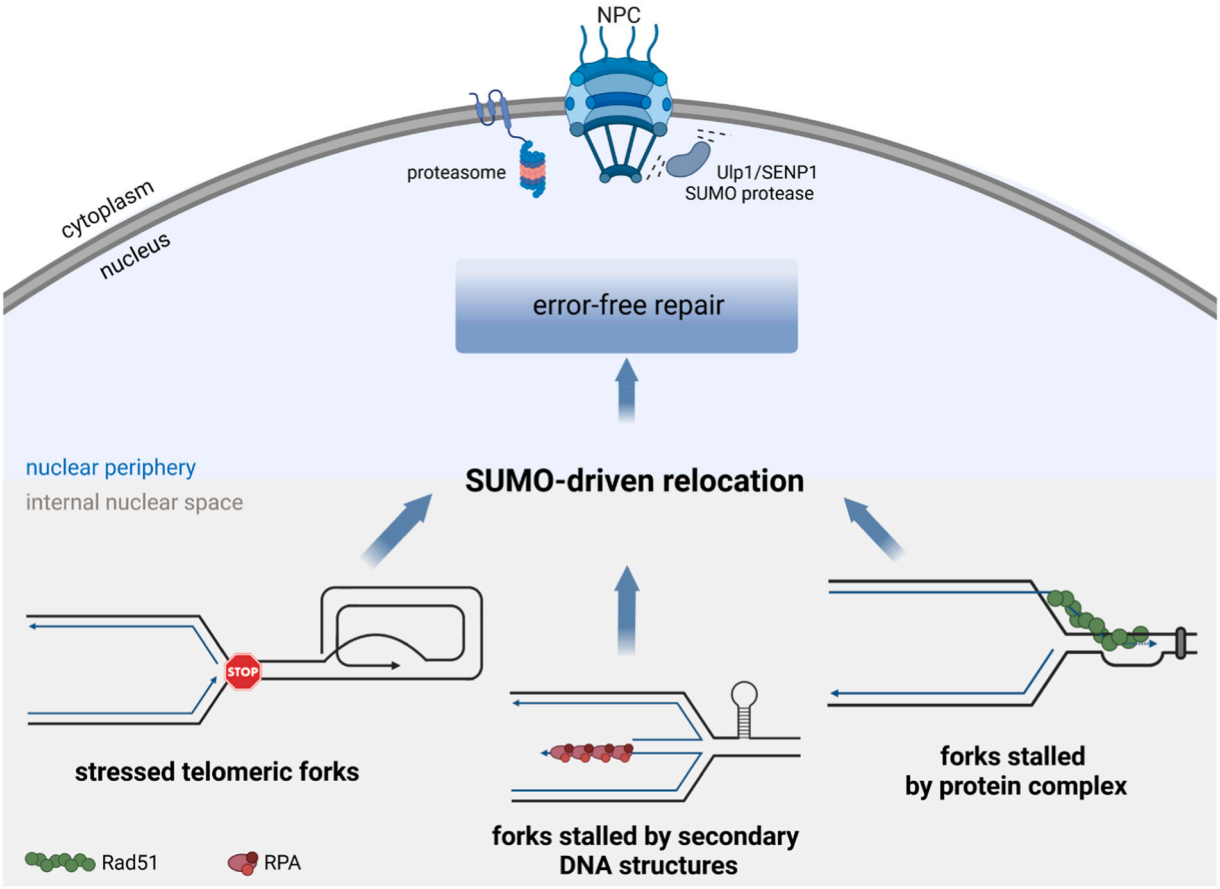

Fig. 4. Several type of stressed replication fork relocate to the nuclear periphery and anchor to nuclear pore complex (NPC) in a SUMO-dependent manner.

which occurs in the nucleoplasm and that is limited by SUMO chains [82,85]. As mentioned above, both RDR and BIR are mutagenic pathways, and one attractive hypothesis is that nuclear positioning may influence their intrinsic mutagenicity, for example by regulating transition from Rad51-dependent to Rad51-independent template switching [44].

5. Concluding remark: what are the key HR functions to prevent genome instability, tumor development and modulate sensitivity to chemotherapies?

Beyond our fundamental understanding of the most prevalent functions of the HR machinery to prevent genome instability, scientists and clinicians face two distinct challenges. The first one is to assign the cancer risk associated to specific BRCA patient mutations. The second is to predict the response to treatment of a tumor defective in BRCA1/2, or more generally in the HR pathway. In this context, multiple cellular (Rad51 foci), molecular (repair efficiency) and genomic assays (mutational signature) have been developed to assign HDR defects in cancer cells. The first challenge is linked to defining which HR defect (unprotected fork, HDR defect, gap suppression and repair) is more prone to generating genome instability fueling cancer development. The second one depends on understanding which replicative function is defective in a certain type of cancer to delineate the best genotoxic-based treatment. It must be taken into account that unrepaired and persistent gaps are converted into collapsed and broken forks at the next round of DNA replication, creating a higher need for HR-mediated fork restart and repair [73]. Both unprotected forks and suppression of gaps have been shown to correlate with chemo-resistance, in particular to cisplatin and PARP inhibitor (reviewed and discussed in [94]). The use of separation-of-function mutated forms of BRCA2 in mice showed that HDR defect is prone to tumorigenesis, unlike fork protection and gap suppression defects [95]. Interestingly, defective fork protection and gap suppression, but not HDR, was observed in BRCA2 heterozygous mice, a situation highly relevant to patients. It is conceivable that defective fork protection and/or gap accumulation favor a “background noise” of genome instability sufficient to accumulate genetic damages. Interestingly, *BRCA* genes are hot spots of fork stalling, undergoing error-prone fork repair in *BRCA* haplo-insufficient cells, a mechanism that may favor loss of heterozygosity [96]. Upon loss of the second allele, cells switch into an HDR defect mode that amplifies genome instability and tumor development. In support of this, DSB repair in BRCA2-deficient cells relies on the use of alternative and error-prone DNA repair pathways, named Alt NHEJ, mediated by the DNA polymerase Theta [97]. Thus, a part of the genome instability that fuels cancer development may result from such mutagenic repair, as discussed in [98].

Declaration of Competing Interest

The authors declare no competing interests.

Data Availability

No data was used for the research described in the article.

Acknowledgement

SAEL acknowledges funding from ANR (ANR-19-CE12-0023-01 and ANR-19-CE12-0016-03), the Fondation Ligue Contre le Cancer “Equipe Labellisée 2020” (EL2020LNCC/Sal), CNRS and the institute Curie. KS has received individual PhD fellowships from the Fondation Ligue Contre le Cancer and the fondation ARC.

References

[1] A. Ait Saada, S.A.E. Lambert, A.M. Carr, Preserving replication fork integrity and competence via the homologous recombination pathway, DNA Repair (Amst.) 71 (2018) 135–147, https://doi.org/10.1016/j.dnarep.2018.08.017.
[2] M.K. Zeman, K.A. Cimprich, Causes and consequences of replication stress, Nat. Cell Biol. 16 (2014) 2–9, https://doi.org/10.1038/ncb2897.
[3] E.M. Taylor, H.D. Lindsay, DNA replication stress and cancer: cause or cure? , Futur. Oncol. 12 (2016) 221–237, https://doi.org/10.2217/fon.15.292.
[4] M. Macheret, T.D. Halazonetis, DNA replication stress as a hallmark of cancer, Annu. Rev. Pathol. Mech. Dis. 10 (2015) 425–448, https://doi.org/10.1146/annurev-pathol-012414-040424.
[5] M. Berti, D. Cortez, M. Lopes, The plasticity of DNA replication forks in response to clinically relevant genotoxic stress, Nat. Rev. Mol. Cell Biol. 21 (2020) 633–651, https://doi.org/10.1038/s41580-020-0257-5.
[6] J. San Filippo, P. Sung, H. Klein, Mechanism of eukaryotic homologous recombination, Annu. Rev. Biochem. 77 (2008) 229–257, https://doi.org/10.1146/annurev.biochem.77.061306.125255.
[7] J.T. Holthausen, C. Wyman, R. Kanaar, Regulation of DNA strand exchange in homologous recombination, DNA Repair (Amst.) 9 (2010) 1264–1272, https://doi.org/10.1016/j.dnarep.2010.09.014.
[8] V. Cloud, Y.L. Chan, J. Grubb, B. Budke, D.K. Bishop, Rad51 is an accessory factor for Dmc1-mediated joint molecule formation during meiosis, Sci. (80-.) 337 (2012) 1222–1225, https://doi.org/10.1126/science.1219379.
[9] Y. Hashimoto, A.R. Chaudhuri, M. Lopes, V. Costanzo, Rad51 protects nascent DNA from Mre11-dependent degradation and promotes continuous DNA synthesis, Nat. Struct. Mol. Biol. 17 (2010) 1305–1311, https://doi.org/10.1038/nsmb.1927.
[10] C.R. Joseph, S. Dusi, M. Giannattasio, D. Branzei, Rad51-mediated replication of damaged templates relies on monoSUMOylated DDK kinase, Nat. Commun. 13 (2022) 2480, https://doi.org/10.1038/s41467-022-30215-9.
[11] X. Wu, A. Malkova, Break-induced replication mechanisms in yeast and mammals, Curr. Opin. Genet. Dev. 71 (2021) 163–170, https://doi.org/10.1016/j.gde.2021.08.002.
[12] L. Liu, Z. Yan, B.A. Osia, J. Twarowski, L. Sun, J. Kramara, R.S. Lee, S. Kumar, R. Elango, H. Li, W. Dang, G. Ira, A. Malkova, Tracking break-induced replication shows that it stalls at roadblocks, Nature 590 (2021) 655–659, https://doi.org/10.1038/s41586-020-03172-w.
[13] B. Osia, J. Twarowski, T. Jackson, K. Lobachev, L. Liu, A. Malkova, Migrating bubble synthesis promotes mutagenesis through lesions in its template, Nucleic Acids Res 50 (2022) 6870–6889, https://doi.org/10.1093/nar/gkac520.
[14] R. Elango, B. Osia, V. Harcy, E. Malc, P.A. Mieczkowski, S.A. Roberts, A. Malkova, Repair of base damage within break-induced replication intermediates promotes kataegis associated with chromosome rearrangements, Nucleic Acids Res 47 (2019) 9666–9684, https://doi.org/10.1093/NAR/GKZ651.
[15] C.J. Sakofsky, S.A. Roberts, E. Malc, P.A. Mieczkowski, M.A. Resnick, D. A. Gordenin, A. Malkova, Break-induced replication is a source of mutation clusters underlying kataegis, Cell Rep. 7 (2014) 1640–1648, https://doi.org/10.1016/j.celrep.2014.04.053.
[16] A. Deem, A. Keszthelyi, T. Blackgrove, A. Vayl, B. Coffey, R. Mathur, A. Chabes, A. Malkova, Break-induced replication is highly inaccurate, PLoS Biol. 9 (2011), e1000594, https://doi.org/10.1371/journal.pbio.1000594.
[17] L. Costantino, S.K. Sotiriou, J.K. Rantala, S. Magin, E. Mladenov, T. Helleday, J. E. Haber, G. Iliakis, O.P. Kallioniemi, T.D. Halazonetis, Break-induced replication repair of damaged forks induces genomic duplications in human cells, Sci. (80-.) 343 (2014) 88–91, https://doi.org/10.1126/science.1243211.
[18] Y. Hashimoto, F. Puddu, V. Costanzo, RAD51-and MRE11-dependent reassembly of uncoupled CMG helicase complex at collapsed replication forks, Nat. Struct. Mol. Biol. 19 (2012) 17–25, https://doi.org/10.1038/nsmb.2177.
[19] N. Saini, S. Ramakrishnan, R. Elango, S. Ayyar, Y. Zhang, A. Deem, G. Ira, J. E. Haber, K.S. Lobachev, A. Malkova, Migrating bubble during break-induced replication drives conservative DNA synthesis, Nature 502 (2013) 389–392, https://doi.org/10.1038/nature12584.
[20] M.A. Wilson, Y. Kwon, Y. Xu, W.H. Chung, P. Chi, H. Niu, R. Mayle, X. Chen, A. Malkova, P. Sung, G. Ira, Pif1 helicase and Polδ promote recombination-coupled DNA synthesis via bubble migration, Nature 502 (2013) 393–396, https://doi.org/10.1038/nature12585.
[21] O. Buzovetsky, Y. Kwon, N.T. Pham, C. Kim, G. Ira, P. Sung, Y. Xiong, Role of the Pif1-PCNA complex in pol δ-dependent strand displacement DNA synthesis and break-induced replication, Cell Rep. 21 (2017) 1707–1714, https://doi.org/10.1016/j.celrep.2017.10.079.
[22] R.A. Donnianni, L.S. Symington, Break-induced replication occurs by conservative DNA synthesis, Proc. Natl. Acad. Sci. U. S. A 110 (2013) 13475–13480, https://doi.org/10.1073/pnas.1309800110.
[23] S. Li, H. Wang, S. Jehi, J. Li, S. Liu, Z. Wang, L. Truong, T. Chiba, Z. Wang, X. Wu, PIF1 helicase promotes break-induced replication in mammalian cells, EMBO J. 40 (2021), e104509, https://doi.org/10.15252/embj.2020104509.
[24] J.R. Lydeard, S. Jain, M. Yamaguchi, J.E. Haber, Break-induced replication and telomerase-independent telomere maintenance require Pol32, Nature 448 (2007) 820–823, https://doi.org/10.1038/nature06047.
[25] R.A. Donnianni, Z.X. Zhou, S.A. Lujan, A. Al-Zain, V. Garcia, E. Glancy, A. B. Burkholder, T.A. Kunkel, L.S. Symington, DNA polymerase delta synthesizes both strands during break-induced replication, e4, Mol. Cell. 76 (2019) 371–381, https://doi.org/10.1016/j.molcel.2019.07.033.
[26] K. Hou, Y. Yu, D. Li, Y. Zhang, K. Zhang, J. Tong, K. Yang, S. Jia, Alternative lengthening of telomeres and mediated telomere synthesis, Cancers 14 (2022) 2194, https://doi.org/10.3390/cancers14092194.

[27] S. Minocherhomji, S. Ying, V.A. Bjerregaard, S. Bursomanno, A. Aleliunaite, W. Wu, H.W. Mankouri, H. Shen, Y. Liu, I.D. Hickson, Replication stress activates DNA repair synthesis in mitosis, Nature 528 (2015) 286–290, https://doi.org/10.1038/nature16139.
[28] A.P. Bertolin, J.S. Hoffmann, V. Gottifredi, Under-replicated DNA: the byproduct of large genomes? Cancers 12 (2020) 1–20, https://doi.org/10.3390/cancers12102764.
[29] R. Bhowmick, S. Minocherhomji, I.D. Hickson, RAD52 facilitates mitotic DNA synthesis following replication stress, Mol. Cell. 64 (2016) 1117–1126, https://doi.org/10.1016/j.molcel.2016.10.037.
[30] S.K. Sotiriou, I. Kamileri, N. Lugli, K. Evangelou, C. Da-Ré, F. Huber, L. Padayachy, S. Tardy, N.L. Nicati, S. Barriot, F. Ochs, C. Lukas, J. Lukas, V.G. Gorgoulis, L. Scapozza, T.D. Halazonetis, Mammalian RAD52 functions in break-induced replication repair of collapsed DNA replication forks, Mol. Cell. 64 (2016) 1127–1134, https://doi.org/10.1016/j.molcel.2016.10.038.
[31] I.E. Wassing, E. Graham, X. Saayman, L. Rampazzo, C. Ralf, A. Bassett, F. Esashi, The RAD51 recombinase protects mitotic chromatin in human cells, Nat. Commun. 12 (2021) 5380, https://doi.org/10.1038/s41467-021-25643-y.
[32] E. Petermann, M.L. Orta, N. Issaeva, N. Schultz, T. Helleday, Hydroxyurea-stalled replication forks become progressively inactivated and require two different RAD51-mediated pathways for restart and repair, Mol. Cell. 37 (2010) 492–502, https://doi.org/10.1016/j.molcel.2010.01.021.
[33] K. Mizuno, S. Lambert, G. Baldacci, J.M. Murray, A.M. Carr, Nearby inverted repeats fuse to generate acentric and dicentric palindromic chromosomes by a replication template exchange mechanism, Genes Dev. 23 (2009) 2876–2886, https://doi.org/10.1101/gad.1863009.
[34] S. Lambert, K. Mizuno, J. Blaisonneau, S. Martineau, R. Chanet, K. Fréon, J. M. Murray, A.M. Carr, G. Baldacci, Homologous recombination restarts blocked replication forks at the expense of genome rearrangements by template exchange, Mol. Cell. 39 (2010) 346–359, https://doi.org/10.1016/j.molcel.2010.07.015.
[35] R. Zellweger, D. Dalcher, K. Mutreja, M. Berti, J.A. Schmid, R. Herrador, A. Vindigni, M. Lopes, Rad51-mediated replication fork reversal is a global response to genotoxic treatments in human cells, J. Cell Biol. 208 (2015) 563–579, https://doi.org/10.1083/jcb.201406099.
[36] J.M. Mason, Y.L. Chan, R.W. Weichselbaum, D.K. Bishop, Non-enzymatic roles of human RAD51 at stalled replication forks, Nat. Commun. 10 (2019) 4410, https://doi.org/10.1038/s41467-019-12297-0.
[37] A. Ait Saada, A. Teixeira-Silva, I. Iraqui, A. Costes, J. Hardy, G. Paoletti, K. Fréon, S.A.E. Lambert, Unprotected replication forks are converted into mitotic sister chromatid bridges, e4, Mol. Cell. 66 (2017) 398–410, https://doi.org/10.1016/j.molcel.2017.04.002.
[38] M.O. Nguyen, M. Jalan, C.A. Morrow, F. Osman, M.C. Whitby, Recombination occurs within minutes of replication blockage by RTS1 producing restarted forks that are prone to collapse, Elife 2015 (2015), e04539, https://doi.org/10.7554/eLife.04539.
[39] K. Naiman, E. Campillo-Funollet, A.T. Watson, A. Budden, I. Miyabe, A.M. Carr, Replication dynamics of recombination-dependent replication forks, Nat. Commun. 12 (2021) 923, https://doi.org/10.1038/s41467-021-21198-0.
[40] I. Miyabe, K. Mizuno, A. Keszthelyi, Y. Daigaku, M. Skouteri, S. Mohebi, T. A. Kunkel, J.M. Murray, A.M. Carr, Polymerase Ĩ replicates both strands after homologous recombination-dependent fork restart, Nat. Struct. Mol. Biol. 22 (2015) 932–938, https://doi.org/10.1038/nsmb.3100.
[41] I. Iraqui, Y. Chekkal, N. Jmari, V. Pietrobon, K. Fréon, A. Costes, S.A.E. Lambert, Recovery of arrested replication forks by homologous recombination is error-prone, PLoS Genet 8 (2012), e1002976, https://doi.org/10.1371/journal.pgen.1002976.
[42] K. Mizuno, I. Miyabe, S.A. Schalbetter, A.M. Carr, J.M. Murray, Recombination-restarted replication makes inverted chromosome fusions at inverted repeats, Nature 493 (2013) 246–249, https://doi.org/10.1038/nature11676.
[43] M. Jalan, J. Oehler, C.A. Morrow, F. Osman, M.C. Whitby, Factors affecting template switch recombination associated with restarted DNA replication, Elife 8 (2019), e41697, https://doi.org/10.7554/eLife.41697.
[44] A. Kishkevich, S. Tamang, M.O. Nguyen, J. Oehler, E. Bulmaga, C. Andreadis, C. A. Morrow, F. Osman, M.C. Whitby, Rad52's DNA annealing activity drives template switching associated with restarted DNA replication, Nat. Commun. 13 (2022) 7293, https://doi.org/10.1038/s41467-022-35060-4.
[45] C. Mocanu, E. Karanika, M. Fernández-Casañas, A. Herbert, T. Olukoga, M. E. Özgürses, K.L. Chan, DNA replication is highly resilient and persistent under the challenge of mild replication stress, Cell Rep. 39 (2022), 110701, https://doi.org/10.1016/j.celrep.2022.110701.
[46] K. Mutreja, J. Krietsch, J. Hess, S. Ursich, M. Berti, F.K. Roessler, R. Zellweger, M. Patra, G. Gasser, M. Lopes, ATR-mediated global fork slowing and reversal assist fork traverse and prevent chromosomal breakage at DNA interstrand cross-links, e5, Cell Rep. 24 (2018) 2629–2642, https://doi.org/10.1016/j.celrep.2018.08.019.
[47] A. Quinet, D. Lemaçon, A. Vindigni, Replication fork reversal: players and guardians, Mol. Cell. 68 (2017) 830–833, https://doi.org/10.1016/j.molcel.2017.11.022.
[48] K. Schlacher, N. Christ, N. Siaud, A. Egashira, H. Wu, M. Jasin, Double-strand break repair-independent role for BRCA2 in blocking stalled replication fork degradation by MRE11, Cell 145 (2011) 529–542, https://doi.org/10.1016/j.cell.2011.03.041.
[49] D. Lemaçon, J. Jackson, A. Quinet, J.R. Brickner, S. Li, S. Yazinski, Z. You, G. Ira, L. Zou, N. Mosammaparast, A. Vindigni, MRE11 and EXO1 nucleases degrade reversed forks and elicit MUS81-dependent fork rescue in BRCA2-deficient cells, Nat. Commun. 8 (2017) 860, https://doi.org/10.1038/s41467-017-01180-5.
[50] A.M. Kolinjivadi, V. Sannino, A. De Antoni, K. Zadorozhny, M. Kilkenny, H. Técher, G. Baldi, R. Shen, A. Ciccia, L. Pellegrini, L. Krejci, V. Costanzo, Smarcal1-mediated fork reversal triggers Mre11-dependent degradation of nascent DNA in the absence of Brca2 and stable Rad51 nucleofilaments, e7, Mol. Cell. 67 (2017) 867–881, https://doi.org/10.1016/j.molcel.2017.07.001.
[51] S. Mijic, R. Zellweger, N. Chappidi, M. Berti, K. Jacobs, K. Mutreja, S. Ursich, A. Ray Chaudhuri, A. Nussenzweig, P. Janscak, M. Lopes, Replication fork reversal triggers fork degradation in BRCA2-defective cells, Nat. Commun. 8 (2017) 859, https://doi.org/10.1038/s41467-017-01164-5.
[52] W. Liu, Y. Saito, J. Jackson, R. Bhowmick, M.T. Kanemaki, A. Vindigni, D. Cortez, RAD51 bypasses the CMG helicase to promote replication fork reversal, Science 380 (2023) 382–387, https://doi.org/10.1126/science.add7328.
[53] A.T. Wang, T. Kim, J.E. Wagner, B.A. Conti, F.P. Lach, A.L. Huang, H. Molina, E. M. Sanborn, H. Zierhut, B.K. Cornes, A. Abhyankar, C. Sougnez, S.B. Gabriel, A. D. Auerbach, S.C. Kowalczykowski, A. Smogorzewska, A dominant mutation in human RAD51 reveals its function in DNA interstrand crosslink repair independent of homologous recombination, Mol. Cell. 59 (2015) 478–490, https://doi.org/10.1016/j.molcel.2015.07.009.
[54] S. Halder, A. Sanchez, L. Ranjha, G. Reginato, I. Ceppi, A. Acharya, R. Anand, P. Cejka, Double-stranded DNA binding function of RAD51 in DNA protection and its regulation by BRCA2, e5, Mol. Cell. 82 (2022) 3553–3565, https://doi.org/10.1016/j.molcel.2022.08.014.
[55] R.P. Wong, K. Petriukov, H.D. Ulrich, Daughter-strand gaps in DNA replication – substrates of lesion processing and initiators of distress signalling, DNA Repair (Amst.) 105 (2021), 103163, https://doi.org/10.1016/j.dnarep.2021.103163.
[56] F. Vanoli, M. Fumasoni, B. Szakal, L. Maloisel, D. Branzei, Replication and recombination factors contributing to recombination-dependent bypass of DNA lesions by template switch, PLoS Genet 6 (2010), e1001205, https://doi.org/10.1371/journal.pgen.1001205.
[57] M. Giannattasio, K. Zwicky, C. Follonier, M. Foiani, M. Lopes, D. Branzei, Visualization of recombination-mediated damage bypass by template switching, Nat. Struct. Mol. Biol. 21 (2014) 884–892, https://doi.org/10.1038/nsmb.2888.
[58] R. González-Prieto, A.M. Muñoz-Cabello, M.J. Cabello-Lobato, F. Prado, Rad51 replication fork recruitment is required for DNA damage tolerance, EMBO J. 32 (2013) 1307–1321, https://doi.org/10.1038/emboj.2013.73.
[59] R.P. Wong, N. García-Rodríguez, N. Zilio, M. Hanulová, H.D. Ulrich, Processing of DNA polymerase-blocking lesions during genome replication is spatially and temporally segregated from replication forks, e4, Mol. Cell. 77 (2020) 3–16, https://doi.org/10.1016/j.molcel.2019.09.015.
[60] A.L. Piberger, A. Bowry, R.D.W. Kelly, A.K. Walker, D. González-Acosta, L. J. Bailey, A.J. Doherty, J. Méndez, J.R. Morris, H.E. Bryant, E. Petermann, PrimPol-dependent single-stranded gap formation mediates homologous recombination at bulky DNA adducts, Nat. Commun. 11 (2020) 5863, https://doi.org/10.1038/s41467-020-19570-7.
[61] M.I. Cano-Linares, A. Yáñez-Vilches, N. García-Rodríguez, M. Barrientos-Moreno, R. González-Prieto, P. San-Segundo, H.D. Ulrich, F. Prado, Non-recombinogenic roles for Rad52 in translesion synthesis during DNA damage tolerance, EMBO Rep. 22 (2021), e50410, https://doi.org/10.15252/embr.202050410.
[62] M.J. Cabello-Lobato, C. González-Garrido, M.I. Cano-Linares, R.P. Wong, A. Yáñez-Vílchez, M. Morillo-Huesca, J.M. Roldán-Romero, M. Vicioso, R. González-Prieto, H.D. Ulrich, F. Prado, Physical interactions between MCM and Rad51 facilitate replication fork lesion bypass and ssDNA gap filling by non-recombinogenic functions, Cell Rep. 36 (2021), 109440, https://doi.org/10.1016/j.celrep.2021.109440.
[63] M. Fumasoni, K. Zwicky, F. Vanoli, M. Lopes, D. Branzei, Error-free DNA damage tolerance and sister chromatid proximity during DNA replication rely on the polα/primase/Ctf4 complex, Mol. Cell. 57 (2015) 812–823, https://doi.org/10.1016/j.molcel.2014.12.038.
[64] B.A. Conti, A. Smogorzewska, Mechanisms of direct replication restart at stressed replisomes, DNA Repair (Amst.) 95 (2020), 102947, https://doi.org/10.1016/j.dnarep.2020.102947.
[65] Y. Benureau, C. Pouvelle, P. Dupaigne, S. Baconnais, E. Moreira Tavares, G. Mazón, E. Despras, E. Le Cam, P.L. Kannouche, Changes in the architecture and abundance of replication intermediates delineate the chronology of DNA damage tolerance pathways at UV-stalled replication forks in human cells, Nucleic Acids Res 50 (2022) 9909–9929, https://doi.org/10.1093/nar/gkac746.
[66] L. Di Biagi, E. Malacaria, F. Antonella Aiello, P. Valenzisi, G. Marozzi, A. Franchitto, P. Pietro, RAD52 prevents accumulation of Polα-dependent replication gaps at perturbed replication forks in human cells, BioRxiv Prepr. Serv. Biol. (2023) 2023.04.12.536536. doi: 10.1101/2023.04.12.536536. https://doi.org/10.1101/2023.04.12.536536.
[67] S.B. Cantor, Revisiting the BRCA-pathway through the lens of replication gap suppression: "gaps determine therapy response in BRCA mutant cancer", DNA Repair 107 (2021), 103209 https://doi.org/10.1016/j.dnarep.2021.103209.
[68] N.J. Panzarino, J.J. Krais, K. Cong, M. Peng, M. Mosqueda, S.U. Nayak, S.M. Bond, J.A. Calvo, M.B. Doshi, M. Bere, J. Ou, B. Deng, L.J. Zhu, N. Johnson, S.B. Cantor, Replication gaps underlie BRCA deficiency and therapy response, Cancer Res. 81 (2021) 1388–1397, https://doi.org/10.1158/0008-5472.CAN-20-1602.
[69] K. Cong, M. Peng, A.N. Kousholt, W.T.C. Lee, S. Lee, S. Nayak, J. Krais, P. S. VanderVere-Carozza, K.S. Pawelczak, J. Calvo, N.J. Panzarino, J.J. Turchi, N. Johnson, J. Jonkers, E. Rothenberg, S.B. Cantor, Replication gaps are a key determinant of PARP inhibitor synthetic lethality with BRCA deficiency, e7, Mol. Cell. 81 (2021) 3128–3144, https://doi.org/10.1016/j.molcel.2021.06.011.
[70] A. Quinet, S. Tirman, J. Jackson, S. Šviković, D. Lemaçon, D. Carvajal-Maldonado, D. González-Acosta, A.T. Vessoni, E. Cybulla, M. Wood, S. Tavis, L.F.Z. Batista, J. Méndez, J.E. Sale, A. Vindigni, PRIMPOL-mediated adaptive response suppresses

replication fork reversal in BRCA-deficient cells, e9, Mol. Cell. 77 (2020) 461–474, https://doi.org/10.1016/j.molcel.2019.10.008.
[71] S. Tirman, A. Quinet, M. Wood, A. Meroni, E. Cybulla, J. Jackson, S. Pegoraro, A. Simoneau, L. Zou, A. Vindigni, Temporally distinct post-replicative repair mechanisms fill PRIMPOL-dependent ssDNA gaps in human cells, e8, Mol. Cell. 81 (2021) 4026–4040, https://doi.org/10.1016/j.molcel.2021.09.013.
[72] A. Taglialatela, G. Leuzzi, V. Sannino, R. Cuella-Martin, J.W. Huang, F. Wu-Baer, R. Baer, V. Costanzo, A. Ciccia, REV1-Polζ maintains the viability of homologous recombination-deficient cancer cells through mutagenic repair of PRIMPOL-dependent ssDNA gaps, e7, Mol. Cell. 81 (2021) 4008–4025, https://doi.org/10.1016/j.molcel.2021.08.016.
[73] A. Simoneau, R. Xiong, L. Zou, The trans cell cycle effects of PARP inhibitors underlie their selectivity toward BRCA1/2-deficient cells, Genes Dev. 35 (2021) 1271–1289, https://doi.org/10.1101/GAD.348479.121.
[74] O. Belan, M. Sebald, M. Adamowicz, R. Anand, A. Vancevska, J. Neves, V. Grinkevich, G. Hewitt, S. Segura-Bayona, R. Bellelli, H.M.R. Robinson, G. S. Higgins, G.C.M. Smith, S.C. West, D.S. Rueda, S.J. Boulton, POLQ seals post-replicative ssDNA gaps to maintain genome stability in BRCA-deficient cancer cells, Mol. Cell. 82 (2022) 4664–4680.e9, https://doi.org/10.1016/j.molcel.2022.11.008.
[75] A. Schrempf, S. Bernardo, E.A. Arasa Verge, M.A. Ramirez Otero, J. Wilson, D. Kirchhofer, G. Timelthaler, A.M. Ambros, A. Kaya, M. Wieder, G.F. Ecker, G. E. Winter, V. Costanzo, J.I. Loizou, POLθ processes ssDNA gaps and promotes replication fork progression in BRCA1-deficient cells, Cell Rep. 41 (2022), 111716, https://doi.org/10.1016/j.celrep.2022.111716.
[76] Z. Kang, P. Fu, A.L. Alcivar, H. Fu, C. Redon, T.K. Foo, Y. Zuo, C. Ye, R. Baxley, A. Madireddy, R. Buisson, A.K. Bielinsky, L. Zou, Z. Shen, M.I. Aladjem, B. Xia, BRCA2 associates with MCM10 to suppress PRIMPOL-mediated repriming and single-stranded gap formation after DNA damage, Nat. Commun. 12 (2021) 5966, https://doi.org/10.1038/s41467-021-26227-6.
[77] R. Bhowmick, M. Lerdrup, S.A. Gadi, G.G. Rossetti, M.I. Singh, Y. Liu, T. D. Halazonetis, I.D. Hickson, RAD51 protects human cells from transcription-replication conflicts, Mol. Cell. 82 (2022) 3366–3381.e9, https://doi.org/10.1016/j.molcel.2022.07.010.
[78] F.J. Groelly, R.A. Dagg, M. Petropoulos, G.G. Rossetti, B. Prasad, A. Panagopoulos, T. Paulsen, A. Karamichali, S.E. Jones, F. Ochs, V.S. Dionellis, E. Puig Lombardi, M. J. Miossec, H. Lockstone, G. Legube, A.N. Blackford, M. Altmeyer, T. D. Halazonetis, M. Tarsounas, Mitotic DNA synthesis is caused by transcription-replication conflicts in BRCA2-deficient cells, Mol. Cell. 82 (2022) 3382–3397.e7, https://doi.org/10.1016/j.molcel.2022.07.011.
[79] B. Pardo, M. Moriel-Carretero, T. Vicat, A. Aguilera, P. Pasero, Homologous recombination and Mus81 promote replication completion in response to replication fork blockage, EMBO Rep. 21 (2020), e49367, https://doi.org/10.15252/embr.201949367.
[80] F. García Fernández, E. Fabre, The dynamic behavior of chromatin in response to DNA double-strand breaks, Genes 13 (2022) 215, https://doi.org/10.3390/genes13020215.
[81] J. Miné-Hattab, I. Chiolo, Complex chromatin motions for DNA repair, Front. Genet. 11 (2020) 800, https://doi.org/10.3389/fgene.2020.00800.
[82] K. Schirmeisen, S.A.E. Lambert, K. Kramarz, SUMO-based regulation of nuclear positioning to spatially regulate homologous recombination activities at replication stress sites, Genes 12 (2021) 2010, https://doi.org/10.3390/genes12122010.
[83] N. Lamm, S. Rogers, A.J. Cesare, Chromatin mobility and relocation in DNA repair, Trends Cell Biol. 31 (2021) 843–855, https://doi.org/10.1016/j.tcb.2021.06.002.
[84] S. Nagai, K. Dubrana, M. Tsai-Pflugfelder, M.B. Davidson, T.M. Roberts, G. W. Brown, E. Varela, F. Hediger, S.M. Gasser, N.J. Krogan, Functional targeting of DNA damage to a nuclear pore-associated SUMO-dependent ubiquitin ligase, Science 322 (2008) 597–602, https://doi.org/10.1126/science.1162790.
[85] K. Kramarz, K. Schirmeisen, V. Boucherit, A. Ait Saada, C. Lovo, B. Palancade, C. Freudenreich, S.A.E. Lambert, The nuclear pore primes recombination-dependent DNA synthesis at arrested forks by promoting SUMO removal, Nat. Commun. 11 (2020) 5643, https://doi.org/10.1038/s41467-020-19516-z.
[86] P. Aguilera, J. Whalen, C. Minguet, D. Churikov, C. Freudenreich, M.N. Simon, V. Géli, The nuclear pore complex prevents sister chromatid recombination during replicative senescence, Nat. Commun. 11 (2020) 160, https://doi.org/10.1038/s41467-019-13979-5.
[87] X.A. Su, V. Dion, S.M. Gasser, C.H. Freudenreich, Regulation of recombination at yeast nuclear pores controls repair and triplet repeat stability, Genes Dev. 29 (2015) 1006–1017, https://doi.org/10.1101/gad.256404.114.
[88] N. Lamm, M.N. Read, M. Nobis, D. Van Ly, S.G. Page, V.P. Masamsetti, P. Timpson, M. Biro, A.J. Cesare, Nuclear F-actin counteracts nuclear deformation and promotes fork repair during replication stress, Nat. Cell Biol. 22 (2020) 1460–1470, https://doi.org/10.1038/s41556-020-00605-6.
[89] A.M. Pinzaru, M. Kareh, N. Lamm, E. Lazzerini-Denchi, A.J. Cesare, A. Sfeir, Replication stress conferred by POT1 dysfunction promotes telomere relocalization to the nuclear pore, Genes Dev. 34 (2020) 1619–1636, https://doi.org/10.1101/gad.337287.120.
[90] D. Churikov, F. Charifi, N. Eckert-Boulet, S. Silva, M.N. Simon, M. Lisby, V. Géli, SUMO-dependent relocalization of eroded telomeres to nuclear pore complexes controls telomere recombination, Cell Rep. 15 (2016) 1242–1253, https://doi.org/10.1016/j.celrep.2016.04.008.
[91] M.N. Simon, D. Churikov, V. Géli, Replication stress as a source of telomere recombination during replicative senescence in Saccharomyces cerevisiae, FEMS Yeast Res 16 (2016) fow085, https://doi.org/10.1093/femsyr/fow085.
[92] R.E. Brown, C.H. Freudenreich, Structure-forming repeats and their impact on genome stability, Curr. Opin. Genet. Dev. 67 (2021) 41–51, https://doi.org/10.1016/j.gde.2020.10.006.
[93] J.M. Whalen, N. Dhingra, L. Wei, X. Zhao, C.H. Freudenreich, Relocation of collapsed forks to the nuclear pore complex depends on sumoylation of DNA repair proteins and permits Rad51 association, Cell Rep. 31 (2020), 107635, https://doi.org/10.1016/j.celrep.2020.107635.
[94] J.L. Hopkins, L. Lan, L. Zou, DNA repair defects in cancer and therapeutic opportunities, Genes Dev. 34 (2022) 278–293, https://doi.org/10.1101/gad.349431.122.
[95] L. PX, Z. M, J. M, , BRCA2 promotes genomic integrity and therapy resistance primarily through its role in homology-directed repair, BioRxiv Prepr. Serv. Biol. 2023 (2023), 04.11.536470. doi: 10.1101/2023.04.11.536470. https://doi.org/10.1101/2023.04.11.536470.
[96] M. Deshpande, T. Paniza, N. Jalloul, G. Nanjangud, J. Twarowski, A. Koren, N. Zaninovic, Q. Zhan, K. Chadalavada, A. Malkova, H. Khiabanian, A. Madireddy, Z. Rosenwaks, J. Gerhardt, Error-prone repair of stalled replication forks drives mutagenesis and loss of heterozygosity in haploinsufficient BRCA1 cells, Mol. Cell. 82 (2022) 3781–3793.e7, https://doi.org/10.1016/j.molcel.2022.08.017.
[97] R. Ceccaldi, J.C. Liu, R. Amunugama, I. Hajdu, B. Primack, M.I.R. Petalcorin, K. W. O'Connor, P.A. Konstantinopoulos, S.J. Elledge, S.J. Boulton, T. Yusufzai, A. D. D'Andrea, Homologous-recombination-deficient tumours are dependent on Polθ-mediated repair, Nature 518 (2015) 258–262, https://doi.org/10.1038/nature14184.
[98] G. Matos-Rodrigues, J. Guirouilh-Barbat, E. Martini, B.S. Lopez, Homologous recombination, cancer and the "RAD51 paradox,", NAR Cancer 3 (2021) zcab016, https://doi.org/10.1093/narcan/zcab016.

Molecular Cell

Article

RNA:DNA hybrids from Okazaki fragments contribute to establish the Ku-mediated barrier to replication-fork degradation

Graphical abstract

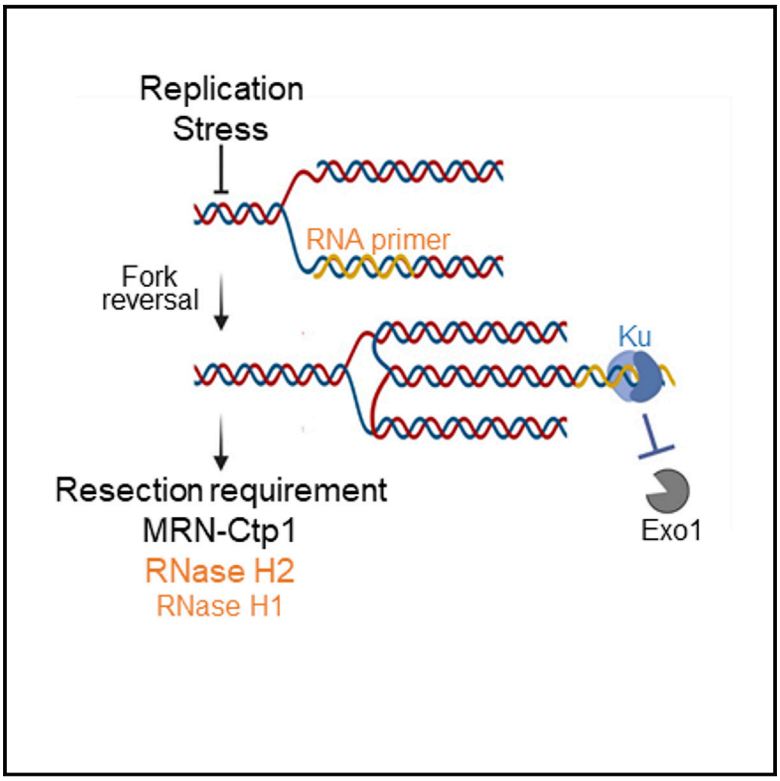

Authors

Charlotte Audoynaud,
Kamila Schirmeisen,
Anissia Ait Saada, ..., Karine Fréon,
Jean-Baptiste Charbonnier,
Sarah A.E. Lambert

Correspondence

sarah.lambert@curie.fr

In brief

Audoynaud et al. find that the RNA primer from Okazaki fragments safeguards the integrity of arrested replication fork by generating an RNA:DNA hybrid that establishes the Ku barrier, making RNaseH2 necessary to engage fork degradation. RNaseH2 and MRN-Ctp1 cooperate to promote cell resistance to replication stress in a Ku-dependent manner.

Highlights

- Unprocessed RNA:DNA hybrids impair nascent strand degradation
- RNase H2 overcomes the Ku barrier to Exo1 by processing RNA:DNA hybrids
- The RNA primer from Okazaki fragments contributes to establish the Ku barrier
- Ku binds RNA:DNA hybrids *in vitro* and *in vivo* upon replication stress

Audoynaud et al., 2023, Molecular Cell *83*, 1061–1074
April 6, 2023
https://doi.org/10.1016/j.molcel.2023.02.008

CellPress

Molecular Cell

CellPress

Article

RNA:DNA hybrids from Okazaki fragments contribute to establish the Ku-mediated barrier to replication-fork degradation

Charlotte Audoynaud,[1,2,4,5] Kamila Schirmeisen,[1,2,4,5] Anissia Ait Saada,[1,2,4,6] Armelle Gesnik,[3,6] Paloma Fernández-Varela,[3,6] Virginie Boucherit,[1,2,4] Virginie Ropars,[3] Anusha Chaudhuri,[1,2,4] Karine Fréon,[1,2,4] Jean-Baptiste Charbonnier,[3] and Sarah A.E. Lambert[1,2,4,7,*]

[1]Institut Curie, Université PSL, CNRS UMR3348, 91400 Orsay, France
[2]Université Paris-Saclay, CNRS UMR3348, 91400 Orsay, France
[3]Université Paris-Saclay, CEA, CNRS, Institute for Integrative Biology of the Cell (I2BC), 91198 Gif-sur-Yvette, France
[4]Ligue Nationale Contre le cancer (équipe labélisée), Orsay, France
[5]These authors contributed equally
[6]These authors contributed equally
[7]Lead contact
*Correspondence: sarah.lambert@curie.fr
https://doi.org/10.1016/j.molcel.2023.02.008

SUMMARY

Nonhomologous end-joining (NHEJ) factors act in replication-fork protection, restart, and repair. Here, we identified a mechanism related to RNA:DNA hybrids to establish the NHEJ factor Ku-mediated barrier to nascent strand degradation in fission yeast. RNase H activities promote nascent strand degradation and replication restart, with a prominent role of RNase H2 in processing RNA:DNA hybrids to overcome the Ku barrier to nascent strand degradation. RNase H2 cooperates with the MRN-Ctp1 axis to sustain cell resistance to replication stress in a Ku-dependent manner. Mechanistically, the need of RNaseH2 in nascent strand degradation requires the primase activity that allows establishing the Ku barrier to Exo1, whereas impairing Okazaki fragment maturation reinforces the Ku barrier. Finally, replication stress induces Ku foci in a primase-dependent manner and favors Ku binding to RNA:DNA hybrids. We propose a function for the RNA:DNA hybrid originating from Okazaki fragments in controlling the Ku barrier specifying nuclease requirement to engage fork resection.

INTRODUCTION

A myriad of unavoidable replication-fork obstacles threaten faithful DNA duplication.[1] As fork obstacles lead to stalling, collapse, or fork breakage, they are direct sources of replication stress-induced genome instability, an underlying cause of human diseases and a well-recognized hallmark of most cancer cells.[2] Therefore, investigating the molecular circuits preserving genome integrity and replication competence at stressed replication fork is critical to the understanding of the etiology of human diseases.

Elongating transcription machineries are one type of fork obstacle causing fork arrest. Head-on collision upon transcription-replication conflict (TRC) triggers unscheduled R-loop formation, i.e., a triple-stranded structure composed of a co-transcriptionally formed RNA:DNA hybrid opposite to a displaced single-stranded DNA (ssDNA).[3,4] Head-on TRC activates an ATR-dependent DNA-damage-response (DDR) pathway, and R-loops formed at TRCs are detrimental to genome stability maintenance,[5] although it remains unclear how the RNA:DNA hybrid itself and/or the stalled RNA polymerase contribute to fork stalling.[6] Nonetheless, several studies have established that a subset of R-loop is genotoxic.[7,8]

RNA:DNA hybrids are also a consequence of double-strand break (DSB) repair.[9,10] Whereas the ways they originate at DSBs are still under debate, they are proposed to act as mediators of DSB repair and signaling.[11,12] RNA:DNA hybrids modulate the activity of DNA repair machineries allowing the recruitment of DNA repair factors from the homologous recombination (HR) and NHEJ pathways.[13–19] RNA:DNA hybrids have been also proposed to mediate RNA-templated DNA repair and to influence the fidelity of DSB repair by NHEJ.[20,21] However, it is also evident that RNA:DNA hybrids at DSBs are removed or degraded to allow the completion of DNA repair, requiring therefore the activity of RNA helicases such as senataxin or RNase H activities.[10,13,16,18,22,23]

Protection, restart, and repair of stressed replication forks is critical to genomic stability, giving rise to the identification of a diversity of fork-rescue pathways, underscoring the plasticity of the replication fork.[24] Error-free repair of replication-born DNA

damage usually relies on the HR pathway to protect nascent strands from hyperdegradation and to resume DNA replication.[25] Recent works support that NHEJ is active during DNA replication to repair stressed forks and to safeguard fork integrity.[15] In both yeast and mammals, several NHEJ-related factors, such as Ku, XLF, RIF1, and 53BP1, are engaged at stalled or broken forks to act as antiresection barriers, independently of their canonical function in NHEJ.[26–33] Moreover, Ku binding at reversed or broken fork precedes HR activity, ensuring coordinated nascent strand degradation or Rad51 loading.[27,34] However, erroneous NHEJ events at halted forks trigger chromosomal rearrangement, and therefore NHEJ-mediated fork processing is tightly regulated by mechanisms that remain poorly understood.[35,36]

Many RNA species are physiologically associated with DNA replication.[21] Ribonucleotides are frequently incorporated by replicative DNA polymerases generating thousands of DNA-embedded RNA species that are further removed by RNase H2.[37,38] During Okazaki fragment (OF) synthesis on the lagging strand, the primase synthetizes a RNA primer of 8–12 ribonucleotides in size, which is successively elongated by Pol α and δ.[38,39] OF is therefore a potential source of RNA:DNA hybrids inherently associated with the DNA replication process. Whether such physiological RNA:DNA hybrids could be modulators of replication-fork repair, as proposed for DSB repair, is currently unknown. In addition, RNAs are well-described *cis*- and *trans*-modulators of NHEJ activity (reviewed by Audoynaud et al.[15]), but the role of RNA-associated DNA replication in regulating NHEJ function at replication stress sites has not been explored yet.

Here, we address the function of RNA:DNA hybrids during fork repair by taking advantage of a transcription-independent replication-fork barrier (RFB).[40] We employed the previously described *RTS1*-RFB that allows the polar block of a single replisome by a DNA-bound protein complex. Forks arrested at the *RTS1*-RFB are restarted in 15–20 min by an HR-dependent but DSB-independent mechanism, called recombination-dependent replication (RDR).[41–43] Nascent strand degradation by nucleases allows ssDNA gaps to form and to recruit HR factors to promote replication restart.[44] The restarted fork is associated to a noncanonical DNA synthesis insensitive to the RFB.[45–47] We found that unprocessed RNA:DNA hybrids at the RFB prevent the degradation of nascent strand and replication restart. Nascent strand degradation relies on the catalytic activity of RNase H2 to overcome the NHEJ factor Ku-mediated barrier. We propose that the unprocessed primer of the last synthetized OF is embedded in the reversed fork, triggering an RNA:DNA hybrid formation to which Ku can bind, revealing that the RNA:DNA hybrid from OF plays a regulatory function in safeguarding fork integrity.

RESULTS

Unresolved RNA:DNA hybrids at arrested forks impair nascent strand degradation

RNA:DNA hybrids have been shown to accumulate both upstream and downstream of the *RTS1*-RFB during S phase.[47] To investigate the dynamics of those RNA:DNA hybrids, we performed real-time microscopy. We asked how frequently the catalytically dead form of RNase H1 fused to GFP (Rnh1-D129N-GFP)—which is used to detect RNA:DNA hybrids[48]—co-localizes with the *LacO*-marked RFB of which nuclear positioning is visualized by mCherry-LacI foci (Figure S1A). Even though *LacO*-arrays led to background co-localization events regardless of the activity of the RFB, RNA:DNA hybrids significantly accumulated in S-phase cells upon activation of the RFB (in 48% of cells in RFB ON versus 30% in RFB OFF, $p < 0.005$) compared with control conditions (Figures S1B–S1C). Most of the co-localization events lasted for less than 40 s, suggesting a short lifetime and fast processing of RNA:DNA hybrids (Figure S1D). We thus questioned the origin of those RFB-induced RNA:DNA hybrids and their potential influence on fork repair.

As reported,[10,49] the lack of RNase H1 and H2 activities resulted in cell sensitivity to replication blocking agents and accumulation of RNA:DNA hybrids (Figures 1A, S2A, and S2B). Thus, we investigated the role of RNase H1 and H2 in promoting replication resumption at the RFB. The absence of RNase H1 and H2 led to a ~2-fold reduction in the frequency of replication slippage occurring downstream the RFB—a mutational signature left by HR-mediated restarted forks[45,46]—indicating a reduced RDR efficiency (Figures 1B and 1C). By analyzing the replication intermediates (RIs) by bidimensional gel electrophoresis (2DGE), the formation of large ssDNA gaps (>100 bp) at the RFB resulted into a specific "tail" DNA structure, emanating from arrested fork signal and descending toward the linear arc (Figures 1D and S2C, red arrow).[27,50] The absence of RNase H1 and H2 led to the disappearance of the tail signal (Figures 1D, 1E, S2D, and S2E). The profile of RPA binding downstream of the RFB revealed no RPA loading in the absence of RNase H1 and H2 (Figure 1F). This lack of ssDNA gap can be caused either by the need to process RNA:DNA hybrids to engage nascent strand degradation or by an accumulation of *de novo*, possibly transcriptionally induced, RNA:DNA hybrids, in a postresection manner, which would compete with RPA loading, as previously proposed[10,51,52] (Figure 1G). To distinguish between these two hypotheses, purified RIs were treated with RNase H1 *in vitro* before resolution by 2DGE. We reasoned that if ssDNA gaps are masked by *de novo* RNA:DNA hybrids *in vivo*, their processing *in vitro* should restore the tail signal (Figure 1G, right panel). In contrast, if RNA:DNA hybrids need to be processed *in vivo* to engage nascent strand resection, the tail signal should not be restored (Figure 1G, left panel). Most RNA:DNA hybrids co-eluted with the ssDNA-enriched fraction and were fully eliminated upon RNase H1 treatment (Figure 1H), without affecting the intensity of the tail signal in wild-type (WT) and *rnh1Δ rnh201Δ* cells (Figures 1D and 1E), supporting the hypothesis that unprocessed RNA:DNA hybrids at arrested fork impair nascent strand degradation *in vivo*.

The short-range resection of nascent strand requires RNA:DNA hybrids processing by RNaseH2

We then analyzed each single RNase H mutant and found that fork resection was 2-times decreased in *rnh201Δ* cells compared with WT, whereas no defect was observed in *rnh1Δ* or in the catalytic dead mutant *rnh1-D129N* cells (Figures 2A and 2B). The profile of RPA binding downstream of the RFB revealed that RPA loading was severely compromised only in

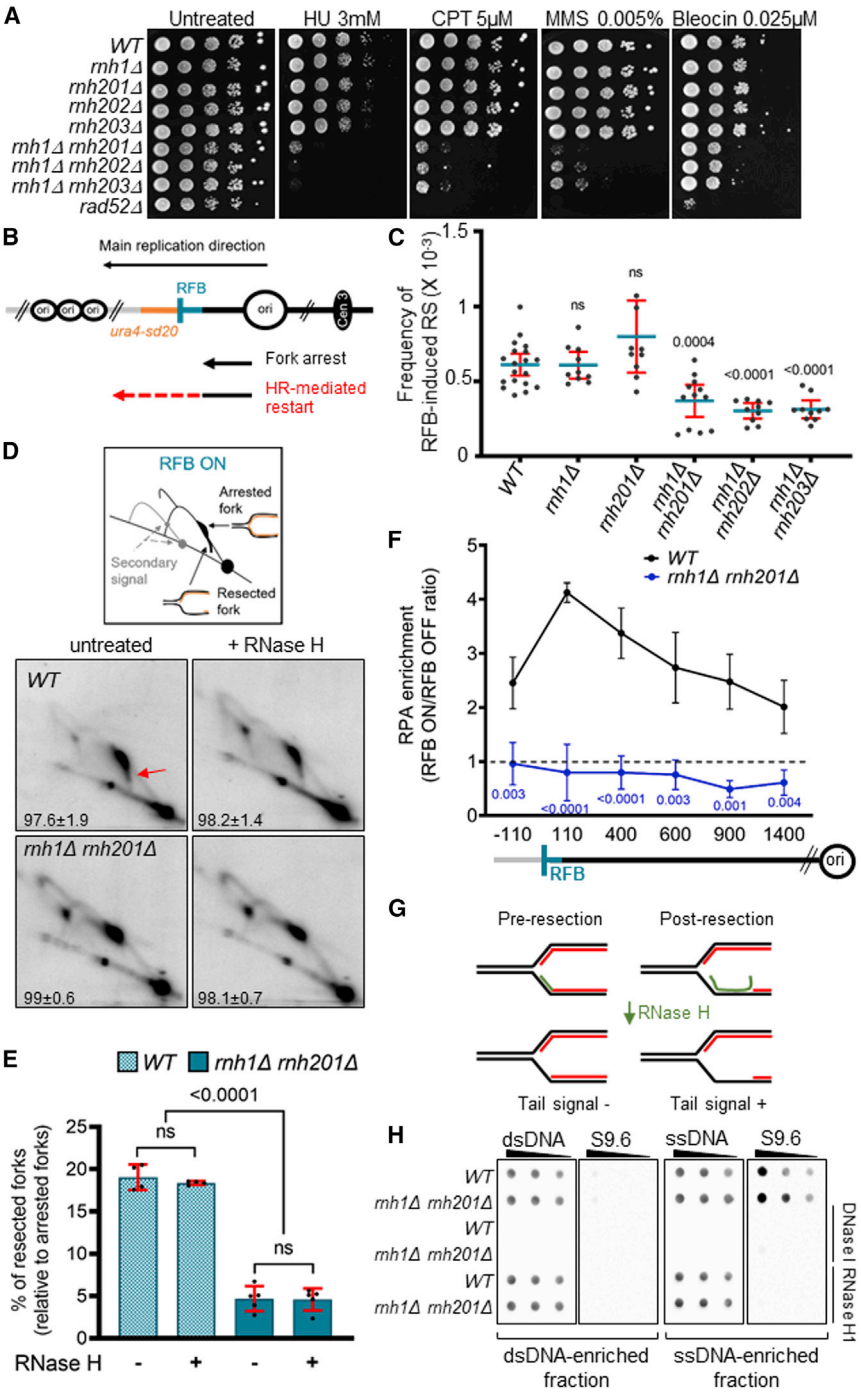

Figure 1. RNaseH activities promote nascent strand degradation and recombination-dependent replication

(A) 10-fold serial dilutions of indicated strains on indicated media conditions (CPT: camptothecin, HU: hydroxyurea, MMS: methyl methane sulfonate).

(B) Diagram of the *t-ura4sd20<ori* construct containing a single *RTS1*-RFB (<, blue bars) that leads to the polar arrest of replisomes traveling from the centromere (Cen3) toward the telomere (t). "Ori" (black circles) indicate the main replication origins upstream and downstream of the RFB. Polar fork arrest is mediated by the binding of Rtf1 to the *RTS1* sequence. Rtf1 expression in under the thiamine-repressible *nmt41* promoter: with thiamine, Rtf1 is repressed and the RFB is poorly active (RFB OFF); without thiamine, Rtf1 is expressed and the RFB is strongly active (RFB ON) (REF). The non-functional *ura4-sd20* allele contains a 20 nt duplication flanked by micro-homology. HR-mediated restart is associated to a non-canonical DNA synthesis prone to frequent replication slippage (RS) leading to the deletion of the duplication, thus restoring a functional *ura4*$^{+}$ marker.[45]

(C) Frequency of RFB-induced RS in indicated strains and conditions. Each dot represents one sample from independent biological replicate. Bars indicate mean values ± 95% confidence interval. Statistics were calculated using Mann-Whitney U test, compare to *WT*.

(D) RIs analysis by neutral-neutral 2DGE. Top: scheme of RIs observed within the *AseI* restriction fragment in RFB ON condition using *ura4* as probe. Gray lines indicate secondary signal caused by partial digestion of psoralencross-linked RIs. Bottom: representative 2DGE analysis in indicated strains in RFB ON condition, with RIs treated or not with RNase H *in vitro*. The red arrow indicates the "tail" signal in WT strain. Numbers indicate the efficiency of the RFB ± standard deviation (SD).

(E) Tail quantification from (C). Dots represent values obtained from independent biological replicates. Bars indicate mean values ± SD. Statistical analysis was performed using Student's t test.

(F) Analysis of RPA recruitment (ON/OFF ratio) to the *RTS1*-RFB by ChIP-qPCR in indicated strains. Distances from the RFB are indicated in base pairs (bp). Values are means of at least three independent experiments ± SD. Statistical analysis was performed using Student's t test, compared with WT.

(G) Scheme of hypothetic models explaining how an RNA:DNA hybrid may interfere with ssDNA gaps in a pre or postresection manner. The green lines indicate an RNA:DNA hybrid.

(H) Separation of digested and psoralen cross-linked DNA samples on BND-cellulose columns resulted in dsDNA and a ssDNA-enriched fractions which were treated *in vitro* with RNase H1 or DNase I and analyzed by dot blot using anti-dsDNA (dsDNA), anti-ssDNA (ssDNA), and S9.6 antibodies.

See also Figures S1 and S2 and Tables S1 and S2.

rnh201Δ cells (Figure 2C), further supporting that, among the two RNase H activities, RNase H2 is mainly responsible for the degradation of nascent strand while RNase H1 may act as a backup activity. Furthermore, RNase H2 was also involved in the hyperresection of arrested forks observed in the absence of Rad3^{ATR} (Figures 2D and 2E).[44] RNase H2 is involved in the processing of RNA:DNA hybrids and promotes ribonucleotide excision repair (RER).[53] The Rnh201-G72S, an analogous Aicardi-Goutières patient mutation, is a nearly catalytically dead form of RNase H2,[54–56] which maintains sufficient activity

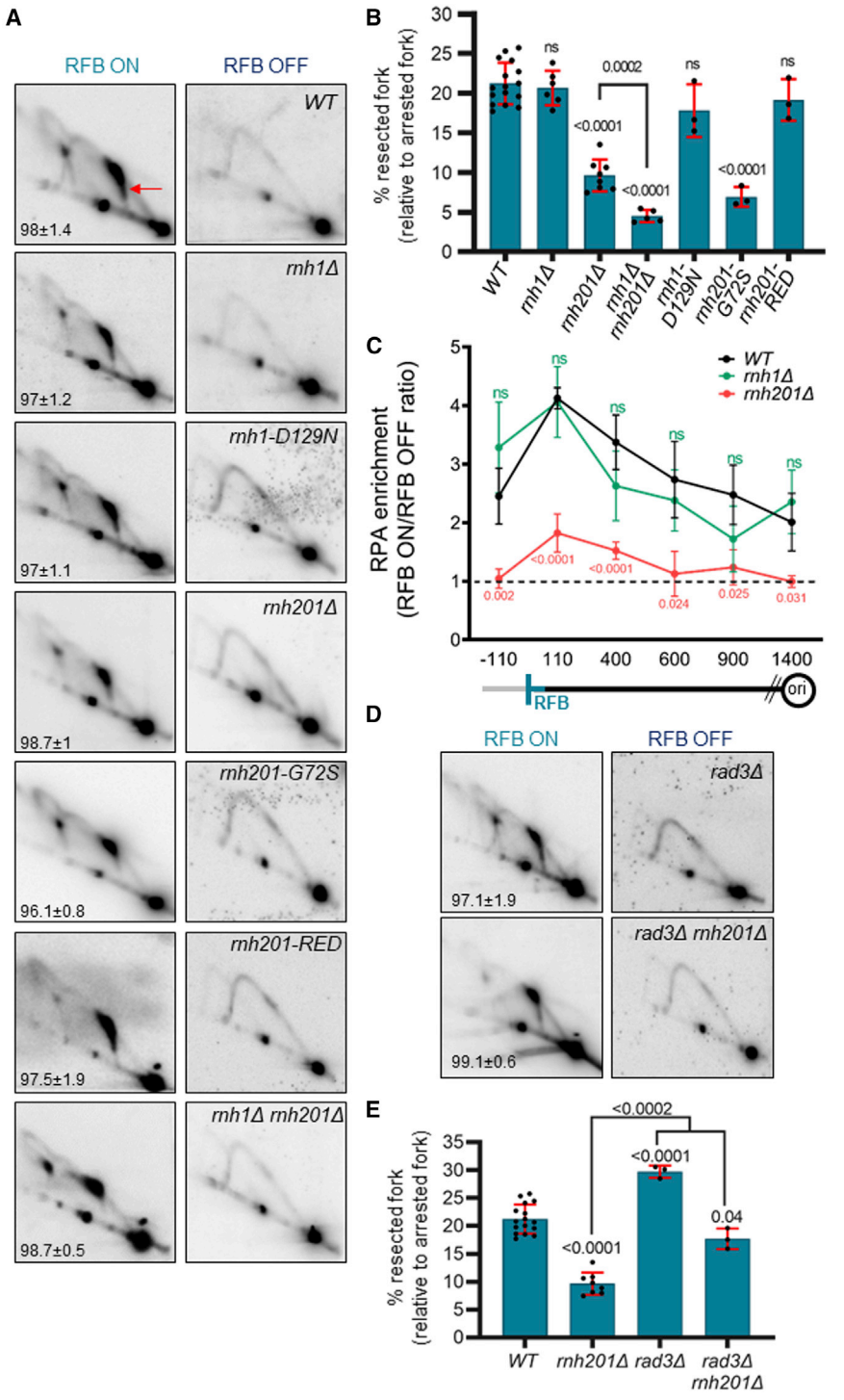

Figure 2. RNase H2-mediated processing of RNA:DNA hybrids engages nascent strand degradation

(A and D) Representative 2DGE analysis in indicated strains and conditions as described in Figure 1D.

(B and E) Tail quantification from (C). Dots represent values obtained from independent biological replicates. Bars indicate mean values ± SD. Statistical analysis was performed using Student's t test.

(C) Analysis of RPA recruitment (ON/OFF ratio) to the *RTS1*-RFB by ChIP-qPCR in indicated strains. Distances from the RFB are indicated in base pairs (bp). Values are means of at least three independent experiments ± SD. Statistical analysis was performed using Student's t test, compared with WT.

See also Figure S2 and Tables S1 and S2.

to prevent global RNA:DNA hybrid accumulation and resistance to replication stress when combined with *rnh1* deletion (Figures S2A and S2B) but was defective enough to exhibit defects in nascent strand degradation at the RFB (Figures 2A and 2B). In contrast, the Rnh201-RED mutant, which is specifically defective for the excision of mono- and diribonucleotides,[56] showed neither accumulation of RNA:DNA hybrids nor defective nascent strand degradation (Figures 2A, 2B, and S2B). Of note, *rnh201-RED* conferred a slight sensitivity to hydroxyurea when combined with *rnh1* deletion (Figure S2A), consistent with a higher incorporation of ribonucleotides during replication under dNTP pool starvation and cell survival relying on the RER pathway.[57,58] We concluded that the ability of RNase H2 to process RNA:DNA hybrids promotes physiological and pathological nascent strand degradation.

RNase H2 counteracts the Ku-mediated barrier to nascent strand degradation by Exo1

In fission yeast and human cells, the degradation of nascent strand is a two-step process with a short-range resection mediated by the Mre11-Rad50-Nbs1 (MRN)-Ctp1 axis generating ~110-bp-sized gaps that are obligatory for subsequent Exo1-mediated long-range resection up to ~1 kb.[27,59,60] The profile of RPA binding downstream of the RFB indicated that RNase H2 was required for both short- and long-range resection, similarly to the MRN-Ctp1 axis (Figure 2C). We therefore investigated the interplays between RNase H2 and the MRN-Ctp1 axis. We found that the defects in fork resection and in the frequency of RFB-induced replication slippage in *rad50Δ rnh201Δ* cells were similar to the ones observed in *rad50Δ* cells, indicating that RNaseH2 cooperates with MRN to promote nascent strand degradation and replication restart (Figures S3A–S3C). Moreover, genetic analysis revealed that defect in both RNase H2 and Rad50, or Ctp1, led to synthetic lethality upon treatment with replication-blocking agents

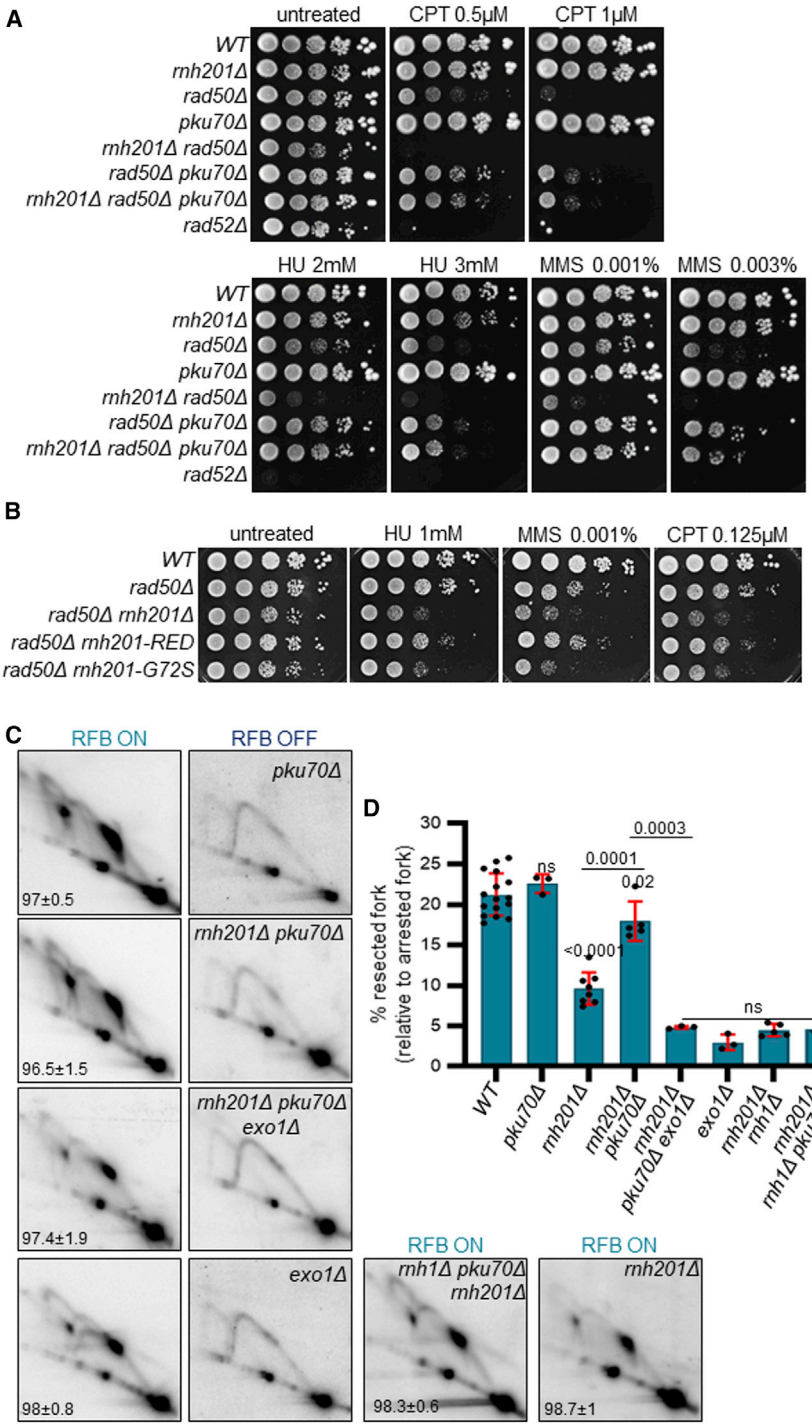

Figure 3. RNase H2 cooperates with MRN to overcome Ku-mediated barrier to resection

(A and B) 10-fold serial dilutions of indicated strains on indicated media conditions, respectively. CPT, camptothecin; HU, hydroxyurea; MMS, methyl methane sulfonate).

(C) Representative 2DGE analysis in indicated strains and conditions as described in Figure 1D.

(D) Tail quantification from (C). Dots represent values obtained from independent biological replicates. Bars indicate mean values ± SD. Statistical analysis was performed using Student's t test.

See also Figures S3 and S4 and Table S1.

(Figures 3A and S3D). This synthetic lethality was dependent on the catalytic activity of RNase H2 but partly alleviated when RNase H2 retains its ability to process RNA:DNA hybrids (Figure 3B). We and others have shown that Ku restricts Exo1 activity at replication forks and that MRN-Ctp1 overcomes the Ku-mediated barrier to engage the long-range resection.[27,60] Interestingly, the synthetic lethality observed between MRN-Ctp1 axis and RNase H2 in response to replication stress was fully dependent on Ku (Figures 3A and S3D), revealing that the ability of RNase H2 to process RNA:DNA hybrids cooperates with the MRN-Ctp1 axis to overcome Ku function during replication stress. To gauge this function, we asked if RNase H2 counteracts the Ku-mediated barrier to nascent strand degradation. The analysis of the tail signal revealed that in the absence of Ku, nascent strand degradation is independent of RNase H2 while remaining Exo1 dependent (Figures 3C and 3D), similarly to MRN-Ctp1 axis defect,[27] indicating that RNase H2 processes an RNA:DNA hybrid that contributes to establish the Ku-mediated barrier to Exo1 resection. Surprisingly, we observed that the deletion of *pku70* did not rescue the fork-resection defect observed in the absence of both RNase H activities, in contrast to the rescue phenotype observed in the single *rnh201* null mutant (Figures 3C and 3D). These data suggest that distinct RNA:DNA hybrids form at the RFB and are processed differently by RNase H1 and H2, the latter having a specific function in regulating Ku function at arrested forks.

The nuclease activity of MRN is dispensable to overcome the Ku-mediated barrier to nascent strand degradation at the RFB,[27] raising the possibility that RNase H2 may compensate for this. Nonetheless, no synthetic lethality was observed when combining *rnh201* deletion with a nuclease-dead allele of *mre11* (*mre11-D65N*), nor was a more drastic defect in nascent strand degradation at the RFB (Figures S3B and S3C). Furthermore, the MRN-Ctp1 axis was proposed to release Ku from replication-born DNA damage.[27,60] Consistent with this, Pku80-GFP foci accumulated in *rad50Δ* cells upon 4 h of CPT treatment but such accumulation did not occur in *rnh201Δ* cells and was not exacerbated in the double mutant (Figures S4A and S4B).[61] Since topoisomerase I inhibition by CPT can result in

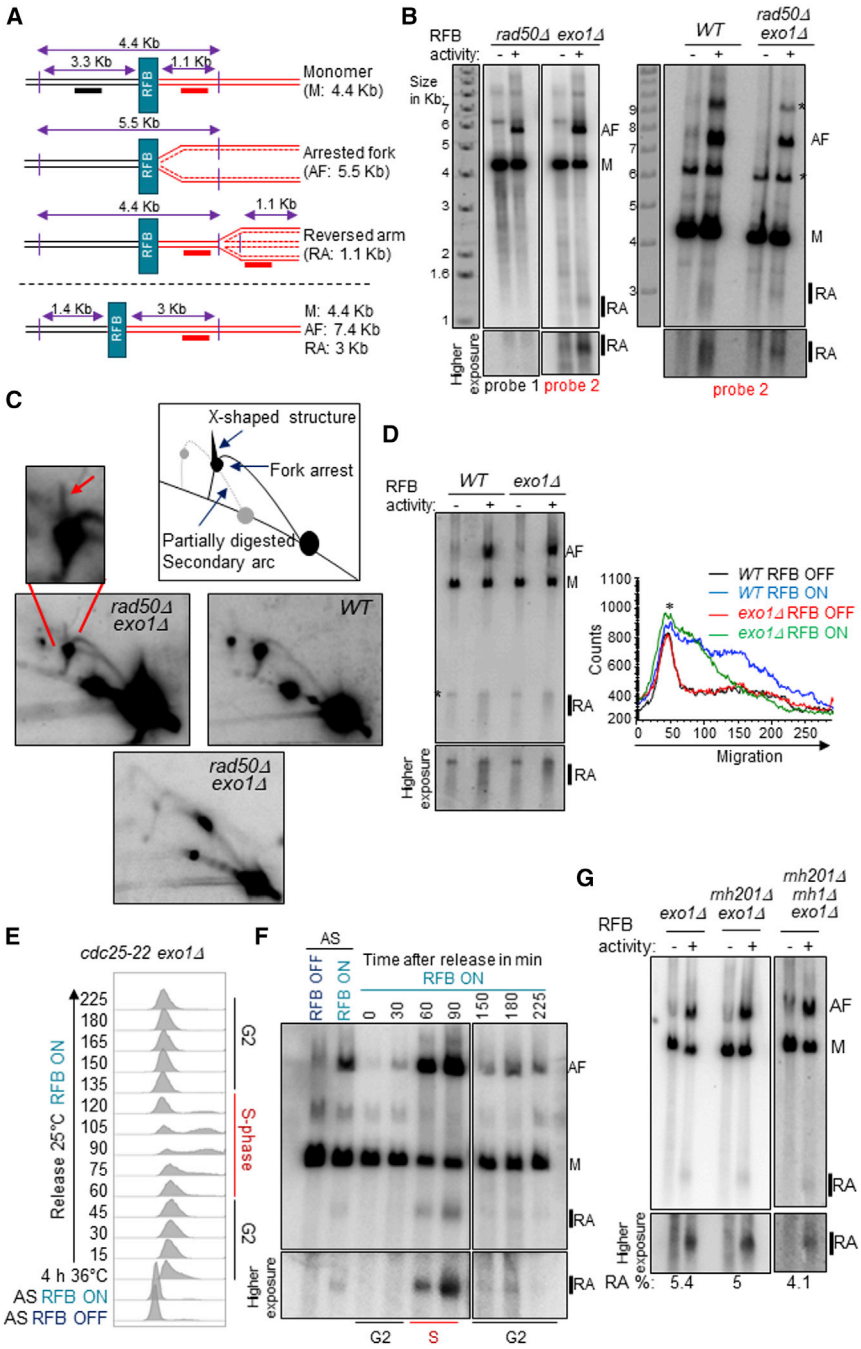

Figure 4. Fork reversal at the RFB is not impaired by unresolved RNA:DNA hybrids

(A) Scheme of the constructs used with the expected mass of RIs species and the probes used (probe 1 and 2 in black and red, respectively).

(B) Representative southern-blot analysis after 1DGE resolution of RIs in indicated strains and conditions, using indicated probes. A higher exposure of the RA is shown. *, partial digestion caused by psoralen cross-links. 1.1 kb-RA and 3 kb-RA constructs, as described in (A), on left and right, respectively.

(C) Top: scheme of RIs observed within the *AseI* restriction fragment in RFB ON condition using the probe 2 (red) and the 3kb-RA construct described in (A). Gray lines indicate secondary signal caused by partial digestion of psoralen cross-linked RIs. Middle: representative 2DGE analysis in indicated strains in RFB ON condition. The red arrow indicates signal corresponding to fork reversal. Bottom panel: 2DGE analysis in RFB ON condition using the probe 2 (red) and the 1-kb-RA construct described in (A).

(D) Left: representative southern-blot analysis after 1DGE resolution of RIs in indicated strains and conditions, using the probe 2 (red) and the 1.1-kb-RA construct described in (A). Right: corresponding scan lines of RA intensity according to migration distance for each strain and condition. *, The unspecific was used as reference.

(E) Flow cytometry analysis of *cdc25-22 exo1Δ* cells synchronized in G2 (4 h at 36°C) and released in cell cycle at 25°C in RFB ON condition. Time points are indicated in minutes. AS, asynchronous cells.

(F) Southern-blot analysis after 1DGE resolution of RIs from cell synchronization described in (E), using the probe 2 (red) and the 3 Kb-RA construct described in (A).

(G) Representative southern-blot analysis after 1DGE resolution of RIs in indicated strains and conditions using the probe 2 (red) and the 1.1-kb-RA construct described in (A). Numbers indicate the estimation of % RA relative to arrested fork (AF) signal.

See also Figure S5 and Table S1.

single-ended DSB, we analyzed Pku80-GFP localization to the *LacO*-marked RFB and obtained similar data (Figure S4C and S4D). Although these data may reflect a role for MRN—in addition to promoting Ku eviction from stressed forks—in limiting Ku accumulation, this function is not shared by RNase H2. We suggest that RNase H2 and MRN-Ctp1 cooperate to overcome the Ku-mediated barrier to Exo1 by providing distinct activity: RNaseH2 processes an RNA:DNA hybrid at arrested forks to offer an entry point for Exo1 activity, while limiting or evicting Ku relies on MRN-Ctp1.

Lack of RNase H activities does not impair fork reversal at the RFB

In human cells, a reversed fork is an entry point for nuclease activities to promote nascent strand degradation[24,59,62] and provides a double-stranded DNA end for Ku binding as recently shown by Moldovan's lab.[60] An unresolved RNA:DNA hybrid at arrested forks may prevent fork reversal and thus nascent strand degradation. To explore this, we investigated the formation of reversed fork at the RFB. We exploited that, following restriction digestion, reversed fork would release a linear DNA fragment specific to the regressed arm, whose length corresponds to the distance between the site of fork arrest and the first restriction site upstream of the RFB (Figure 4A).[63] First, we employed a construct and a restriction digest for which the expected size

of the reversed arm is of 1.1 kb in a *rad50Δ exo1Δ* background to avoid its degradation. After RIs enrichment and resolution by 1DGE, we detected signals corresponding to the monomer (M), the arrested fork (AF), and a linear fragment of ~1.1 kb (RA) (Figure 4B, left panel). This last signal was restricted to the RFB ON condition and detected exclusively when using a probe specific to the reversed arm (compare red and black probes), consistent with fork reversal occurring at the active RFB. Similar results were obtained with a construct for which the expected size of the reversed arm is of 3 kb. Consistent with this linear fragment corresponding to the reversed arm, it migrated as a smear in WT cells in which nascent strand degradation occurs (Figure 4B, right panel). The reversed fork is an X-shaped DNA structure detectable by 2DGE as a diagonal spike emanating from the arrested fork signal.[63] Such a conical signal has been reported at the fork-pausing site *MPS1* in *Schizosaccharomyces pombe* and upon global replication stress in *Physarum polycephalum*.[64,65] To date, such a signal was undetectable in our 2DGE blots when using a restriction enzyme cutting 1.1 kb away from the RFB even when fork resection is abolished in *rad50Δ exo1Δ* cells (Figure 4C, bottom panel). One explanation is that the reversed arm is cut by the restriction enzyme, leading to the loss of the X-shaped structure. To test this, we performed 2DGE using a restriction enzyme cutting 3 kb upstream the RFB and observed an X-shaped structure emanating from the fork-arrest signal in *rad50Δ exo1Δ* cells but not in WT cells (Figure 4C, top panels). These data indicate that the detection of reversed fork by 2DGE is sensitive to the position of the restriction site relative to the fork-arrest site and requires a reversed arm not being resected, consistent with fork reversal undergoing nascent strand degradation.

Breakage of the arrested fork would similarly result in the detection of the observed linear fragment. To exclude this possibility, we analyzed the dynamics of the linear fragment during cell cycle. Because of difficulties in getting well-synchronized population in a *rad50Δ exo1Δ* cells, we shifted to the single *exo1Δ* mutant in which the reversed arm, while moderately resected, was detectable by 1DGE (Figure 4D). The reversed arm appeared and disappeared concomitantly to the AF signal during S phase progression and was not persistent in G2 cells, indicating similar kinetics resolution (Figure 4E and 4F). While the repair of a broken arm would rely on the HR pathway, the intensity of the linear fragment in *rad51Δ* or *rad52Δ* cells was not significantly different from WT cells (Figures S5B and S5C). We also excluded the hypothesis that the linear fragment resulted from Mus81-dependent fork cleavage (Figure S5).[66,67] Although we cannot formally rule out that the linear fragment signal results in part from fork breakage, our data converge on most of this signal exhibiting the hallmarks of a reversed arm, consistent with arrested forks undergoing fork reversal at the RFB. Of note, despite initial studies reporting that checkpoint kinases prevent fork reversal in response to HU treatment in yeast, reversed fork was observed in checkpoint proficient yeast cells upon CPT treatment.[68–70] However, we found no variation in the intensity of the reversed arm in the absence of $Rad3^{Mec1/ATR}$ (Figures S5D and S5E).

The lack of RNase H2 or both RNase H activities did not impact the intensity of the reversed arm (Figure 4G), revealing that fork reversal was not impaired by an unresolved RNA:DNA hybrid at the RFB and placing RNase H2 function downstream of fork remodeling to overcome the Ku-mediated barrier to nascent strand degradation.

The RNA primer from Okazaki fragments is an RNase H2 substrate at arrested forks

To address the origin of the RNA:DNA hybrid at arrested forks, making RNase H2 necessary to engage nascent strand degradation, we focused on Okazaki fragment (OF) metabolism as recurrent synthesis of RNA primer on the lagging strand is a source of RNA:DNA hybrids coupled to DNA replication.[38] We made use of two temperature sensitive alleles of *spp1* that encode the primase catalytic subunit: *spp1-4* (D275G, L429P) and *spp1-21* (D74E, V180G) (Figure 5A). These mutations are consistent with a global destabilization of the Spp1 protein in a temperature-dependent manner, leading to an unstable Polα-primase complex even at 25°C, affecting the synthesis of RNA primers.[71] Compared with WT, both primase mutants led to an hyperresection of nascent strand that was no longer dependent on RNase H2, at both 25°C and 32°C (Figures 5B, 5C, S5A, and S5B). This rescue phenotype cannot be explained by a cell-growth defect or cell-cycle distribution, which were similar between the strains at 25°C and 32°C (Figures 5A and S6C). Hence, compromising RNA primer synthesis of OF bypasses the RNase H2 requirement, supporting the idea that OF synthesis generates an RNA:DNA hybrid processed by RNase H2 to engage Exo1 resection. Moreover, the RNA primer from OF appears critical to limit nascent strand degradation, raising the possibility that the Ku-mediated barrier to Exo1 is not fully established when the RNA primer synthesis is compromised. In support of this, CPT-induced Pku80-GFP foci were reduced by nearly 2 times in *spp1-4* and *spp1-21* cells, compared with WT (Figures 5D and 5E). We concluded that the RNA primer from OF synthesis generates an RNA:DNA hybrid that contributes to establish the Ku-mediated barrier, making RNase H2 necessary to engage nascent strand degradation.

To strengthen this conclusion, we reasoned that increasing the half-life of OF by mutating the prominent OF maturation factor $Rad2^{Fen1}$ should reinforce the Ku-mediated barrier and dampen nascent strand degradation in a Ku-dependent manner. Fork resection was decreased by 2 times in *rad2Δ* cells and this phenotype was rescued by deleting *pku70* (Figures 5B and 5C). In contrast, a defect in Sen1, an RNA helicase involved in R-loop processing[22,23,72] did not affect nascent strand degradation (Figures 5B and 5C), supporting that the RNA primer from OF, but unlikely from R-loop, generates an RNA:DNA hybrid to play a pivotal role in regulating nascent strand degradation by modulating the Ku-mediated barrier.

Ku binds to OF *in vitro* and to RNA:DNA hybrids *in vivo* upon replication stress

Collectively, our data led us to hypothesize that the reversed arm embeds the last unligated OF being annealed to its complementary nascent leading strand, making RNase H2 necessary to process the resulting RNA:DNA hybrid to offer an entry point to Exo1 activity—thus counteracting Ku-mediated barrier to nascent strand degradation. This model implies that Ku binds to

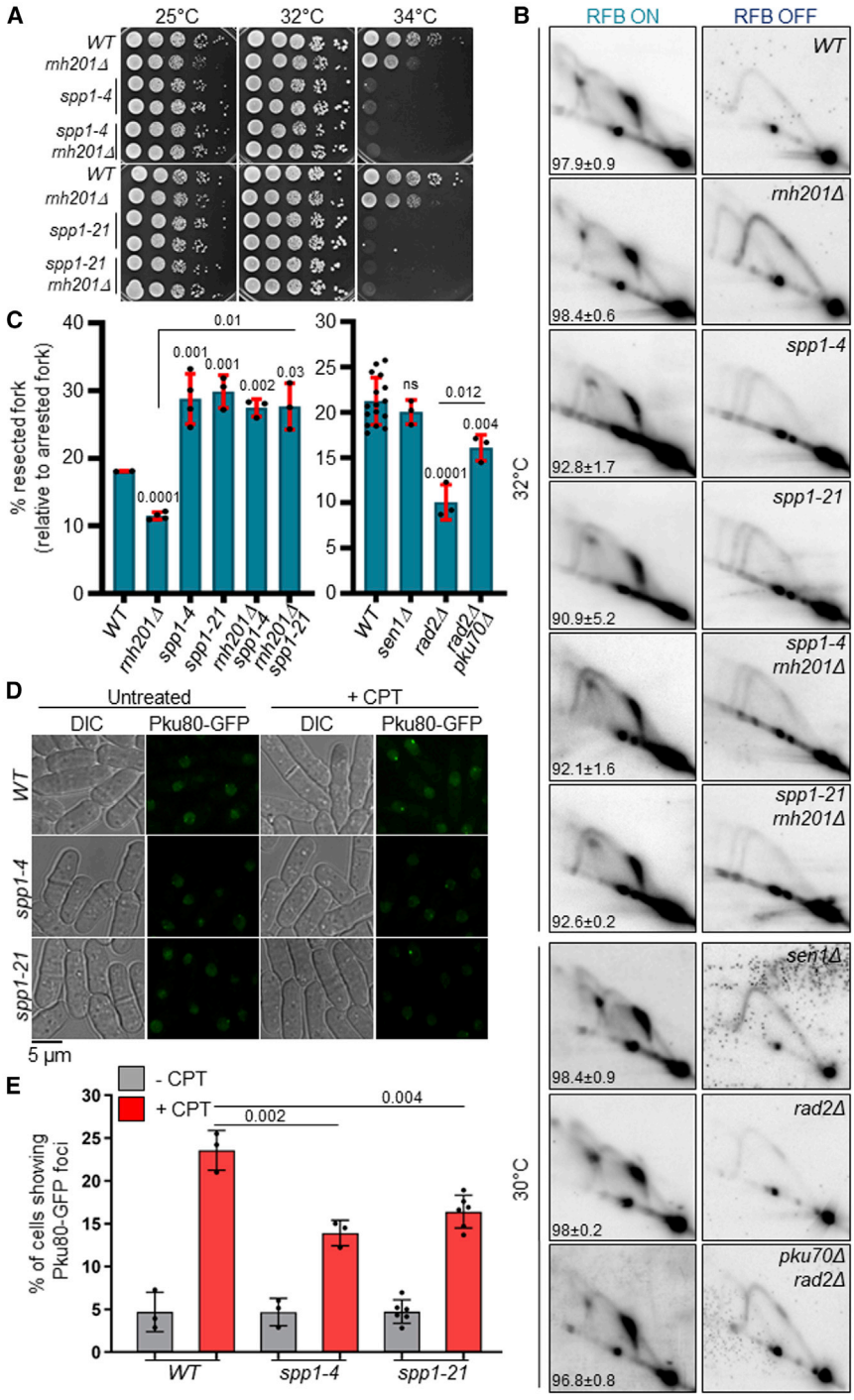

Figure 5. Interfering with Okazaki fragment synthesis and maturation affects the requirement for RNase H2 activity and the Ku-mediated barrier

(A) 10-fold serial dilutions of indicated strains at indicated temperatures.

(B) Representative 2DGE analysis in indicated strains and conditions as described in Figure 1D. The 32°C panels correspond to strains that were grown at 25°C and shifted at 32°C for 19 h.

(C) Tail quantification from (B). Dots represent values obtained from independent biological replicates. Bars indicate mean values ± SD. Statistical analysis was performed using Student's t test.

(D) Examples of cells showing Pku80-GFP foci in indicated strains and conditions (CPT at 20µM for 4 h). Strains were grown at 25°C and shifted to 32°C for 19 h before CPT treatment.

(E) Quantification of (D). Dots represent values obtained from independent biological replicates. Bars indicate mean values ± SD. At least 500 nuclei were analyzed for each experiment. Statistical analysis was performed using Student's t test.

See also Figure S6 and Table S1.

RNA:DNA hybrids. In CPT (4 h, 20µM)-treated cells, immunoprecipitated Pku70-HA associated with RNA:DNA hybrids, as revealed with the S9.6 antibody. No S9.6 signal was enriched in control strains and untreated condition (Figure 6A). Such Ku-RNA:DNA hybrid interaction did not result from an higher expression of Pku70-HA upon CPT treatment (Figure 6B). To gauge if RNA:DNA hybrids are direct substrates of Ku, we investigated the interaction of purified *S. pombe* Ku (SpKu) with RNA:DNA hybrid by biophysical methods. We co-expressed *S. pombe* Pku70 and Pku80 in insect cells and purified the complex at homogeneity in large quantity for calorimetry analyses (Figure S7A). We first measured the affinity of SpKu for double-strand DNA (dsDNA), the classical DNA substrate of Ku in canonical NHEJ and measured a dissociation constant (Kd) of 0.9 ± 0.04 nM (Figures 6C–6E, substrate A) (Figure S7, sequences). This represents a slightly higher affinity compared with the affinity measured by calorimetry with human Ku and the same DNA substrate.[73] We then designed two substrates with one biotin at an extremity or two biotins at both extremities to block them with streptavidin (Figure 6D, substrates B and C, respectively). We observed an interaction with one extremity blocked in the nanomolar range though with a weaker affinity (Kd, 41 ± 3 nM) and no interaction with the DNA blocked at the two ends (Figures 6C and 6E, substrates B and C). We then designed a DNA with the same sequence except that one strand contains 10 ribonucleotides in 5′ followed by 8 deoxyribonucleotides. This molecule mimics an OF substrate. We blocked one end by using a biotin and streptavidin (Figure 6D, substrate D compared with B). We measured an interaction with a tight affinity (Kd, 5.8 ± 2.9 nM) (Figures 6C and 6E, substrate D). We then designed a substrate with an hairpin as an alternative way to block one extremity. We also observed a tight interaction in the nanomolar range (Kd, 10 ± 0.2 nM) (Figures 6C and 6E, substrate

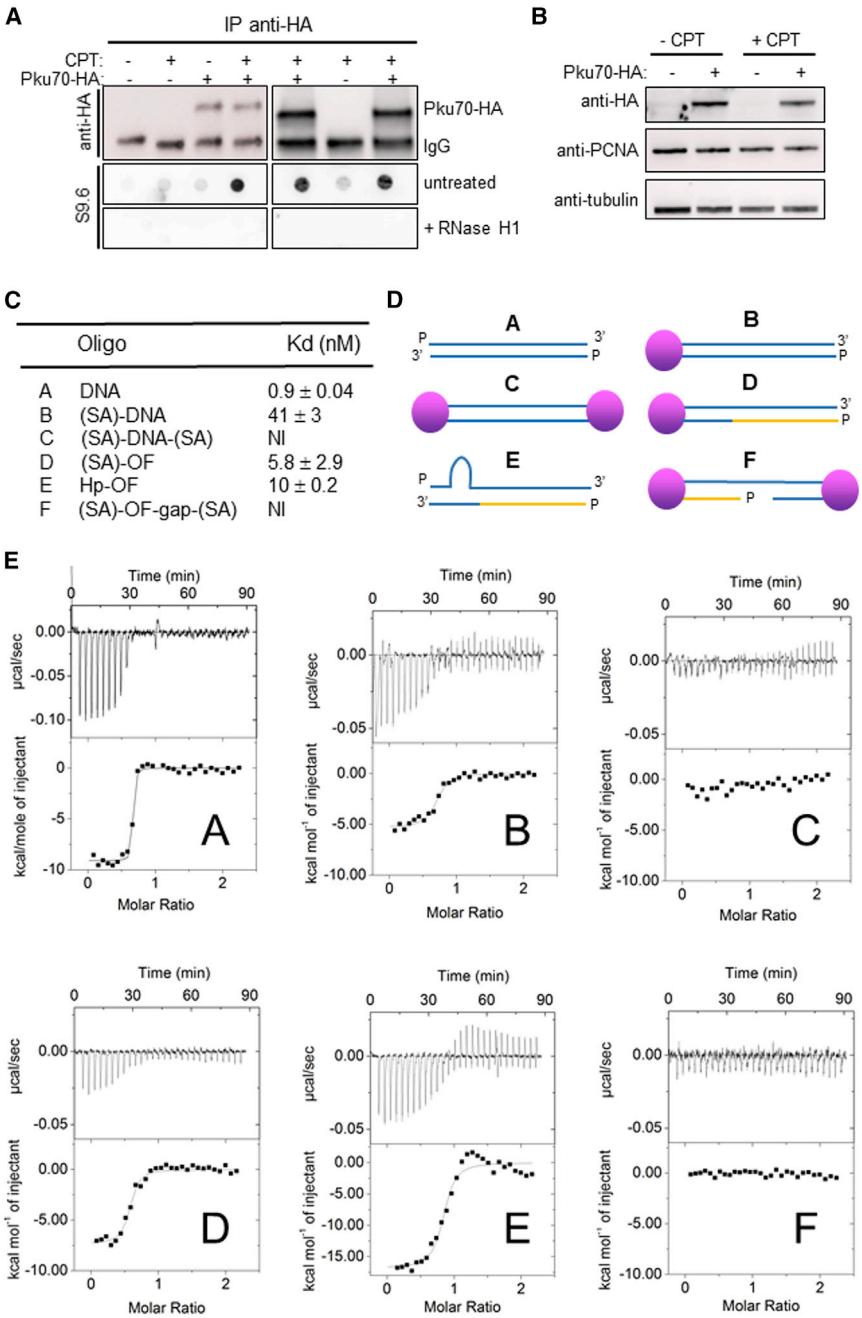

Figure 6. Ku binds RNA:DNA hybrids related substrates *in vivo* and *in vitro*

(A) Analysis of RNA:DNA hybrids co-immunoprecipitated with anti-HA antibody in indicated strains and conditions. Top: immunoblots using anti-HA antibody. The position of Pku70-HA and IgG are indicated. Bottom: detection of RNA:DNA hybrids by dot blot using S9.6 antibody. Treatment with RNaseH1 *in vitro* revealed the specificity of the signal.

(B) Expression of Pku70-HA by immunoblot in indicated strains and conditions. Tubulin and PCNA were used as loading control.

(C and D) Calorimetry measurements of the interaction between SpKu and several substrates: dsDNA 18 bp, without (A) or with one (B) or two streptavidin (C) blocking the extremities. Substrate (D) equivalent to (B) with an OF fragment at one end. Substrate (E) with an OF fragment and an hairpin as a blocking function. Substrate (F) with an OF fragment in the internal position and 4 nucleotides gaps (see Figure S7 for sequences of the substrates).

(E) Thermograms and isothermal titration curves of SpKu with the substrates (A)–(F).

See also Figure S7 and Tables S1 and S2.

E). These two last measurements indicate that SpKu interacts tightly *in vitro* with OF substrates. Finally, we designed a substrate that mimics an OF not present at an extremity but in an internal position as in a lagging strand (Figure 6D, substrate F). We observed no interaction of SpKu with this molecule, suggesting that Ku interaction with OF requires the RNA:DNA hybrid to be accessible from an extremity (Figure 6E, substrate F). We cross-validated these calorimetry results with electrophoretic mobility shift assay (EMSA) analyses, which showed a similar interaction between dsDNA and a substrate containing an OF (Figures S7B–S7D). Overall, we concluded that RNA:DNA hybrids are physiological substrates for Ku binding in response to replication stress and that Ku is able to bind substrates mimicking OF *in vitro*.

DISCUSSION

Collectively, this study uncovers an RNA:DNA hybrid-related mechanism to regulate the Ku-mediated barrier to nascent strand degradation. We propose that the RNA primer originating from OF synthesis is embedded in the reversed arms of reversed forks, creating a substrate for Ku binding and specifying a nuclease requirement to engage fork resection (Figure 7). The coordinated action of MRN-Ctp1 axis and RNase H2 promotes Ku eviction and the RNA:DNA hybrid degradation, respectively, allowing Exo1 to degrade nascent strands. This RNA:DNA hybrid-based mechanism contributes to safeguard fork integrity and timely replication resumption, revealing an underappreciated function for DNA-embedded RNA species in maintaining genome stability.

Several individual NHEJ-related factors are involved in fork protection, in repairing replication-induced DSBs, and in restarting replication forks.[15] In fission yeast, Ku binding to arrested forks is necessary for recovery from replication stress by promoting timely fork restart and fork protection.[27,47] Human RIF1, 53BP1, and KU have been proposed to act as barriers against nascent strand degradation and thus to contribute to

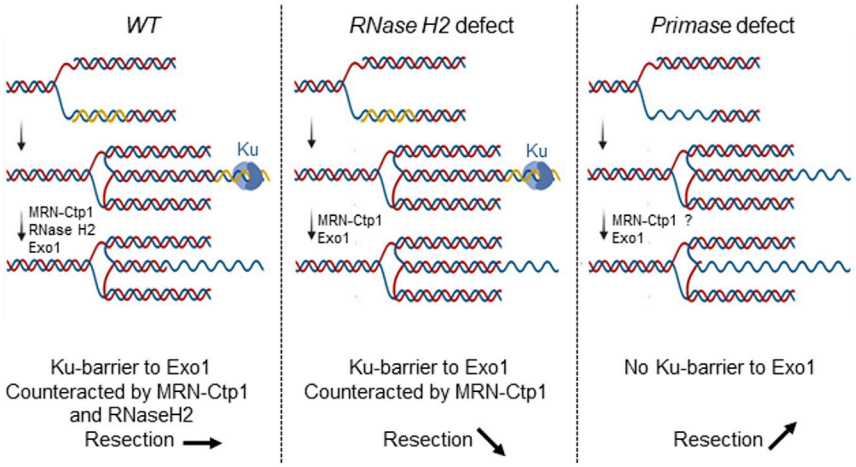

Figure 7. The RNA primer from Okazaki fragment contributes to establish the Ku-mediated barrier and thus specifying nuclease requirement

See text for details.

fork protection and prevent under-replicating DNA leading to chromosome breakage.[26–29] Recently, Moldovan's lab demonstrated that human KU association to HU-stalled forks depends on fork reversal at which the KU-PARP14 axis is part of a multistep process to regulate nascent strand degradation.[60] In contrast, Smolka's lab showed that KU-DNAPK stabilizes HU-stalled forks by promoting fork reversal and subsequent nascent strand degradation.[74] While these reports underscore the importance of regulating NHEJ-mediated fork-protection pathways, they also suggest that human KU may act at multiple steps during fork protection. Since there is no DNAPK ortholog identified so far in yeast, we favor the hypothesis that *S. pombe* Ku is recruited at arrested forks downstream of fork reversal, but this remains to be formally demonstrated.

RNAs are known *cis*- and *trans*-modulators of NHEJ activity, in particular during DSB repair.[15] Here, we propose that RNA:DNA hybrids are *cis*-regulators of Ku function at reversed forks to regulate nascent strand degradation. Beyond the *RTS1*-RFB scenario, we establish that Ku binds RNA:DNA hybrids upon replication stress and substrates mimicking OF. Moreover, defects in RNase H2 and MRN lead to synthetic lethality upon replication stress in a Ku-dependent manner. The synthesis of OF on the lagging strand is a recurrent source of RNA:DNA hybrids associated with DNA replication. Compromising the RNA primer synthesis of OF bypasses RNase H2 requirement and impairs the Ku-mediated barrier to nascent strand degradation. In human cells, two pathways of replication-fork protection were identified providing distinct nuclease substrates and engagement of distinct fork protection factors.[28] We speculate that the presence of the last unprocessed OF, embedded as an RNA:DNA hybrid within the reversed arm of the reversed fork, may provide substrate specificity for nucleases and Ku binding. In this scenario, overcoming the Ku barrier would require nucleases able to process the RNA:DNA hybrid from OF such as RNase H2, whereas the absence of RNA:DNA hybrids may generate a reversed arm with an extremity not suitable for Ku binding (Figure 7). Of note, RIF1 and 53BP1 promote fork protection by counteracting DNA2-dependent resection, a nuclease previously involved in OF processing.[26,28,29]

At DSBs, short- and long-range resection are coordinated by a complex interplay between Ku and MRN-CtIP^{Ctp1}, with Ku being an early responder to restrict the long-range resection.[75] In both fission yeast and mammalian cells, Ku eviction from DSB ends depends on MRN-CtIP^{Ctp1} and Mre11 nuclease activity.[34,76] Recently, Ku protein block was proposed to stimulate Mre11-mediated initial endonucleolytic cleavage of 5′-terminated DNA strands, promoting a switch toward short-range resection.[60,77] In yeasts, MRN promotes nascent strand degradation at the *RTS1*-RFB and stalled forks in a nuclease-independent manner.[27,78] The presence of an RNA:DNA hybrid within the reversed arm constitutes an additional level of complexity in the understanding of MRN and Ku antagonism in controlling fork resection. One hypothesis is that MRN-Ctp1 is inefficient in promoting 5′ incision at an RNA:DNA hybrid, as previously suggested,[79] requiring additional nuclease activities to promote long-range resection. However, we obtained no evidence that nascent strand degradation depends on the nuclease activity of Mre11 in primase mutants. We propose that RNase H2, by processing RNA:DNA hybrids, likely provides nicks used as an entry point for Exo1 activity, therefore overcoming the Ku-mediated barrier.[80] In such a scenario, Ku eviction remains dependent on MRN-Ctp1 but independent of Mre11 nuclease activity, a mechanism that remains to be understood. Moreover, in the absence of RNase H2 and Ku, nascent strand degradation depends on Exo1, suggesting that Exo1 is able to process the RNA moiety of an RNA:DNA hybrid. *In vitro*, Exo1 can degrade RNA:DNA hybrids containing up to 10 consecutive ribonucleotides, but not 15.[81] The RNA primer during OF synthesis ranges from 8 to 12 ribonucleotides[38] raising the possibility that Exo1 can process them at a low rate, explaining the partial fork-resection defect in the absence of RNase H2, unless additional nucleases are acting at an RNA:DNA hybrid-containing reversed fork (Figure 7).

Mutations in any of the 3 subunits of RNase H2 account for more than half of the Aicardi-Goutières syndrome (AGS) cases, an autoimmune genetic disorder characterized by an upregulation of type I interferon (IFN) expression and microcephaly.[54] To date, the molecular tenants of this pathology are still unclear. Another gene frequently mutated in AGS is SAMHD1, which has been recently involved in nascent strand degradation at HU-stalled forks in human cells.[82] Mechanistically, SAMHD1 stimulates the exonuclease activity of MRE11 to allow replication restart. In SAMHD1-depleted cells, alternative processing of stalled forks by RECQ1 leads to ssDNA accumulation in the cytoplasm, which in turn triggers cGAS-STING pathway

activation and IFN production. Our work establishes that fission yeast RNase H2 also contributes to fork resection, further linking AGS to defects in nascent strand degradation and fork restart, consistent with patient-derived AGS cells carrying defects in RNase H2 exhibit signs of replication stress and chronic activation of the DDR, in particular of the postreplication repair pathway.[83]

The role of DNA-embedded RNA species in regulating fork repair has received little attention so far. We propose that RNA:DNA hybrids embedded in reversed fork and originating from OF are *cis*-regulators of Ku function to maintain replication-fork integrity. We uncover a role for RNA:DNA hybrids in dictating requirement for specific dismantling activities to ensure proper replication-fork processing and restart.

Limitations of the study

We propose reversed fork as an entry point for Ku binding and nuclease activities, as suggested in humans. So far, we are unable to delineate the genetic requirement for fork reversal in yeast, likely because multiple helicases or translocases are involved as found in humans, preventing us to test the model further. However, we do not exclude that fork resection can occur independently of fork reversal. Moreover, our data establish that the primase activity is critical to control the Ku-mediated barrier to nascent strand degradation and our results indicate a role of OF in this process. Nonetheless, we cannot exclude that the primase may also fill in the resected reversed arm via the fission yeast ST complex, an analog to the human CST complex. Finally, consistent with the defect of fork resection in the absence of RNase H activities being not rescued by the deletion of Ku, we do not exclude that additional replication stress-induced RNA:DNA hybrids may be at work at replication stress sites to regulate DNA repair pathways and maintain genome integrity.

STAR★METHODS

Detailed methods are provided in the online version of this paper and include the following:

- KEY RESOURCES TABLE
- RESOURCE AVAILABILITY
  - Lead contact
  - Materials availability
  - Data and code availability
- EXPERIMENTAL MODEL AND SUBJECT DETAILS
- METHOD DETAILS
  - Standard yeast genetics
  - Replication slippage assay
  - Analysis of replication intermediates by 2DGE
  - Fork reversal detection by 1DGE
  - Nucleic acid extraction
  - Dot blot
  - Flow cytometry
  - Live cell imaging
  - Movie analysis
  - Chromatin Immunoprecipitation (ChIP)
  - Whole protein extract analysis
  - Purification of S. pombe Ku70-80
  - Calorimetry
  - EMSA
- QUANTIFICATION AND STATISTICAL ANALYSIS

SUPPLEMENTAL INFORMATION

Supplemental information can be found online at https://doi.org/10.1016/j.molcel.2023.02.008.

ACKNOWLEDGMENTS

The authors thank Vincent Vanoosthuyse, Stefania Francesconi, Antony Carr, and Theresa Wang for exchanging strains and reagents. We thank A. Bourand-Plantefol (I2BC, Gif sur Yvette) for protocol for EMSA and the I2BC platform for Protein Interactions and French Infrastructure for Integrated Structural Biology (FRISBI) ANR-10-INBS-0005 for access to calorimetry. We also thank the PICT-IBiSA@Orsay Imaging Facility of the Institut Curie (particularly Laetitia Besse) and the Flow Cytometry Facility of the Orsay site of Institut Curie (particularly Charlene Lasgi and Lucie Martin from the team). We thank Stephan Vagner for his helpful comments on this work. This study was supported by grants from the Institut Curie, the CNRS, the Fondation LIGUE "Equipe Labellisée 2020" (EL2020LNCC/Sal), and the ANR grant REDEFINE (ANR-19-CE12-0016-03) to S.A.E.L. J.B.C. is supported by grants from ANR-20-CE11-0026, ANR-21-CE12-0019, and ANR-22-CE12-0037. C.A. was funded by a French governmental fellowship and a fourth-year PhD grant from Fondation ARC. K.S. was funded by a three-year PhD fellowship from the Fondation LIGUE. The funders had no role in study design, data collection and analysis, the decision to publish, or preparation of the manuscript.

AUTHOR CONTRIBUTIONS

C.A. performed the experiments shown in Figures 1, 2, 3, 5B, 5C (*rad2Δ* and *sen1Δ*), 6A, 6B, S1, S2, S3D–S3F, and S4. A.A.S. and V.B. performed the experiments in Figures 4 and S5. P.F.V., A.G., and V.R. performed the experiments in Figures 6C, 6D, and S7. K.S. performed the experiments in Figures 5A–5C, S3A–S3C, and S6. A.C. performed the experiments on Figures 5D and 5E. K.B.F.L. contributed to all experiments, except those in Figures 6C, 6D, and S7, via her contribution to lab management and direct involvement in performing experiments. C.A., K.F., K.S., J.B.C., and S.A.E.L. contributed to experimental design and data analysis and presentation. C.A., J.B.C., and S.A.E.L. wrote the manuscript. J.B.C. and S.A.E.L. edited the manuscript.

DECLARATION OF INTERESTS

The authors declare no competing interests.

Received: December 14, 2021
Revised: December 9, 2022
Accepted: February 4, 2023
Published: March 2, 2023

REFERENCES

1. Zeman, M.K., and Cimprich, K.A. (2014). Causes and consequences of replication stress. Nat. Cell Biol. *16*, 2–9. https://doi.org/10.1038/ncb2897.
2. Gaillard, H., García-Muse, T., and Aguilera, A. (2015). Replication stress and cancer. Nat. Rev. Cancer *15*, 276–289. https://doi.org/10.1038/nrc3916.
3. García-Muse, T., and Aguilera, A. (2019). R loops: from physiological to pathological roles. Cell *179*, 604–618. https://doi.org/10.1016/j.cell.2019.08.055.

4. Crossley, M.P., Bocek, M., and Cimprich, K.A. (2019). R-loops as cellular regulators and genomic threats. Mol. Cell *73*, 398–411. https://doi.org/10.1016/j.molcel.2019.01.024.

5. Hamperl, S., Bocek, M.J., Saldivar, J.C., Swigut, T., and Cimprich, K.A. (2017). Transcription-replication conflict orientation modulates R-loop levels and activates distinct DNA damage responses. Cell *170*, 774–786.e19. https://doi.org/10.1016/j.cell.2017.07.043.

6. Kemiha, S., Poli, J., Lin, Y.L., Lengronne, A., and Pasero, P. (2021). Toxic R-loops: cause or consequence of replication stress? DNA Repair (Amst) *107*, 103199. https://doi.org/10.1016/j.dnarep.2021.103199.

7. Promonet, A., Padioleau, I., Liu, Y., Sanz, L., Biernacka, A., Schmitz, A.L., Skrzypczak, M., Sarrazin, A., Mettling, C., Rowicka, M., et al. (2020). Topoisomerase 1 prevents replication stress at R-loop-enriched transcription termination sites. Nat. Commun. *11*, 3940. https://doi.org/10.1038/s41467-020-17858-2.

8. Costantino, L., and Koshland, D. (2018). Genome-wide map of R-loop-induced damage reveals how a subset of R-loops contributes to genomic instability. Mol. Cell *71*, 487–497.e3. https://doi.org/10.1016/j.molcel.2018.06.037.

9. Marnef, A., and Legube, G. (2021). R-loops as Janus-faced modulators of DNA repair. Nat. Cell Biol. *23*, 305–313. https://doi.org/10.1038/s41556-021-00663-4.

10. Ohle, C., Tesorero, R., Schermann, G., Dobrev, N., Sinning, I., and Fischer, T. (2016). Transient RNA-DNA hybrids are required for efficient double-strand break repair. Cell *167*, 1001–1013.e7. https://doi.org/10.1016/j.cell.2016.10.001.

11. Domingo-Prim, J., Bonath, F., and Visa, N. (2020). RNA at DNA double-strand breaks: the challenge of dealing with DNA:RNA hybrids. BioEssays *42*, e1900225. https://doi.org/10.1002/bies.201900225.

12. Pessina, F., Giavazzi, F., Yin, Y., Gioia, U., Vitelli, V., Galbiati, A., Barozzi, S., Garre, M., Oldani, A., Flaus, A., et al. (2019). Functional transcription promoters at DNA double-strand breaks mediate RNA-driven phase separation of damage-response factors. Nat. Cell Biol. *21*, 1286–1299. https://doi.org/10.1038/s41556-019-0392-4.

13. D'Alessandro, G., Whelan, D.R., Howard, S.M., Vitelli, V., Renaudin, X., Adamowicz, M., Iannelli, F., Jones-Weinert, C.W., Lee, M.Y., Matti, V., et al. (2018). BRCA2 controls DNA:RNA hybrid level at DSBs by mediating RNase H2 recruitment. Nat. Commun. *9*, 5376. https://doi.org/10.1038/s41467-018-07799-2.

14. Michelini, F., Pitchiaya, S., Vitelli, V., Sharma, S., Gioia, U., Pessina, F., Cabrini, M., Wang, Y., Capozzo, I., Iannelli, F., et al. (2017). Damage-induced lncRNAs control the DNA damage response through interaction with DDRNAs at individual double-strand breaks. Nat. Cell Biol. *19*, 1400–1411. https://doi.org/10.1038/ncb3643.

15. Audoynaud, C., Vagner, S., and Lambert, S. (2021). Non-homologous end-joining at challenged replication forks: an RNA connection? Trends Genet. *37*, 973–985. https://doi.org/10.1016/j.tig.2021.06.010.

16. Sessa, G., Gómez-González, B., Silva, S., Pérez-Calero, C., Beaurepere, R., Barroso, S., Martineau, S., Martin, C., Ehlén, Å., Martínez, J.S., et al. (2021). BRCA2 promotes DNA-RNA hybrid resolution by DDX5 helicase at DNA breaks to facilitate their repair. EMBO J. *40*, e106018. https://doi.org/10.15252/embj.2020106018.

17. Dang, T.T., and Morales, J.C. (2020). Xrn2 links RNA: dna hybrid resolution to double strand break repair pathway choice. Cancers (Basel) *12*, 1–15. https://doi.org/10.3390/cancers12071821.

18. Li, L., Germain, D.R., Poon, H.-Y., Hildebrandt, M.R., Monckton, E.A., McDonald, D., Hendzel, M.J., and Godbout, R. (2016). DEAD box 1 facilitates removal of RNA and homologous recombination at DNA double-strand breaks. Mol. Cell. Biol. *36*, 2794–2810. https://doi.org/10.1128/MCB.00415-16.

19. Bhatia, V., Valdés-Sánchez, L., Rodriguez-Martinez, D., and Bhattacharya, S.S. (2018). Formation of 53BP1 foci and ATM activation under oxidative stress is facilitated by RNA:DNA hybrids and loss of ATM-53BP1 expression promotes photoreceptor cell survival in mice. F1000Res *7*, 1233. https://doi.org/10.12688/F1000RESEARCH.15579.1.

20. Chakraborty, A., Tapryal, N., Venkova, T., Horikoshi, N., Pandita, R.K., Sarker, A.H., Sarkar, P.S., Pandita, T.K., and Hazra, T.K. (2016). Classical non-homologous end-joining pathway utilizes nascent RNA for error-free double-strand break repair of transcribed genes. Nat. Commun. *7*, 13049. https://doi.org/10.1038/ncomms13049.

21. Zong, D., Oberdoerffer, P., Batista, P.J., and Nussenzweig, A. (2020). RNA: a double-edged sword in genome maintenance. Nat. Rev. Genet. *21*, 651–670. https://doi.org/10.1038/s41576-020-0263-7.

22. Cohen, S., Puget, N., Lin, Y.L., Clouaire, T., Aguirrebengoa, M., Rocher, V., Pasero, P., Canitrot, Y., and Legube, G. (2018). Senataxin resolves RNA:DNA hybrids forming at DNA double-strand breaks to prevent translocations. Nat. Commun. *9*, 533. https://doi.org/10.1038/s41467-018-02894-w.

23. Rawal, C.C., Zardoni, L., Di Terlizzi, M., Galati, E., Brambati, A., Lazzaro, F., Liberi, G., and Pellicioli, A. (2020). Senataxin ortholog Sen1 limits DNA:RNA hybrid accumulation at DNA double-strand breaks to control end resection and repair fidelity. Cell Rep. *31*, 107603. https://doi.org/10.1016/j.celrep.2020.107603.

24. Berti, M., Cortez, D., and Lopes, M. (2020). The plasticity of DNA replication forks in response to clinically relevant genotoxic stress. Nat. Rev. Mol. Cell Biol. *21*, 633–651. https://doi.org/10.1038/s41580-020-0257-5.

25. Ait Saada, A., Lambert, S.A.E., and Carr, A.M. (2018). Preserving replication fork integrity and competence via the homologous recombination pathway. DNA Repair (Amst) *71*, 135–147. https://doi.org/10.1016/j.dnarep.2018.08.017.

26. Mukherjee, C., Tripathi, V., Manolika, E.M., Heijink, A.M., Ricci, G., Merzouk, S., de Boer, H.R., Demmers, J., van Vugt, M.A.T.M., and Ray Chaudhuri, A. (2019). RIF1 promotes replication fork protection and efficient restart to maintain genome stability. Nat. Commun. *10*, 3287. https://doi.org/10.1038/s41467-019-11246-1.

27. Teixeira-Silva, A., Ait Saada, A., Hardy, J., Iraqui, I., Nocente, M.C., Fréon, K., and Lambert, S.A.E. (2017). The end-joining factor Ku acts in the end-resection of double strand break-free arrested replication forks. Nat. Commun. *8*, 1982. https://doi.org/10.1038/s41467-017-02144-5.

28. Liu, W., Krishnamoorthy, A., Zhao, R., and Cortez, D. (2020). Two replication fork remodeling pathways generate nuclease substrates for distinct fork protection factors. Sci. Adv. *6*, eabc3598. https://doi.org/10.1126/sciadv.abc3598.

29. Garzón, J., Ursich, S., Lopes, M., Hiraga, S.I., and Donaldson, A.D. (2019). Human RIF1-protein phosphatase 1 prevents degradation and breakage of nascent DNA on replication stalling. Cell Rep. *27*, 2558–2566.e4. https://doi.org/10.1016/j.celrep.2019.05.002.

30. Chen, B.R., Quinet, A., Byrum, A.K., Jackson, J., Berti, M., Thangavel, S., Bredemeyer, A.L., Hindi, I., Mosammaparast, N., Tyler, J.K., et al. (2019). XLF and H2AX function in series to promote replication fork stability. J. Cell Biol. *218*, 2113–2123. https://doi.org/10.1083/jcb.201808134.

31. Sánchez, A., and Russell, P. (2015). Ku Stabilizes replication forks in the absence of Brc1. PLOS One *10*, e0126598. https://doi.org/10.1371/journal.pone.0126598.

32. Miyoshi, T., Kanoh, J., and Ishikawa, F. (2009). Fission yeast Ku protein is required for recovery from DNA replication stress. Genes Cells *14*, 1091–1103. https://doi.org/10.1111/j.1365-2443.2009.01337.x.

33. Joshi, R.R., Ali, S.I., and Ashley, A.K. (2019). DNA ligase IV prevents replication fork stalling and promotes cellular proliferation in triple negative breast cancer. J. Nucleic Acids *2019*, 9170341. https://doi.org/10.1155/2019/9170341.

34. Chanut, P., Britton, S., Coates, J., Jackson, S.P., and Calsou, P. (2016). Coordinated nuclease activities counteract Ku at single-ended DNA double-strand breaks. Nat. Commun. *7*, 12889. https://doi.org/10.1038/ncomms12889.

35. Balmus, G., Pilger, D., Coates, J., Demir, M., Sczaniecka-Clift, M., Barros, A.C., Woods, M., Fu, B., Yang, F., Chen, E., et al. (2019). ATM orchestrates the DNA-damage response to counter toxic non-homologous end-joining at broken replication forks. Nat. Commun. *10*, 87. https://doi.org/10.1038/s41467-018-07729-2.

36. Britton, S., Chanut, P., Delteil, C., Barboule, N., Frit, P., and Calsou, P. (2020). ATM antagonizes NHEJ proteins assembly and DNA-ends synapsis at single-ended DNA double strand breaks. Nucleic Acids Res. *48*, 9710–9723. https://doi.org/10.1093/nar/gkaa723.

37. Lazzaro, F., Novarina, D., Amara, F., Watt, D.L., Stone, J.E., Costanzo, V., Burgers, P.M., Kunkel, T.A., Plevani, P., and Muzi-Falconi, M. (2012). RNase H and postreplication repair protect cells from ribonucleotides incorporated in DNA. Mol. Cell *45*, 99–110. https://doi.org/10.1016/j.molcel.2011.12.019.

38. Burgers, P.M.J., and Kunkel, T.A. (2017). Eukaryotic DNA replication fork. Annu. Rev. Biochem. *86*, 417–438. https://doi.org/10.1146/annurev-biochem-061516-044709.

39. Balakrishnan, L., and Bambara, R.A. (2013). Okazaki fragment metabolism. Cold Spring Harb. Perspect. Biol. *5*, a010173. https://doi.org/10.1101/cshperspect.a010173.

40. Lambert, S., Watson, A., Sheedy, D.M., Martin, B., and Carr, A.M. (2005). Gross chromosomal rearrangements and elevated recombination at an inducible site-specific replication fork barrier. Cell *121*, 689–702. https://doi.org/10.1016/j.cell.2005.03.022.

41. Lambert, S., Mizuno, K., Blaisonneau, J., Martineau, S., Chanet, R., Fréon, K., Murray, J.M., Carr, A.M., and Baldacci, G. (2010). Homologous recombination restarts blocked replication forks at the expense of genome rearrangements by template exchange. Mol. Cell *39*, 346–359. https://doi.org/10.1016/j.molcel.2010.07.015.

42. Mizuno, K., Miyabe, I., Schalbetter, S.A., Carr, A.M., and Murray, J.M. (2013). Recombination-restarted replication makes inverted chromosome fusions at inverted repeats. Nature *493*, 246–249. https://doi.org/10.1038/nature11676.

43. Nguyen, M.O., Jalan, M., Morrow, C.A., Osman, F., and Whitby, M.C. (2015). Recombination occurs within minutes of replication blockage by RTS1 producing restarted forks that are prone to collapse. eLife *4*, e04539. https://doi.org/10.7554/eLife.04539.

44. Tsang, E., Miyabe, I., Iraqui, I., Zheng, J., Lambert, S.A.E., and Carr, A.M. (2014). The extent of error-prone replication restart by homologous recombination is controlled by Exo1 and checkpoint proteins. J. Cell Sci. *127*, 2983–2994. https://doi.org/10.1242/jcs.152678.

45. Iraqui, I., Chekkal, Y., Jmari, N., Pietrobon, V., Fréon, K., Costes, A., and Lambert, S.A.E. (2012). Recovery of arrested replication forks by homologous recombination is error-prone. PLoS Genet. *8*, e1002976. https://doi.org/10.1371/journal.pgen.1002976.

46. Jalan, M., Oehler, J., Morrow, C.A., Osman, F., and Whitby, M.C. (2019). Factors affecting template switch recombination associated with restarted DNA replication. eLife *8*, e41697. https://doi.org/10.7554/eLife.41697.

47. Naiman, K., Campillo-Funollet, E., Watson, A.T., Budden, A., Miyabe, I., and Carr, A.M. (2021). Replication dynamics of recombination-dependent replication forks. Nat. Commun. *12*, 923. https://doi.org/10.1038/s41467-021-21198-0.

48. Chédin, F., Hartono, S.R., Sanz, L.A., and Vanoosthuyse, V. (2021). Best practices for the visualization, mapping, and manipulation of R-loops. EMBO J. *40*, e106394. https://doi.org/10.15252/embj.2020106394.

49. Zhao, H., Zhu, M., Limbo, O., and Russell, P. (2018). RNase H eliminates R-loops that disrupt DNA replication but is nonessential for efficient DSB repair. EMBO Rep. *19*, e45335. https://doi.org/10.15252/embr.201745335.

50. Ait Saada, A., Teixeira-Silva, A., Iraqui, I., Costes, A., Hardy, J., Paoletti, G., Fréon, K., and Lambert, S.A.E. (2017). Unprotected replication forks are converted into mitotic sister chromatid bridges. Mol. Cell *66*, 398–410.e4. https://doi.org/10.1016/j.molcel.2017.04.002.

51. Liu, S., Hua, Y., Wang, J., Li, L., Yuan, J., Zhang, B., Wang, Z., Ji, J., and Kong, D. (2021). RNA polymerase III is required for the repair of DNA double-strand breaks by homologous recombination. Cell *184*, 1314–1329.e10. https://doi.org/10.1016/j.cell.2021.01.048.

52. Šviković, S., Crisp, A., Tan-Wong, S.M., Guilliam, T.A., Doherty, A.J., Proudfoot, N.J., Guilbaud, G., and Sale, J.E. (2019). R-loop formation during S phase is restricted by PrimPol-mediated repriming. EMBO J. *38*, e99793. https://doi.org/10.15252/embj.201899793.

53. Nava, G.M., Grasso, L., Sertic, S., Pellicioli, A., Muzi Falconi, M.M., and Lazzaro, F. (2020). One, no one, and one hundred thousand: the many forms of ribonucleotides in DNA. Int. J. Mol. Sci. *21*, 1706. https://doi.org/10.3390/ijms21051706.

54. Crow, Y.J., Leitch, A., Hayward, B.E., Garner, A., Parmar, R., Griffith, E., Ali, M., Semple, C., Aicardi, J., Babul-Hirji, R., et al. (2006). Mutations in genes encoding ribonuclease H2 subunits cause Aicardi-Goutières syndrome and mimic congenital viral brain infection. Nat. Genet. *38*, 910–916. https://doi.org/10.1038/ng1842.

55. Rohman, M.S., Koga, Y., Takano, K., Chon, H., Crouch, R.J., and Kanaya, S. (2008). Effect of the disease-causing mutations identified in human ribonuclease (RNase) H2 on the activities and stabilities of yeast RNase H2 and archaeal RNase HII. FEBS J. *275*, 4836–4849. https://doi.org/10.1111/j.1742-4658.2008.06622.x.

56. Chon, H., Sparks, J.L., Rychlik, M., Nowotny, M., Burgers, P.M., Crouch, R.J., and Cerritelli, S.M. (2013). RNase H2 roles in genome integrity revealed by unlinking its activities. Nucleic Acids Res. *41*, 3130–3143. https://doi.org/10.1093/nar/gkt027.

57. Cerritelli, S.M., and El Hage, A. (2020). RNases H1 and H2: guardians of the stability of the nuclear genome when supply of dNTPs is limiting for DNA synthesis. Curr. Genet. *66*, 1073–1084. https://doi.org/10.1007/s00294-020-01086-8.

58. Meroni, A., Nava, G.M., Bianco, E., Grasso, L., Galati, E., Bosio, M.C., Delmastro, D., Muzi-Falconi, M., and Lazzaro, F. (2019). RNase H activities counteract a toxic effect of polymerase in cells replicating with depleted dNTP pools. Nucleic Acids Res. *47*, 4612–4623. https://doi.org/10.1093/nar/gkz165.

59. Lemaçon, D., Jackson, J., Quinet, A., Brickner, J.R., Li, S., Yazinski, S., You, Z., Ira, G., Zou, L., Mosammaparast, N., et al. (2017). MRE11 and EXO1 nucleases degrade reversed forks and elicit MUS81-dependent fork rescue in BRCA2-deficient cells. Nat. Commun. *8*, 860. https://doi.org/10.1038/s41467-017-01180-5.

60. Dhoonmoon, A., Nicolae, C.M., and Moldovan, G.L. (2022). The KU-PARP14 axis differentially regulates DNA resection at stalled replication forks by MRE11 and EXO1. Nat. Commun. *13*, 5063. https://doi.org/10.1038/s41467-022-32756-5.

61. Jones, C.E., and Forsburg, S.L. (2021). Monitoring Schizosaccharomyces pombe genome stress by visualizing end-binding protein Ku. Biol. Open *10*, bio054346. https://doi.org/10.1242/bio.054346.

62. Mijic, S., Zellweger, R., Chappidi, N., Berti, M., Jacobs, K., Mutreja, K., Ursich, S., Ray Chaudhuri, A., Nussenzweig, A., Janscak, P., et al. (2017). Replication fork reversal triggers fork degradation in BRCA2-defective cells. Nat. Commun. *8*, 859. https://doi.org/10.1038/s41467-017-01164-5.

63. Neelsen, K.J., and Lopes, M. (2015). Replication fork reversal in eukaryotes: from dead end to dynamic response. Nat. Rev. Mol. Cell Biol. *16*, 207–220. https://doi.org/10.1038/nrm3935.

64. Maric, C., and Bénard, M. (2014). Replication forks reverse at high frequency upon replication stress in Physarum polycephalum. Chromosoma *123*, 577–585. https://doi.org/10.1007/s00412-014-0471-z.

65. Vengrova, S., and Dalgaard, J.Z. (2004). RNase-sensitive DNA modification(s) initiates S. pombe mating-type switching. Genes Dev. *18*, 794–804. https://doi.org/10.1101/gad.289404.

66. Hanada, K., Budzowska, M., Davies, S.L., Van Drunen, E., Onizawa, H., Beverloo, H.B., Maas, A., Essers, J., Hickson, I.D., and Kanaar, R. (2007). The structure-specific endonuclease Mus81 contributes to replication restart by generating double-strand DNA breaks. Nat. Struct. Mol. Biol. *14*, 1096–1104. https://doi.org/10.1038/nsmb1313.

67. Froget, B., Blaisonneau, J., Lambert, S., and Baldacci, G. (2008). Cleavage of stalled forks by fission yeast Mus81/Eme1 in absence of DNA replication checkpoint. Mol. Biol. Cell *19*, 445–456. https://doi.org/10.1091/mbc.E07-07-0728.

68. Sogo, J.M., Lopes, M., and Foiani, M. (2002). Fork reversal and ssDNA accumulation at stalled replication forks owing to checkpoint defects. Science *297*, 599–602. https://doi.org/10.1126/science.1074023.

69. Hu, J., Sun, L., Shen, F., Chen, Y., Hua, Y., Liu, Y., Zhang, M., Hu, Y., Wang, Q., Xu, W., et al. (2012). The intra-S phase checkpoint targets Dna2 to prevent stalled replication forks from reversing. Cell *149*, 1221–1232. https://doi.org/10.1016/j.cell.2012.04.030.

70. Menin, L., Ursich, S., Trovesi, C., Zellweger, R., Lopes, M., Longhese, M.P., and Clerici, M. (2018). Tel1/ ATM prevents degradation of replication forks that reverse after topoisomerase poisoning. EMBO Rep. *19*, e45535. https://doi.org/10.15252/embr.201745535.

71. Griffiths, D.J.F., Liu, V.F., Nurse, P., and Wang, T.S.F. (2001). Role of fission yeast primase catalytic subunit in the replication checkpoint. Mol. Biol. Cell *12*, 115–128. https://doi.org/10.1091/mbc.12.1.115.

72. San Martin-Alonso, M., Soler-Oliva, M.E., García-Rubio, M., García-Muse, T., and Aguilera, A. (2021). Harmful R-loops are prevented via different cell cycle-specific mechanisms. Nat. Commun. *12*, 4451. https://doi.org/10.1038/s41467-021-24737-x.

73. Nemoz, C., Ropars, V., Frit, P., Gontier, A., Drevet, P., Yu, J., Guerois, R., Pitois, A., Comte, A., Delteil, C., et al. (2018). XLF and APLF bind Ku80 at two remote sites to ensure DNA repair by non-homologous end joining. Nat. Struct. Mol. Biol. *25*, 971–980. https://doi.org/10.1038/s41594-018-0133-6.

74. Dibitetto, D., Marshall, S., Sanchi, A., Liptay, M., Badar, J., Lopes, M., Rottenberg, S., and Smolka, M.B. (2022). DNA-PKcs promotes fork reversal and chemoresistance. Mol. Cell *82*, 3932–3942.e6. https://doi.org/10.1016/j.molcel.2022.08.028.

75. Reginato, G., and Cejka, P. (2020). The MRE11 complex: A versatile toolkit for the repair of broken DNA. DNA Repair (Amst) *91–92*, 102869. https://doi.org/10.1016/j.dnarep.2020.102869.

76. Langerak, P., Mejia-Ramirez, E., Limbo, O., and Russell, P. (2011). Release of Ku and MRN from DNA ends by Mre11 nuclease activity and Ctp1 is required for homologous recombination repair of double-strand breaks. PLoS Genet. *7*, e1002271. https://doi.org/10.1371/journal.pgen.1002271.

77. Reginato, G., Cannavo, E., and Cejka, P. (2017). Physiological protein blocks direct the Mre11-Rad50-Xrs2 and Sae2 nuclease complex to initiate DNA end resection. Genes Dev. *31*, 2325–2330. https://doi.org/10.1101/gad.308254.117.

78. Delamarre, A., Barthe, A., de la Roche Saint-André, C., Luciano, P., Forey, R., Padioleau, I., Skrzypczak, M., Ginalski, K., Géli, V., Pasero, P., et al. (2020). MRX increases chromatin accessibility at stalled replication forks to promote nascent DNA resection and cohesin loading. Mol. Cell *77*, 395–410.e3. https://doi.org/10.1016/j.molcel.2019.10.029.

79. Chang, E.Y.C., Tsai, S., Aristizabal, M.J., Wells, J.P., Coulombe, Y., Busatto, F.F., Chan, Y.A., Kumar, A., Dan Zhu, Y., Wang, A.Y.H., et al. (2019). MRE11-RAD50-NBS1 promotes fanconi anemia R-loop suppression at transcription–replication conflicts. Nat. Commun. *10*, 4265. https://doi.org/10.1038/s41467-019-12271-w.

80. Wang, W., Daley, J.M., Kwon, Y., Xue, X., Krasner, D.S., Miller, A.S., Nguyen, K.A., Williamson, E.A., Shim, E.Y., Lee, S.E., et al. (2018). A DNA nick at Ku-blocked double-strand break ends serves as an entry site for exonuclease 1 (Exo1) or Sgs1–Dna2 in long-range DNA end resection. J. Biol. Chem. *293*, 17061–17069. https://doi.org/10.1074/jbc.RA118.004769.

81. Daley, J.M., Tomimatsu, N., Hooks, G., Wang, W., Miller, A.S., Xue, X., Nguyen, K.A., Kaur, H., Williamson, E., Mukherjee, B., et al. (2020). Specificity of end resection pathways for double-strand break regions containing ribonucleotides and base lesions. Nat. Commun. *11*, 3088. https://doi.org/10.1038/s41467-020-16903-4.

82. Coquel, F., Silva, M.J., Técher, H., Zadorozhny, K., Sharma, S., Nieminuszczy, J., Mettling, C., Dardillac, E., Barthe, A., Schmitz, A.L., et al. (2018). SAMHD1 acts at stalled replication forks to prevent interferon induction. Nature *557*, 57–61. https://doi.org/10.1038/s41586-018-0050-1.

83. Pizzi, S., Sertic, S., Orcesi, S., Cereda, C., Bianchi, M., Jackson, A.P., Lazzaro, F., Plevani, P., and Muzi-Falconi, M. (2015). Reduction of hRNase H2 activity in Aicardi-Goutières syndrome cells leads to replication stress and genome instability. Hum. Mol. Genet. *24*, 649–658. https://doi.org/10.1093/hmg/ddu485.

84. Kramarz, K., Saada, A.A., and Lambert, S.A.E. (2021). The analysis of recombination-dependent processing of blocked replication forks by bidimensional gel electrophoresis. Methods Mol. Biol. *2153*, 365–381. https://doi.org/10.1007/978-1-0716-0644-5_25.

85. Sabatinos, S.A., and Forsburg, S.L. (2009). Measuring DNA content by flow cytometry in fission yeast. Methods Mol. Biol. *521*, 449–461. https://doi.org/10.1007/978-1-60327-815-7_25.

86. Knutsen, J.H.J., da Rein, I.D., Rothe, C., Stokke, T., Grallert, B., and Boye, E. (2011). Cell-cycle analysis of fission yeast cells by flow cytometry. PLoS One *6*, e17175. https://doi.org/10.1371/journal.pone.0017175.

STAR★METHODS

KEY RESOURCES TABLE

REAGENT or RESOURCE	SOURCE	IDENTIFIER
Antibodies		
S9.6	Protein Expression and Purification Core facility, Institut Curie	N/A
Anti-dsDNA	Santa Cruz Biotechnology	Cat# sc-58749; RRID: AB_783088
Anti-ssDNA	Millipore	Cat# MAB3034; RRID: AB_11212688
Anti-GFP	Invitrogen	Cat# A11122; RRID: AB_221569
Normal Rabbit IgG	Cell Signaling Technology	Cat# 2729S; RRID: AB_1031062
Pierce™ Anti-HA magnetic beads	Thermo Scientific	Cat# 88837; RRID: AB_2861399
Anti-HA	Santa Cruz Biotechnology	Cat# sc-57592; RRID: AB_629568
Anti-tubulin	Abcam	Cat# Ab6160; RRID: AB_305328
HRP-AffiniPure Goat Anti-Mouse IgG	Jackson ImmunoResearch	Cat# 115-035-003; RRID: AB_10015289
Chemicals, peptides, and recombinant proteins		
Trioxsalen (Tri-methyl psoralen)	Sigma	T6137
Proteinase K	Euromedex	EU0090
RNase, DNase-free	Roche	11119915001
RNase T1	Thermo Scientific	EN0541
RNase A	Sigma	R5503
Sytox Green nucleic acid stain	Invitrogen	S7020
NuSieve™ GTG™ agarose	Lonza	50081
Lysing enzymes	Sigma	L1412
Zymolyase 100T	Amsbio	120493-1
Benzoylated Naphthoylated DEAE-cellulose (BND)	Sigma	B6385
Dynabeads protein G	Invitrogen	10003D
AvaI	New England Biolabs	R0152M
AseI	New England Biolabs	R0526M
NEB Buffer 2.1	New England Biolabs	B7202S
NEB Buffer 3.1	New England Biolabs	B7203S
Beta agarase	New England Biolabs	M0392L
5-FOA	Euromedex	1555
Methyl methane sulfonate (MMS)	Sigma	129925
Hydroxyurea (HU)	Sigma	H8627
Campthotecin (CPT)	Sigma	C9911
Ultra-Hyb buffer	Invitrogen	AM8669
DMA	Thermo Scientific	20660
Glycogen	Roche	10901393001
Caffeine	Sigma	C-8960
DEOXYCYTIDINE 5′-triphosphate [alpha-32P]	Perkin Elmer	BLU013Z250UC
Formaldehyde	Sigma	F-8775
Complete EDTA-free protease inhibitor cocktail tablets	Roche	1873580
Trichloroacetic acid	Sigma	T9159
Ethidium bromide solution	Sigma	E1510
UltraPure™ Agarose	Invitrogen	16500
N-lauryl sarcosine sodium salt solution	Sigma	61747
RNasIN® Plus	Promega	N261B
Protease inhibitor cocktail	Sigma	P8215

(*Continued on next page*)

Continued		
REAGENT or RESOURCE	SOURCE	IDENTIFIER
RNase III	New England Biolabs	M0245L
RNase H	New England Biolabs	M0297L
DNase I	Worthington Biochemical	LS006333
Critical commercial assays		
*Bca*BEST™ Labeling Kit	TaKaRa	6046
iQ SYBR green supermix	Biorad	1708882
Qiaquick PCR purification	Qiagen	28104
Deposited data		
Source Data Figure 1 unprocessed images and raw values	This study	Mendeley Data: https://doi.org/10.17632/k5xm5fpyxt.2
Source Data Figure 2 unprocessed images and raw values	This study	Mendeley Data: https://doi.org/10.17632/k5xm5fpyxt.2
Source Data Figure 3 unprocessed images and raw values	This study	Mendeley Data: https://doi.org/10.17632/k5xm5fpyxt.2
Source Data Figure 4 unprocessed images and raw values	This study	Mendeley Data: https://doi.org/10.17632/k5xm5fpyxt.2
Source Data Figure 5 unprocessed images and raw values	This study	Mendeley Data: https://doi.org/10.17632/k5xm5fpyxt.2
Source Data Figure 6 unprocessed images and raw values	This study	Mendeley Data: https://doi.org/10.17632/k5xm5fpyxt.2
Source Data Supplementary Figure S1 unprocessed images and raw values	This study	Mendeley Data: https://doi.org/10.17632/k5xm5fpyxt.2
Source Data Supplementary Figure S2 unprocessed images and raw values	This study	Mendeley Data: https://doi.org/10.17632/k5xm5fpyxt.2
Source Data Supplementary Figure S3 unprocessed images and raw values	This study	Mendeley Data: https://doi.org/10.17632/k5xm5fpyxt.2
Source Data Supplementary Figure S4 unprocessed images and raw values	This study	Mendeley Data: https://doi.org/10.17632/k5xm5fpyxt.2
Source Data Supplementary Figure S5 unprocessed images and raw values	This study	Mendeley Data: https://doi.org/10.17632/k5xm5fpyxt.2
Source Data Supplementary Figure S6 unprocessed images and raw values	This study	Mendeley Data: https://doi.org/10.17632/k5xm5fpyxt.2
Raw data Figure 6E	This study	Mendeley Data: https://doi.org/10.17632/k5xm5fpyxt.2
Figure Supplementary S6 FACS raw data	This study	Mendeley Data: https://doi.org/10.17632/k5xm5fpyxt.2
Figure 4E FACS raw data	This study	Mendeley Data: https://doi.org/10.17632/k5xm5fpyxt.2
Experimental models: Organisms/strains		
See Supplementary Table S1 for a list of yeast strains used in this study	Lambert's lab	Strain number
Oligonucleotides		
See Supplementary Table S2 for a list of oligonucleotides used in this study	Sigma	N/A
Software and algorithms		
Image processing and analysis in Java	Image J	https://imagej.nih.gov/ij/
Image Quant TL	GE Healthcare	http://gelifesciences.com
MetaMorph Microscopy Automation and Image Analysis Software	Molecular devices	https://www.moleculardevices.com
Other		
MicroSpin™ G-50 columns	GE Healthcare	27-5330-01
Poly-prep Chromatography columns	Biorad	731-1550
Gene Screen Plus nylon membrane	Perkin Elmer	NEF988001PK
Slide for microscopy 8 wells 6mm	Thermo Scientific	ER-201B-CE24
Mini-PROTEAN TGX Precast Gel 4-15 %	Biorad	4561086

RESOURCE AVAILABILITY

Lead contact

Further information and requests for reagents and resources should be directed to and will be fulfilled by the Lead Contact, Dr. Sarah A.E. Lambert (sarah.lambert@curie.fr).

Materials availability

All unique/stable reagents generated in this study are available from the lead contact without restriction.

Data and code availability

- Data have been deposited to Mendeley data and are publicly available as the date of publication. DOIs are listed in the key resources table (Mendeley Data: https://data.mendeley.com/datasets/k5xm5fpyxt).
- This paper does not report original code.
- Any additional information required to reanalyze the data reported in this paper is available from the lead contact upon request.

EXPERIMENTAL MODEL AND SUBJECT DETAILS

Yeast strains were freshly thawed from frozen stocks and grown at 25 °C or 30 °C using standard yeast genetics practices.

METHOD DETAILS

Standard yeast genetics

Yeast strains used in this study are listed in Table S1. The *rnh201-G72S* mutant was obtained by classical genetic techniques. Strains carrying the *RTS1*-RFB system were grown in supplemented EMM-glutamate, where the *RTS1*-RFB barrier was kept inactive by adding 60 μM thiamine (condition RFB OFF). To induce fork blockade, cells were washed twice in water and cultivated in fresh thiamine-free medium for 24 hours incubation (condition RFB ON). For *spp1-4* temperature-sensitive mutants, cells were grown at the permissive temperature of 25 °C in the RFB OFF condition, and then shifted to the semi-permissive temperature of 32 °C for 19 hours prior RFB induction. To assess the sensitivity of chosen mutants to genotoxic drugs, exponentially growing cultures were serially diluted and spotted onto plates containing hydroxyurea (HU), campthotecin (CPT) or methyl methanesulfonate (MMS).

Replication slippage assay

5-FOA (EUROMEDEX, 1555) resistant colonies were grown on uracil-containing plates with or without thiamine for 2 days at 30 °C. They were subsequently inoculated into EMMg supplemented with uracil, with or without thiamine, for 24 hours. Cells were diluted and plated on EMMg complete (for cell survival) and on EMMg uracil-free plates, both supplemented with 60 μM thiamine. To determine the reversion frequency, colonies were counted after 5 to 7 days of incubation at 30 °C as previously described.[45]

Analysis of replication intermediates by 2DGE

Exponentially growing cells ($2.5x10^9$) were treated with 0.1% sodium azide and mixed with frozen EDTA. Genomic DNA was cross-linked upon trimethyl psoralen (0.01 mg/mL, TMP, Sigma, T6137) addition to cell suspensions, for 5 min in the dark with occasional swirling. Then, cells were irradiated with UV-A (365 nm) for 90 s at a constant flow of 50 mW/cm^2.[84] Cell lysis was performed using 0.625 mg/mL lysing enzymes (Sigma, L1412) and 0.5 mg/mL zymolyase 100 T (Amsbio, 120493–1). Resulting spheroplasts were embedded into 2 % low-melting agarose (Lonza, 50081) plugs. Next, plugs were incubated overnight at 55 °C, in a digestion buffer with 1 mg/mL of proteinase K (Euromedex, EU0090), prior washing and storage in TE buffer (50 mM Tris, 10 mM EDTA) at 4 °C. DNA digestion was performed using 60 units per plug of restriction enzyme *Ase*I (NEB, R0526M). Samples were treated with beta-agarase (NEB, M0392L) and RNase A (Roche, 11119915001) and equilibrated to 0.3 M NaCl. Replication intermediates (RIs) were purified using BND cellulose columns (Sigma, B6385; Biorad, 731-1550), as previously described.[41] Double-stranded DNA (dsDNA) was eluted by washing with 0.8 M NaCl, 10mM Tris-HCl (pH 7.5), and 1 mM EDTA. DNA containing single-stranded regions (ssDNA), such as RIs, was eluted by addition of 3 ml of 1 M NaCl, 10 mM Tris-HCl (pH 7.5), 1 mM EDTA, and 1.8% caffeine (Sigma, C-8960). RIs were precipitated with glycogen (Roche, 1090139001) and then separated by two-dimensional electrophoresis using 0.35 % and 0.9 % (+EtBr) agarose gels (1xTBE) for the first and second dimensions, respectively. Migrated DNA was transferred to a nylon membrane (Perkin-Elmer, NEF988001PK) in 10x SSC and probed with ^{32}P-radiolabeled *ura4* probe (TaKaRa *Bca*BEST™ Labeling Kit, 6046 and alpha-^{32}P dCTP, Perkin-Elmer, BLU013Z250UC) in Ultra-Hyb buffer (Invitrogen, AM8669) at 42°C. Signal of replication intermediates was collected in phosphor-imager software (Typhoon-trio) and quantified by densitometric analysis with ImageQuantTL software (GE healthcare). The 'tail signal' was normalized to the overall signal corresponding to arrested forks (see Figure S2A for a detailed explanation)

For the *in vitro* treatment of purified RIs with RNase H1 (NEB, M0297L), the following modifications were performed. Samples were treated with RNase T1 (Thermo Scientific, EN0541) instead of RNase A. Eluted DNA fractions enriched in dsDNA and ssDNA were

both precipitated and washed with 70 % EtOH. 3 μg of isolated DNA was saved for the dotblot analysis. The rest was processed for 2DGE analysis: half was digested 2 hours at 37 °C with RNase H1 before migration on the first dimension.

Fork reversal detection by 1DGE

RIs were prepared as described above for 2DGE analysis. For *AscI*-containing constructs (Figures 4D–4G and S5), DNA digestion was done with 30 units per plug of restriction enzyme *AvaI* (NEB, R0152M). After the first dimensional migration, 0.35 % agarose gels were stained with EtBr. Crosslinks were reversed by UV-c (254nm) irradiation (5.555 kJ/m^2) before transfer to a nylon membrane. Transfer was performed using a vacuum machine in 0.5N NaOH for 1 hour and 50 min, at 50mBar. Membranes' probing was performed as for 2DGE. Probe 1 (Figure 4B, left panel) and Probe 2 used to detect the 3Kb-RA (Figure 4B, right panel) correspond to the *ura4* probe. The probes used to detect the 1Kb-RA (Figures 4 and S4) were made using *L3* primer combined either with *L600* (Figure 4B, left panel) or *Ase1Cen* (see primers list in Table S2, related to key resources table).

Nucleic acid extraction

$2.5x10^8$ cells from exponentially growing cultures were harvested, washed in water and resuspended in 600 μL of lysis solution (2% Triton X-100, 1% SDS, 0.1 M NaCl, 10 mM Tris pH 8, 1 mM EDTA) and 600 μL phenol-chloroform. Cell lysis was performed with a Precellys homogenizer. After lysate clarification, nucleic acids were precipitated by adding cold 100% EtOH. Resulting pellets were then washed in cold 70% EtOH, air dried and let to resuspend into 100μL of water overnight at 4 °C.

Dot blot

Before blotting, all DNA samples were evenly split and submitted to the following digestions. 4μg DNA of each sample were treated with 6U RNase III (NEB, M0245L) for 2 hours at 37°C, followed by inactivation for 20 min at 65°C. As controls, for each sample, the same amount of DNA was additionally treated with 10U RNase H1 (NEB, M0297L) or 50U DNase I (Worthington Biochemical, LS006333). All digested products were diluted to an equal concentration in 2x SSC and then serially diluted. 200μL of the resulting dilutions were spotted onto a Nylon membrane (Perkin-Elmer, NEF988001PK), using a dot blot apparatus. Spotting was performed in replicates on the same membrane, that is subsequently cut to isolate replicates that will be incubated for 2 hours 30 min with the following antibodies: S9.6 (I. Curie, 1:5.000 in TBS-Tween 5% milk), α-dsDNA (Santa Cruz, Sc-58749; 1:5.000 in TBS-Tween 5% BSA) or α-ssDNA (Millipore, MAB3034; 1:10.000 in TBS-Tween 5% BSA). Goat anti-mouse HRP conjugate (Jackson ImmunoResearch, 115-035-003) was used as secondary antibody and was incubated with all membranes (1:10.000 in TBS-Tween 5% milk) for 1 hour. Blotting and all incubations were done at room temperature.

Flow cytometry

Flow cytometry analysis of DNA content was performed as described previously.[85] Briefly, cells fixed in 70 % EtOH were washed with 50 mM sodium citrate then digested with RNase A (Sigma, R5503) for 2 hours and stained with 1μM Sytox Green nucleic acid stain (Invitrogen, S7020). Samples were subjected to flow cytometry using FACSCANTO II (BD Biosciences). For Figure S6C, asynchronous cell populations were analysed using the flow cytometric method that exploit the width and the total area of the DNA-associated signal to discriminate G1 and G2 phases.[86]

Live cell imaging

All image acquisition was performed on the PICT-IBiSA Orsay Imaging facility of Institut Curie. For snapshot microscopy, in RFB OFF and RFB ON conditions, cells were grown in filtered supplemented EMM-glutamate, with or without thiamine respectively, for 24 hours. Exponentially growing cultures were centrifuged and resuspended in 50 μL of fresh medium. 2 μL from this concentrated solution was dropped onto a Thermo Scientific slide (ER-201B-CE24) covered with a thin layer of 1.4 % agarose in filtered EMMg. 13 z-stack pictures (each z step of 300 nm) were captured using a Spinning Disk Nikon inverted microscope equipped with the Perfect Focus System, Yokogawa CSUX1 confocal unit, Photometrics Evolve512 EM-CCD camera, 100X/1.45-NA PlanApo oil immersion objective and a laser bench (Errol) with 491 and 561 nm diode lasers, 100 mX (Cobolt). Pictures were collected with METAMORPH software and analyzed with ImageJ. To investigate the colocalization between Pku80-GFP and *lacO*-bound mCherry-LacI, both channels were merged. Foci that merged or partially overlap were counted as colocalization event.

For the analysis of Pku80-GFP foci formation in response to CPT treatment, cells were grown in complete media and 20μM CPT was added 4 hours prior slide preparation. Cells were visualized with a Nikon inverted microscope as described above, using only a 491 nm diode laser, 100 mX (Cobolt). Pictures were collected with METAMORPH software and analyzed with ImageJ.

Pku80-GFP foci required observer-based thresholding before analysis.[61] Threshold was put as the same level for each genetic background analyzed within the same experiment. Data were collected from at least 3 independent biological repeats.

Movie analysis

To study the colocalization time between the *LacO*-marked RFB (LacI foci) and Rnh1-D129N-GFP foci, cells were prepared and visualized with a Nikon inverted microscope as described above, using two fluorescent channels with 491 and 561 nm diode lasers, 100 mX (Cobolt). Images were captured every 10 s with 21 optical slices (each z step of 200 nm) for 45 min with 200 ms exposure time both for GFP and mCherry channels, using METAMORPH software. Movies have been mounted using ImageJ. To investigate the

colocalization between Rnh1-D129N-GFP and *lacO*-bound mCherry-LacI, both channels were merged. The duration of colocalization events was estimated based on the overlap of *RTS1*-RFB *LacO*/lacI-mCherry and Rnh1-D129N-GFP signals (Figure S1).

Chromatin Immunoprecipitation (ChIP)

Chromatin immunoprecipitations against RPA (Ssb3-YFP) were performed as described in [44] with the following modifications. 2x100 mL of culture (at $1x10^7$ Cells/ml density) for each condition (*RTS1*-RFB OFF/ON) was crosslinked with 10 mM DMA (dimethyl adipimidate, thermo scientific, 20660) and subsequently 1% formaldehyde (Sigma, F-8775). Each duplicate was frozen in liquid nitrogen and then lysed by bead beating in 400 μL of lysis buffer (50 mM HEPES pH 7.5, 1 % Triton X100, 0.1 % Nadeoxycholate, 1 mM EDTA with 1 mM PMSF and Complete EDTA-free protease inhibitor cocktail tablets (Roche, 1873580). Chromatin sonication was performed using a Diagenode Bioruptor in a High mode (10 cycles of 30s ON and 30s OFF). For each condition, duplicates were pooled (2x400 μL of sonicated chromatin) and overnight immunoprecipitation was performed as follows: 300 μL was incubated with anti-GFP antibody (Invitrogen, A11122) at 1:150 while 300 μL was incubated with Normal Rabbit IgG antibody (Cell Signaling Technology, #2729S) at concentration 1:75. 5 μL was preserved as INPUT fraction. Next morning Dynabeads Protein G (Invitrogen, 10003D) were added for 1 hour and immunoprecipitated complexes have been decrosslinked for 2 hours at 65°C. DNA was purified with a Qiaquick PCR purification kit (QIAGEN, 28104) and eluted in 400 μL of water. qPCR (iQ SYBR green supermix, Biorad, 1708882, primers listed in Table S2, Related to key resources table) was performed to determine the relative amounts of DNA. Calculated starting quantity values (based on standard curves for each pair of primers) were normalized by substracting the rabbit IgG control signal from the specific GFP signal. RPA enrichment is presented as ON/OFF ratio.

Pku70-3xHA ChIP was performed as described in [27]. Briefly, experiments were performed as follows: samples were crosslinked with 1 % formaldehyde for 15 min. Sonication was performed using a Diagenod Bioruptor at High setting for 8 cycles (30s ON and 30s OFF). Immunoprecipitation was performed using 50 μl anti-HA antibody coupled to magnetic beads (Thermo Scientific, Pierce 88837) for 600μl of sonicated chromatin. Cell lysis and immunoprecipitation steps were performed in presence of RNase inhibitors (10 units/sample of RNasIN® Plus, Promega, N261B). Crosslink was reversed over night at 70 °C, followed by proteinase K treatment. DNA was purified using Qiaquick PCR purification kit and eluted in 40 μl of water.

Whole protein extract analysis

Aliquots of $2x10^7$ cells from the cultures used for Pku70-3HA ChIP experiments were collected. Cells were disrupted by bead beating in 1 mL of 20 % TCA (Sigma, T9159). Pellets of denatured proteins were washed with 1M Tris pH 8 and resuspended in 2x Laemmli buffer (62.5 mM Tris pH 6.8, 20 % glycerol, 2 % SDS, 5 % β-mercaptoethanol with bromophenol blue). Samples were boiled before being subjected to SDS-PAGE on Mini-PROTEAN TGX Precast Gel 4-15 % (Biorad, 4561086). Western blot using anti-HA (Santa Cruz Biotechnology, sc-57592) or anti-tubulin (Abcam, Ab6160) antibodies was performed.

Purification of S. pombe Ku70-80

Full-length PKu70 and PKu80 were co-expressed in Sf21 insect cells and used for calorimetry and EMSA analyses. A 10His-tag was added on the N terminus of PKu80. Protein production was initiated in Sf21 cells by infection with the baculovirus stock at MOI of 5x10-3 and cells were collected 5-6 days after the infection (3-4 days after the proliferation arrest). Cells were sonicated and the supernatant was incubated with Benzonase (300 units for 30 min at 4°C). The Ku heterodimer was purified on a NiNTA-Agarose affinity column (Protino, Macherey Nagel) with a 1M NaCl wash step to remove DNA excess. The eluted Ku was then bound onto an anion exchange column (Resource Q, GE Healthcare) equilibrate with buffer Q (20 mM Tris pH 8.0, 50 mM NaCl, 50 mM KCl, 10 mM β-mercaptoethanol). The final yield was ~4 mg of purified heterodimer by liter of culture.[73]

Calorimetry

Interactions between Ku and DNA or RNA:DNA substrates were determined by isothermal titration calorimetry (ITC) using a VP-ITC calorimeter (Malvern). Prior to measurements, all solutions were degassed under vacuum. The reaction cell of the ITC (volume 1.8 mL) was loaded with Ku heterodimers. Proteins were extensively dialyzed against 20 mM Tris, pH 8.0, 150 mM NaCl, and 5 mM β-mercaptoethanol. The Ku heterodimer present in the cell was titrated by automatic injections of 10 μL of the different DNA and OF substrates. Enthalpy ΔH (in $kcal.mol^{-1}$), stoichiometry of the reaction N, and association constant Ka (in M^{-1}) were obtained by nonlinear least-squares fitting of the experimental data using the single set of independent binding sites model of the Origin software provided with the instrument. Control experiments were performed with DNA and OF molecules injected into the buffer to evaluate the heat of the dilution. The experiments were performed at 25°C. The sequences of the substrates used for the calorimetry are reported in Figure S7.

EMSA

Binding reactions (10 μL) were performed by incubating Ku and the annealed oligonucleotides listed above. One oligonucleotides is labelled with a FAM fluorophore. They are used at a final concentration of 40nM, with the indicated final concentrations of proteins in 10mM Tris-HCl pH8, 50mM NaCl (with 5% Glycerol). Reactions were incubated at 4°C for 30 minutes and fractionated by 6% PAGE (19%/1% [w/v] Acrylamide:Bis-acrylamide) in 0.5x standard Tris-borate- EDTA (TBE) buffer at 80 V for 45 min at 4°C. After electrophoresis, DNA was visualized using a ChemiDoc MP imaging system (Bio-Rad) by direct detection of the fluorescently labeled DNA (FAM).

The sequences of the substrates used for EMSA are reported in Table S2 (list of primers used in this study, Related to Key Resources Table of STAR methods section).

QUANTIFICATION AND STATISTICAL ANALYSIS

Quantitative densitometric analysis of Southern-blots was performed using ImageQuant software. The 'tail signal' of resected forks was normalized to the overall signal of arrested forks.

Cell images were collected using METAMORPH software. They were processed and analyzed using ImageJ software.

Definitions of represented values and error bars are mentioned within the figure legends. For most experiments, the number of samples is $n > 3$, obtained from independent biological replicate to ensure biological reproducibility.

Statistical analysis was carried using Mann-Whitney U tests and Student's t test, as mentioned within the figure legends.

Extended Summary in French

Résumé étendu en français

INTRODUCTION

Le maintien de la stabilité du génome est crucial pour garantir la transmission à fidèle de l'information génétique. Des défauts dans le processus de réplication de l'ADN, connus sous le nom de stress de réplicatif, ont émergé comme une source majeure d'instabilité génomique, contribuant au développement du cancer. La principale cause du stress réplicatif est l'altération de la progression des fourches de réplication causée par différents types d'obstacles ou de barrières physiques, ou encore par un déséquilibre métabolique conduisant à des ressources limitées pour la duplication de la chromatine. La perte de capacité de réplication du génome conduit souvent à des défauts de ségrégation des chromosomes en mitose. Pour éviter une duplication incomplète des chromosomes, les cellules exploitent des voies de réparation multiples pour i) rétablir la compétence de synthèse de l'ADN au niveau des fourches dysfonctionnelles ou cassées, ii) protéger l'intégrité des fourches de réplication bloquées, iii) combler des brèches d'ADN simple brin laissées derrières les fourches de réplication.

Parmi les mécanismes de réparation de l'ADN qui contribuent à tolérer le stress de réplication, la voie de la recombinaison homologue (RH) est essentielle pour assurer une synthèse continue de l'ADN et une duplication complète du génome (Chakraborty et al., 2023). Des études menées chez la levure ont montré que la machinerie de RH contribue à la réplication complète de l'ADN en rétablissant la compétence de réplication des fourches dysfonctionnelles via le mécanisme de réplication dépendante de la recombinaison (RDR). Contrairement à de nombreux modèles établis dans la littérature, ce mécanisme de RDR survient en absence de cassures double-brin de l'ADN. De façon surprenante, le mécanismes de RDR s'accompagne d'une synthèse d'ADN non canonique, associée à une fréquence de mutation plus élevée, comparée à la synthèse de l'ADN réplicative (Mizuno et al., 2009; Lambert et al., 2010). Cela indique qu'en cas d'échec de la réplication, l'achèvement de la duplication des chromosomes s'accompagne de l'utilisation de mécanismes mutagènes, ce qui peut entraîner une instabilité du génome accrue.

Le noyau des cellules eucaryotes se compose de différents compartiments, suivant la nature de la chromatine, montrant des capacités de réparation de l'ADN distinctes. De plus, les machineries de réparation de l'ADN sont également spatialement organisées (Kalousi and Soutoglou, 2016; Lemaitre et al., 2014). Un exemple correspond aux régions d'hétérochromatine ou le nucléole qui sont réfractaires à certains modes de réparation, alors que la région des pores nucléaires sont plus favorables à des modes de réparation alternatifs. Par conséquent, dans certains cas, la chromatine endommagée peut présenter une certaine mobilité afin de changer de compartiments nucléaires pour une réparation de l'ADN plus adaptée.

Chez différents organismes eucaryotes, des études ont montré que des cassures double-brin se produisant dans l'hétérochromatine échappent à leur compartiment afin de favoriser un mode de réparation par la RH. De plus, les cassures d'ADN difficiles à réparer et les télomères érodés se déplacent vers les complexes des pores nucléaires (NPC). Ces phénomènes de relocalisation vers la périphérie nucléaire ont aussi été observés dans le cas de dommages réplicatifs. En effet, chez la levure, les fourches de réplication bloquées soit par des séquences formant des structures secondaires, soit par des protéines liées à l'ADN, soit dans les séquences télomériques, se déplacent vers la périphérie nucléaire pour s'ancrer au NPC (Nagai et al., 2008; Su et al., 2015; Whalen et al., 2020; Aguilera et al., 2020; Kramarz et al., 2020). Des observations similaires ont été faites lorsque la réplication des télomères humains est perturbée. (Pinzaru et al., 2020). Enfin, l'inhibition globale de la synthèse d'ADN chez l'homme conduit à une relocalisation des fourches altérées vers la périphérie nucléaire (Lamm et al., 2020).

Des études pionnières ont indiqué que la SUMOylation sert de signal majeur pour coordonner la position nucléaire des cassures double-brin de l'ADN et des fourches de réplication bloquées. La SUMOylation est une modification post-traductionnelle basée sur la fixation covalente d'une particule SUMO à une protéine cible (Celen and Sahin, 2020). La SUMOylation se produit à travers une cascade enzymatique impliquant l'enzyme activatrice E1, l'enzyme de conjugaison E2 et la ligase E3 SUMO qui catalyse la conjugaison de SUMO à un substrat. SUMO peut être attaché comme un monomère sur une lysine acceptrice unique, générant la monoSUMOylation. Les substrats peuvent également être modifiés avec une particule monoSUMO sur plusieurs lysines, ce qui est appelé multiSUMOylation. De plus, SUMO a la capacité de former des chaînes polymériques (polySUMOylation) dans lesquelles les particules SUMO successives sont conjuguées à une lysine interne de la particule SUMO, conduisant à la formation de

chaines de SUMOylation (Pichler et al., 2017). Tout comme d'autres modifications post-traductionnelles, la SUMOylation est hautement dynamique et réversible. Le clivage de la particule SUMO des cibles est réalisé par des protéases spécifiques de la SUMO, qui appartiennent à la famille Ulp/SENP.

Au niveau moléculaire, la SUMOylation peut avoir diverses conséquences biologiques en affectant l'activité, la localisation et/ou la stabilité de la protéine cible (Geiss-Friedlander and Melchior, 2007; Wilkinson and Henley, 2010). La SUMOylation peut également servir de signal de recrutement pour d'autres protéines. Celles-ci comprennent une classe spécifique d'ubiquitine E3 ligases appelées ligases d'ubiquitine ciblées par SUMO (STUbL, pour SUMO-targeted ubiquitin ligases). En général, toutes les STUbL se caractérisent par deux éléments structurels clés qui déterminent leurs fonctions enzymatiques : un ensemble de motifs d'interaction SUMO (SIMs, pour SUMO interacting motifs) permet le recrutement et la liaison à des substrats multiSUMOylés et polySUMOylés, tandis qu'un domaine de type E3 RING est nécessaire pour l'activité de ligase d'ubiquitine. Des études génétiques et biochimiques ont montré que les STUbL régulent l'homéostasie de la SUMOylation en ciblant les protéines SUMOylées pour une dégradation médiée par le protéasome (Chang et al., 2021).

Le métabolisme lié à la SUMOylation est spatialement ségrégé dans les cellules eucaryotes. La localisation nucléaire des enzymes liées au métabolisme SUMO détermine leur spécificité de substrat, offrant ainsi un autre moyen de contrôler les niveaux de SUMOylation. Par exemple, la séquestration des SUMO protéases à proximité du NPC a été démontrée. Des études chez les levures de fission et de bourgeonnement ont révélé que la localisation de l'Ulp1 à la périphérie nucléaire nécessite des nucléoporines du NPC, soit du complexe Y soit du panier nucléaire. Dans les deux systèmes de levure, l'altération de l'ancrage de Ulp1 aux NPCs conduit à une mauvaise localisation dans le nucléoplasme et à une dégradation médiée par le protéasome subséquente (Zhao et al., 2004; Palancade et al., 2007; Nie et al., 2015). De même, comme chez les levures, la protéase SUMO SENP2 de mammifères est enrichie aux NPCs, et la perte de cet ancrage entraîne une diminution globale de la SUMOylation (Zhang et al., 2002). Ces données mettent en évidence un rôle des NPCs en tant que centre pour la signalisation médiée par la SUMOylation, role conservé au cours de l'évolution.

Des études chez les levures et les mammifères ont décrit de nombreuses cibles de SUMO, incluant des composants du réplisome et des protéines de réparation de l'ADN, y compris les facteurs de la RH. De façon intéressante, le niveau de SUMOylation augmente en réponse à des stress de réplication ou aux dommages de l'ADN (Zhao and Blobel, 2005; Watts et al., 2007; Psakhye and Jentsch, 2012; Cremona et al., 2012; Jentsch and Psakhye, 2013). Les levures portant des mutations dans la voie de SUMOylation sont sensibles à des agents génotoxiques, mais l'abrogation des sites accepteurs de SUMO sur des protéines cibles individuelles de la RH ne conduit qu'à des phénotypes légers (Psakhye and Jentsch, 2012). Cette contradiction entre les phénotypes forts affichés par les mutations dans les enzymes liées au métabolisme de la SUMOylation et l'absence de phénotypes notables des mutants défectueux en SUMOylation semble caractéristique de la voie SUMO et peut être expliquée par ce qu'on appelle « l'effet d'ensemble ». Lorsque la SUMOylation est limitée à une zone locale spécifique, elle favorise la modification d'un groupe de protéines. Ces protéines SUMOylées agissent ensuite de manière synergique par une combinaison d'interactions SUMO:SIM. Ceci est particulièrement important dans le cas de processus qui nécessitent l'action coordonnée de plusieurs composants.

OBJECTIFS

Des études menées chez plusieurs organismes modèles ont démontré que différents types de fourches de réplication dont la progression est entravée se déplacent vers la périphérie nucléaire et s'ancrent aux NPCs de manière dépendante de la SUMOylation. Une telle relocalisation médiée par SUMO est un mécanisme de protection important pour maintenir la stabilité du génome. Un travail récent de notre équipe a révélé que, chez la levure de fission, les fourches de réplication bloquées par une protéine liée à l'ADN se relocalisent et s'ancrent aux NPCs, une étape nécessaire pour la reprise de l'a synthèse d'ADN (Kramarz et al., 2020). Ce déplacement vers la périphérie nucléaire dépend de la formation de chaines SUMO et la SUMO E3 ligase Pli1. Cependant, les chaînes SUMO limitent l'efficacité de la reprise de la réplication, nécessitant ainsi d'être éliminées par la protéase SENP Ulp1 et le protéasome, dont les activités sont enrichies à la périphérie nucléaire. Nous avons précédemment constaté que le complexe Y du NPC joue un rôle critique dans la reprise de la synthèse de l'ADN médiée par la RH. Cette fonction a été liée au rôle de la nucléoporine Nup132 dans la promotion de la localisation d'Ulp1 à la périphérie nucléaire. De plus, nous avons montré que la SUMOylation par Pli1 protège l'intégrité des fourche bloquées et restant localisées dans le nucléoplasme.

Cependant, en raison de certaines limitations de notre travail précédent, de nombreux aspects du modèle proposé sont restés inexplorés. Par conséquent, en combinant différentes approches moléculaires et génétiques, j'ai cherché à décrypter comment la ségrégation spatiale du métabolisme de SUMOylation, en combinaison avec les NPCs, protège l'intégrité des fourches de réplication et leur compétence de réplication. Une grande partie de mon projet de doctorat a été consacrée à mieux comprendre les aspects dynamiques des mécanismes engagés à la périphérie nucléaire qui sont impliqués dans le redémarrage des fourches bloquées par un mécanisme dépendant de la recombinaison homologue. De plus, j'ai cherché à caractériser la vague de SUMOylation qui se produit au site de blocage de fourche. J'ai également abordé les déterminants clés de l'intégrité des fourches de réplication au sein d'un noyau compartimenté.

SYSTÈME EXPÉRIMENTAL

Pour atteindre mes objectifs, j'ai utilisé une barrière de fourche de réplication (RFB, pour Replication fork Barrier) conditionnelle et site-spécifique dans le génome de la levure de fission. Dans ce système, l'activité de la RFB est médiée par la protéine Rft1 qui se lie à la séquence *RTS1* pour bloquer la progression du réplisome de manière polaire. Afin de créer un système inductible, le gène endogène codant pour Rtf1 a été placé sous le promoteur nmt41 répressible par la thiamine. Si la thiamine est présente dans le milieu de culture, Rtf1 n'est pas exprimée et la *RTS1*-RFB reste inactive (condition appelée OFF). Inversement, après élimination de la thiamine, nmt41 n'est plus réprimé et Rtf1 est exprimée, conduisant à l'activation de la *RTS1*-RFB (condition appelée ON). Les fourches bloquées par la barrière de réplication deviennent dysfonctionnelles et peuvent être sauvées de deux manières. Elles sont soit résolues par une fourche convergente, soit, si cela ne se produit pas à temps, elles sont redémarrées par la réplication dépendante de la recombinaison (RDR) en 20 minutes. Le mécanisme de RDR est associé à une synthèse d'ADN non canonique, les deux brins étant répliqués par la polymérase delta (Lambert et al., 2010; Mizuno et al., 2013; Tsang et al., 2014; Miyabe et al., 2015; Nguyen et al., 2015). Des essais génétiques, cellulaires et moléculaires complémentaires ont été développés au laboratoire pour étudier les mécanismes moléculaires et les acteurs clés impliqués dans les événements se produisant au niveau du blocage de la fourche de réplication au locus *RTS1*-RFB. Ces techniques permettent : (1) de mesurer l'efficacité de redémarrage des fourches par la voie de la recombinaison homologue (essai génétique); (2) d'analyser les intermédiaires de réplication générés au niveau des fourches bloquées (électrophorèse

bidimensionnelle en gel d'agarose, 2DGE); (3) de suivre le recrutement de protéines sur le locus en condition de blocage de fourche en cellules uniques (microscopie combinée à un système rapporteur fluorescent) ou dans une population cellulaire (immuno-précipitation de la chromatine, ChIP); (4) de suivre in vivo le destin et la position nucléaire du locus (microscopie combinée à un système rapporteur fluorescent) (Ait Saada et al., 2017; Teixeira-Silva et al., 2017; Hardy et al., 2019; Kramarz et al., 2020).

RÉSULTATS

Le panier nucléaire favorise la réplication dépendante de la recombinaison de manière pré- et post-ancrage.

Nous avons précédemment montré que la nucléoporine Nup132 (ScNup133, HsNUP133), un composant du complexe Y du NPC, joue un rôle après l'ancrage en favorisant le redémarrage des fourches par la recombinaison en assurant la séquestration d'Ulp1 à la périphérie nucléaire (Kramarz et al., 2020). Cette séquestration d'Ulp1 est nécessaire pour contrer l'effet inhibiteur des chaînes SUMO sur l'efficacité de la RDR.

Durant mon doctorat, j'ai montré que les nucléoporines du panier nucléaire, un autre sous-complexe du NPC, sont également impliquées dans le redémarrage des fourches médiées par la recombinaison de deux manières différentes. En combinant notre analyse génétique et notre approche de microscopie sur cellules vivantes, j'ai découvert que la nucléoporine du panier nucléaire Nup60 favorise une reprise efficace des fourches de manière post-ancrage en assurant la séquestration d'Ulp1 à la périphérie nucléaire. Cela est cohérent avec la situation dans la levure bourgeonnante, où il a été démontré que ScNup60 était nécessaire pour localiser et stabiliser la SUMO-protéase Ulp1 à la périphérie nucléaire (Zhao et al., 2004).

J'ai en outre démontré qu'un autre composant du panier nucléaire, la nucléoporine Alm1, contribue également à la reprise de la réplication au niveau des fourches arrêtées par la RFB, à la fois avant et après l'ancrage. J'ai révélé que la perte d'Alm1 entraînait une absence de relocalisation/ancrage des fourches arrêtées au NPC. L'absence de relocalisation dans les cellules déficientes en Alm1 est plutôt un effet indirect dû à deux caractéristiques, à savoir les altérations de la morphologie nucléaire et la réduction de l'abondance des NPC. De manière intrigante, l'ancrage artificiel de la RFB aux NPC n'est pas suffisant pour sauver le défaut de RDR des cellules *alm1*Δ, ce qui indique qu'Alm1 est également nécessaire pour favoriser le redémarrage des fourches arrêtées lors de

leur relocalisation aux NPC. Contrairement à Nup60, ce rôle post-ancrage d'Alm1 n'est pas lié à la séquestration spatiale d'Ulp1 à la périphérie nucléaire. Néanmoins, le défaut de RDR des cellules *alm1*Δ n'a pas été contourné en empêchant la formation de chaînes SUMO, confirmant que ce mutant ne souffre pas d'une incapacité à annuler la toxicité des chaînes SUMO. Il a été également démontré que plusieurs sous-unités du protéasome étaient délocalisées depuis la périphérie nucléaire dans les cellules *alm1*Δ (Salas-Pino et al., 2017). Nous avons précédemment identifié que l'activité du protéasome est nécessaire pour promouvoir le mécanisme de RDR de manière post-ancrage (Kramarz et al., 2020). Par conséquent, le deuxième rôle d'Alm1 repose vraisemblablement sur sa capacité à enrichir les composants du protéasome à la périphérie nucléaire.

Dans l'ensemble, mon travail identifie des rôles distincts des composants du panier nucléaire dans la promotion d'une reprise efficace de la réplication au niveau des fourches arrêtées, Nup60 étant impliqué dans la séquestration spatiale d'Ulp1 et Alm1 garantissant l'enrichissement des sous-unités du protéasome à la périphérie nucléaire.

Les activités d'Ulp1 et du protéasome régulent différemment la dynamique de reprise de la synthèse d'ADN au niveau des fourches de réplication arrêtées.

Nous avons précédemment montré que la SUMO-protéase Ulp1et le protéasome sont nécessaires pour un redémarrage efficace des fourches de réplication par la recombinaison (Kramarz et al., 2020). Ici, en cartographiant l'utilisation des ADN polymérases, je révèle que ces deux facteurs, Ulp1 et le protéasome, assurent une dynamique de synthèse d'ADN optimale au niveau des fourches redémarrées par deux mécanismes distincts.

Tout d'abord, j'ai identifié un rôle pour Ulp1 pour engager la synthèse d'ADN Polδ/Polδ au niveau des fourches redémarrées. Ce mécanisme nécessite la séquestration d'Ulp1 à la périphérie nucléaire, coordonnée par la nucléoporine Nup132 du complexe Y et la nucléoporine du panier nucléaire Nup60, et permet de contrecarrer les effets toxiques des chaines SUMO. Ainsi, les NPC associés à Ulp1 favorisent une initiation efficace de la reprise de la synthèse d'ADN, sans toutefois affecter la vitesse des fourches de réplication redémarrées.

De plus, j'ai établi que l'activité du protéasome contribue au maintien d'une dynamique de synthèse de l'ADN médiée par la recombinaison en favorisant la progression des polymérases d'ADN au niveau des fourches redémarrées. Cette fonction se produit indépendamment de l'effet toxiques des chaines SUMO, bien que nous ayons précédemment identifié un rôle de l'ubiquitine E3 ligase qui cible les protéines SUMOylées pour la dégradation (STUbL) dans le mécanisme du RDR. Cela peut donc indiquer que les facteurs monoSUMOylés ou les cibles multiSUMOylées sans chaîne (modifiées avec des motifs SUMO individuels à de multiples sites) peuvent être les cibles potentielles de la voie dépendante de STUbL et du protéasome pour garantir la vitesse des polymérases d'ADN redémarrées.

Dans l'ensemble, mes données fournissent de nouvelles informations mécanistiques sur la régulation du redémarrage de la réplication dépendante de la recombinaison au NPC, montrant ainsi la nécessité pour les fourches dysfonctionnelles de changer de positionnement au sein du noyau. Les NPC associées à Ulp1, en luttant contre l'effet inhibiteur des chaînes SUMO, contribuent à une initiation efficace de la synthèse d'ADN réparatrice, tandis que les NPC associées au protéasome favorisent la progression de la synthèse d'ADN réparatrice, et ceci de manière indépendante des chaînes SUMO. Il est intéressant de noter que les activités d'Ulp1 et du protéasome ne peuvent pas se substituer l'une à l'autre, et plusieurs cibles SUMOylées et/ou ubiquitinées sont probablement impliquées pour réguler finement la synthèse d'ADN dépendante de la HR.

Les fourches arrêtées au niveau de la RFB subissent une vague locale de SUMOylation dépendante de Pli1.

Les événements de SUMOylation dépendants de Pli1 sont impliqués dans la relocalisation des fourches arrêtées vers la périphérie nucléaire. Ils contrôlent finement la réplication dépendante de la recombinaison dans le nucléoplasme et assurent la protection des fourches de réplication arrêtées (Kramarz et al., 2020). Cependant, la contribution de Pli1 à l'accumulation de SUMO conjugés aux fourches arrêtées n'avait pas été abordée.

En utilisant un anticorps SUMO généré dans notre laboratoire, j'ai montré pour la première fois une accumulation locale de formes conjuguées de SUMO au niveau des fourches bloquées. Cet enrichissement détectable de la SUMOylation lors de l'activation de la RFB soutient le modèle selon lequel de multiples cibles, au lieu d'une

seule, sont modifiées par SUMO. En effet, en cas de dommages à l'ADN, il est connu que la SUMOylation affecte un ensemble de protéines plutôt que des protéines individuelles, ce qui entraîne des modifications simultanées à plusieurs sites de différents facteurs (Psakhye and Jentsch, 2012).

Chez la levure à fission, deux ligases SUMO E3 ont été identifiées à ce jour : Pli1 et Nse2. Chacune d'entre elles a des cibles spécifiques et au moins certaines fonctions non redondantes dans le maintien de la stabilité du génome (Watts et al., 2007). J'ai donc examiné la répartition des rôles de ces deux ligases SUMO E3 de la levure à fission. Pour ce faire, j'ai généré des formes mutées de Pli1 et Nse2 spécifiquement affectés pour leur activité SUMO ligase en introduisant des mutations ponctuelles dans leurs domaines RING. Ces mutations ont été rapportées pour abolir la fonction ligase SUMO des deux ligases (Xhemalce et al., 2004; Andrews et al., 2005).

J'ai observé que la relocalisation des RFB actives vers le NPC dépend de l'activité SUMO E3 ligase de Pli1, mais pas de Nse2. En utilisant notre test génétique d'efficacité de redémarrage des fourches, j'ai constaté que la réplication dépendante de la recombinaison ne nécessite pas la SUMOylation médiée par Nse2. J'ai également observé que la SUMOylation médiée par la SUMO E3 ligase Pli1 est essentielle pour maintenir l'intégrité des fourches de réplication arrêtées, tandis que la seconde SUMO E3 ligase Nse2 semble être dispensable. Il est important de noter que j'ai confirmé que la fonction de Pli1 dans la protection des fourches de réplication dépend de son activité SUMO E3 ligase. Plus précisément, la monoSUMOylation est suffisante pour limiter la dégradation des brins naissants au niveau des fourches de réplication arrêtées qui échouent à changer de position nucléaire et restent localisées dans le nucléoplasme.

Quel pourrait être le mécanisme par lequel Pli1 assure la régulation négative de la dégradation des brins naissants ? La SUMOylation peut recruter et/ou favoriser la rétention optimale de facteurs de RH connus pour leur rôle dans la protection des fourches de réplication. En effet, j'ai découvert qu'en cas d'activation de la RFB, Pli1 favorise une vague de SUMOylation localisée et favorise également l'enrichissement de Rad51 au niveau de la RFB active. En soutien à l'idée que la SUMOylation médiée par Pli1 favorise le recrutement de Rad51 aux fourches de réplication arrêtées, les SUMO E3 ligases humaines PIAS1 et PIAS4, ont également été montrées comme

nécessaires pour l'accumulation de RAD51 sur les sites contenant des dommages à l'ADN (Shima et al., 2013).

Le métabolisme spatialement confiné de la SUMOylation assure l'intégrité de la fourche de réplication dans un noyau compartimenté.

La résection des extrémités d'ADN doit être étroitement régulée, car une résection insuffisante ou excessive menace la stabilité du génome (Ronato et al., 2020; Cejka and Symington, 2021). En particulier, la persistance de longs fragment d'ADN simple brin, générées par exemple au niveau des fourches de réplication arrêtées, sont extrêmement vulnérables aux agents endommageant l'ADN et sont propices à une hyper-mutation (Saini and Gordenin, 2020). Par conséquent, protéger les fourches de réplication contre une dégradation importante est essentiel pour prévenir l'instabilité du génome.

Mes données indiquent que l'interaction entre la localisation de la SUMO-protéase Ulp1 et la position nucléaire contribue à maintenir l'intégrité des fourches de réplication arrêtées. Les fourches arrêtées, qui ont échoué à s'ancrer aux NPC, étaient plus fréquemment soumises à une longue résection médiée par la nucléase Exo1 lorsque Ulp1 n'était plus localisé à la périphérie nucléaire (dans la mutation *nup131*Δ *nup132*Δ). En revanche, lorsque Ulp1 était correctement distribué à la périphérie nucléaire, les fourches arrêtées positionnées dans le nucléoplasme ne subissaient pas de dégradation importante (dans les mutations *alm1*Δ et *sumo-KallR*). Mes résultats indiquent que la délocalisation de Ulp1 de la périphérie nucléaire rend le nucléoplams particulièrement permissif à une dégradation des brins naissants par la nuclease Exo1. Comment l'absence de séquestration d'Ulp1 à la périphérie nucléaire rend-elle le compartiment nucléoplasmique plus perméable à une longue résection médiée par Exo1 ? Conformément à mes observations, je propose que la délocalisation d'Ulp1 de la périphérie nucléaire nuit à l'intégrité des fourches de réplication en défavorisant la monoSUMOylation dépendante de Pli1, qui est essentielle à la protection des fourches de réplication dans le nucléoplasme. J'émet l'hypothèse que, dans ces conditions, le compartiment nucléoplasmique devient moins efficace pour assurer la protection des fourches, tandis que la périphérie nucléaire offre un environnement plus propice pour la protection des fourches par des mécanismes qui restent à découvrir. Deux mécanismes possibles pourraient expliquer ce phénomène.

La SUMO E3 ligase Pli1 de la levure à fission est auto-SUMOylée et accumule des chaînes SUMO qui peuvent servir de sites de liaison pour STUbL (Nie et al., 2015). Dans des conditions normales, Ulp1 déSUMOyle Pli1 pour le protéger de la dégradation par la protéasome médiée par l'ubiquitination. Cependant, lorsque Ulp1 est délocalisée, Pli1 est dégradée. Par conséquent, Pli1 polySUMOylée est soumise à une dégradation médiée par STUbL, ce qui entraîne des défauts profonds dans la voie SUMO (Nie et al., 2015). Cette diminution globale de la SUMOylation dépendante de Pli1 peut empêcher la modification de substrats clés impliqués dans la protection contre la dégradation des brins naissants, lorsque les fourches arrêtées se trouvent dans le nucléoplasme. Ainsi, le défaut de protection des fourches dans le double mutant *nup131*Δ *nup132*Δ pourrait découler de la déstabilisation de Pli1. D'autre part, il est également supposé que la délocalisation de Ulp1 dans le nucléoplasme, même en faible quantité, pourrait déSUMOyler certains substrats nucléaires et réduire la quantité de leurs formes SUMOylées (Panse et al., 2003; Li and Hochstrasser, 2003; Palancade et al., 2007). Cette étude indique que Ulp1 délocalisée dans le nucléoplasme acquiert la capacité de déSUMOyler des substrats normalement spécifiques à Ulp2 (Li and Hochstrasser, 2003). Ainsi, la séquestration de Ulp1 peut empêcher la déSUMOylation non régulée de protéines nucléoplasmiques. Par conséquent, il n'est pas exclu que la délocalosation de Ulp1 dans le double mutant *nup131*Δ *nup132*Δ conduise à une déSUMOylation non programmée d'un facteur nucléoplasmique, dont la SUMOylation est cruciale pour favoriser la protection des fourches.

CONCLUSIONS

En résumé, mes résultats fournissent des informations clés sur la ségrégation spatiale du métabolisme de la SUMOylation en situation de stress de réplication et mettent en évidence un rôle central du panier nucléaire dans le redémarrage de la fourche de réplication médiée par la recombinaison et la protection de son intégrité. Ces découvertes soulignent le rôle potentiel des chaînes SUMO dans la régulation de l'efficacité du mécanisme de RDR, soulignant ainsi un aspect méconnu du métabolisme de SUMOylation en situation de stress de réplication. En fin de compte, ces observations offrent une base solide pour de futures investigations sur les mécanismes moléculaires de la régulation de la réplication en situation de stress et de l'intégrité du génome dans un environnement nucléaire complexe et compartimenté.

REFERENCES

Abugable AA, Morris JLM, Palminha NM, Zaksauskaite R, Ray S, El-Khamisy SF. (2019). DNA repair and neurological disease: From molecular understanding to the development of diagnostics and model organisms. DNA Repair, 81:102669. doi: 10.1016/j.dnarep.2019.102669.

Achar YJ, Balogh D, Haracska L. (2011). Coordinated protein and DNA remodeling by human HLTF on stalled replication fork. Proc Natl Acad Sci U S A, 108(34):14073-8. doi: 10.1073/pnas.1101951108.

Ackerson SM, Romney C, Schuck PL, Stewart JA. (2021) To Join or Not to Join: Decision Points Along the Pathway to Double-Strand Break Repair vs. Chromosome End Protection. Front Cell Dev Biol. 9:708763. doi: 10.3389/fcell.2021.708763.

Aguilar-Martinez E, Guo B, Sharrocks AD. (2017) RNF4 interacts with multiSUMOylated ETV4. Wellcome Open Res. 1:3. doi: 10.12688/wellcomeopenres.9935.2.

Ait Saada A, Lambert SAE, Carr AM. (2018). Preserving replication fork integrity and competence via the homologous recombination pathway. DNA Repair, 71:135-147. doi: 10.1016/j.dnarep.2018.08.017.

Ait Saada A, Teixeira-Silva A, Iraqui I, Costes A, Hardy J, Paoletti G, Fréon K, Lambert SAE. (2017). Unprotected Replication Forks Are Converted into Mitotic Sister Chromatid Bridges. Mol Cell., 66(3):398-410.e4. doi: 10.1016/j.molcel.2017.04.002.

Altmannova V, Eckert-Boulet N, Arneric M, Kolesar P, Chaloupkova R, Damborsky J, Sung P, Zhao X, Lisby M, Krejci L. (2010). Rad52 SUMOylation affects the efficiency of the DNA repair. Nucleic Acids Res., 38(14):4708-21. doi: 10.1093/nar/gkq195.

Alvarez S, Díaz M, Flach J. Rodriguez-Acebes S, López-Contreras AJ, Martínez D, Cañamero M, Fernández-Capetillo O, Isern J, Passegué E, Méndez J. (2015). Replication stress caused by low MCM expression limits fetal erythropoiesis and hematopoietic stem cell functionality. Nat Commun, 6, 8548. doi: 10.1038/ncomms9548

Amitai A, Seeber A, Gasser SM, Holcman D. (2017). Visualization of Chromatin Decompaction and Break Site Extrusion as Predicted by Statistical Polymer Modeling of Single-Locus Trajectories. Cell Rep., 18(5):1200-1214. doi: 10.1016/j.celrep.2017.01.018.

Andrews EA, Palecek J, Sergeant J, Taylor E, Lehmann AR, Watts FZ. (2005). Nse2, a component of the Smc5-6 complex, is a SUMO ligase required for the response to DNA damage. Mol Cell Biol., 25(1):185-96. doi: 10.1128/MCB.25.1.185-196.2005.

Antoniuk-Majchrzak J., Enkhbaatar T. Długajczyk A. Kaminska J. Skoneczny M. Klionsky DJ, Skoneczna A. (2023). Stability of Rad51 recombinase and persistence of Rad51 DNA repair foci depends on post-translational modifiers, ubiquitin and SUMO. Biochim Biophys Acta Mol Cell Res, 1870(7):119526. doi: 10.1016/j.bbamcr.2023.119526.

Aravind L, Watanabe H, Lipman DJ, Koonin EV. (2000). Lineage-specific loss and divergence of functionally linked genes in eukaryotes. Proc Natl Acad Sci U S A., 97(21):11319-24. doi: 10.1073/pnas.200346997.

Ashour ME, Mosammaparast N. (2021). Mechanisms of damage tolerance and repair during DNA replication. Nucleic Acids Res., 49(6):3033-3047. doi: 10.1093/nar/gkab101.

Aten JA, Stap J, Krawczyk PM, van Oven CH, Hoebe RA, Essers J, Kanaar R. (2004). Dynamics of DNA double-strand breaks revealed by clustering of damaged chromosome domains. Science, 303(5654):92-5. doi: 10.1126/science.1088845.

Bachrati CZ, Borts RH, Hickson ID. (2006). Mobile D-loops are a preferred substrate for the Bloom's syndrome helicase. Nucleic Acids Res., 34(8):2269-79. doi: 10.1093/nar/gkl258.

Bartek J, Lukas C, Lukas J. Checking on DNA damage in S phase. (2004). Nat Rev Mol Cell Biol., 5(10):792-804. doi: 10.1038/nrm1493.

Bartkova J, Rezaei N, Liontos M, Karakaidos P, Kletsas D, Issaeva N, Vassiliou LV, Kolettas E, Niforou K, Zoumpourlis VC, Takaoka M, Nakagawa H, Tort F, Fugger K, Johansson F, Sehested M, Andersen CL, Dyrskjot L, Ørntoft T, Lukas J, Kittas C, Helleday T, Halazonetis TD, Bartek J, Gorgoulis VG. (2006). Oncogene-induced senescence is part of the tumorigenesis barrier imposed by DNA damage checkpoints. Nature, 444(7119):633-7. doi: 10.1038/nature05268.

Balmus G, Pilger D, Coates J, Demir M, Sczaniecka-Clift M, Barros AC, Woods M, Fu B, Yang F, Chen E, Ostermaier M, Stankovic T, Ponstingl H, Herzog M, Yusa K, Martinez FM, Durant ST, Galanty Y, Beli P, Adams DJ, Bradley A, Metzakopian E, Forment JV, Jackson SP. (2019). ATM orchestrates the DNA-damage response to counter toxic non-homologous end-joining at broken replication forks. Nat Commun., 10(1):87. doi: 10.1038/s41467-018-07729-2.

Bassett A, Cooper S, Wu C, Travers A. (2009). The folding and unfolding of eukaryotic chromatin. Curr Opin Genet Dev., 19(2):159-65. doi: 10.1016/j.gde.2009.02.010.

Baumann P, West SC. (1998). Role of the human RAD51 protein in homologous recombination and double-stranded-break repair. Trends Biochem Sci., 23(7):247-51. doi: 10.1016/s0968-0004(98)01232-8.

Beck H, Nähse-Kumpf V, Larsen MS, O'Hanlon KA, Patzke S, Holmberg C, Mejlvang J, Groth A, Nielsen O, Syljuåsen RG, Sørensen CS. (2012). Cyclin-dependent kinase suppression by WEE1 kinase protects the genome through control of replication initiation and nucleotide consumption. Mol Cell Biol., 32(20):4226-36. doi: 10.1128/MCB.00412-12.

Belan O, Sebald M, Adamowicz M, Anand R, Vancevska A, Neves J, Grinkevich V, Hewitt G, Segura-Bayona S, Bellelli R, Robinson HMR, Higgins GS, Smith GCM, West SC, Rueda DS, Boulton SJ. (2022). POLQ seals post-replicative ssDNA gaps to maintain genome stability in BRCA-deficient cancer cells. Mol Cell., 82(24):4664-4680.e9. doi: 10.1016/j.molcel.2022.11.008.

Bell SP, Labib K. (2016). Chromosome Duplication in Saccharomyces cerevisiae. Genetics, 203(3):1027-67. doi: 10.1534/genetics.115.186452.

Bell SP, Kaguni JM. (2013). Helicase loading at chromosomal origins of replication. Cold Spring Harb Perspect Biol., 5(6):a010124. doi: 10.1101/cshperspect.a010124.

Bell SP, Stillman B. (1992). ATP-dependent recognition of eukaryotic origins of DNA replication by a multiprotein complex. Nature, 357(6374):128-34. doi: 10.1038/357128a0.

Bellelli R, Boulton SJ. (2021). Spotlight on the Replisome: Aetiology of DNA Replication-Associated Genetic Diseases. Trends Genet., 37(4):317-336. doi: 10.1016/j.tig.2020.09.008.

Bennett CB, Lewis LK, Karthikeyan G, Lobachev KS, Jin YH, Sterling JF, Snipe JR, Resnick MA. (2001). Genes required for ionizing radiation resistance in yeast. Nat Genet., 29(4):426-34. doi: 10.1038/ng778.

Benson FE, Baumann P, West SC. (1998). Synergistic actions of Rad51 and Rad52 in recombination and DNA repair. Nature, 391(6665):401-4. doi: 10.1038/34937.

Benureau Y, Pouvelle C, Dupaigne P, Baconnais S, Moreira Tavares E, Mazón G, Despras E, Le Cam E, Kannouche PL. (2022). Changes in the architecture and abundance of replication intermediates delineate the chronology of DNA damage tolerance pathways at UV-stalled replication forks in human cells. Nucleic Acids Res., 50(17):9909-9929. doi: 10.1093/nar/gkac746.

Beranek DT. (1990). Distribution of methyl and ethyl adducts following alkylation with monofunctional alkylating agents. Mutat Res., 231(1):11-30. doi: 10.1016/0027-5107(90)90173-2.

Berg H.C. (1993). Random Walks in Biology. Princeton University Press, Princeton, NJ.

Bergink S, Ammon T, Kern M, Schermelleh L, Leonhardt H, Jentsch S. (2013). Role of Cdc48/p97 as a SUMO-targeted segregase curbing Rad51-Rad52 interaction. Nat Cell Biol., 15(5):526-32. doi: 10.1038/ncb2729.

Berti M, Ray Chaudhuri A, Thangavel S, Gomathinayagam S, Kenig S, Vujanovic M, Odreman F, Glatter T, Graziano S, Mendoza-Maldonado R, Marino F, Lucic B, Biasin V, Gstaiger M, Aebersold R, Sidorova JM, Monnat RJ Jr, Lopes M, Vindigni A. (2013). Human RECQ1 promotes restart of replication forks reversed by DNA topoisomerase I inhibition. Nat Struct Mol Biol., 20(3):347-54. doi: 10.1038/nsmb.2501.

Berti M, Teloni F, Mijic S, Ursich S, Fuchs J, Palumbieri MD, Krietsch J, Schmid JA, Garcin EB, Gon S, Modesti M, Altmeyer M, Lopes M. (2020). Sequential role of RAD51 paralog complexes in replication fork remodeling and restart. Nat Commun., 11(1):3531. doi: 10.1038/s41467-020-17324-z.

Bester AC, Roniger M, Oren YS, Im MM, Sarni D, Chaoat M, Bensimon A, Zamir G, Shewach DS, Kerem B. (2011). Nucleotide deficiency promotes genomic instability in early stages of cancer development. Cell., 145(3):435-46. doi: 10.1016/j.cell.2011.03.044.

Bétous R, Mason AC, Rambo RP, Bansbach CE, Badu-Nkansah A, Sirbu BM, Eichman BF, Cortez D. (2012). SMARCAL1 catalyzes fork regression and Holliday junction migration to maintain genome stability during DNA replication. Genes Dev., 26(2):151-62. doi: 10.1101/gad.178459.111.

Bhargava R, Onyango DO, Stark JM. (2016). Regulation of Single-Strand Annealing and its Role in Genome Maintenance. Trends Genet., 32(9):566-575. doi: 10.1016/j.tig.2016.06.007.

Bhowmick R, Minocherhomji S, Hickson ID. (2016). RAD52 Facilitates Mitotic DNA Synthesis Following Replication Stress. Mol Cell., 64(6):1117-1126. doi: 10.1016/j.molcel.2016.10.037.

Bhowmick R, Hickson ID. (2017). The "enemies within": regions of the genome that are inherently difficult to replicate. F1000Res., 6:666. doi: 10.12688/f1000research.11024.1.

Bianchi J, Rudd SG, Jozwiakowski SK, Bailey LJ, Soura V, Taylor E, Stevanovic I, Green AJ, Stracker TH, Lindsay HD, Doherty AJ. (2013). PrimPol bypasses UV photoproducts during eukaryotic chromosomal DNA replication. Mol Cell., 52(4):566-73. doi: 10.1016/j.molcel.2013.10.035.

Biffi G, Tannahill D, McCafferty J, Balasubramanian S. (2013). Quantitative visualization of DNA G-quadruplex structures in human cells. Nat Chem., 5(3):182-6. doi: 10.1038/nchem.1548.

Blastyák A, Hajdú I, Unk I, Haracska L. (2010). Role of double-stranded DNA translocase activity of human HLTF in replication of damaged DNA. Mol Cell Biol., 30(3):684-93. doi: 10.1128/MCB.00863-09.

Bochman ML, Schwacha A. (2008). The Mcm2-7 complex has in vitro helicase activity. Mol Cell., 31(2):287-93. doi: 10.1016/j.molcel.2008.05.020.
Bochman ML, Paeschke K, Zakian VA. (2012). DNA secondary structures: stability and function of G-quadruplex structures. Nat Rev Genet., 13(11):770-80. doi: 10.1038/nrg3296.

Boddy MN, Gaillard PHL, McDonald WH, Shanahan P, Yates JR 3rd, Russell P. (2001). Mus81-Eme1 are essential components of a Holliday junction resolvase. Cell, 107(4):537-48. doi: 10.1016/s0092-8674(01)00536-0.

Bologna S, Altmannova V, Valtorta E, Koenig C, Liberali P, Gentili C, Anrather D, Ammerer G, Pelkmans L, Krejci L, Ferrari S. (2015). Sumoylation regulates EXO1 stability and processing of DNA damage. Cell Cycle, 14(15):2439-50. doi: 10.1080/15384101.2015.1060381.

Boulanger M, Chakraborty M, Tempé D, Piechaczyk M, Bossis G. (2021). SUMO and Transcriptional Regulation: The Lessons of Large-Scale Proteomic, Modifomic and Genomic Studies. Molecules, 26(4):828. doi: 10.3390/molecules26040828.

Bouwman P, Aly A, Escandell JM, Pieterse M, Bartkova J, van der Gulden H, Hiddingh S, Thanasoula M, Kulkarni A, Yang Q, Haffty BG, Tommiska J, Blomqvist C, Drapkin R, Adams DJ, Nevanlinna H, Bartek J, Tarsounas M, Ganesan S, Jonkers J. (2010). 53BP1 loss rescues BRCA1 deficiency and is associated with triple-negative and BRCA-mutated breast cancers. Nat Struct Mol Biol., 17(6):688-95. doi: 10.1038/nsmb.1831.

Boyle S, Gilchrist S, Bridger JM, Mahy NL, Ellis JA, Bickmore WA. (2001). The spatial organization of human chromosomes within the nuclei of normal and emerin-mutant cells. Hum Mol Genet., 10(3):211-9. doi: 10.1093/hmg/10.3.211.
Branzei D. (2011). Ubiquitin family modifications and template switching. FEBS Lett., 585(18):2810-7. doi: 10.1016/j.febslet.2011.04.053.

Branzei D, Foiani M. (2005). The DNA damage response during DNA replication. Curr Opin Cell Biol., 17(6):568-75. doi: 10.1016/j.ceb.2005.09.003.

Branzei D, Foiani M. (2008). Regulation of DNA repair throughout the cell cycle. Nat Rev Mol Cell Biol., 9(4):297-308. doi: 10.1038/nrm2351.

Branzei D, Sollier J, Liberi G, Zhao X, Maeda D, Seki M, Enomoto T, Ohta K, Foiani M. (2006). Ubc9- and mms21-mediated sumoylation counteracts recombinogenic events at damaged replication forks. Cell, 127(3):509-22. doi: 10.1016/j.cell.2006.08.050.

Brenner KA, Nandakumar J. (2022). Consequences of telomere replication failure: the other end-replication problem. Trends Biochem Sci., 47(6):506-517. doi: 10.1016/j.tibs.2022.03.013.

Brewer BJ, Lockshon D, Fangman WL. (1992). The arrest of replication forks in the rDNA of yeast occurs independently of transcription. Cell, 71(2):267-76. doi: 10.1016/0092-8674(92)90355-g.

Brown RE, Freudenreich CH. (2021). Structure-forming repeats and their impact on genome stability. Curr Opin Genet Dev., 67:41-51. doi: 10.1016/j.gde.2020.10.006.

Bugreev DV, Yu X, Egelman EH, Mazin AV. (2007). Novel pro- and anti-recombination activities of the Bloom's syndrome helicase. Genes Dev., 21(23):3085-94. doi: 10.1101/gad.1609007.

Buis J, Wu Y, Deng Y, Leddon J, Westfield G, Eckersdorff M, Sekiguchi JM, Chang S, Ferguson DO. (2008). Mre11 nuclease activity has essential roles in DNA repair and genomic stability distinct from ATM activation. Cell, 135(1):85-96. doi: 10.1016/j.cell.2008.08.015.

Bunting SF, Callén E, Wong N, Chen HT, Polato F, Gunn A, Bothmer A, Feldhahn N, Fernandez-Capetillo O, Cao L, Xu X, Deng CX, Finkel T, Nussenzweig M, Stark JM, Nussenzweig A. (2010). 53BP1 inhibits homologous recombination in Brca1-deficient cells by blocking resection of DNA breaks. Cell, 141(2):243-54. doi: 10.1016/j.cell.2010.03.012.

Burdine RD, Preston CC, Leonard RJ, Bradley TA, Faustino RS. (2020). Nucleoporins in cardiovascular disease. J Mol Cell Cardiol.,141:43-52. doi: 10.1016/j.yjmcc.2020.02.010.

Burkovics P. Sebesta M. Sisakova A. Plault N. Szukacsov V. Robert T. Pinter L. Marini V. Kolesar P. Haracska L. Gangloff S. Krejci L. (2013). Srs2 mediates PCNA-SUMO-dependent inhibition of DNA repair synthesis. EMBO J. 32(5):742-55. doi: 10.1038/emboj.2013.9.

Burgers P, Kunkel T. (2017). Eukaryotic DNA Replication Fork Annu Rev Biochem., 86:417-438. doi: 10.1146/annurev-biochem-061516-044709.

Burgess RC, Lisby M, Altmannova V, Krejci L, Sung P, Rothstein R. (2009). Localization of recombination proteins and Srs2 reveals anti-recombinase function in vivo. J Cell Biol., 185(6):969-81. doi: 10.1083/jcb.200810055.

Burgess RC, Rahman S, Lisby M, Rothstein R, Zhao X. (2007). The Slx5-Slx8 complex affects sumoylation of DNA repair proteins and negatively regulates recombination. Mol Cell Biol., 27(17):6153-62. doi: 10.1128/MCB.00787-07.

Bystricky K, Heun P, Gehlen L, Langowski J, Gasser SM. (2004). Long-range compaction and flexibility of interphase chromatin in budding yeast analyzed by high-resolution imaging techniques. Proc Natl Acad Sci USA, 101(47):16495-500. doi: 10.1073/pnas.0402766101.

Byun TS, Pacek M, Yee MC, Walter JC, Cimprich KA. (2005). Functional uncoupling of MCM helicase and DNA polymerase activities activates the ATR-dependent checkpoint. Genes Dev., 19(9):1040-52. doi: 10.1101/gad.1301205.

Cadet J, Wagner JR. (2013). DNA base damage by reactive oxygen species, oxidizing agents, and UV radiation. Cold Spring Harb Perspect Biol. 5(2):a012559. doi: 10.1101/cshperspect.a012559.

Caridi CP, D'Agostino C, Ryu T, Zapotoczny G, Delabaere L, Li X, Khodaverdian VY, Amaral N, Lin E, Rau AR, Chiolo I. (2018). Nuclear F-actin and myosins drive relocalization of heterochromatic breaks. Nature. 559(7712):54-60. doi: 10.1038/s41586-018-0242-8.

Carr A, Lambert S. (2021). Recombination-dependent replication: new perspectives from site-specific fork barriers. Curr Opin Genet Dev. 71:129-135. doi: 10.1016/j.gde.2021.07.008.

Carré-Simon À, Fabre E. (2021). 3D Genome Organization: Causes and Consequences for DNA Damage and Repair. Genes (Basel). 13(1):7. doi: 10.3390/genes13010007.

Carreira A, Hilario J, Amitani I, Baskin RJ, Shivji MK, Venkitaraman AR, Kowalczykowski SC. (2009). The BRC repeats of BRCA2 modulate the DNA-binding selectivity of RAD51. Cell. 136(6):1032-43. doi: 10.1016/j.cell.2009.02.019.

Caspari T, Murray JM, Carr AM. (2002). Cdc2-cyclin B kinase activity links Crb2 and Rqh1-topoisomerase III. Genes Dev. 16(10):1195-208. doi: 10.1101/gad.221402.

Ceballos SJ, Heyer WD. (2011). Functions of the Snf2/Swi2 family Rad54 motor protein in homologous recombination. Biochim Biophys Acta. 1809(9):509-23. doi: 10.1016/j.bbagrm.2011.06.006.

Cejka P, Plank JL, Bachrati CZ, Hickson ID, Kowalczykowski SC. (2010). Rmi1 stimulates decatenation of double Holliday junctions during dissolution by Sgs1-Top3. Nat Struct Mol Biol. 17(11):1377-82. doi: 10.1038/nsmb.1919.

Cejka P. (2015). DNA End Resection: Nucleases Team Up with the Right Partners to Initiate Homologous Recombination. J Biol Chem. 290(38):22931-8. doi: 10.1074/jbc.R115.675942.

Cejka P, Symington LS. (2021). DNA End Resection: Mechanism and Control. Annu Rev Genet. 55:285-307. doi: 10.1146/annurev-genet-071719-020312.

Chabes A, Stillman B. (2007). Constitutively high dNTP concentration inhibits cell cycle progression and the DNA damage checkpoint in yeast Saccharomyces cerevisiae. Proc Natl Acad Sci U S A. 104(4):1183-8. doi: 10.1073/pnas.0610585104.

Chabosseau P, Buhagiar-Labarchède G, Onclercq-Delic R, Lambert S, Debatisse M, Brison O, Amor-Guéret M. (2011). Pyrimidine pool imbalance induced by BLM helicase deficiency contributes to genetic instability in Bloom syndrome. Nat Commun. 2:368. doi: 10.1038/ncomms1363.

Challa K, Schmid CD, Kitagawa S, Cheblal A, Iesmantavicius V, Seeber A, Amitai A, Seebacher J, Hauer MH, Shimada K, Gasser SM. (2021). Damage-induced chromatome dynamics link Ubiquitin ligase and proteasome recruitment to histone loss and efficient DNA repair. Mol Cell. 81(4):811-829.e6. doi: 10.1016/j.molcel.2020.12.021.

Chan YW, West SC. (2018). A new class of ultrafine anaphase bridges generated by homologous recombination. Cell Cycle. 17(17):2101-2109. doi: 10.1080/15384101.2018.1515555.

Chang YC, Oram MK, Bielinsky AK. (2021). SUMO-Targeted Ubiquitin Ligases and Their Functions in Maintaining Genome Stability. Int J Mol Sci. 22(10):5391. doi: 10.3390/ijms22105391.

Chang HHY, Pannunzio NR, Adachi N, Lieber MR. (2017). Non-homologous DNA end joining and alternative pathways to double-strand break repair. Nat Rev Mol Cell Biol. 18(8):495-506. doi: 10.1038/nrm.2017.48.

Chapman JR, Taylor MR, Boulton SJ. (2012). Playing the end game: DNA double-strand break repair pathway choice. Mol Cell. 47(4):497-510. doi: 10.1016/j.molcel.2012.07.029.

Charlier CF, Martins RAP. (2020). Protective Mechanisms Against DNA Replication Stress in the Nervous System. Genes (Basel). 11(7):730. doi: 10.3390/genes11070730.

Chavdarova M, Marini V, Sisakova A, Sedlackova H, Vigasova D, Brill SJ, Lisby M, Krejci L. (2015). Srs2 promotes Mus81-Mms4-mediated resolution of recombination intermediates. Nucleic Acids Res. 43(7):3626-42. doi: 10.1093/nar/gkv198.

Cheblal A, Challa K, Seeber A, Shimada K, Yoshida H, Ferreira HC, Amitai A, Gasser SM. (2020). DNA Damage-Induced Nucleosome Depletion Enhances Homology Search Independently of Local Break Movement. Mol Cell. 80(2):311-326.e4. doi: 10.1016/j.molcel.2020.09.002.

Chen XB, Melchionna R, Denis CM, Gaillard PHL, Blasina A, Van de Weyer I, Boddy MN, Russell P, Vialard J, McGowan CH. (2001). Human Mus81-associated endonuclease cleaves Holliday junctions in vitro. Mol Cell. 8(5):1117-27. doi: 10.1016/s1097-2765(01)00375-6.

Chen Q, Ijpma A, Greider CW. (2001). Two survivor pathways that allow growth in the absence of telomerase are generated by distinct telomere recombination events. Mol Cell Biol. 21(5):1819-27. doi: 10.1128/MCB.21.5.1819-1827.2001.

Chiolo I, Minoda A, Colmenares SU, Polyzos A, Costes SV, Karpen GH. (2011). Double-strand breaks in heterochromatin move outside of a dynamic HP1a domain to complete recombinational repair. Cell. 144(5):732-44. doi: 10.1016/j.cell.2011.02.012.

Cho NW, Dilley RL, Lampson MA, Greenberg RA. (2014). Interchromosomal homology searches drive directional ALT telomere movement and synapsis. Cell. 159(1):108-121. doi: 10.1016/j.cell.2014.08.030.

Chung DK, Chan JN, Strecker J, Zhang W, Ebrahimi-Ardebili S, Lu T, Abraham KJ, Durocher D, Mekhail K. (2015). Perinuclear tethers license telomeric DSBs for a broad kinesin- and NPC-dependent DNA repair process. Nat Commun. 6:7742. doi: 10.1038/ncomms8742.

Chung I, Zhao X. (2015). DNA break-induced sumoylation is enabled by collaboration between a SUMO ligase and the ssDNA-binding complex RPA. Genes Dev. 29(15):1593-8. doi: 10.1101/gad.265058.115.

Churikov D, Charifi F, Eckert-Boulet N, Silva S, Simon MN, Lisby M, Géli V. (2016). SUMO-Dependent Relocalization of Eroded Telomeres to Nuclear Pore Complexes

Controls Telomere Recombination. Cell Rep. 15(6):1242-53. doi: 10.1016/j.celrep.2016.04.008.

Ciccia A, Constantinou A, West SC. (2003). Identification and characterization of the human mus81-eme1 endonuclease. J Biol Chem. 278(27):25172-8. doi: 10.1074/jbc.M302882200.

Ciccia A, Elledge SJ. (2010). The DNA damage response: making it safe to play with knives. Mol Cell. 40(2):179-204. doi: 10.1016/j.molcel.2010.09.019.

Clausen AR, Zhang S, Burgers PM, Lee MY, Kunkel TA. (2013). Ribonucleotide incorporation, proofreading and bypass by human DNA polymerase δ. DNA Repair (Amst). 12(2):121-7. doi: 10.1016/j.dnarep.2012.11.006.

Cloud V, Chan YL, Grubb J, Budke B, Bishop DK. (2012). Rad51 is an accessory factor for Dmc1-mediated joint molecule formation during meiosis. Science. 337(6099):1222-5. doi: 10.1126/science.1219379.

Cvetic C, Walter JC. (2005). Eukaryotic origins of DNA replication: could you please be more specific? Semin Cell Dev Biol. 16(3):343-53. doi: 10.1016/j.semcdb.2005.02.009.

Codlin S, Dalgaard JZ. (2003). Complex mechanism of site-specific DNA replication termination in fission yeast. EMBO J. 22(13):3431-40. doi: 10.1093/emboj/cdg330.

Conway AB, Lynch TW, Zhang Y, Fortin GS, Fung CW, Symington LS, Rice PA. (2004). Crystal structure of a Rad51 filament. Nat Struct Mol Biol. 11(8):791-6. doi: 10.1038/nsmb795.

Cooper JA, Schafer DA. (2000). Control of actin assembly and disassembly at filament ends. Curr Opin Cell Biol. 12(1):97-103. doi: 10.1016/s0955-0674(99)00062-9.

Cortez D. (2015). Preventing replication fork collapse to maintain genome integrity. DNA Repair (Amst). 32:149-157. doi: 10.1016/j.dnarep.2015.04.026.

Costantino L, Sotiriou SK, Rantala JK, Magin S, Mladenov E, Helleday T, Haber JE, Iliakis G, Kallioniemi OP, Halazonetis TD. (2014). Break-induced replication repair of damaged forks induces genomic duplications in human cells. Science. 343(6166):88-91. doi: 10.1126/science.1243211.

Costes A, Lambert SA. (2012). Homologous recombination as a replication fork escort: fork-protection and recovery. Biomolecules. 3(1):39-71. doi: 10.3390/biom3010039.

Cremer M, Grasser F, Lanctôt C, Müller S, Neusser M, Zinner R, Solovei I, Cremer T. (2008). Multicolor 3D fluorescence in situ hybridization for imaging interphase chromosomes. Methods Mol Biol. 463:205-39. doi: 10.1007/978-1-59745-406-3_15.

Cremer T, Cremer M. (2010). Chromosome territories. Cold Spring Harb Perspect Biol. 22(3):a003889. doi: 10.1101/cshperspect.a003889.

Cremer T, Cremer C, Baumann H, Luedtke EK, Sperling K, Teuber V, Zorn C. (1982). Rabl's model of the interphase chromosome arrangement tested in Chinese hamster cells by premature chromosome condensation and laser-UV-microbeam experiments. Hum Genet. 60(1):46-56. doi: 10.1007/BF00281263.

Cremona CA, Sarangi P, Yang Y, Hang LE, Rahman S, Zhao X. (2012). Extensive DNA damage-induced sumoylation contributes to replication and repair and acts in addition to the mec1 checkpoint. Mol Cell. 45(3):422-32. doi: 10.1016/j.molcel.2011.11.028.

Croft JA, Bridger JM, Boyle S, Perry P, Teague P, Bickmore WA. (1999). Differences in the localization and morphology of chromosomes in the human nucleus. J Cell Biol. 145(6):1119-31. doi: 10.1083/jcb.145.6.1119.

Crow YJ, Leitch A, Hayward BE, Garner A, Parmar R, Griffith E, Ali M, Semple C, Aicardi J, Babul-Hirji R, Baumann C, Baxter P, Bertini E, Chandler KE, Chitayat D, Cau D, Déry C, Fazzi E, Goizet C, King MD, Klepper J, Lacombe D, Lanzi G, Lyall H, Martínez-Frías ML, Mathieu M, McKeown C, Monier A, Oade Y, Quarrell OW, Rittey CD, Rogers RC, Sanchis A, Stephenson JB, Tacke U, Till M, Tolmie JL, Tomlin P, Voit T, Weschke B, Woods CG, Lebon P, Bonthron DT, Ponting CP, Jackson AP. (2006). Mutations in genes encoding ribonuclease H2 subunits cause Aicardi-Goutières syndrome and mimic congenital viral brain infection. Nat Genet. 238(8):910-6. doi: 10.1038/ng1842.

Dalgaard JZ, Klar AJ. (2001). Does S. pombe exploit the intrinsic asymmetry of DNA synthesis to imprint daughter cells for mating-type switching? Trends Genet. 17(3):153-7. doi: 10.1016/s0168-9525(00)02203-4.

D'Angelo MA, Hetzer MW. (2008). Structure, dynamics and function of nuclear pore complexes. Trends Cell Biol. 18(10):456-66. doi: 10.1016/j.tcb.2008.07.009.

Davis AP, Symington LS. (2001). The yeast recombinational repair protein Rad59 interacts with Rad52 and stimulates single-strand annealing. Genetics. 159(2):515-25. doi: 10.1093/genetics/159.2.515.

Davies AA, Masson JY, McIlwraith MJ, Stasiak AZ, Stasiak A, Venkitaraman AR, West SC. (2001). Role of BRCA2 in control of the RAD51 recombination and DNA repair protein. Mol Cell. 7(2):273-82. doi: 10.1016/s1097-2765(01)00175-7.

Davidson PM, Cadot B. (2021). Actin on and around the Nucleus. Trends Cell Biol. 31(3):211-223. doi: 10.1016/j.tcb.2020.11.009.

Deegan TD, Diffley JF. (2016). MCM: one ring to rule them all. Curr Opin Struct Biol. 37:145-51. doi: 10.1016/j.sbi.2016.01.014.

Deem A, Keszthelyi A, Blackgrove T, Vayl A, Coffey B, Mathur R, Chabes A, Malkova A. (2011). Break-induced replication is highly inaccurate. PLoS Biol. 9(2):e1000594. doi: 10.1371/journal.pbio.1000594.

Dekker J, Alber F, Aufmkolk S, Beliveau BJ, Bruneau BG, Belmont AS, Bintu L, Boettiger A, Calandrelli R, Disteche CM, Gilbert DM, Gregor T, Hansen AS, Huang B, Huangfu D, Kalhor R, Leslie CS, Li W, Li Y, Ma J, Noble WS, Park PJ, Phillips-Cremins JE, Pollard KS, Rafelski SM, Ren B, Ruan Y, Shav-Tal Y, Shen Y, Shendure J, Shu X, Strambio-De-Castillia C, Vertii A, Zhang H, Zhong S. (2023). Spatial and temporal organization of the genome: Current state and future aims of the 4D nucleome project. Mol Cell. 83(15):2624-2640. doi: 10.1016/j.molcel.2023.06.018.

Dekker J, Heard E. (2015). Structural and functional diversity of Topologically Associating Domains. FEBS Lett. 589(20 Pt A):2877-84. doi: 10.1016/j.febslet.2015.08.044.

De Septenville AL, Duigou S, Boubakri H, Michel B. (2012). Replication fork reversal after replication-transcription collision. PLoS Genet. 8(4):e1002622. doi: 10.1371/journal.pgen.1002622.

Dewar JM, Budzowska M, Walter JC. (2015). The mechanism of DNA replication termination in vertebrates. Nature. 2015 Sep 17;525(7569):345-50. doi: 10.1038/nature14887.

Dhingra N, Wei L, Zhao X. (2019). Replication protein A (RPA) sumoylation positively influences the DNA damage checkpoint response in yeast. J Biol Chem. 294(8):2690-2699. doi: 10.1074/jbc.RA118.006006.

Dhingra N, Zhao X. (2019). Intricate SUMO-based control of the homologous recombination machinery. Genes Dev. 33(19-20):1346-1354. doi: 10.1101/gad.328534.119.

Di Antonio M, Ponjavic A, Radzevičius A, Ranasinghe RT, Catalano M, Zhang X, Shen J, Needham LM, Lee SF, Klenerman D, Balasubramanian S. (2020). Single-molecule visualization of DNA G-quadruplex formation in live cells. Nat Chem. 12(9):832-837. doi: 10.1038/s41557-020-0506-4.

Di Biagi L, Malacaria E, Aiello FA, Valenzisi P, Marozzi G, Franchitto A, Pichierri P. (2023). RAD52 prevents accumulation of Polα-dependent replication gaps at perturbed replication forks in human cells. bioRxiv [Preprint]. doi: 10.1101/2023.04.12.536536.

Dilley RL, Verma P, Cho NW, Winters HD, Wondisford AR, Greenberg RA. (2016). Break-induced telomere synthesis underlies alternative telomere maintenance. Nature. 539(7627):54-58. doi: 10.1038/nature20099.

Di Micco R, Fumagalli M, Cicalese A, Piccinin S, Gasparini P, Luise C, Schurra C, Garre' M, Nuciforo PG, Bensimon A, Maestro R, Pelicci PG, d'Adda di Fagagna F. (2006). Oncogene-induced senescence is a DNA damage response triggered by DNA hyper-replication. Nature. 444(7119):638-42. doi: 10.1038/nature05327.

Dimitrova N, Chen YC, Spector DL, de Lange T. (2008). 53BP1 promotes non-homologous end joining of telomeres by increasing chromatin mobility. Nature. 456(7221):524-8. doi: 10.1038/nature07433.

Ding R, West RR, Morphew DM, Oakley BR, McIntosh JR. (1997). The spindle pole body of Schizosaccharomyces pombe enters and leaves the nuclear envelope as the cell cycle proceeds. Mol Biol Cell. 8(8):1461-79. doi: 10.1091/mbc.8.8.1461.

Dion V, Kalck V, Horigome C, Towbin BD, Gasser SM. (2012). Increased mobility of double-strand breaks requires Mec1, Rad9 and the homologous recombination machinery. Nat Cell Biol. 14(5):502-9. doi: 10.1038/ncb2465.

Dion V, Kalck V, Seeber A, Schleker T, Gasser SM. (2013). Cohesin and the nucleolus constrain the mobility of spontaneous repair foci. EMBO Rep. 14(11):984-91. doi: 10.1038/embor.2013.142. Epub 2013 Sep 10.

Dixon JR, Selvaraj S, Yue F, Kim A, Li Y, Shen Y, Hu M, Liu JS, Ren B. (2012). Topological domains in mammalian genomes identified by analysis of chromatin interactions. Nature. 485(7398):376-80. doi: 10.1038/nature11082.

Doğan ES, Liu C. (2018). Three-dimensional chromatin packing and positioning of plant genomes. Nat Plants. 4(8):521-529. doi: 10.1038/s41477-018-0199-5.
Dohmen RJ. (2004). SUMO protein modification. Biochim Biophys Acta. 1695(1-3):113-31. doi: 10.1016/j.bbamcr.2004.09.021.

Donnianni RA, Symington LS. (2013). Break-induced replication occurs by conservative DNA synthesis. Proc Natl Acad Sci USA. 110(33):13475-80. doi: 10.1073/pnas.1309800110.

Donnianni RA, Zhou ZX, Lujan SA, Al-Zain A, Garcia V, Glancy E, Burkholder AB, Kunkel TA, Symington LS. (2019). DNA Polymerase Delta Synthesizes Both Strands during Break-Induced Replication. Mol Cell. 76(3):371-381.e4. doi: 10.1016/j.molcel.2019.07.033.

Dou H, Huang C, Singh M, Carpenter PB, Yeh ET. (2010). Regulation of DNA repair through deSUMOylation and SUMOylation of replication protein A complex. Mol Cell. 39(3):333-45. doi: 10.1016/j.molcel.2010.07.021.

Douglas ME, Ali FA, Costa A, Diffley JFX. (2018). The mechanism of eukaryotic CMG helicase activation. Nature. 555(7695):265-268. doi: 10.1038/nature25787.

Drinnenberg IA, Fink GR, Bartel DP. (2011). Compatibility with killer explains the rise of RNAi-deficient fungi. Science. 333(6049):1592. doi: 10.1126/science.1209575.

Duckett DR, Murchie AI, Diekmann S, von Kitzing E, Kemper B, Lilley DM. (1988). The structure of the Holliday junction, and its resolution. 55(1):79-89. doi: 10.1016/0092-8674(88)90011-6.

Dungrawala H, Rose KL, Bhat KP, Mohni KN, Glick GG, Couch FB, Cortez D. (2015). The Replication Checkpoint Prevents Two Types of Fork Collapse without Regulating Replisome Stability. Mol Cell. 59(6):998-1010. doi: 10.1016/j.molcel.2015.07.030.

Durocher D, Jackson SP. (2001). DNA-PK, ATM and ATR as sensors of DNA damage: variations on a theme? Curr Opin Cell Biol. doi: 10.1016/s0955-0674(00)00201-5.

Egel R, Egel-Mitani M. (1974). Premeiotic DNA synthesis in fission yeast. Exp Cell Res. 88(1):127-34. doi: 10.1016/0014-4827(74)90626-0.

Elango R, Osia B, Harcy V, Malc E, Mieczkowski PA, Roberts SA, Malkova A. (2019). Repair of base damage within break-induced replication intermediates promotes kataegis associated with chromosome rearrangements. Nucleic Acids Res. 47(18):9666-9684. doi: 10.1093/nar/gkz651.

Enoch T, Carr AM, Nurse P. (1992). Fission yeast genes involved in coupling mitosis to completion of DNA replication. Genes Dev. 6(11):2035-46. doi: 10.1101/gad.6.11.2035.

Escribano-Díaz C, Orthwein A, Fradet-Turcotte A, Xing M, Young JT, Tkáč J, Cook MA, Rosebrock AP, Munro M, Canny MD, Xu D, Durocher D. (2013). A cell cycle-dependent regulatory circuit composed of 53BP1-RIF1 and BRCA1-CtIP controls DNA repair pathway choice. Mol Cell. 49(5):872-83. doi: 10.1016/j.molcel.2013.01.001.

Eydmann T, Sommariva E, Inagawa T, Mian S, Klar AJ, Dalgaard JZ. (2008). Rtf1-mediated eukaryotic site-specific replication termination. Genetics. 180(1):27-39. doi: 10.1534/genetics.108.089243. Epub 2008 Aug 24. PMID: 18723894; PMCID: PMC2535681.

Fantes P. (1989). Yeast cell cycle. Curr Opin Cell Biol. 1(2):250-5. doi: 10.1016/0955-0674(89)90096-3.

Fantes PA, Hoffman CS. (2016). A Brief History of Schizosaccharomyces pombe Research: A Perspective Over the Past 70 Years. Genetics. 203(2):621-9. doi: 10.1534/genetics.116.189407.

Fasching CL, Cejka P, Kowalczykowski SC, Heyer WD. (2015). Top3-Rmi1 dissolve Rad51-mediated D loops by a topoisomerase-based mechanism. Mol Cell. 57(4):595-606. doi: 10.1016/j.molcel.2015.01.022.

Fasching CL, Neumann AA, Muntoni A, Yeager TR, Reddel RR. (2007). DNA damage induces alternative lengthening of telomeres (ALT) associated promyelocytic leukemia bodies that preferentially associate with linear telomeric DNA. Cancer Res. 67(15):7072-7. doi: 10.1158/0008-5472.CAN-07-1556.

Felsenfeld G, Groudine M. (2003). Controlling the double helix. Nature. 421(6921):448-53. doi: 10.1038/nature01411.

Feng W, Di Rienzi SC, Raghuraman MK, Brewer BJ. (2011). Replication stress-induced chromosome breakage is correlated with replication fork progression and is preceded by single-stranded DNA formation. G3 (Bethesda). 1(5):327-35. doi: 10.1534/g3.111.000554.

Feng L, Li N, Li Y, Wang J, Gao M, Wang W, Chen J. (2015). Cell cycle-dependent inhibition of 53BP1 signaling by BRCA1. Cell Discov. 1:15019. doi: 10.1038/celldisc.2015.19.

Fielden J, Ruggiano A, Popović M, Ramadan K. (2018). DNA protein crosslink proteolysis repair: From yeast to premature aging and cancer in humans. DNA Repair (Amst). 71:198-204. doi: 10.1016/j.dnarep.2018.08.025.

Fishman-Lobell J, Rudin N, Haber JE. (1992). Two alternative pathways of double-strand break repair that are kinetically separable and independently modulated. Mol Cell Biol. 12(3):1292-303. doi: 10.1128/mcb.12.3.1292-1303.1992.

Forget AL, Kowalczykowski SC. (2012). Single-molecule imaging of DNA pairing by

RecA reveals a three-dimensional homology search. Nature. 482(7385):423-7. doi: 10.1038/nature10782.

Forsburg SL, Rhind N. (2006). Basic methods for fission yeast. Yeast. 23(3):173-83. doi: 10.1002/yea.1347.

Fouché N, Ozgür S, Roy D, Griffith JD. (2006). Replication fork regression in repetitive DNAs. Nucleic Acids Res. 34(20):6044-50. doi: 10.1093/nar/gkl757.

Fragkos M, Ganier O, Coulombe P, Méchali M. (2015). DNA replication origin activation in space and time. Nat Rev Mol Cell Biol. 16(6):360-74. doi: 10.1038/nrm4002.

Freudenreich CH, Kantrow SM, Zakian VA. (1998). Expansion and length-dependent fragility of CTG repeats in yeast. Science. 279(5352):853-6. doi: 10.1126/science.279.5352.853.

Fricke WM, Brill SJ. (2003). Slx1-Slx4 is a second structure-specific endonuclease functionally redundant with Sgs1-Top3. Genes Dev. 17(14):1768-78. doi: 10.1101/gad.1105203.

Friedberg EC. (2005). Suffering in silence: the tolerance of DNA damage. Nat Rev Mol Cell Biol. 6(12):943-53. doi: 10.1038/nrm1781.

Fritz AJ, Sehgal N, Pliss A, Xu J, Berezney R. (2019). Chromosome territories and the global regulation of the genome. Genes Chromosomes Cancer. 58(7):407-426. doi: 10.1002/gcc.22732.

Fu H, Redon CE, Thakur BL, Utani K, Sebastian R, Jang SM, Gross JM, Mosavarpour S, Marks AB, Zhuang SZ, Lazar SB, Rao M, Mencer ST, Baris AM, Pongor LS, Aladjem MI. (2021). Dynamics of replication origin over-activation. Nat Commun. 12(1):3448. doi: 10.1038/s41467-021-23835-0.

Fujita M. (2006). Cdt1 revisited: complex and tight regulation during the cell cycle and consequences of deregulation in mammalian cells. Cell Div. 1:22. doi: 10.1186/1747-1028-1-22.

Fumasoni M, Zwicky K, Vanoli F, Lopes M, Branzei D. (2015). Error-free DNA damage tolerance and sister chromatid proximity during DNA replication rely on the Polα/Primase/Ctf4 Complex. Mol Cell. 57(5):812-823. doi: 10.1016/j.molcel.2014.12.038.

Gaillard H, García-Muse T, Aguilera A. (2015). Replication stress and cancer. Nat Rev Cancer. 15(5):276-89. doi: 10.1038/nrc3916.

Gaillard H, Santos-Pereira JM, Aguilera A. (2019). The Nup84 complex coordinates the DNA damage response to warrant genome integrity. Nucleic Acids Res. 47(8):4054-4067. doi: 10.1093/nar/gkz066.

Galanty Y, Belotserkovskaya R, Coates J, Jackson SP. (2012). RNF4, a SUMO-targeted ubiquitin E3 ligase, promotes DNA double-strand break repair. Genes Dev. 26(11):1179-95. doi: 10.1101/gad.188284.112.

Galanty Y, Belotserkovskaya R, Coates J, Polo S, Miller KM, Jackson SP. (2009). Mammalian SUMO E3-ligases PIAS1 and PIAS4 promote responses to DNA double-strand breaks. Nature. 462(7275):935-9. doi: 10.1038/nature08657.

Gallardo P, Barrales RR, Daga RR, Salas-Pino S. (2019). Nuclear Mechanics in the Fission Yeast. Cells. 8(10):1285. doi: 10.3390/cells8101285.

Gan W, Guan Z, Liu J, Gui T, Shen K, Manley JL, Li X. (2011). R-loop-mediated genomic instability is caused by impairment of replication fork progression. Genes Dev. 25(19):2041-56. doi: 10.1101/gad.17010011.

García-Gómez S, Reyes A, Martínez-Jiménez MI, Chocrón ES, Mourón S, Terrados G, Powell C, Salido E, Méndez J, Holt IJ, Blanco L. (2013). PrimPol, an archaic primase/polymerase operating in human cells. Mol Cell. 52(4):541-53. doi: 10.1016/j.molcel.2013.09.025.

García-Muse T, Aguilera A. (2016). Transcription-replication conflicts: how they occur and how they are resolved. Nat Rev Mol Cell Biol. 17(9):553-63. doi: 10.1038/nrm.2016.88.

Garcia V, Phelps SE, Gray S, Neale MJ. (2011). Bidirectional resection of DNA double-strand breaks by Mre11 and Exo1. Nature. 479(7372):241-4. doi: 10.1038/nature10515.
García-Rodríguez N, Wong RP, Ulrich HD. (2018). The helicase Pif1 functions in the template switching pathway of DNA damage bypass. Nucleic Acids Res. 46(16):8347-8356. doi: 10.1093/nar/gky648.

Ge XQ, Blow JJ. (2010). Chk1 inhibits replication factory activation but allows dormant origin firing in existing factories. J Cell Biol. 191(7):1285-97. doi: 10.1083/jcb.201007074.

Géli V, Lisby M. (2015). Recombinational DNA repair is regulated by compartmentalization of DNA lesions at the nuclear pore complex. Bioessays. 37(12):1287-92. doi: 10.1002/bies.201500084.

Georgescu RE, Langston L, Yao NY, Yurieva O, Zhang D, Finkelstein J, Agarwal T, O'Donnell ME. (2014). Mechanism of asymmetric polymerase assembly at the eukaryotic replication fork. Nat Struct Mol Biol. 21(8):664-70. doi: 10.1038/nsmb.2851.

Georgescu R, Yuan Z, Bai L, de Luna Almeida Santos R, Sun J, Zhang D, Yurieva O, Li H, O'Donnell ME. (2017). Structure of eukaryotic CMG helicase at a replication fork and implications to replisome architecture and origin initiation. Proc Natl Acad Sci U S A. 114(5):E697-E706. doi: 10.1073/pnas.1620500114.

Giannattasio M, Zwicky K, Follonier C, Foiani M, Lopes M, Branzei D. (2014). Visualization of recombination-mediated damage bypass by template switching. Nat Struct Mol Biol. 21(10):884-92. doi: 10.1038/nsmb.2888.

Goeres J, Chan PK, Mukhopadhyay D, Zhang H, Raught B, Matunis MJ. (2011). The SUMO-specific isopeptidase SENP2 associates dynamically with nuclear pore complexes through interactions with karyopherins and the Nup107-160 nucleoporin subcomplex. Mol Biol Cell. 22(24):4868-82. doi: 10.1091/mbc.E10-12-0953.

Gotta M, Laroche T, Formenton A, Maillet L, Scherthan H, Gasser SM. (1996). The clustering of telomeres and colocalization with Rap1, Sir3, and Sir4 proteins in wild-type Saccharomyces cerevisiae. J Cell Biol. 134(6):1349-63. doi: 10.1083/jcb.134.6.1349.

Gong L, Millas S, Maul GG, Yeh ET. (2000). Differential regulation of sentrinized proteins by a novel sentrin-specific protease. J Biol Chem. 275(5):3355-9. doi: 10.1074/jbc.275.5.3355.

Guilbaud G, Murat P, Wilkes HS, Lerner LK, Sale JE, Krude T. (2022). Determination of human DNA replication origin position and efficiency reveals principles of initiation zone organisation. Nucleic Acids Res. 50(13):7436-7450. doi: 10.1093/nar/gkac555.

Haahr P, Hoffmann S, Tollenaere MA, Ho T, Toledo LI, Mann M, Bekker-Jensen S, Räschle M, Mailand N. (2016). Activation of the ATR kinase by the RPA-binding protein ETAA1. Nat Cell Biol. 18(11):1196-1207. doi: 10.1038/ncb3422.

Hagan IM, Grallert A, Simanis V. (2016). Synchronizing Progression of Schizosaccharomyces pombe Cells from G2 through Repeated Rounds of Mitosis and S Phase with cdc25-22 Arrest Release. Cold Spring Harb Protoc. 2016(8). doi: 10.1101/pdb.prot091264.

Halazonetis TD, Gorgoulis VG, Bartek J. (2008). An oncogene-induced DNA damage model for cancer development. Science. 319(5868):1352-5. doi: 10.1126/science.1140735.

Hamperl S, Bocek MJ, Saldivar JC, Swigut T, Cimprich KA. (2017). Transcription-Replication Conflict Orientation Modulates R-Loop Levels and Activates Distinct DNA Damage Responses. Cell. 170(4):774-786.e19. doi: 10.1016/j.cell.2017.07.043.

Han J, Wan L, Jiang G, Cao L, Xia F, Tian T, Zhu X, Wu M, Huen MSY, Wang Y, Liu T, Huang J. (2021). ATM controls the extent of DNA end resection by eliciting sequential posttranslational modifications of CtIP. Proc Natl Acad Sci U S A. 118(12):e2022600118. doi: 10.1073/pnas.2022600118.

Hang J, Dasso M. (2020). Association of the human SUMO-1 protease SENP2 with the nuclear pore. J Biol Chem. 277(22):19961-6. doi: 10.1074/jbc.M201799200.

Harami GM, Pálinkás J, Seol Y, Kovács ZJ, Gyimesi M, Harami-Papp H, Neuman KC, Kovács M. (2022). The toposiomerase IIIalpha-RMI1-RMI2 complex orients human Bloom's syndrome helicase for efficient disruption of D-loops. Nat Commun. 13(1):654. doi: 10.1038/s41467-022-28208-9.

Hardeland U, Steinacher R, Jiricny J, Schär P. (2002). Modification of the human thymine-DNA glycosylase by ubiquitin-like proteins facilitates enzymatic turnover. EMBO J. 21(6):1456-64. doi: 10.1093/emboj/21.6.1456.

Harding SM, Boiarsky JA, Greenberg RA. (2015). ATM Dependent Silencing Links Nucleolar Chromatin Reorganization to DNA Damage Recognition. Cell Rep. 13(2):251-9. doi: 10.1016/j.celrep.2015.08.085.

Hardy J, Dai D, Ait Saada A, Teixeira-Silva A, Dupoiron L, Mojallali F, Fréon K, Ochsenbein F, Hartmann B, Lambert S. (2019). Histone deposition promotes recombination-dependent replication at arrested forks. PLoS Genet. 15(10):e1008441. doi: 10.1371/journal.pgen.1008441.

Hariharasudhan G, Jeong SY, Kim MJ, Jung SM, Seo G, Moon JR, Lee S, Chang IY, Kee Y, You HJ, Lee JH. (2022). TOPORS-mediated RAD51 SUMOylation facilitates homologous recombination repair. Nucleic Acids Res. 50(3):1501-1516. doi: 10.1093/nar/gkac009.

Harrigan JA, Belotserkovskaya R, Coates J, Dimitrova DS, Polo SE, Bradshaw CR, Fraser P, Jackson SP. (2011). Replication stress induces 53BP1-containing OPT domains in G1 cells. J Cell Biol. 193(1):97-108. doi: 10.1083/jcb.201011083.

Hartwell LH, Weinert TA. (1989). Checkpoints: controls that ensure the order of cell cycle events. Science. 1989 Nov 3;246(4930):629-34. doi: 10.1126/science.2683079.

Hashimoto Y, Puddu F, Costanzo V. (2011). RAD51- and MRE11-dependent reassembly

of uncoupled CMG helicase complex at collapsed replication forks. Nat Struct Mol Biol. 19(1):17-24. doi: 10.1038/nsmb.2177.

Hashimoto Y, Ray Chaudhuri A, Lopes M, Costanzo V. (2010). Rad51 protects nascent DNA from Mre11-dependent degradation and promotes continuous DNA synthesis. Nat Struct Mol Biol. 17(11):1305-11. doi: 10.1038/nsmb.1927.

Hauer MH, Gasser SM. (2017). Chromatin and nucleosome dynamics in DNA damage and repair. Genes Dev. 31(22):2204-2221. doi: 10.1101/gad.307702.117.

Hayles J, Nurse P. (2018). Introduction to Fission Yeast as a Model System. Cold Spring Harb Protoc. 2018(5). doi: 10.1101/pdb.top079749.

Hecker CM, Rabiller M, Haglund K, Bayer P, Dikic I. (2006). Specification of SUMO1- and SUMO2- interacting motifs. J Biol Chem. 281(23):16117-27. doi: 10.1074/jbc.M512757200.

Heckman DS, Geiser DM, Eidell BR, Stauffer RL, Kardos NL, Hedges SB. (2001). Molecular evidence for the early colonization of land by fungi and plants. Science. 293(5532):1129-33. doi: 10.1126/science.1061457.

Hector RE, Ray A, Chen BR, Shtofman R, Berkner KL, Runge KW. (2012). Mec1p associates with functionally compromised telomeres. Chromosoma. 121(3):277-90. doi: 10.1007/s00412-011-0359-0.

Hedges SB. (2002). The origin and evolution of model organisms. Nat Rev Genet. 3(11):838-49. doi: 10.1038/nrg929.

Heichinger C, Penkett CJ, Bähler J, Nurse P. (2006). Genome-wide characterization of fission yeast DNA replication origins. EMBO J. 25(21):5171-9. doi: 10.1038/sj.emboj.7601390.

Helmrich A, Ballarino M, Nudler E, Tora L. (2013). Transcription-replication encounters, consequences and genomic instability. Nat Struct Mol Biol. 20(4):412-8. doi: 10.1038/nsmb.2543.

Heitzer E, Tomlinson I. (2014). Replicative DNA polymerase mutations in cancer. Curr Opin Genet Dev. 24(100):107-13. doi: 10.1016/j.gde.2013.12.005. Epub 2014 Feb 26.

Heller RC, Kang S, Lam WM, Chen S, Chan CS, Bell SP. (2011). Eukaryotic origin-dependent DNA replication in vitro reveals sequential action of DDK and S-CDK kinases. Cell. 146(1):80-91. doi: 10.1016/j.cell.2011.06.012.

Herbert S, Brion A, Arbona JM, Lelek M, Veillet A, Lelandais B, Parmar J, Fernández FG, Almayrac E, Khalil Y, Birgy E, Fabre E, Zimmer C. (2017). Chromatin stiffening underlies enhanced locus mobility after DNA damage in budding yeast. EMBO J. 36(17):2595-2608. doi: 10.15252/embj.201695842.

Hill TM, Marians KJ. (1990). Escherichia coli Tus protein acts to arrest the progression of DNA replication forks in vitro. Proc Natl Acad Sci U S A. 87(7):2481-5. doi: 10.1073/pnas.87.7.2481.

Hills SA, Diffley JF. (2014). DNA replication and oncogene-induced replicative stress. Curr Biol. 24(10):R435-44. doi: 10.1016/j.cub.2014.04.012. Erratum in: Curr Biol. 2014 Jul 7;24(13):1563.

Ho JC, Warr NJ, Shimizu H, Watts FZ. (2001). SUMO modification of Rad22, the Schizosaccharomyces pombe homologue of the recombination protein Rad52. Nucleic Acids Res. 29(20):4179-86. doi: 10.1093/nar/29.20.4179.

Hockemeyer D, Sfeir AJ, Shay JW, Wright WE, de Lange T. (2005). POT1 protects telomeres from a transient DNA damage response and determines how human chromosomes end. EMBO J. 24(14):2667-78. doi: 10.1038/sj.emboj.7600733.

Hoeijmakers JH. (2009). DNA damage, aging, and cancer. N Engl J Med. 361(15):1475-85. doi: 10.1056/NEJMra0804615. Erratum in: N Engl J Med. 2009 Nov 5;361(19):1914.
Hoelz A, Debler EW, Blobel G. (2011). The structure of the nuclear pore complex. Annu Rev Biochem. 80:613-43. doi: 10.1146/annurev-biochem-060109-151030.

Hoffman CS, Wood V, Fantes PA. (2015). An Ancient Yeast for Young Geneticists: A Primer on the Schizosaccharomyces pombe Model System. Genetics. 201(2):403-23. doi: 10.1534/genetics.115.181503. Erratum in: Genetics. 2016 Mar;202(3):1241.

Horigome C, Bustard DE, Marcomini I, Delgoshaie N, Tsai-Pflugfelder M, Cobb JA, Gasser SM. (2016). PolySUMOylation by Siz2 and Mms21 triggers relocation of DNA breaks to nuclear pores through the Slx5/Slx8 STUbL. Genes Dev. 30(8):931-45. doi: 10.1101/gad.277665.116.

Horigome C, Unozawa E, Ooki T, Kobayashi T. (2019). Ribosomal RNA gene repeats associate with the nuclear pore complex for maintenance after DNA damage. PLoS Genet. 15(4):e1008103. doi: 10.1371/journal.pgen.1008103.

Hu J, Sun L, Shen F, Chen Y, Hua Y, Liu Y, Zhang M, Hu Y, Wang Q, Xu W, Sun F, Ji J, Murray JM, Carr AM, Kong D. (2012). The intra-S phase checkpoint targets Dna2 to prevent stalled replication forks from reversing. Cell. 149(6):1221-32. doi: 10.1016/j.cell.2012.04.030.

Huertas P, Cortés-Ledesma F, Sartori AA, Aguilera A, Jackson SP. (2008). CDK targets Sae2 to control DNA-end resection and homologous recombination. Nature. 455(7213):689-92. doi: 10.1038/nature07215. Epub 2008 Aug 20.

Husnjak K, Keiten-Schmitz J, Müller S. (2016). Identification and Characterization of SUMO-SIM Interactions. Methods Mol Biol. 1475:79-98. doi: 10.1007/978-1-4939-6358-4_6.

Ibarra A, Schwob E, Méndez J. (2008). Excess MCM proteins protect human cells from replicative stress by licensing backup origins of replication. Proc Natl Acad Sci U S A. 105(26):8956-61. doi: 10.1073/pnas.0803978105.

Ide H, Shoulkamy MI, Nakano T, Miyamoto-Matsubara M, Salem AM. (2010). Repair and biochemical effects of DNA-protein crosslinks. Mutat Res. 711(1-2):113-22. doi: 10.1016/j.mrfmmm.2010.12.007.

IJpma AS, Greider CW. (2003). Short telomeres induce a DNA damage response in Saccharomyces cerevisiae. Mol Biol Cell. 14(3):987-1001. doi: 10.1091/mbc.02-04-0057.

Ira G, Pellicioli A, Balijja A, Wang X, Fiorani S, Carotenuto W, Liberi G, Bressan D, Wan L, Hollingsworth NM, Haber JE, Foiani M. (2004). DNA end resection, homologous recombination and DNA damage checkpoint activation require CDK1. Nature. 431(7011):1011-7. doi: 10.1038/nature02964.

Iraqui I, Chekkal Y, Jmari N, Pietrobon V, Fréon K, Costes A, Lambert SA. (2012). Recovery of arrested replication forks by homologous recombination is error-prone. PLoS Genet. 8(10):e1002976. doi: 10.1371/journal.pgen.1002976.

Ivessa AS, Lenzmeier BA, Bessler JB, Goudsouzian LK, Schnakenberg SL, Zakian VA. (2003). The Saccharomyces cerevisiae helicase Rrm3p facilitates replication past nonhistone protein-DNA complexes. Mol Cell. 12(6):1525-36. doi: 10.1016/s1097-2765(03)00456-8.

Jackson SP, Bartek J. (2009). The DNA-damage response in human biology and disease. Nature. 461(7267):1071-8. doi: 10.1038/nature08467.

Jakob B, Splinter J, Conrad S, Voss KO, Zink D, Durante M, Löbrich M, Taucher-Scholz G. (2011). DNA double-strand breaks in heterochromatin elicit fast repair protein recruitment, histone H2AX phosphorylation and relocation to euchromatin. Nucleic Acids Res. 39(15):6489-99. doi: 10.1093/nar/gkr230.

Jakob B, Splinter J, Taucher-Scholz G. (2009). Positional stability of damaged chromatin domains along radiation tracks in mammalian cells. Radiat Res. 171(4):405-18. doi: 10.1667/RR1520.1.

Jalan M, Oehler J, Morrow CA, Osman F, Whitby MC. (2019). Factors affecting template switch recombination associated with restarted DNA replication. Elife. 8:e41697. doi: 10.7554/eLife.41697.

Janssen A, Breuer GA, Brinkman EK, van der Meulen AI, Borden SV, van Steensel B, Bindra RS, LaRocque JR, Karpen GH. (2016). A single double-strand break system reveals repair dynamics and mechanisms in heterochromatin and euchromatin. Genes Dev. 30(14):1645-57. doi: 10.1101/gad.283028.116.

Jasin M, Rothstein R. (2013). Repair of strand breaks by homologous recombination. Cold Spring Harb Perspect Biol. 5(11):a012740. doi: 10.1101/cshperspect.a012740.

Jazayeri A, Balestrini A, Garner E, Haber JE, Costanzo V. (2008). Mre11-Rad50-Nbs1-dependent processing of DNA breaks generates oligonucleotides that stimulate ATM activity. EMBO J. 27(14):1953-62. doi: 10.1038/emboj.2008.128.

Jensen RB, Carreira A, Kowalczykowski SC. (2010). Purified human BRCA2 stimulates RAD51-mediated recombination. Nature. 467(7316):678-83. doi: 10.1038/nature09399.

Jentsch S, Psakhye I. (2013). Control of nuclear activities by substrate-selective and protein-group SUMOylation. Annu Rev Genet. 47:167-86. doi: 10.1146/annurev-genet-111212-133453.

Jin QW, Fuchs J, Loidl J. (2000). Centromere clustering is a major determinant of yeast interphase nuclear organization. J Cell Sci. 113 (Pt 11):1903-12. doi: 10.1242/jcs.113.11.1903.

Johnson ES. (2004). Protein modification by SUMO. Annu Rev Biochem. 73:355-82. doi: 10.1146/annurev.biochem.73.011303.074118.

Johnson RD, Jasin M. (2000). Sister chromatid gene conversion is a prominent double-strand break repair pathway in mammalian cells. EMBO J. 19(13):3398-407. doi: 10.1093/emboj/19.13.3398.

Joseph CR, Dusi S, Giannattasio M, Branzei D. (2022). Rad51-mediated replication of damaged templates relies on monoSUMOylated DDK kinase. Nat Commun. 13(1):2480. doi: 10.1038/s41467-022-30215-9.

Kalocsay M, Hiller NJ, Jentsch S. (2009). Chromosome-wide Rad51 spreading and SUMO-H2A.Z-dependent chromosome fixation in response to a persistent DNA double-strand break. Mol Cell. 33(3):335-43. doi: 10.1016/j.molcel.2009.01.016.

Kalousi A, Soutoglou E. (2016). Nuclear compartmentalization of DNA repair. Curr Opin Genet Dev. 37:148-157. doi: 10.1016/j.gde.2016.05.013.

Kan Y, Batada NN, Hendrickson EA. (2017). Human somatic cells deficient for RAD52 are impaired for viral integration and compromised for most aspects of homology-directed repair. DNA Repair (Amst). 55:64-75. doi: 10.1016/j.dnarep.2017.04.006.

Karanam K, Kafri R, Loewer A, Lahav G. (2012). Quantitative live cell imaging reveals a gradual shift between DNA repair mechanisms and a maximal use of HR in mid S phase. Mol Cell. 47(2):320-9. doi: 10.1016/j.molcel.2012.05.052.

Karras GI, Fumasoni M, Sienski G, Vanoli F, Branzei D, Jentsch S. (2013). Noncanonical role of the 9-1-1 clamp in the error-free DNA damage tolerance pathway. Mol Cell. 49(3):536-46. doi: 10.1016/j.molcel.2012.11.016.

Katyal S, McKinnon PJ. (2008). DNA strand breaks, neurodegeneration and aging in the brain. Mech Ageing Dev. 129(7-8):483-91. doi: 10.1016/j.mad.2008.03.008.

Kawabata T, Luebben SW, Yamaguchi S, Ilves I, Matise I, Buske T, Botchan MR, Shima N. (2011). Stalled fork rescue via dormant replication origins in unchallenged S phase promotes proper chromosome segregation and tumor suppression. Mol Cell. 41(5):543-53. doi: 10.1016/j.molcel.2011.02.006.

Kerscher O. (2007). SUMO junction-what's your function? New insights through SUMO-interacting motifs. EMBO Rep. 8(6):550-5. doi: 10.1038/sj.embor.7400980.

Kerzendorfer C, O'Driscoll M. (2009). Human DNA damage response and repair deficiency syndromes: linking genomic instability and cell cycle checkpoint proficiency. DNA Repair (Amst). 8(9):1139-52. doi: 10.1016/j.dnarep.2009.04.018.

Keszthelyi A, Minchell NE, Baxter J. (2016). The Causes and Consequences of Topological Stress during DNA Replication. Genes (Basel). 7(12):134. doi: 10.3390/genes7120134.

Khadaroo B, Teixeira MT, Luciano P, Eckert-Boulet N, Germann SM, Simon MN, Gallina I, Abdallah P, Gilson E, Géli V, Lisby M. (2009). The DNA damage response at eroded telomeres and tethering to the nuclear pore complex. Nat Cell Biol. 11(8):980-7. doi: 10.1038/ncb1910.

Khatri GS, MacAllister T, Sista PR, Bastia D. (1989). The replication terminator protein of E. coli is a DNA sequence-specific contra-helicase. Cell. 59(4):667-74. doi: 10.1016/0092-8674(89)90012-3.

Kishkevich A, Tamang S, Nguyen MO, Oehler J, Bulmaga E, Andreadis C, Morrow CA, Jalan M, Osman F, Whitby MC. (2022). Rad52's DNA annealing activity drives template switching associated with restarted DNA replication. Nat Commun. 13(1):7293. doi: 10.1038/s41467-022-35060-4.

Knutsen JH, Rein ID, Rothe C, Stokke T, Grallert B, Boye E. (2011). Cell-cycle analysis of fission yeast cells by flow cytometry. PLoS One. 6(2):e17175. doi: 10.1371/journal.pone.0017175.

Kobayashi T, Horiuchi T. (1996). A yeast gene product, Fob1 protein, required for both replication fork blocking and recombinational hotspot activities. Genes Cells. 1(5):465-74. doi: 10.1046/j.1365-2443.1996.d01-256.x.

Kohzaki M, Hatanaka A, Sonoda E, Yamazoe M, Kikuchi K, Vu Trung N, Szüts D, Sale JE, Shinagawa H, Watanabe M, Takeda S. (2007). Cooperative roles of vertebrate Fbh1 and Blm DNA helicases in avoidance of crossovers during recombination initiated by replication fork collapse. Mol Cell Biol. 27(8):2812-20. doi: 10.1128/MCB.02043-06.

Kolinjivadi AM, Sannino V, De Antoni A, Zadorozhny K, Kilkenny M, Técher H, Baldi G, Shen R, Ciccia A, Pellegrini L, Krejci L, Costanzo V. (2017). Smarcal1-Mediated Fork Reversal Triggers Mre11-Dependent Degradation of Nascent DNA in the Absence of Brca2 and Stable Rad51 Nucleofilaments. Mol Cell. 67(5):867-881.e7. doi: 10.1016/j.molcel.2017.07.001.

Kosoy A, Calonge TM, Outwin EA, O'Connell MJ. (2007). Fission yeast Rnf4 homologs are required for DNA repair. J Biol Chem. 282(28):20388-94. doi: 10.1074/jbc.M702652200.

Kramara J, Osia B, Malkova A. (2018). Break-Induced Replication: The Where, The Why, and The How. Trends Genet. 34(7):518-531. doi: 10.1016/j.tig.2018.04.002.

Kramarz K, Mucha S, Litwin I, Barg-Wojas A, Wysocki R, Dziadkowiec D. (2017). DNA Damage Tolerance Pathway Choice Through Uls1 Modulation of Srs2 SUMOylation in *Saccharomyces cerevisiae*. Genetics. 206(1):513-525. doi: 10.1534/genetics.116.196568.

Kramarz K, Schirmeisen K, Boucherit V, Ait Saada A, Lovo C, Palancade B, Freudenreich C, Lambert SAE. (2020). The nuclear pore primes recombination-dependent DNA

synthesis at arrested forks by promoting SUMO removal. Nat Commun. 11(1):5643. doi: 10.1038/s41467-020-19516-z.

Krawczyk PM, Borovski T, Stap J, Cijsouw T, ten Cate R, Medema JP, Kanaar R, Franken NA, Aten JA. (2012). Chromatin mobility is increased at sites of DNA double-strand breaks. J Cell Sci. 125(Pt 9):2127-33. doi: 10.1242/jcs.089847.

Krings G, Bastia D. (2005). Sap1p binds to Ter1 at the ribosomal DNA of Schizosaccharomyces pombe and causes polar replication fork arrest. J Biol Chem. 280(47):39135-42. doi: 10.1074/jbc.M508996200.

Kruhlak MJ, Celeste A, Dellaire G, Fernandez-Capetillo O, Müller WG, McNally JG, Bazett-Jones DP, Nussenzweig A. (2006). Changes in chromatin structure and mobility in living cells at sites of DNA double-strand breaks. J Cell Biol. 172(6):823-34. doi: 10.1083/jcb.200510015.

Kumar R, González-Prieto R, Xiao Z, Verlaan-de Vries M, Vertegaal ACO. (2017). The STUbL RNF4 regulates protein group SUMOylation by targeting the SUMO conjugation machinery. Nat Commun. 8(1):1809. doi: 10.1038/s41467-017-01900-x.

Kumar D, Viberg J, Nilsson AK, Chabes A. (2010). Highly mutagenic and severely imbalanced dNTP pools can escape detection by the S-phase checkpoint. Nucleic Acids Res. 38(12):3975-83. doi: 10.1093/nar/gkq128.

Kunnev D, Rusiniak ME, Kudla A, Freeland A, Cady GK, Pruitt SC. (2010). DNA damage response and tumorigenesis in Mcm2-deficient mice. Oncogene. 29(25):3630-8. doi: 10.1038/onc.2010.125.

Lallemand-Breitenbach V, Jeanne M, Benhenda S, Nasr R, Lei M, Peres L, Zhou J, Zhu J, Raught B, de Thé H. (2008). Arsenic degrades PML or PML-RARalpha through a SUMO-triggered RNF4/ubiquitin-mediated pathway. Nat Cell Biol. 10(5):547-55. doi: 10.1038/ncb1717.

Lambert S, Mizuno K, Blaisonneau J, Martineau S, Chanet R, Fréon K, Murray JM, Carr AM, Baldacci G. (2010). Homologous recombination restarts blocked replication forks at the expense of genome rearrangements by template exchange. Mol Cell. 39(3):346-59. doi: 10.1016/j.molcel.2010.07.015.

Lambert S, Watson A, Sheedy DM, Martin B, Carr AM. (2005). Gross chromosomal rearrangements and elevated recombination at an inducible site-specific replication fork barrier. Cell. 121(5):689-702. doi: 10.1016/j.cell.2005.03.022.

Lamm N, Read MN, Nobis M, Van Ly D, Page SG, Masamsetti VP, Timpson P, Biro M, Cesare AJ. (2020). Nuclear F-actin counteracts nuclear deformation and promotes fork

repair during replication stress. Nat Cell Biol. 22(12):1460-1470. doi: 10.1038/s41556-020-00605-6.

Lavin MF, Kozlov S, Gatei M, Kijas AW. (2015). ATM-Dependent Phosphorylation of All Three Members of the MRN Complex: From Sensor to Adaptor. Biomolecules. 5(4):2877-902. doi: 10.3390/biom5042877.

Lazzaro F, Novarina D, Amara F, Watt DL, Stone JE, Costanzo V, Burgers PM, Kunkel TA, Plevani P, Muzi-Falconi M. (2012). RNase H and postreplication repair protect cells from ribonucleotides incorporated in DNA. Mol Cell. 45(1):99-110. doi: 10.1016/j.molcel.2011.12.019.

Lee EH, Kornberg A, Hidaka M, Kobayashi T, Horiuchi T. (1989). Escherichia coli replication termination protein impedes the action of helicases. Proc Natl Acad Sci U S A. 86(23):9104-8. doi: 10.1073/pnas.86.23.9104.

Lee JH, Paull TT. (2004). Direct activation of the ATM protein kinase by the Mre11/Rad50/Nbs1 complex. Science. 304(5667):93-6. doi: 10.1126/science.1091496.

Lee JH, Paull TT. (2005). ATM activation by DNA double-strand breaks through the Mre11-Rad50-Nbs1 complex. Science. 308(5721):551-4. doi: 10.1126/science.1108297.

Lemaçon D, Jackson J, Quinet A, Brickner JR, Li S, Yazinski S, You Z, Ira G, Zou L, Mosammaparast N, Vindigni A. (2017). MRE11 and EXO1 nucleases degrade reversed forks and elicit MUS81-dependent fork rescue in BRCA2-deficient cells. Nat Commun. 8(1):860. doi: 10.1038/s41467-017-01180-5.

Lemaître C, Grabarz A, Tsouroula K, Andronov L, Furst A, Pankotai T, Heyer V, Rogier M, Attwood KM, Kessler P, Dellaire G, Klaholz B, Reina-San-Martin B, Soutoglou E. (2014). Nuclear position dictates DNA repair pathway choice. Genes Dev. 28(22):2450-63. doi: 10.1101/gad.248369.114.

Lemaître C, Fischer B, Kalousi A, Hoffbeck AS, Guirouilh-Barbat J, Shahar OD, Genet D, Goldberg M, Betrand P, Lopez B, Brino L, Soutoglou E. (2012). The nucleoporin 153, a novel factor in double-strand break repair and DNA damage response. Oncogene. 31(45):4803-9. doi: 10.1038/onc.2011.638.

Lescasse R, Pobiega S, Callebaut I, Marcand S. (2013). End-joining inhibition at telomeres requires the translocase and polySUMO-dependent ubiquitin ligase Uls1. EMBO J. 32(6):805-15. doi: 10.1038/emboj.2013.24.

Leupold U. (1950). Die Vererbung von Homothallie und Heterothallie bei Schizosaccharomyces pombe. CR Lab Carlsberg Sér Physiol 24: 381–480

Lewis A, Felberbaum R, Hochstrasser M. (2007). A nuclear envelope protein linking nuclear pore basket assembly, SUMO protease regulation, and mRNA surveillance. J Cell Biol. 178(5):813-27. doi: 10.1083/jcb.200702154.

Li SJ, Hochstrasser M. (2003). The Ulp1 SUMO isopeptidase: distinct domains required for viability, nuclear envelope localization, and substrate specificity. J Cell Biol. 160(7):1069-81. doi: 10.1083/jcb.200212052.

Li SJ, Hochstrasser M. (2000). The yeast ULP2 (SMT4) gene encodes a novel protease specific for the ubiquitin-like Smt3 protein. Mol Cell Biol. 20(7):2367-77. doi: 10.1128/MCB.20.7.2367-2377.2000.

Li X, Stith CM, Burgers PM, Heyer WD. (2009). PCNA is required for initiation of recombination-associated DNA synthesis by DNA polymerase delta. Mol Cell. 36(4):704-13. doi: 10.1016/j.molcel.2009.09.036.

Li S, Wang H, Jehi S, Li J, Liu S, Wang Z, Truong L, Chiba T, Wang Z, Wu X. (2021). PIF1 helicase promotes break-induced replication in mammalian cells. EMBO J. 40(8):e104509. doi: 10.15252/embj.2020104509.

Li X, Zhang XP, Solinger JA, Kiianitsa K, Yu X, Egelman EH, Heyer WD. (2007). Rad51 and Rad54 ATPase activities are both required to modulate Rad51-dsDNA filament dynamics. Nucleic Acids Res. 35(12):4124-40. doi: 10.1093/nar/gkm412.

Liang F, Han M, Romanienko PJ, Jasin M. (1998). Homology-directed repair is a major double-strand break repair pathway in mammalian cells. Proc Natl Acad Sci U S A. 95(9):5172-7. doi: 10.1073/pnas.95.9.5172.

Liebelt F, Jansen NS, Kumar S, Gracheva E, Claessens LA, Verlaan-de Vries M, Willemstein E, Vertegaal ACO. (2019). The poly-SUMO2/3 protease SENP6 enables assembly of the constitutive centromere-associated network by group deSUMOylation. Nat Commun. 10(1):3987. doi: 10.1038/s41467-019-11773-x.

Lieberman-Aiden E, van Berkum NL, Williams L, Imakaev M, Ragoczy T, Telling A, Amit I, Lajoie BR, Sabo PJ, Dorschner MO, Sandstrom R, Bernstein B, Bender MA, Groudine M, Gnirke A, Stamatoyannopoulos J, Mirny LA, Lander ES, Dekker J. (2009). Comprehensive mapping of long-range interactions reveals folding principles of the human genome. Science. 326(5950):289-93. doi: 10.1126/science.1181369.

Lindahl T, Barnes DE. (2000). Repair of endogenous DNA damage. Cold Spring Harb Symp Quant Biol.65:127-33. doi: 10.1101/sqb.2000.65.127.

Linder P. (1893). *Schizosaccharomyces pombe* n.sp., ein neuer Gährungserreger. Wochenschrift für Brauerei. 10:1298–1300

Lisby M, Barlow JH, Burgess RC, Rothstein R. (2004). Choreography of the DNA damage response: spatiotemporal relationships among checkpoint and repair proteins. Cell. 118(6):699-713. doi: 10.1016/j.cell.2004.08.015.

Lisby M, Mortensen UH, Rothstein R. (2003). Colocalization of multiple DNA double-strand breaks at a single Rad52 repair centre. Nat Cell Biol. 5(6):572-7. doi: 10.1038/ncb997.

Liu L, Yan Z, Osia BA, Twarowski J, Sun L, Kramara J, Lee RS, Kumar S, Elango R, Li H, Dang W, Ira G, Malkova A. (2021). Tracking break-induced replication shows that it stalls at roadblocks. Nature. 590(7847):655-659. doi: 10.1038/s41586-020-03172-w.

Liu S, Miné-Hattab J, Villemeur M, Guerois R, Pinholt HD, Mirny LA, Taddei A. (2023). In vivo tracking of functionally tagged Rad51 unveils a robust strategy of homology search. Nat Struct Mol Biol. doi: 10.1038/s41594-023-01065-w.

Liu J, Renault L, Veaute X, Fabre F, Stahlberg H, Heyer WD. (2011). Rad51 paralogues Rad55-Rad57 balance the antirecombinase Srs2 in Rad51 filament formation. Nature. 479(7372):245-8. doi: 10.1038/nature10522.

Liu W, Saito Y, Jackson J, Bhowmick R, Kanemaki MT, Vindigni A, Cortez D. (2023). RAD51 bypasses the CMG helicase to promote replication fork reversal. Science. 380(6643):382-387. doi: 10.1126/science.add7328.

Liu L, Sugawara N, Malkova A, Haber JE. (2021). Determining the kinetics of break-induced replication (BIR) by the assay for monitoring BIR elongation rate (AMBER). Methods Enzymol. 661:139-154. doi: 10.1016/bs.mie.2021.09.004.

Loayza D, De Lange T. (2003). POT1 as a terminal transducer of TRF1 telomere length control. Nature. 423(6943):1013-8. doi: 10.1038/nature01688.

Locke AJ, Hossain L, McCrostie G, Ronato DA, Fitieh A, Rafique TA, Mashayekhi F, Motamedi M, Masson JY, Ismail IH. (2021). SUMOylation mediates CtIP's functions in DNA end resection and replication fork protection. Nucleic Acids Res. 49(2):928-953. doi: 10.1093/nar/gkaa1232.

Loeillet S, Palancade B, Cartron M, Thierry A, Richard GF, Dujon B, Doye V, Nicolas A. (2005). Genetic network interactions among replication, repair and nuclear pore deficiencies in yeast. DNA Repair (Amst). 4(4):459-68. doi: 10.1016/j.dnarep.2004.11.010.

Lopes M, Cotta-Ramusino C, Pellicioli A, Liberi G, Plevani P, Muzi-Falconi M, Newlon CS, Foiani M. (2001). The DNA replication checkpoint response stabilizes stalled replication forks. Nature. 412(6846):557-61. doi: 10.1038/35087613.

Lopes M, Foiani M, Sogo JM. (2006). Multiple mechanisms control chromosome integrity after replication fork uncoupling and restart at irreparable UV lesions. Mol Cell. 21(1):15-27. doi: 10.1016/j.molcel.2005.11.015.

Lopez-Mosqueda J, Maas NL, Jonsson ZO, Defazio-Eli LG, Wohlschlegel J, Toczyski DP. (2010). Damage-induced phosphorylation of Sld3 is important to block late origin firing. Nature. 467(7314):479-83. doi: 10.1038/nature09377.

Lottersberger F, Karssemeijer RA, Dimitrova N, de Lange T. (2015). 53BP1 and the LINC Complex Promote Microtubule-Dependent DSB Mobility and DNA Repair. Cell. 163(4):880-93. doi: 10.1016/j.cell.2015.09.057.

Lubelsky Y, Sasaki T, Kuipers MA, Lucas I, Le Beau MM, Carignon S, Debatisse M, Prinz JA, Dennis JH, Gilbert DM. (2011). Pre-replication complex proteins assemble at regions of low nucleosome occupancy within the Chinese hamster dihydrofolate reductase initiation zone. Nucleic Acids Res. 39(8):3141-55. doi: 10.1093/nar/gkq1276.

Lundblad V, Blackburn EH. (1993). An alternative pathway for yeast telomere maintenance rescues est1- senescence. Cell. 73(2):347-60. doi: 10.1016/0092-8674(93)90234-h.

Lydeard JR, Jain S, Yamaguchi M, Haber JE. (2007). Break-induced replication and telomerase-independent telomere maintenance require Pol32. Nature. 448(7155):820-3. doi: 10.1038/nature06047.

Mackenroth B, Alani E. (2021). Collaborations between chromatin and nuclear architecture to optimize DNA repair fidelity. DNA Repair (Amst). 97:103018. doi: 10.1016/j.dnarep.2020.103018.

Maeda D, Seki M, Onoda F, Branzei D, Kawabe Y, Enomoto T. (2004). Ubc9 is required for damage-tolerance and damage-induced interchromosomal homologous recombination in S. cerevisiae. DNA Repair (Amst). 3(3):335-41. doi: 10.1016/j.dnarep.2003.11.011.

Maestroni L, Matmati S, Coulon S. (2017). Solving the Telomere Replication Problem. Genes (Basel). 8(2):55. doi: 10.3390/genes8020055.

Mahaney BL, Meek K, Lees-Miller SP. (2009). Repair of ionizing radiation-induced DNA double-strand breaks by non-homologous end-joining. Biochem J. 417(3):639-50. doi: 10.1042/BJ20080413.

Mahajan R, Delphin C, Guan T, Gerace L, Melchior F. (1997). A small ubiquitin-related polypeptide involved in targeting RanGAP1 to nuclear pore complex protein RanBP2. Cell. 88(1):97-107. doi: 10.1016/s0092-8674(00)81862-0.

Makhnevych T, Ptak C, Lusk CP, Aitchison JD, Wozniak RW. (2007). The role of karyopherins in the regulated sumoylation of septins. J Cell Biol. 177(1):39-49. doi: 10.1083/jcb.200608066.

Malkova A, Ivanov EL, Haber JE. (1996). Double-strand break repair in the absence of RAD51 in yeast: a possible role for break-induced DNA replication. Proc Natl Acad Sci U S A. 93(14):7131-6. doi: 10.1073/pnas.93.14.7131.

Malkova A, Signon L, Schaefer CB, Naylor ML, Theis JF, Newlon CS, Haber JE. (2001). RAD51-independent break-induced replication to repair a broken chromosome depends on a distant enhancer site. Genes Dev. 15(9):1055-60. doi: 10.1101/gad.875901. PMID: 11331601; PMCID: PMC312680.

Maloisel L, Fabre F, Gangloff S. (2008). DNA polymerase delta is preferentially recruited during homologous recombination to promote heteroduplex DNA extension. Mol Cell Biol. 28(4):1373-82. doi: 10.1128/MCB.01651-07.

Manivasakam P, Aubrecht J, Sidhom S, Schiestl RH. (2001). Restriction enzymes increase efficiencies of illegitimate DNA integration but decrease homologous integration in mammalian cells. Nucleic Acids Res. 29(23):4826-33. doi: 10.1093/nar/29.23.4826.

Mankouri HW, Ashton TM, Hickson ID. (2011). Holliday junction-containing DNA structures persist in cells lacking Sgs1 or Top3 following exposure to DNA damage. Proc Natl Acad Sci U S A. 108(12):4944-9. doi: 10.1073/pnas.1014240108.

González-Prieto R, Muñoz-Cabello AM, Cabello-Lobato MJ, Prado F. (2013). Rad51 replication fork recruitment is required for DNA damage tolerance. EMBO J. 32(9):1307-21. doi: 10.1038/emboj.2013.73.

Marcomini I, Gasser SM. (2015). Nuclear organization in DNA end processing: Telomeres vs double-strand breaks. DNA Repair (Amst). 32:134-140. doi: 10.1016/j.dnarep.2015.04.024.

Maric M, Mukherjee P, Tatham MH, Hay R, Labib K. (2017). Ufd1-Npl4 Recruit Cdc48 for Disassembly of Ubiquitylated CMG Helicase at the End of Chromosome Replication. Cell Rep. 18(13):3033-3042. doi: 10.1016/j.celrep.2017.03.020.

Masai H, Matsumoto S, You Z, Yoshizawa-Sugata N, Oda M. (2010). Eukaryotic chromosome DNA replication: where, when, and how? Annu Rev Biochem. 2010;79:89-130. doi: 10.1146/annurev.biochem.052308.103205.

Mason JM, Chan YL, Weichselbaum RW, Bishop DK. (2019). Non-enzymatic roles of human RAD51 at stalled replication forks. Nat Commun. 10(1):4410. doi: 10.1038/s41467-019-12297-0.

Mathews CK. (2016). The Most Interesting Enzyme in the World. Structure. 24(6):843-4. doi: 10.1016/j.str.2016.05.006.

Matos J, West SC. (2014). Holliday junction resolution: regulation in space and time. DNA Repair (Amst). 19(100):176-81. doi: 10.1016/j.dnarep.2014.03.013.

Matos DA, Zhang JM, Ouyang J, Nguyen HD, Genois MM, Zou L. (2020). ATR Protects the Genome against R Loops through a MUS81-Triggered Feedback Loop. Mol Cell. 77(3):514-527.e4. doi: 10.1016/j.molcel.2019.10.010.

Matunis MJ, Coutavas E, Blobel G. (1996) A novel ubiquitin-like modification modulates the partitioning of the Ran-GTPase-activating protein RanGAP1 between the cytosol and the nuclear pore complex. J Cell Biol. 135(6 Pt 1):1457-70. doi: 10.1083/jcb.135.6.1457.

Mayer R, Brero A, von Hase J, Schroeder T, Cremer T, Dietzel S. (2005). Common themes and cell type specific variations of higher order chromatin arrangements in the mouse. BMC Cell Biol. 6:44. doi: 10.1186/1471-2121-6-44.

McEachern MJ, Haber JE. (2006). Break-induced replication and recombinational telomere elongation in yeast. Annu Rev Biochem. 75:111-35. doi: 10.1146/annurev.biochem.74.082803.133234.

McCulloch SD, Kunkel TA. (2008). The fidelity of DNA synthesis by eukaryotic replicative and translesion synthesis polymerases. Cell Res. 18(1):148-61. doi: 10.1038/cr.2008.4.

McCully EK, Robinow CF. (1971). Mitosis in the fission yeast Schizosaccharomyces pombe: a comparative study with light and electron microscopy. J Cell Sci. 9(2):475-507. doi: 10.1242/jcs.9.2.475.

Nick McElhinny SA, Kumar D, Clark AB, Watt DL, Watts BE, Lundström EB, Johansson E, Chabes A, Kunkel TA. (2010). Genome instability due to ribonucleotide incorporation into DNA. Nat Chem Biol. 6(10):774-81. doi: 10.1038/nchembio.424.

McIlwraith MJ, Vaisman A, Liu Y, Fanning E, Woodgate R, West SC. (2005). Human DNA polymerase eta promotes DNA synthesis from strand invasion intermediates of homologous recombination. Mol Cell. 20(5):783-92. doi: 10.1016/j.molcel.2005.10.001.

McIntosh D, Blow JJ. (2012). Dormant origins, the licensing checkpoint, and the response to replicative stresses. Cold Spring Harb Perspect Biol. 4(10):a012955. doi: 10.1101/cshperspect.a012955.

Méchali M. (2010). Eukaryotic DNA replication origins: many choices for appropriate answers. Nat Rev Mol Cell Biol. 11(10):728-38. doi: 10.1038/nrm2976.

Mehta KPM, Thada V, Zhao R, Krishnamoorthy A, Leser M, Lindsey Rose K, Cortez D. (2022). CHK1 phosphorylates PRIMPOL to promote replication stress tolerance. Sci Adv. 8(13):eabm0314. doi: 10.1126/sciadv.abm0314.

Menin L, Ursich S, Trovesi C, Zellweger R, Lopes M, Longhese MP, Clerici M. (2018). Tel1/ATM prevents degradation of replication forks that reverse after topoisomerase poisoning. EMBO Rep. 19(7):e45535. doi: 10.15252/embr.201745535.

Michel B, Boubakri H, Baharoglu Z, LeMasson M, Lestini R. (2007). Recombination proteins and rescue of arrested replication forks. DNA Repair (Amst). 6(7):967-80. doi: 10.1016/j.dnarep.2007.02.016.

Mijic S, Zellweger R, Chappidi N, Berti M, Jacobs K, Mutreja K, Ursich S, Ray Chaudhuri A, Nussenzweig A, Janscak P, Lopes M. (2017). Replication fork reversal triggers fork degradation in BRCA2-defective cells. Nat Commun. 8(1):859. doi: 10.1038/s41467-017-01164-5.

Milne GT, Weaver DT. (1993). Dominant negative alleles of RAD52 reveal a DNA repair/recombination complex including Rad51 and Rad52. Genes Dev. 7(9):1755-65. doi: 10.1101/gad.7.9.1755.

Mimitou EP, Symington LS. (2011). DNA end resection-unraveling the tail. DNA Repair (Amst). 10(3):344-8. doi: 10.1016/j.dnarep.2010.12.004.

Mimitou EP, Symington LS. (2008). Sae2, Exo1 and Sgs1 collaborate in DNA double-strand break processing. Nature. 455(7214):770-4. doi: 10.1038/nature07312.

Mimitou EP, Yamada S, Keeney S. (2017). A global view of meiotic double-strand break end resection. Science. 355(6320):40-45. doi: 10.1126/science.aak9704.

Miné-Hattab J, Chiolo I. (2020). Complex Chromatin Motions for DNA Repair. Front Genet. 11:800. doi: 10.3389/fgene.2020.00800.

Miné-Hattab J, Heltberg M, Villemeur M, Guedj C, Mora T, Walczak AM, Dahan M, Taddei A. (2021). Single molecule microscopy reveals key physical features of repair foci in living cells. Elife. 10:e60577. doi: 10.7554/eLife.60577.

Miné-Hattab J, Rothstein R. (2012). Increased chromosome mobility facilitates homology search during recombination. Nat Cell Biol. 14(5):510-7. doi: 10.1038/ncb2472.

Miné-Hattab J, Rothstein R. (2013). DNA in motion during double-strand break repair. Trends Cell Biol. 23(11):529-36. doi: 10.1016/j.tcb.2013.05.006.

Miné-Hattab J, Recamier V, Izeddin I, Rothstein R, Darzacq X. (2017). Multi-scale tracking reveals scale-dependent chromatin dynamics after DNA damage. Mol Biol Cell. 28(23):3323–32. doi: 10.1091/mbc.E17-05-0317.

Minocherhomji S, Ying S, Bjerregaard VA, Bursomanno S, Aleliunaite A, Wu W, Mankouri HW, Shen H, Liu Y, Hickson ID. (2015). Replication stress activates DNA repair synthesis in mitosis. Nature. 528(7581):286-90. doi: 10.1038/nature16139.

Misteli T. (2020). The Self-Organizing Genome: Principles of Genome Architecture and Function. Cell. 183(1):28-45. doi: 10.1016/j.cell.2020.09.014.
Mirkin SM. (2007). Expandable DNA repeats and human disease. Nature. 447(7147):932-40. doi: 10.1038/nature05977.

Mitchison JM, Nurse P. (1985). Growth in cell length in the fission yeast Schizosaccharomyces pombe. J Cell Sci. 75:357-76. doi: 10.1242/jcs.75.1.357.
Mitchison JM. (1957). The growth of single cells. I. Schizosaccharomyces pombe. Exp Cell Res. 13(2):244-62. doi: 10.1016/0014-4827(57)90005-8.

Mitchison JM. (1990). The fission yeast, Schizosaccharomyces pombe. Bioessays. 12(4):189-91. doi: 10.1002/bies.950120409.

Miteva M, Keusekotten K, Hofmann K, Praefcke GJ, Dohmen RJ. (2010). Sumoylation as a signal for polyubiquitylation and proteasomal degradation. Subcell Biochem. 54:195-214. doi: 10.1007/978-1-4419-6676-6_16.

Miyabe I, Mizuno K, Keszthelyi A, Daigaku Y, Skouteri M, Mohebi S, Kunkel TA, Murray JM, Carr AM. (2015). Polymerase δ replicates both strands after homologous recombination-dependent fork restart. Nat Struct Mol Biol. 22(11):932-8. doi: 10.1038/nsmb.3100.

Miyazaki T, Bressan DA, Shinohara M, Haber JE, Shinohara A. (2004). In vivo assembly and disassembly of Rad51 and Rad52 complexes during double-strand break repair. EMBO J. 23(4):939-49. doi: 10.1038/sj.emboj.7600091.

Mizuno K, Lambert S, Baldacci G, Murray JM, Carr AM. (2009). Nearby inverted repeats fuse to generate acentric and dicentric palindromic chromosomes by a replication template exchange mechanism. Genes Dev. 23(24):2876-86. doi: 10.1101/gad.1863009.

Mizuno K, Miyabe I, Schalbetter SA, Carr AM, Murray JM. (2013). Recombination-restarted replication makes inverted chromosome fusions at inverted repeats. Nature. 493(7431):246-9. doi: 10.1038/nature11676.

Mocanu C, Karanika E, Fernández-Casañas M, Herbert A, Olukoga T, Özgürses ME, Chan KL. (2022). DNA replication is highly resilient and persistent under the challenge of mild replication stress. Cell Rep. 39(3):110701. doi: 10.1016/j.celrep.2022.110701.

Moiseeva TN, Yin Y, Calderon MJ, Qian C, Schamus-Haynes S, Sugitani N, Osmanbeyoglu HU, Rothenberg E, Watkins SC, Bakkenist CJ. (2019). An ATR and CHK1 kinase signaling mechanism that limits origin firing during unperturbed DNA replication. Proc Natl Acad Sci USA. 116(27):13374-13383. doi: 10.1073/pnas.1903418116.

Moreno SP, Bailey R, Campion N, Herron S, Gambus A. (2014). Polyubiquitylation drives replisome disassembly at the termination of DNA replication. Science. 346(6208):477-81. doi: 10.1126/science.1253585.

Moreno A, Carrington JT, Albergante L, Al Mamun M, Haagensen EJ, Komseli ES, Gorgoulis VG, Newman TJ, Blow JJ. (2016). Unreplicated DNA remaining from unperturbed S phases passes through mitosis for resolution in daughter cells. Proc Natl Acad Sci U S A.;113(39):E5757-64. doi: 10.1073/pnas.1603252113.

Morris JR, Boutell C, Keppler M, Densham R, Weekes D, Alamshah A, Butler L, Galanty Y, Pangon L, Kiuchi T, Ng T, Solomon E. (2009). The SUMO modification pathway is involved in the BRCA1 response to genotoxic stress. Nature. 462(7275):886-90. doi: 10.1038/nature08593.

Mossessova E, Lima CD. (2000). Ulp1-SUMO crystal structure and genetic analysis reveal conserved interactions and a regulatory element essential for cell growth in yeast. Mol Cell. 5(5):865-76. doi: 10.1016/s1097-2765(00)80326-3.

Moudry P, Lukas C, Macurek L, Neumann B, Heriche JK, Pepperkok R, Ellenberg J, Hodny Z, Lukas J, Bartek J. (2012). Nucleoporin NUP153 guards genome integrity by promoting nuclear import of 53BP1. Cell Death Differ. 19(5):798-807. doi: 10.1038/cdd.2011.150.

Mourón S, Rodriguez-Acebes S, Martínez-Jiménez MI, García-Gómez S, Chocrón S, Blanco L, Méndez J. (2013). Repriming of DNA synthesis at stalled replication forks by human PrimPol. Nat Struct Mol Biol. 20(12):1383-9. doi: 10.1038/nsmb.2719.

Moyer SE, Lewis PW, Botchan MR. (2006). Isolation of the Cdc45/Mcm2-7/GINS (CMG) complex, a candidate for the eukaryotic DNA replication fork helicase. Proc Natl Acad Sci U S A. 103(27):10236-10241. doi: 10.1073/pnas.0602400103.

Nacson J, Krais JJ, Bernhardy AJ, Clausen E, Feng W, Wang Y, Nicolas E, Cai KQ, Tricarico R, Hua X, DiMarcantonio D, Martinez E, Zong D, Handorf EA, Bellacosa A, Testa JR, Nussenzweig A, Gupta GP, Sykes SM, Johnson N. (2018). BRCA1 Mutation-Specific Responses to 53BP1 Loss-Induced Homologous Recombination and PARP Inhibitor Resistance. Cell Rep. 24(13):3513-3527.e7. doi: 10.1016/j.celrep.2018.08.086.

Nagai S, Dubrana K, Tsai-Pflugfelder M, Davidson MB, Roberts TM, Brown GW, Varela E, Hediger F, Gasser SM, Krogan NJ. (2008). Functional targeting of DNA damage to a nuclear pore-associated SUMO-dependent ubiquitin ligase. Science. 322(5901):597-602. doi: 10.1126/science.1162790.

Naiman K, Campillo-Funollet E, Watson AT, Budden A, Miyabe I, Carr AM. (2021). Replication dynamics of recombination-dependent replication forks. Nat Commun. 12(1):923. doi: 10.1038/s41467-021-21198-0.

Nakamura K, Kustatscher G, Alabert C, Hödl M, Forne I, Völker-Albert M, Satpathy S, Beyer TE, Mailand N, Choudhary C, Imhof A, Rappsilber J, Groth A. (2021). Proteome dynamics at broken replication forks reveal a distinct ATM-directed repair response suppressing DNA double-strand break ubiquitination. Mol Cell. 81(5):1084-1099.e6. doi: 10.1016/j.molcel.2020.12.025.

Nam EA, Cortez D. (2011). ATR signaling: more than meeting at the fork. Biochem J. 436(3):527-36. doi: 10.1042/BJ20102162.

Nayak A, Müller S. (2014). SUMO-specific proteases/isopeptidases: SENPs and beyond. Genome Biol. 15(7):422. doi: 10.1186/s13059-014-0422-2.

Neelsen KJ, Lopes M. (2015). Replication fork reversal in eukaryotes: from dead end to dynamic response. Nat Rev Mol Cell Biol. 16(4):207-20. doi: 10.1038/nrm3935.

Nelms BE, Maser RS, MacKay JF, Lagally MG, Petrini JH. (1998). In situ visualization of DNA double-strand break repair in human fibroblasts. Science. 280(5363):590-2. doi: 10.1126/science.280.5363.590.

New JH, Sugiyama T, Zaitseva E, Kowalczykowski SC. (1998). Rad52 protein stimulates DNA strand exchange by Rad51 and replication protein A. Nature. 391(6665):407-10. doi: 10.1038/34950.

Neumann FR, Dion V, Gehlen LR, Tsai-Pflugfelder M, Schmid R, Taddei A, Gasser SM. (2012). Targeted INO80 enhances subnuclear chromatin movement and ectopic homologous recombination. Genes Dev. 26(4):369-83. doi: 10.1101/gad.176156.111.

Neumaier T, Swenson J, Pham C, Polyzos A, Lo AT, Yang P, Dyball J, Asaithamby A, Chen DJ, Bissell MJ, Thalhammer S, Costes SV. (2012). Evidence for formation of DNA repair centers and dose-response nonlinearity in human cells. Proc Natl Acad Sci U S A. 109(2):443-8. doi: 10.1073/pnas.1117849108.

Nguyen MO, Jalan M, Morrow CA, Osman F, Whitby MC. (2015). Recombination occurs within minutes of replication blockage by RTS1 producing restarted forks that are prone to collapse. Elife. 4:e04539. doi: 10.7554/eLife.04539.

Nguyen JHG, Viterbo D, Anand RP, Verra L, Sloan L, Richard GF, Freudenreich CH. (2017). Differential requirement of Srs2 helicase and Rad51 displacement activities in replication of hairpin-forming CAG/CTG repeats. Nucleic Acids Res. 45(8):4519-4531. doi: 10.1093/nar/gkx088.

Nie M, Boddy MN. (2015). Pli1(PIAS1) SUMO ligase protected by the nuclear pore-associated SUMO protease Ulp1 SENP1/2. J Biol Chem. 290(37):22678-85. doi: 10.1074/jbc.M115.673038.

Nieduszynski CA, Hiraga S, Ak P, Benham CJ, Donaldson AD. (2006). OriDB: a DNA replication origin database. Nucleic Acids Res. 35:D40-6. doi: 10.1093/nar/gkl758.

Nimonkar AV, Genschel J, Kinoshita E, Polaczek P, Campbell JL, Wyman C, Modrich P, Kowalczykowski SC. (2011). BLM-DNA2-RPA-MRN and EXO1-BLM-RPA-MRN constitute two DNA end resection machineries for human DNA break repair. Genes Dev. 25(4):350-62. doi: 10.1101/gad.2003811.

Niño CA, Guet D, Gay A, Brutus S, Jourquin F, Mendiratta S, Salamero J, Géli V, Dargemont C. (2016). Posttranslational marks control architectural and functional

plasticity of the nuclear pore complex basket. J Cell Biol. 212(2):167-80. doi: 10.1083/jcb.201506130.

Nishida T, Tanaka H, Yasuda H. (2000). A novel mammalian Smt3-specific isopeptidase 1 (SMT3IP1) localized in the nucleolus at interphase. Eur J Biochem. 267(21):6423-7. doi: 10.1046/j.1432-1327.2000.01729.x.

Noll DM, Mason TM, Miller PS. (2006). Formation and repair of interstrand cross-links in DNA. Chem Rev. 106(2):277-301. doi: 10.1021/cr040478b.

Nordlund P, Reichard P. (2006). Ribonucleotide reductases. Annu Rev Biochem. 75:681-706. doi: 10.1146/annurev.biochem.75.103004.142443. PMID: 16756507.

O'Driscoll M, Jeggo PA. (2008). The role of the DNA damage response pathways in brain development and microcephaly: insight from human disorders. DNA Repair (Amst). 7(7):1039-50. doi: 10.1016/j.dnarep.2008.03.018.

Okazaki R, Okazaki T, Sakabe K, Sugimoto K, Sugino A. (1968). Mechanism of DNA chain growth. I. Possible discontinuity and unusual secondary structure of newly synthesized chains. Proc Natl Acad Sci U S A. 59(2):598-605. doi: 10.1073/pnas.59.2.598.

Orthwein A, Noordermeer SM, Wilson MD, Landry S, Enchev RI, Sherker A, Munro M, Pinder J, Salsman J, Dellaire G, Xia B, Peter M, Durocher D. (2015). A mechanism for the suppression of homologous recombination in G1 cells. Nature. 528(7582):422-6. doi: 10.1038/nature16142.

Oshidari R, Strecker J, Chung DKC, Abraham KJ, Chan JNY, Damaren CJ, Mekhail K. (2018). Nuclear microtubule filaments mediate non-linear directional motion of chromatin and promote DNA repair. Nat Commun. 9(1):2567. doi: 10.1038/s41467-018-05009-7.

Osia B, Twarowski J, Jackson T, Lobachev K, Liu L, Malkova A. (2022). Migrating bubble synthesis promotes mutagenesis through lesions in its template. Nucleic Acids Res. 50(12):6870-6889. doi: 10.1093/nar/gkac520.

Oza P, Jaspersen SL, Miele A, Dekker J, Peterson CL. (2009). Mechanisms that regulate localization of a DNA double-strand break to the nuclear periphery. Genes Dev. 23(8):912-27. doi: 10.1101/gad.1782209.

Paeschke K, Capra JA, Zakian VA. (2011). DNA replication through G-quadruplex motifs is promoted by the Saccharomyces cerevisiae Pif1 DNA helicase. Cell. 145(5):678-91. doi: 10.1016/j.cell.2011.04.015.

Palancade B, Liu X, Garcia-Rubio M, Aguilera A, Zhao X, Doye V. (2007). Nucleoporins prevent DNA damage accumulation by modulating Ulp1-dependent sumoylation processes. Mol Biol Cell. 18(8):2912-23. doi: 10.1091/mbc.e07-02-0123.

Panse VG, Küster B, Gerstberger T, Hurt E. (2003). Unconventional tethering of Ulp1 to the transport channel of the nuclear pore complex by karyopherins. Nat Cell Biol. 5(1):21-7. doi: 10.1038/ncb893.

Panzarino NJ, Krais JJ, Cong K, Peng M, Mosqueda M, Nayak SU, Bond SM, Calvo JA, Doshi MB, Bere M, Ou J, Deng B, Zhu LJ, Johnson N, Cantor SB. (2021). Replication Gaps Underlie BRCA Deficiency and Therapy Response. Cancer Res. 81(5):1388-1397. doi: 10.1158/0008-5472.CAN-20-1602.

Papouli E, Chen S, Davies AA, Huttner D, Krejci L, Sung P, Ulrich HD. (2005). Crosstalk between SUMO and ubiquitin on PCNA is mediated by recruitment of the helicase Srs2p. Mol Cell. 219(1):123-33. doi: 10.1016/j.molcel.2005.06.001.

Parisis N, Krasinska L, Harker B, Urbach S, Rossignol M, Camasses A, Dewar J, Morin N, Fisher D. (2017). Initiation of DNA replication requires actin dynamics and formin activity. EMBO J. 36(21):3212-3231. doi: 10.15252/embj.201796585.

Parker JL, Ulrich HD. (2012). A SUMO-interacting motif activates budding yeast ubiquitin ligase Rad18 towards SUMO-modified PCNA. Nucleic Acids Res. 40(22):11380-8. doi: 10.1093/nar/gks892.

Paull TT, Lee JH. (2005). The Mre11/Rad50/Nbs1 complex and its role as a DNA double-strand break sensor for ATM. Cell Cycle. 4(6):737-40. doi: 10.4161/cc.4.6.1715.

Paulsen RD, Cimprich KA. (2007). The ATR pathway: fine-tuning the fork. DNA Repair (Amst). 6(7):953-66. doi: 10.1016/j.dnarep.2007.02.015.

Paulsen RD, Soni DV, Wollman R, Hahn AT, Yee MC, Guan A, Hesley JA, Miller SC, Cromwell EF, Solow-Cordero DE, Meyer T, Cimprich KA. (2009). A genome-wide siRNA screen reveals diverse cellular processes and pathways that mediate genome stability. Mol Cell. 35(2):228-39. doi: 10.1016/j.molcel.2009.06.021.

Pavlov YI, Zhuk AS, Stepchenkova EI. (2020). DNA Polymerases at the Eukaryotic Replication Fork Thirty Years after: Connection to Cancer. Cancers (Basel). 12(12):3489. doi: 10.3390/cancers12123489.

Paulovich AG, Hartwell LH. (1995). A checkpoint regulates the rate of progression through S phase in S. cerevisiae in response to DNA damage. Cell. 82(5):841-7. doi: 10.1016/0092-8674(95)90481-6.

Pellegrini L, Yu DS, Lo T, Anand S, Lee M, Blundell TL, Venkitaraman AR. (2002). Insights into DNA recombination from the structure of a RAD51-BRCA2 complex. Nature. 420(6913):287-93. doi: 10.1038/nature01230.

Perry JJ, Tainer JA, Boddy MN. (2008). A SIM-ultaneous role for SUMO and ubiquitin. Trends Biochem Sci. 33(5):201-8. doi: 10.1016/j.tibs.2008.02.001.

Petermann E, Orta ML, Issaeva N, Schultz N, Helleday T. (2010). Hydroxyurea-stalled replication forks become progressively inactivated and require two different RAD51-mediated pathways for restart and repair. Mol Cell. 37(4):492-502. doi: 10.1016/j.molcel.2010.01.021.

Petermann E, Woodcock M, Helleday T. (2010). Chk1 promotes replication fork progression by controlling replication initiation. Proc Natl Acad Sci U S A. 107(37):16090-5. doi: 10.1073/pnas.1005031107.

Petrini JH, Stracker TH. (2003). The cellular response to DNA double-strand breaks: defining the sensors and mediators. Trends Cell Biol. 13(9):458-62. doi: 10.1016/s0962-8924(03)00170-3.

Petryk N, Kahli M, d'Aubenton-Carafa Y, Jaszczyszyn Y, Shen Y, Silvain M, Thermes C, Chen CL, Hyrien O. (2016). Replication landscape of the human genome. Nat Commun. 7:10208. doi: 10.1038/ncomms10208.

Pfander B, Moldovan GL, Sacher M, Hoege C, Jentsch S. (2005). SUMO-modified PCNA recruits Srs2 to prevent recombination during S phase. Nature. 436(7049):428-33. doi: 10.1038/nature03665.

Piazza A, Wright WD, Heyer WD. (2017). Multi-invasions Are Recombination Byproducts that Induce Chromosomal Rearrangements. Cell. 170(4):760-773.e15. doi: 10.1016/j.cell.2017.06.052.

Piberger AL, Bowry A, Kelly RDW, Walker AK, González-Acosta D, Bailey LJ, Doherty AJ, Méndez J, Morris JR, Bryant HE, Petermann E. (2020). PrimPol-dependent single-stranded gap formation mediates homologous recombination at bulky DNA adducts. Nat Commun. 11(1):5863. doi: 10.1038/s41467-020-19570-7.

Pichler A, Fatouros C, Lee H, Eisenhardt N. (2017). SUMO conjugation - a mechanistic view. Biomol Concepts. 8(1):13-36. doi: 10.1515/bmc-2016-0030.

Pichler A, Knipscheer P, Oberhofer E, van Dijk WJ, Körner R, Olsen JV, Jentsch S, Melchior F, Sixma TK. (2005). SUMO modification of the ubiquitin-conjugating enzyme E2-25K. Nat Struct Mol Biol. 12(3):264-9. doi: 10.1038/nsmb903.

Pinzaru AM, Hom RA, Beal A, Phillips AF, Ni E, Cardozo T, Nair N, Choi J, Wuttke DS, Sfeir A, Denchi EL. (2016). Telomere Replication Stress Induced by POT1 Inactivation Accelerates Tumorigenesis. Cell Rep. 15(10):2170-2184. doi: 10.1016/j.celrep.2016.05.008.

Pinzaru AM, Kareh M, Lamm N, Lazzerini-Denchi E, Cesare AJ, Sfeir A. (2020). Replication stress conferred by POT1 dysfunction promotes telomere relocalization to the nuclear pore. Genes Dev. 34(23-24):1619-1636. doi: 10.1101/gad.337287.120.

Poli J, Tsaponina O, Crabbé L, Keszthelyi A, Pantesco V, Chabes A, Lengronne A, Pasero P. (2012). dNTP pools determine fork progression and origin usage under replication stress. EMBO J. 31(4):883-94. doi: 10.1038/emboj.2011.470.

Polleys EJ, Freudenreich CH. (2021). Homologous recombination within repetitive DNA. Curr Opin Genet Dev. 71:143-153. doi: 10.1016/j.gde.2021.08.005.

Polleys EJ, House NCM, Freudenreich CH. (2017). Role of recombination and replication fork restart in repeat instability. DNA Repair (Amst). 56:156-165. doi: 10.1016/j.dnarep.2017.06.018.

Pombo A, Dillon N. (2015). Three-dimensional genome architecture: players and mechanisms. Nat Rev Mol Cell Biol. 16(4):245-57. doi: 10.1038/nrm3965.

Pommier Y, Marchand C. (2011). Interfacial inhibitors: targeting macromolecular complexes. Nat Rev Drug Discov. 11(1):25-36. doi: 10.1038/nrd3404.

Poole LA, Cortez D. (2017). Functions of SMARCAL1, ZRANB3, and HLTF in maintaining genome stability. Crit Rev Biochem Mol Biol. 52(6):696-714. doi: 10.1080/10409238.2017.1380597.

Pouokam M, Cruz B, Burgess S, Segal MR, Vazquez M, Arsuaga J. (2019). The Rabl configuration limits topological entanglement of chromosomes in budding yeast. Sci Rep. 9(1):6795. doi: 10.1038/s41598-019-42967-4.

Prado F. (2021). Non-Recombinogenic Functions of Rad51, BRCA2, and Rad52 in DNA Damage Tolerance. Genes (Basel). 12(10):1550. doi: 10.3390/genes12101550.

Pray, L. (2008) Discovery of DNA structure and function: Watson and Crick. Nature Education 1(1):100

Prudden J, Pebernard S, Raffa G, Slavin DA, Perry JJ, Tainer JA, McGowan CH, Boddy MN. (2007). SUMO-targeted ubiquitin ligases in genome stability. EMBO J. 26(18):4089-101. doi: 10.1038/sj.emboj.7601838.

Przetocka S, Porro A, Bolck HA, Walker C, Lezaja A, Trenner A, von Aesch C, Himmels SF, D'Andrea AD, Ceccaldi R, Altmeyer M, Sartori AA. (2018). CtIP-Mediated Fork Protection Synergizes with BRCA1 to Suppress Genomic Instability upon DNA Replication Stress. Mol Cell. 72(3):568-582.e6. doi: 10.1016/j.molcel.2018.09.014.

Psakhye I, Castellucci F, Branzei D. (2019). SUMO-Chain-Regulated Proteasomal Degradation Timing Exemplified in DNA Replication Initiation. Mol Cell. 76(4):632-645.e6. doi: 10.1016/j.molcel.2019.08.003.

Psakhye I, Jentsch S. (2012). Protein group modification and synergy in the SUMO pathway as exemplified in DNA repair. Cell. 151(4):807-820. doi: 10.1016/j.cell.2012.10.021.

Qi Z, Redding S, Lee JY, Gibb B, Kwon Y, Niu H, Gaines WA, Sung P, Greene EC. (2015). DNA sequence alignment by microhomology sampling during homologous recombination. Cell. 160(5):856-869. doi: 10.1016/j.cell.2015.01.029.

Qiu Y, Antony E, Doganay S, Koh HR, Lohman TM, Myong S. (2013). Srs2 prevents Rad51 filament formation by repetitive motion on DNA. Nat Commun. 4:2281. doi: 10.1038/ncomms3281.

Quinet A, Lemaçon D, Vindigni A. (2017). Replication Fork Reversal: Players and Guardians. Mol Cell. 68(5):830-833. doi: 10.1016/j.molcel.2017.11.022.

Quinet A, Tirman S, Jackson J, Šviković S, Lemaçon D, Carvajal-Maldonado D, González-Acosta D, Vessoni AT, Cybulla E, Wood M, Tavis S, Batista LFZ, Méndez J, Sale JE, Vindigni A. (2020). PRIMPOL-Mediated Adaptive Response Suppresses Replication Fork Reversal in BRCA-Deficient Cells. Mol Cell. 77(3):461-474.e9. doi: 10.1016/j.molcel.2019.10.008.

Rabl C. (1885) Über Zelltheilung. Morphologisches Jahrbuch 10

Ragu S, Matos-Rodrigues G, Lopez BS. (2020). Replication Stress, DNA Damage, Inflammatory Cytokines and Innate Immune Response. Genes (Basel). 11(4):409. doi: 10.3390/genes11040409.

Ramsay AJ, Quesada V, Foronda M, Conde L, Martínez-Trillos A, Villamor N, Rodríguez D, Kwarciak A, Garabaya C, Gallardo M, López-Guerra M, López-Guillermo A, Puente XS, Blasco MA, Campo E, López-Otín C. (2013). POT1 mutations cause telomere dysfunction in chronic lymphocytic leukemia. Nat Genet. 45(5):526-30. doi: 10.1038/ng.2584.

Ranjha L, Levikova M, Altmannova V, Krejci L, Cejka P. (2019). Sumoylation regulates the stability and nuclease activity of *Saccharomyces cerevisiae* Dna2. Commun Biol. 2:174. doi: 10.1038/s42003-019-0428-0.

Rao SS, Huntley MH, Durand NC, Stamenova EK, Bochkov ID, Robinson JT, Sanborn AL, Machol I, Omer AD, Lander ES, Aiden EL. (2014). A 3D map of the human genome at kilobase resolution reveals principles of chromatin looping. Cell. 159(7):1665-80. doi: 10.1016/j.cell.2014.11.021.

Rass U, Compton SA, Matos J, Singleton MR, Ip SC, Blanco MG, Griffith JD, West SC. (2010). Mechanism of Holliday junction resolution by the human GEN1 protein. Genes Dev. 24(14):1559-69. doi: 10.1101/gad.585310.

Rawal CC, Caridi CP, Chiolo I. (2019). Actin' between phase separated domains for heterochromatin repair. DNA Repair (Amst). 81:102646. doi: 10.1016/j.dnarep.2019.102646.

Ray Chaudhuri A, Callen E, Ding X, Gogola E, Duarte AA, Lee JE, Wong N, Lafarga V, Calvo JA, Panzarino NJ, John S, Day A, Crespo AV, Shen B, Starnes LM, de Ruiter JR, Daniel JA, Konstantinopoulos PA, Cortez D, Cantor SB, Fernandez-Capetillo O, Ge K, Jonkers J, Rottenberg S, Sharan SK, Nussenzweig A. (2016). Replication fork stability confers chemoresistance in BRCA-deficient cells. Nature. 535(7612):382-7. doi: 10.1038/nature18325. Erratum in: Nature. 2016 Nov 17;539(7629):456.

Ray Chaudhuri A, Hashimoto Y, Herrador R, Neelsen KJ, Fachinetti D, Bermejo R, Cocito A, Costanzo V, Lopes M. (2012). Topoisomerase I poisoning results in PARP-mediated replication fork reversal. Nat Struct Mol Biol. 19(4):417-23. doi: 10.1038/nsmb.2258.

Reverter D, Lima CD. (2005). Insights into E3 ligase activity revealed by a SUMO-RanGAP1-Ubc9-Nup358 complex. Nature. 435(7042):687-92. doi: 10.1038/nature03588.

Renkawitz J, Lademann CA, Jentsch S. (2014). Mechanisms and principles of homology search during recombination. Nat Rev Mol Cell Biol. 15(6):369-83. doi: 10.1038/nrm3805.

Rijkers T, Van Den Ouweland J, Morolli B, Rolink AG, Baarends WM, Van Sloun PP, Lohman PH, Pastink A. (1998). Targeted inactivation of mouse RAD52 reduces homologous recombination but not resistance to ionizing radiation. Mol Cell Biol. 18(11):6423-9. doi: 10.1128/MCB.18.11.6423.

Robles-Espinoza CD, Harland M, Ramsay AJ, Aoude LG, Quesada V, Ding Z, Pooley KA, Pritchard AL, Tiffen JC, Petljak M, Palmer JM, Symmons J, Johansson P, Stark MS, Gartside MG, Snowden H, Montgomery GW, Martin NG, Liu JZ, Choi J, Makowski M, Brown KM, Dunning AM, Keane TM, López-Otín C, Gruis NA, Hayward NK, Bishop DT, Newton-Bishop JA, Adams DJ. (2014). POT1 loss-of-function variants predispose to familial melanoma. Nat Genet. 46(5):478-481. doi: 10.1038/ng.2947.

Ronato DA, Mersaoui SY, Busatto FF, Affar EB, Richard S, Masson JY. (2020). Limiting the DNA Double-Strand Break Resectosome for Genome Protection. Trends Biochem Sci. 45(9):779-793. doi: 10.1016/j.tibs.2020.05.003.

Rothkamm K, Krüger I, Thompson LH, Löbrich M. (2003). Pathways of DNA double-strand break repair during the mammalian cell cycle. Mol Cell Biol. 2003 23(16):5706-15. doi: 10.1128/MCB.23.16.5706-5715.2003.

Rouet P, Smih F, Jasin M. (1994). Introduction of double-strand breaks into the genome of mouse cells by expression of a rare-cutting endonuclease. Mol Cell Biol. 14(12):8096-106. doi: 10.1128/mcb.14.12.8096-8106.1994.

Roukos V, Voss TC, Schmidt CK, Lee S, Wangsa D, Misteli T. (2013). Spatial dynamics of chromosome translocations in living cells. Science. 341(6146):660-4. doi: 10.1126/science.1237150.

Roumelioti FM, Sotiriou SK, Katsini V, Chiourea M, Halazonetis TD, Gagos S. (2016). Alternative lengthening of human telomeres is a conservative DNA replication process with features of break-induced replication. EMBO Rep. 17(12):1731-1737. doi: 10.15252/embr.201643169.

Rowley MJ, Nichols MH, Lyu X, Ando-Kuri M, Rivera ISM, Hermetz K, Wang P, Ruan Y, Corces VG. (2017). Evolutionarily Conserved Principles Predict 3D Chromatin Organization. Mol Cell. 67(5):837-852.e7. doi: 10.1016/j.molcel.2017.07.022.

Rowley MJ, Corces VG. (2018). Organizational principles of 3D genome architecture. Nat Rev Genet. 19(12):789-800. doi: 10.1038/s41576-018-0060-8.

Ryu T, Spatola B, Delabaere L, Bowlin K, Hopp H, Kunitake R, Karpen GH, Chiolo I. (2015). Heterochromatic breaks move to the nuclear periphery to continue recombinational repair. Nat Cell Biol. 17(11):1401-11. doi: 10.1038/ncb3258.

Sacher M, Pfander B, Jentsch S. (2005). Identification of SUMO-protein conjugates. Methods Enzymol. 399:392-404. doi: 10.1016/S0076-6879(05)99027-7.

Sacher M, Pfander B, Hoege C, Jentsch S. (2006). Control of Rad52 recombination activity by double-strand break-induced SUMO modification. Nat Cell Biol. 8(11):1284-90. doi: 10.1038/ncb1488.
Saini N, Gordenin DA. (2020). Hypermutation in single-stranded DNA. DNA Repair (Amst). 91-92:102868. doi: 10.1016/j.dnarep.2020.102868.

Saini N, Ramakrishnan S, Elango R, Ayyar S, Zhang Y, Deem A, Ira G, Haber JE, Lobachev KS, Malkova A. (2013). Migrating bubble during break-induced replication drives conservative DNA synthesis. Nature. 2502(7471):389-92. doi: 10.1038/nature12584.

Saitoh H, Pizzi MD, Wang J. (2002). Perturbation of SUMOlation enzyme Ubc9 by distinct domain within nucleoporin RanBP2/Nup358. J Biol Chem. 277(7):4755-63. doi: 10.1074/jbc.M104453200.

Sakofsky CJ, Roberts SA, Malc E, Mieczkowski PA, Resnick MA, Gordenin DA, Malkova A. (2014). Break-induced replication is a source of mutation clusters underlying kataegis. Cell Rep. 7(5):1640-1648. doi: 10.1016/j.celrep.2014.04.053.

Salas-Pino S, Gallardo P, Barrales RR, Braun S, Daga RR. (2017). The fission yeast nucleoporin Alm1 is required for proteasomal degradation of kinetochore components. J Cell Biol. 216(11):3591-3608. doi: 10.1083/jcb.201612194.

Sale JE. (2013). Translesion DNA synthesis and mutagenesis in eukaryotes. Cold Spring Harb Perspect Biol. 5(3):a012708. doi: 10.1101/cshperspect.a012708.

Saldivar JC, Cortez D, Cimprich KA. (2017). The essential kinase ATR: ensuring faithful duplication of a challenging genome. Nat Rev Mol Cell Biol. 18(10):622-636. doi: 10.1038/nrm.2017.67. Epub 2017 Aug 16. Erratum in: Nat Rev Mol Cell Biol. 2017 Dec;18(12):783.

Sale JE. (2012). Competition, collaboration and coordination-determining how cells bypass DNA damage. J Cell Sci. 125(Pt 7):1633-43. doi: 10.1242/jcs.094748.

Santiago A, Li D, Zhao LY, Godsey A, Liao D. (2013). p53 SUMOylation promotes its nuclear export by facilitating its release from the nuclear export receptor CRM1. Mol Biol Cell. 24(17):2739-52. doi: 10.1091/mbc.E12-10-0771.

Sarangi P, Steinacher R, Altmannova V, Fu Q, Paull TT, Krejci L, Whitby MC, Zhao X. (2015). Sumoylation influences DNA break repair partly by increasing the solubility of a conserved end resection protein. PLoS Genet. 11(1):e1004899. doi: 10.1371/journal.pgen.1004899.

Sarangi P, Zhao X. (2015). SUMO-mediated regulation of DNA damage repair and responses. Trends Biochem Sci. 40(4):233-42. doi: 10.1016/j.tibs.2015.02.006.
Sarni D, Kerem B. (2017). Oncogene-Induced Replication Stress Drives Genome Instability and Tumorigenesis. Int J Mol Sci. 18(7):1339. doi: 10.3390/ijms18071339.
Schärer OD. (2005). DNA interstrand crosslinks: natural and drug-induced DNA adducts that induce unique cellular responses. Chembiochem. 6(1):27-32. doi: 10.1002/cbic.200400287.

Schirmeisen K, Lambert SAE, Kramarz K. (2021). SUMO-Based Regulation of Nuclear Positioning to Spatially Regulate Homologous Recombination Activities at Replication Stress Sites. Genes (Basel). 12(12):2010. doi: 10.3390/genes12122010.

Schlacher K, Christ N, Siaud N, Egashira A, Wu H, Jasin M. (2011). Double-strand break repair-independent role for BRCA2 in blocking stalled replication fork degradation by MRE11. Cell. 145(4):529-42. doi: 10.1016/j.cell.2011.03.041.

Schmit M, Bielinsky AK. (2021). Congenital Diseases of DNA Replication: Clinical Phenotypes and Molecular Mechanisms. Int J Mol Sci. 222(2):911. doi: 10.3390/ijms22020911.

Schrank BR, Aparicio T, Li Y, Chang W, Chait BT, Gundersen GG, Gottesman ME, Gautier J. (2018). Nuclear ARP2/3 drives DNA break clustering for homology-directed repair. Nature. 559(7712):61-66. doi: 10.1038/s41586-018-0237-5.

Schwartz TU. (2016). The Structure Inventory of the Nuclear Pore Complex. J Mol Biol. 428(10 Pt A):1986-2000. doi: 10.1016/j.jmb.2016.03.015.

Seeber A, Dion V, Gasser SM. (2014). Remodelers move chromatin in response to DNA damage. Cell Cycle. 13(6):877-8. doi: 10.4161/cc.28200.

Seeler JS, Dejean A. (2003). Nuclear and unclear functions of SUMO. Nat Rev Mol Cell Biol. 4(9):690-9. doi: 10.1038/nrm1200.

Seigneur M, Bidnenko V, Ehrlich SD, Michel B. (1998). RuvAB acts at arrested replication forks. Cell. 95(3):419-30. doi: 10.1016/s0092-8674(00)81772-9.

Sen D, Gilbert W. (1988). Formation of parallel four-stranded complexes by guanine-rich motifs in DNA and its implications for meiosis. Nature. 334(6180):364-6. doi: 10.1038/334364a0.

Sender R, Milo R. (2021). The distribution of cellular turnover in the human body. Nat Med. 27(1):45-48. doi: 10.1038/s41591-020-01182-9.

Sexton T, Cavalli G. (2015). The role of chromosome domains in shaping the functional genome. Cell. 160(6):1049-59. doi: 10.1016/j.cell.2015.02.040.

Sfeir A, Kosiyatrakul ST, Hockemeyer D, MacRae SL, Karlseder J, Schildkraut CL, de Lange T. (2009). Mammalian telomeres resemble fragile sites and require TRF1 for efficient replication. Cell. 138(1):90-103. doi: 10.1016/j.cell.2009.06.021.

Sharma S. (2011). Non-B DNA Secondary Structures and Their Resolution by RecQ Helicases. J Nucleic Acids. 2011:724215. doi: 10.4061/2011/724215.

Shechter D, Costanzo V, Gautier J. (2004). ATR and ATM regulate the timing of DNA replication origin firing. Nat Cell Biol. 6(7):648-55. doi: 10.1038/ncb1145.

Shen Z, Pardington-Purtymun PE, Comeaux JC, Moyzis RK, Chen DJ. (1996). UBL1, a human ubiquitin-like protein associating with human RAD51/RAD52 proteins. Genomics. 36(2):271-9. doi: 10.1006/geno.1996.0462.

Shibata A. (2017). Regulation of repair pathway choice at two-ended DNA double-strand breaks. Mutat Res. 803-805:51-55. doi: 10.1016/j.mrfmmm.2017.07.011.

Shibata A, Conrad S, Birraux J, Geuting V, Barton O, Ismail A, Kakarougkas A, Meek K, Taucher-Scholz G, Löbrich M, Jeggo PA. (2011). Factors determining DNA double-strand break repair pathway choice in G2 phase. EMBO J. 30(6):1079-92. doi: 10.1038/emboj.2011.27.

Shima H, Suzuki H, Sun J, Kono K, Shi L, Kinomura A, Horikoshi Y, Ikura T, Ikura M, Kanaar R, Igarashi K, Saitoh H, Kurumizaka H, Tashiro S. (2013). Activation of the SUMO modification system is required for the accumulation of RAD51 at sites of DNA damage. J Cell Sci. 126(Pt 22):5284-92. doi: 10.1242/jcs.133744.

Shinohara A, Ogawa T. (1998). Stimulation by Rad52 of yeast Rad51-mediated recombination. Nature. 391(6665):404-7. doi: 10.1038/34943.

Shinohara A, Ogawa H, Ogawa T. (1992). Rad51 protein involved in repair and recombination in S. cerevisiae is a RecA-like protein. Cell. 69(3):457-70. doi: 10.1016/0092-8674(92)90447-k.

Short JM, Liu Y, Chen S, Soni N, Madhusudhan MS, Shivji MK, Venkitaraman AR. (2016). High-resolution structure of the presynaptic RAD51 filament on single-stranded DNA by electron cryo-microscopy. Nucleic Acids Res. 44(19):9017-9030. doi: 10.1093/nar/gkw783.

Shrivastav M, De Haro LP, Nickoloff JA. (2008). Regulation of DNA double-strand break repair pathway choice. Cell Res. 18(1):134-47. doi: 10.1038/cr.2007.111.

Simon M, Giot L, Faye G. (1991). The 3' to 5' exonuclease activity located in the DNA polymerase delta subunit of Saccharomyces cerevisiae is required for accurate replication. EMBO J. 10(8):2165-70. doi: 10.1002/j.1460-2075.1991.tb07751.x.

Simon MN, Churikov D, Géli V. (2016). Replication stress as a source of telomere recombination during replicative senescence in Saccharomyces cerevisiae. FEMS Yeast Res. 16(7):fow085. doi: 10.1093/femsyr/fow085.

Smith MJ, Bryant EE, Joseph FJ, Rothstein R. (2019). DNA damage triggers increased mobility of chromosomes in G1-phase cells. Mol Biol Cell. 30(21):2620-2625. doi: 10.1091/mbc.E19-08-0469.

Smith MJ, Bryant EE, Rothstein R. (2018). Increased chromosomal mobility after DNA damage is controlled by interactions between the recombination machinery and the checkpoint. Genes Dev. 32(17-18):1242-1251. doi: 10.1101/gad.317966.118.

Sneeden JL, Grossi SM, Tappin I, Hurwitz J, Heyer WD. (2013). Reconstitution of recombination-associated DNA synthesis with human proteins. Nucleic Acids Res. 241(9):4913-25. doi: 10.1093/nar/gkt192.

Sriramachandran AM, Meyer-Teschendorf K, Pabst S, Ulrich HD, Gehring NH, Hofmann K, Praefcke GJK, Dohmen RJ. (2019). Arkadia/RNF111 is a SUMO-targeted ubiquitin ligase with preference for substrates marked with SUMO1-capped SUMO2/3 chain. Nat Commun. 10(1):3678. doi: 10.1038/s41467-019-11549-3.

Sogo JM, Lopes M, Foiani M. (2002). Fork reversal and ssDNA accumulation at stalled replication forks owing to checkpoint defects. Science. 297(5581):599-602. doi: 10.1126/science.1074023.

Solinger JA, Kiianitsa K, Heyer WD. (2002). Rad54, a Swi2/Snf2-like recombinational repair protein, disassembles Rad51:dsDNA filaments. Mol Cell. 10(5):1175-88. doi: 10.1016/s1097-2765(02)00743-8.

Sollier J, Cimprich KA. (2015). Breaking bad: R-loops and genome integrity. Trends Cell Biol. 25(9):514-22. doi: 10.1016/j.tcb.2015.05.003.

Song J, Durrin LK, Wilkinson TA, Krontiris TG, Chen Y. (2004). Identification of a SUMO-binding motif that recognizes SUMO-modified proteins. Proc Natl Acad Sci U S A. 101(40):14373-8. doi: 10.1073/pnas.0403498101.

Soria-Bretones I, Cepeda-García C, Checa-Rodriguez C, Heyer V, Reina-San-Martin B, Soutoglou E, Huertas P. (2017). DNA end resection requires constitutive sumoylation of CtIP by CBX4. Nat Commun. 8(1):113. doi: 10.1038/s41467-017-00183-6.

Sotiriou SK, Kamileri I, Lugli N, Evangelou K, Da-Ré C, Huber F, Padayachy L, Tardy S, Nicati NL, Barriot S, Ochs F, Lukas C, Lukas J, Gorgoulis VG, Scapozza L, Halazonetis TD. (2016). Mammalian RAD52 Functions in Break-Induced Replication Repair of Collapsed DNA Replication Forks. Mol Cell. 264(6):1127-1134. doi: 10.1016/j.molcel.2016.10.038.

Souquet B, Freed E, Berto A, Andric V, Audugé N, Reina-San-Martin B, Lacy E, Doye V. (2018). Nup133 Is Required for Proper Nuclear Pore Basket Assembly and Dynamics in Embryonic Stem Cells. Cell Rep. 23(8):2443-2454. doi: 10.1016/j.celrep.2018.04.070.

Soutoglou E, Dorn JF, Sengupta K, Jasin M, Nussenzweig A, Ried T, Danuser G, Misteli T. (2007). Positional stability of single double-strand breaks in mammalian cells. Nat Cell Biol. 9(6):675-82. doi: 10.1038/ncb1591.

Spector I, Shochet NR, Kashman Y, Groweiss A. (1983). Latrunculins: novel marine toxins that disrupt microfilament organization in cultured cells. Science. 219(4584):493-5. doi: 10.1126/science.6681676.

Srikumar T, Lewicki MC, Raught B. (2013). A global S. cerevisiae small ubiquitin-related modifier (SUMO) system interactome. Mol Syst Biol. 9:668. doi: 10.1038/msb.2013.23.
Sriramachandran AM, Dohmen RJ. (2014). SUMO-targeted ubiquitin ligases. Biochim Biophys Acta. 1843(1):75-85. doi: 10.1016/j.bbamcr.2013.08.022.

Steinacher R, Osman F, Lorenz A, Bryer C, Whitby MC. (2013). Slx8 removes Pli1-dependent protein-SUMO conjugates including SUMOylated topoisomerase I to promote genome stability. PLoS One. 28(8):e71960. doi: 10.1371/journal.pone.0071960.

Steitz, T. A. (1999). DNA polymerases: structural diversity and common mechanisms. J. Biol. Chem. 274, 17395–17398. doi: 10.1074/jbc.274.25.17395

Stingele J, Bellelli R, Boulton SJ. (2017). Mechanisms of DNA-protein crosslink repair. Nat Rev Mol Cell Biol. 18(9):563-573. doi: 10.1038/nrm.2017.56.

Strachan J. Leidecker O. Spanos C. Le Coz C. Chapman E. Arsenijevic A. Zhang H. Zhao N. Bayne EH. (2022). SUMOylation regulates Lem2 function in centromere clustering and silencing. bioRxiv doi: https://doi.org/10.1101/2022.11.02.514898

Strecker J, Gupta GD, Zhang W, Bashkurov M, Landry MC, Pelletier L, Durocher D. (2016). DNA damage signaling targets the kinetochore to promote chromatin mobility. Nat Cell Biol. 18(3):281-90. doi: 10.1038/ncb3308.

Su XA, Dion V, Gasser SM, Freudenreich CH. (2015). Regulation of recombination at yeast nuclear pores controls repair and triplet repeat stability. Genes Dev. 29(10):1006-17. doi: 10.1101/gad.256404.114.

Sugawara N, Pâques F, Colaiácovo M, Haber JE. (1997). Role of Saccharomyces cerevisiae Msh2 and Msh3 repair proteins in double-strand break-induced recombination. Proc Natl Acad Sci U S A. 94(17):9214-9. doi: 10.1073/pnas.94.17.9214.

Sugawara N, Wang X, Haber JE. (2003). In vivo roles of Rad52, Rad54, and Rad55 proteins in Rad51-mediated recombination. Mol Cell. 12(1):209-19. doi: 10.1016/s1097-2765(03)00269-7.

Sung P. (1997). Function of yeast Rad52 protein as a mediator between replication protein A and the Rad51 recombinase. J Biol Chem. 272(45):28194-7. doi: 10.1074/jbc.272.45.28194.

Suwaki N, Klare K, Tarsounas M. (2011). RAD51 paralogs: roles in DNA damage signalling, recombinational repair and tumorigenesis. Semin Cell Dev Biol. 22(8):898-905. doi: 10.1016/j.semcdb.2011.07.019.

Symington LS, Gautier J. (2011). Double-strand break end resection and repair pathway choice. Annu Rev Genet. 45:247-71. doi: 10.1146/annurev-genet-110410-132435.

Szostak JW, Orr-Weaver TL, Rothstein RJ, Stahl FW. (1983). The double-strand-break repair model for recombination. Cell. 33(1):25-35. doi: 10.1016/0092-8674(83)90331-8.

Taddei A, Hediger F, Neumann FR, Bauer C, Gasser SM. (2004). Separation of silencing from perinuclear anchoring functions in yeast Ku80, Sir4 and Esc1 proteins. EMBO J. 23(6):1301-12. doi: 10.1038/sj.emboj.7600144.

Taglialatela A, Leuzzi G, Sannino V, Cuella-Martin R, Huang JW, Wu-Baer F, Baer R, Costanzo V, Ciccia A. (2021). REV1-Polζ maintains the viability of homologous recombination-deficient cancer cells through mutagenic repair of PRIMPOL-dependent ssDNA gaps. Mol Cell. 81(19):4008-4025.e7. doi: 10.1016/j.molcel.2021.08.016.

Tanabe H, Müller S, Neusser M, von Hase J, Calcagno E, Cremer M, Solovei I, Cremer C, Cremer T. (2002). Evolutionary conservation of chromosome territory arrangements in

cell nuclei from higher primates. Proc Natl Acad Sci U S A. 99(7):4424-9. doi: 10.1073/pnas.072618599.

Taylor DL, Ho JC, Oliver A, Watts FZ. (2002). Cell-cycle-dependent localisation of Ulp1, a Schizosaccharomyces pombe Pmt3 (SUMO)-specific protease. J Cell Sci. 115(Pt 6):1113-22. doi: 10.1242/jcs.115.6.1113.

Técher H, Koundrioukoff S, Nicolas A, Debatisse M. (2017). The impact of replication stress on replication dynamics and DNA damage in vertebrate cells. Nat Rev Genet. 18(9):535-550. doi: 10.1038/nrg.2017.46.

Teixeira-Silva A, Ait Saada A, Hardy J, Iraqui I, Nocente MC, Fréon K, Lambert SAE. (2017). The end-joining factor Ku acts in the end-resection of double strand break-free arrested replication forks. Nat Commun. 8(1):1982. doi: 10.1038/s41467-017-02144-5.

Thangavel S, Berti M, Levikova M, Pinto C, Gomathinayagam S, Vujanovic M, Zellweger R, Moore H, Lee EH, Hendrickson EA, Cejka P, Stewart S, Lopes M, Vindigni A. (2015). DNA2 drives processing and restart of reversed replication forks in human cells. J Cell Biol. 208(5):545-62. doi: 10.1083/jcb.201406100.

Therizols P, Duong T, Dujon B, Zimmer C, Fabre E. (2010). Chromosome arm length and nuclear constraints determine the dynamic relationship of yeast subtelomeres. Proc Natl Acad Sci U S A. 107(5):2025-30. doi: 10.1073/pnas.0914187107.

Thomä NH, Czyzewski BK, Alexeev AA, Mazin AV, Kowalczykowski SC, Pavletich NP. (2005). Structure of the SWI2/SNF2 chromatin-remodeling domain of eukaryotic Rad54. Nat Struct Mol Biol. 12(4):350-6. doi: 10.1038/nsmb919.

Toledo LI, Altmeyer M, Rask MB, Lukas C, Larsen DH, Povlsen LK, Bekker-Jensen S, Mailand N, Bartek J, Lukas J. (2013). ATR prohibits replication catastrophe by preventing global exhaustion of RPA. Cell. 155(5):1088-103. doi: 10.1016/j.cell.2013.10.043.

Toledo L, Neelsen KJ, Lukas J. (2017). Replication Catastrophe: When a Checkpoint Fails because of Exhaustion. Mol Cell. 66(6):735-749. doi: 10.1016/j.molcel.2017.05.001.

Torres-Rosell J, Sunjevaric I, De Piccoli G, Sacher M, Eckert-Boulet N, Reid R, Jentsch S, Rothstein R, Aragón L, Lisby M. (2007). The Smc5-Smc6 complex and SUMO modification of Rad52 regulates recombinational repair at the ribosomal gene locus. Nat Cell Biol. 9(8):923-31. doi: 10.1038/ncb1619.

Tretyakova NY, Groehler A 4th, Ji S. (2015). DNA-Protein Cross-Links: Formation, Structural Identities, and Biological Outcomes. Acc Chem Res. 48(6):1631-44. doi: 10.1021/acs.accounts.5b00056.

Tsang E, Miyabe I, Iraqui I, Zheng J, Lambert SA, Carr AM. (2014). The extent of error-prone replication restart by homologous recombination is controlled by Exo1 and checkpoint proteins. J Cell Sci. 127(Pt 13):2983-94. doi: 10.1242/jcs.152678.

Tsouroula K, Furst A, Rogier M, Heyer V, Maglott-Roth A, Ferrand A, Reina-San-Martin B, Soutoglou E. (2016). Temporal and Spatial Uncoupling of DNA Double Strand Break Repair Pathways within Mammalian Heterochromatin. Mol Cell. 63(2):293-305. doi: 10.1016/j.molcel.2016.06.002.

Tye S, Ronson GE, Morris JR. (2021). A fork in the road: Where homologous recombination and stalled replication fork protection part ways. Semin Cell Dev Biol. 113:14-26. doi: 10.1016/j.semcdb.2020.07.004.

Urulangodi M, Sebesta M, Menolfi D, Szakal B, Sollier J, Sisakova A, Krejci L, Branzei D. (2015). Local regulation of the Srs2 helicase by the SUMO-like domain protein Esc2 promotes recombination at sites of stalled replication. Genes Dev. 29(19):2067-80. doi: 10.1101/gad.265629.115.

Uziel T, Lerenthal Y, Moyal L, Andegeko Y, Mittelman L, Shiloh Y. (2003). Requirement of the MRN complex for ATM activation by DNA damage. EMBO J. 22(20):5612-21. doi: 10.1093/emboj/cdg541.

Uzunova K, Göttsche K, Miteva M, Weisshaar SR, Glanemann C, Schnellhardt M, Niessen M, Scheel H, Hofmann K, Johnson ES, Praefcke GJ, Dohmen RJ. (2007). Ubiquitin-dependent proteolytic control of SUMO conjugates. J Biol Chem. 282(47):34167-75. doi: 10.1074/jbc.M706505200.

Vallerga MB, Mansilla SF, Federico MB, Bertolin AP, Gottifredi V. (2015). Rad51 recombinase prevents Mre11 nuclease-dependent degradation and excessive PrimPol-mediated elongation of nascent DNA after UV irradiation. Proc Natl Acad Sci U S A. 112(48):E6624-33. doi: 10.1073/pnas.1508543112.

van Sluis M, McStay B. (2015). A localized nucleolar DNA damage response facilitates recruitment of the homology-directed repair machinery independent of cell cycle stage. Genes Dev. 29(11):1151-63. doi: 10.1101/gad.260703.115.

van Steensel B, Belmont AS. (2017). Lamina-Associated Domains: Links with Chromosome Architecture, Heterochromatin, and Gene Repression. Cell. 169(5):780-791. doi: 10.1016/j.cell.2017.04.022.

Vanoli F, Fumasoni M, Szakal B, Maloisel L, Branzei D. (2010). Replication and recombination factors contributing to recombination-dependent bypass of DNA lesions by template switch. PLoS Genet. 6(11):e1001205. doi: 10.1371/journal.pgen.1001205.

Varberg JM, Unruh JR, Bestul AJ, Khan AA, Jaspersen SL. (2022). Quantitative analysis of nuclear pore complex organization in *Schizosaccharomyces pombe*. Life Sci Alliance. 5(7):e202201423. doi: 10.26508/lsa.202201423.

Vare D, Groth P, Carlsson R, Johansson F, Erixon K, Jenssen D. (2012). DNA interstrand crosslinks induce a potent replication block followed by formation and repair of double strand breaks in intact mammalian cells. DNA Repair (Amst). 11(12):976-85. doi: 10.1016/j.dnarep.2012.09.010.

Vaz B, Popovic M, Ramadan K. (2017). DNA-Protein Crosslink Proteolysis Repair. Trends Biochem Sci. 42(6):483-495. doi: 10.1016/j.tibs.2017.03.005.

Vyas A, Freitas AV, Ralston ZA, Tang Z. (2021). Fission Yeast Schizosaccharomyces pombe: A Unicellular "Micromammal" Model Organism. Curr Protoc. 1(6):e151. doi: 10.1002/cpz1.151.

Waga S, Stillman B. (1994). Anatomy of a DNA replication fork revealed by reconstitution of SV40 DNA replication in vitro. Nature. 369(6477):207-12. doi: 10.1038/369207a0.

Waga S, Stillman B. (1998). The DNA replication fork in eukaryotic cells. Annu Rev Biochem. 67:721-51. doi: 10.1146/annurev.biochem.67.1.721.

Wang X, Ira G, Tercero JA, Holmes AM, Diffley JF, Haber JE. (2004). Role of DNA replication proteins in double-strand break-induced recombination in Saccharomyces cerevisiae. Mol Cell Biol. 24(16):6891-9. doi: 10.1128/MCB.24.16.6891-6899.2004.

Wang Z, Jones GM, Prelich G. (2006). Genetic analysis connects SLX5 and SLX8 to the SUMO pathway in Saccharomyces cerevisiae. Genetics. 172(3):1499-509. doi: 10.1534/genetics.105.052811.

Wang S, Su JH, Beliveau BJ, Bintu B, Moffitt JR, Wu CT, Zhuang X. (2016). Spatial organization of chromatin domains and compartments in single chromosomes. Science. 353(6299):598-602. doi: 10.1126/science.aaf8084.

Wassing IE, Graham E, Saayman X, Rampazzo L, Ralf C, Bassett A, Esashi F. (2021). The RAD51 recombinase protects mitotic chromatin in human cells. Nat Commun. 12(1):5380. doi: 10.1038/s41467-021-25643-y.

Waters LS, Minesinger BK, Wiltrout ME, D'Souza S, Woodruff RV, Walker GC. (2009). Eukaryotic translesion polymerases and their roles and regulation in DNA damage tolerance. Microbiol Mol Biol Rev. 73(1):134-54. doi: 10.1128/MMBR.00034-08.

Watson JD, Crick FH. (1953). Molecular structure of nucleic acids; a structure for deoxyribose nucleic acid. Nature. 171(4356):737-8. doi: 10.1038/171737a0.

Watts FZ, Skilton A, Ho JC, Boyd LK, Trickey MA, Gardner L, Ogi FX, Outwin EA. (2007). The role of Schizosaccharomyces pombe SUMO ligases in genome stability. Biochem Soc Trans. 35(Pt 6):1379-84. doi: 10.1042/BST0351379.

Wei X, Samarabandu J, Devdhar RS, Siegel AJ, Acharya R, Berezney R. (1998). Segregation of transcription and replication sites into higher order domains. Science. 281(5382):1502-6. doi: 10.1126/science.281.5382.1502.

Wei Y, Diao LX, Lu S, Wang HT, Suo F, Dong MQ, Du LL. (2017). SUMO-Targeted DNA Translocase Rrp2 Protects the Genome from Top2-Induced DNA Damage. Mol Cell. 66(5):581-596.e6. doi: 10.1016/j.molcel.2017.04.017.

Wang W, Klein KN, Proesmans K, Yang H, Marchal C, Zhu X, Borrman T, Hastie A, Weng Z, Bechhoefer J, Chen CL, Gilbert DM, Rhind N. (2021). Genome-wide mapping of human DNA replication by optical replication mapping supports a stochastic model of eukaryotic replication. Mol Cell. 81(14):2975-2988.e6. doi: 10.1016/j.molcel.2021.05.024.

Werner A, Flotho A, Melchior F. (2012). The RanBP2/RanGAP1*SUMO1/Ubc9 complex is a multisubunit SUMO E3 ligase. Mol Cell. 46(3):287-98. doi: 10.1016/j.molcel.2012.02.017.

Whalen JM, Dhingra N, Wei L, Zhao X, Freudenreich CH. (2020). Relocation of Collapsed Forks to the Nuclear Pore Complex Depends on Sumoylation of DNA Repair Proteins and Permits Rad51 Association. Cell Rep. 31(6):107635. doi: 10.1016/j.celrep.2020.107635.

Willaume S, Rass E, Fontanilla-Ramirez P, Moussa A, Wanschoor P, Bertrand P. (2021). A Link between Replicative Stress, Lamin Proteins, and Inflammation. Genes (Basel). 12(4):552. doi: 10.3390/genes12040552.

Wilson MA, Kwon Y, Xu Y, Chung WH, Chi P, Niu H, Mayle R, Chen X, Malkova A, Sung P, Ira G. (2013). Pif1 helicase and Polδ promote recombination-coupled DNA synthesis via bubble migration. Nature. 502(7471):393-6. doi: 10.1038/nature12585.

Willis N, Rhind N. (2011). Studying S-phase DNA damage checkpoints using the fission yeast Schizosaccharomyces pombe. Methods Mol Biol. 782:13-21. doi: 10.1007/978-1-61779-273-1_2.

Winey M, Bloom K. (2012). Mitotic spindle form and function. Genetics. 190(4):1197-224. doi: 10.1534/genetics.111.128710.

Wold MS. (1997). Replication protein A: a heterotrimeric, single-stranded DNA-binding protein required for eukaryotic DNA metabolism. Annu Rev Biochem. 66:61-92. doi: 10.1146/annurev.biochem.66.1.61.

Wold MS, Kelly T. (1988). Purification and characterization of replication protein A, a cellular protein required for in vitro replication of simian virus 40 DNA. Proc Natl Acad Sci U S A. 5(8):2523-7. doi: 10.1073/pnas.85.8.2523.

Wolner B, Peterson CL. (2005). ATP-dependent and ATP-independent roles for the Rad54 chromatin remodeling enzyme during recombinational repair of a DNA double strand break. J Biol Chem. 280(11):10855-60. doi: 10.1074/jbc.M414388200.

Wong RP, Petriukov K, Ulrich HD. (2021). Daughter-strand gaps in DNA replication - substrates of lesion processing and initiators of distress signalling. DNA Repair (Amst). 2021 Sep;105:103163. doi: 10.1016/j.dnarep.2021.103163.

Wong RP, García-Rodríguez N, Zilio N, Hanulová M, Ulrich HD. (2020). Processing of DNA Polymerase-Blocking Lesions during Genome Replication Is Spatially and Temporally Segregated from Replication Forks. Mol Cell. 77(1):3-16.e4. doi: 10.1016/j.molcel.2019.09.015.

Wood V, Gwilliam R, Rajandream MA, Lyne M, Lyne R, Stewart A, Sgouros J, Peat N, Hayles J, Baker S, Basham D, Bowman S, Brooks K, Brown D, Brown S, Chillingworth T, Churcher C, Collins M, Connor R, Cronin A, Davis P, Feltwell T, Fraser A, Gentles S, Goble A, Hamlin N, Harris D, Hidalgo J, Hodgson G, Holroyd S, Hornsby T, Howarth S, Huckle EJ, Hunt S, Jagels K, James K, Jones L, Jones M, Leather S, McDonald S, McLean J, Mooney P, Moule S, Mungall K, Murphy L, Niblett D, Odell C, Oliver K, O'Neil S, Pearson D, Quail MA, Rabbinowitsch E, Rutherford K, Rutter S, Saunders D, Seeger K, Sharp S, Skelton J, Simmonds M, Squares R, Squares S, Stevens K, Taylor K, Taylor RG, Tivey A, Walsh S, Warren T, Whitehead S, Woodward J, Volckaert G, Aert R, Robben J, Grymonprez B, Weltjens I, Vanstreels E, Rieger M, Schäfer M, Müller-Auer S, Gabel C, Fuchs M, Düsterhöft A, Fritzc C, Holzer E, Moestl D, Hilbert H, Borzym K, Langer I, Beck A, Lehrach H, Reinhardt R, Pohl TM, Eger P, Zimmermann W, Wedler H, Wambutt R, Purnelle B, Goffeau A, Cadieu E, Dréano S, Gloux S, Lelaure V, Mottier S, Galibert F, Aves SJ, Xiang Z, Hunt C, Moore K, Hurst SM, Lucas M, Rochet M, Gaillardin C, Tallada VA, Garzon A, Thode G, Daga RR, Cruzado L, Jimenez J, Sánchez M, del Rey F, Benito J,

Domínguez A, Revuelta JL, Moreno S, Armstrong J, Forsburg SL, Cerutti L, Lowe T, McCombie WR, Paulsen I, Potashkin J, Shpakovski GV, Ussery D, Barrell BG, Nurse P. (2002). The genome sequence of Schizosaccharomyces pombe. Nature. 415(6874):871-80. doi: 10.1038/nature724.
Woodcock CL. (2006). Chromatin architecture. Curr Opin Struct Biol. 16(2):213-20. doi: 10.1016/j.sbi.2006.02.005.

Wright WD, Heyer WD. (2014). Rad54 functions as a heteroduplex DNA pump modulated by its DNA substrates and Rad51 during D loop formation. Mol Cell. 53(3):420-32. doi: 10.1016/j.molcel.2013.12.027.

Wu L, Hickson ID. (2003). The Bloom's syndrome helicase suppresses crossing over during homologous recombination. Nature. 426(6968):870-4. doi: 10.1038/nature02253.

Wyatt HD, Sarbajna S, Matos J, West SC. (2013). Coordinated actions of SLX1-SLX4 and MUS81-EME1 for Holliday junction resolution in human cells. Mol Cell. 52(2):234-47. doi: 10.1016/j.molcel.2013.08.035.

Xiao Z, Chen Z, Gunasekera AH, Sowin TJ, Rosenberg SH, Fesik S, Zhang H. (2003). Chk1 mediates S and G2 arrests through Cdc25A degradation in response to DNA-damaging agents. J Biol Chem. 278(24):21767-73. doi: 10.1074/jbc.M300229200.

Xie Y, Kerscher O, Kroetz MB, McConchie HF, Sung P, Hochstrasser M. (2007). The yeast Hex3.Slx8 heterodimer is a ubiquitin ligase stimulated by substrate sumoylation. J Biol Chem. 282(47):34176-84. doi: 10.1074/jbc.M706025200.

Xu W, Aparicio JG, Aparicio OM, Tavaré S. (2006). Genome-wide mapping of ORC and Mcm2p binding sites on tiling arrays and identification of essential ARS consensus sequences in S. cerevisiae. BMC Genomics. 7:276. doi: 10.1186/1471-2164-7-276.

Xhemalce B, Riising EM, Baumann P, Dejean A, Arcangioli B, Seeler JS. (2007). Role of SUMO in the dynamics of telomere maintenance in fission yeast. Proc Natl Acad Sci U S A. 104(3):893-8. doi: 10.1073/pnas.0605442104.

Xie Z, Jay KA, Smith DL, Zhang Y, Liu Z, Zheng J, Tian R, Li H, Blackburn EH. (2015). Early telomerase inactivation accelerates aging independently of telomere length. Cell. 160(5):928-939. doi: 10.1016/j.cell.2015.02.002.

Xu Z, Fallet E, Paoletti C, Fehrmann S, Charvin G, Teixeira MT. (2015). Two routes to senescence revealed by real-time analysis of telomerase-negative single lineages. Nat Commun. 6:7680. doi: 10.1038/ncomms8680.

Yamaguchi-Iwai Y, Sonoda E, Buerstedde JM, Bezzubova O, Morrison C, Takata M, Shinohara A, Takeda S. (1998). Homologous recombination, but not DNA repair, is reduced in vertebrate cells deficient in RAD52. Mol Cell Biol. 18(11):6430-5. doi: 10.1128/MCB.18.11.6430.

Yang H, Li Q, Fan J, Holloman WK, Pavletich NP. (2005). The BRCA2 homologue Brh2 nucleates RAD51 filament formation at a dsDNA-ssDNA junction. Nature. 433(7026):653-7. doi: 10.1038/nature03234.

Yekezare M, Gómez-González B, Diffley JF. (2013). Controlling DNA replication origins in response to DNA damage - inhibit globally, activate locally. J Cell Sci. 126(Pt 6):1297-306. doi: 10.1242/jcs.096701.

Ying S, Hamdy FC, Helleday T. (2012). Mre11-dependent degradation of stalled DNA replication forks is prevented by BRCA2 and PARP1. Cancer Res. 72(11):2814-21. doi: 10.1158/0008-5472.CAN-11-3417.

Zaratiegui M, Vaughn MW, Irvine DV, Goto D, Watt S, Bähler J, Arcangioli B, Martienssen RA. (2011). CENP-B preserves genome integrity at replication forks paused by retrotransposon LTR. Nature. 469(7328):112-5. doi: 10.1038/nature09608.

Zidovska A, Weitz DA, Mitchison TJ. (2013). Micron-scale coherence in interphase chromatin dynamics. Proc Natl Acad Sci USA. 110(39):15555-60. doi: 10.1073/pnas.1220313110.

Zagelbaum J, Schooley A, Zhao J, Schrank BR, Callen E, Zha S, Gottesman ME, Nussenzweig A, Rabadan R, Dekker J, Gautier J. (2023) Multiscale reorganization of the genome following DNA damage facilitates chromosome translocations via nuclear actin polymerization. Nat Struct Mol Biol. 30(1):99-106. doi: 10.1038/s41594-022-00893-6.

Zegerman P, Diffley JF. (2010). Checkpoint-dependent inhibition of DNA replication initiation by Sld3 and Dbf4 phosphorylation. Nature. 467(7314):474-8. doi: 10.1038/nature09373.

Zellweger R, Dalcher D, Mutreja K, Berti M, Schmid JA, Herrador R, Vindigni A, Lopes M. (2015). Rad51-mediated replication fork reversal is a global response to genotoxic treatments in human cells. J Cell Biol. 208(5):563-79. doi: 10.1083/jcb.201406099.

Zeman MK, Cimprich KA. (2014). Causes and consequences of replication stress. Nat Cell Biol. 16(1):2-9. doi: 10.1038/ncb2897.

Zhang YW, Jones TL, Martin SE, Caplen NJ, Pommier Y. (2009). Implication of checkpoint kinase-dependent up-regulation of ribonucleotide reductase R2 in DNA damage response. J Biol Chem. 284(27):18085-95. doi: 10.1074/jbc.M109.003020.

Zhang H, Saitoh H, Matunis MJ. (2002). Enzymes of the SUMO modification pathway localize to filaments of the nuclear pore complex. Mol Cell Biol. 22(18):6498-508. doi: 10.1128/MCB.22.18.6498-6508.2002.

Zhang L, Meng J, Liu H, Huang Y. (2012). A nonparametric Bayesian approach for clustering bisulfate-based DNA methylation profiles. BMC Genomics. 13 Suppl 6(Suppl 6):S20. doi: 10.1186/1471-2164-13-S6-S20.

Zhao F, Kim W, Kloeber JA, Lou Z. (2020). DNA end resection and its role in DNA replication and DSB repair choice in mammalian cells. Exp Mol Med. 52(10):1705-1714. doi: 10.1038/s12276-020-00519-1.

Zhao X, Wu CY, Blobel G. (2004). Mlp-dependent anchorage and stabilization of a desumoylating enzyme is required to prevent clonal lethality. J Cell Biol. 167(4):605-11. doi: 10.1083/jcb.200405168.

Zhao X, Blobel G. (2005). A SUMO ligase is part of a nuclear multiprotein complex that affects DNA repair and chromosomal organization. Proc Natl Acad Sci U S A. 102(13):4777-82. doi: 10.1073/pnas.0500537102.

Zhu Z, Chung WH, Shim EY, Lee SE, Ira G. (2008). Sgs1 helicase and two nucleases Dna2 and Exo1 resect DNA double-strand break ends. Cell. 134(6):981-94. doi: 10.1016/j.cell.2008.08.037.

Zong D, Oberdoerffer P, Batista PJ, Nussenzweig A. (2020). RNA: a double-edged sword in genome maintenance. Nat Rev Genet. 21(11):651-670. doi: 10.1038/s41576-020-0263-7.